



Advanced High-Strength Steels Application Guidelines Version 6.0

Technical Editors:

Stuart Keeler, Sc.D. Mechanical Metallurgy

Menachem Kimchi, M.Sc. Welding Engineering

Peter J. Mooney, Managing Director, 3S-Superior Stamping Solutions, LLC



Table of Contents

(In PDF form, section titles can be clicked to navigate)

	Preface	vii
1.0	Section 1.0 Introduction, Development and Growth of AHSS	1-1
1.A.	Development History	1-1
1.B.	Today's AHSS	1-2
1.C.	Automotive Steel Performance Advantages (ASPA)	1-5
	1.C.1. Cost	1-5
	1.C.2. Safety	1-6
	1.C.3. Emissions	1-7
	1.C.3.a. Life Cycle Assessment (LCA)	1-9
1.D.	AHSS – In Use Applications and Requirement	1-10
	1.D.1. Crash Performance.	1-10
	1.D.2. Stiffness	1-11
	1.D.3. Formability and Manufacturing	1-11
	1.D.4. Current Vehicle Examples	1-12
	1.D.4.a. 2016-17 Chevy Cruze	1-12
	1.D.4.b. 2017 Kia Sportage	1-12
	1.D.4.c. 2017 Chrysler Pacifica	1-13
	1.D.4.d. FutureSteelVehicle (FSV)	1-14
1.E.	Using These Guidelines	1-17
2.0	Section 2.0 Metallurgy of AHSS	2-1
2.A.	Defining Steels	2-1
2.B.	Metallurgy of AHSS	2-2
	2.B.1. Dual Phase (DP) Steel	2-2
	2.B.2. Transformation Induced Plasticity (TRIP) Steel	2-5
	2.B.3. Complex (CP) Steel	2-8
	2.B.4. Martensitic (MS) Steel	2-10
	2.B.5. Ferritic-Bainitic (FB) Steel	2-12
	2.B.6. Twinning Induced Plasticity (TWIP) Steel	2-14
	2.B.7. Hot-Formed (HF) Steel	2-16
	2.B.8. Post-Forming Heat-Treatable (PFHT) Steel	2-16
	2.B.9. Special Processed Steels	2-17
	2.B.10. Evolving AHSS Types	2-17
2.C.	Conventional Low & High-Strength Automotive Sheet Steels	2-19
	2.C.1. Mild Steels	2-14
	2.C.2. Interstitial-free (IF) Steels (Low-Strength And High-Strength)	2-19
	2.C.3. Bake Hardenable (BH) Steels	2-19
	2.C.4. Carbon-Manganese (CM) Steels	2-19
	2.C.5. High-Strength Low-Alloy (HSLA) Steels	2-19

2.D	Understanding Mechanical Properties	2-20
2.D.1	Elastic Stresses – Young’s Modulus	2-21
2.D.2	Yield Strength vs. Yield Stress	2-21
2.D.3	Work Hardening – n-value	2-23
2.D.4	Diffuse/Width Neck – Tensile Strength	2-25
2.D.5	Local/Thickness Neck – Forming Limit Curve	2-25
2.D.6	Fracture – Total Elongation	2-26
2.D.7	Directionality of Properties (Anisotropy Ratio) – r-value	2-26
2.D.8	Bake Hardening and Aging	2-26
2.D.9	Strain Rate Effects	2-26
2.D.10	Key Points	2-29
2.E	Corrosion Resistant Coatings on AHSS	2-30
2.E.1	Hot Dipped and Electrogalvanized Coatings	2-30
2.E.2	Electrogalvanized Coatings	2-31
3.0	Section 3.0 Forming and Manufacturing	3-1
3.A.	General Comments	3-1
3.B.	Sheet Metal Forming	3-2
3.B.1.	Global Versus Local Formability	3-2
3.B.2.	Stress-strain Curves	3-3
3.B.3.	Deformation Limits	3-11
	3.B.3.a. Forming Limit Curves (FLC) Global Formability	3-11
	3.B.3.b. Edge Stretching Limits – Local Formability	3-12
	3.B.3.c. Stretch Bend Limits – Local Formability	3-20
	3.B.3.d. Key Points	3-24
3.B.4.	Cold Forming Modes	3-25
	3.B.4.a. Stretching	3-25
	3.B.4.b. Bending	3-30
	3.B.4.c. Deep Drawing – Cup Drawing	3-31
	3.B.4.d. Roll Forming	3-33
	3.B.4.e. Key Points	3-35
3.B.5.	Hot Forming	3-36
	3.B.5.a. Direct Hot-Forming Process	3-36
	3.B.5.b. Indirect Hot-Forming Process	3-38
	3.B.5.c. Benefits of Hot Forming	3-39
	3.B.5.d. Typical Parts	3-40
	3.B.5.e. Key Points	3-40
3.C.	Tooling and Design Considerations	3-41
3.C.1.	Tool and Part Design	3-41
	3.C.1.a. Multiple Stage Forming	3-44
	3.C.1.b. Prototype Tools	3-45
3.C.2.	Tool Materials and Die Wear	3-45
	3.C.2.a. Tool Materials	3-46
	3.C.2.b. Key Points	3-48
	3.C.2.c. Tool Wear, Clearance and Burr Height	3-49
	3.C.2.d. Key Points	3-52

	3.C.3.	Springback Management	3-53
		3.C.3.a. Springback and AHSS	3-53
		3.C.3.b. Origins of Springback	3-54
		3.C.3.c. Types of Springback	3-54
		3.C.3.d. Three Methods of Correction	3-58
		3.C.3.e. Key Points	3-70
	3.C.4.	Blanking, Shearing and Trim Operations	3-71
		3.C.4.a. General Comments	3-71
		3.C.4.b. Trim Blade Design & Blanking Clearances	3-71
	3.C.5.	Computerized Die Tryout (Virtual Forming)	3-75
		3.C.5.a. Short Explanation of Process	3-75
		3.C.5.b. Advantages for AHSS Forming	3-75
		3.C.5.c. Key Points	3-77
	3.C.6.	Press Requirements	3-78
		3.C.6.a. Servpro Presses	3-78
		3.C.6.b. Force versus Energy	3-82
		3.C.6.c. Prediction of Press Forces Using Simulative Tests	3-85
		3.C.6.d. Extrapolation From Existing Production Data	3-85
		3.C.6.e. Computerized Forming-Process Development	3-86
		3.C.6.f. Case Study for Press Energy	3-87
		3.C.6.g. Setting Draw Beads	3-87
		3.C.6.h. Key Points	3-88
	3.C.7.	Straightening and Precision Levelling AHSS	3-89
3.D.		Die Surface Treatments and Lubrication	3-92
	3.D.1.	Die Surface Treatments	3-92
		3.D.1.a. Surface hardening vs. Surface Coating	3-92
	3.D.2.	Lubricant Overview	3-94
		3.D.2.a. AHSS Energy, Heat and Lubrication	3-94
		3.D.2.b. New Lubricants for AHSS Stampings	3-96
		3.D.2.c. Key Points	3-97
3.E.		Other Steel Processing Technologies	3-98
	3.E.1.	Laser (Tailor) Welded Blanks	3-98
	3.E.2.	Laser Welded Coil	3-99
	3.E.3.	Tailor Rolled Coil	3-100
	3.E.4.	Laser Blanking	3-100
	3.E.5.	Traditional Tube Forming	3-101
		3.E.5.a. High Frequency Welded Tubes	3-101
		3.E.5.a. Laser Welded Tailored Tubes	3-105
		3.E.5.c. Variable (Multiple) Walled Tubes	3-107
		3.E.5.d. Key Points	3-108
	3.E.6.	Hydroforming Tubes	3-109
		3.E.6.a. Pre-Form Bending	3-109

		3.E.6.b. Forming	3-110
		3.E.6.c. Post Forming Trimming	3-111
		3.E.6.d. Design Considerations	3-111
		3.E.6.e. Key Points	3-111
3.F.		Process Maintenance and Quality Control	3-112
	3.F.1.	Reference Panels	3-112
	3.F.2.	Key Points	3-114
3.G.		In-Service Requirements	3-115
	3.G.1.	Crash Management	3-115
	3.G.2.	Fatigue	3-116
	3.G.3.	Key Points	3-117
4.0		Section 4.0 Joining	4-1
4.A.		Introduction	4-1
4.B.		Joining Processes	4-1
4.C.		Resistance Welding Processes	4-2
	4.C.1.	Fundamentals and Principles of Resistance Welding	4-2
	4.C.2.	Resistance Welding Processes	4-6
	4.C.3.	Heat Balance – Material Balance – Thickness Balance	4-16
	4.C.4.	Welding Current Mode	4-17
	4.C.5.	Electrode Geometry	4-19
	4.C.6.	Part Fit-Up	4-19
	4.C.7.	Coating Effects	4-19
	4.C.8.	Judging Weldability using Carbon Equivalence (CE)	4-21
	4.C.9.	Process Simulation	4-21
4.D.		Resistance Spot Welding Joint Test Performance	4-23
	4.D.1.	Destructive and In-Process Weld Testing	4-24
	4.D.2.	Shear Tension Strength of Welds and Fracture Modes	4-26
	4.D.3.	Fracture Mode	4-29
	4.D.4.	Fatigue Strength of Spot Weld	4-31
	4.D.5.	Improvement in CTS by Post-Heat Conduction	4-33
	4.D.6.	Embrittlement Phenomenon	4-35
4.E.		Spot Welding of Three Steel Sheets with Large Thickness Ratios	4-37
4.F.		Application of Spot Welding to Hollow Members	4-40
4.G.		Arc Welding Processes	4-42
	4.G.1.	Fundamental and Principles of Arc Welding	4-42
		4.G.1.a. Shielding	4-43
		4.G.1.b. Weld Joints and Weld Types for Arc Welding	4-44
		4.G.1.c. Electrode Feed Rate	4-45
		4.G.1.d. Welding Travel Speed	4-45
		4.G.1.e. Arc Welding Safety	4-45
	4.G.2.	Arc Welding Procedures	4-46

4.H.	Gas Metal Arc Welding (GMAW)	4-51
4.H.1.	GMAW Procedures	4-53
4.I.	Arc Stud Welding	4-58
4.I.1.	Gas Arc Stud Welding	4-59
4.J.	High Energy Density Welding Processes (Laser Welding)	4-60
4.J.1.	Fundamentals and Principles of High Energy Density Welding Processes	4-60
4.J.2.	Laser Beam Welding	4-61
4.J.3.	Laser Welding Processes	4-63
	4.J.3.a. Butt Welds and Tailor-Welded Products	4-64
	4.J.3.b. Assembly Laser Welding	4-65
	4.J.3.c. Remote Laser Welding	4-66
	4.J.3.d. Body-in-White (BIW) Joining	4-68
4.K.	Hybrid Welding Processes	4-71
4.K.1.	Fundamentals and Principles of Hybrid Welding	4-71
4.K.2.	Hybrid Welding Processes	4-71
	4.K.2.a. Hybrid Laser and MIG Welding	4-72
	4.K.2.b. Hybrid RSW and Adhesives	4-73
4.L.	Solid-State Welding Processes	4-76
4.L.1.	Friction Welding Processes	4-76
	4.L.1.a. Friction Stir Welding (FSW)	4-76
4.L.2.	High Frequency (HF) Welding	4-79
	4.L.2.a. Fundamentals and Principles of HF Welding	4-79
	4.L.2.b. Advantages/Disadvantages of HF Welding	4-81
	4.L.2.c. Induction Seam Welding of Pipe and Tubing	4-82
	4.L.2.d. Contact Seam Welding of Pipe and Tubing	4-83
	4.L.3. HF Induction Welding Procedures	4-84
	4.L.4. Safe Practices	4-86
4.M.	Magnetic Pulse Welding (MPW)	4-87
4.M.1.	Physics of the Process	4-87
4.M.2.	Power Source	4-88
4.M.3.	Tubular Structures	4-89
4.M.4.	Applications	4-90
4.M.5.	Safe Practices	4-90
	4.M.5.a. Mechanical	
	4.M.5.b. Electrical	4-90
	4.M.5.c. Personal Protection	4-90
4.N.	Brazing and Soldering	4-91
4.N.1.	Fundamentals and Principles of Brazing and Soldering	4-91
4.N.2.	Brazing Procedures	4-92
4.O.	Adhesive Bonding	4-94
4.O.1.	Fundamentals and Principles of Adhesive Bonding	4-94

	4.O.2.	Adhesive Bonding Procedures	4-94
4.P.		Mechanical Joining	4-96
4.Q.		Material Issues for Field Weld Repair and Replacement	4-100
4.R.		Joint Performance in Use	4-101
4.S.		Joint Performance Comparisons	4-107
	4.S.1.	All Processes General Comparison	4-108
	4.S.2.	Spot Welding Compared to Spot/Laser Welding Mixture	4-115
		4.S.2.a. Cost Effectiveness	4-115
	4.S.3.	GMAW Compared to Laser Welding	4-116
5.0		Section 5.0 Glossary	5-1
6.0		Section 6.0 References	6-1

This document is intended to provide technical application guidelines. The user of such information is encouraged to consult the steel supplier for specific applications. The World Steel Association and WorldAutoSteel have exercised reasonable diligence in preparing this document but are not responsible for any errors or omissions therein. The material in this document is protected by copyright. Use, distribution to third parties or reproduction in any format is allowed, provided WorldAutoSteel is acknowledged as the source of this information.

© *WorldAutoSteel 2017*

Preface

New global standards for vehicle safety (crash), fuel economy and tailpipe emissions are firmly in place through 2020, with aggressive targets being negotiated for the next ten years. Interestingly, regional regulations that were very different converge between 2020 and 2025, as shown in Figure P-1. Automakers are searching for advanced designs and materials that help them meet these tough standards, while still being manufacturable. Today's vehicle programs must balance performance, safety, fuel efficiency, affordability and the environment, while maintaining designs that are appealing to customers. Innovative steel designs must achieve significant increases in strength, while offering thinner gauges to reduce vehicle mass.

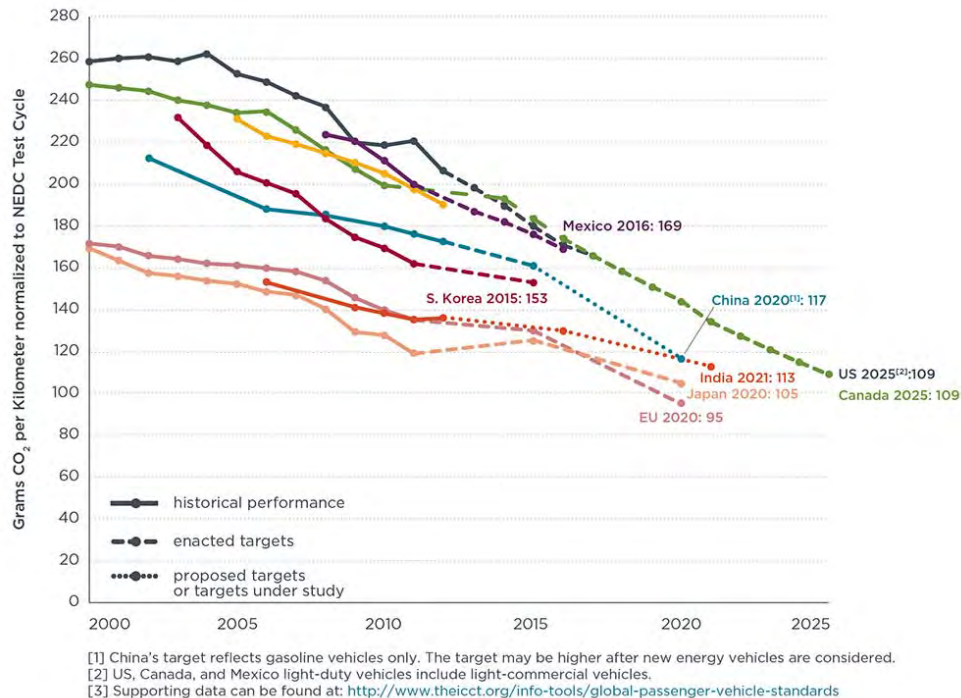


Figure P-1: Global Emissions Regulations¹⁻²

During the next ten years, applications of Advanced High-Strength Steels (AHSS) into OEM and supplier plants will proliferate, and users of AHSS will need to rapidly accumulate application knowledge. Additional research and press shop experiences have resulted in greater understanding of these unique steels, and so we present this update of the AHSS Application Guidelines - Version 6.0, to capture global best practices. These guidelines are the leading AHSS information resource for engineers and press shop personnel. Experts from WorldAutoSteel and our partners developed previous versions of the AHSS Application Guidelines covering metallurgy, forming, and joining. Version 6.0 reflects new content highlighting the broader materials portfolio, advanced fabrication technologies, and optimized joining processes.

In addition, a joint effort by WorldAutoSteel and A/SP created a common Glossary of Terms that encompass the entire field of AHSS. Other mutual interchanges of data and technology information continue.

Our appreciation is given to the many steel company experts throughout the world who have contributed to this and previous AHSS Application Guidelines. We have enjoyed contributions from Carrie

Tamarelli, and the Steel Market Development Institute (SMDI), who completed a comprehensive internal document entitled *AHSS 101: The Evolving Use of Advanced High-Strength Steels for Automotive Applications*. This is just one of many SMDI contributions. Special thanks to the Auto/Steel Partnership, who contributed from their vast database of projects and manufacturing experiences, jointly developing content with WorldAutoSteel, to add to the Guidelines' robustness and practical insight.

WorldAutoSteel acknowledges Dr Stuart Keeler of Keeler Technologies LLC, who has contributed for many years as the Technical Editor of the Metallurgy and Forming sections, and Professor Menachem Kimchi of The Ohio State University, who continues as the Technical Editor for Joining. Both have accomplished much in their distinguished careers, and we're thankful for their devotion to this body of work. Finally, appreciation and acknowledgement is given to Peter Mooney, 3S-Superior Stamping Solutions, LLC, who provided key metallurgical and formability details to this Version 6.0.

These Guidelines and other WorldAutoSteel information can be found at www.worldautosteel.org. WorldAutoSteel member companies who sponsored this work and provided expert reviews are listed following.

George Coates
Technical Director, WorldAutoSteel
World Steel Association

Members of WorldAutoSteel are:

- AK Steel
- Anshan Iron and Steel Group Corporation
- Arcelor Mittal
- Baoshan Iron & Steel Co. Ltd.
- China Steel Corporation
- Ereğli Demir ve Çelik Fabrikaları T.A.Ş.
- HBIS Group Co., Ltd.
- Hyundai-Steel Company
- JFE Steel Corporation
- JSW Steel Limited
- Kobe Steel, Ltd.
- Nippon Steel & Sumitomo Metal Corporation
- Nucor Corporation
- POSCO
- SeverStal
- SSAB
- Tata Steel
- ThyssenKrupp Steel Europe AG
- United States Steel Corporation
- Usinas Siderúrgicas de Minas Gerais S.A.
- voestalpine Stahl GmbH

SECTION 1.0 – INTRODUCTION TO ADVANCED HIGH-STRENGTH STEELS (AHSS)

With escalating concerns about human-induced green-house gases, global legislators have passed more stringent vehicle emissions regulations through 2020, while considering further, aggressive targets for the next ten years. Automakers are searching for new materials and engineering capabilities to meet requirements that often conflict. As an example, structural applications require materials characterized by high strength and stiffness, often achieved with greater thickness. But fuel economy and emissions are positively impacted when component thickness is reduced. New vehicle designs with complex geometries are aesthetically pleasing, but difficult to form and join, compromised further by thickness reduction to achieve mass reduction targets. The global steel industry continues to develop new grades of steel, defined by ever-increasing strength and formability capabilities, continually reinventing this diverse material to address these opposing demands. These Advanced High-Strength Steels (AHSS) are characterized by unique microstructures and metallurgical properties that allow OEM's to meet the diverse functional requirements of today's vehicles.

Worldwide working groups within the WorldAutoSteel organization created the AHSS Application Guidelines to explain how and why AHSS steels were different from traditional higher strength steels in terms of press-forming, fabrication and joining for automotive underbody, structural, and body panels designed for higher strength steels. This Version 6.0 document provides in-depth current information on a wide range of topics related to successful application of these steels.

1.A. Development History

In 1994, a consortium of 35 sheet steel producers began the UltraLight Steel Auto Body (ULSAB)^{W-1} program to design a lightweight steel auto body structure that would meet a wide range of safety and performance targets.^{S-6} The body-in-white (BIW) unveiled in 1998 validated the design concepts of the program, and ULSAB proved to be lightweight, structurally sound, safe, executable and affordable. One of the major contributors to the success of the ULSAB was a group of new steel types and grades called Advanced High-Strength Steels (AHSS). The AHSS family had unique microstructures utilizing complex deformation and phase transformation processes to achieve strength and ductility combinations that were never-before realized. Better still, these materials would utilize existing stamping and assembly fabrication equipment and production methods.

More projects followed to demonstrate and communicate the capability of steel to meet demands for increased safety and fuel efficiency through light-weighting of various vehicle structures, as captured in Figure 1.A-1. For example, the UltraLight Steel Auto Closures (ULSAC) program developed mass-efficient hoods, doors and decklids from AHSS. The UltraLight Steel Auto Body Advanced Vehicle Concepts (ULSAB-AVC) program further refined fabrication methods in conjunction with these new materials, to achieve even greater mass reduction with AHSS.^{A-8} In 2008, WorldAutoSteel began yet another program called FutureSteelVehicle^{W-2}, where steel members accelerated the development of new AHSS grades, further stretching the envelope for strength and ductility levels. The FutureSteelVehicle (FSV) program took automotive steel applications to GigaPascal strength AHSS and added the dimension of designing for reduced life cycle emissions.^{W-7} Through engineering optimization, FSV achieved 39% mass reduction in the body structure.^{G-5} The engineering reports for this project, available at www.worldautosteel.org, are still being downloaded today by engineers around the world, and used to guide steel technology selection and application.

The Auto/Steel Partnership (A/SP) engaged in research and demonstrated the value of AHSS through several programs.^{S-6} One such project, Lightweight Front End Structure, used a holistic approach to meet goals of more than 20 percent weight reduction while maintaining crash worthiness.

Manufacturability was examined and emphasized throughout this project. Another key program, the Future Generation Passenger Compartment project, particularly examined the effect of mass compounding. Over the years since ULSAB, the successes of AHSS have motivated steel companies to continue research on both new types and grades of AHSS and to then bring these new steels to production. Essential for the growing use of AHSS has been the simultaneous development of new processes and equipment to produce and form the material. Some of these processes are described in later sections of these guidelines.



Figure 1.A-1: WorldAutoSteel vehicle development programs.

1.B. Today's AHSS

AHSS are complex, sophisticated materials, with carefully selected chemical compositions and multiphase microstructures resulting from precisely controlled heating and cooling processes. Various strengthening mechanisms are employed to achieve a range of strength, ductility, toughness, and fatigue properties.

The AHSS family includes Dual Phase (DP), Complex-Phase (CP), Ferritic-Bainitic (FB), Martensitic (MS), Transformation-Induced Plasticity (TRIP), Hot-Formed (HF), and Twinning-Induced Plasticity (TWIP). These 1st and 2nd Generation AHSS grades are uniquely qualified to meet the functional performance demands of certain parts. For example, DP and TRIP steels are excellent in the crash zones of the car for their high energy absorption. For structural elements of the passenger compartment, extremely high-strength steels, such as Martensitic and boron-based Press Hardened Steels (PHS) result in improved safety performance. Recently there has been increased funding and research for the development of the "3rd Generation" of AHSS. These are steels with special alloying and thermo-mechanical processing to achieve improved strength-ductility combinations compared to present grades, with potential for more efficient joining capabilities, at lower costs. For example, in the U.S., a DOE-sponsored program is enabling the development of 1200 MPa steels with three-fold improvements in ductility. The broad range of properties is best illustrated by the famous Steel Strength Ductility Diagram, captured in Figure 1.B-1.

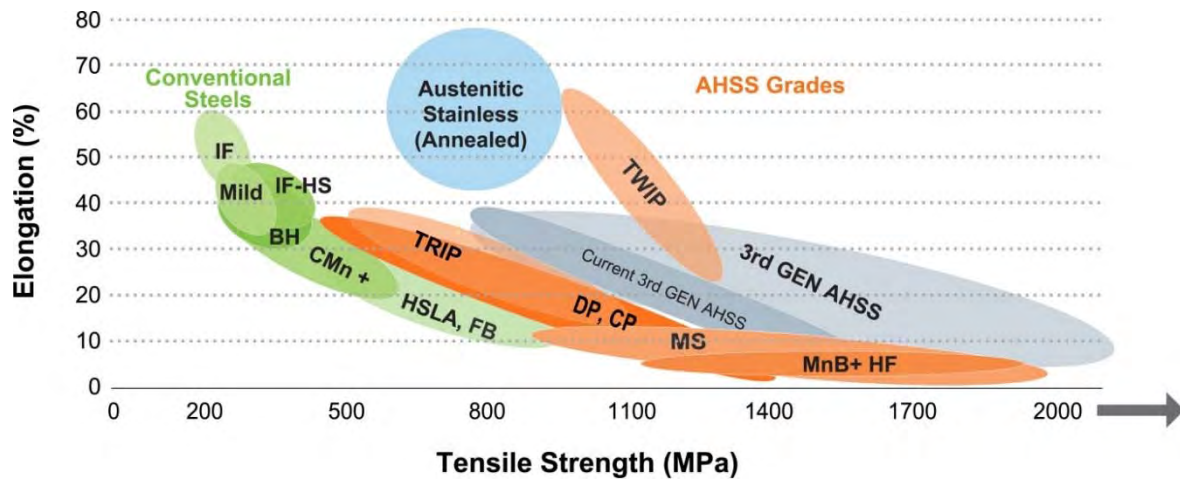


Figure 1.B-1: Steel Strength Ductility Diagram, illustrating the range of properties available from today's AHSS grades.^{W-5}

Advanced high-strength steel (AHSS) grades contain significant alloying and two or more phases. The multiple phases provide increased strength and ductility not attainable with single phase steels, such as high strength, low alloy (HSLA) grades. HSLA materials achieve their strength through alloying and solid solution hardening, whereas AHSS are produced by using specific alloys and precise thermomechanical processing.

In the past, steels with tensile strength (UTS) levels ≥ 550 MPa and greater were generally categorized as AHSS, and the name “ultra-high-strength steels” was reserved for tensile strengths exceeding 780 MPa. However, today there are multiple phase AHSS with tensile strengths as low as 440 MPa, and so using strength as the threshold for whether a steel qualifies as “AHSS” is no longer suitable.

AHSS with tensile strengths of at least 1000 MPa are often called “GigaPascal steel” (1000 MPa = 1GPa). Please note another category of steels, represented with a bubble in Figure 1.B-1: Austenitic Stainless Steel. These materials have excellent strength combined with excellent ductility, and thus meet many vehicle functional requirements. Third Generation AHSS seeks to offer comparable or improved capabilities at significantly lower cost.

Because the nomenclature for steel differs around the world, this particular report adopts the generic classification “XX aaa/bbb” where:

- XX = Type of steel (abbreviations expanded in Table 1-1 below)
- aaa = Minimum yield strength (YS) in MPa
- bbb = Minimum ultimate tensile strength (UTS) in Mega Pascal (MPa)^{W-7}

These various steel product families are shown in Table 1.B-1, in accordance with this nomenclature.

Table 1.B-1: Steel type designators.^{W-7}

XX	Type of steel	XX	Type of steel
HSLA	High Strength, Low Alloy	TRIP	Transformation Induced Plasticity
DP	Dual Phase	MS	Martensitic (MART)
CP	Complex Phase	TWIP	Twinning-Induced Plasticity
FB	Ferritic Bainitic	HF	Hot Formed (and quenched)
Q & P	Quenching & Partitioning	TPN	Three Phase Nano-Precipitation

Previous AHSS Application Guidelines showcased a materials portfolio driven by the FSV program, with more than twenty new grades of AHSS acknowledged as commercially available by 2015-2020. The AHSS materials portfolio continues to grow, as the steel industry responds to requirements for high strength, light weight steels. Thus, Table 1.B-2 below is a current reflection of available AHSS grades today. More details about these grades and their applications are provided in the following sections of this report.

Table 1.B-2: AHSS Version 6.0 Materials Portfolio (including HSLA)

No.	Steel Grade	Min Yield Strength	Min Tensile Strength
		MPa	MPa
1	DP 210/440	210	440
2	DP 300/500	300	500
3	FB 330/450	330	450
4	HSLA 350/450	350	450
5	DP 350/600	350	600
6	TRIP 350/600	350	600
7	TRIP 400/700	400	700
8	HSLA 420/500	420	500
9	FB 450/600	450	600
10	TRIP 450/800	450	800
11	HSLA 490/600	490	600
12	CP 500/800	500	800
13	DP 500/800	500	800
14	TWIP 500/900	500	900
15	TWIP 500/980	500	980
16	HSLA 550/650	550	650
17	CP 600/900	600	900
18	TWIP 600/900	600	900
19	DP 600/980	600	980
20	TRIP 600/980	600	980
21	Q&P 650/980	650	980
22	CP 680/780	680	780
23	TPN 680/780	680	780
24	HSLA 700/780	700	780
25	DP 700/1000	700	1000
26	CP 750/900	750	900
27	TPN 750/900	750	900
28	DP 750/980	750	900
29	TRIP 750/980	750	980
30	TWIP 750/1000	750	1000
31	CP 800/1000	800	1000
32	DP 800/1180	800	1180
33	CP 850/1180	850	1180
34	MS 950/1200	950	1200
35	TWIP 950/1200	950	1200
36	CP 1000/1200	1000	1200
37	MS 1050/1470	1050	1470
38	CP1050/1470	1050	1470
39	HF 1050/1500	1050	1500
40	DP 1150/1270	1150	1270
41	MS 1150/1400	1150	1400
42	HF 1200/1900	1200	1900
43	MS 1250/1500	1250	1500

When considering AHSS application benefits for vehicles, the steel industry has adopted the acronym **SAFE**—for crash protection (**S**afety), for **A**ffordability and cost, for **F**uel efficiency, and for the **E**nvironment. The following are highlights of research that summarize these automotive steel performance advantages.

1.C. Automotive Steel Performance Advantages (ASPA)

AHSS uniquely satisfy safety, efficiency, emissions, manufacturability, durability, and cost requirements.

1.C.1. Cost



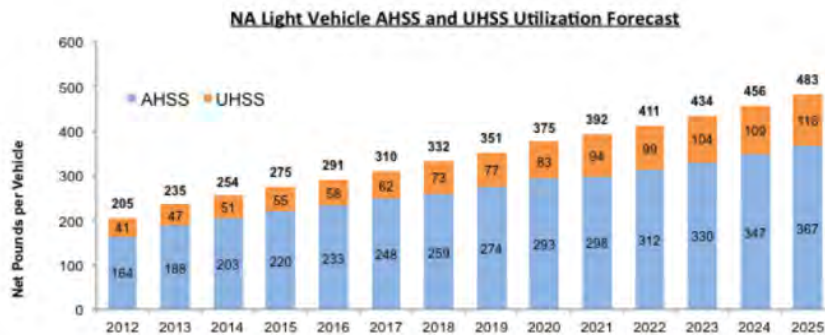
Key reasons to utilize AHSS are (1) better performance in crash energy management, and (2) superior strength allowing this performance to be achieved with thinner materials, translating into lower vehicle weight. It is important to note that the auto industry has adopted light-weighting as a greenhouse gas reduction strategy; this strategy, however, must be executed in an **affordable manner**. In the WorldAutoSteel vehicle programs and competitive benchmarking studies^{W-5}, it has been clearly demonstrated that optimized steel body structures can be constructed with

very modest increases in total system cost relative to conventional body structures. Thus, today's steels enable significant mass reduction, while meeting crash and other functional requirements, while preserving affordability.

As a result, the steel industry is seeing unprecedented growth in AHSS automotive applications. Independent marketing research suggests that they are the fastest growing materials for future automotive applications^{D-2} as shown in Figure 1.C-1.

AHSS Forecast

The 2014 average AHSS use in North American produced light vehicles is 254 pounds and expected to nearly double to 483 pounds by 2025



Source: Ducker Analysis

Figure 1.C-1: AHSS is the fastest growing automotive material.^{D-2}

Most steel companies are extending their research and development efforts to expand the range of properties available through these new steels, to enable safe and environmentally friendly vehicles. In North America, light vehicle metallic material trends^{D-2} show the use of AHSS will grow significantly (Figure 1.C-2).

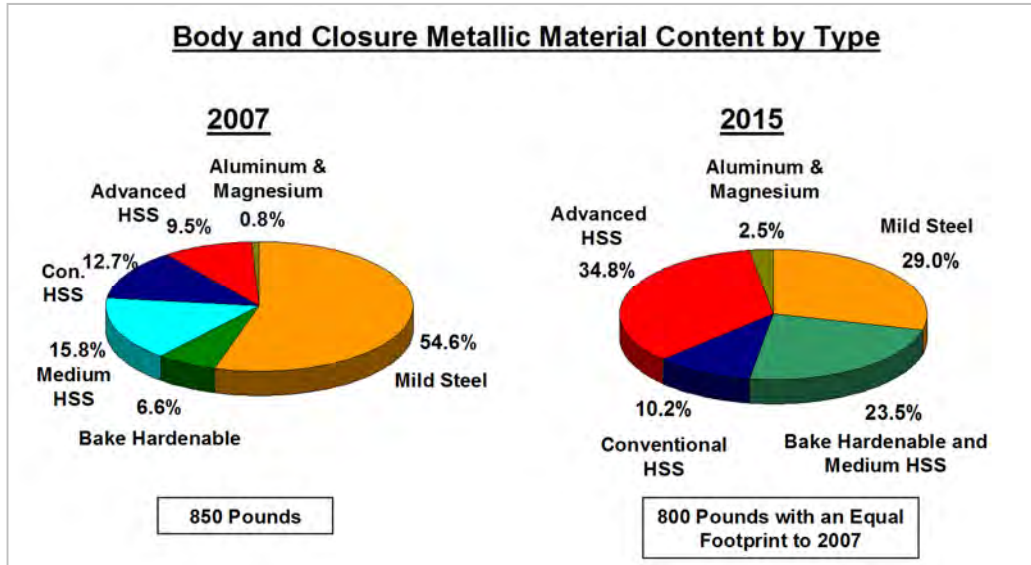


Figure 1.C-2: The use of high-strength steel (HSS) and AHSS grades are growing rapidly.^{D-2}

1.C.2. Safety



The percentage of high strength steels used in light vehicles relative to other materials continues to grow, and much of the growth has been fueled by increasingly stringent safety regulations and ratings systems. Consumers are demanding safe cars, and governments are responding with new tests and standards that **influence auto body structures, design and materials**. The results of vehicle safety performance tests are then a strong incentive affecting consumer purchasing decisions.

In the U.S., the National Highway Traffic Safety Administration (NHTSA) sets standards for vehicle safety, such as those for impact resistance, restraints, and fuel economy.^{N-4} Similarly, the European New Car Assessment Program (NCAP) measures vehicle performance in a variety of crash tests, including front, side and pole impacts, and impacts with pedestrians. Testing by the U.S. Insurance Institute for Highway Safety (IIHS) also has encouraged improved frontal, side, and rear impact ratings, as well as roof strength and rollover ratings, for automobiles on the road today.^{I-3} Meeting these standards often requires the addition of weight to the vehicle.

There is consensus in the automotive supply chain that **safe vehicles can be designed with reduced weight** if care is taken in the **design phase**. In other words, material properties can be optimized through engineering design to avoid excess or redundant mass in the structure. The FSV program showed that natural, non-linear load paths allow for more effective crash management and lighter weight structures, attainable through design optimization and rigorous application of AHSS.^{W-7}

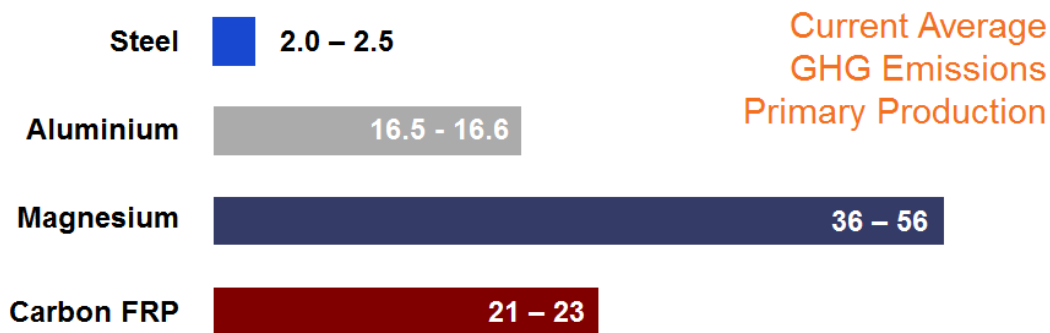


1.C.3. Emissions

As environmental and climate change concerns escalate, pressure is being applied in every industry to reduce the greenhouse gas (GHG) produced by our modern lifestyles. Consequently, the automotive industry is receiving increasing pressure to reduce its environmental impact while maintaining safety and affordability. In the process, **an erroneous perception has emerged that automotive light-weighting and**

reduced GHG emissions are primarily associated with the application of low-density materials, like aluminium, magnesium and composites.

These low density materials are currently being used in luxury class vehicles, where their costs are more easily absorbed into the high sales price. These same materials are now finding their way into higher volume vehicles to reach light-weighting goals, where their high costs can be somewhat justified against penalties for violating fuel economy or emissions mandates, or to reduce costly batteries for electric vehicles. However, low density materials create an offsetting emissions problem, as the production of these materials is GHG-intensive, and therefore costly to the environment.^{P-3} The production of these alternative materials can produce 7 to 20 times more emissions than steel, as shown in Figure 1.C-3.



Footnotes:

- All steel and aluminium grades included in ranges.
- Difference between AHSS and conventional steels less than 5%.
- Aluminium data - global for ingots; European only for process from ingot to final products .

Figure 1.C-3: Material average GHG emissions from primary production, in kg CO₂e/kg material.^{W-7, G-4}

Per kilogram emissions are not the whole story, of course. The idea behind the use of these lower density materials is that you can use less material. Doesn't this reduction in material offset the higher GHG emissions? Not necessarily. To illustrate this point, consider the material production emissions of a typical automotive component. The mid-range GHG values for each material are taken from the above chart and then multiplied by the actual material weight that is required to make the reference component; this is depicted for a hypothetical component in Figure 1.C-4. The actual mass for an equivalent component varies based on the material(s) utilized, and the design of the component.

Material Production GHG comparison for a functionally equivalent component - typical example

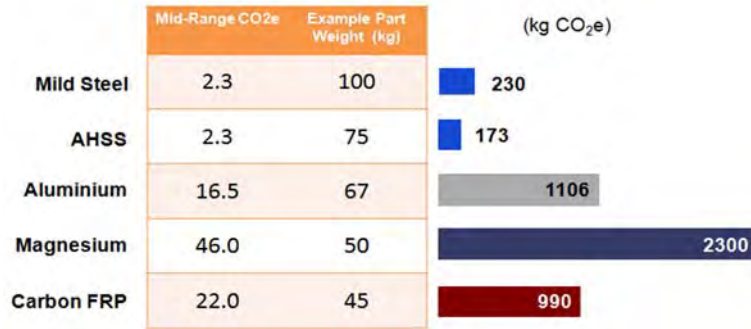


Figure 1.C-4: Material GHG emissions for typical functional unit.

Though less weight is required for some alternative materials to achieve the same component functional performance, the material production emissions can still be many times higher than those of the baseline component. Thus, the increase in material production emissions may outweigh the reduction in use phase emissions even considering the mass savings benefit.^{G-4}

This kind of unintended consequence is an issue today, and it will only get worse in the future if the focus remains solely on tailpipe emissions. For a typical gasoline-powered vehicle today, approximately 65-70% of GHG emissions come from the tailpipe, with the remaining 30-35% caused by vehicle and fuel production and vehicle disposal.

However, as the automotive industry’s efforts to reduce GHG emissions are increasingly moving towards more advanced powertrains and fuel sources, material production accounts for a much larger percentage of total GHG.^{P-4} These powertrains greatly reduce the tailpipe GHG emissions, which means that the material production phase emissions make up a greater percentage of total vehicle emissions (Figure 1.C-5). For example, in a battery electric vehicle powered entirely by renewable electricity, vehicle production emissions, including material production, could account for as much as 95% of total emissions—a more than complete reversal of the current figures. Therefore, use of low GHG material such as steel becomes even more important.

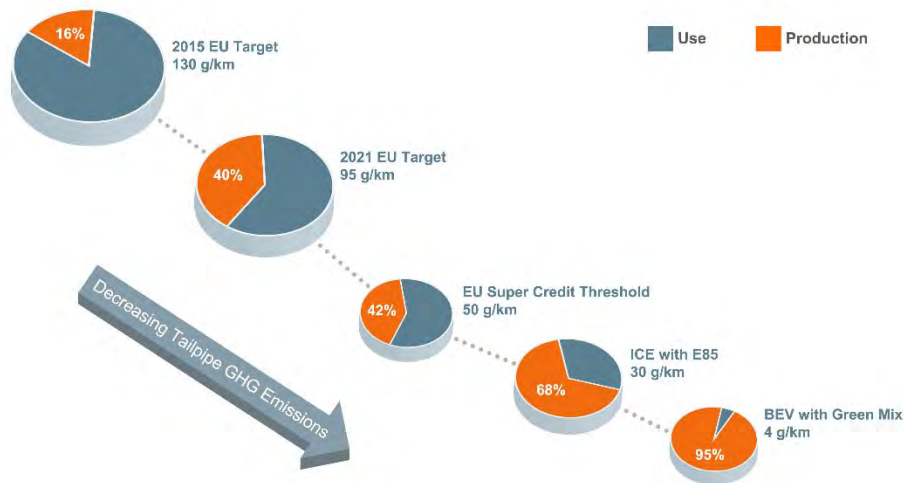


Figure 1.C-5: Share of production emissions at various levels of tailpipe emissions.^{G-4}

1.C.3.a. Life Cycle Assessment (LCA)

Reducing vehicle GHG emissions is a longstanding challenge taken on by the automotive industry and material suppliers with ever increasing pressure from policymakers. Climate change and the increasing number of vehicles on the road are the two essential catalysts. To measure emission levels, the reference tool has primarily been tailpipe emissions.

However, the environmental challenge is greater than just reducing the weight of materials and resulting tailpipe emissions. A true assessment of a vehicle's environmental footprint, with a view to effectively make a difference in the total emissions, will consider all life phases, including emissions resulting from material production, the vehicle's use and end-of-life treatments, i.e. a Life Cycle Assessment (LCA), as illustrated in Figure 1.C-6.^{G-4} The principles, framework, requirements and guidelines for LCA are laid out in ISO standards 14040 and 14044.

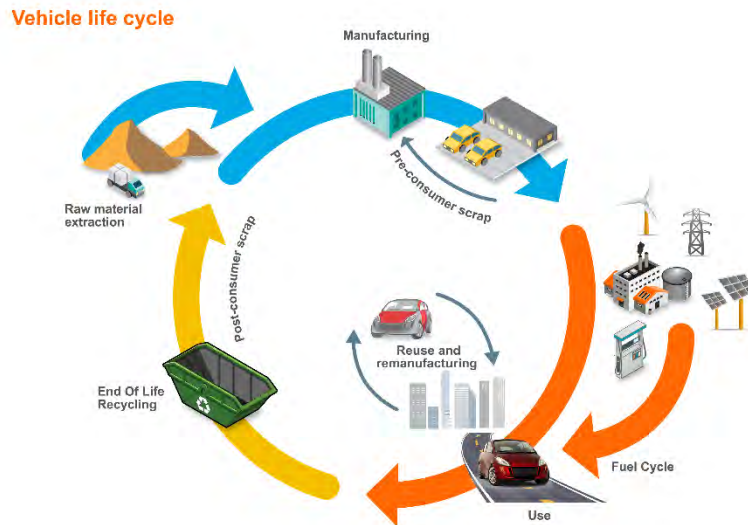


Figure 1.C-6: Vehicle total life cycle^{G-4}

This is important, because environmental policies are enacted to achieve a total net reduction in emissions, including GHG (measured in Carbon dioxide equivalents, or CO₂e). Properly applied, LCA enables automakers to ensure that improvements in one phase are not offset by worse performance in another phase. This assessment of potential trade-offs is critical to environmental improvement. For example, if the increase in production emissions of a lightweight material is greater than the decrease in use phase emissions, vehicle light-weighting can actually *increase* total emissions - an **unintended consequence**.

LCA reveals a key environmental performance advantages of steel: lower GHG emissions in all phases of the life cycle - the only material that can claim this distinction. Another advantage is steel's 100% recyclability. In fact, steel is the most recycled material on our planet, with mature vehicle collection and recycling systems already long established in the automotive industry.

It's also important to note that LCA can be used to assess a broad array of environmental impacts beyond Global Warming Potential. Other important impacts that are often considered include acidification, ecotoxicity, and ozone depletion. Although today's emphasis is on global warming potential and the reduction of greenhouse gases, with time there will be added emphasis on understanding and mitigating other environmental impacts.

Tailpipe-only regulation will become increasingly inadequate as the auto industry moves forward, limiting design choices and increasing production costs for OEMs while failing to fully account for automotive GHG emissions. Only when a vehicle's total life cycle emissions are accounted for can a true picture of its environmental impact emerge.

1.D. AHSS – In Use Applications and Requirements

Several key considerations drive material selection for automotive applications, including safety, fuel efficiency, environmental performance, manufacturability, durability, and quality. For exposed parts, aesthetic concerns related to paint finish and dent resistance are also important. These factors manifest themselves differently in each component of the vehicle, and materials are selected to match each set of performance requirements in the most efficient means possible.

1.D.1. Crash Performance

The ability to carry the required static and dynamic loads, particularly in a crash event, is one of the key design considerations for vehicle structures. Both materials strategy and geometric design play important roles in determining the final load paths and part details. Two generalized areas of the car have very different safety requirements, as shown in Figure 1.D-1 and Table 1.D-1. The passenger compartment, enclosed in a rigid “safety cage,” is designed to protect the passengers in the event of a low or high-speed crash; the structure should prevent any deformation or intrusions that would compromise the integrity of the cage structure and impinge on the space around the passengers. The so-called “crumple zones,” located at the front and rear of the vehicle, are designed to absorb as much energy as possible in the event of a front or rear collision. By absorbing the energy over a distance, the crumple zone will cushion the impact and help preserve the structure of the passenger compartment. The general guidelines for materials selection in these zones are outlined below:

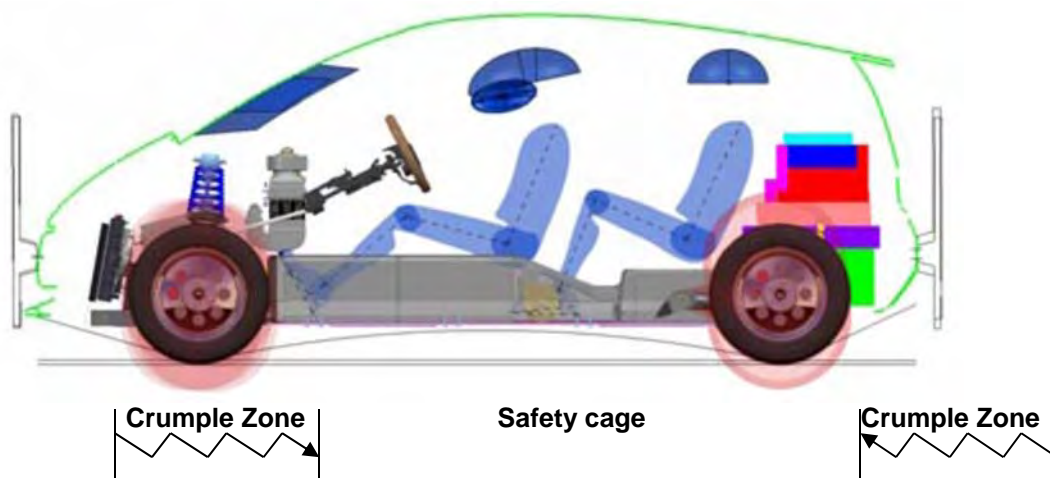


Figure 1.D-1: The Major crash management zones of a vehicle.^{W-7}

Table 1.D-1: Differing Safety Requirements of Vehicle Structures.

Crash Zone	Performance Requirements	Material properties to meet need	Evidence of Performance	Potential Steel Selection
<i>Crumple Zone</i>	High energy absorption over a distance in crash event	High work hardening, strength, and ductility	Large area under the stress-strain curve	Dual Phase, Complex Phase, Transformation-Induced Plasticity
<i>Passenger Compartment</i>	No deformation/intrusion during crash event	High yield strength	Ultimate tensile strength of σ - ϵ curves	Martensitic, Hot Formed, Dual Phase (>980 MPa)

Clearly, the choice of steel properties, such as those shown in Figure 1.D-2, guides steel-types selections for specific applications. The components are designed so that together they form a structure that meets all requirements, particularly all crash cases, both those enforced by regional regulatory bodies and those set internally by car companies.

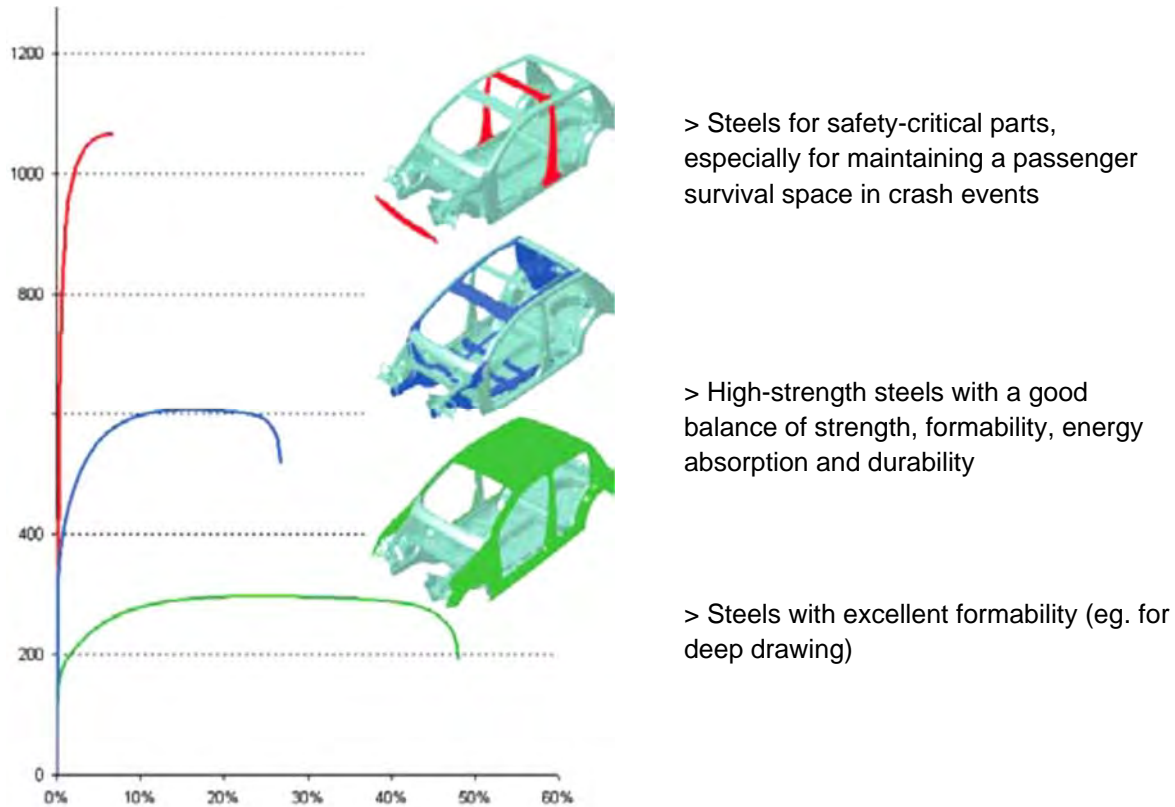


Figure 1.D-2: Stress (in MPa) vs. percent elongation for different steel types and their applications in body structure [Adapted from C-5]

1.D.2. Stiffness

Stiffness is a function of part geometry and elastic modulus, not YS or UTS, and is related to handling, safety, as well as noise, vibration, and harshness concerns. Although using AHSS helps to increase strength and decrease weight by using thinner material, stiffness can suffer as a result. Geometry, specifically the moment of inertia of the cross-section about the primary load axis, plays a significant role in determining stiffness. The flexibility to adjust cross sectional and overall geometries allows for structural design solutions that more efficiently carry loads in the vehicle. The use of AHSS offers many advantages in this process because high work hardening rates increase formability, allowing for improved shapes for optimal efficiency.^{S-7} Additionally, AHSS typically possess high bake-hardening ability which can improve the final strength of a component after forming and paint-baking (curing).

1.D.3. Forming and Manufacturability

AHSS were developed partly to address decreased formability with increased strength in conventional steels. As steels became increasingly stronger, they simultaneously became increasingly difficult to form into automotive parts. AHSS, although much stronger than conventional low- to high-strength steel, also offer high work hardening and bake hardening capabilities that allow increased formability and opportunities for optimization of part geometries.^{S-7} Both overall elongation and local elongation

properties are important for formability; for some difficult-to-form parts, high stretchability at sheared edges is important (as discussed regarding Complex Phase and Ferritic-Bainitic steels in Section 2.0 following).

1.D.4. Current Vehicle Examples

Manufacturers continue to embrace AHSS to provide affordable materials solutions to their functional and regulatory requirements. The following are just a few examples where automakers have attributed improved performance and lightweighting due to the use of these remarkable steels.

1.D.4.a. 2016-17 Chevy Cruze

The new-generation 2016 Chevrolet Cruze represents GM's newest entry in the midsize compact car segment. It was developed by GM's global R&D team, which gave the Cruze a new clean-sheet design and brand-new architecture. The team's goal was to set new benchmarks in the segment for fuel economy, handling and intelligent technology. The redesign has been carried into 2017 models, including the new hatchback version.

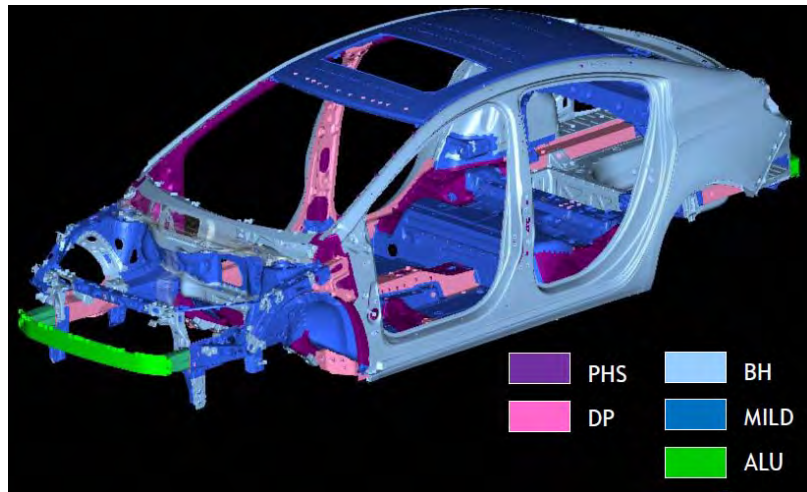


Figure 1.D-3: Cruze Material Breakdown.^{K-7}

According to a presentation by Michael Kupper and Klaus-Peter Eckhardt at the 2014 Aachen Body Engineering Days, the design team's goal was to utilize as much high-strength steel as possible (Figure 1.D-3). Seventy-two percent of the new Cruze's body consists of AHSS, enhancing fuel economy without compromising safety. These efforts, along with clean sheet redesign of the entire structure, resulted in a 52 kg mass reduction in the BIW. According to Kupper, even with these aggressive measures, the team did not exhaust the potential of AHSS mass reduction capabilities.

1.D.4.b. 2017 Kia Sportage

The structure of the 2017 Kia Sportage (Figure 1.D-4) was significantly improved due to the extensive use of AHSS, the automaker claims. With 51 percent of the Sportage's BIW consisting of AHSS, versus the outgoing model's 18 percent, torsional rigidity improved 39 percent. As well, the Sportage earned the highest safety designation possible – Top Safety Pick Plus (TSP+) – from the Insurance Institute for Highway Safety (IIHS) when equipped with optional front crash prevention systems. The rating reflects top scores in each of five crashworthiness tests as well as the integration of driver assistance technologies to aid in crash prevention.



Figure 1.D-4: Kia Sportage body structure is 51% AHSS.^{K-8}

1.D.4.c. 2017 Chrysler Pacifica

Lighter by approximately 250 pounds (model to model), stiffer and more aerodynamic than the outgoing model, the 2017 Chrysler Pacifica (Figure 1.D-5) claims to be noticeably more responsive with lower levels of body roll and enhanced agility to absorb and distribute road inputs. The redesigned vehicle was recognized at the North American International Auto Show as 2017 Utility of the Year. FCA gives much of the credit to the extensive use of advanced, hot-stamped/high-strength steels, application of structural adhesives where necessary and an intense focus on mass optimization. The Pacifica utilizes approximately 22 percent more HSS than its predecessor, of which 48 percent is AHSS for maximizing stiffness and strength while optimizing weight efficiency – the first FCA U.S. sliding door offering to blend AHSS and material mass optimization to this extent. Specific steel components that contribute to the lightweight suspension system include:

- Thin-gauged front suspension cradle constructed of HSS with “lightening holes” (e.g. “non-contributing” material was removed) on all models, as well as hydroformed front cradle side rails that enable a weight savings.
- Thin-gauged steel trailing arms in the rear suspension enabled by a “blade-style” design that ensures strength and durability without adding mass.



Figure 1.D-5: 2017 Pacifica “Utility of the Year”.^{F-3}

1.D.4.d. WorldAutoSteel FutureSteelVehicle Program - *Nature's Way to Mobility*

Begun in 2008, the FSV (Figure 1.D-6) is the latest technology demonstration project of the global steel industry.



Figure 1.D-6: FutureSteelVehicle Battery Electric Vehicle Concept.^{W-7}

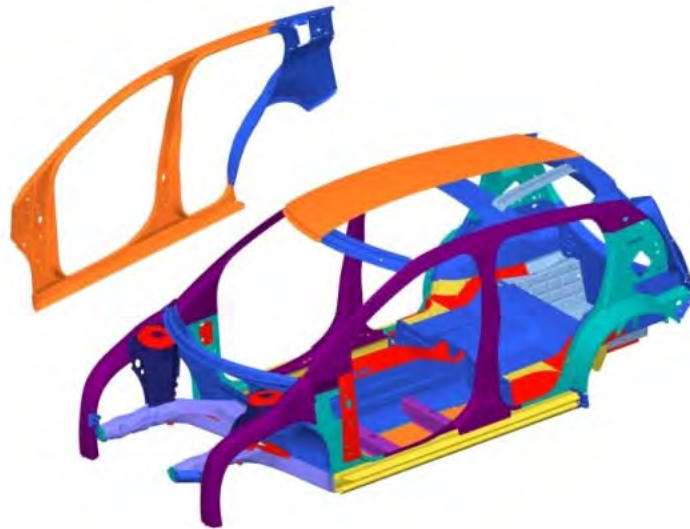
This three-year program builds on 13 years of pioneering work to find ways to decrease vehicle mass, reduce cost and meet comprehensive crash safety standards, all in pursuit of a smaller environmental footprint. FSV is a global steel industry investment in advancing the state of the art of automobile bodies that contribute to lower emission vehicles. It validates wide ranging research into the practical use of AHSS, innovative design and manufacturing technologies, and proposes specific examples for electrified vehicles.

The FSV draws from a broad portfolio of steel types and grades, in a range of properties from mild to GigaPascal strength levels, applying a vast array of manufacturing processes. With advanced optimization algorithms and computing power, FSV incorporated hundreds of variables in the design process to identify a wide band of solutions. This FSV approach integrates vehicle design, powertrain design and packaging, occupant space, passenger ingress/egress, driver sight angles, NVH, and aerodynamics to achieve a body structure that works in harmony with all vehicle requirements. This more vigorous process mimics nature, yielding non-intuitive results beyond what has been previously possible.^{W-7} FSV shows the way forward for a full range of more efficient steel designs for electric powertrains (Figure 1.D-7). An important conclusion is that these same design attributes can be applied to conventional ICE-powered vehicles as well.

The FSV aims to help automakers respond effectively to more stringent emissions and fuel efficiency standards and to reduce the effects of greenhouse gases while meeting other absolutes, such as safety (crash) standards and affordability. It comprehends new electric-drive powertrains, whose use is leading to even greater focus on vehicle weight reduction and, hence, material selection. The project includes structural variants for battery electric (BEV), plug-in hybrids (PHEV-20 and -40) and fuel cell (FCEV) powertrains.

FSV relies on new developments in AHSS that are stronger and yet more formable. It employs a holistic design approach that applies the latest computer-aided optimization techniques to leverage steel's exceptional design flexibility. Also, for the first time, FSV uses LCA to select the steels and manufacturing techniques that result in the lowest total carbon footprint, going beyond accounting only for emissions in the use phase.^{W-7}

FSV relies on new developments in AHSS that are stronger and yet more formable. It employs a holistic design approach that applies the latest computer-aided optimization techniques to leverage steel's exceptional design flexibility. Also, for the first time, FSV uses LCA to select the steels and manufacturing techniques that result in the lowest total carbon footprint, going beyond accounting only for emissions in the use phase.^{W-7}



FSV BEV Steel Types
as % of Body Structure Mass

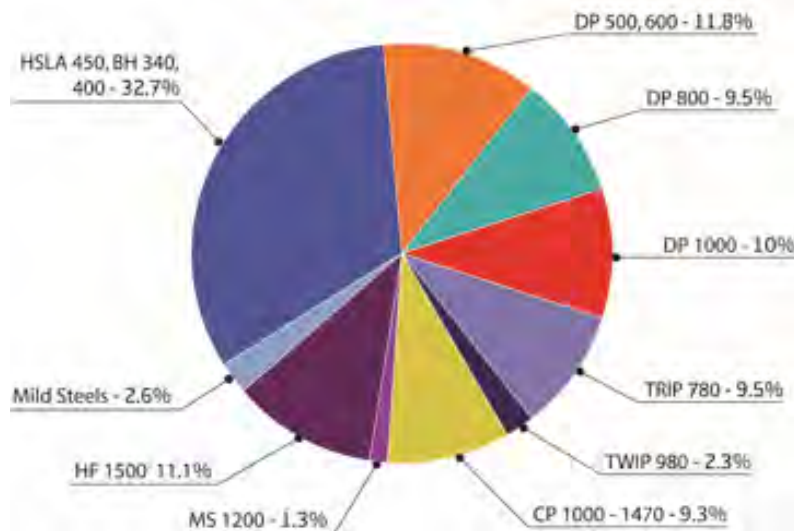


Figure 1.D-7: FutureSteelVehicle material usage.^{W-7}

Lower Weight

Extensive use of a broad portfolio of AHSS grades, coupled with engineering design optimization, enables a robust body structure that is feasible to produce and achieves 5-star crash performance against all global crash standards, while also exceeding mass reduction targets. A lower weight, mass-efficient body creates opportunities for downsizing sub-systems, including the powertrain, and promotes reductions in overall vehicle mass. As an example, the body structure mass achievement for the FSV BEV variant is 177 kg^{W-6}, including the battery tray (unique to a BEV product). This compares quite favorably with the 2010 VW Polo, at 231 kg, which was recognized as Car of the Year in Europe because of its mass-efficient design, but carries a lighter ICE gasoline powertrain. Please note Table 1.D-2 for benchmarking comparisons.

Table 1.D-2: FSV benchmarking.

Vehicle	Class	Powertrain	Curb Weight	Body Mass	Fuel Consumption (NEDC)
FSV – BEV	B+	BEV	958 kg	177 kg	2.42 l/100 km (equiv)
ULSAB - AVC	C	ICE-G	933 kg	202 kg	4.40 l/100 km
VW Polo	B	ICE-G	1067 kg	231 kg	5.70 l/100 km

Lower Cost

Steel is the most cost-competitive material for car bodies. It is economical to fabricate into components and sub-systems and to assemble into the total body-structure assembly. The resulting cost estimate of \$1,115 to manufacture and assemble the complete FSV body validates this proposition and represents no cost penalty compared to today’s vehicles.

Lowest Total Lifetime Emissions

FSV demonstrates the importance of LCA as an integral element of a vehicle design process. In combination with optimizing the design for mass, cost and functionality, the FSV integrates into all analyses an accounting for its complete environmental footprint as measured in CO₂e. It more appropriately comprehends the entire lifetime carbon footprint of the vehicle, not simply the use phase. This not only includes the entire fuel production cycle (well to pump) and fuel usage cycle (pump to wheels), but also the production of raw materials and disposal/recycling.

FSV amply demonstrates that the coupling of a light weight, AHSS body structure with a battery-electric powertrain results in a 50 to 70 percent reduction in total life cycle emissions, compared to equivalently-sized vehicles with conventional gasoline ICEs.^{W-7} Furthermore, based on the new steels’ light weighting capabilities, steel is the only material to realize emission reductions in **all** life cycle phases. Table 1.D-3 summarizes total vehicle carbon footprint and emissions performance by life cycle phase.

Table 1.D-3: FSV comparison between U.S. and Europe energy grids

Vehicle/Powertrain	Material & Recycling (kg CO ₂ e)	Use Phase (kg CO ₂ e)	Total Life Cycle (kg CO ₂ e)
Polo V ICEg	1,479	32,655	34,134
FSV BEV USA grid	1,328	13,844	15,172
FSV BEV Europe grid	1,328	9,670	10,998
FSV vs. Polo V - USA grid		- 56% CO₂e reduction	
FSV vs. Polo V – Europe grid		- 68% CO₂e reduction	

Safety

The FSV design anticipates increasingly stringent crash safety standards over the next decade and meets European and U.S. 5-Star crash safety performance requirements.^{W-7} It applies the latest holistic design and material optimization approaches made possible by more powerful computing capabilities. In this way, by best using steel’s unmatched capabilities for design and manufacturing efficiency, the final FSV design comprises optimized, mass-efficient shapes that meet or exceed a global reach of crash safety requirements.

1.E. Using These Guidelines

Worldwide working groups within WorldAutoSteel membership created the AHSS Application Guidelines to explain how and why AHSS were different from traditional higher strength steels in terms of press-forming, fabrication, and joining for automotive underbody, structural, and body panels designed for AHSS. This Version 6.0 document provides in-depth current information on a wide range of topics.

It is important to note that different automotive companies throughout the world have adopted different specification criteria and that steel companies have different production capabilities and commercial availability. Therefore, the typical mechanical properties provided in this document simply illustrate the broad range of AHSS grades that may be available worldwide. In addition, regional test procedures will cause a systematic variation in some properties measured on the same steel sample. One example is total elongation, where measurement gauge length can be 50-mm or 80-mm plus different gauge widths depending on the worldwide region in which the test is conducted. In addition, minimum values can be defined relative to either the rolling direction or transverse direction. Therefore, communication directly with individual steel companies is imperative to determine grade availability along with specific test procedures, associated parameters and steel properties.

SECTION 2 – METALLURGY OF AHSS

2.A. Defining Steels

Automotive steels can be classified in several different ways. One is a metallurgical designation providing some process information. Common designations include low-strength steels (interstitial-free and mild steels); conventional HSS, such as bake hardenable and high-strength, low-alloy steels (HSLA); and Advanced High-Strength Steels, or AHSS (for example, dual phase and transformation-induced plasticity steels). Additional higher strength steels for the automotive market include hot-formed, post-forming heat-treated steels, and steels designed for unique applications that have improved edge stretch and stretch bending characteristics.

A second classification method important to part designers is strength of the steel. This document will use the general terms HSLA and AHSS to designate all higher strength steels. This classification system has a problem with the on-going development of the many new grades for each type of steel. Therefore, a DP or TRIP steel can have strength grades that encompass two or more strength ranges.

A third classification method presents various mechanical properties or forming parameters of different steels, such as total elongation, work hardening exponent (n-value), or hole expansion ratio (λ). As an example, Figure 2.A-1 compares total elongations – a steel property related to formability – to the tensile strength for the current types of steel. These properties are important for press shop operations and virtual forming analyses.

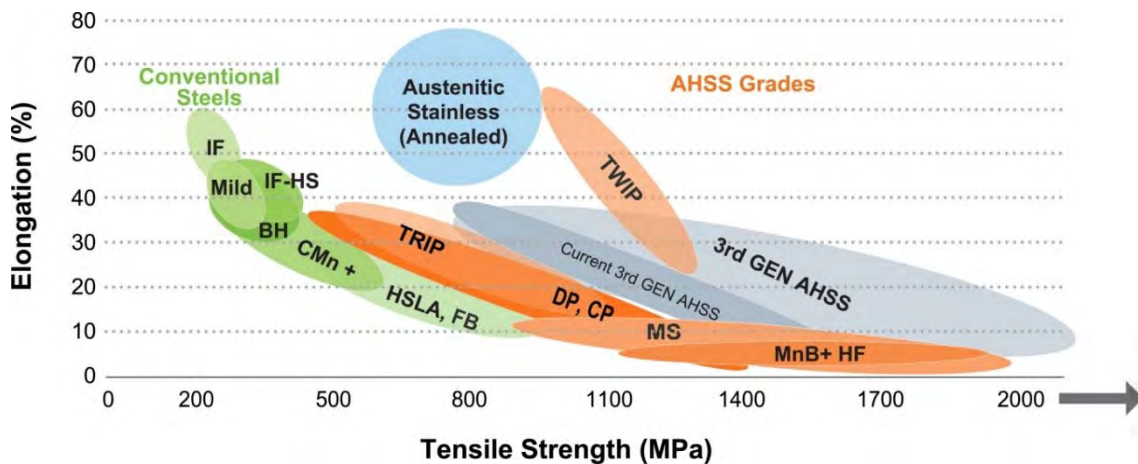


Figure 2.A-1: Global Formability Diagram for Today's AHSS Grades (includes comparison of traditional low-strength and high-strength steels).^{w-1}

The principal difference between conventional HSLA steels and AHSS is their microstructure. Conventional HSLA steels are single-phase ferritic steels with a potential for some pearlite in C-Mn steels. AHSS are primarily steels with a multiphase microstructure containing one or more phases other than ferrite, pearlite, or cementite - for example martensite, bainite, austenite, and/or retained austenite in quantities sufficient to produce unique mechanical properties. Some types of AHSS have a higher strain hardening capacity resulting in a strength-ductility balance superior to conventional steels. Other types have ultra-high yield and tensile strengths and show a bake hardening behavior.

Since the terminology used to classify steel products varies considerably throughout the world, this document uses the WorldAutoSteel format to define the steels. Each steel grade is identified by metallurgical type, minimum yield strength (in MPa), and minimum tensile strength (in MPa). As an example, DP 500/800 means a dual phase steel with 500 MPa minimum yield strength and 800 MPa minimum ultimate tensile strength. The ULSAB-AVC programme^{w-1} first used this classification system.

2.B. Metallurgy of AHSS

Manufacturers and users of steel products generally understand the fundamental metallurgy of conventional low- and high-strength steels. Section 2.B. provides a brief description of these common steel types. Since the metallurgy and processing of AHSS grades are somewhat novel compared to conventional steels, they are described here to provide a baseline understanding of how their remarkable mechanical properties evolve from their unique processing and structure. All AHSS are produced by controlling the chemistry and cooling rate from the austenite or austenite plus ferrite phase, either on the runout table of the hot mill (for hot-rolled products) or in the cooling section of the continuous annealing furnace (continuously annealed or hot-dip coated products). Research has provided chemical and processing combinations that have created many additional grades and improved properties within each type of AHSS.

2.B.1. Dual Phase (DP) Steel

DP steels consist of a ferritic matrix containing a hard martensitic second phase in the form of islands.

Increasing the volume fraction of hard second phases generally increases the strength. DP (ferrite plus martensite) steels are produced by controlled cooling from the austenite phase (in hot-rolled products) or from the two-phase ferrite plus austenite phase (for continuously annealed cold-rolled and hot-dip coated products) to transform some austenite to ferrite before a rapid cooling transforms the remaining austenite to martensite. Due to the production process, a small amount of other phases (bainite and retained austenite) may be present.

Depending on the composition and process route, steels requiring enhanced capability to resist cracking on a stretched edge (as typically measured by hole expansion capacity) can have a microstructure containing significant quantities of bainite.

Figure 2.B-1 shows a schematic microstructure of DP steel, which contains ferrite plus islands of martensite. The soft ferrite phase is generally continuous, giving these steels excellent ductility. When these steels deform, strain is concentrated in the lower-strength ferrite phase surrounding the islands of martensite, creating the unique high initial work-hardening rate (n-value) exhibited by these steels. Figure 2.B-2 is an actual micrograph showing the ferrite and martensite constituents.

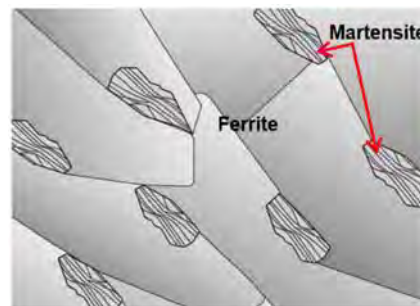
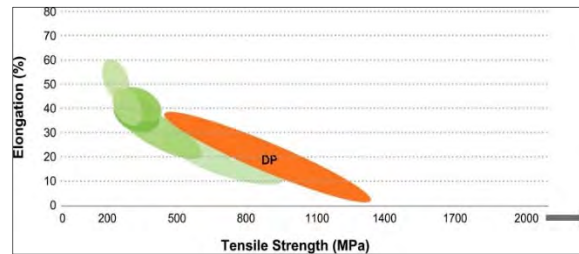


Figure 2.B-1: Schematic shows islands of martensite in a matrix of ferrite.

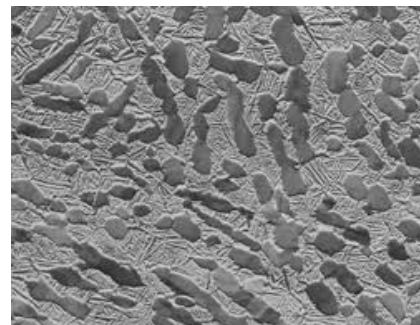


Figure 2.B-2: Micrograph of DP steel.

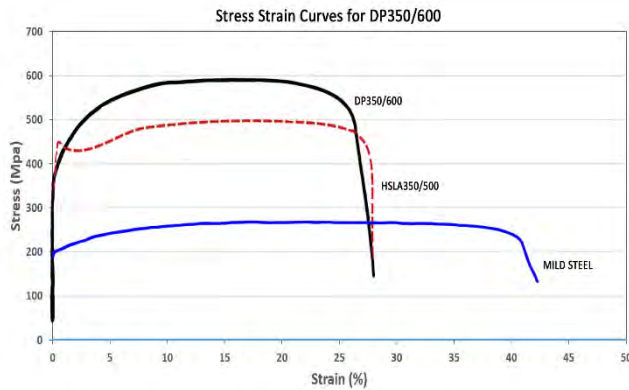


Figure 2.B-3: The DP 350/600 with higher TS than the HSLA 350/450^{K-1}

The work hardening rate plus excellent elongation creates DP steels with much higher ultimate tensile strengths than conventional steels of similar yield strength. Figure 2.B-3 compares the engineering stress-strain curve for HSLA steel to a DP steel curve of similar yield strength. The DP steel exhibits higher initial work hardening rate, higher ultimate tensile strength, and lower YS/TS ratio than the HSLA with comparable yield strength. Additional engineering and true stress-strain curves for DP steel grades are located in Figure 2.B-4.

DP and other AHSS also have a bake hardening effect that is an important benefit compared to conventional higher strength steels. The bake hardening effect is the increase in yield strength resulting from elevated temperature aging (created by the curing temperature of paint bake ovens) after pre-straining (generated by the work hardening due to deformation during stamping or other manufacturing process). The extent of the bake hardening effect in AHSS depends on an adequate amount of forming strain for the specific chemistry and thermal history of the steel. Additional bake hardening information is located in Section 2.D.8. – Bake Hardening and Aging.

DP and other AHSS also have a bake

In DP steels, carbon enables the formation of martensite at practical cooling rates by increasing the hardenability of the steel. Manganese, chromium, molybdenum, vanadium, and nickel, added individually or in combination, also help increase hardenability. Carbon also strengthens the martensite as a ferrite solute strengthener, as do silicon and phosphorus. These additions are carefully balanced, not only to produce unique mechanical properties, but also to maintain the generally good resistance spot welding capability. However, when welding the higher strength grades (DP 700/1000 and above) to themselves, the spot weldability may require adjustments to the welding practice. Examples of current production grades of DP steels and typical automotive applications are shown below:

DP 300/500	Roof outer, door outer, body side outer, package tray, floor panel
DP 350/600	Floor panel, hood outer, body side outer, cowl, fender, floor reinforcements
DP 500/800	Body side inner, quarter panel inner, rear rails, rear shock reinforcements
DP 600/980	Safety cage components (B-pillar, floor panel tunnel, engine cradle, front sub-frame package tray, shotgun, seat),
DP 700/1000	Roof rails
DP 800/1180	B-pillar upper

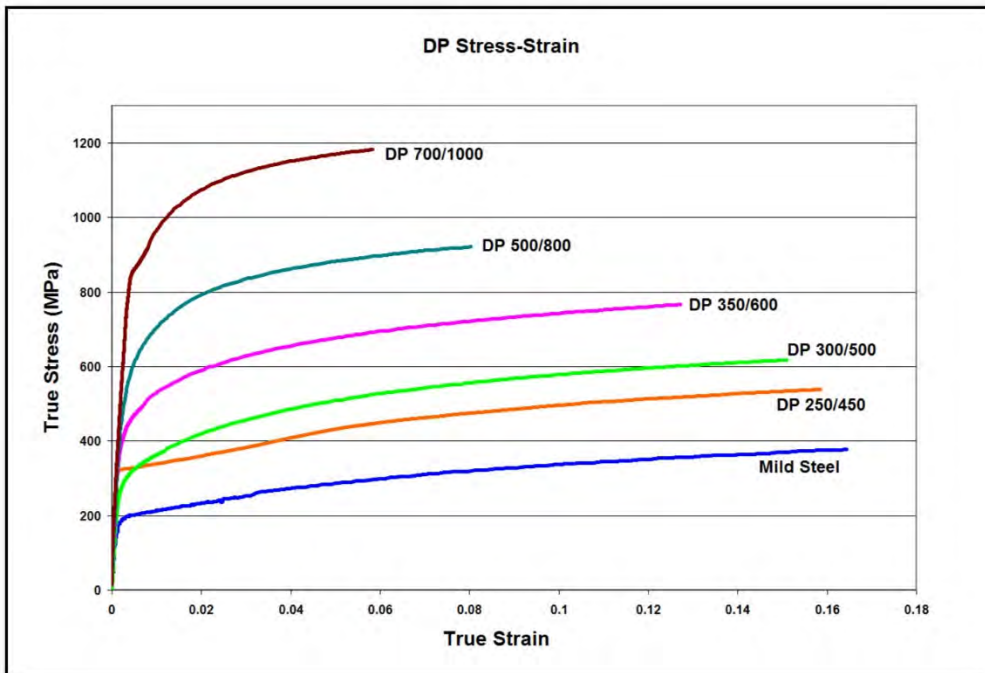
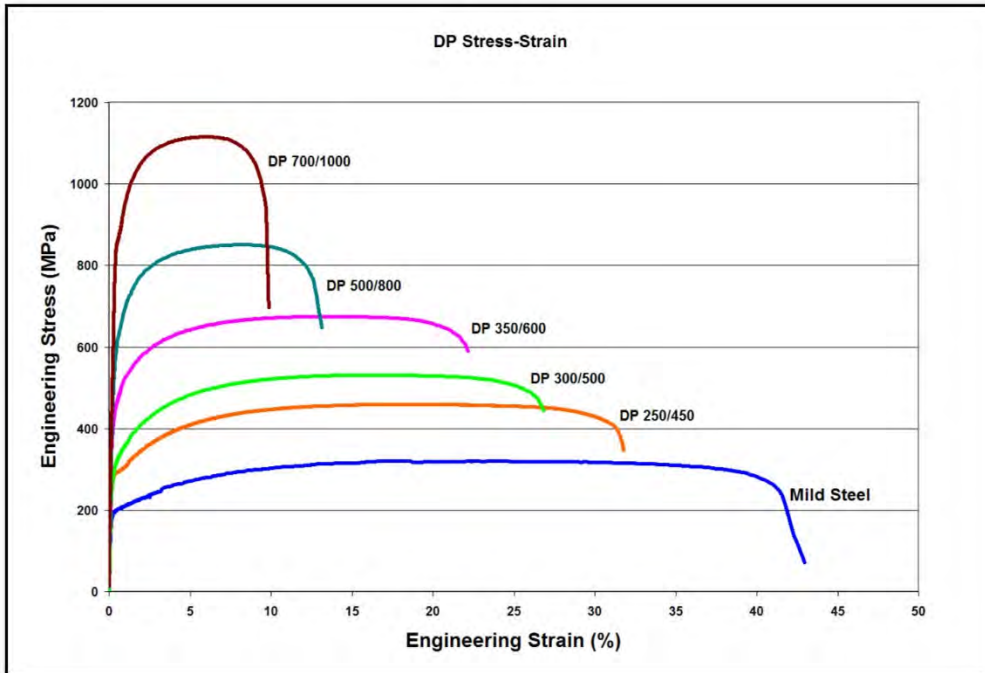


Figure 2.B-4: Engineering stress-strain (upper graphic) and true stress-strain (lower graphic) curves for a series of DP steel grades.^{S-5, V-1} Sheet thicknesses: DP 250/450 and DP 500/800 = 1.0mm. All other steels were 1.8-2.0mm.

2.B.2. Transformation Induced Plasticity (TRIP) Steel

The microstructure of TRIP steels is retained austenite embedded in a primary matrix of ferrite. In addition to a minimum of five volume percent of retained austenite, hard phases such as martensite and bainite are present in varying amounts. TRIP steels typically require the use of an isothermal hold at an intermediate temperature, which produces some bainite. The higher silicon and carbon content of TRIP steels also result in significant volume fractions of retained austenite in the final microstructure. Figure 2.B-5 shows a schematic of TRIP steel microstructure. Figure 2.B-6 is a micrograph of TRIP 690. Figure 2.B-7 compares the engineering stress-strain curve for HSLA steel to a DP steel curve of similar yield strength.

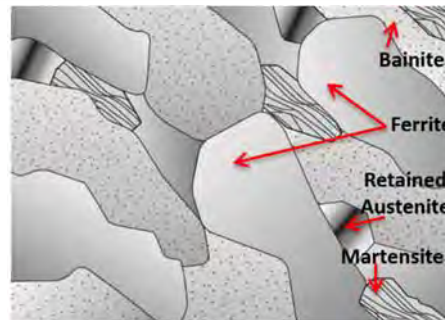
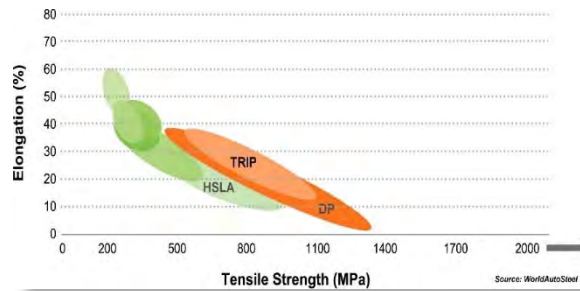


Figure 2.B-5: Bainite and retained austenite are additional phases in TRIP steels

During deformation, the dispersion of hard second phases in soft ferrite creates a high work hardening rate, as observed in the DP steels. However, in TRIP steels the retained austenite also progressively transforms to martensite with increasing strain, thereby increasing the work hardening rate at higher strain levels. This is illustrated in Figure 2.B-8, where the engineering stress-strain behavior of HSLA, DP and TRIP steels of approximately similar yield strengths are compared. The TRIP steel has a lower initial work hardening rate than the DP steel, but the hardening rate persists at higher strains where work hardening of the DP begins to diminish. Additional engineering and true stress-strain curves for TRIP steel grades are located in Figure 2.B-9.

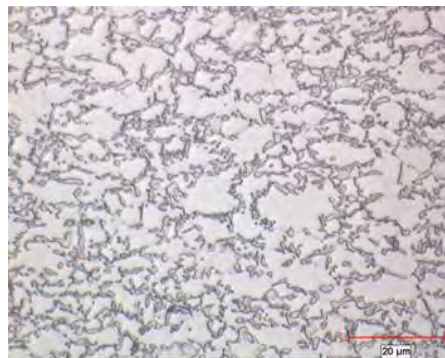


Figure 2.B-6: Micrograph of TRIP 690 steel

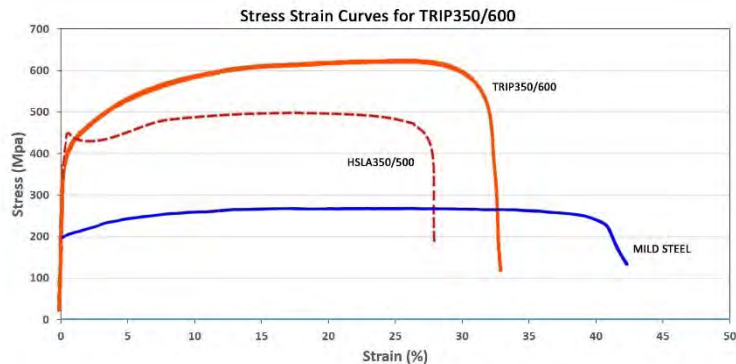


Figure 2.B-7: TRIP 350/600 compared to similar yield strength HSLA.

The work hardening rates of TRIP steels are substantially higher than for conventional HSS, providing significant stretch forming. This is particularly useful when designers take advantage of the high work hardening rate (and increased bake hardening effect) to design a part utilizing the as-formed mechanical properties. The high work hardening rate persists to higher strains in TRIP steels, providing a slight advantage over DP in the most severe stretch forming applications.

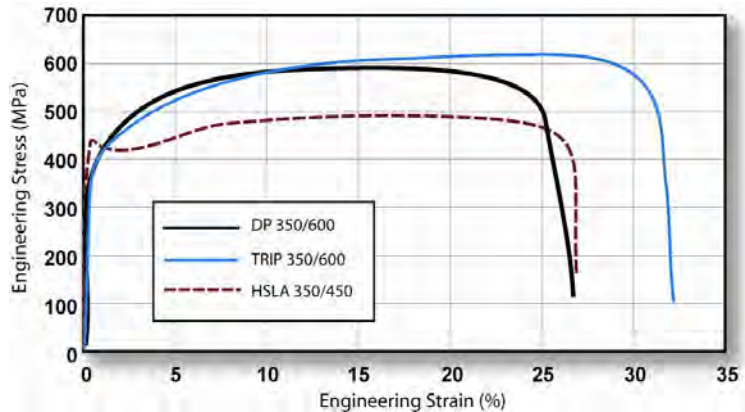


Figure 2.B-8: TRIP 350/600 with a greater total elongation than DP 350/600 and HSLA 350/450^{K-1}

TRIP steels use higher quantities of carbon than DP steels to obtain sufficient carbon content for stabilizing the retained austenite phase to below ambient temperature. Higher contents of silicon and/or aluminium accelerate the ferrite/bainite formation. These elements assist in maintaining the necessary carbon content within the retained austenite. Suppressing the carbide precipitation during bainitic transformation appears to be crucial for TRIP steels. Silicon and aluminium are used to avoid carbide precipitation in the bainite region.

The strain level at which retained austenite begins to transform to martensite is controlled by adjusting the carbon content. At lower carbon levels, the retained austenite begins to transform almost immediately upon deformation, increasing the work hardening rate and formability during the stamping process. At higher carbon contents, the retained austenite is more stable and begins to transform only at strain levels beyond those produced during forming. At these carbon levels, the retained austenite persists into the final part. It transforms to martensite during subsequent deformation, such as a crash event.

TRIP steels therefore can be engineered or tailored to provide excellent formability for manufacturing complex AHSS parts or exhibit high work hardening during crash deformation for excellent crash energy absorption. The additional alloying requirements of TRIP steels degrade their resistance spot-welding behavior. This can be addressed somewhat by modification of the welding cycles used (for example, pulsating welding or dilution welding).

Current production grades of TRIP steels and example automotive applications:

TRIP 350/600	Frame rails, rail reinforcements
TRIP 400/700	Side rail, crash box
TRIP 450/800	Dash panel, roof rails
TRIP 600/980	B-pillar upper, roof rail, engine cradle, front and rear rails, seat frame

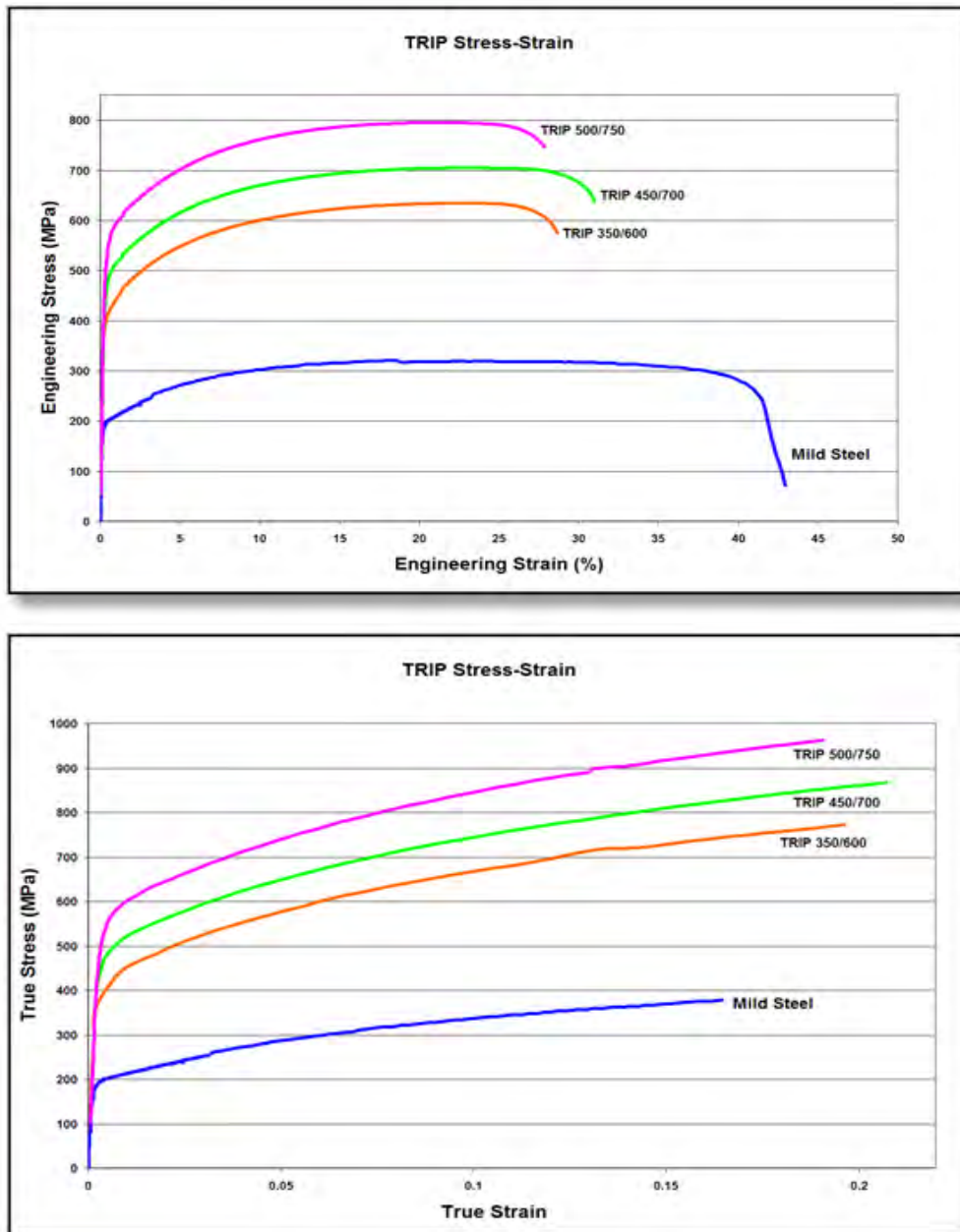


Figure 2.B-9: Engineering stress-strain (upper graphic) and true stress-strain (lower graphic) curves for a series of TRIP steel grades.^{V-1}

Sheet thickness: TRIP 350/600 = 1.2mm, TRIP 450/700 = 1.5mm,
TRIP 500/750 = 2.0mm, and Mild Steel = approx. 1.9mm

2.B.3. Complex Phase (CP) Steel

CP steels typify the transition to steel with very high ultimate tensile strengths. The microstructure of CP steels contains small amounts of martensite, retained austenite and pearlite within the ferrite/bainite matrix. An extreme grain refinement is created by retarded recrystallization or precipitation of microalloying elements like Ti or Nb. Figure 2.B-10 shows a schematic of CP steel microstructure. Figure 2.B-11 shows the grain structure for hot rolled CP 800/1000. Figure 2.B-12 compares the engineering stress-strain curve for HSLA steel to a CP 1000/1200 steel curve.

In comparison to DP steels, CP steels show significantly higher yield strengths at equal tensile strengths of 800 MPa and greater. CP steels are characterized by high energy absorption, high residual deformation capacity and good hole expansion. Engineering and true stress-strain curves for CP steel grades are located in Figure 2.B-13.

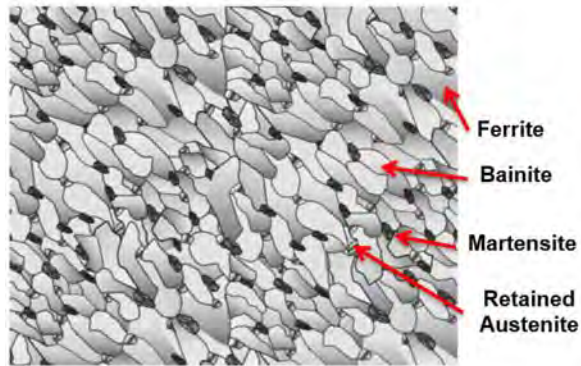
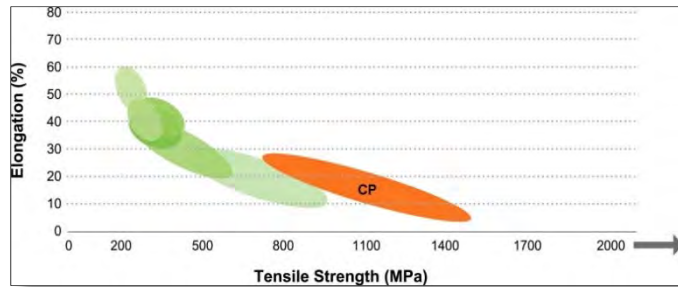


Figure 2.B-10: Schematic of CP steel microstructure.

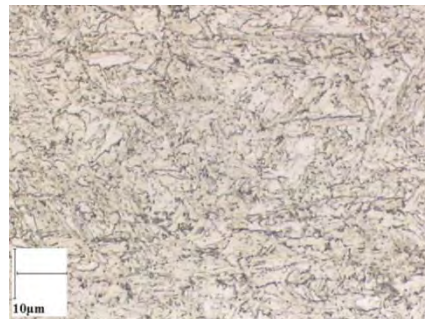


Figure 2.B-11: Micrograph of CP 800/1000 hot rolled steel.

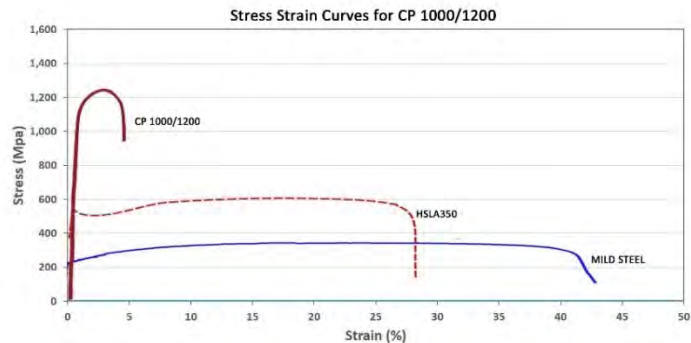


Figure 2.B-12: CP 1000/1200 compared to HSLA.

Current production grades of CP steels and example automotive applications:

CP 600/900	Frame rails, B-pillar reinforcements
CP 680/780	Frame rails, chassis components, transverse beams
CP 750/900	B-pillar reinforcements, tunnel stiffener
CP 800/1000	Rear suspension brackets, fender beam
CP1000/1200	Rear frame rail reinforcements, rocker outer
CP1050/1470	Rocker panels, bumper beams

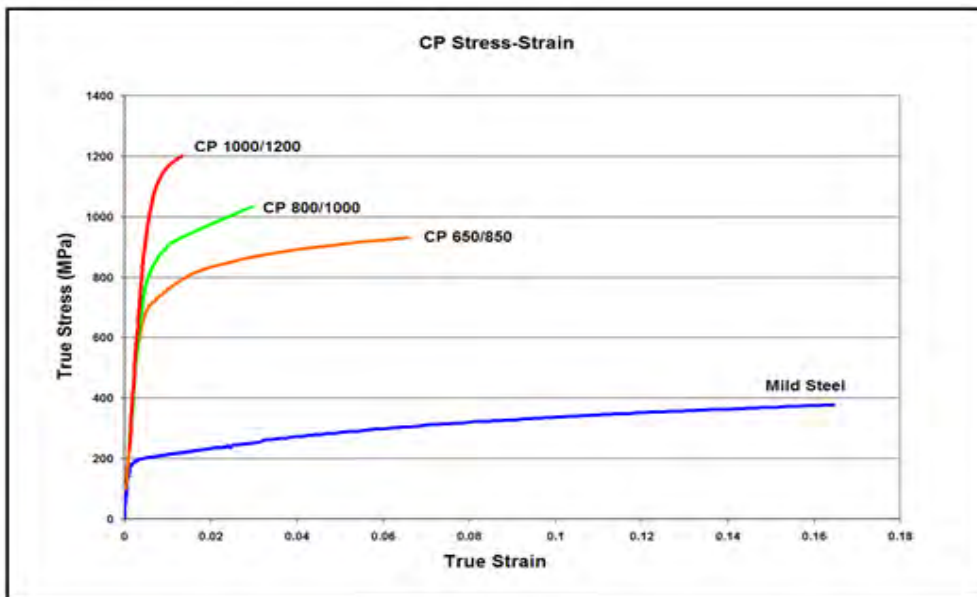
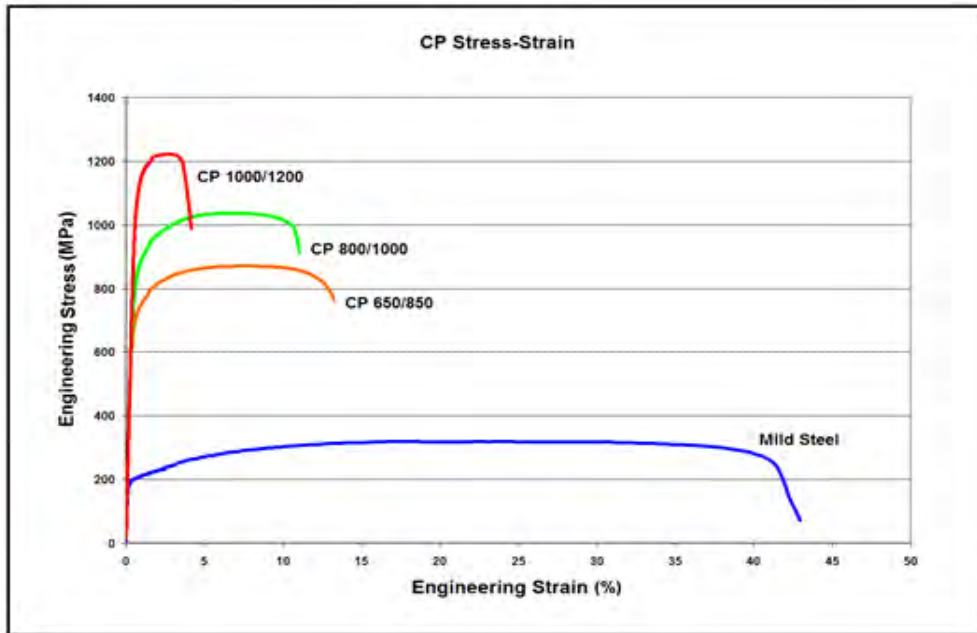


Figure 2.B-13: Engineering stress-strain (upper graphic) and true stress-strain (lower graphic) curves for a series of CP steel grades.^{V-1} Sheet thickness: CP650/850 = 1.5mm, CP 800/1000 = 0.8mm, CP 1000/1200 = 1.0mm, and Mild Steel = approx. 1.9mm.

2.B.4. Martensitic (MS) Steel

To create MS steels, the austenite that exists during hot-rolling or annealing is transformed almost entirely to martensite during quenching on the run-out table or in the cooling section of the continuous annealing line. The MS steels are characterized by a martensitic matrix containing small amounts of ferrite and/or bainite (note Figure 2.B-14 and 2.B-15). Within the group of multiphase steels, MS steels show the highest tensile strength level. This structure also can be developed with post-forming heat treatment. MS steels provide the highest strengths, up to 1700 MPa ultimate tensile strength. MS steels are often subjected to post-quench tempering to improve ductility, and can provide adequate formability even at extremely high strengths. Figure 2.B.-16 shows MS950/1200 compared to HSLA. Engineering and true stress-strain curves for MS steel grades are located in Figure 2.B-17.

Adding carbon to MS steels increases hardenability and strengthens the martensite. Manganese, silicon, chromium, molybdenum, boron, vanadium, and nickel are also used in various combinations to increase hardenability. MS steels are produced from the austenite phase by rapid quenching to transform most of the austenite to martensite.

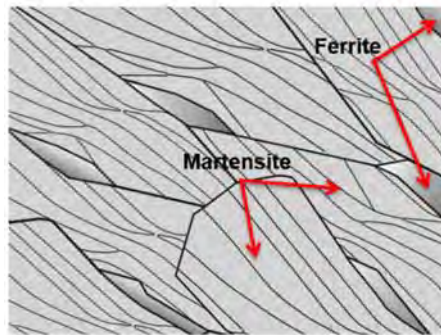
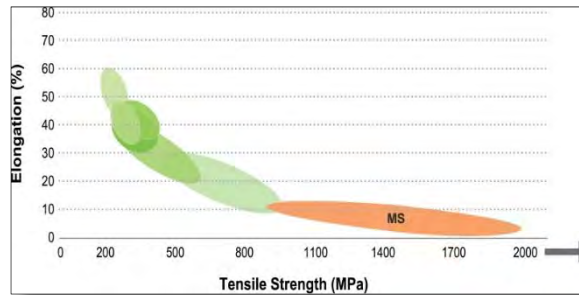


Figure 2.B-14: Schematic of Martensitic steel microstructure.

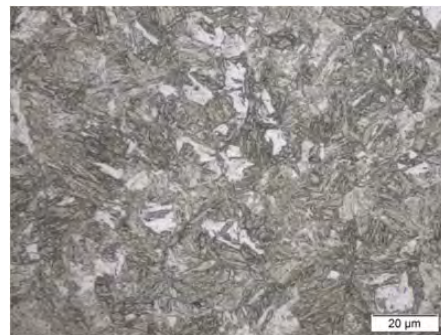


Figure 2.B-15: Microstructure for MS 950/1200.

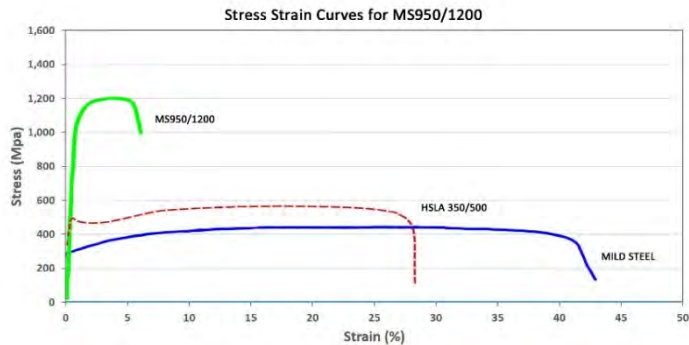


Figure 2.B.-16: MS950/1200 steel compared to HSLA.

Current production grades of MS steels and example automotive applications:

MS 950/1200	Cross-members, side intrusion beams, bumper beams, bumper reinforcements
MS 1150/1400	Rocker outer, side intrusion beams, bumper beams, bumper reinforcements
MS 1250/1500	Side intrusion beams, bumper beams, bumper reinforcements

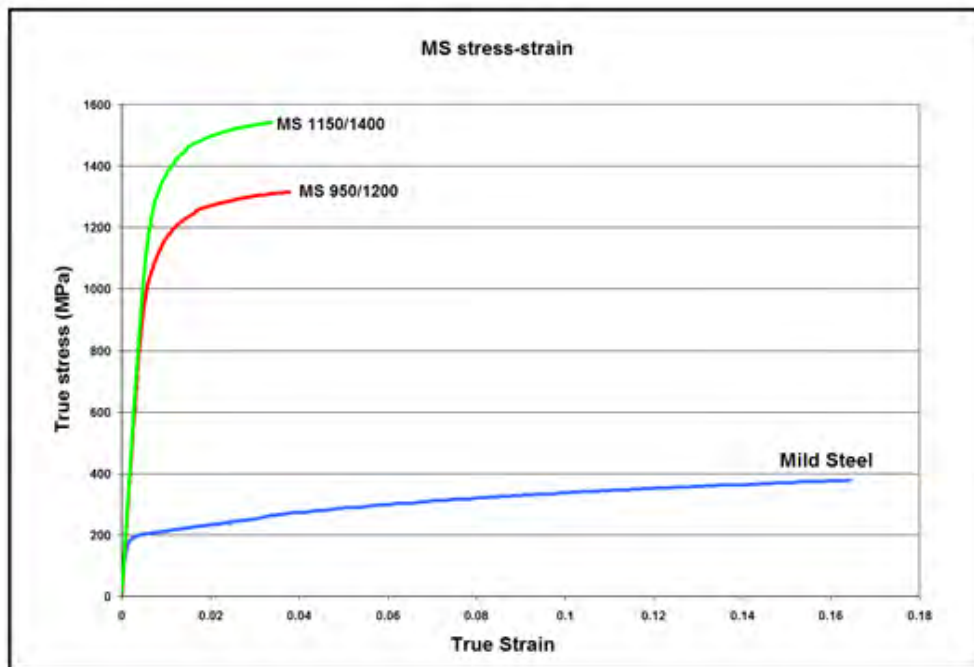
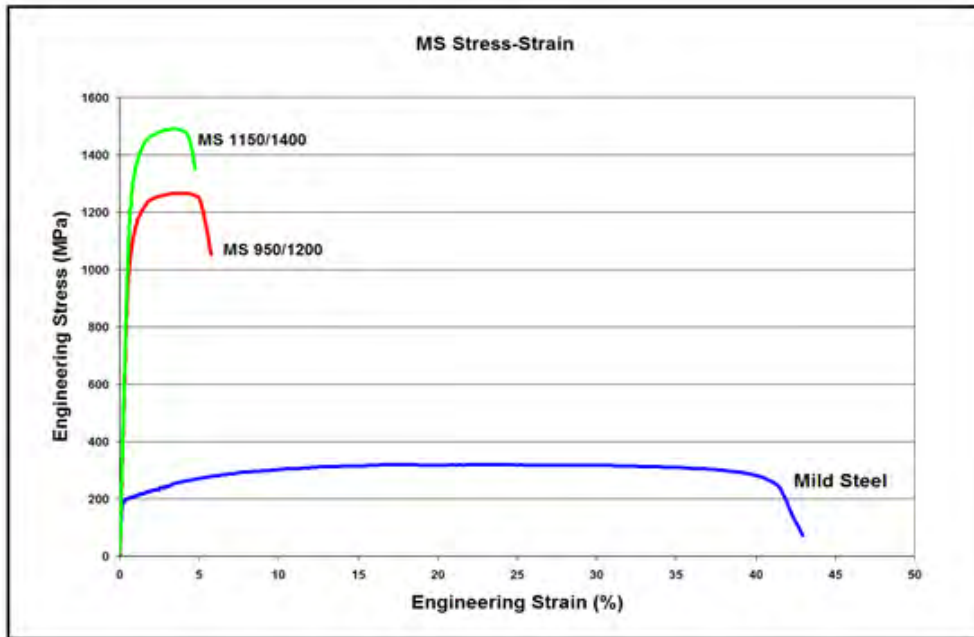


Figure 2.B-17: Engineering stress-strain (upper graphic) and true stress-strain (lower graphic) curves for a series of MS steel grades^{S-5}. All Sheet thicknesses were 1.8-2.0 mm.

2.B.5. Ferritic-Bainitic (FB) Steel

FB steels sometimes are utilized to meet specific customer application requirements that require Stretch Flangeable (SF) or High Hole Expansion (HHE) capabilities for improved edge stretch capability.

FB steels have a microstructure of fine ferrite and bainite. Strengthening is obtained by both grain refinement and second phase hardening with bainite. Figure 2.B-18 is a schematic of Ferritic-Bainitic steel micro-structure. Figure 2.B-19 is a micrograph of FB 450/600. FB steels are available as hot-rolled products.

The primary advantage of FB steels over HSLA and DP steels is the improved stretchability of sheared edges as measured by the hole expansion test (λ). Compared to HSLA steels with the same level of strength, FB steels also have a higher strain hardening exponent (n-value) and increased total elongation. Figure 2.B.-20 compares FB 450/600 with HSLA 350/500 steel. Engineering and true stress-strain curves for FB steel grades are located in Figure 2.B.21.

Because of their good weldability, FB steels are considered for tailored blank applications. These steels also are characterized by both good crash performances and good fatigue properties.

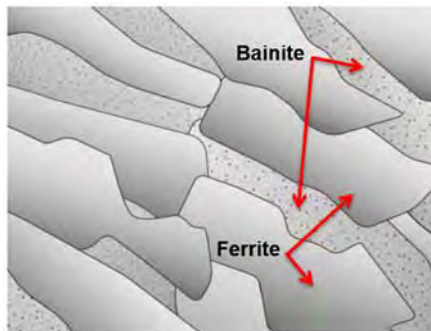
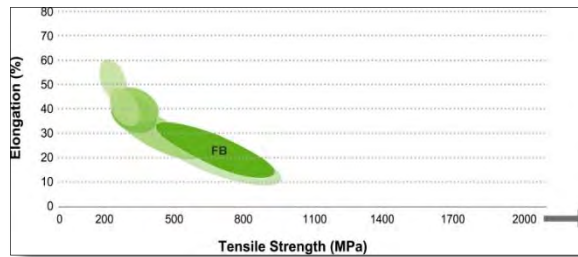


Figure 2.B-18: Schematic of Ferritic-Bainitic steel microstructure.

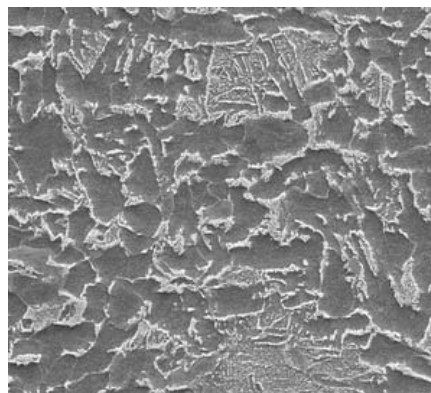


Figure 2-19: Micrograph of FB 450/600.

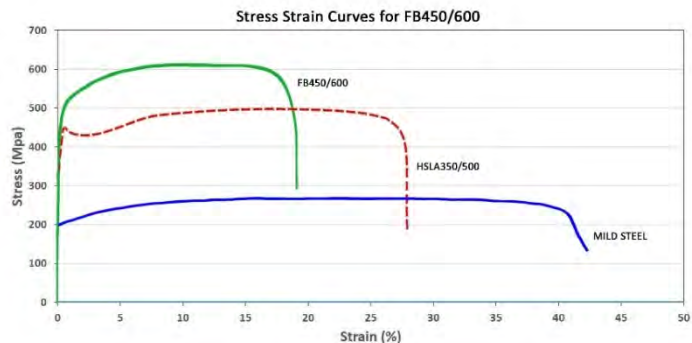


Figure 2.B-20 FB 450/600 compared to HSLA 350/500 steel.

Current production grades of FB steels and example automotive applications:

FB 330/450	Rim, brake pedal arm, seat cross member, suspension arm
FB 450/600	Lower control arm, rim, bumper beam, chassis parts, rear twist beam

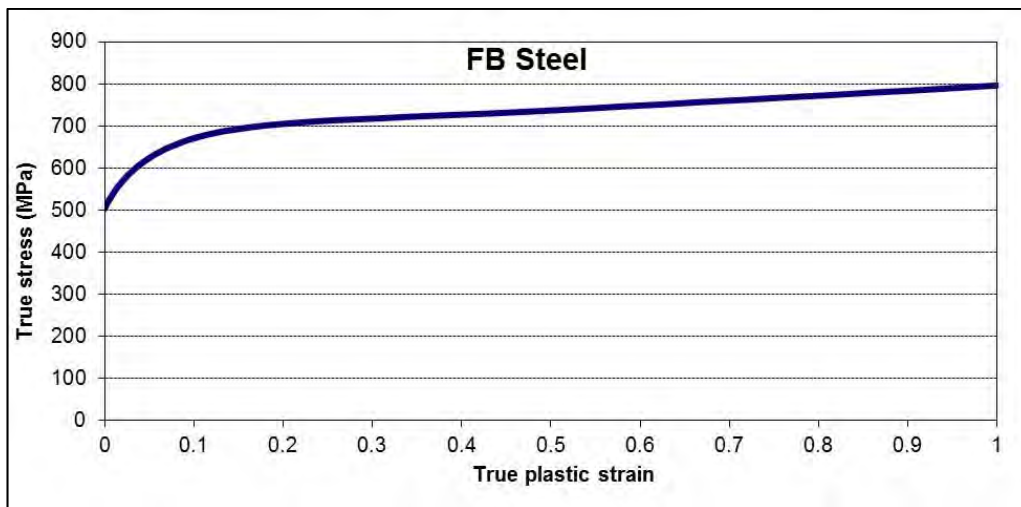
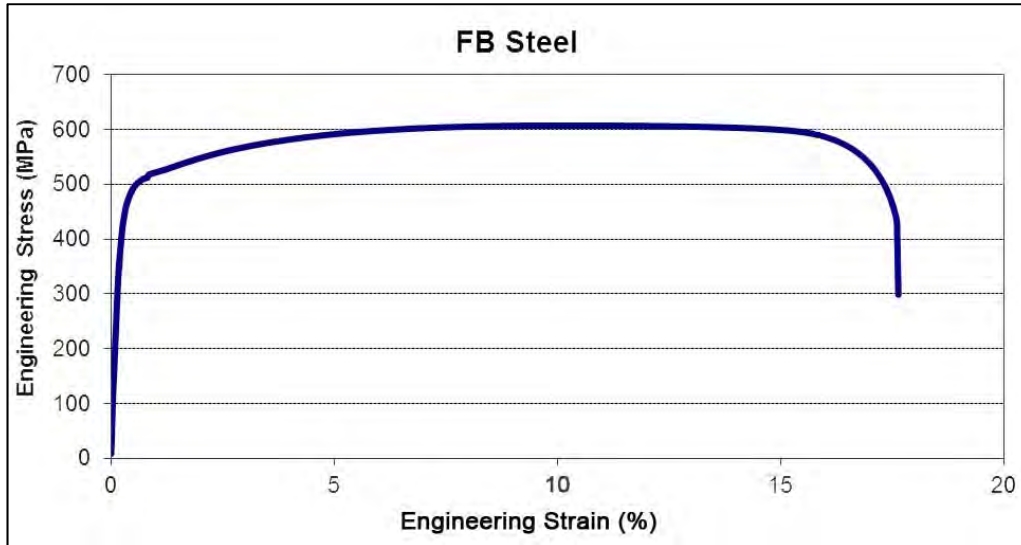


Figure 2.B-21: Engineering stress-strain (upper graphic) and true stress-strain (lower graphic) curve for FB 450/600.^{T-10}

2.B.6. Twinning-Induced Plasticity (TWIP) Steel

TWIP steels^{C-4} have a high manganese content (17-24%) that causes the steel to be fully austenitic at room temperatures. A large amount of deformation is driven by the formation of deformation twins. This deformation mode leads to the naming of this steel class. The twinning causes a high value of the instantaneous hardening rate (n-value) as the microstructure becomes finer and finer. The resultant twin boundaries act like grain boundaries and strengthen the steel. Figure 2.B.-22 provides a schematic of TWIP steel. Figure 2.B.-23 shows the as annealed microstructure for a TWIP steel.

TWIP steels combine extremely high strength with extremely high stretchability. The n-value increases to a value of 0.4 at an approximate engineering strain of 30% and then remains constant until both uniform and total elongation reach 50%. The tensile strength is higher than 1000 MPa.

Figure 2.B.-24 compares TWIP 750/1000 to HSLA steel. Engineering and true stress-strain curves for TWIP steel grades are located in Figure 2.B.-25.

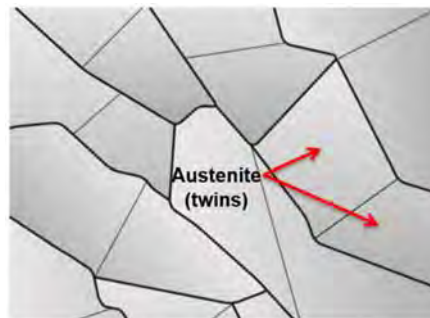
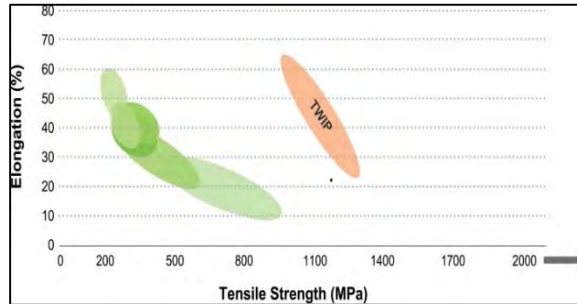


Figure 2.B.-22: Schematic of TWIP steel.

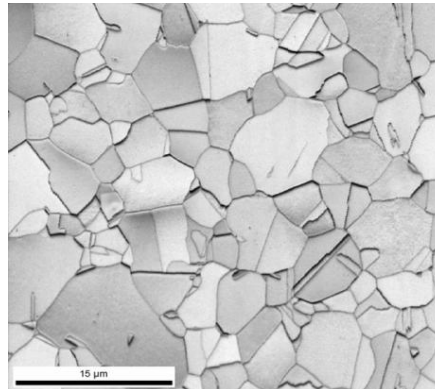


Figure 2.B.-23: Photomicrograph of TWIP steel as annealed.

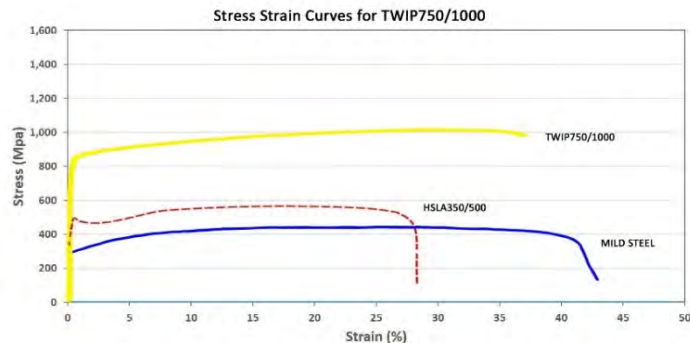


Figure 2.B.-24: TWIP 750/1000 compared to HSLA steel.

Current production grades of TWIP steels and example automotive applications:

TWIP 500/900	A-Pillar, wheelhouse, front side member
TWIP 500/980	Wheel, lower control arm, front and rear bumper beams, B-pillar, wheel rim
TWIP 600/900	Floor cross-member, wheelhouse
TWIP 750/1000	Door impact beam
TWIP 950/1200	Door impact beam

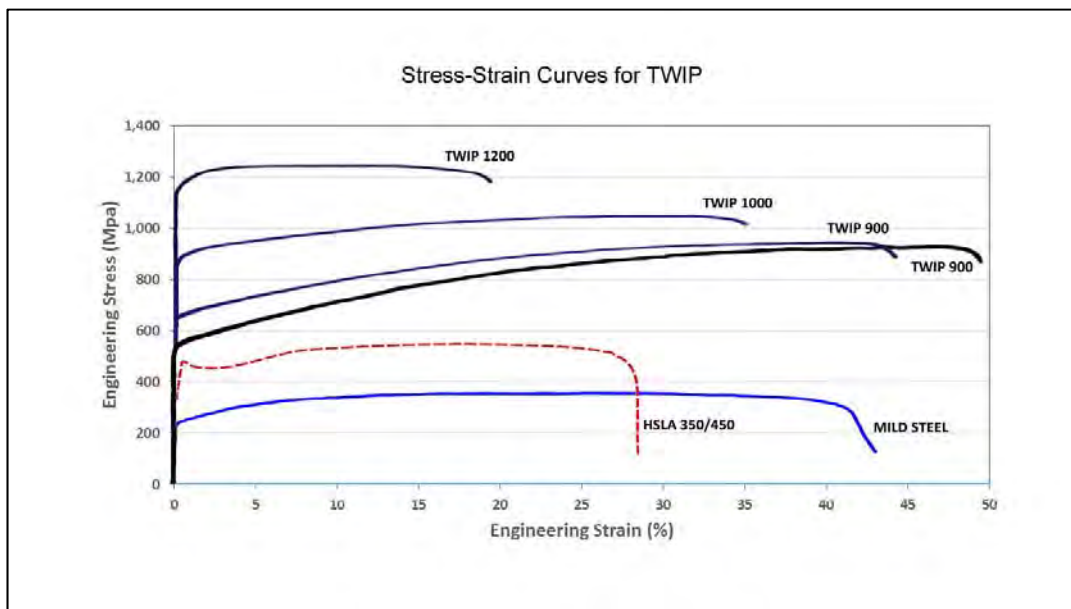
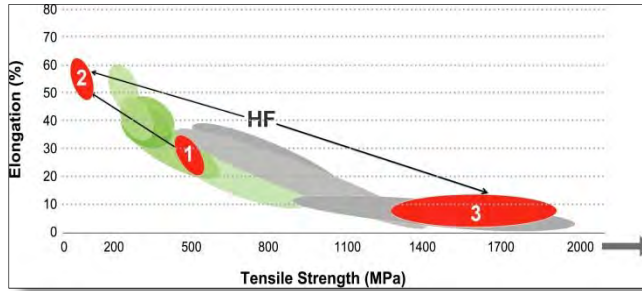


Figure 2.B-25: Engineering stress-strain curve for TWIP^{P-2}

2.B.7. Hot-Formed (HF) Steel

The implementation of press-hardening applications and the utilization of hardenable steels are promising alternatives for optimized part geometries with complex shapes and no springback issues. Boron-based hot-forming steels (between 0.001% and 0.005% boron) have been in use since the 1990s for body-in-white construction. A typical minimum temperature of 850 °C must be maintained during the forming process (austenitization) followed by a cooling rate greater than 50 °C/s to ensure that the desired mechanical properties are achieved. Two types of press-hardening or hot-forming applications are currently available:



- Direct Hot-Forming
- Indirect Hot-Forming

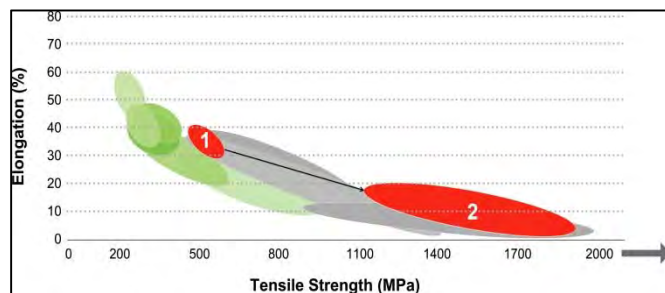
During Direct Hot-Forming, all deformation of the blank is done in the high temperature austenitic range followed by quenching. Indirect Hot-Forming preforms the blank at room temperature to a high percentage of the final part shape followed by additional high temperature forming and quenching. The final microstructure of HF steel is similar to Martensite. Stress-strain curves after quenching are similar to martensitic (MS) steels shown in Figure 2-13.

Additional information on Hot-Forming is located in Section 3.B.5 – Hot-Forming Modes. Current production grades of HF steels and automotive applications:

HF 340/480	As-received room temperature
HF 1050/1500	Heat treated after forming A-pillar, B-pillar, cross beam
HF 1200/1900	Heat treated after forming

2.B.8. Post-Forming Heat-Treatable (PFHT) Steel

Post-forming heat treatment is a general method to develop an alternative higher strength steel. The major issue holding back widespread implementation of HSS typically has been maintaining part geometry during and after the heat treatment process. To address distortion problems, the part is fixtured, then heated (via furnace or induction) followed by immediate quenching. This has been a more effective solution for production applications because, the stamping is formed at a lower strength (ellipse 1) and then raised to a much higher strength by heat treatment (ellipse 2).



Another process is air-hardening of alloyed tempering steels that feature very good forming properties in the soft-state (deep-drawing properties) and high strength after heat treatment (air-hardening). Apart from direct application as sheet material, air-hardening steels are suitable for tube welding. These tubes are excellent for hydroforming applications.

A third option is in-die quenching. A version of Indirect Hot-Forming completes all forming of the part at room temperature, heats the part to about 850-900 °C, and then uses a water cooled die to quench the part to martensite. This process is called Form Hardening.

Current production grades of PFHT steel and example automotive applications:

PFHT 340/480	As-received room temperature
PFHT 1050/1500	Heat treated after forming
PFHT 1200/1900	Heat treated after forming

2.B.9. Special Processed Steels

The microstructures of DP, TRIP and other AHSS have islands or particles of different phases. One example is the martensite islands. When forming steels, these particles cause localization of strain during edge stretching, stretch-bending over tight radii, or other deformation modes whereby strain can localize to generate high peak strains. These steels then are subject to failure at deformations less than that predicted by the properties. Steel companies have been conducting extensive research to develop specialized steels for such applications that minimize the negative effect of these phases or particles. More information is contained in Section 3.B.3 – Deformation Limits.

2.B.10. Evolving AHSS Types

In response to automotive demands for additional AHSS capabilities, research laboratories in the steel industry and academic institutions continue to search for new types of steel or modification of existing types. The goal of the primary research (Enhanced Multiphase Products) is improving formability for a given strength range while reducing the cost and welding problems associated with steels having a high percent of austenite. Other examples of these developing steels are ultrafine (nano) grain, low density, and high Young's modulus steels.

As an example, the Figure 2.B-26 shows multiple pathways with different AHSS grades, which are being modified to achieve vastly improved ductility.

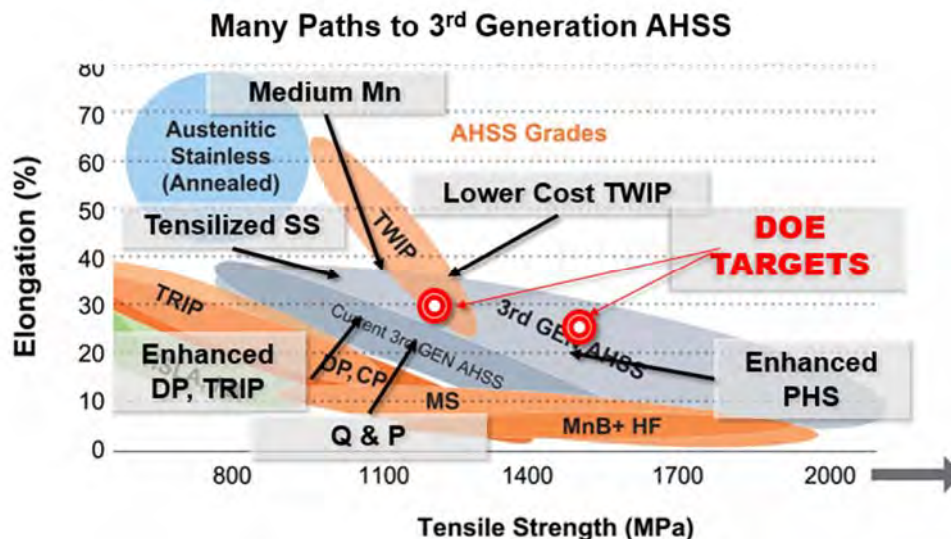


Figure 2.B.26: There are many pathways to achieve improved ductility with Gen 3 steels. Laboratory elongation data approach 2 to 3 times the values commonly reported for DP steels.^{W-10}

TPN – Three-Phase Steel with Nano-Precipitation

A new family of high-performance cold forming steels consists of a ferritic matrix containing bainite, residual austenite and nano-precipitations. During the forming, a high percentage of retained austenite is converted to martensite. This work-induced transformation has a positive effect on the hardening behavior of the material to create a good combination of high formability and high strength. Due to their high resistance to local thinning, these grades allow component geometries that are very difficult to achieve with other high-strength steels of the same strength class. The following nano-precipitation grades are produced for automotive applications.

TPN 680/780: HR660Y760T-TP	B-pillar, Crossmember, longitudinal members, side panel reinforcement
TPN 750/900: HR730Y880T-TP	B-pillar, Crossmember, longitudinal members, bumper, side panel reinforcement

Q&P – Quenching and Partitioning

Q&P steels are a series of C-Si-Mn, C-Si-Mn-Al or other likely compositions subjected to the quenching and partitioning (Q&P) heat treatment process. With a final microstructure of ferrite (in the case of partial austenitization), martensite and retained austenite, Q&P steels exhibit an excellent combination of strength and ductility, which permitted their use in a new generation of advanced high strength steels (AHSS) for automobiles. Q&P steels are suitable for cold stamping for those structure and safety parts of automotive with relatively complicated shape to improve fuel economy while promoting passenger safety.

2.C. Conventional Low- and High-Strength Automotive Sheet Steels

2.C.1. Mild Steels

Mild steels have an essentially ferritic microstructure. Drawing Quality (DQ) and Aluminium Killed (AKDQ) steels are examples of mild steels and often serve as a reference base because of their widespread application and large production volume over the past decades.

2.C.2. Interstitial-Free (IF) Steels (Low Strength and High Strength)

IF steels have ultra-low carbon levels designed for lower yield strengths and higher work hardening exponents (n-values). These steels have more stretchability than Mild steels. The IF-HS grades utilize a combination of elements for solid solution strengthening, precipitation of carbides and/or nitrides, and grain refinement. Another common element added to increase strength is phosphorous (another solid solution strengthener). The higher strength grades of IF steel are widely used for both structural and closure applications.

2.C.3. Bake Hardenable (BH) Steels

BH steels have a basic ferritic microstructure and solid solution strengthening. A unique feature of these steels is the chemistry and processing designed to keep carbon in solution during steelmaking and then allowing this carbon to come out of solution during paint baking or several weeks at room temperature. This increases the yield strength of the formed part for increased dent resistance without reduction in formability. Common applications are automotive outer body panels where increased dent resistance is required.

2.C.4. Carbon-Manganese (CM) Steels

CM steels utilize solid solution strengthening for higher strength.

2.C.5. High-Strength Low-Alloy (HSLA) Steels

HSLA steels increase strength primarily by micro-alloying elements contributing to fine carbide precipitation, substitutional and interstitial strengthening, and grain-size refinement. HSLA steels are found in many body-in-white and underbody structural applications where strength is needed for increased in-service loads.

2.D. Understanding Mechanical Properties

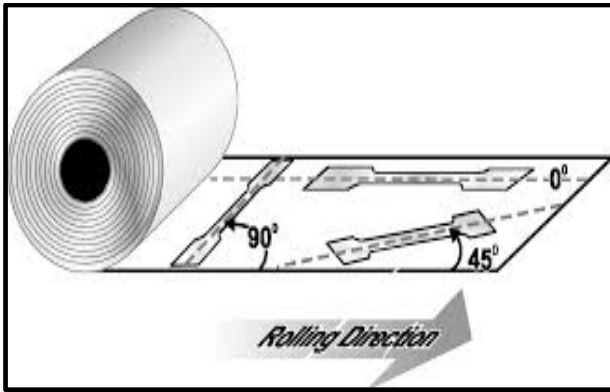


Figure 2.D-1: Typical tensile test specimen orientation as taken from coil.^{M-5}

For decades, the single phase ferritic mild and high-strength low-alloy steels were commonly known by yield strength, tensile strength, and total elongation – usually tested in the longitudinal (0°) transverse (90°) and 45° position relative to the rolling direction (see Figure 2.D-1). Often hardness readings were included, but hardness readings are of little use in assessing formability requirements for steel and are best used to quantify the durability of tooling used to roll, stamp, and trim steel. Sometimes work hardening exponents (n-values) and anisotropy ratios (r-values) were specified to attain improved and consistent formability. The formability limits of different grades of conventional mild and HSLA steels were learned by correlating press performance with as-received mechanical properties.

Today the AHSS are more complex with press performance capabilities modified by changing chemistry, annealing temperature, amount of deformation, time, and even deformation path. By developing new microstructures, these steels become “Designer Steels” with properties tailored not only for initial forming of the stamping but in-service performance requirements for crash resistance, energy absorption, fatigue life, and other needs. An extended list of properties is now needed to evaluate total performance with virtual forming prior to cutting the first die, to ensure ordering and receipt of the correct steel, and to enable successful troubleshooting if problems occur.

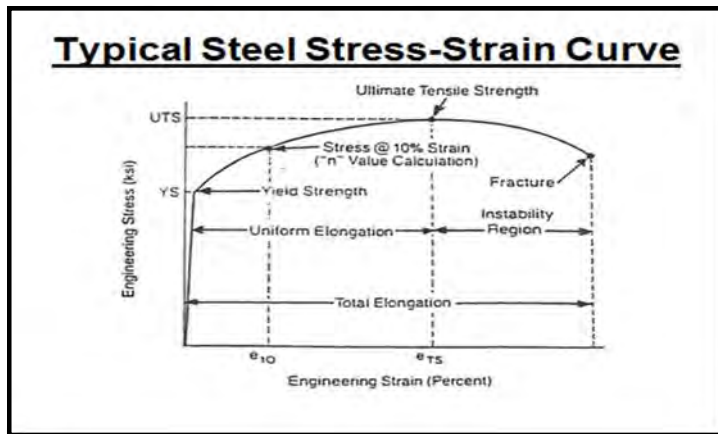
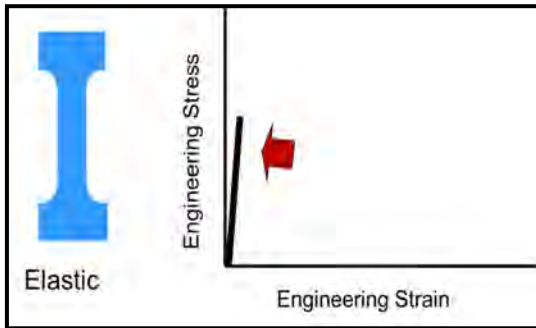


Figure 2.D-2: Typical engineering stress-strain curve showing some of the key formability parameters

As the use of formability parameters is spreading out from OEMs to the tier suppliers, it becomes even more important that all levels of suppliers and users understand both how to measure the parameters and how they affect the forming process. This section provides a short introduction to these parameters. Many of these parameters are measured during a tensile test, which commonly provides an engineering stress-strain curve (Figure 2.D-2). The following section explains each of the tensile test parameters.

2.D.1. Elastic Stresses – Young’s Modulus



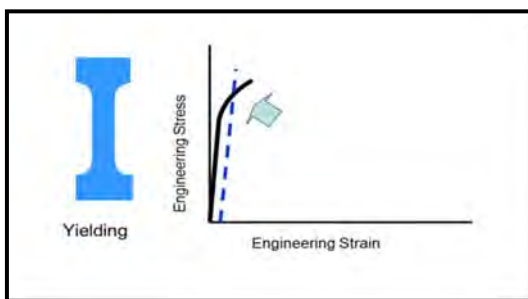
The first deformation of a stamping is created by the external forces of the tooling (pulling or pushing) the atoms in the atomic cell away from their neutral state. At the atomic level, these forces are called elastic stresses and the deformation elastic strain. These forces within the atomic cell are extremely strong, creating small magnitudes of elastic strain for high values of elastic stress. The curve of elastic stress plotted against elastic strain is called Young’s modulus or elastic modulus. For steel this is a steep straight line for

most of its length – often called proportional straining. This elastic strain becomes non-proportional with the onset of plastic (permanent) deformation.

The slope of the modulus line depends on the atomic structure of the metal. Most steels have an atomic unit cell of nine iron atoms – one on each corner of the cube and one in the center of the cube. This is labeled BCC or Body Centered Cubic. The common value for the slope of steel is 210 GPa (30 million psi). In contrast, aluminum and many other non-ferrous metals have 14 atoms – one on each corner of the cube and one on each face of the cube. This is labeled FCC or Face Centered Cubic. The common number for the slope of aluminum is 70 GPa (10 million psi). Removing the forming forces to zero causes the atomic spacing to return back to its initial dimensions. The elastic stresses and elastic strain are now at zero. This return to initial dimensions is called springback – a major factor in achieving consistent stamping shape and dimensions. The amount of springback is inversely proportional to the modulus of elasticity. Therefore, for the same yield stress, steel with three times the modulus of aluminum will have one-third the amount of springback.

Springback deformation usually cannot return the stamping back to its zero elastic stress state due to plastic deformation. The elastic stress remaining in the stamping is called the residual or trapped stress. Any additional change to the stamping conditions (blank trim, hole punching, bracket welding, reshaping, or other plastic deformation) will change the amount of residual stresses and therefore potentially change the stamping shape and dimensions.

2.D.2. Yield Strength vs. Yield Stress



After elongating by elastic deformation, regions of the metal will begin adding plastic (permanent) deformation to sheet metal. Instead of a sharp change from elastic to plastic deformation, a gradual transition occurs. Two measurement techniques are used to assign a yield strength (Figure 2.D-3). The first is drawing a line parallel to the modulus line at an offset strain of 0.2%. The intersection stress becomes the yield strength. The second technique is drawing a vertical line at the 0.5% strain value until it crosses the stress-strain curve. The yield strengths of the two techniques are nearly equal.

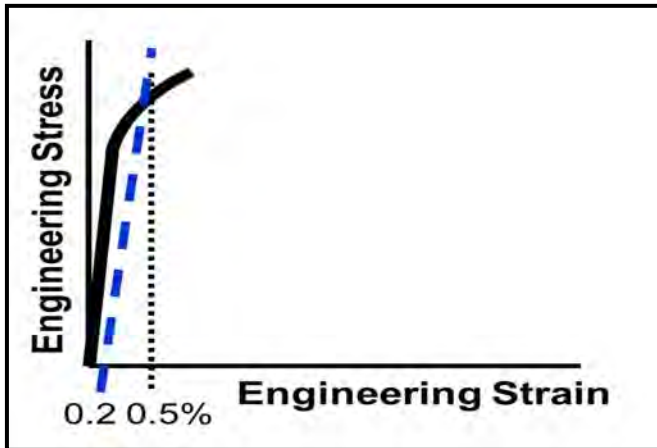


Figure 2.D-3: Determining yield strength with a line parallel to the modulus line and offset by 0.2% or a vertical line offset by 0.5%.

Some metals have yield point elongation (YPE) or Lüder's bands. This occurs when a band of deformation breaks free from being pinned by interstitial carbon atoms and other restrictive features of the microstructure. The stress drops immediately and is called the upper yield stress (Figure 2.D-4). The stress drops to the lower yield stress. Deformation continues at approximately a constant stress until the entire tensile sample has yielded and the sample begins to work harden.

Since springback is proportional to the yield strength of the steel, knowing the yield strength allows some estimation of relative springback (Figure 2.D-5). In this figure compared to mild steel, HSLA can

attain four times more springback and MS AHSS can attain eight times more springback due to increased yield strength.

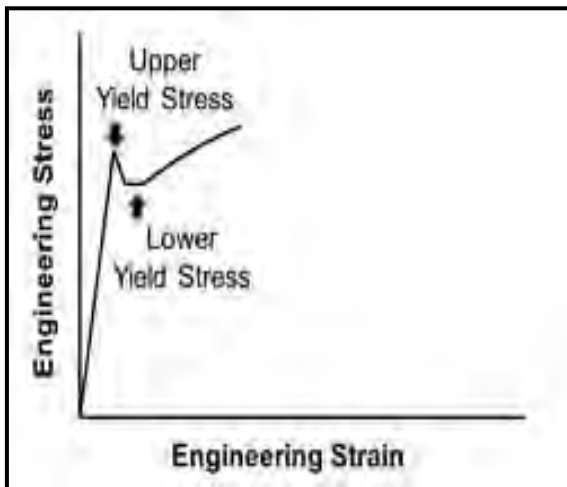


Figure 2.D-4: Defining upper/lower yield stress.

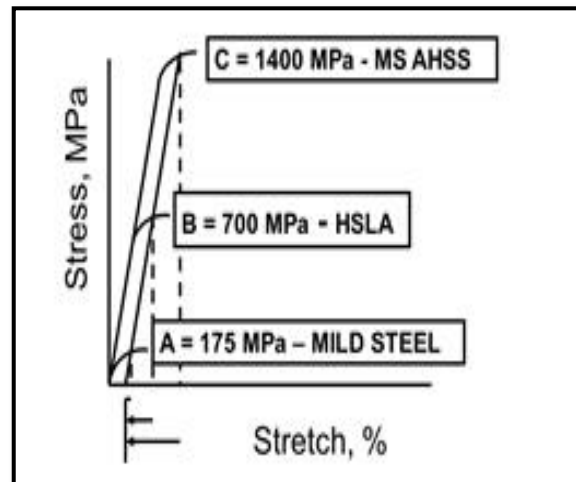
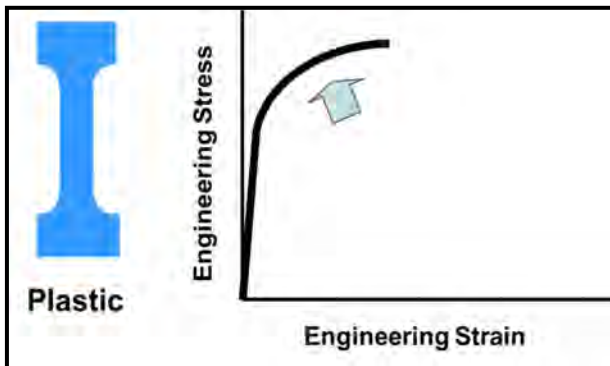


Figure 2.D-5: The springback is proportional to the yield strength.

2.D.3. Work Hardening – n-value



Deformation in the plastic region causes the metal to work harden, which has both advantages and disadvantages. The metal in the area of greater deformation is strengthened by work hardening to reduce the formation of strain gradients (localization of strain) observed in Figure 2.D-6. Assume the design of the die caused the stamping to greatly increase deformation in one zone relative to the remainder of the stamping. Without work hardening, this deformation zone would become thinner as the metal is stretched to create more surface area. This thinning increases the local surface stress to

cause more thinning until the metal reaches its forming limit. With work hardening the reverse occurs. The metal becomes stronger in the higher deformation zone and reduces the tendency for localized thinning. The surface deformation becomes more uniformly distributed.

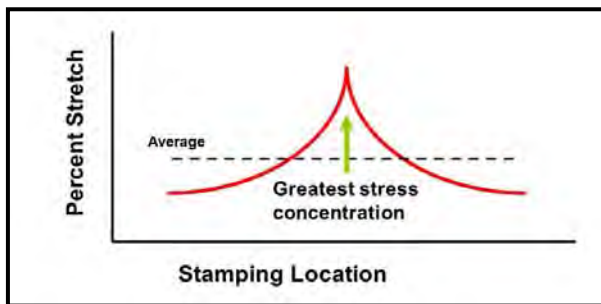


Figure 2.D-6: Strain gradients grow in high stress areas of the stamping.

For sheet metal forming the work hardening is commonly defined by the power law equation:

$$\sigma_T = K \epsilon^n$$

The work hardening exponent (n-value) is the measure for comparing stretching capability of various metals. For decades conventional steels (mild steels, HSLA, etc) had an n-value that was constant with deformation. The n-value measurements commonly were made from 10% to 20%

elongation. A more robust measurement is 10% elongation to elongation at maximum load. This avoids elongation measurements for tests that have an onset of necking less than 20% and includes measurement data for metals that have maximum loads in excess of 20%. Although the yield strength, tensile strength, yield/tensile ratio and percent elongation are helpful when assessing a steel's formability, it is the n-value along with steel thickness that determines the position of the forming limit curve (FLC) on the forming limit diagram (FLD) (to be discussed further in Section 3.B.3 – Deformation Limits). The n-value, therefore, is the mechanical property that one should always analyze when global formability concerns exist. That is also why the n-value is one of the key material related inputs used in virtual forming simulations.

Today many of the AHSS grades have n-values that change value with increased deformation (or engineering strain). For example, Figure 2.D-7 compares the instantaneous n-value of a DP350/600 with a conventional HSLA350/450 grade where the DP steel has a relatively high n-value at lower strain levels, then drops to a range very similar to the conventional HSLA grade after about 7-8% strain. The actual strain gradient of the two steels will be very different due to this initial higher work hardening rate of the dual phase steel. As a result of this unique characteristic of certain AHSS grades with respect to n-value, many OEM's and Tier suppliers create steel specifications for these

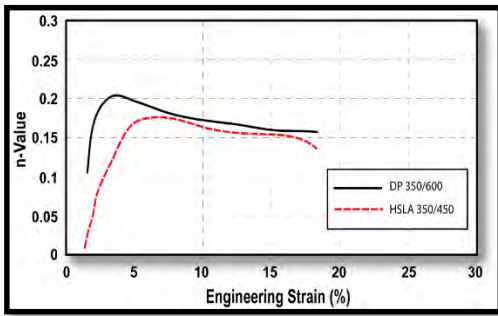


Figure 2.D-7: Instantaneous n-values versus strain for DP 350/600 and HSLA 350/450 steels.^{K-1}

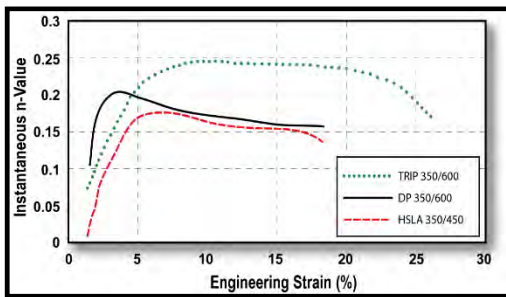


Figure 2.D-7: Instantaneous n-values versus strain for DP 350/600, TRIP 350/600 and HSLA 350/450 steels.^{K-1}

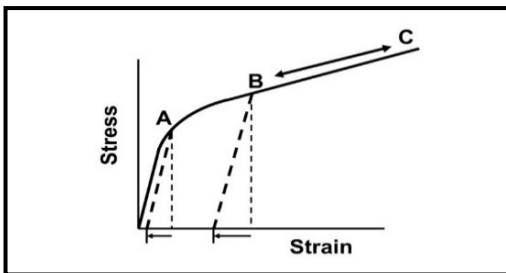


Figure 2.D-8: Deformation of the steel causes the stress at each location in the stamping to change due to work hardening. The resultant stress is called flow stress.

grades that have one minimum n-value, typically in the 4-6% strain range and a second lower minimum n-value at 10% to the end of uniform elongation. Plots of n-value against strain (instantaneous n-values) are helpful in defining the stretchability of these newer steels. The work hardening also plays an important role in determining the amount of total stretchability as measured by various deformation limits (see Section 3.B.3 – Deformation Limits).

Among the AHSS grades available, DP exhibits the greatest initial work hardening rate at strains below 8%. Whereas DP steels perform well under global formability conditions, TRIP steels offer additional advantages derived from a unique, multiphase microstructure that also adds retained austenite and bainite to the DP microstructure. During deformation, the retained austenite is transformed into martensite to increase the strength level, and this transformation allows the steel to maintain a very high n-value throughout the entire deformation process (see Figure 2.D-7). This characteristic allows for more complex geometries and/or reduced thickness for mass reduction. After the part is formed, there is usually additional retained austenite remaining in the microstructure that will subsequently be transformed into martensite in a crash event, making TRIP ideal for parts in crush zones on a vehicle.

Figure 2.D-5 showed the relationship between springback and yield strength for as-received metal. However, forming the stamping also work hardens the metal, thereby increasing the flow stress (yield strength plus increase in stress due to work hardening). Figure 2.D-8 shows this new flow stress as location B for one location in the stamping. The increased stress also increases the elastic stress and the total springback for this point in the stamping. Other locations in the stamping will have different values of flow stress and springback. The stamping will take whatever shape is necessary to minimize total residual stresses.

Process changes, production modifications, uncontrolled lubricant quantities, and many other variables can cause the flow stress at this location to vary (often randomly) from B to C in Figure 2.D-8. The variation at this one location interacting with variations at all other stamping locations can generate a synergistic final output that produces a stamping completely out of print specifications.

2.D.4. Diffuse/Width Neck – Tensile Strength

The elongation of the tensile test sample activates two primary deformation modes. One is a geometrical softening created by the reduction in the sample cross-section. This reduction is necessary to maintain constancy of volume. The other is work hardening. Initially the work hardening is greater than geometric softening to create increasing forming load and stress. Because the work hardening rate (n-value) is a constant when true stress-strain is plotted on log paper, the work hardening is a parabolic curve when plotted as engineering stress-strain. At some level of strain, the geometrical softening of the cross-section becomes greater than work hardening. At this point a load maximum (ultimate tensile strength) is observed and the tensile sample develops a width or diffuse neck – usually in the middle of the sample. The amount of elongation in the gage length of the extensometer at the onset of the neck is called the uniform elongation. As the diffuse neck grows the load is dropping. The portions of the sample above and below the neck stop deforming.

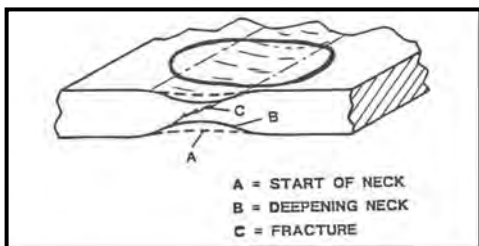
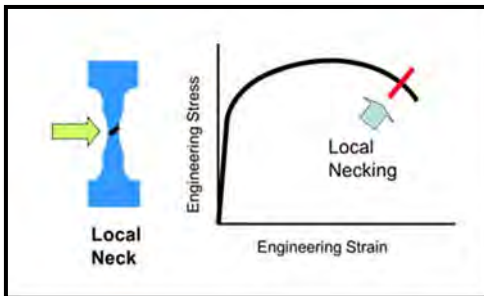
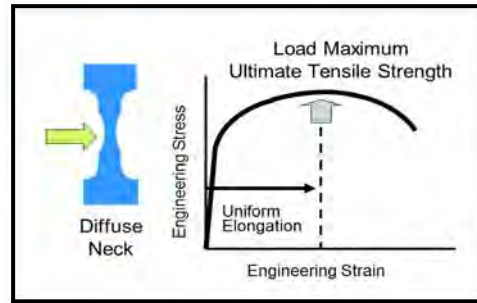
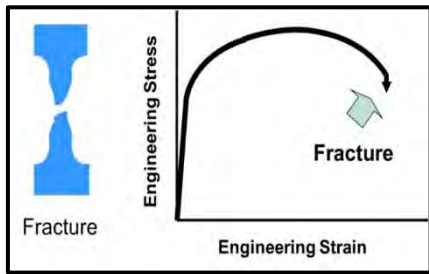


Figure 2.D-9: The maximum useful deformation of a stamping terminates when the local neck just begins to form.

2.D.5. Local/Thickness Neck – and the Forming Limit Curve

A very important parameter in stretch forming is the maximum allowable strain combinations within the plane of the sheet. This maximum stretch in the tensile test is the onset of a local or thickness neck – usually observed as a narrow band oriented about 54-degrees from the axis of the tensile sample. No deformation occurs along the width of the neck – only increased elongation and thinning (Figure 2.D-9). This limit is not the uniform elongation or total elongation observed in the tensile test. This local or through-thickness neck occurs shortly before the traditional fracture of the specimen. When the local neck begins, deformation stops in the remainder of the stamping. Even though high strains can occur in the neck, the stamping has already gone over the edge of the “Deformation Cliff.” The local neck also spoils a class A surface. This local neck is the source of the Forming Limit Diagram and Forming Limit Curve (see Section 3.B.3. Deformation Limits).

2.D.6. Fracture – Total Elongation



Deformation continues in the local neck until fracture occurs. The amount of additional strain in the neck depends on the microstructure. Inclusions, particles, and grain boundary cracking can accelerate early fracture. Total elongation is measured from start of deformation to start of fracture. Two extensometer gage lengths are commonly used: A50 (50mm or 2-inches) and A80 (80 mm or 3 inches). Past procedures attempted to position the two fractured strips back together and hand measure the distance between two gage marks on the sample. Today

computer data acquisition identifies the data point at one-half maximum load and records the elongation of the previous data point.

2.D.7. Directionality of Properties (Anisotropy Ratio) – r-value

The normal anisotropy ratio (r_m) defines the ability of the metal to deform in the thickness direction relative to deformation in the plane of the sheet. For r_m values greater than one, the sheet metal resists thinning. Values greater than one improve cup drawing, hole expansion, and other forming modes where metal thinning is detrimental.

High-strength steels with UTS greater than 450 MPa and hot-rolled steels have r_m values approximating one. Therefore, conventional HSLA and AHSS at similar yield strengths perform equally in forming modes influenced by the r_m value. However, r-value for higher strength grades of AHSS (800 MPa or higher) can be lower than one and any performance influenced by r-value would be not as good as HSLA of similar strength. For example AHSS grades may struggle to form part geometries that require a deep draw, including corners where the steel is under circumferential compression on the binder. This is one of the reasons why higher strength level AHSS grades should have part designs and draw dies developed as “open ended” (to be discussed in detail in Section 3.B.10 – Springback Compensation).

2.D.8. Bake Hardening and Aging

Strain aging was measured using typical values for an automotive paint/bake cycle consisting of 2% uniaxial pre-strain followed by baking at 170°C for 30 minutes. Figure 2.D-10 defines the measurement for work hardening (B minus A), unloading to C for baking, and reloading to yielding at D for measurement of bake hardening (D minus B).

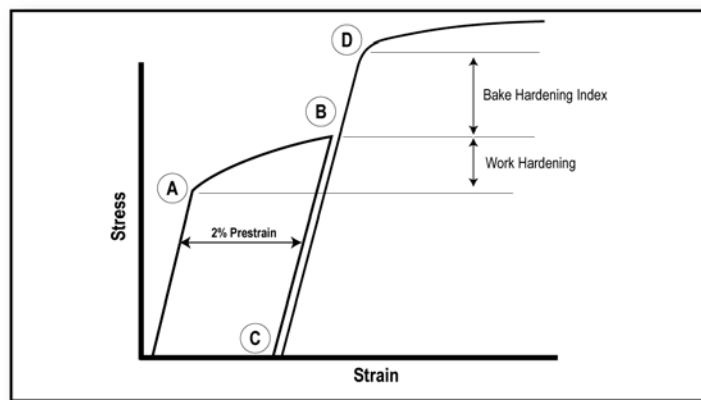


Figure 2.D-10: Measurement of work hardening index and bake hardening index

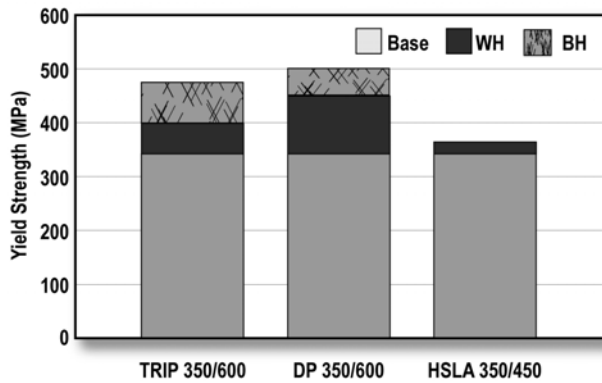


Figure 2.D-11: Comparison of work hardening (WH) and bake hardening (BH) for TRIP, DP, and HSLA steels given a 2% prestrain.^{S-1, K-3}

Figure 2D-11 shows the work hardening and bake hardening increases for the 2% prestrained and baked tensile specimen. The HSLA shows little or no bake hardening, while AHSS such as DP and TRIP steels show a large positive bake hardening index. The DP steel also has significantly higher work hardening than HSLA or TRIP steel because of higher strain hardening at low strains. No aging behavior of AHSS has been observed due to storage of as-received coils or blanks over a significant length of time at normal room temperatures. Hence, significant mechanical property changes of shipped AHSS products during normal storage conditions are unlikely.

2.D.9. Strain Rate Effects

To characterize the strain rate sensitivity, medium strain rate tests were conducted at strain rates ranging from 10^{-3} /sec (commonly found in tensile tests) to 10^3 /sec. For reference, 10^1 /sec approximates the strain rate observed in a typical stamping. As expected, the results showed that YS (Figure 2.D-12A) and UTS (Figure 2D-12B) increase with increasing strain rate.

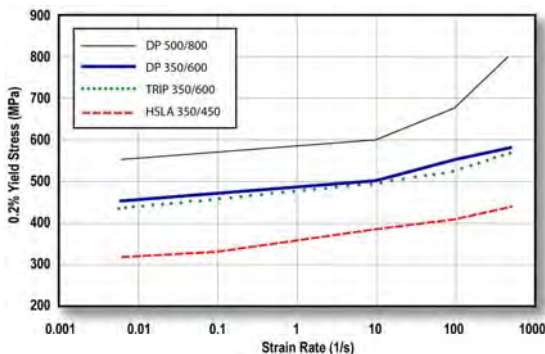


Figure 2D-12A: Increase in yield stress as a function of strain rate.^{Y-1}

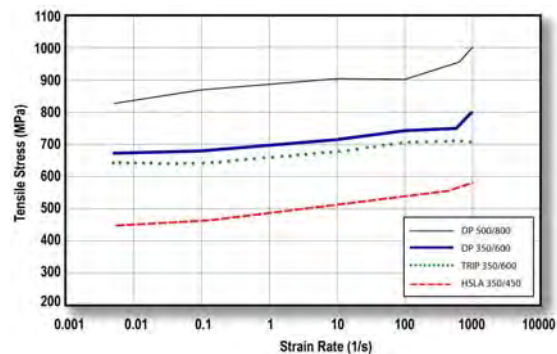


Figure 2D-12B: Increase in tensile stress as a function of strain rate.^{Y-1}

Up to a strain rate of 10^1 /sec, both the YS and UTS only increased about 16-20 MPa per order of magnitude increase in strain rate. These increases are less than those measured for low strength steels. This means the YS and UTS values active in the sheet metal are somewhat greater than the reported quasi-static values traditionally reported. However, the change in YS and UTS from small changes in press strokes per minute are very small and are less than the changes experienced from one coil to another. The change in n-value with increase in strain rate is shown in Figure 2.D-13. Steels with YS greater than 300 MPa have an almost constant n-value over the full strain rate range, although some variation from one strain rate to another is possible.

Figure 2.D-14 shows the true stress-true strain curves at several strain rates for HF steel after heat treatment and quenching to MS. The yield stress increases approximately five MPa for one order of magnitude increase in strain rate. It should also be noted that strain rate effects can be very different for different materials in very high strain rate modes (e.g. automotive crash). Refer to Section 3.G.1 – Crash Management for more information.

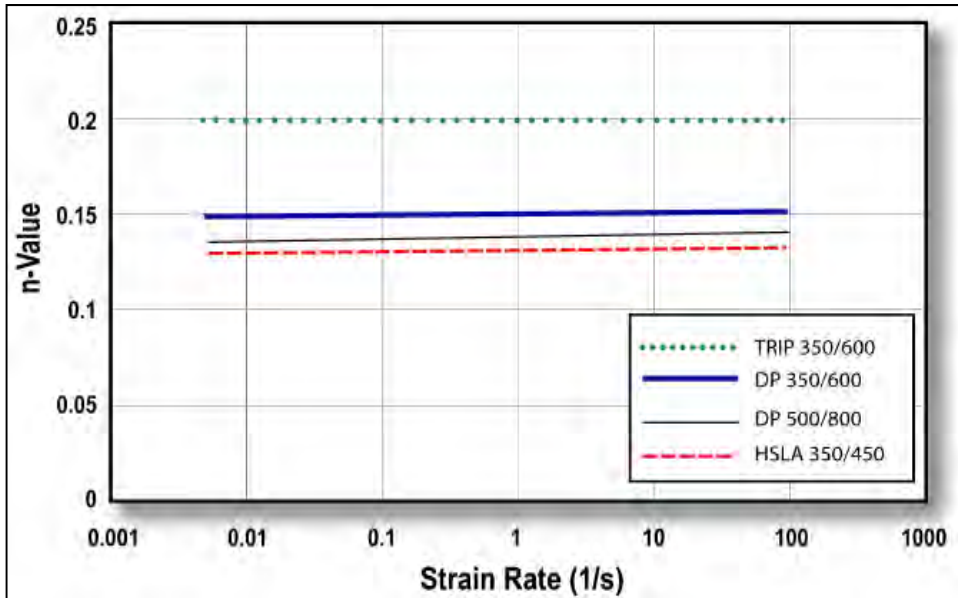


Figure 2.D-13: Relationship between n-value and strain rate showing relatively no overall increase.^{V-1}

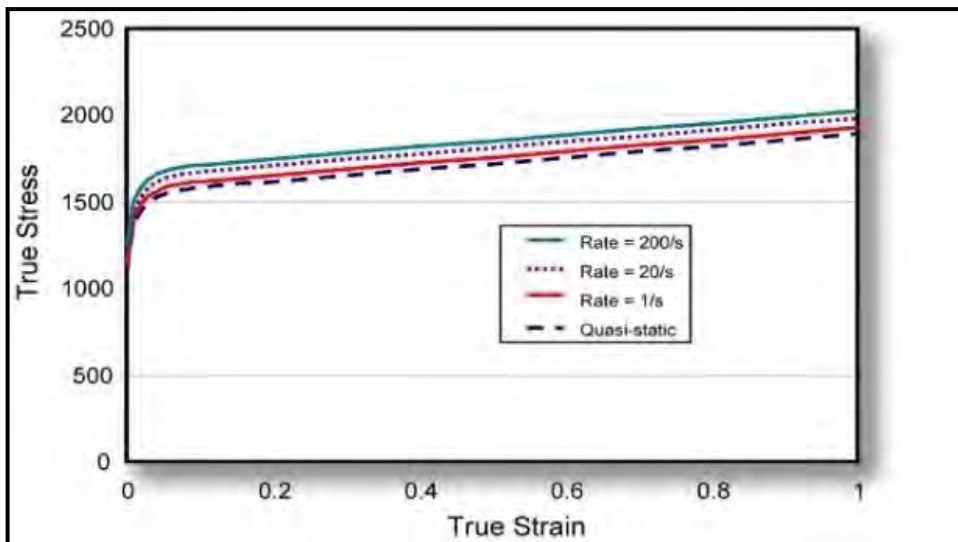


Figure 2.D-14: Extended true stress-strain curves for HF steel with different strain rates.^{V-1} Steel is 1.0 mm thick after heat treatment and quenching.

2.D.10. Key Points

- The multiphase microstructure in AHSS results in properties that change as the steel is deformed. An in-depth understanding of formability properties is necessary for proper application of these steels. Close supplier/user communication is required for proper material selection.
- Tensile test data is very useful for assessing a steel's ability to perform with respect to global (tensile) formability.
- DP steels have increased n-values in the initial stages of deformation compared to conventional HSLA. These higher n-values help distribute deformation more uniformly in the presence of a stress gradient and thereby reduce local thinning.
- Certain AHSS grades such as DP have an n-value that varies, with a very high n-value in the first 0-8% strain, then a drop as strain increases.
- TRIP steels have less initial increase in n-value than DP steels during forming but sustain the increase throughout the entire deformation process, allowing them to achieve more complex geometries or further reduce thickness for weight savings.
- TRIP steels have retained austenite after forming that will transform into martensite during a crash event, enabling improved crash performance.
- Most cold-rolled and coated AHSS and conventional HSLA steels with UTS greater than 450 MPa, and all hot-rolled steels have normal anisotropy values (r_m) around a value of one.
- AHSS work hardens with increasing strain rate, but the effect is less than observed with Mild steel. The n-value changes very little over a 10^5 increase in strain rate.
- As-received AHSS does not age-harden in storage.
- DP and TRIP steels have substantial increase in YS due to a bake hardening effect, while conventional HSLA steels have almost none.

2.E. – Corrosion Resistant Coatings on AHSS

2.E.1. – Hot Dipped and Electrogalvanized Coatings

Many steel parts on a vehicle require corrosion protection, regardless of whether they are exposed or unexposed applications. Today's AHSS products are primarily used on unexposed structural parts. The most common way to accomplish corrosion protection is to coat the steel with zinc by means of a hot dipped galvanizing process.

The hot dipped galvanizing process requires the steel to pass through a molten bath of zinc (at ~460° C/860° F), and the steel is preheated to the same approximate temperature as the molten pot to facilitate adhesion. The steel is under tension during the process, and thus formability properties may be affected very slightly. . Figure 2.E-1 shows a schematic of a typical hot dipped galvanized coating section

Hot dipped galvanizing lines at different steel companies have similar processes that result in similar surfaces with respect to coefficient of friction. Surface finish and texture (and resultant frictional characteristics) are primarily due to roll textures, based on the customer specification. Converting from one coating line to another using the same specification is usually not of major significance with respect to coefficient of friction and formability.

There are several types of hot dipped coatings for automotive applications, with unique characteristics that affect their corrosion protection, lubricity for forming, weldability and paintability. One of the primary hot dipped galvanized coatings is a pure zinc coating (HDGI), sometime referred to as free zinc. This coating has small traces of aluminum in the molten zinc bath to improve adhesion among other things. The end-result is a very shiny surface with a very low coefficient of friction and Figure 2.E-2 shows a schematic of a cross section of typical hot dipped galvanized steel.

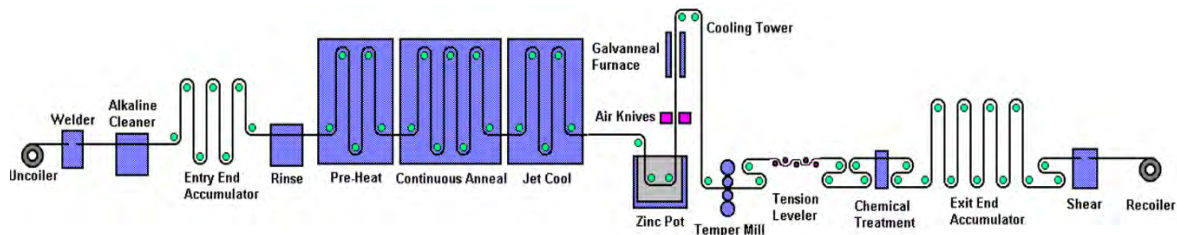


Figure 2.E-1: Schematic of a typical hot dipped galvanizing line.



Figure 2.E-2: Cross section of free zinc hot dipped galvanized steel.

The other primary hot dipped coating used for corrosion protection is hot dipped galvanneal (HDGA). This steel goes through the same process as free zinc hot dipped steel, but after exiting the zinc pot, the steel strip passes through a galvannealing furnace where the zinc coating is reheated while still molten. Iron in the substrate diffuses into the zinc coating, creating an iron-zinc alloy with typical iron content in the 8-12% range. The iron content improves weldability, which is a key attribute of the galvanneal coatings. The iron content can be unevenly distributed throughout the coating (see Figure

2.E-3), ranging from 5% at the surface (where the coating contacts the die) to as much as 25% iron content at the steel/coating interface. The lower iron content at the surface creates a softer surface, resulting in an increased coefficient of friction and potential formability impacts. For difficult to form parts with HDGA, most automakers add press-applied lubricants; for example, phosphate is a dry film lubricant applied to the coil after the zinc coating process to improve formability.

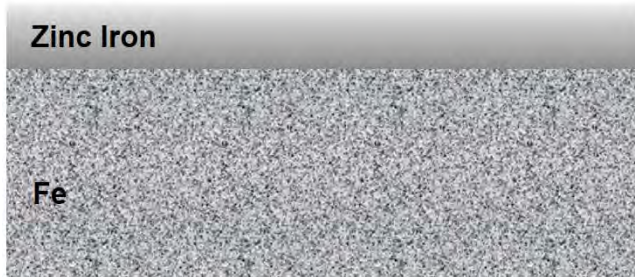


Figure 2.E-3: Cross section of galvanneal coating, showing higher iron content at the interface.

Hot dipped galvanizing is a desirable coating for structural steel applications requiring corrosion protection, as it is a relatively low cost solution because the steel can be annealed and coated in the same operation. However, the thermal cycle for this type of coating process inhibits the ability to produce some of the higher strength AHSS grades, where rapid cooling is required to achieve very high strengths (980 MPa and above). Most hot dip galvanizing lines are limited to coating steels up to 780 MPa in tensile strength.

The furnace section before the zinc pot in a hot dipped galvanizing or galvannealing line heats the steel to at least the temperature of the molten zinc (460°C/860°F), and is capable of continuously annealing cold rolled steel and recrystallizing the microstructure, dramatically improving forming characteristics. The temperature in this furnace can be adjusted to produce the desired microstructure in the final product; for example, temperatures can be set to prevent large changes in microstructure or properties. Thus, full-hard high strength steels can be recovery annealed, and hot rolled HSLA steels can be coated with only minor changes in mechanical properties. For Dual Phase steels the zinc bath serves as an aging section, maintaining the elevated temperature of the steel long enough to achieve the dual phase microstructure.

Martensitic steels and many advanced high strength steels with strengths above 980 MPa cannot attain their microstructure with the thermal profile of a hot dipped galvanizing line (with limited rapid quenching capabilities), and many AHSS grades have chemistries that produce surface oxides which prevent good adhesion of the zinc to the surface. These grades must be produced on a Continuous Annealing Line, or CAL. The CAL line features a furnace with variable and rapid quenching operations that enable the thermal processing required to achieve very high strength levels. If corrosion protection is required, these grades of steel are coated on an electrogalvanizing line (EG) in a separate operation, after being processed on a CAL line.

2.E.2 – Electrogalvanized Coatings

Electrogalvanizing is an alternative zinc deposition process, where the zinc is electrolytically bonded to steel in order to protect against corrosion (Figure 2.E-4) The process involves electroplating, running a current of electricity through a saline/zinc solution with a zinc anode and steel conductor. Since the electroplating process doesn't elevate the temperature of the steel substrate significantly, the microstructure and physical properties of AHSS products achieved on a continuous anneal line (CAL) are largely unchanged after the EG process. As a result, there are three chief advantages of electrogalvanizing compared to hot dipped galvanizing: (1) lower processing temperatures, (2) thinner coatings with comparable corrosion performance, and (3) brighter, more aesthetically appealing coatings.

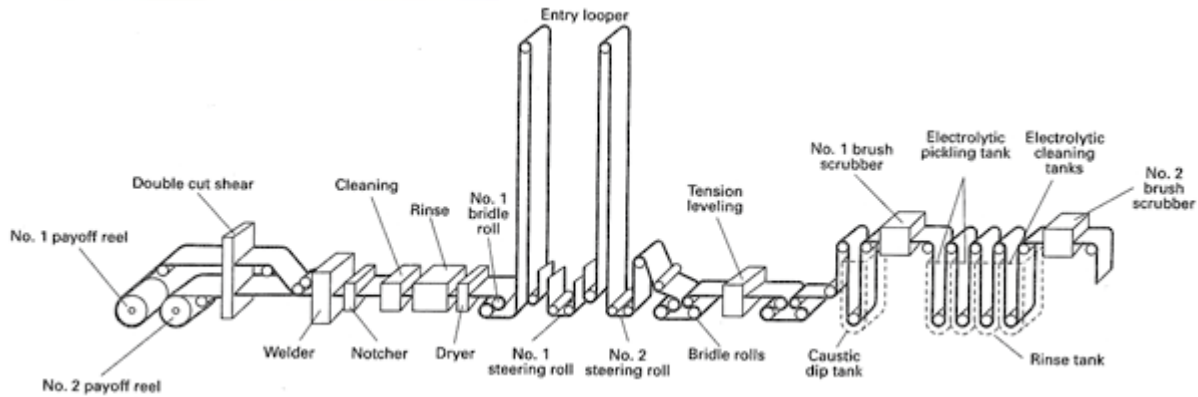


Figure 2.E-4: Schematic of a typical electrogalvanizing line with vertical plating cells.^{A-19}

The overwhelming majority of electrogalvanizing lines can only apply pure (free) zinc coatings. There are no concerns about coating phases as with galvaneal coatings and there is no aluminum on the coating, which improves weldability. The biggest concern with electrogalvanizing lines is the coefficient of friction. Figure 2.E-4 is a chart that compares the approximate coefficient of friction for various coatings. As can be seen, electrogalvanized (EG) coatings have the second highest coefficient of friction, behind HDGA. With EG, some automakers will apply a more viscous oil, commonly called pre-lube, that also improves formability versus the typical mill oil that is normally applied and serves mainly as a rust inhibitor.

Different EG lines may use different technologies to apply the zinc crystals. These different processes lead to a potentially different surface morphology and, subsequently, a different coefficient of friction as the zinc crystals are deposited in a different fashion. Under dry conditions, the coefficient of friction can be quite high, yet the “stacked plate-like surface morphology” allows these coatings to trap and hold lubrication better than the smoother surfaces of hot dipped galvanizing coatings. Auto manufacturers should therefore consult the steel supplier for specific lubricant recommendations based on the forming needs.

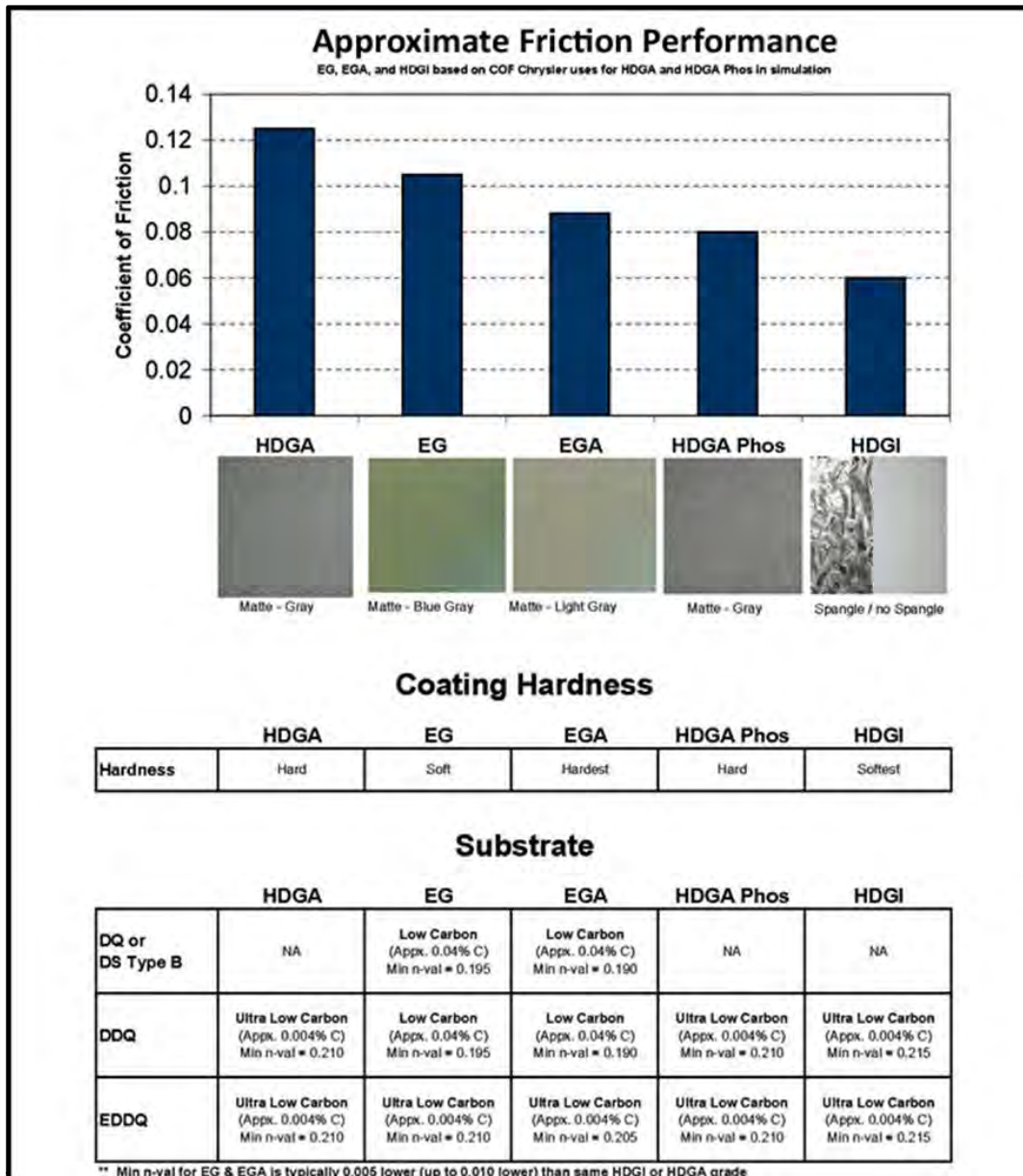


Figure 2.E-4: Chart comparing the approximate coefficient of friction for various coating types.^{M-4}

2.E.3 – Key Points

- Many AHSS parts require corrosion protection, achieved through the application of some type of zinc coating. The primary methods of applying zinc are through a hot dipped galvanizing line, or through an electro-galvanizing process.
- Most hot dipped galvanized lines result in very similar coefficients of friction for a given steel type. Electrogalvanized coating lines have varying surface morphologies, which can result in significantly different formability characteristics.
- Hot dipped galvanized coatings have improved joining, but have different phases that can vary in their composition, and can cause adhesion or formability problems.
- Identifying the intended steel production source should be accomplished early in the die construction and die try-out process. Steel application engineers should be consulted regarding part design and intended processing parameters as early as possible, to ensure robust stamping and joining performance.

SECTION 3 – FORMING AND MANUFACTURING

3.A. General Comments

Forming of Advanced High-Strength Steel (AHSS) is not a radical change from forming conventional High Strength Low Alloy (HSLA). The major acquisition of new knowledge and experience needed for forming higher strength steels in general has increased gradually over the years as ever-increasing strengths became available with the HSLA grades. New demands for improved crash performance, while reducing mass and cost, have spawned a new group of steels that improve on the current conventional base of HSLA.

The AHSS solve two distinct automotive needs by two different groups of steels. The first group as a class has higher strength levels with improved formability and crash-energy absorption compared to the current HSLA grades. This requirement is fulfilled by the DP, TRIP, FB, and TWIP grades of steel, which have increased values of the work hardening exponent (n -value). The second is to extend the availability of steel in strength ranges above the HSLA grades. This area is covered by the CP and MS grades. Originally targeted for chassis, suspension, and body-in-white components, AHSS are now being applied to doors and other body panels. New variations in microstructure are designed to meet specific process requirements, including increased edge stretch, flangeability, strengthening after forming, or tighter property tolerances.

The progressive increases in yield and tensile strength with these new AHSS grades magnifies existing forming issues with conventional HSLA grades, and creates new challenges. Concerns include higher loads on processing equipment including presses, levellers, straighteners, roll forming equipment, blanking, and coil slitting lines. Additionally, there are material and surface treatment considerations required for tooling in the stamping plants: draw dies, trim steels, and flange steels. Compared to conventional HSLA steels, greater energy requirements result from higher AHSS yield strengths, tensile strengths and significantly higher work hardening rates. This places new requirements on press capacity, leveller, straightener and slitting capabilities, tool construction/protection, lubricant capabilities, part and process design, and maintenance. Springback management becomes more critical as yield strengths continue to increase. Conventional and hot formed AHSS parts have a very high final strength after forming, and post forming operations should be avoided. Trimming, cutting, and piercing equipment must be constructed to overcome the extremely high strength of the final stamping. Post forming laser cutting cells are commonly used on hot formed parts to produce a finished part that avoids pushing the limits of trim and pierce tools and dies utilized for conventional HSLA.

This Applications Guidelines document utilizes a steel designation system to minimize regional confusion about the mechanical properties when comparing AHSS to conventional high-strength low alloy steels. The format is Steel Type YS/TS in MPa. Therefore, HSLA 350/450 would have a minimum yield strength of 350 MPa and minimum tensile strength of 450 MPa. The designation also highlights different yield strengths for steel grades with equal tensile strengths, thereby allowing some assessment of the stress-strain curves and amount of work hardening.

There are an ever-increasing number of AHSS multiphase microstructure grades available, each designed to resist various forming failure modes while achieving final part performance requirements. Thus, it's critical that information regarding the planned part geometry, die and stamping processing, and final part application be shared with steel suppliers, product and die process engineering, and end users so the right steel grade will be selected for the application. This becomes especially relevant with respect to two distinctly different forming failure modes called global formability and local formability.

3.B. Sheet Metal Forming

3.B.1. Global versus Local Formability

Measuring steel's ability to address global formability failure modes has traditionally utilized the tensile test properties (described in detail in 2.D. Understanding Mechanical Properties), and the conventional forming limit curve (FLC), where performance is defined by resistance to local necking. These global formability modes include stretch forming, drawing and plane strain tension, where relatively large regions of material are deformed simultaneously (hence, "global"). Strain localization occurs as a material response to relatively uniform applied deformation. Strain distribution is the key to global formability, and conventional indicators are the FLC, and steel mechanical properties including the work-hardening exponent (n-value), uniform elongation and total elongation.

Global formability failures can also be described as tensile failures, and the ability to predict these for both conventional and AHSS using tensile test data is quite accurate when the proper inputs are used. Forming simulation software uses tensile test data to predict formability conditions and hot spots. In global formability conditions, the steel progressively thins as it is formed/stretched. Strains are initially distributed over large areas, but then the steel thins or "necks", the load becomes concentrated and failure ultimately occurs.

Local formability failure modes are an entirely different failure condition, where fractures occur from applied concentrated (local) deformation. Local forming modes include stretch flanging, hole extrusion and tight-radius bending. Failures are observed in these operations, with particular sensitivity to cutting conditions and edge stresses developed in blanking and slitting operations. Trim steel clearances, shear angles, trim steel materials, tool sharpness and design, steel rolling direction, and part design considerations are all important, and are discussed in more detail in Section 3.C.7. – Straightening and Precision Levelling AHSS.

Local formability failures are absent significant thinning, or the onset of a detectable neck" prior to failure. They are often described as edge or shear fractures, and are not predicted through most traditional virtual forming simulations when using the forming limit as the failure criterion. AHSS grades, such as DP and TRIP, are more prone to these local formability failures. AHSS grades within a given tensile strength level that enhance global formability performance may be detrimental to local formability performance, and vice versa, thus it is important to understand the manufacturing and conversion processes to select the appropriate steel grade. New tests are being utilized to better quantify and characterize the optimal AHSS grade choice for each intended application.

Mechanical tests now being utilized to better describe unique local formability related failure modes associated with AHSS include:

- Hole Expansion Test (HET),
- Bend Under Tension (BUT) Test, and
- 2D Sheared Edge Tension Test (SET).

The Forming Section of these Guidelines addresses the forming limits, global and local formability modes before covering the more traditional areas of tooling, springback, press loads and other steel processing technologies. Most data and experience are available for DP steels that have been in production and automotive use for some time. Increased application of other AHSS, however, are providing extensive new data and performance information.

3.B.2. Stress-strain Curves

Stress-strain curves are extremely valuable for comparing different steel types and even different grades within a single type of steel. Engineering stress–strain curves are developed using initial gage length and initial cross-sectional area of the specimen. These curves highlight yield point elongation, ultimate tensile strength, uniform elongation, total elongation, and other strain events. In contrast, the true stress–strain curves are based on instantaneous gage length and instantaneous cross-sectional area of the specimen. Therefore, the area under the curve up to a specific strain is proportional to the energy required to create that level of strain or the energy absorbed (crash management) when that level of strain is imparted to a part.

Figure 3.B-1 through 3.B-7 are a collection of typical stress-strain curves, both engineering and true, for different grades of HSLA, DP, TRIP, CP, FB, TWIP and MS steels. A typical stress-strain curve for mild steel is included in most of the graphs for reference purposes. This will permit one to compare potential forming parameters, press loads, press energy requirements, and other parameters when switching among different steel types and grades. Sample stress-strain curves contained in this section illustrate general trends and reasons why these trends differ from conventional HSLA. Specific type and grade curves and data can only be obtained by selecting the exact type, grade, and thickness of AHSS and then contacting your steel supplier for properties expected with their processing of the order so that this data can be used for successful computerized (virtual) forming simulations to effectively evaluate potential global formability issues.

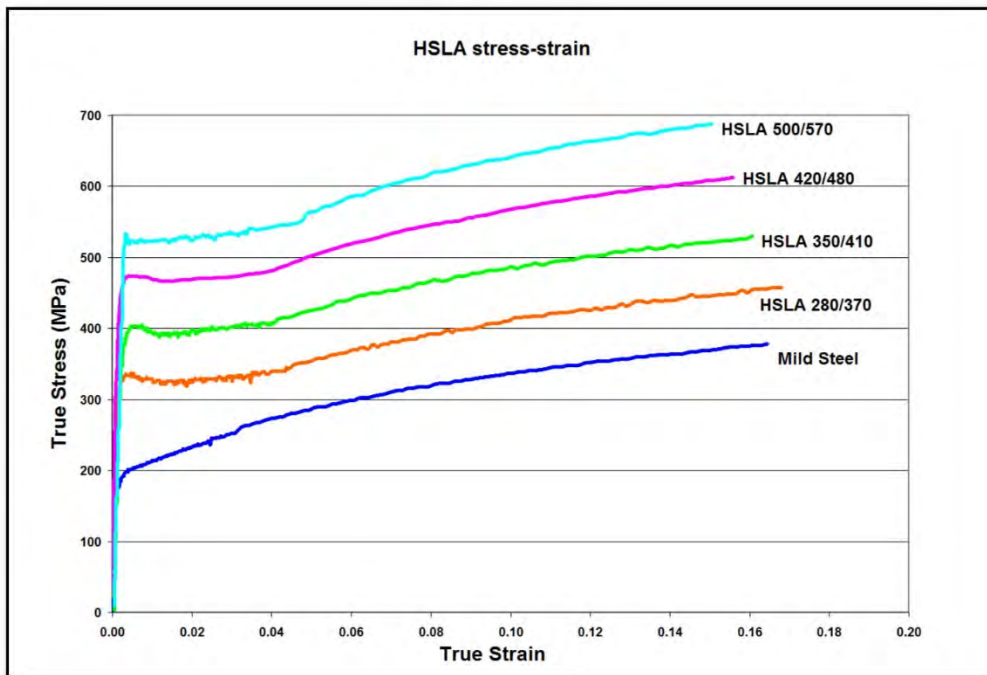
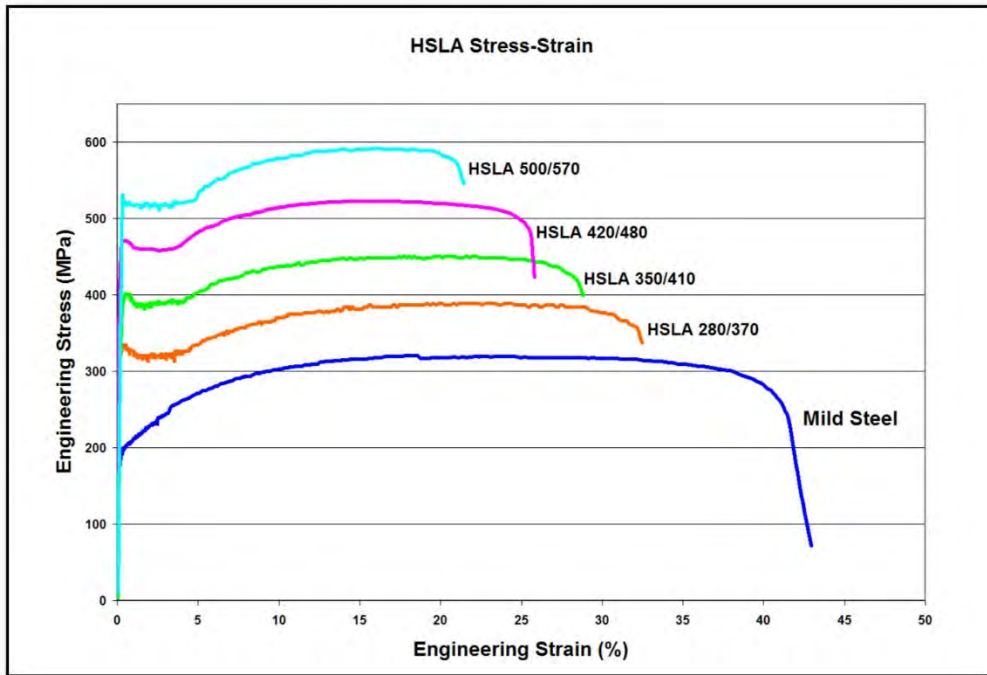


Figure 3.B-1: Engineering stress-strain (upper graphic) and true stress-strain (lower graphic) curves for a series of cold-rolled HSLA steel grades.^{S-5}

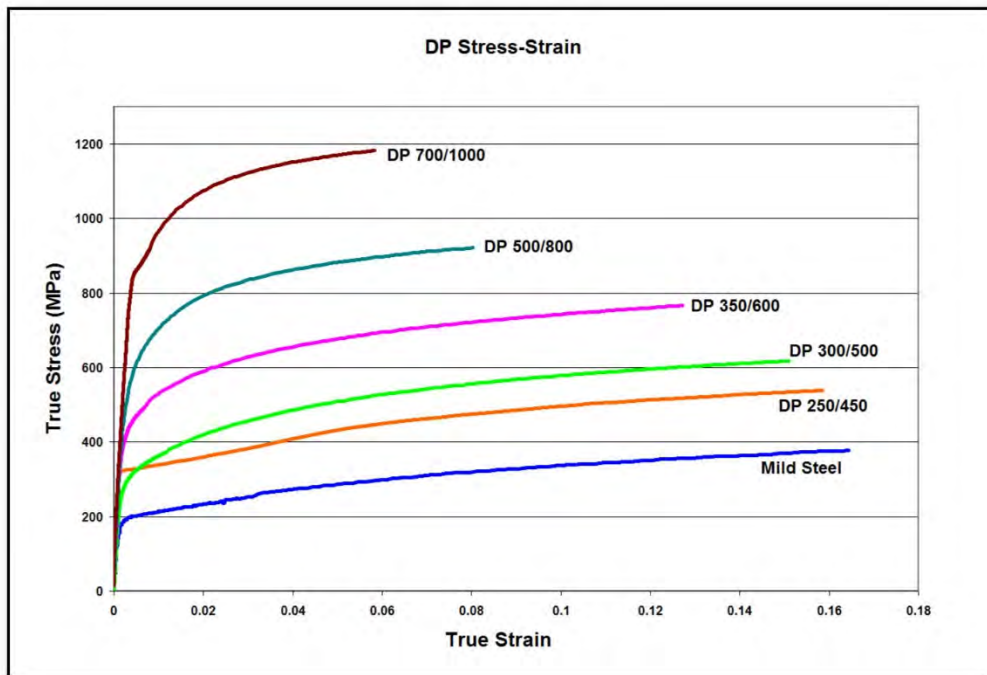
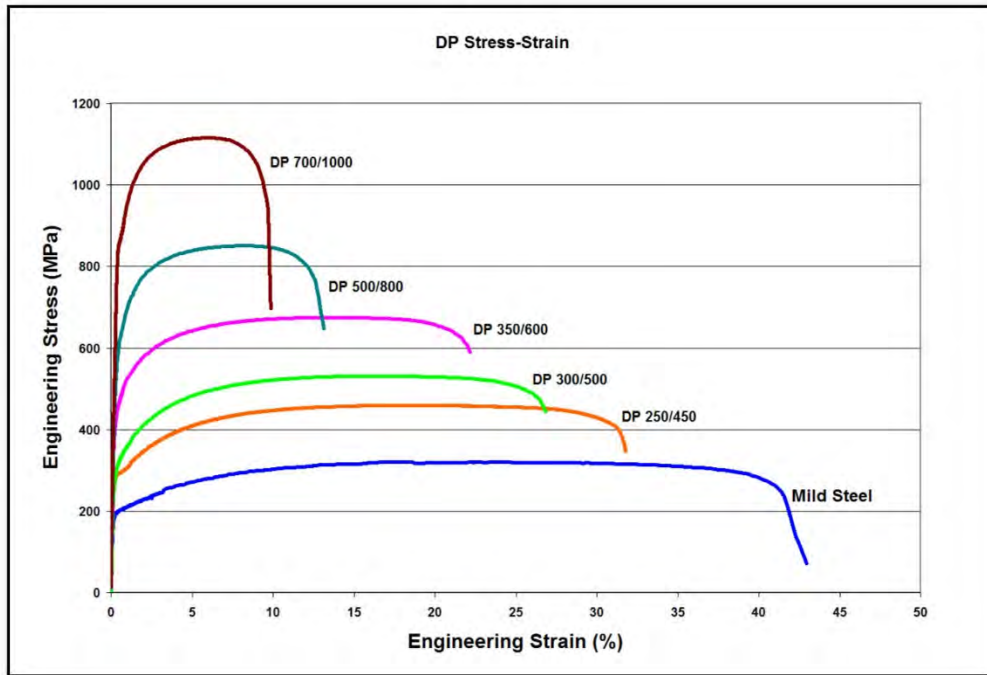


Figure 3.B-2: Engineering stress-strain (upper graphic) and true stress-strain (lower graphic) curves for a series of DP steel grades. ^{S-5, V-1} Sheet thicknesses: DP 250/450 and DP 500/800 = 1.0mm. All other steels were 1.8-2.0mm.

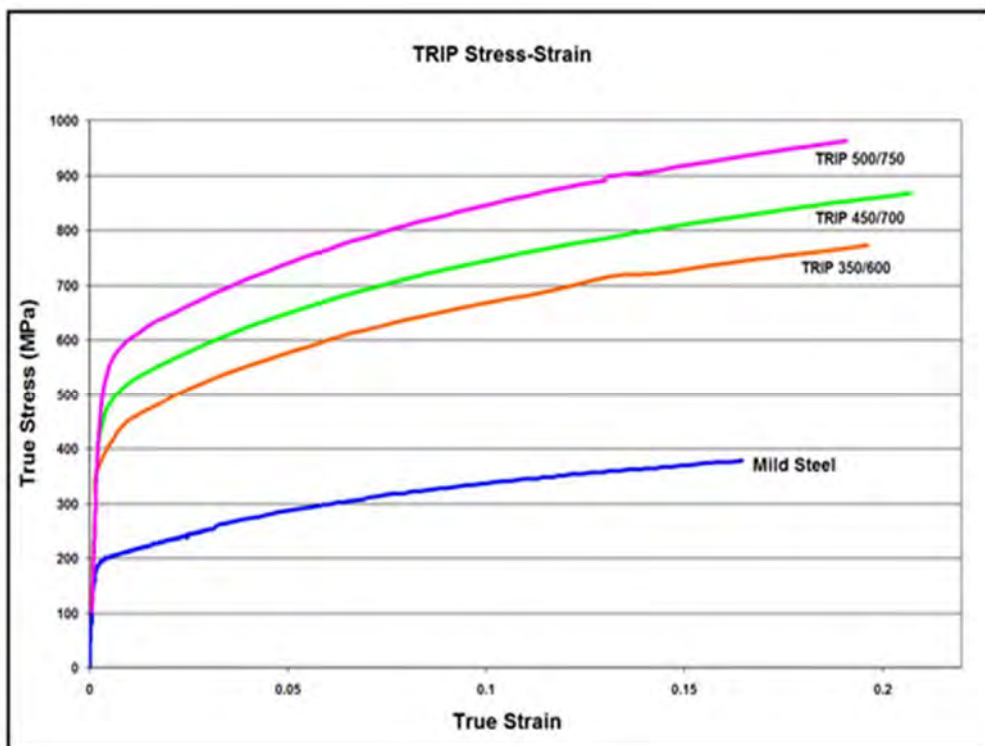
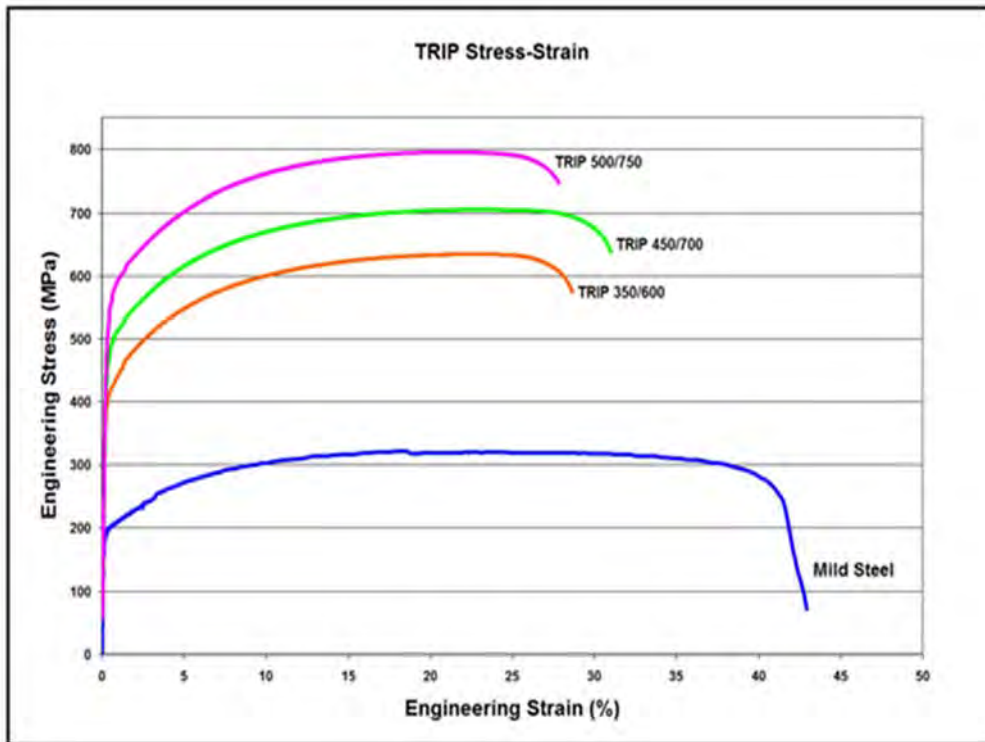


Figure 3.B-3: Engineering stress-strain (upper graphic) and true stress-strain (lower graphic) curves for a series of TRIP steel grades.^{V-1} Sheet thickness: TRIP 350/600 = 1.2mm, TRIP 450/700 = 1.5mm, TRIP 500/750 = 2.0mm, and Mild Steel = approx. 1.9mm.

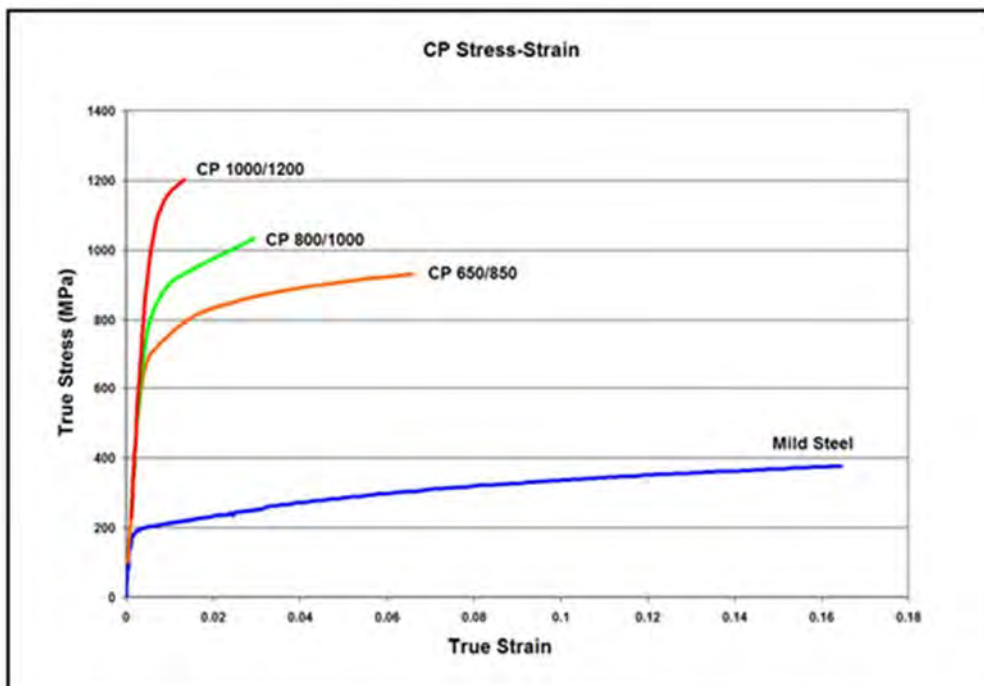
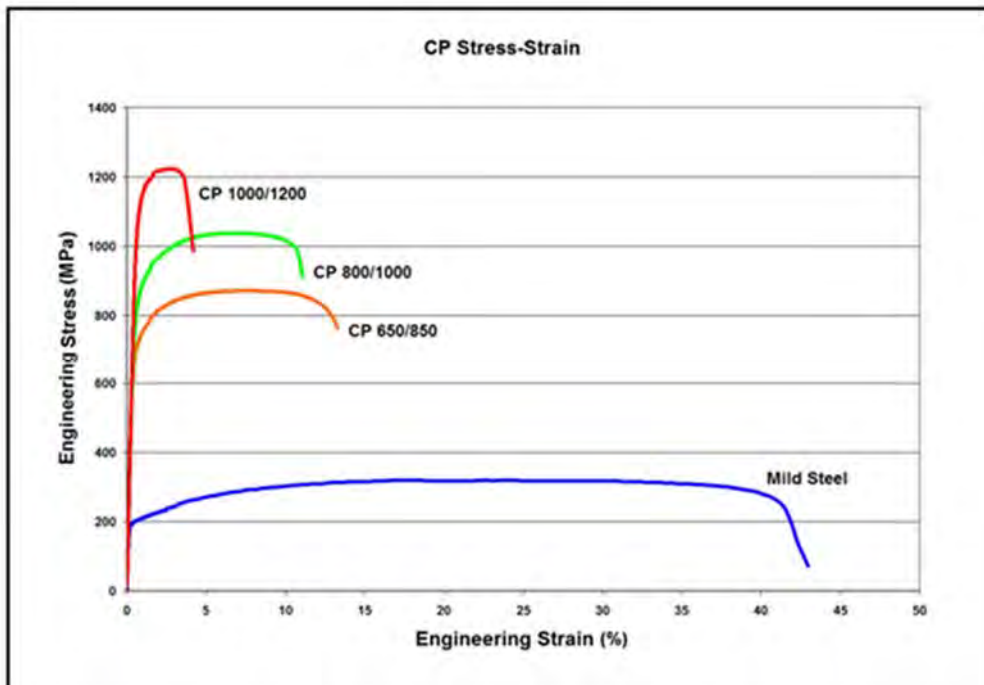


Figure 3.B-4: Engineering stress-strain (upper graphic) and true stress-strain (lower graphic) curves for a series of CP steel grades.^{V-1} Sheet thickness: CP650/850 = 1.5mm, CP 800/1000 = 0.8mm, CP 1000/1200 = 1.0mm, and Mild Steel = approx. 1.9mm.

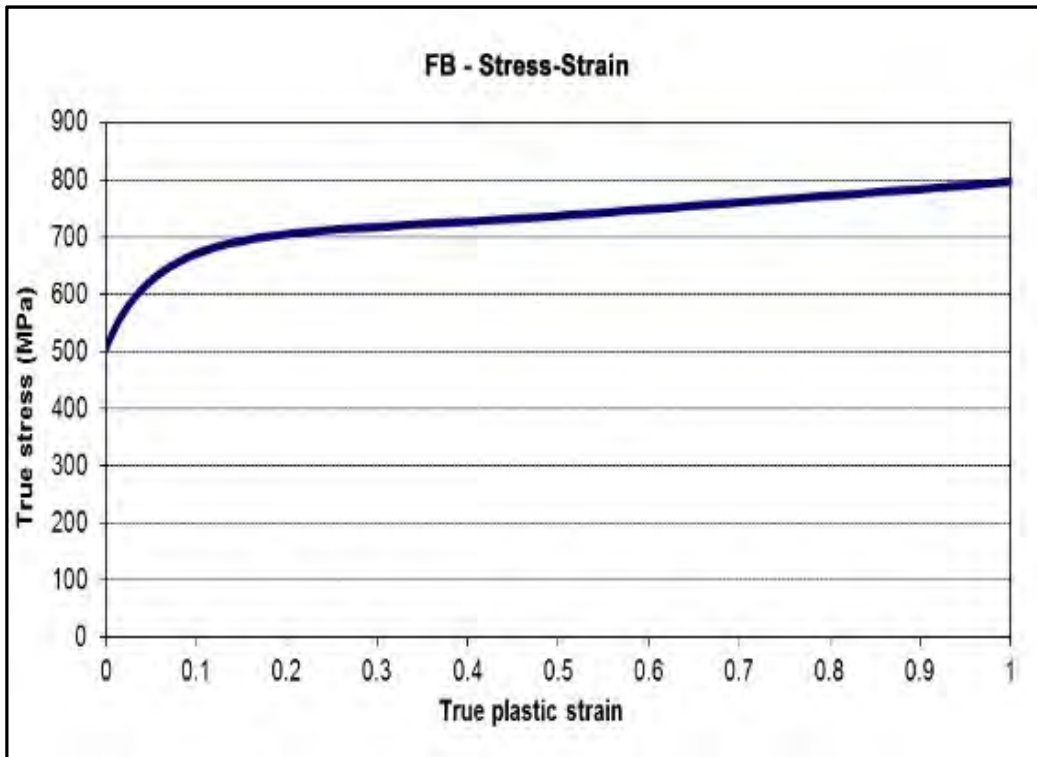
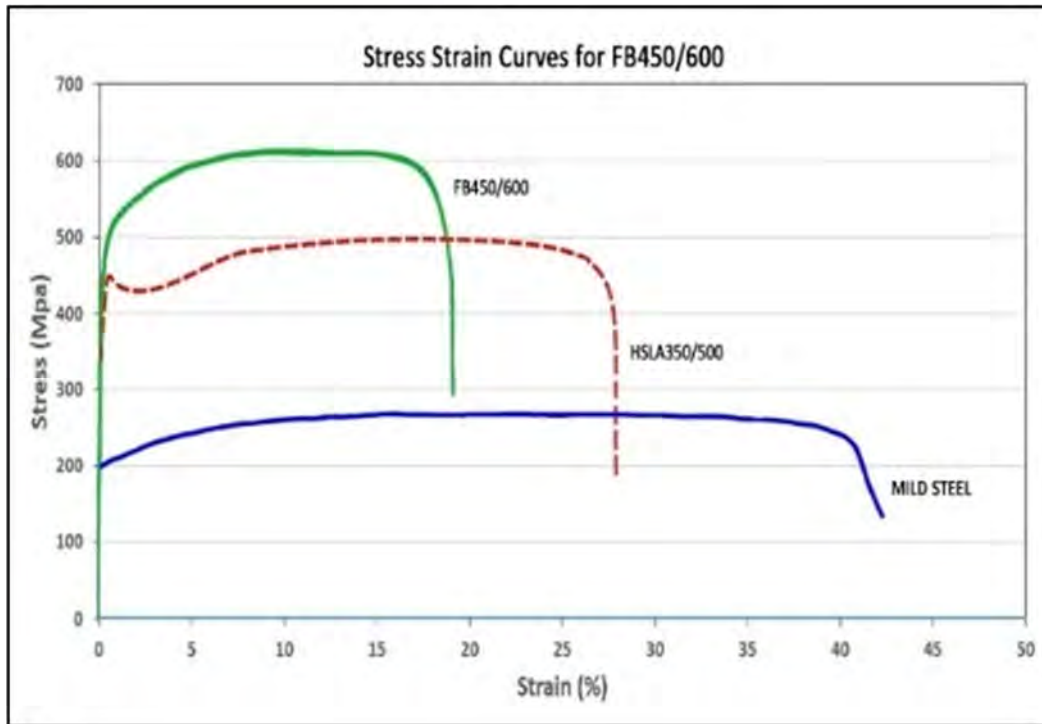


Figure 3.B-5: Engineering stress-strain (upper graphic) and true stress-strain (lower graphic) curves for FB 450/600.^{T-10}

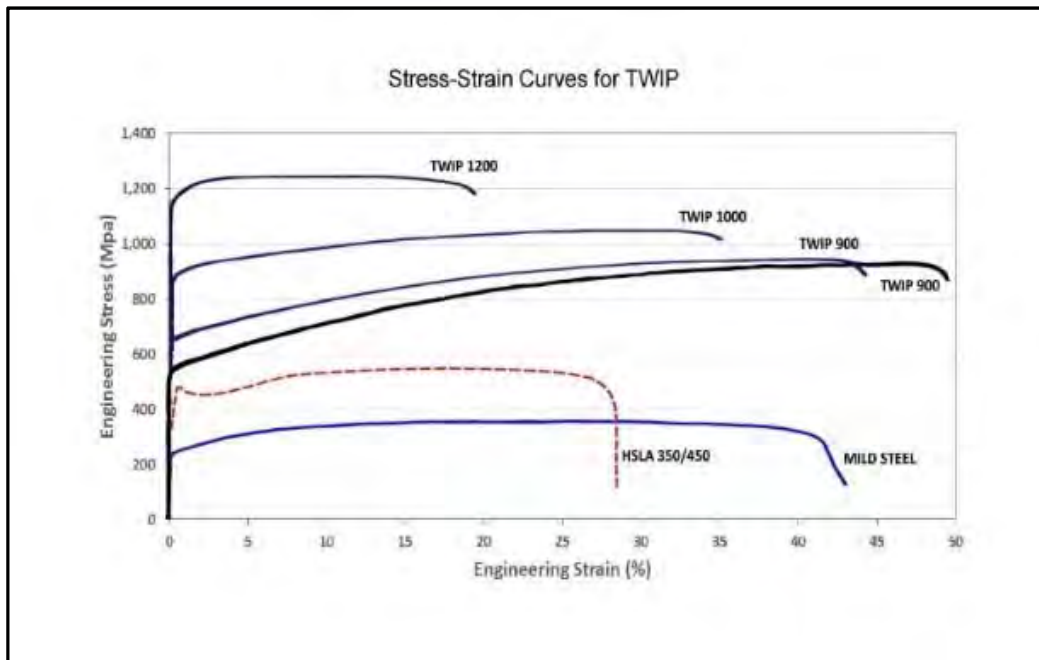


Figure 3.B-6: Engineering stress-strain curves for TWIP steel grades.^{P-2}

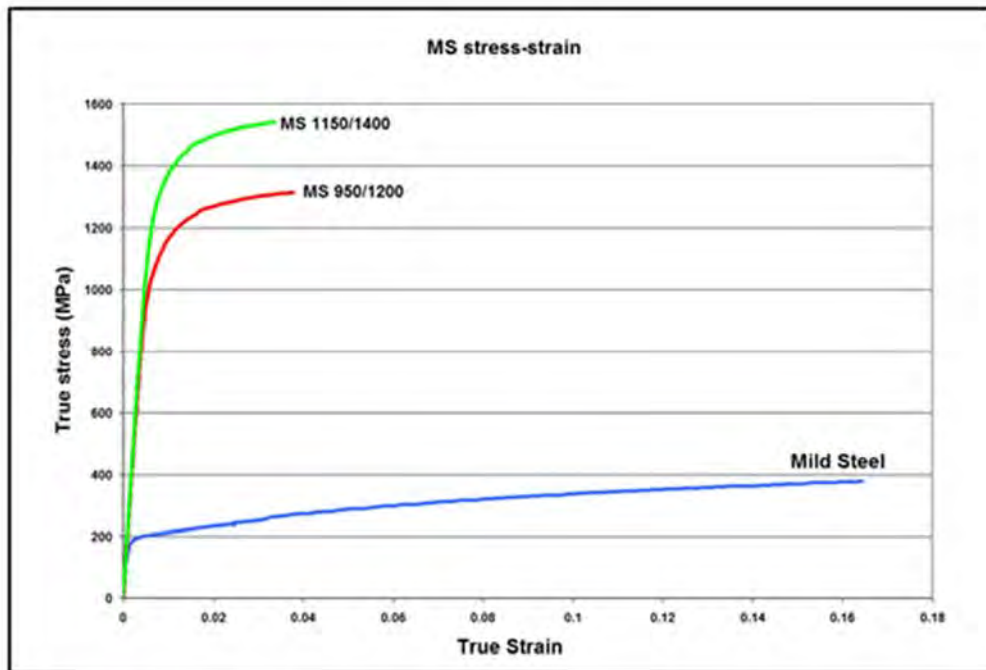
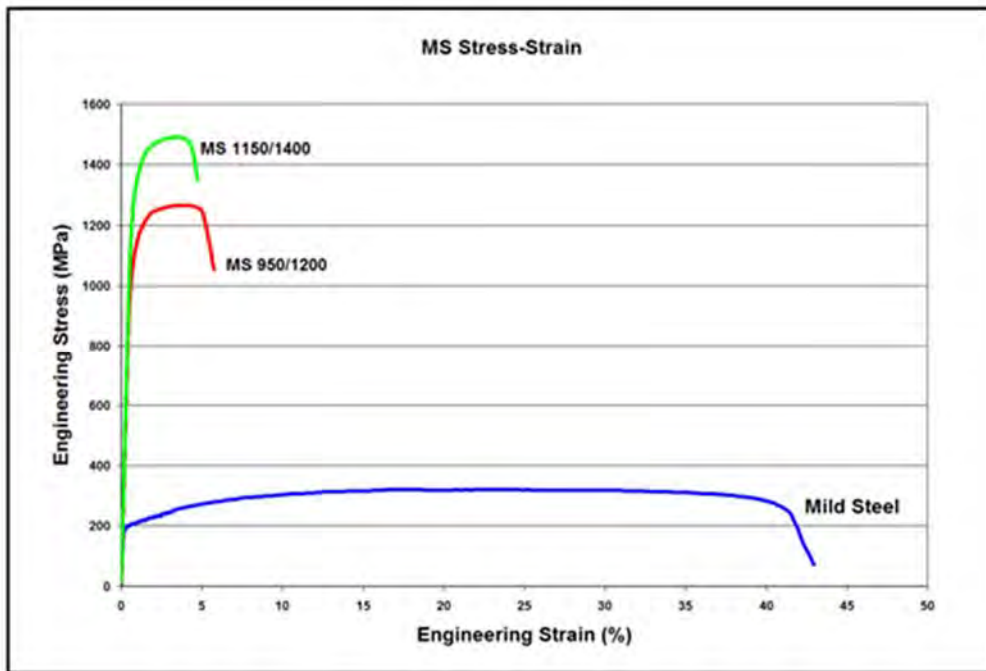


Figure 3.B-7: Engineering stress-strain (upper graphic) and true stress-strain (lower graphic) curves for a series of MS steel grades^{S-5}. All sheet thicknesses were 1.8-2.0 mm

3.B.3. Deformation Limits

Knowledge of forming limits is important throughout the entire product design to production cycle. First is the computerized forming-process development (virtual die tryout), which requires forming limits for the selected steel type and grade to assess the forming severity (hot spots) for each point on the stamping. Next is the process and tool design stage where specific features of the tooling are established and again computer-validated against forming limits for the specific steel. Troubleshooting tools for die tryout on the press shop floor utilize forming limits to assess the final severity of the part and to track process improvements. Finally, forming limits are used to track part severity throughout the production life of the stamping as the tooling undergoes both intentional (engineering) modifications and unintentional (wear or damage) changes. It is common to use circle grid or thinning strain analysis in conjunction with calculated forming limits to monitor part performance and nearness to failure (associated with global formability) during the production life of the part.

This sub-section presents three different types of forming limits. First is the traditional forming limit curve applicable to stretching modes of sheet metal forming (global formability). Second is an edge stretching limit that applies to the problem of stretching (hole expansion, stretch flanging and blank edge extension) the cut edge of sheet metal (local formability). Third is a shear fracture encountered during small radii bending of DP and TRIP steels (also local formability).

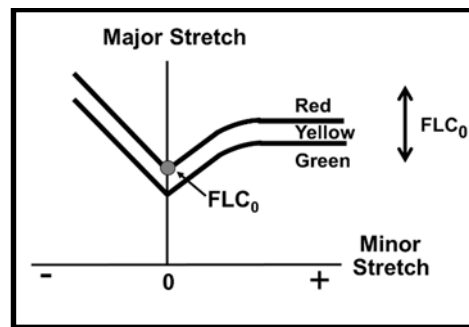
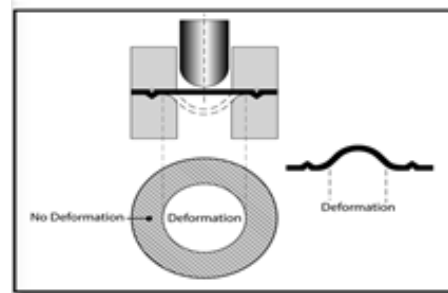


Figure 3.B-8: General graphical form of the Forming Limit Curve.

3.B.3.a. Forming Limit Curves (FLC) – Global Formability

Forming limit curves (FLC) are used routinely in many areas around the world during the design, tryout, and production stages of a stamping. An FLC is a map of strains that indicate the onset of critical local (through thickness) necking for different strain paths, represented by major and minor strains (Figure 3.B-8). These critical strains not only become the limit of useful deformation but are also the points below from which safety margins are calculated.



Experimental determination of FLCs involves stretching sheet specimens of different widths over a hemispherical dome to generate different strain paths from which critical strains are determined. This is shown in Figure 3.B.9^{P-9}

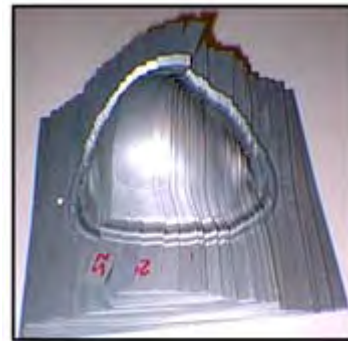


Figure 3.B.9: Limited dome height test coupons, showing variation in sample width which affect deformation mode, and allow creation of the forming limit curve. ^{P-9}

Considerable prior work has been done with respect to characterizing the minimum value of the FLC as a function of mechanical properties. The original FLC height was based on sheet thickness and n-value. New studies in Europe also found a correlation with three properties – total elongation, tensile strength and sheet thickness^{T-11} Regional differences also may be observed in the

generation, shape, and application of forming limit curves. Some curves are determined by equations. ISO12004 is applicable to other forming limit diagrams.

The above mentioned FLC's are strain-based with deformation measured by circular grids easily applied in the press shops. New procedures^{S-8} are being developed that are stress-based, which are readily applicable to virtual forming. Stress-based FLC's also correct for the previous problem dealing with non-linear strain paths during the forming of the stamping^{S-8}

Specific FLC comparisons for mild, HSLA, DP, and TRIP steels are discussed in Section 3.B.4.a. – Stretching.

3.B.3.b. Edge Stretching Limits – Local Formability

Extensive research work is being conducted in various parts of the world to study the capability of AHSS to withstand tensile stretching on sheared edges (edge fracture) as well as bending over a radius (shear fracture), with or without tension. This sheared edge can be created at many different times during the transition from the steel mill to final assembly. This includes coil slitting, blanking (straight and configured), offal trimming (external edges or internal cut-outs), hole punching, and other operations that change the edge condition. Tensile stretching is most commonly created during hole expansion, stretch flanging, and blank extension processes. Presently, there are no reliable edge stretching failure criteria available for use in forming simulations, to predict local formability failures with AHSS. The forming limit curve developed from virgin material is no longer appropriate to predict edge failure due to edge damage associated with blanking and trimming processes. This section enables better understanding of the many variables and their interactions affecting edge stretch performance during forming.

Hole Expansion Test

The Hole Expansion Test (HET) is one of the most common tests to quantify the local formability related edge fracture failure mode associated with AHSS. The HET is also useful for relative comparisons of various AHSS products in local formability performance. The results are then used to tailor steel performance for the intended application, through modifications of chemistry, rolling and thermal practices to achieve the desired edge stretching performance.

There are two main versions of the HET, one using a flat bottom punch and the other using a conical or hemispherical punch. The flat punch test often results in an early strain concentration during the test due to the free edge. Therefore, the hole expansion ration (HER) generated by a conical punch was consistently higher than that created by a flat bottom punch, so when companies test results for various conventional and AHSS grades, the HET test method needs to be specified. Either one could be used to compare edge stretching of different metals. The conical punch test has become more common because it is more simulative of a stretch flanging operation. Widely used standards for conducting the HET include ISO/TS 16630-2003 and JFS T 1001-1996. In both versions, a square steel blank is cut and a hole pierced in the sample. The quality of the punched hole is critical when trying to obtain consistent data. Special effort is needed to keep the tools sharp and damage free in the lab test environment to maintain the consistency in edge conditions. Hard and wear resistant tools, preferably a coated PM grade are highly recommended. Clearances should be monitored, especially if thickness changes are made to the tested material as trim clearances are a critical variable when working with AHSS. If different steel thicknesses are being tested, different diameter punch dies may have to be used to maintain a consistent clearance for varying sheet thicknesses during the hole piercing process.

The flat blank with pierced hole is then clamped in the hole expansion test device, and either a flat or conical punch is pushed up into the hole. The test continues while the hole edge is examined, until a through-thickness edge crack is observed, at which time the punch is stopped. Detecting the point at which edge fracture initiates can be done visually or more commonly, with a camera magnified to get a

close-up of the specimen during the test. The hole expansion ratio (HER) or percent hole expansion is then calculated. The increase in the ratio of the final/initial hole diameter is typically given by the symbol lambda (λ) and is the percentage increase in the size of the hole before edge fracture is observed. The greater the hole expansion ratio of the material, the more likely that the material will have improved local formability characteristics. Figure 3.B-10 shows a HET sample after being tested with a conical punch. Figure 3.B-11 shows a schematic of a typical HET conical punch/die setup.

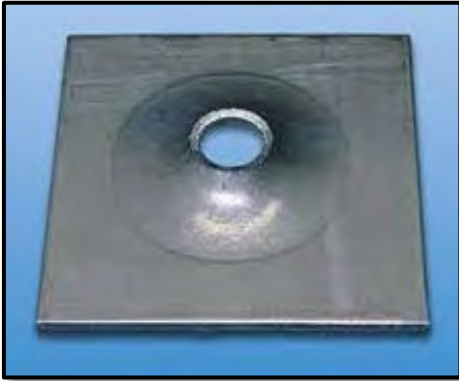


Figure 3.B-10: AHSS sample after a hole expansion test using a conical punch.^{M-5}

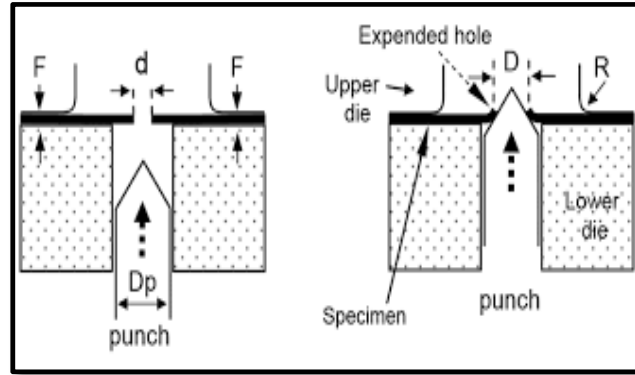


Figure 3.B-11: Schematic of a typical hole expansion test (HET) conical punch/die setup.^{M-5}

HET studies have been conducted under different cutting conditions, such as milled edge, laser cut edge, waterjet cut edge, burr, no burr, different trim clearances, etc. The hole expansion test edge simulates a circular tensile test sample with similar width and thickness reductions.

The chart in Figure 3.B-12 can be explained as the reduction in the degree of edge damage on edge stretch performance of the steel due to differences in the severity of damage created during the cutting operation. Improved edge quality and reduced mechanical work hardening of the edge can be attained by laser cutting, EDM cutting, water jet cutting, or fine blanking processes to improve the hole expansion ratio (HER). Trim steel clearances, shear angles, and tool steel types and sharpness also impact HET results and are of much greater significance with AHSS due to their multiphase microstructure. This severe work hardening generated during the edge shearing prevents the use of traditional FLC's based on the as-received properties of the steel to determine allowable sheared edge stretching.

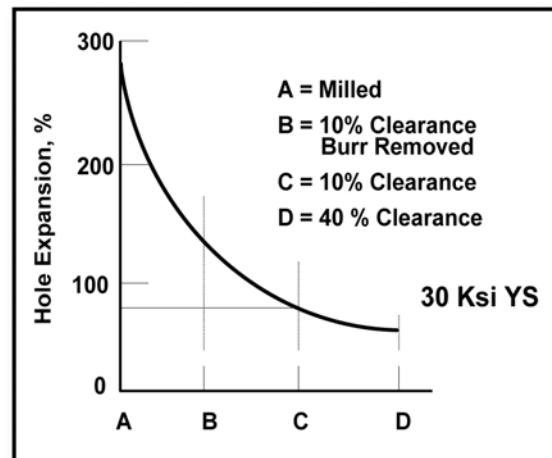


Figure 3.B-12: Schematic showing hole expansion capability for a 200 MPa mild steel for various punch conditions.^{H-1}

Research^{V-1} similar to Figure 3.B-12 but devoted to AHSS and conventional HSLA is presented in Figure 3.B-13. Note that the hole expansion % is significantly lower for punched holes than for machined holes – the result of more edge damage. The reduction in the hole expansion % for DP and TRIP steels compared to conventional HSLA and CP steels is due to the islands of

martensite which can increase interfacial shearing between the ductile ferrite matrix and the harder martensite phases. A more detailed study of sheared edge stretching is available in reference K-6.

Production studies found that DP and TRIP steels had a unique type of edge stretch failure. These steels had early edge failure for edges pulled in tension. These local formability failures are classic examples of edge fracture, characterized by no localized neck during edge stretching. Research shows that multiphase microstructures, specifically islands of the very hard martensite surrounded by a softer ferrite matrix, may crack along the ferrite-martensite interface as seen in Figure 3.B-14. The larger the size of the initiated damage site (due to edge shearing), the smaller the critical stress required for crack propagation.

The absence of global thinning followed by the onset of localized necking makes it very important to clearly define the actual mode of failure before selecting solutions. Examination of the edge of the part where the failure is occurring is the best way to accomplish this. Figure 3.B-15 is a close-up of an edge fracture showing no observable thinning or necking.

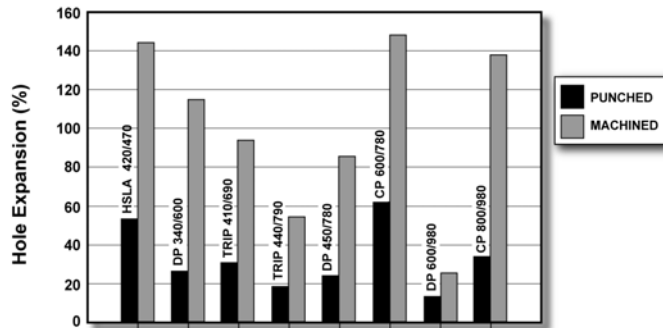


Figure 3.B-13: HET results for punched and machined holes showing edge effect of damage to sheet metal stretchability.^{V-1}

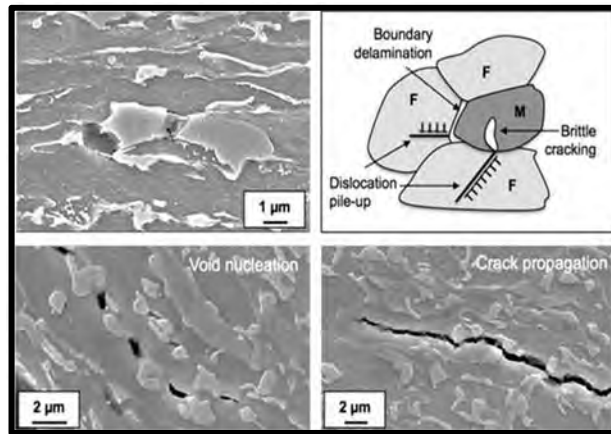


Figure 3.B-14: Features and mechanisms of damage initiation and propagation in DP steel.^{M-6}

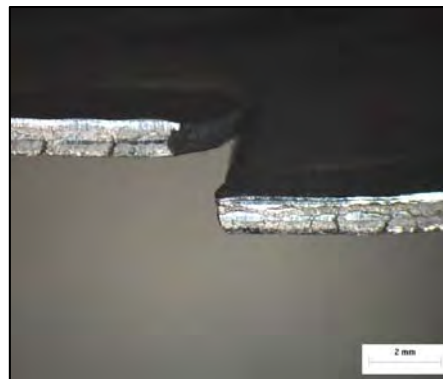


Figure 3.B-15: Close-up of same edge fracture.^{M-4}

A study^{C-1} evaluated the hole expansion ratio created by hole punching tools as they wore in a production environment. The powder metallurgy (PM) tools had a 60 HRC. The tools were uncoated. Data in Figure 3.B.16 show the percent hole expansion from newly ground punches and dies (Sharp Tools) and from used production punches and dies (Worn Tools). The radial clearance was 0.1 mm. A rust preventative oil was applied to the steels during the punching; a lubricant oil was applied during hole expansion. The poor edge condition after punching was caused by tool wear and possible micro-chipping. The clearance was hardly affected, but the steels suffered cold work which dramatically affected their hole expansion results.

The conclusions from this study were: 1) When exposing a DP steel to edge deformation, make sure the best quality edge condition is utilized and the burr, if possible, should be facing downward, and 2) Use hard wear-resistant tooling, preferably coated PM grades, for punching. Additional information on tool materials is available in Section 3.C.2 – Tool Materials and Die Wear.

One solution for improved sheared edge stretchability is homogeneous microstructure, so steel suppliers have customized product offerings like complex phase steel, where extensive grain refinement (reducing the size of the ferrite and martensite grains) is achieved. Consequently, the size of the initial damage resulting from shearing is reduced, raising the critical stress for crack propagation to higher levels and reducing the likelihood for crack propagation. Additionally, reducing the difference in hardness between the soft ferrite phase and the hard martensite phase improves the hole expansion ratio. Changes in chemistry, hot rolling conditions and intercritical annealing temperatures are some of the methods used to achieve this. Such metallurgical trends can include a single phase of bainite or multiple phases including bainite and removal of large particles of martensite. This trend is shown in Figure 3.B-17.

Figure 3.B-18 shows SEM images of a regular DP780 grade and a modified DP780 grade designed to improve the hole expansion ratio for greater resistance to local formability failures such as edge fracture and shear fracture. Note that the modified DP grade has more homogeneous distribution of martensite with smaller ferrite grains.

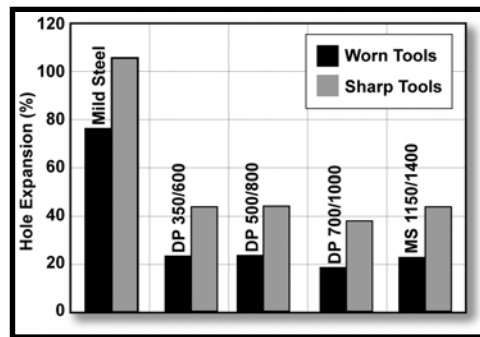


Figure 3.B-16: Impact of production tooling condition on hole expansion performance. (tests conducted w 50 mm diameter conical punch).^{C-1}

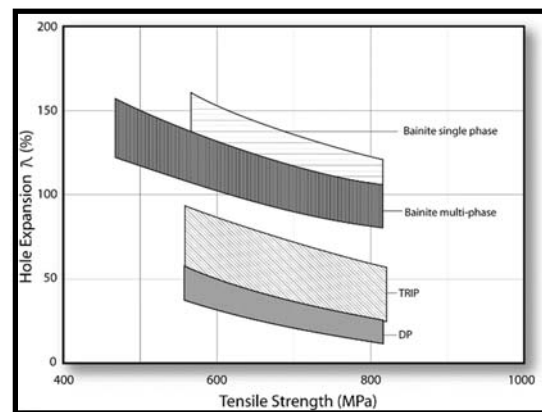


Figure 3.B-17: Improvements in hole expansion by modification of microstructure.^{N-1}

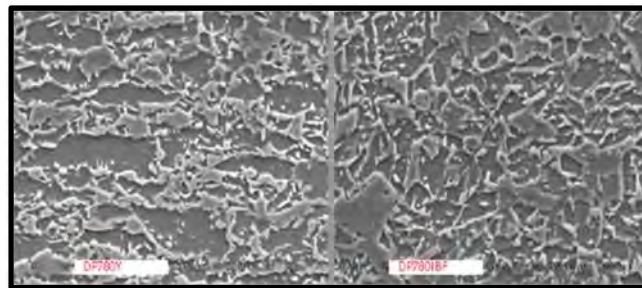


Figure 3.B-18: SEM images of the microstructure of a regular DP780 (left) and a DP780 grade modified (right) to improve the hole expansion ratio to improve local formability performance.^{M-5}

Again, note that the differences in microstructure that enhance local formability characteristics can also be detrimental to global formability characteristics and vice versa. Figure 3.B-19 shows a system developed to classify and rate the formability of Advanced High-Strength Steels. Formability classification is based upon the local/global strain ratio, while the formability rating is based upon the overall formability index. These parameters are defined below.

The ratio between true fracture strain (*TFS*) and true uniform strain (ϵ_u) is useful in understanding relative intrinsic formability characteristics; this graph refers to the ratio as fracture resistance. Materials with higher *TFS* values are naturally expected to perform better under localized formability conditions, including flanging, edge stretching and tight-radius bending. Materials with higher uniform strain values (*i.e.* higher terminal *n* values) are better suited for stretch forming and are able to distribute strain more uniformly, conditions suitable for global formability requirements.^{H-4}

Figure 3.B.20 shows the general comparison between total elongation and the hole expansion ratio for conventional HSLA and various AHSS “designer steels” targeting specific formability concerns.

HET studies have also shown that edge fracture on multiphase AHSS is sensitive to rolling direction as well. When testing a sample, the edge fractures will typically occur first at the hole edge along the rolling direction. Tests consistently confirm that performance is worse in the transverse direction. Figure 3.B-21 shows a photo of an actual part in production where the edge fractures are following the rolling direction. With this being the case, when designing and developing the part and die process, locating stretch flanges perpendicular to the rolling direction when possible will increase resistance to edge fracture. If this cannot be done, identifying locations where scallops/notches can be inserted in the stretch flange without negatively impacting the part structure, fit or die processing should be investigated.

During early die development and die try-out, it’s important to both select the correct grade of AHSS for and process the trial blank with the rolling direction aligned with production intent. Prototype blanks are regularly cut by laser, EDM, water jet or even by hand when the final blank size hasn’t been established

AHSS 980 Grades: TFS vs. True Uniform Strain

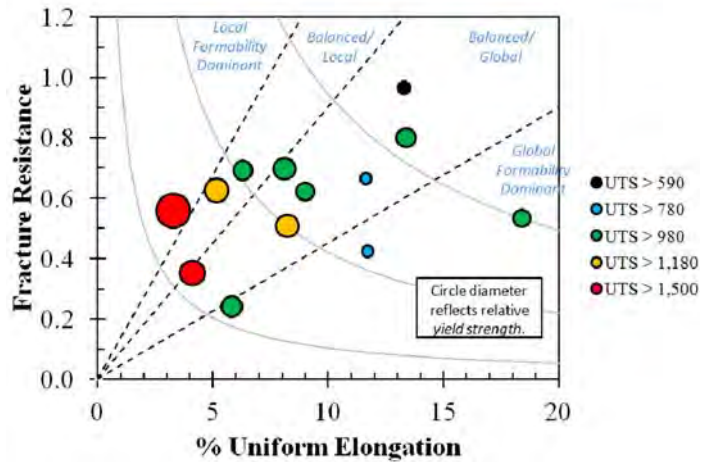


Figure 3.B-19: Chart showing the relationship between tensile elongation and fracture resistance as they relate to global and local formability of AHSS.^{H-4}

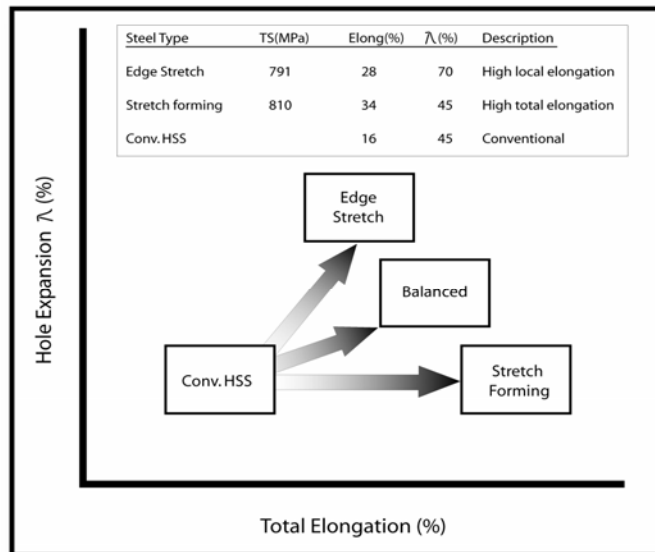


Figure 3.B-20: Schematic showing AHSS tailored for high total elongation or high local elongation as defined by the HET.^{T-1}

yet and a blank die has yet to be constructed. Using the incorrect rolling direction during try-out can create misleading conclusions about process robustness.

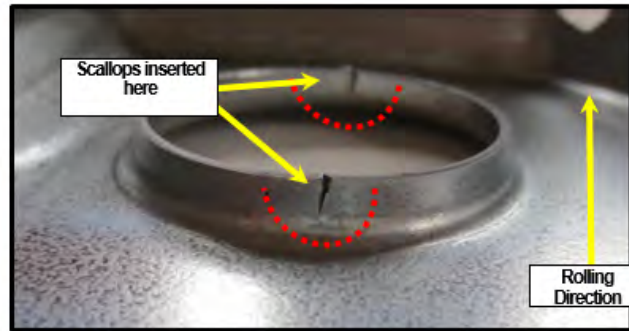


Figure 3.B-21: Actual part where the edge fractures are following the rolling direction. In this case, as the flange wasn't needed around the entire perimeter of the hole, scallops were inserted in the locations of the fractures.^{M-7}

Previous sections compared HET results for punched versus machined holes, and sharp versus worn tools and the results confirm that steel conversion process variables are of great significance and need to be better understood to optimize the overall process.

The HET has been used by many researchers to change punch materials, clearances and shear angles to more clearly define optimal conditions to maximize HET results and the associated local formability performance (λ). Changes to some of these process variables can have a significant effect on the performance of AHSS in the HET. Historically, for conventional steels, a clearance of 10% of metal thickness on punches and trim steels has been used as a rule of thumb and flat punches are used in many instances, due in part to ease of sharpening. Trim steels for long shear blades might have a 2-3° angle on them to minimize peak tonnages and target 10% of metal thickness as a standard clearance.

The same clearance rules of thumb hold true for slitting knives on slitting lines when dealing with conventional steels. The HET studies, however, show that these historical rules of thumb do not apply for AHSS with a multiphase microstructure. Optimum clearances for multiphase AHSS appear to be 13-15% of metal thickness, and a punch bevelled up to 6 degrees seems to generate the highest HER, depending on metal thickness. This is true for punched holes as is used in the HET, but the HET has some limitations in terms of what it can simulate. Laser EDM and water jet cut edges have essentially no clearance or bevel, and side trimmed edges are straight. Trying to achieve a 6° shear angle on a long shear blade or slitting knives is impractical as well.

Two-Dimensional (2-D) Edge Tension Test

Additional tests have been developed to further investigate process parameters and more clearly understand and optimize non-steel related variables. One of the tests, used to evaluate edge stretchability is a two-dimensional (2-D) edge tension test. There are multiple versions of this type of test, but they all are based on the same concept.

The 2-D edge tension test is similar to a standard tensile test in that a steel specimen is pulled under tension until failure. Unlike a standard tensile test where both sides of the tensile specimen are milled into a “dog bone”, the 2D tension test only mills one edge of the sample whereas the other edge is cut under a predetermined set of conditions. This could involve laser cutting, EDM, water jet cutting, milling, slitting or mechanical cutting at various trim clearances, shear angles, rake angles or with different die materials. Alternative AHSS grades can also obviously be compared. The output data is typically measured as total elongation and comparisons can be made with different process parameters using the same material to better define optimum process parameters. Figure 3.B-22 shows a 2D edge tension test sample with a milled edge on one side and an as-trimmed edge on the other side where edge fracture will typically initiate.

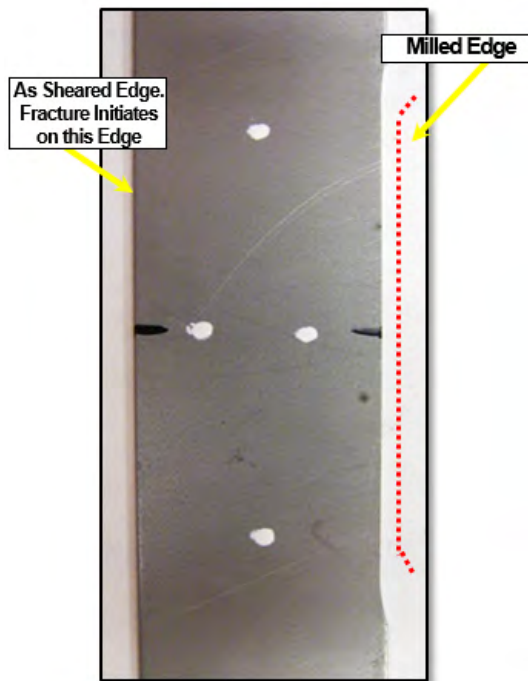


Figure 3.B-22: 2D edge tension test specimen sometimes referred to as a “half dog bone” as only one side is milled.

One study used the 2D tension test to evaluate:

- the rolling direction and how it impacts failure on multiphase AHSS such as DP and TRIP, and
- how shear angles on mechanical trim conditions can impact total elongation.

The material was DP600 and used 5 different shear trim angles tested in both the longitudinal and transverse direction relative to the rolling direction of the coil. Figure 3.B-23 shows the results of this study, which confirms that the longitudinal (rolling direction) always outperforms the transverse (coil width), and the shear angle and clearance of the shearing process also contributed to differences in total elongation. Another study investigated 5 different shear angles and also compared milling, laser cutting, and water jet cutting processes.

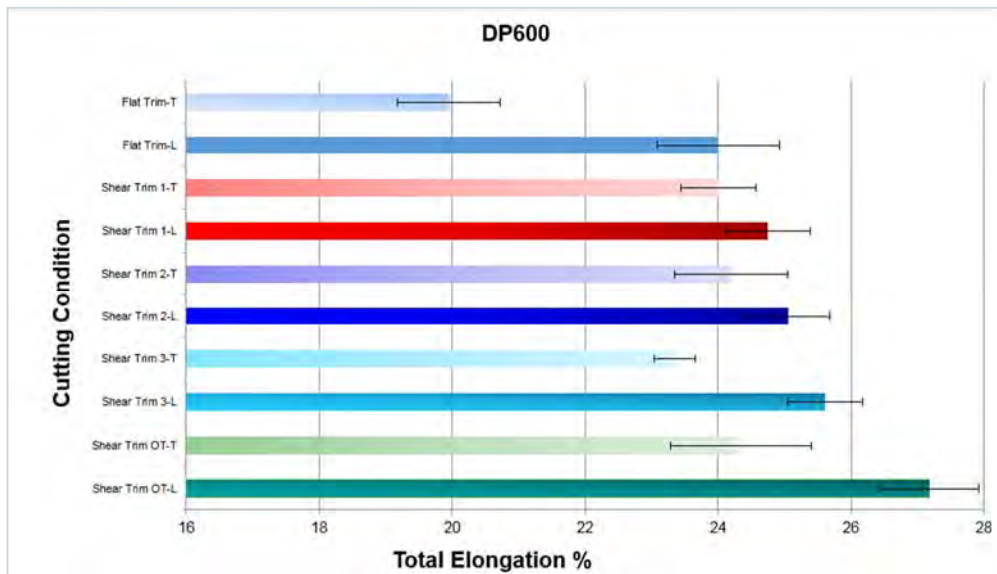


Figure 3.B-23: Chart shows: 1) longitudinal direction always has a greater total elongation than the transverse direction; 2) cutting condition significantly impacts total elongation.^{S-10}

This study was conducted on DP600 and DP980 grades. Figures 3.B-24A and 3.B-24B show results, which correlate with HET studies on the same subjects. As shown in the charts, non-cold worked edges (laser cut, water jet cut and milled) always outperformed mechanically sheared edges.^{S-10}

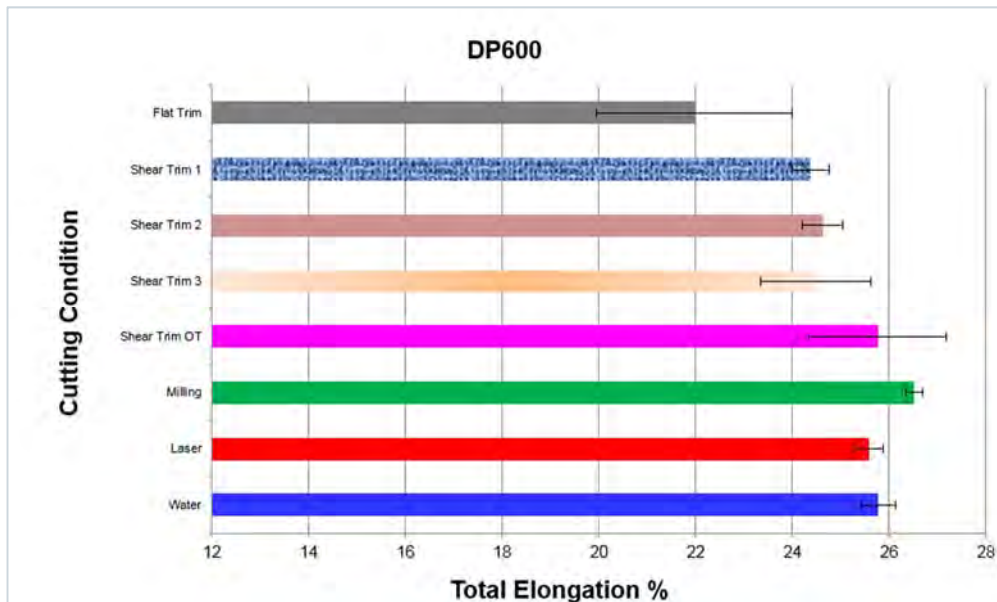


Figure 3.B-24A: Edge stretchability for DP600 based on various trim conditions.^{S-10}

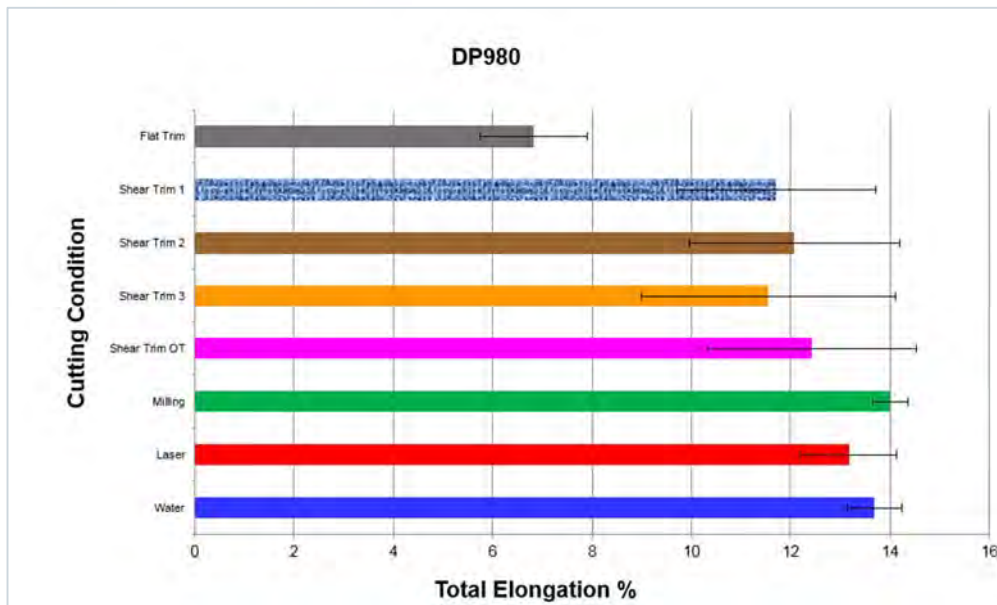


Figure 3.B-24B: Edge stretchability for DP980 based on various trim conditions ^{S-10}

As discussed earlier, mechanically shearing the edge cold works the steel and reduces the work hardening exponent (n -value), leading to less edge stretchability. These studies, however, show that shearing parameters such as clearance, shear angle and rake angle also play a large part in improving edge stretch. Since local formability failures are not preceded by significant thinning and necking of the steel, and won't be predicted by forming simulations using the forming limit curve for failure criteria;

Edge condition was also examined in detail. Please refer to Section 3.C.7 – Straightening and Precision Levelling AHSS for sheared/trimmed edge conditions.

3.B.3.c. Stretch Bend Limits – Local Formability

Automotive product designers utilize small radii for springback control, sectional stiffness, packaging constraints, and design features. Increased sensitivity to crack formation is observed for AHSS at small die radius to material thickness (R/t) ratios. Traditional forming limit curves or other press shop criteria do not predict these fractures. Likewise, usual forming simulations, such as computerized forming-process development, also do not flag these fractures. However, these shear fractures have occurred in die tryout. These shear fractures are the other main form of local formability failure associated with multiphase AHSS such as DP and TRIP.

Substantial research is underway to develop one or more tests that will predict the onset of these shear failures. Reference W-3 presents angular stretch-bend test results. Reference W-4 details pulling metal strips over radii with back tension. Most of the research results show significant reduction in available deformation for different grades of DP and TRIP steels. All the research focuses on finding a procedure that will predetermine at what level of strain specific steels will fail. This data is then used in Computerized Forming-Process Development analyses to determine feasibility of any given part design.

As shear fracture is another failure mechanism affected by local formability, AHSS users need improved understanding. Shear fractures on AHSS may exhibit similarities to edge fracture: of the absence of necking prior to failure (as is observed with global formability failures). Figure 3.B-25 shows a photo of a typical shear fracture on a DP780 part. Figure 3.B-26 shows the same part from a different angle where the actual radius at the punch opening can be seen. The shear fracture occurred on the sharp radius on the left whereas the larger radius on the right experienced no failure. Depth of draw and draw bead configuration were the same on both sides of the draw panel. Restraining force was also similar on both sides of the blankholder. The significant variable was the die radius.

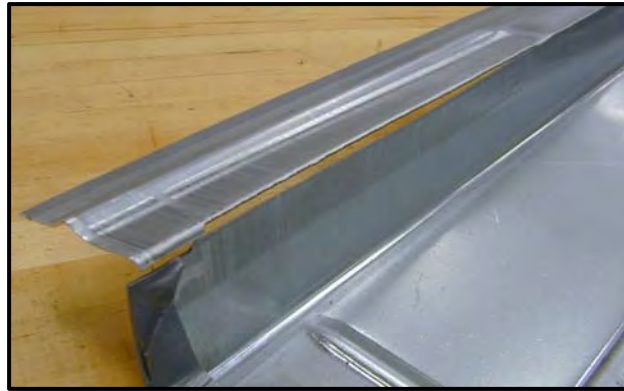


Figure 3.B-25: Typical shear fracture on a DP780 part. ^{M-7}

It is well understood that smaller die radii can lead to formability failures. When the ratio of a die radius over sheet thickness is large enough beyond the shear fracture limit, the failure occurs outside the radius. In this case, the conventional forming limit curve can be used to assess part robustness and predict failure. When the ratio of a die radius over sheet thickness is within the shear fracture limit but above the simple bending limit (no stretching imposed to bending), the failure may occur in the radius or outside the radius, depending upon the tension level applied during forming. If the failure occurs inside the radius, the failure limit derived from the shear fracture tests should be used as the criterion to predict failure. Finally, when the ratio of a die radius over sheet thickness is smaller than the limit from the simple bending test, the failure occurs in the radius.

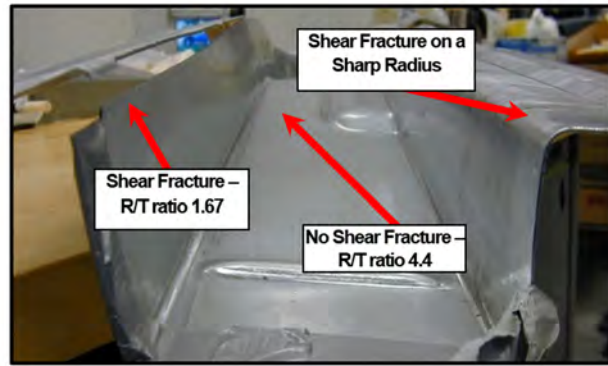


Figure 3.B-26: Side view of the same part showing shear fracture on the left side of the part where the R/T ratio was 1.67. The right side of the same part with the same depth of draw, draw bead configuration, and restraining force had no shear fracture and had an R/T ratio of 4.4. ^{M-7}

Therefore, it is important for the part designer to design an appropriate die radius for a given AHSS product and forming conditions / processes used to manufacture the part. The computer simulation is an excellent tool to derive an appropriate die radius for the specified part and forming process, recognizing that the failure limit from the shear fracture test should be used as the failure criterion in the simulation.

The schematic in Figure 3.B-27 shows the typical global formability failure occurring at the radius tangent on the part sidewall. With shear fractures, the failures occur on the radius opposed to the tangent to the radius (Note Figure 3.B-28). No thinning or localized necking is observed at the fracture site.

Numerous studies have shown that radius to thickness ratios (R/T) are significant indicators of performance with respect to shear fracture on AHSS, and thus R/T ratio guidelines have been established. One test utilized to better characterize various steel grades and their resistance to shear fracture is called the bend test. The results of the bend test are typically reported as a ratio of thickness to radius ($R/T = 1T, 2T, 3T, \text{etc.}$). Samples are bent at various radii until shear fracture is observed. The test results are then used to categorize a product's ability to resist shear fracture. Many steel companies report minimum bend test limits for various grades and certain automakers include minimum bend test requirements in their specifications as well. Different steel companies and automakers may have different bend test methods and/or requirements, so it is important to understand those requirements and procedures to better match the material characteristics with the customer's design and process expectations. The test methods could involve a bend of $60^\circ, 90^\circ, 180^\circ$ as well as various radii, die materials, speeds, etc.

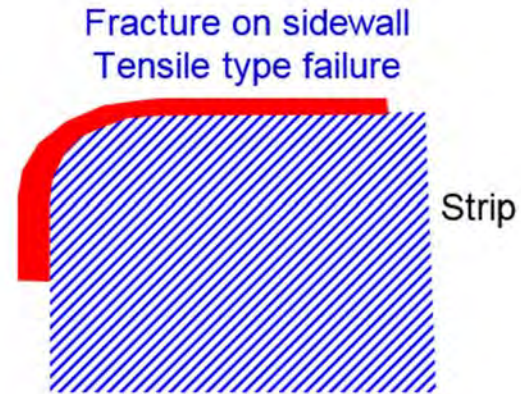


Figure 3.B-27: Schematic showing the location of a typical global formability failure located at the tangent to the radius. ^{M-7}

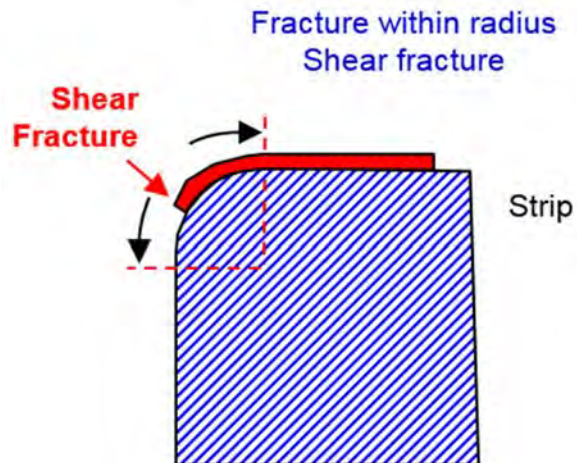


Figure 3.B-28: Schematic showing the location of a typical local formability shear fracture located on the actual die radius. ^{M-7}

Figure 3.B-29 shows etched cross sections of bend test samples at 180° with two different radii for reference purposes.

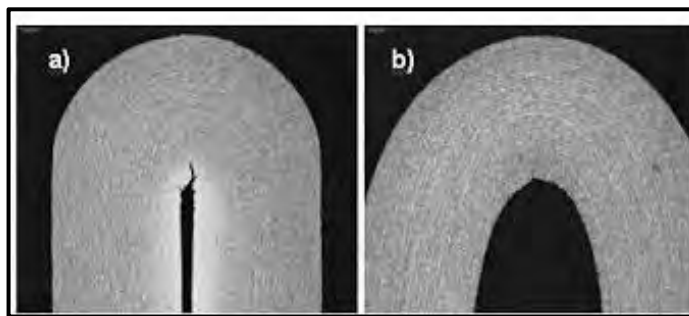


Figure 3.B-29: Cross sections of two samples after undergoing a 180° bend test with a different radius on the bend test die. ^{M-7}

As strength levels increase, R/T ratios need to be increased to avoid shear fractures. As with edge fracture, “designer grades” of AHSS can also be tailored to change the R/T ratio before fracture as well. Guidelines have been established for minimum R/T ratios based on bend test results as well as real world case studies. For DP600 and above, the R/T ratio should be at least 3T for product features such as embossments. On DP600 and above, die radii that are pulled over a punch radius or through a draw bead under tension, the R/T ratio should be at least 5T. Auto-Steel Partnership Case Study #7 has a specific example of shear fracture where the radius on a DP980 center pillar outer upper reinforcement was 1T instead of 3T, resulting in shear fracture on the radius.

As with edge fracture, shear fracture is also sensitive to rolling direction. If the radius is running in the rolling direction, the bend will be transverse to the rolling direction which is the worst-case scenario when trying to avoid shear fracture. Unfortunately, many DP and TRIP parts are very long rails, rockers, sills, cross members, etc., where a wide master coil is produced, then slit into multiple narrower coils (mults) for further processing. In many instances, the part is too long in one direction to take advantage of the fact that these AHSS grades are rolling direction sensitive and the optimum rolling direction cannot be utilized. As a result, it’s especially critical to understand minimum R/T ratios when designing the part to avoid shear fractures. Figures 3.B-30 shows a shear fracture on a DP60 rocker where the bend radius is in the non-optimum rolling direction.



Figure 3.B-30: Shear fracture running in the rolling direction (left). Close-up of the same shear fracture (right) where the fracture is on the radius, not on the tangent to the radius. Note also there is no sign of thinning or necking at the fracture. ^{M-5}

3.B.3.d. Key Points

Forming Limit Curves

- Differences in determination and interpretation of FLCs exist in different regions of the world. These Application Guidelines utilize one current system of commonly used Forming Limit Curves (FLCs) positioned with FLC_0 determined by terminal n-value and thickness.
- This system of FLCs commonly used for low strength and conventional HSLA is generally applicable to experimental FLCs obtained for DP steels for global formability.
- The left side of the FLC (negative minor strains) is in good agreement with experimental data for DP and TRIP steels. The left side depicts a constant thinning strain as a forming limit.
- Determination of FLCs for TRIP, MS, TWIP, and other special steels present measurement and interpretation problems and need further development.

Sheared Edge Stretching Limits

- Sheared edge stretching limits are important for hole expansion and stretch flanging. All steels have reduced hole expansion limits caused by the cold work and reduced n-value of the metal adjacent to the cut edge.
- The hole expansion limits for sheared edges of DP and TRIP steels suffer additional reduction because of edge fracture associated with the interfaces between the ductile ferrite and the hard martensite phase in the microstructure. This reduction becomes more severe as the volume of martensite increases for increased strength.
- 2D tension tests have been developed by many research centers to investigate alternative sheared edge conditions under various process parameters. It has been shown that edge condition is a significant variable independent of burr height alone.
- The microstructure of AHSS can be modified to enhance either total elongation for general stretch forming or local elongation for sheared edge stretching limits. The same microstructure generally does not provide high values for both total and local elongation-values. However, some increases in both can be created to provide a balance of total and local elongation.

Stretch Bend Limits

- Early shear type fractures have been encountered without a sheared edge when a small tool radius to sheet thickness (r/t ratio) is encountered within a stamping. It is therefore important to use guidelines developed over the years as a baseline when determining R/T ratios.
- Shear fractures are not predicted by the forming limit curve or computerized forming-process development.
- Several research programs are attempting to develop a new bending test that will quantify when these failures will occur in any specific sheet metal.
- As with edge fractures, shear fractures are also sensitive to rolling direction. When designing parts, and conducting die try-outs with prototype steel, this variable must be taken into account.

3.B.4. Cold Forming Modes

Stamping and die designers are interested in the forming capabilities of the steels they specify. This is true of conventional HSLA and even more so for AHSS. Unfortunately, complex stampings are composed of several different basic forming modes, which react to a different set of mechanical properties. Likewise, formability of steel, and especially AHSS, cannot be characterized by a single number. Therefore, formability comparisons of AHSS to conventional HSLA must be done for each basic forming mode. In this section, four general groups (stretching, bending, cup drawing, roll forming) are reviewed.

3.B.4.a. Stretching

Sheet metal stretching, especially the biaxial tension mode, is a critical form of deformation. The biaxial increase in surface area rapidly reduces the metal thickness as shown by the constancy of volume equation. The thinning soon reaches the onset of the local neck and failure as defined by the various forming limit diagrams. This mode of failure is global formability related. The *n*-value plays an important role in the amount of allowable deformation at failure. The conventional mild steels and the higher strength steels, such as HSLA, have an *n*-value that is approximately constant with deformation. More important, the *n*-value is strongly related to the yield strength of the conventional steels (Fig. 3.B-31).

Two specific modes of stretch forming are controlled by the *n*-value:

1) The *n*-value suppresses the highly localized deformation found in strain gradients (Figure 3.B-32).

A stress concentration created by character lines, small features, embossments, etc. can trigger a strain gradient. Usually formed in the plane strain mode, the major (peak) strain can climb rapidly as the thickness of the steel within the gradient becomes thinner. This peak strain can increase more rapidly than the general deformation in the stamping, causing failure early in the press stroke. Until failure is reached, the gradient has increased sensitivity to variations in process inputs. The change in peak strains causes variations in elastic stresses, which can cause dimensional variations in the stamping. The corresponding thinning at the gradient site can reduce corrosion life, fatigue life, crash management and stiffness.

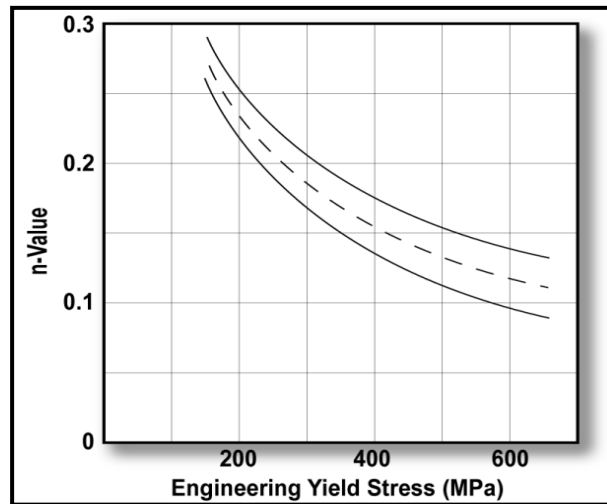


Figure 3.B-31: Experimental relationship between *n*-value and engineering yield stress for a wide range of mild and conventional HSS types and grades.^{K-2}

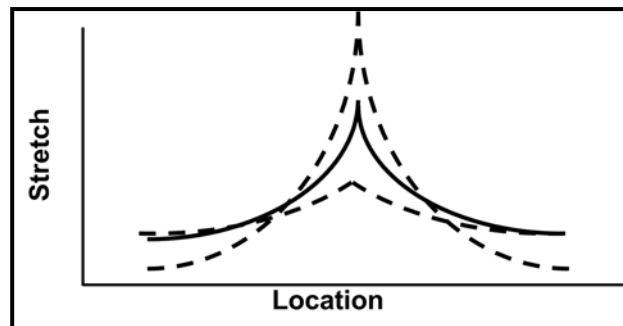


Figure 3.B-32: Strain gradients can be unstable causing different peak values.^{S-12}

As the gradient begins to form, low n-value metal within the gradient undergoes less work hardening and lower stresses can continue major peak deformation. In contrast, higher n-values create greater work hardening, thereby keeping the peak strain low and well below the forming limits. This allows the stamping to reach completion.

Unfortunately, comparison of n-value for DP steel to HSLA steel requires more than a simple comparison of their reported n-values for a given yield strength.

The instantaneous n-value curves for the DP 350/600 and HSLA 350/450 shown in Figure 3.B-33 clearly indicate the significantly higher peak n-value (0.20) for DP steel versus (0.13) for HSLA steel at 4% strain. The higher initial n-value tends to restrict the onset of strain localization and growth of sharp strain gradients. Minimization of sharp gradients in the length of line also reduces the amount of localized sheet metal thinning.

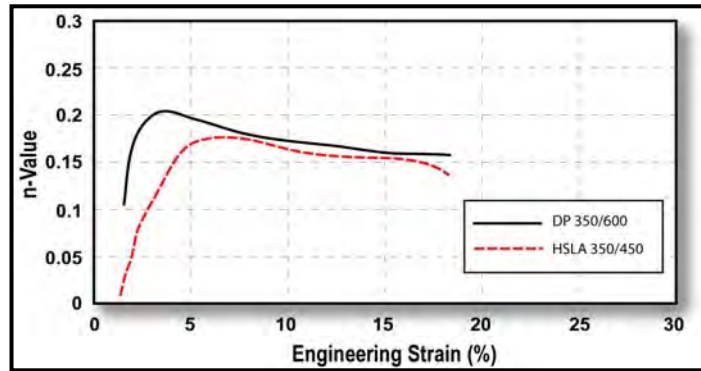


Figure 3.B-33: Instantaneous n-values versus strain for DP 350/600 and HSLA 350/450 steels.^{K-1}

2) The n-value determines the allowable biaxial stretch within the stamping as defined by the forming limit curve (FLC).

The traditional n-value measurements over the strain range of 10% - 20% would show no difference between the two steels. The approximately constant n-value plateau extending beyond the 10% strain range provides the terminal or high strain n-value. This terminal n-value is a major input in determining the maximum allowable strain in stretching as defined by the forming limit curve. Experimental FLC curves (Figure 3.B-34) for the two steels show this overlap.

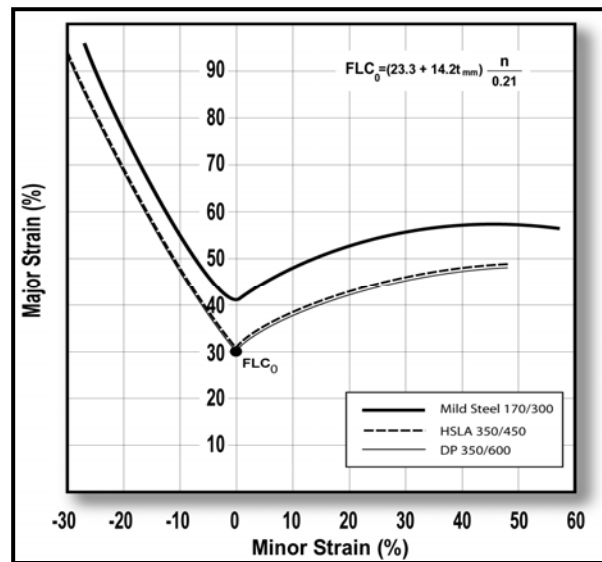


Figure 3.B-34: Experimental FLCs for one sample each of Mild, HSLA, and DP steels with thicknesses equal to 1.2 mm.^{K-1}

Both HSLA 350/450 and DP 350/600 steels have terminal n-values (measured at high values of strain) equal to 0.17. These two steels have approximately the same YS and total elongations but the UTS values are very different. More interesting are the Mild 170/300 and TRIP 400/600 steels because both have terminal n-values of 0.23. However, this FLC₀ equation based on n-value currently cannot be applied to TRIP steels and must be further researched. The modified microstructures of the AHSS allow different property relationships to tailor each steel type and grade to specific application needs. Even more important is the requirement to obtain property data from the steel supplier for the types and grades being considered for specific applications.

Unlike the DP steels where the increase in n-value is restricted to the low strain-values, the TRIP steels constantly create new islands of martensite that maintain the high n- values over large ranges of strain (Figure 3.B-35). An n-value of 0.25 can be found in VD-IF (vacuum-degassed interstitial-free) steels.

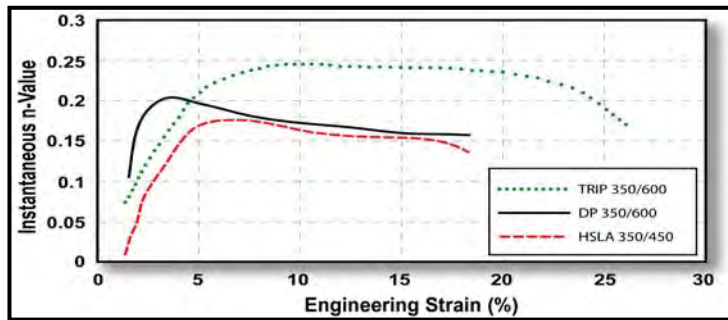


Figure 3.B-35: Instantaneous n-values versus strain for TRIP, DP, and HSLA steels.^{K-1}

The continued high n-value of the TRIP steel relative to the HSLA steel contributes to the increase in total elongation observed in Table 3.B-1. The increased n-value at higher strain levels further restricts strain localization and increases the height of the FLC (Figure 3.B-36). This diagram shows that the height of the TRIP FLC is equivalent to the height of the FLC for mild steel.

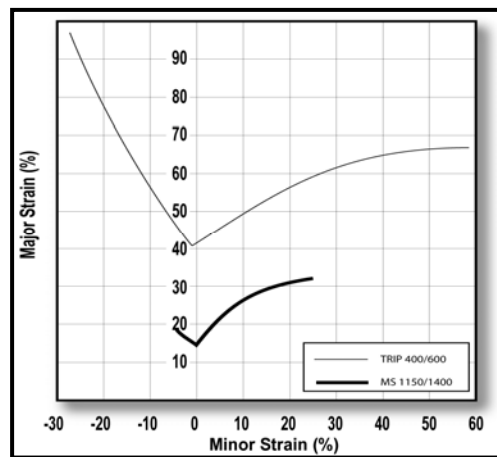


Figure 3.B-36: Preliminary experimental FLCs for t=1.2 mm TRIP steel and t=1.5 mm MS steel.^{K-1, C-1}

Table 3.B-1 - Properties of steels used in Figures 3.B-39 and 3.B-41.^{K-1, C-1}

Type & Grade	UTS (MPa)	Tot. El (%)	YPE (%)	Terminal n
Mild Steel 170/300	314	42.9	0	0.23
HSLA 350/450	443	28.4	2.8	0.17
DP 350/600	602	29.0	0	0.17
TRIP 400/600	631	34.0	0	0.23
MS 1150/1400	1546	5.0	0	N.A.

Terminal n-values (except MS steel) are the average n-value measured between strain levels of 10% and uniform elongation.

The set of general schematics in Figure 3.B.37 illustrates the difference among HSLA, DP, and TRIP steels in terms of gradients and height of FLCs.

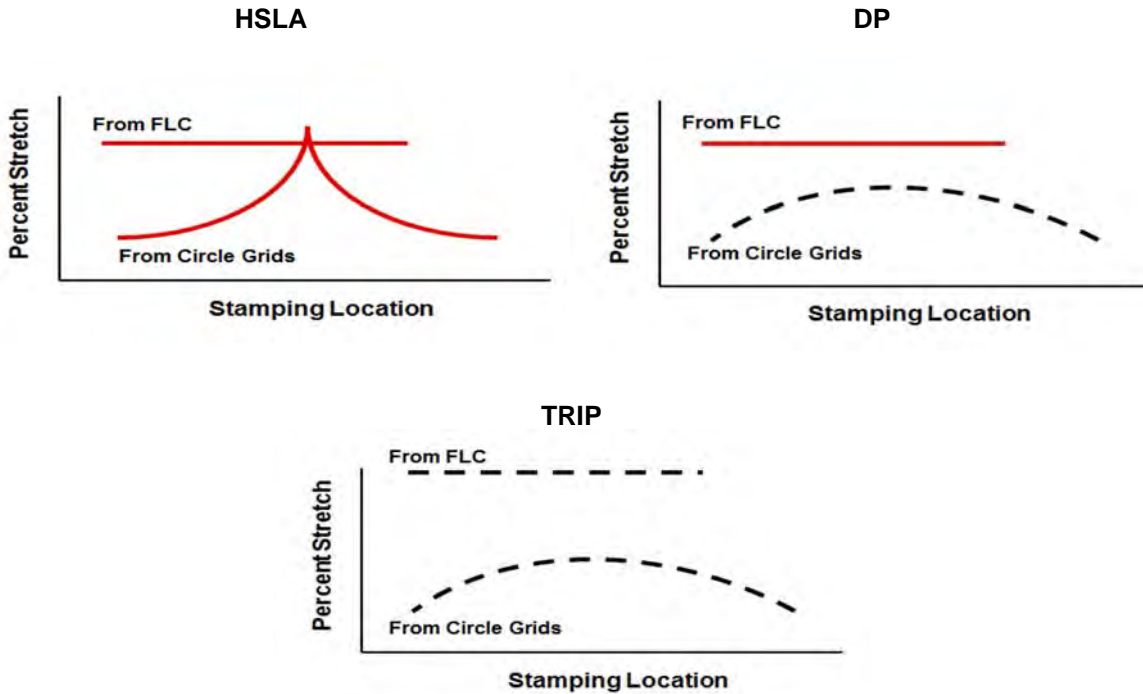


Figure 3.B.-37: Schematics showing the improvements of DP and TRIP over HSLA (not to scale).

The hemispherical dome test often is used to determine the relative stretchability of different metals and lubricants (Figure 3.B-38). Usually a 100mm diameter hemispherical punch is driven into a completely clamped blank. This ensures pure biaxial stretch without metal flowing from the blank into the deformation zone.

Figure 3.B-39 illustrates a typical test output. Note the maximum dome height (H/d) at failure decreased as the yield strength increased and the n-value decreased.

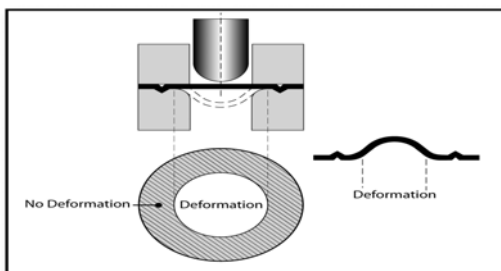


Figure 3.B.-38: Stretch forming generated by a hemispherical punch stretching a locked circular blank.

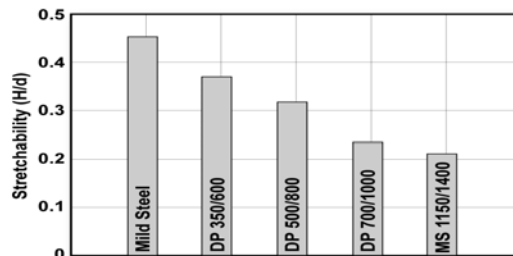


Figure 3.B.-39: Dome stretch tests using a 100 mm hemispherical punch and a clamped blank. Sheet thickness is 1.2 mm except for the MS thickness of 1.5 mm.^{C-1}

Advanced High-Strength Steels Application Guidelines

Additional stretch tests can be performed with the hemispherical dome tester other than the dome height at failure shown above. The limiting dome height (LDH) test stretches rectangular strips of metal that are locked in the longitudinal direction (Figure 3.B-40). Blanks are coated with conventional anti-rust oil and held with a circular lock bead of 165 mm diameter. Strips of different width are tested and their maximum dome height at failure is recorded. Figure 3.B-40 shows the minimum hemispherical dome height is substantially higher for the TRIP steel compared to the equivalent HSLA steel.

The Limiting Dome Height test results for EDDQ (vacuum-degassed Interstitial-free) steel and three AHSS are in Figure 3.B-41. Instead of plotting the various dome heights (as in Figure 3.B-40) to find the minimum value, Figure 3.B-41 simply shows the minimum value for each steel.

The same tooling, steels, and lubricant from Figure 3.B-40 generated the thinning strains in Figure 3.B-42. Instead of forming to failure, the 50 mm radius hemispherical punch stretched the dome height to only 25 mm for both steels. The increased capability of the TRIP steel to minimize localized thinning is observed.

TWIP (Twinning Induced Plasticity) steel has unique properties for stretchability and total elongation. The Steel Strength Ductility Diagram (Figure 2.A-1) shows TWIP steel positioned with the austenitic (Series 300) stainless steels. TWIP steels have n-values in the 0.4 range. Stretchability exceeds even that of EDDQ IF steel (Figure 3.B-41).

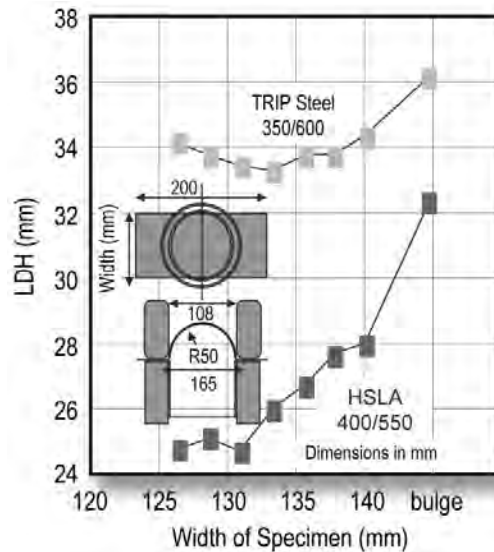


Figure 3.B-40: Limiting Dome Height is greater for TRIP than HSLA for the two steel grades tested.^{T-2}

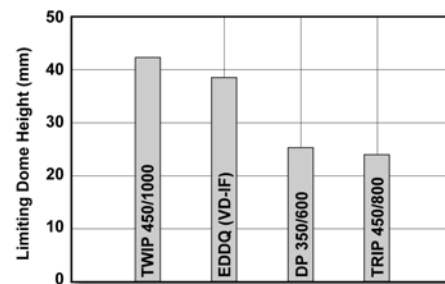


Figure 3.B-41: Limiting Dome Height values reflect relative stretchability of three AHSS compared to a low strength IF steel.^{P-2}

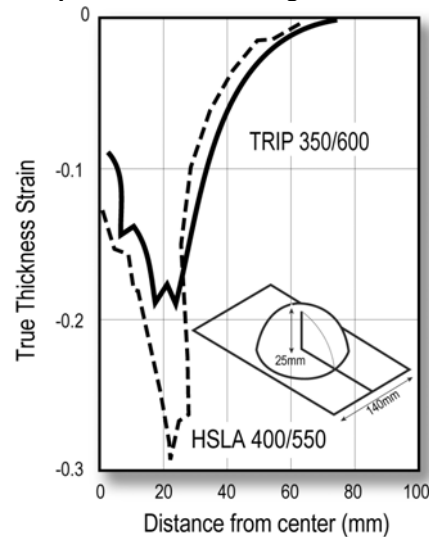


Figure 3.B-42: Local thinning is smaller for TRIP than HSLA at a constant dome height.^{T-2}

3.B.4.b. Bending

The usual mode of bending is curvature around a straight-line radius (Figure 3.B-43). Across the radius is a gradient of strains from maximum outer fibre tension through a neutral axis to inner fibre compression. No strain (plane strain) occurs along the bend axis. For this discussion, any edge effects are excluded and only bulk deformation is considered.

Deformation at the outer surface during three-point bending depends on the stretchability capacity of the metal. The failure strain in the bend is related to the total elongation of conventional steel, but as discussed in Section 3.B.3.c. – Stretch Bend Limits, AHSS with multiphase microstructures such as DP and TRIP experience shear fracture that severely reduces the bendability before failure occurs. A higher total elongation helps sustain a larger outer fibre stretch of the bend before surface fracture, thereby permitting a smaller bend radius. Since total elongation decreases with increasing strength for a given sheet thickness, the achievable minimum design bend radius must be increased (Figure 3.B-44).

For equal strengths, most AHSS have greater total elongations than conventional HSLA (Figures 2.A-1). As discussed in Section 3.B.3.b – Edge Stretching Limits, the multiphase microstructures of DP and TRIP steels cause low local formability as measured by the HET and 2D tension test.

Several cases of early radii cracking of production bending DP and TRIP steels have been attributed to these local formability failures (See Section 3.B.4. – Cold Forming Modes). As an illustration, bend tests were performed and compared to virtual forming simulations for both HSLA and DP780 steels. The HSLA global formability failure aligned with simulation predictions, and was accompanied by a visible neck (see Figures 3.B-45A-B). In contrast, the DP780 showed no visible neck at the failure site and no correlation between the simulation and actual test results (see Figures 3.B-46A-B).

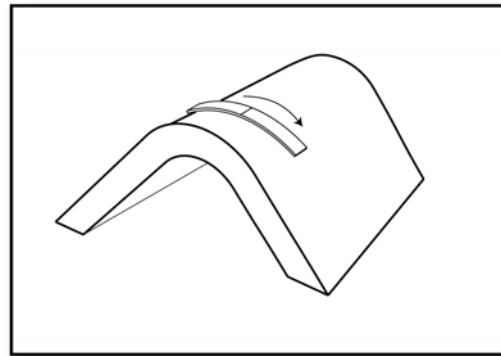


Figure 3.B-43: Typical three-point bend has outer fibre tension and inner fibre compression with a neutral axis in the centre.

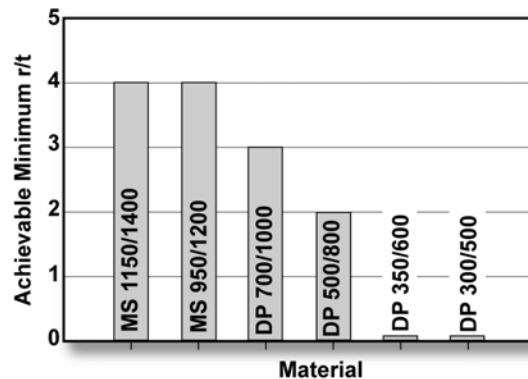


Figure 3.B-44: Achievable minimum bend radius (r/t) in a three-point bend test increases as the total elongation of the steel decreases.^{S-5}

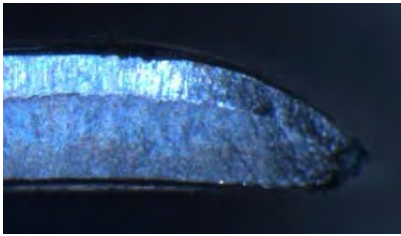


Figure 3.B-45A: Close-up of visible necking before tensile failure of a conventional HSLA. ^{S-11}

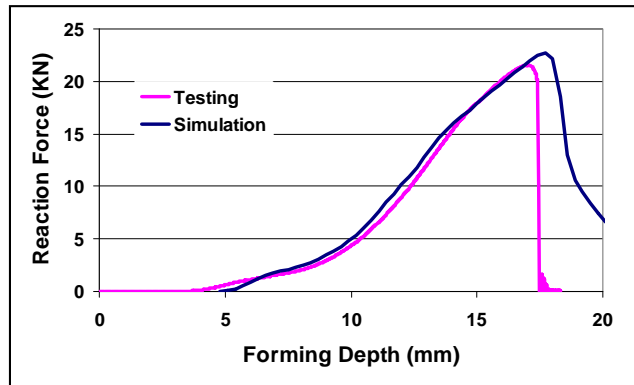


Figure 3.B-45B: Virtual forming simulation of the conventional HSLA with strong correlation to actual testing. ^{S-11}

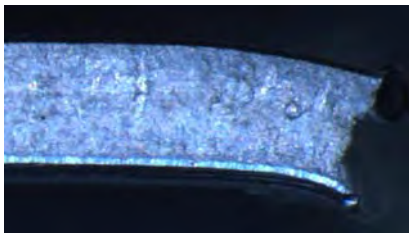


Figure 3.B-46A: Close-up of local formability failure on DP780 with no visible necking before failure. ^{S-11}

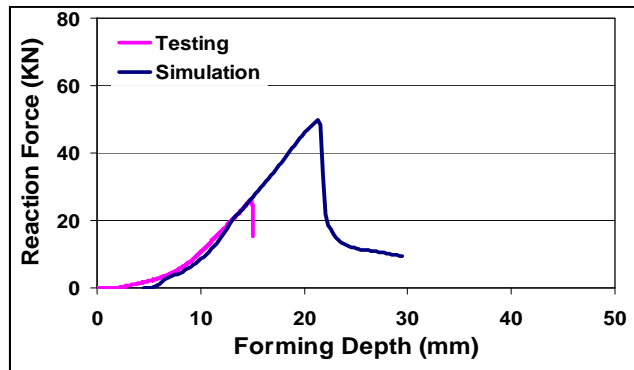


Figure 3.B-46B: Comparison of a virtual forming simulation with actual testing of the DP780 showing no correlation between the two. ^{S-11}

3.B.4.c. Deep Drawing - Cup Drawing

Deep drawing is defined as radial drawing or cup drawing (Figure 3.B-47). The flange of a circular blank is subjected to a radial tension and a circumferential compression as the flange moves in a radial direction towards the circular die radius in response to a pull generated by a flat bottom punch. In addition to forming cylindrical cups, segments of a deep drawn cup are found in corners of box-shaped stampings and at the ends of closed channels.

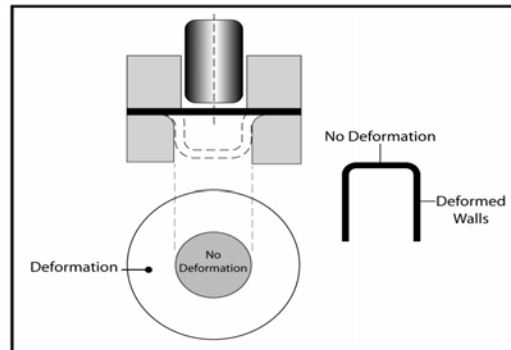


Figure 3.B-47: A circular blank is formed into a cylindrical cup by the deep drawing, radial drawing, or cup drawing method of deformation.

Advanced High-Strength Steels Application Guidelines

The steel property that improves cup drawing or radial drawing is the normal anisotropy or r_m value. Values greater than one allow an increase in the limiting draw ratio (LDR), which is the maximum ratio of blank diameter to punch diameter allowed in the first draw. In contrast, the LDR is insensitive to the strength of the steel and the n -value. High-strength steels with UTS greater than 450 MPa and hot-rolled steels have r_m values approximating one and LDR values between 2.0 – 2.2. Therefore, DP and HSLA steels have a very similar LDR. However, the TRIP steels have a slightly improved LDR deep drawability.^{T-2} Since the transformation of retained austenite to martensite is influenced by the deformation mode (Figure 3.B-48), the amount of transformed austenite to martensite generated by shrink flanging in the flange area is less than the plane strain deformation in the cup wall. This difference in transformation from retained austenite to martensite makes the wall area stronger than the flange area, thereby increasing the LDR.

Laboratory cup drawing experiments show an approximate LDR of 2.0 – 2.2 for the DP steels tested (Figure 3.B-49). Note that a doubling of the yield strength has no effect on the LDR. An increased r_m value of mild steel created a small increase in LDR over DP steel.

The MS (martensitic) steel has reduced bendability going over the die radius.

Photos of the cups formed for Figure 3.B-48 are shown in Figure 3.B-50.

The absolute value of the LDR, however, also depends on the lubrication, blank holder load, die radius and other system inputs.

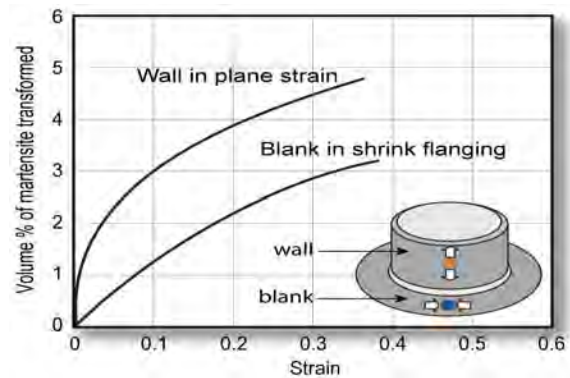


Figure 3.B-48: The cup wall is strengthened more than the flange due to increased amounts of transformed martensite in TRIP steels.^{T-2}

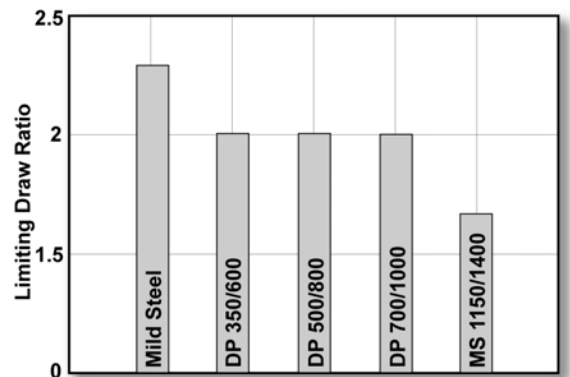


Figure 3.B-49: LDR tests for Mild, DP, and MS steels.^{C-1}

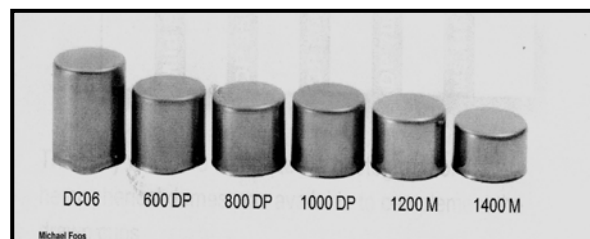


Figure 3.B-50: Cups plotted in Figure 3-66 above.^{F-3}

3.B.4.d. Roll Forming

The roll forming process forms a flat metal strip by successive bending into the desired shape. Each bending operation can be distributed along several sets of rolls to minimize strain localization and compensate for springback. Therefore, roll forming is well suited for generating many complex shapes from AHSS, especially those with low total elongations such as MS steel. Figure 3.B-51 shows example automotive applications that are ideal for this process.

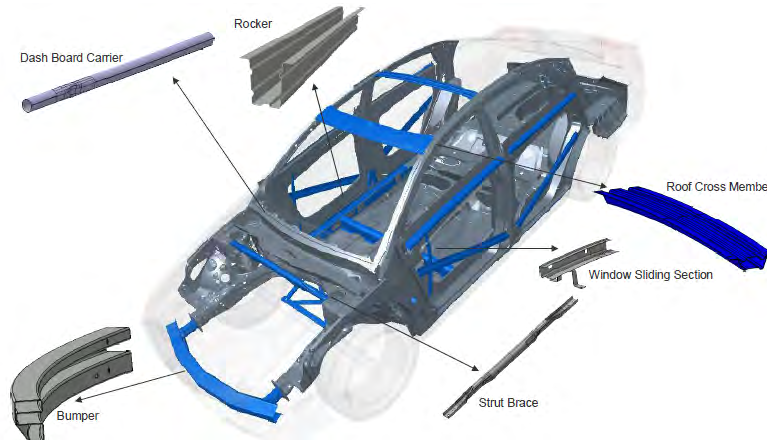


Figure 3.B-51: Body components that are ideally suited for roll-forming.

Roll forming can produce AHSS parts with:

- Steels of all levels of mechanical properties and different microstructures.
- Small radii depending on the thickness and mechanical properties of the steel.
- Reduced number of forming stations compared with lower strength steel.

However, the forces on the rollers and frames are higher. A rule of thumb says that the force is proportional to the strength and thickness squared. Therefore, structural strength ratings of the roll forming equipment must be checked to avoid bending of the shafts. Typical values of the minimum radius and springback can be determined for the different AHSS with tests on simple U shapes performed with six stations (Figure 3.B-52). The value of minimum internal radius of a roll formed component depends primarily on the thickness and the tensile strength of the steel (Figure 3.B-53). Roll forming allows smaller radii than a bending process.

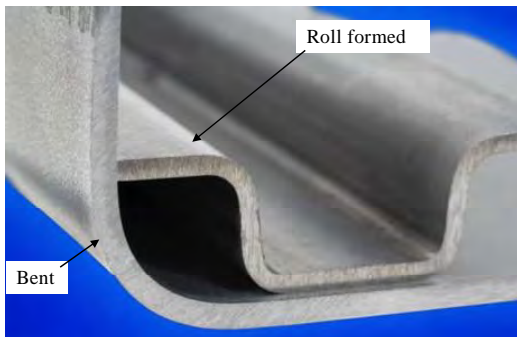


Figure 3.B-52: Comparison between the minimum obtainable radii made by roll forming and bending a 2 mm MS 1050/1400 steel.^{S-5}

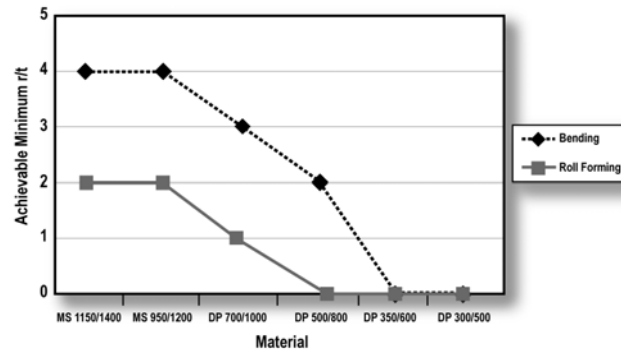


Figure 3.B-53: Achievable minimum r/t values for bending and roll forming for different strength and types of steel.^{S-5}

The main parameters having an influence on the springback are the radius of the component, the sheet thickness, and the strength of the steel. The effects of these parameters are shown in Figure 3.B-54. As expected, angular change increases for increased tensile strength and bend radius. Figure 3.B-55, shows a profile made with the same tool setup for three steels having different strengths and the same thickness. Even with the large difference in strength, the springback is almost the same. ^{S-5}

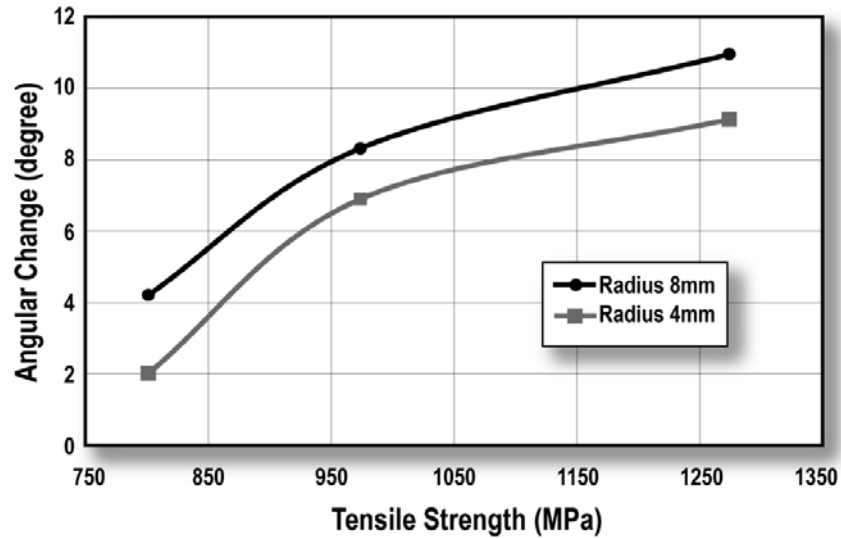


Figure 3.B-54: Angular change increases with increasing tensile strength and bend radii. ^{A-4}



Figure 3.B-55: Profile made with the same tool setup for three different steels. ^{S-5}

3.B.4.e. Key Points

Stretching

- DP steel has a higher initial n-value than TRIP steel, which helps flatten emerging strain gradients and localized thinning. Stretch form features such as embossments can be slightly sharper or deeper. DP steel does not have a higher FLC compared to conventional HSLA with comparable YS.
- TRIP steels benefit from a higher n-value throughout the deformation process, which helps to flatten emerging strain gradients and reduce localized thinning. In addition, the height of the FLC is increased and higher values of strain are allowed before failure.
- The limited stretchability of both conventional HSLA and AHSS (compared to Mild steels) increases the importance of product design, change of forming mode, utilization of a preform stage, lubricant selection, and other process design options.

Bending

- For equal strengths, most AHSS have greater total elongations than conventional HSLA.
- Shear fractures are not predicted by the forming limit curve or forming simulations. Early shear-type fractures have been encountered when a small tool radius to sheet thickness (R/T) ratio is experienced, thus it's important to use die design guidelines for minimum R/T ratios.
- Roll forming can produce AHSS parts with steels of all levels of mechanical properties and different microstructures with a reduced R/T ratio versus conventional bending.
- Roll forming retards springback primarily through over-bending without particularly complex tools.

Deep Drawing (Cup Drawing)

- The LDR for both HSS and DP steels is approximately two because the r_m values for most HSS and AHSS are approximately one.
- The LDR for TRIP steel is slightly greater than two because martensitic transformation strengthening for plane strain deformation in the cup wall is greater than the strengthening for shrink flange deformation in the blank. This delays the onset of the local neck.

3.B.5. Hot-Forming

Today many product designs tend to combine geometry complexity and part consolidation with the highest possible final strength steel required for in-service applications. Maximum part complexity usually requires superior stretchability as evidenced by high work hardening capability and defined by the n-value. Part consolidation might take three non-severe stampings and make one very severe large part. Imagine three separate stampings formed with extensive metal flow from the binder to provide maximum part depth. Lay the three stampings side-by-side in a straight line and successfully connect them with welds to make the final part. Now attempt to make all three attached stampings from a single blank in one die. There is no binder area to feed the middle stamping, which now must form almost completely by excessive stretch forming. Making the problem worse, increasing the strength of the as-received steel reduces the stretching capacity of the steel because the work hardening exponent (n-value) decreases with increasing strength for each type of steel. Finally, springback problems increase as the yield strength increases.

The hot-forming process can minimize all the above problems. Since first used in the Saab 9000 in 1984, hot-forming has steadily increased in popularity. In recent years, the use of hot formed AHSS components has rapidly increased. For instance, the number of production stampings from hot-forming went up from 8 million per year in 1997 to 107 million per year in 2007, and continues to rise in all regions of the globe. For some recent vehicles, the percentage of these steels is close to 25% of the body in white (BIW) weight. Today, hot-forming is used to form stamping geometries with relatively complex shapes such as A-pillars, B-pillars, front/rear side members, cross members, etc.

The following steps (Figure 3.B-56) present details of the direct hot-forming process.^{M-2, I-1} While several steels are applicable, the data below represent 22MnB5 - the most common hot forming steel. The initial microstructure is composed of ferrite and pearlite.

3.B.5.a. Direct Hot-Forming Process

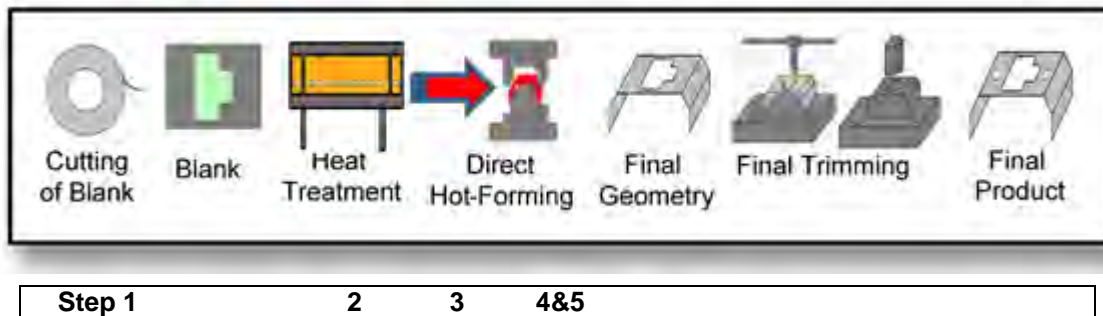


Figure 3.B-56: Graphic showing steps in the Direct Hot-Forming process.^{V-2}

Step 1 in Figure 3.B-56– Cut the blank (Marker 1 in Figure 3.B-57): The as-received HF steel is at room temperature with yield strength of 350-400 MPa, a tensile strength of 550-600 MPa, and a total elongation around 25%. Blanking dies must withstand these properties (See true stress-strain curves in Figure 3.B-58 upper graph).

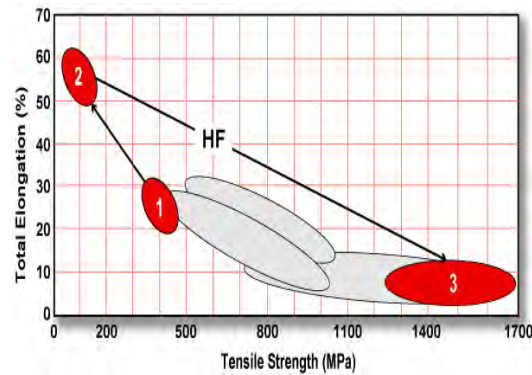


Figure 3.B-57: Steel properties during the forming process.

Step 2- Heat the blank (Marker 2 in Figure 3.B-57): To enable the material to harden, it must first be heated above 900 °C to change the microstructure to austenite. Generally, this is accomplished in continuous furnaces to ensure a continuous heating process. Typical furnace time is 5-8 minutes. The exposure of the tool steel to the high temperatures necessary for hot-forming can result in large variations in friction as a result of changes in the surface topography, removal of oxide layers, and excessive wear of the tool. One approach to overcome the issues of friction is to apply suitable coatings or various surface treatments to the tool steel.

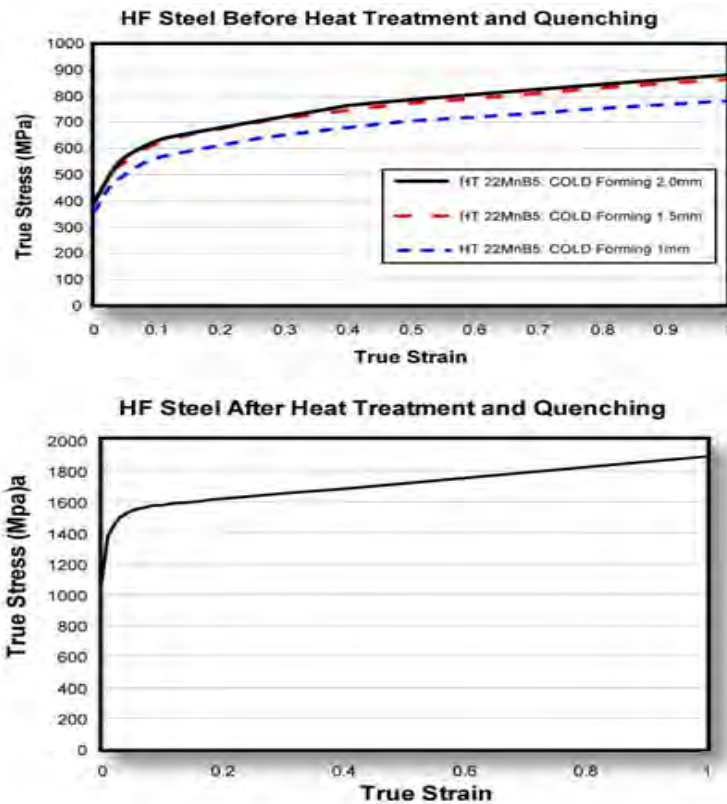


Figure 3.B-58: True stress-strain curves for different sheet thickness of as-received boron-based HF steel tested at room temperature (upper curve) and tested after heat treatment and quenching (lower curve).^{V-1}

Currently, an aluminium-silicon (AS) coating is the most common coating applied to blanks to prevent the formation of this surface oxide. Other coatings include hot-dipped galvanized (GI), galvanized (GA), zinc-nickel (GP), and organic substances. Inert gasses can be used for special applications. The coatings also help prevent in-service corrosion in part areas difficult to shot blast or otherwise remove the surface oxide prior to application of additional corrosion protection treatments.

Step 3 – Transfer blank to die: Robots or linear transfer systems (feeders) can transfer the blank to the water-cooled die in about three seconds. To protect the transfer system from overheating and minimize the heat loss of the blank, insulation should be used – an example is the placement of heat shields between the blanks and the transfer system. Once transferred, positioning aids ensure that the blank is located precisely in the die.

Step 4 – Forming the stamping: Forming temperature typically starts at 850 °C and ends at 650 °C. While in the austenitic range, the true yield stress is relatively constant at 40 MPa with high elongations greater than 50%. This enables stampings with complex geometries and part consolidation to form successfully with limited springback issues.

Step 5 – In-die quenching (Marker 3 in Figure 3.B-57): When forming is completed, the stamping now contacts both the punch and die for both side quenching. The minimum quench rate is 50 °C/sec. Some actual cooling rates are two or three times the minimum rate. Quenching the formed part leads to a significant increase in the strength of the material and a greater precision in its final dimensions. The quench process transforms the austenite to martensite throughout the entire stamping, which accounts for the increase in strength. The room temperature properties of the final stamping are 1000-1250 MPa yield strength, 1400 -1700 tensile strength, and 4-8% elongations (See the true stress-strain curve in Figure 3.B-58 lower graph). Total time for robot transfer, forming, and quenching is about 20-30 seconds and depends heavily on the quench rate and quenching system. With smaller stampings, forming and quenching of multiple stampings in the die reduces per stamping processing time.

Step 6 – Post-forming operations: The very high strength and low elongations of the final stamping restrict these final operations. The room temperature stamping should not undergo additional forming. Any special cutting, trimming, and piercing equipment must withstand the high loads generated during these operations.

3.B.5.b. Indirect Hot-Forming Process

The indirect hot-forming process (Figure 3.B-59) accomplishes initial forming and trimming prior to hot forming, shown as preform Step 1A. Here, 90-95% of the stamping geometry is pre-formed in conventional dies at room temperature, based on incoming steel properties. The stamping is trimmed (2A) and then subjected to the usual heating cycle in Step 3A above. Additional hot-forming (4A/5A) is now possible for areas of the stamping too severe to form at room temperature. However, the in-direct forming process has a cost increase over the direct hot-forming process – two forming dies are required instead of one.

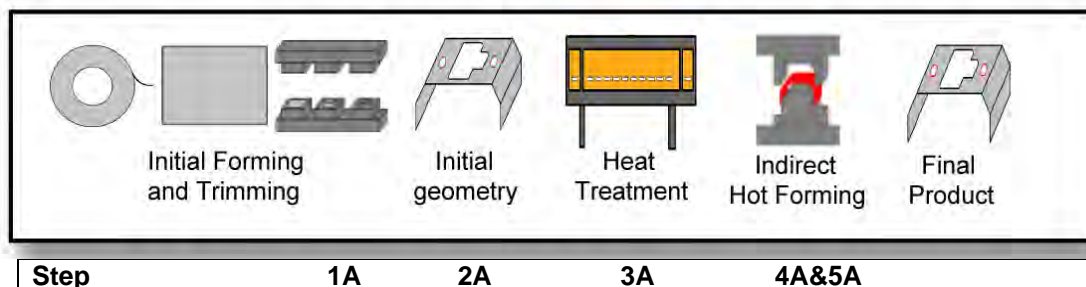


Figure 3.B-59: Graphic showing steps in the In-Direct Hot-Forming process.^{V-2}

Indirect hot-forming was developed to reduce wear on the tool when dealing with uncoated steel. The added cold forming stage reduced movement between the steel and the tool, thus leading to less wear on the tool. On the contrary, in direct hot-forming, rapid cooling of the finished stamping takes place via the surfaces of the tool. Indirect hot-forming process is introduced to develop stampings with more complex form features. Since the stamping cavity depth is formed during cold stamping and the detail features are formed thereafter in the hot-forming press, more complex geometry can be achieved, and distortion is minimized.

Another process similar to the indirect hot-forming process is PFHT (post-forming heat-treating). Very high strength steels generally have greatly reduced stretchability. The PFHT goal is to create the stamping from lower strength but more formable steels (Marker 1 in Figure 3.B-60) by traditional cold-forming processes. The final processing heat and quench sequence creates a very high strength stamping (Marker 2 in Figure 3.B-60). The major issue restricting widespread implementation of PFHT typically has been maintaining stamping geometry during and after the heat treatment process. Fixturing the stamping and then heating (furnace or induction) and immediate quenching appear to be the solution for production applications. Current quenching processes are water, air hardening, or water cooled die.

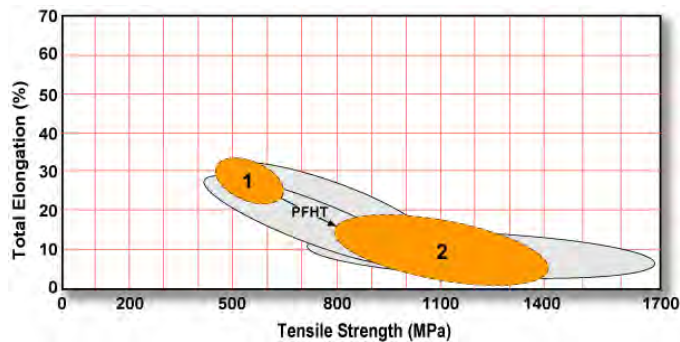


Figure 3.B-60: Post forming heat treating. Lower strength, more formable steel is formed to final shape (Marker 1), heated, and quenched to achieve the final high strength (Marker 2).

3.B.5.c. Benefits of Hot Forming

1. Springback issues eliminated, which is remarkable considering the extremely high final part strength.
2. Very high strength resists stamping deformation
3. Manufactured stampings have low distortion.
4. Stamping consolidation has high feasibility for success.
5. Both high yield strength and steep cyclic stress-strain response create excellent fatigue performance.
6. Stampings have low directionality of properties measured by r-value anisotropy.
7. A 10% increase in yield strength (about 100 MPa) bake hardening effect can further increase in-service strength.
8. Hot-forming has the highest potential for weight reduction of crash components.
9. Tailored welded blanks with different combinations of thickness, properties, and surface coatings can be hot-formed as a single stamping.
10. Controlling the temperature in various locations of the forming die can create zones with different strength levels in the final stamping.

3.B.5.d. Typical Parts

Typical parts are as follows:

- A-pillar upper
- B-pillar outer and reinforcement
- Tunnel
- Front/rear side members
- Cross members
- Door ring

Some of these parts are often made with tailored welded blanks, mixing different thicknesses and different grades (500 MPa for the areas which must allow buckling during crash and 1500 MPa for areas where no deformation under crash is accepted).

3.B.5.e. Key Points

The goal of hot-forming is to achieve complex geometries and part consolidation at strength levels previously unimaginable.

- **Hot forming will heat a steel to temperatures high enough to**
 - a) **increase forming parameters to allow successful forming of difficult stampings**
 - b) **quench the stamping to form very high strength martensite**
 - c) **avoid springback problems associated with higher strength steels.**
- **Steel usually utilized is a 22Mn/B5 with yield strength of 340 MPa, tensile strength of 480 MPa and 20-30% total elongation.**
- **Heated above 850° C, reduces the tensile strength to 100 MPa and increases the total elongation to 50-60%. The steel is formed in a die in this condition.**
- **The forming die is chilled to provide a quenching action while the stamping is still held in the die. The quenching action:**
 - a) **Transforms the steel microstructure to martensite (HF 1050/1500 or HF 1200/1900)**
 - b) **The stamping shape is retained with almost zero springback.**
- **Press speed is approximately two strokes per minute to allow sufficient quenching.**
- **The reduced forming strength may allow for multiple stampings in one die without over loading press capacity.**
- **The very high final strength of the stamping severely limits post forming operations. No additional forming should be attempted. Trimming, cutting, and piercing equipment must be built to overcome the strength of the final stamping. Laser welding is often used.**

3.C. Tooling and Design Considerations

AHSS characteristics must be determined when designing draw dies. First is the initial, as-received yield strength, which is the minimum yield strength throughout the entire sheet. Second is the increase in strength level, which can be substantial for stampings that undergo high strain levels. These two factors acting in tandem can greatly increase the local load. This local load increase mostly accelerates the wear of draw radii with a less pronounced effect on other surfaces. It's important to understand these affects when making die design and die processing decisions. This section describes the re-thinking of tool and part design to extend the life and performance of tooling in press shops.

3.C.1. Tool and Part Design

PART DESIGN: Part design features should be considered as early as possible in the concept stage to allow for proper process and tooling design decisions to be made. Successful application of any material requires close coordination of part design and the manufacturing process. Consult product and manufacturing process engineers when designing AHSS parts to understand the limitations/advantages of the material and the proper forming process to be employed.

- Design structural frames (such as rails, sills, cross members, and roof bows) as open-ended channels to permit forming operations rather than draw die processes. AHSS stampings requiring draw operations (closed ends) are limited due to a reduced depth of draw (see Figure 3.C-1 for schematic comparing an open ended versus closed ended design). The rule of thumb for AHSS such as DP 350/600 is half the draw depth permitted for mild and IF. Less complex, open-ended stamped channels are less limited in depth.

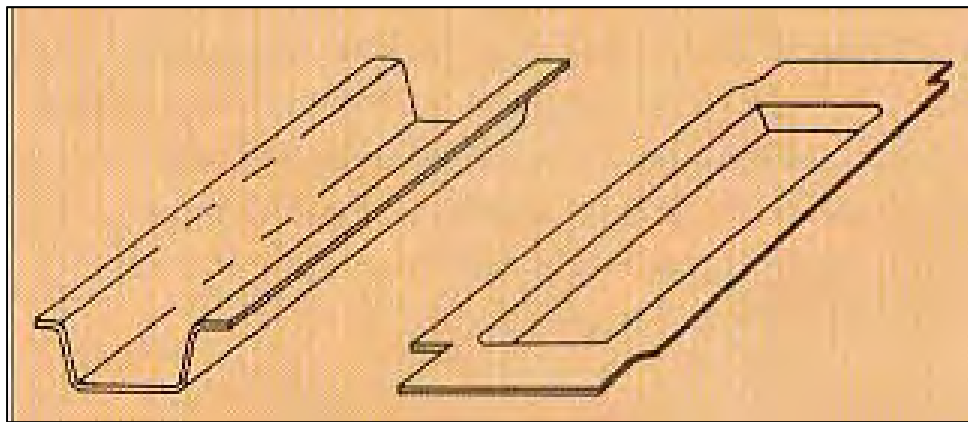


Figure 3.C-1: Schematic of an opened ended part design (left) and a closed ended part design (right). The open-ended design allows for greater depths when utilizing AHSS versus the closed ended design historically used with mild steel.

- Structural parts such as rails, sills, etc., aren't the only parts that can benefit from being developed open ended. This applies more specifically to draw die developments, not just the final part geometry, and improves the ability to make more complex geometries with AHSS. Even though the final part or sections of the final part may be an open ended "hat" section, there may not be a need to "wrap" the end of the part in the draw die as is done many cases. Wrapping ends of "hat" sections increases forming loads, increases the chances of circumferential compression wrinkling on the binder, specifically in the corners, and increases wrinkling on the draw wall if the blank edge runs through the draw bead. Draw die developments that include a closed (or wrapped) end development usually also require a larger blank size. During draw die development, it is best to identify parts that have a "hat" section geometry in certain locations and develop the draw die

accordingly to maximize the positive formability attributes of AHSS while minimizing the limitations of AHSS.

- These same draw die development criteria can be used regardless of whether the steel is conventional mild, IF, BH and HSLA or AHSS. Figure 3.C-2A-B compares a draw die development on a DP600 cowl side with a closed (wrapped) end with a very similar DP600 cowl side developed with an open end. Both final part geometries are very similar, but the close ended development led to significant global formability failures due to the excessive stretch that, ironically initiated in the addendum and propagated into final product. In contrast, the open-ended development had virtually no global formability related failures. Other design and die developmental differences are also noted including the use of stake beads to control springback and embossments to eliminate wavy metal on the part on the right. The additional benefit of the open-ended development is the potential to reduce the blank size for material utilization savings.

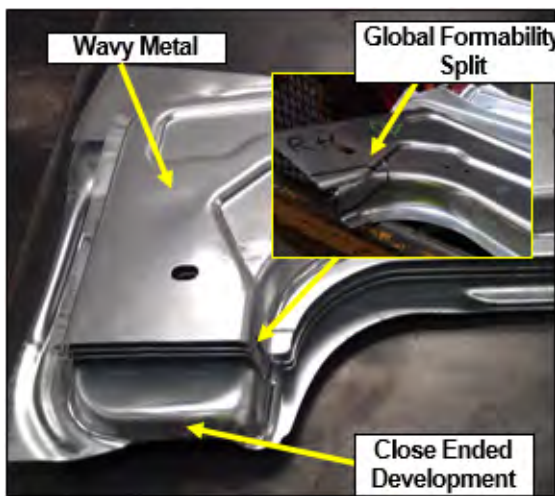


Figure 3.C-2A: Draw die development with closed end development and significant global formability failures. There are no stake beads and no embossments to eliminate wavy metal on the flat portion of the part, both not desirable with AHSS.

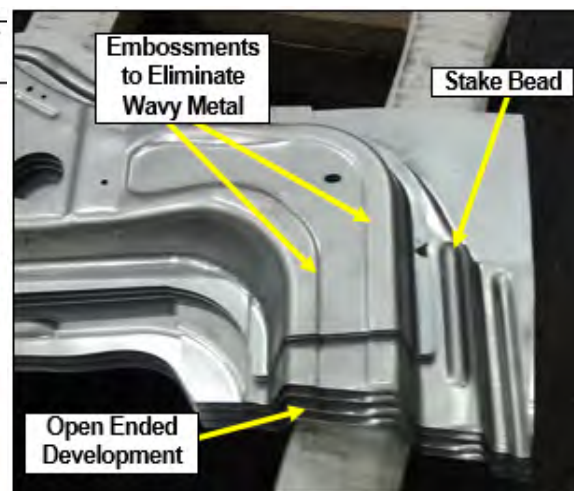


Figure 3.C-2B: Draw die development with open end and virtually no global formability failures. Embossments take out potential wavy metal, and stake beads control springback.

- The automotive industry has adopted a strategy for “lighter dies and fewer dies”, to reduce cost. One key element is “part consolidation”, such as one-piece body side outers and inners. As AHSS is considered for these applications, consolidation will be challenged by the very high strength levels of these steels. Parts previously made with one set of dies may have to be split up into 2 or more separate parts, then welded together, or laser welded before stamping. Figure 3.C-3 shows a rocker panel that in the past would have been stamped as a one-piece part with conventional mild or HSLA steel. Today, this component requires higher strength and reduced thickness to meet weight and crash requirements, and therefore is produced with DP980. Limitations on the formability of this grade necessitated splitting the part up, putting a more formable grade where needed on the wrapped (or closed) end.

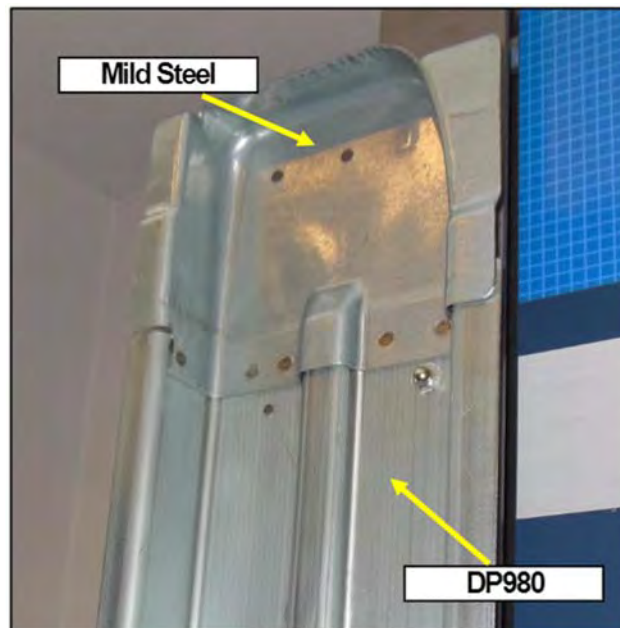


Figure 3.C-3: DP980 rail stamped open ended. A second mild steel part is stamped separately and spot welded to the end of the AHSS rail.

Design AHSS channel shaped part depth as consistent as possible to avoid forming distortions. All shape transitions should be gradual to avoid distortions, especially in areas of metal compression. Minimize stretch/compression flanges whenever possible.

Section 3.C.3 – Springback Management describes in detail tool design and processing to manage springback; in general, you should design out springback in the first draw stage to eliminate additional, costly corrective operations (a restrike, a post-form operation, etc.). The die geometry will dictate the material strain path; by reducing the number of bend/unbend scenarios, this will result less distortion and tool wear.

Design recommendations for other line die operations follow.

Trim and pierce tool design:

- Engineer trim tools to withstand higher loads since AHSS have higher tensile strengths than conventional high-strength steels.
- Proper support for the trim stock during trim operation is very important to minimize edge cracking.
- Modify trim schedule to minimize elastic recovery.
- Shedding of scrap can be a problem because springback of AHSS can cause scrap to stick very firmly in the tool.

Flange design:

- Design more formable flanges to reduce need for extra re-strike operations.
- Areas to be flanged should have a “break-line” or initial bend radius drawn in the first die to reduce springback.
- Adapt die radii for material strength and blank thickness.

Draw beads:

- Draw beads can generate large amounts of work hardening and increased press loads.
- Optimize blank size and shape to reduce the reliance on draw beads, which can excessively work harden the material before entering the die opening.
- Utilize draw beads to induce strain and therefore reduce elastic recovery.

Guidelines to avoid edge cracking during stretch flanging:

- Abrupt changes in flange length cause local stress raisers leading to edge cracks. Hence, the transition of flange length should be gradual.
- Grinding on the draw die to reduce the length of line is commonly done with conventional steel to eliminate splits. This practice can cause the transfer of edge fractures from the draw operation to the flange die since AHSS work hardens at a very high rate (Figure 3.C-4). To stretch flange after forming, consider the addition of metal gainers in the draw die, which provides additional length of line for the subsequent stretch flange.
- Use metal gainers (see Figure 3.C-5 following) in the draw die or in the die prior to the stretch flange operation to compensate for change in length of line that occurs. This can avoid edge cracking of a stretch flange.
- Avoid the use of sharp notch features in curved flanges.
- Edge preparation (quality of cut) is a critical factor.



Figure 3.C-4: Edge fractures transferred from the draw die to flange die.

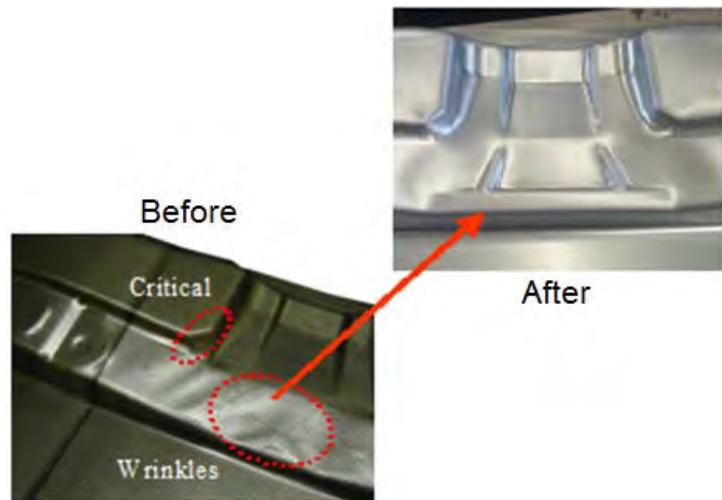


Figure 3.C-5: Insertion of metal gainers to avoid insufficient stretched areas and eliminate buckles.^{T-3}

Correcting loose metal:

- The higher strength of AHSS makes it more difficult to pull out loose metal or achieve a minimum stretch in flat sections of stampings.
- Increase the use of addendum, metal gainers (Figure 3.C-5), and other tool features to balance lengths of line or to locally increase stretch.

3.C.1.a. Multiple Stage Forming

If possible, form all mating areas in the first stage of a forming process and avoid reworking the same area in the next stages. In addition, take care to design stamping processes to minimize the number of forming stages. Address potential springback issues as early as possible in the product design stage (design for springback):

- Avoid right or acute angles.
- Use larger open wall angles.
- Avoid large transition radii between two walls.

Multiple stage forming is recommended for stamping rails or other parts with hat-like cross section, which consist of right angles. In this case, using a two-stage forming process gives much better geometry control than a single stage process. An example of such a process is shown in Figure 3.C-6.

In the first operation (Figure 3.C-6), all 90-degree radii and mating surfaces are formed using “gull-wing” processes with over bending to compensate for springback (note that a large radius is used in the top of the hat area). In the second stage, the top of the rail is flattened. Certain cases may require an over bending of the flat top section.

Multiple forming is also recommended for parts that consist of small geometrical features of severe geometry that can be formed only in the re-strike operation.

A part that has a variable cross section in combination with small geometrical features may need a coining operation in the second or last stage of the forming process. This is the only way to control the geometry.

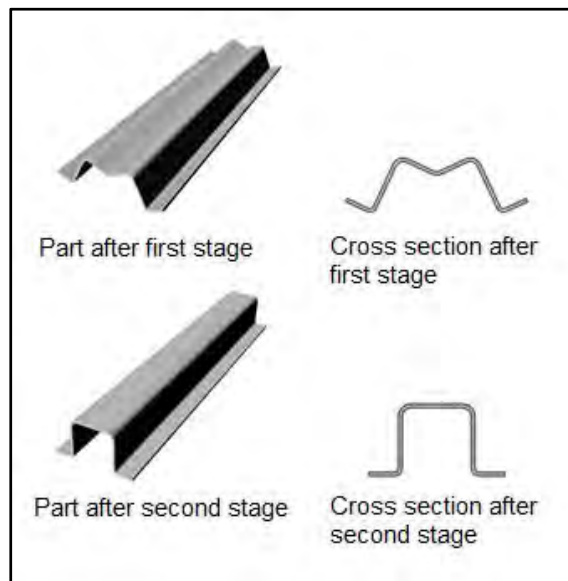


Figure 3.C-6: Two-stage forming to achieve a hat section with small radii.^{R-1}

3.C.1.b. Prototype Tools

For prototyping tools, normally soft tool materials are used and tool surfaces are not protected by wear resistant coatings during tool try out. Soft tools may be used for manufacturing prototype parts and inserts used to eliminate local wrinkles or buckles, however, soft tools should not be used to assess manufacturability and springback of AHSS parts.

When laser cut blanks of AHSS are used during try out, the blank holder surface may be damaged due to the high hardness in the laser cut edges. Laser cutting parameters should be closely controlled to reduce burrs and edge hardness. Laser cut blanks should then be deburred prior to forming in the soft tool.

3.C.2. Tool Materials and Die Wear

Tool and die wear is caused by friction that results from the contact formed between the surface of the die and the blank sheet metal. This damage to the surface of the die can cause a gradual loss of material.

Tool wear is affected by, but not limited to, strength of material, contact pressure, surface finish of the material in contact, sliding velocity, temperature, coating of the die, and lubrication used. When the material is hardened and its strength is increased, an increase in die wear occurs which leads to quality errors in the stamping. In addition, frequent die wear calls for replacement of the current die, which leads to turnaround times and to production losses.

Actions can be taken to prevent excessive wear on the tool and die materials when forming AHSS. To prevent such wear on the tool and die materials, new die materials and better die coatings have been developed.

- These new die materials include the following: wrought and cast tool steels, powder metallurgy tool steels.
- These die materials have been developed to maintain their hardness without compromising the toughness of the material.
- Hard material coatings and nitriding have also been used to improve the tribological properties of die surfaces.

3.C.2.a. Tool Materials

In general, the existing tool and die shop procedures to select the appropriate die material can be used to select dies made to stamp AHSS grades. However, the considerably higher strength level of these grades exerts proportionally increased load on the die material. AHSS might reach hardness values 4-5 times higher than Mild steel grades. This is partially due to the microstructure of the sheet metal itself since some grades include martensitic phases for the required strength. For the martensitic grades (MS), the basic structure is martensite with tensile strengths approaching 1700 MPa.

The higher forces required to form AHSS require increased attention to tool specifications. The three primary areas are:

- Stiffness and toughness of the tool substrate for failure protection.
- Harder tool surface finishes for wear protection.
- Surface roughness of the tool.

Life and performance of a particular draw die is determined by the accepted amount of wear/galling between maintenance periods. When selecting die material, some of the key elements that affect the specification of the die material are:

- Sheet metal being processed, characterized by strength, thickness, and surface coating.
- Die construction, machinability, radii sharpness, surface finish, and die hardness, specifically on draw beads and radii.
- Lubrication.
- Cost per part.

Whereas AHSS delivers significant increases in the applied load, counteracting this load increase can be a reduction in sheet thickness. Thickness reduction for weight saving is one primary reason for applications of AHSS. Unfortunately, the reduced thickness of the steel increases the tendency to wrinkle. Higher blankholder loads are required to suppress these wrinkles. Any formation of wrinkles will increase the local load and accelerate the wear effects. Figure 3.C-7 shows a draw die with severe die wear due to excessive wrinkling on a DP780 part. It is not uncommon to replace these high wear areas with a more durable tool steel insert to minimize this type of excessive wear condition.



Figure 3.C-7: Draw die with significant wear due to excessive wrinkling on a DP780 part.

Tool steel inserts for forming dies must be selected according to the work material and the severity of the forming. Surface coatings are recommended for DP 350/600 and higher grades. When coatings are used, it is important that the substrate has sufficient hardness/strength to avoid plastic deformation of the tool surface - even locally. Therefore, a separate surface hardening, such as nitriding, can be used before the coating is applied. Before coating, it is important to use the tool as a pre-production tool to allow the tool to set, and to provide time for tool to adjust. Surface roughness must be as low as possible before coating. R_a values below $0.2 \mu\text{m}$ are recommended. Steel inserts of 1.2379 or 1.2382 with a TiC/TiN coating are recommended for local high-pressure die areas wearing the zinc off galvanized blanks.

The following table provided by the Auto/Steel Partnership describes recommended materials of construction for stamping dies and components, based on significant research efforts. Naams Standards is the product of a consortium between Ford, GM and FCA North America.

Table 3:C-1 – Recommended Materials for Specific Die Components – NAAMS Standards^{A-20}

Die Component	Recommended Tool Material
Die Shoes (Upper & Lower), Draw Dies	G2500 (non-alloyed gray cast iron)
Draw Die Inserts (high wear areas)	TD2 or D2 tool steel (high wear, low shock)
Restrike Dies: Bottom Pad and Cap	S0050A (alloyed steel, surface hardenable)
Restrike Dies: Upper and Lower Rings, Rails	TD2 or D2 tool steel (high wear, low shock)
Trim & Flange inserts (Upper & Lower), Scrap Cutters	TD2 or D2 tool steel (high wear, low shock)
Flange Dies, Bottom Flange Pads	S0050A (alloyed steel, surface hardenable)

Tool steels for cutting, trimming, and punching tools must be similarly selected. For these operations, tensile strength is more important than yield strength. Tool hardness between 58 and 62 HRC is recommended. Coatings may be used to reduce tool wear, but for the highest strength steels (above 1000 MPa tensile strength) coatings may fail due to local deformation of the die material substrate. To prevent this, hardening of the substrate prior to coating is strongly recommended. Heat-treated (hardened) cutter knives of 1.2379 or 1.2383 show minor wear of the cutter edge. The radial shear gap should be around 15% of the blank thickness. High performance tool steels, such as powder metallurgy (PM) grades, are almost always economical, despite their higher price, because of their low wear rate.

Ceramic tool inserts have extreme hardness for wear resistance, high heat resistance, and optimum tribological behaviour, but have poor machinability and severe brittleness. High costs are offset by reduced maintenance and increased productivity. While not commonly used, the ceramic tool inserts offer a possible solution to high interface loading and wear.

Additional information on tool wear follows in Section 3.C.2.c. – Tool Wear, Clearances, and Burr Height.

3.C.2.b. Key Points

- Areas of concern are the higher working loads that require better tool materials and coatings for both failure protection and wear protection.
- The higher initial yield strengths of AHSS, plus the increased work hardening of DP and TRIP steels can increase the working loads of these steels by a factor 3 or 4 compared to Mild steels.
- AHSS hardness values might increase by a factor 4 or 5 over those of Mild steel.
- Powder metallurgy (PM) tools may be recommended for some AHSS applications.
- Parameters for normal tool design must be modified to incorporate more aggressive springback management techniques.

Design process to minimize wrinkling. Wrinkling leads to higher loads and more tool wear.

3.C.2.c. Tool Wear, Clearances, and Burr Height

Cutting and punching clearances should be increased with increasing sheet material strength. The clearances range from about 6% of the sheet material thickness for Mild steel up to 10%, 16% or even higher for the highest grades with tensile strengths reaching 1400 MPa or higher.

Two-hole punching studies^{C-2} were conducted with Mild steel and AHSS. The first measured tool wear, while the second studied burr height formation. The studies showed that wear when punching AHSS with surface treated high quality (PM) tool steels is comparable with punching Mild steel with conventional tools. If burr height is the criterion, high quality tool steels may be used with longer intervals between sharpening when punching AHSS, since the burr height does not increase as quickly with tool wear as when punching Mild steel with conventional tool steels.

Tested were 1.0 mm sheet metals: Mild 140/270, A80 = 38%, DP 350/600, A80 = 20%, DP 500/800, A80=8%, and MS1150/1400, A80 = 3%. Tool steels were W.Nr. 1.2363 / AISI A2 with a hardness of 61 HRC and a 6% clearance for Mild steel tests. PM tools with a hardness range of 60-62 HRC were used for the AHSS tests. For the DP 350/600, the punch was coated with CVD (TiC) and the clearance was 6%. Tool clearances were 10 % for the MS 1150/1400 and 14 % for DP 500/800.

In the punching test results: The worn cross section of the punch was measured after 200,000 punchings. For comparison, relative tool wear with AHSS was compared to Mild steel with A2 tooling, which was about 2000 μm^2 for the 200,000 punchings. Test results are shown in Figure 3.C-8.

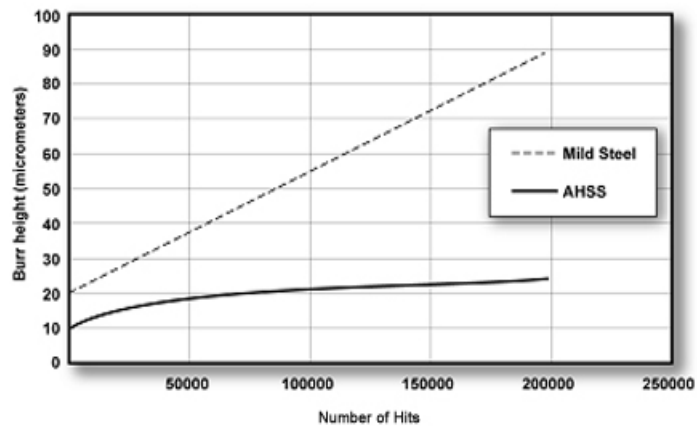


Figure 3.C-8: Punching up to DP 500/800 with surface treated high quality tool steels can be comparable to Mild steel with conventional tools.^{C-2}

Burr height tests: The increasing burr height is often the reason for sharpening punching tools. For Mild steels the burr height increases continuously with tool wear. This was found not to be the case for the AHSS in Figure 3.C-9. Two AHSS tested were DP 500/800 and MS 1150/1400. The burr heights were measured in four locations and averaged. The averages for the two AHSS were so close that they are plotted as a single line.

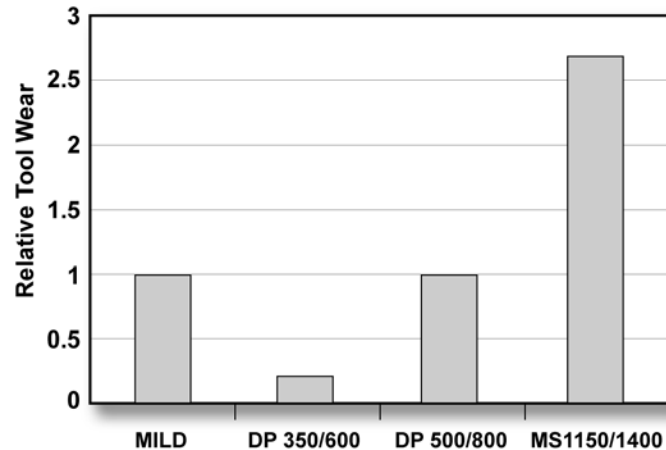


Figure 3.C-9: Burr height comparison for Mild steel and AHSS as a function of the number of hits. Results for DP 500/800 and MS 1150/1400 are identical and shown as the AHSS curve.^{C-2}

The plausible explanation for Figure 3.C-9 is that both materials initially have a burr height related to the material strength and the sharpness of the tools. AHSS fractures at a maximum possible height. This height is reached when the maximum local elongation is obtained during the punching, after which the

fracture occurs. This height is reached when the maximum local elongation is obtained during the punching, after which the

burr height does not increase. The Mild steel, which is more formable, will continue to generate higher burr height with increased tool wear.

The burr height increased with tool wear and increasing die clearance when punching Mild steel. AHSS may require a higher-grade tool steel or surface treatment to avoid tool wear, but tool regrinding because of burrs should be less of a problem. If the tool has been surface treated, grinding the tool will remove the surface treatment, so if possible, the tool must be retreated.

As there are many different tool steels, tool steel treatments, and tool steel coatings, the best thing to do is to identify the dominant mode of tool failure to select the tool steel with the properties to combat that failure mode. It is recommended that the tool material supplier be consulted to select the tool steel with the correct balance of properties to combat the dominant mode of failure. There are 5 main types of cold work failure modes involving tool steels – wear, plastic deformation, chipping cracking, and galling. Figure 3.C-10 shows examples of these 5 failure modes.

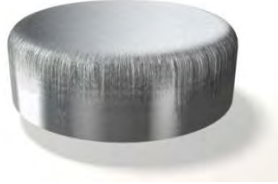

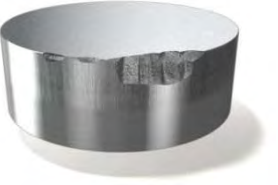
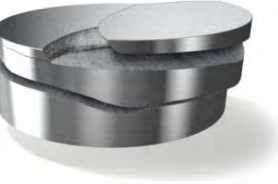

	<p>Wear results in material loss from the tooling material and is related to the tooling material hardness, carbide type and carbide volume. Wear can also be related to material type and process conditions and involves sliding contact between the tooling and the material.</p>
	<p>Plastic Deformation occurs if the process stresses are higher than the yield strength of the tool steel and is related to contact pressure.</p>
	<p>Chipping is related to the stresses in the process and the fatigue resistance of the tooling material.</p>
	<p>Cracking occurs if the process stresses are higher than the tensile strength of the tool steel and can also be fatigue related.</p>
	<p>Galling is a physical/chemical adhesion of the work material to the tool surface. The severity of the galling depends on the surface finish and chemical composition of the material and the tool steel and involves sliding contact between the tooling and the material.</p>

Figure 3.C-10: Five main modes of tooling failure. ^{M-5}

The following case study illustrates the importance of clearly identifying the mode(s) of failure on the part as well as the mode of failure on the tooling to improve the problem-solving path. A dash reinforcement that had been in production for several years, using a 280Mpa yield strength conventional HSLA steel. To improve side impact ratings, the material was converted to DP600. Immediately after implementation, scrap rates increased significantly. The failures were all determined to be local formability edge fractures; investigation revealed that the blank for this part was configured and that the blanked edge at the edge fracture was part of the final product edge. Figure 3.C-11 shows one of the blanked cut-outs which is then drawn and flanged. The edge condition had burrs and a poor burnish to fracture zone. See Figure 3.C-12 for photo of edge fracture.

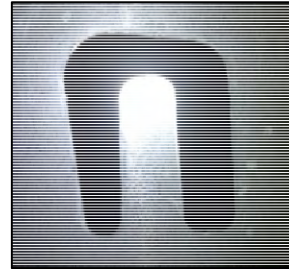


Figure 3.C-11: End of a blank on a dash reinforcement where the blanked cut-out ends up being part of product on the finished part. Close examination shows a poor edge condition.^{M-5}

The blank die was then examined. It was discovered that the tool steel being used was the same as was being used with the conventional HSLA grade, D2. It was also found that the clearances were the same as well, around 10% of metal thickness. Additionally, the inserts used to make the u-shaped cut-out were wearing and failing at an alarming rate. The failures were so frequent that a series of back-up inserts had been constructed so the worn/damaged inserts could be quickly replaced. Figure 3.C-13 shows worn and broken inserts.

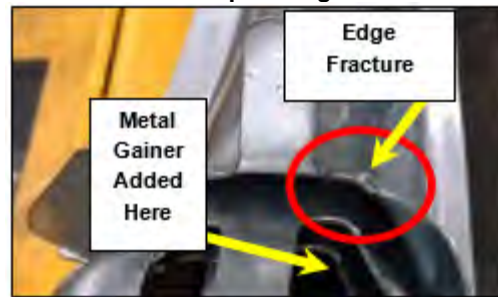


Figure 3.C-12: Local formability edge fracture emanating from a blanked edge in a stretch flange operation and location of metal gainer eventually added to the draw die.

It became clear that the failure mode of the tooling involved both wear and cracking. Additionally, the die clearances were at 10% as opposed to the optimum 15%. As a result, an alternative, more durable tool steel (trade name caldie) with an increased clearance was inserted in the blanking die. This change resulted in a change from constant monitoring, sharpening and replacement of the inserts to over 90,000 hits with virtually no insert maintenance required (other than routine cleaning).

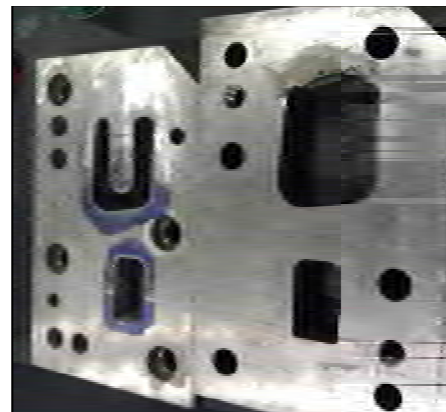


Figure 3.C-13: Worn and broken D2 inserts being used on a DP600 AHSS steel.

This change significantly reduced the scrap rate, but sporadic edge fractures were still being experienced. As a result, breakdown panels of the draw, trim and flange operations were examined. It was found that the draw die at the location in question was not forming the part to the final length of line. After grinding on the draw die, the flanging operation was stretch flanging the blanked edge due to a mismatch in the length of line between the two operations. As DP steels have a very high work hardening rate, stretch flanging a blanked edge significantly increases the potential for edge fracture. As a result, a small metal gainer was added to the draw die to make sure that the flanging operation engaged in only bending and straightening, not additional stretch (see also Figure 3.C-12). After these two process changes, scrap rates for edge fractures dropped to virtually zero.

Given the edge condition sensitivity of AHSS, the importance of selecting the proper tool steel for a given grade of AHSS is of significance. Long term maintenance, repair and scrap/rework costs can be greatly reduced by doing so. Some of these more elaborate tool steels, however, can be significantly more expensive than tool steels that have been used for conventional grades of steel. As a result, some automakers and steel processors don't use the more durable, but more expensive tool steels on the entire working surface of the die. They strategically identify high wear and difficult to maintain areas and install these more expensive tool steels as inserts in those locations. Figures 3.C-14 and 3.C-15 show caldie inserts installed on blank dies in difficult to maintain locations.

Additional information on tool wear is contained in Section 3.C.1.b – Tool Materials.

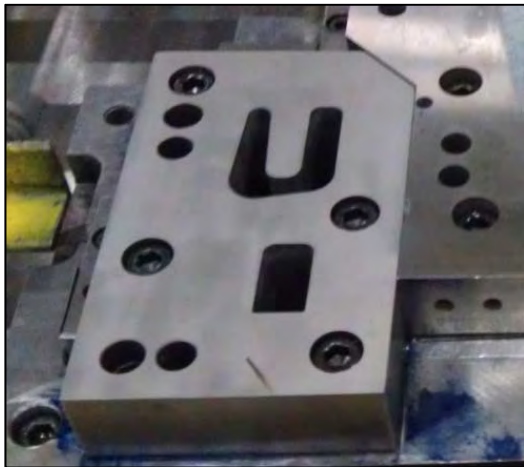


Figure 3.C-14: Caldie insert used to address wear and cracking issues on the blank die. ^{M-5}



Figure 3.C-15: Caldie insert in a difficult to maintain location on a blank die. ^{M-5}

3.C.2.d. Key Points

- Clearances for blanking and shearing should increase as the strength of the material increases.
- Burr height increases with tool wear and increasing die clearances for shearing Mild steel, but AHSS tends to maintain a constant burr height. This means extended intervals between tool sharpening may be applicable to AHSS parts.
- Laser cut blanks used during early tool tryout may not represent normal blanking, shearing, and punching quality. Production intent tooling should be used as early as possible in the development stage.
- The dominant mode of failure of tool steels should be identified and communicated to the tool steel supplier to select the tool steel with the best properties to combat the tool failure mode for a given AHSS grade.

Current research is showing optimum shearing of AHSS can be achieved with the correct shear angle, shear oriented in the metal rolling direction, and greater clearances.

3.C.3. Springback Management

3.C.3.a. Springback and AHSS

Decades ago, the major concern in sheet metal forming was elimination of necks and tears. These forming problems were a function of plastic strain and generally were addressed by maintaining strain levels in the part below specific critical strains. These critical strains were dictated by various forming limits, which included forming limit diagrams, sheared edge stretch tests, and in-service structural requirements.

Today the primary emphasis has shifted to accuracy and consistency of product dimensions. These dimensional problems are a function of the elastic stresses created during the forming of the part and the relief of these stresses, or lack thereof, during the unloading of part after each forming operation. These dimensional problems or springback have always existed in sheet metal forming. However, the magnitude of springback generally increases as the yield strength of the steel increases. As AHSS usage expands due to the combination of higher strength and ductility (for enhanced formability characteristics), countering springback relative to final part dimension becomes critical. First, many of the panels generate higher flow stresses, which are the combination of yield strength and work hardening during deformation. This creates higher elastic stresses in the part. Second, applying AHSS for weight reduction also requires the application of thinner sheet metal that is less capable of maintaining part shape. Third, very little or no prior experience has been generated in most companies relative to AHSS springback management procedures. Many companies have attacked springback problems with proprietary in-house compensation procedures developed over years of trial and error in the production of various parts. An example would be specific over-crowning of a hood panel or over-bending a channel to allow the parts to springback to part print dimensions.

Many reports state that springback problems are much greater for AHSS than for conventional HSLA. However, a better description would be that the springback of AHSS is different from springback of HSLA steels due in large part to the progressively higher initial yield strengths and the greater work hardening rate that significantly increases the yield strength during forming. An example of this difference is shown in Figure 3.C-16. The two channels were made sequentially in a draw die with a pad on the post. The draw die was developed to attain part print dimensions with the HSLA 350/450 steel. The strain distributions between the two parts were very close with almost identical lengths of line. However, the stress distributions were very different because of the steel property differences between DP and HSLA steels.



Figure 3.C-16: Two channels made sequentially in the same die.

3.C.3.b. Origins of Springback

When sheet metal is plastically deformed into a part, the shape of the part always deviates somewhat from the shape of punch and die after removal from the tooling. This dimensional deviation of the part is known as springback. Springback is caused by elastic recovery of the part, which can be illustrated simply on the stress-strain curves shown in Figure 3.C-17.

Unloading (by removing all external forces and moments) from the plastic deformation level A would follow line AB to B, where OB is the permanent deformation (plastic) and BC is the recovered deformation (elastic). Although this elastic recovered deformation at a given location is very small, it can cause significant shape change due to its mechanical multiplying effect on other locations when bending deformation and/or curved surfaces are involved.

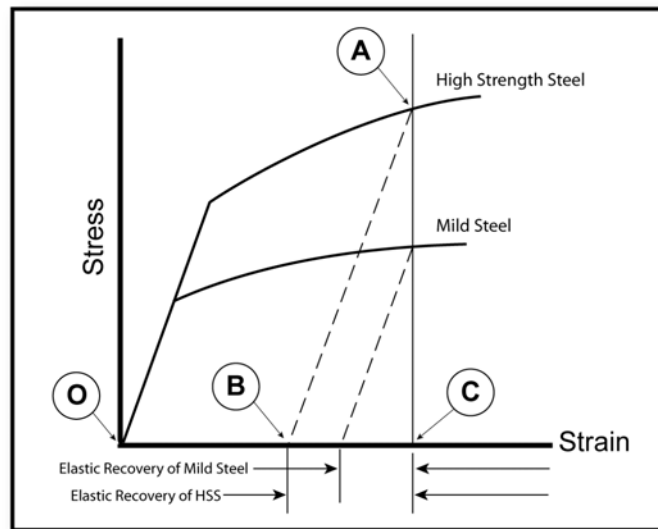


Figure 3.C-17: Schematic showing amount of springback is proportional to stress.

The magnitude of springback is governed by the tooling and component geometry. When part geometry prevents complete unloading (relaxing) of the elastic stresses, the elastic stresses remaining in the part are called residual stresses. The part then will assume whatever shape it can to minimize the total remaining residual stresses. If not all elastic stresses can be relieved, then creating a uniformly distributed residual stress pattern across the sheet and through the thickness will help eliminate the source of mechanical multiplier effects and thus lead to reduced springback problems.

In general, springback experienced in AHSS parts is greater than that experienced in mild or conventional HSLA steels. The expected springback is a function of the as-formed flow stress. Since AHSS have higher as-formed flow stresses for equal part-forming strains, springback generally will be higher for AHSS.

3.C.3.c. Types of Springback

Three modes of springback commonly found in channels and underbody components are angular change, sidewall curl, and twist.

Angular Change

Angular change, sometimes called springback, is the angle created when the bending edge line (the part) deviates from the line of the tool. The springback angle is measured off the punch radius (Figure 3.C-18). If there is no sidewall curl, the angle is constant up the wall of the channel.

Angular/cross section change is caused by stress difference in the sheet thickness direction when a sheet metal bends over a die radius. This stress difference in the sheet thickness direction creates a bending moment at the bending radius after dies are released, which results in the angular change. The key to eliminating or minimizing the angular change is to eliminate or to minimize this bending moment.

Sidewall Curl

Sidewall curl is the curvature created in the side wall of a channel (Figures 3.C-19 and 3.C-20). This curvature occurs when a sheet of metal is drawn over a die/punch radius or through a draw bead. The primary cause is uneven stress distribution or stress gradient through the thickness of the sheet metal. This stress is generated during the bending and unbending process.

During the bending and unbending sequence, the deformation histories for both sides of the sheet are unlikely to be identical. This usually manifests itself by flaring the flanges, which is an important area for joining to other parts. The resulting sidewall curl can cause assembly difficulties for rail or channel sections that require tight tolerance of mating faces during assembly. In the worst case, a gap resulting from the sidewall curl can be so large that welding is not possible.

Figure 3.C-19 illustrates in detail what happens when sheet metal is drawn over the die radius (a bending and unbending process). The deformation in side A changes from tension (A_1) during bending to compression (A_2) during unbending. In contrast, the deformation in side B changes from compression (B_1) to tension (B_2) during bending and unbending. As the sheet enters the sidewall, side A is in

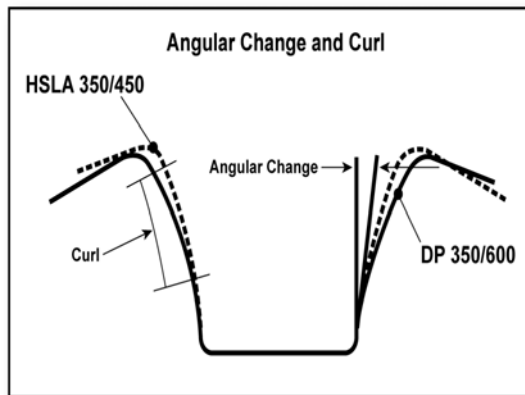


Figure 3.C-18: Schematic showing difference between angular change and sidewall curl.

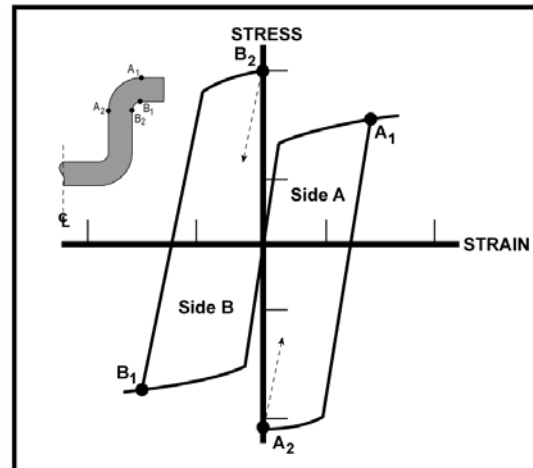


Figure 3.C-19: Origin and mechanism of sidewall curl.

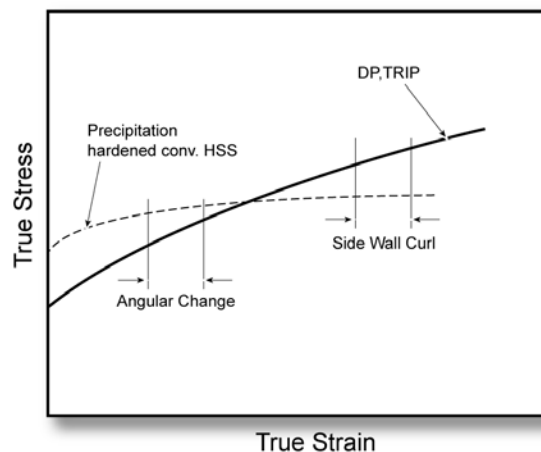


Figure 3.C-19: Schematic description of the effect of hardening properties on springback.^{K-4}

Advanced High-Strength Steels Application Guidelines

compression and side B is in tension, although both sides may have similar amounts of strain. Once the punch is removed from the die cavity (unloading), side A tends to elongate and side B to contract due to the elastic recovery causing a curl in the sidewall.

This difference in elastic recovery in side A and side B is the main source of variation in sidewall curl along the wall. The higher the strength of the deformed metal, the greater the magnitude and difference in elastic recovery between sides A and B and the increase in sidewall curl. The strength of the deformed metal depends not only on the as-received yield strength, but also on the *work hardening capacity*. This is one of the key differences between conventional HSLA and AHSS. Clearly, the rule for minimizing the sidewall curl is to minimize the stress gradient through the sheet thickness.

The difference in strain hardening between conventional HSLA and AHSS explains how the relationship between angular change and sidewall curl can alter part behaviour. Figure 3.C-19 shows the crossover of the true stress – true strain curves when the two steels are specified by equal tensile strengths. The AHSS have lower yield strengths than conventional HSLA for equal tensile strengths. At the lower strain levels usually encountered in angular change at the punch radius, AHSS have a lower level of stress and therefore less springback.

This difference for steels of equal tensile strength (but different yield strengths) is shown in Figure 3.C-21. Of course, the predominant trend is increasing angular change for increasing steel strength.

Sidewall curl is a higher strain event because of the bending and unbending of the steel going over the die radius and any draw beads. For the two stress–strain curves shown in Figure 3.C-20, the AHSS now are at a higher stress level with increased elastic stresses. Therefore, the sidewall curl is greater for the AHSS (Figure 3.C-21).

Now assume that the comparison is made between a conventional HSLA and an AHSS specified with the same yield stress. Figure 3.C-21 would then show the stress–strain curve for the AHSS is always greater (and sometimes substantially greater) than the curve for HSLA. Now the AHSS channel will have greater springback for both angular change and sidewall curl compared to the HSLA channel. This result would be similar to the channels shown in Figure 3.C-16.

These phenomena are dependent on many factors, such as part geometry, tooling design, process parameter, lubrication and material properties. However, the high work-hardening rate of the DP and TRIP steels causes higher increases in the strength of the deformed steel for the same amount of strain.

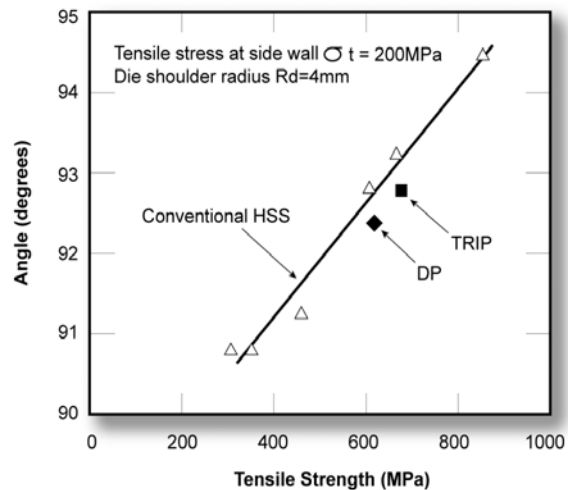


Figure 3.C-20: The AHSS have less angular change at the punch radius for equal tensile strength steels.^{K-4}

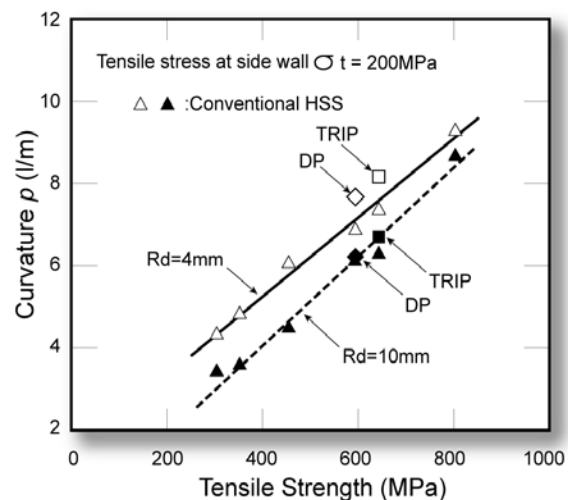


Figure 3.C-21: The AHSS have greater sidewall curl for equal tensile strength steels.^{N-2}

Therefore, any differences in tool build, die and press deflection, location of pressure pins, and other inputs to the stamping can cause varying amounts of springback - even for completely symmetrical parts.

Twist

Twist is defined as two cross sections rotating differently along their axis. Twist is caused by torsion moments in the cross section of the part. The torsional displacement (twist) develops because of unbalanced springback and residual stresses acting in the part to create a force couple, which tends to rotate one end of the part relative to another. As shown in Figure 3.C-22 the torsional moment can come from the in-plane residual stresses in the flange, the sidewall, or both.

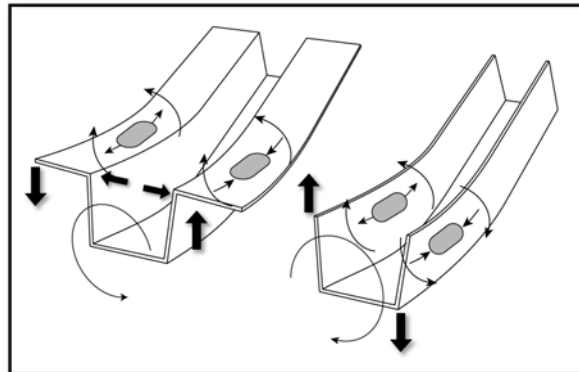


Figure 3.C-22: Torsion Moment created flange or sidewall residual stresses.^{Y-2}

The actual magnitude of twist in a part will be determined by the relationship between unbalanced stresses on the part and the stiffness of the part in the direction of the twist. Low torsional stiffness values in long, thin parts are the reason high aspect ratio parts have significantly higher tendencies to twist. There is also a lever effect, whereby the same amount of twist will result in a larger displacement in a long part than would be the case in a shorter part with a similar twist angle.

The tendency for parts to twist can be overcome by reducing the imbalance in the residual stresses forming the force couple that creates the torsional movement. Unbalanced forces are more likely in unsymmetrical parts, parts with wide flanges or high sidewalls, and in parts with sudden changes in cross section. Parts with unequal flange lengths or non-symmetric cut outs will be susceptible to twist due to unbalanced springback forces generated by these non-symmetrical features.

Even in geometrically symmetrical parts, unbalanced forces can be generated if the strain gradients in the parts are non-symmetrical. Some common causes of non-symmetrical strains in symmetrical parts are improper blank placement, uneven lubrication, uneven die polishing, uneven blankholder pressure, misaligned presses, or broken/worn draw beads. These problems will result in uneven material draw-in with higher strains and higher elastic recoveries on one side of the part compared to the other, thereby generating a force couple and inducing twist.

Twist can also be controlled by maximizing the torsional stiffness of the part - by adding ribs or other geometrical stiffeners or by redesigning or combining parts to avoid long, thin sections that will have limited torsional stiffness.

Global Shape Change

Global shape changes, such as reduced curvature when unloading the panel in the die, are usually corrected by springback management measures. The key problem is minimizing springback variation during the run of the part and during die transition. One study showed that the greatest global shape (dimensional) changes were created during die transition.^{A-1}

Surface Disturbances

Surface disturbances develop from reaction to local residual stress patterns within the body of the part. Common examples are high and low spots, oil canning, and other local deformations that form to balance total residual stresses to their lowest value.

3.C.3.d. Three Methods of Correction

Forming of a part creates elastic stresses unless the forming is performed at a higher temperature range where stress relief is accomplished before the part leaves the die. An example of the latter condition is HF steels. In contrast, cold forming requires some form of springback correction to bring the stamping back to part print. This springback correction can take many forms.

The first approach is to apply an additional process that changes undesirable elastic stresses to less damaging elastic stresses. One example is a post-stretch operation that reduces sidewall curl by changing the tensile-to-compressive elastic stress gradient through the thickness of the sidewall to all tensile elastic stresses through the thickness. Another example is over-forming panels and channels so that the release of elastic stresses brings the part dimensions back to part print instead of becoming undersized.

A second approach is to modify the process and/or tooling to reduce the level of elastic stresses imparted to the part during the forming operation. An example would be to reduce sidewall curl by replacing sheet metal flowing through draw beads and over a die radius with a simple 90 degree bending operation.

A third approach for correcting springback problems is to modify product design to resist the release of the elastic stresses. Mechanical stiffeners are added to the part design to lock in the elastic stresses to maintain desired part shape.

All three approaches are discussed in detail in this unit. While most are applicable to all higher strength steels, the very high flow stresses encountered with AHSS make springback correction high on the priority list. In addition, most of the corrective actions presented here apply to angular change and sidewall curl.

A. Change the Elastic Stresses

POST-STRETCH: One of the leading techniques for significant reduction of both angular change and sidewall curl is a post-stretch operation. An in-plane tension is applied after the bending operations in draw beads and die radii to change tensile to compressive elastic stress gradients to all tensile elastic stresses. When the part is still in the die, the outer surface of the bend over the punch radius is in tension (Point A in Figure 3.C-23), while the inner surface is in compression (B). Upon release from the deforming force, the tensile elastic stresses (A) tend to shrink the outer layers and the compressive elastic forces (B) tend to elongate the inner layers. These opposite forces form a mechanical advantage to magnify the angular change. The differential stress $\Delta\sigma$ can be considered the driver for the dimensional change.

In the case of side wall curl this differential stress $\Delta\sigma$ increases as the sheet metal is work hardened going through draw beads and around the die radius into the wall of the part.

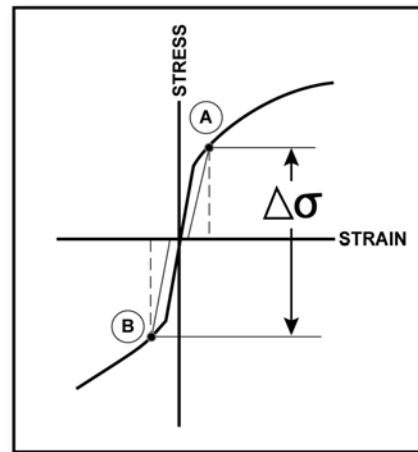


Figure 3.C-23: Sheet metal bent over a punch radius has elastic stresses of the opposite sign creating a mechanical advantage to magnify angular change. Similar effects create sidewall curl for sheet metal pulled through draw beads and over die radii.

To correct this angular change and sidewall curl, a tensile stress is applied to the flange end of the wall until an approximate minimum tensile strain of 2% is generated within the sidewall of the stamping. The sequence is shown in Figure 3.C-24. The initial elastic states are tensile (A1) and compressive (B1). When approximately 2% tensile strain is added to A1, the strain point work hardens and moves up slightly to A2. However, when 2% tensile strain is added to B1, the compressive elastic stress state first decreases to zero, then climbs to a positive level and work hardens slightly to point B2. The neutral axis is moved out of the sheet metal. The differential stress $\Delta\sigma$ now approaches zero. Instead of bending or curving outward, the wall simply shortens by a small amount similar to releasing the load on a tensile test sample. This shortening of the wall length can be easily corrected by an increased punch stroke.

There are two common die design methods used to create the desired minimum 2% post-stretch on the sidewall of AHSS parts, both of which utilize what are commonly called stake beads.

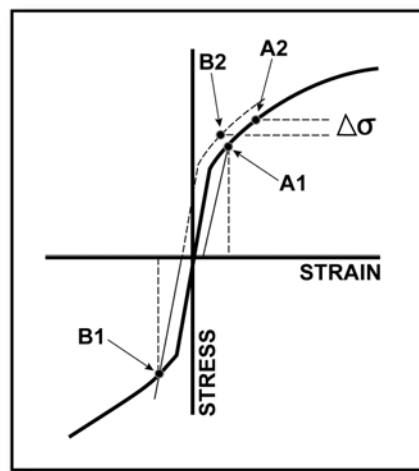


Figure 3.C-24: When subjected to a 2% tensile strain, the positive to compressive stress differential shown in Figure 3.B-110 is now reduced to a very small amount.

The first method involves retractable beads located in machined slots in the lower blankholder. The upper blankholder has machined stake bead pockets. Adjustable stop blocks are located directly under the retractable stake beads and can be shimmed after the timing when the stake bead engages the stamping if required. Studies have shown that the height and geometry of the stake bead can impact springback control. If approximately 2% post-stretch is not achieved, springback might still be excessive. If the restraining force of the stake bead is too great, it could lead to shear fracture at the bead or punch opening radius. At the correct amount of punch stroke, the retractable beads hit the stop blocks, move up, and are forced into the sheet metal flange. This creates a blank locking action while the punch continues to deform the part. As the die opens, the stake beads retract and the cycle repeats itself from press stroke to press stroke. Adjustability of the draw bead height has advantages, particularly during initial die tryout.

As the retractable beads are inserts, removing them to be hardened, coated, polished, etc., is much easier than moving an entire die to perform bead work. Duplicate inserts can also be made, even utilizing alternative tool steels to increase durability. Locating the retractable stake bead on the blankholder, however, can lead to a larger required blank size. Die construction costs for retractable stake beads are also higher due to the additional machining required. Care must also be taken to ensure that there is adequate structural die support to avoid breaking the die. Significantly greater lateral thrust forces can cause catastrophic die failure if the stake beads are located too close to the punch opening. This is also true for many other die components, so die construction standards for mild and HSLA steels may not apply to AHSS.

The second common method is to locate the stake beads on the punch. The stake beads can be machined directly in the punch casting and the stake bead pockets machined into the upper die cavity. This allows for a potential reduced blank size as less material is needed outside the punch opening to accommodate both the draw bead and the stake bead. Figure 3.C-25 shows a photo of a DP590 B-pillar draw panel with draw beads located on the blankholder and stake beads located on the punch just inboard of the draw beads.

Figure 3.C-26A shows a draw die punch with stake beads machined at the very edge of the punch opening. Figure 3.C-26B shows the upper section of the same die with the stake beads and stake bead pockets machined out as well. Although draw beads have historically been featured in the draw die to control metal flow, as material strength levels continue to increase along with work hardening rates, draw beads may become less functional. The natural material deformation (bending and straightening) as it is pulled through the punch opening radius, combined with bearing on the binder surface may be sufficient to control metal flow.

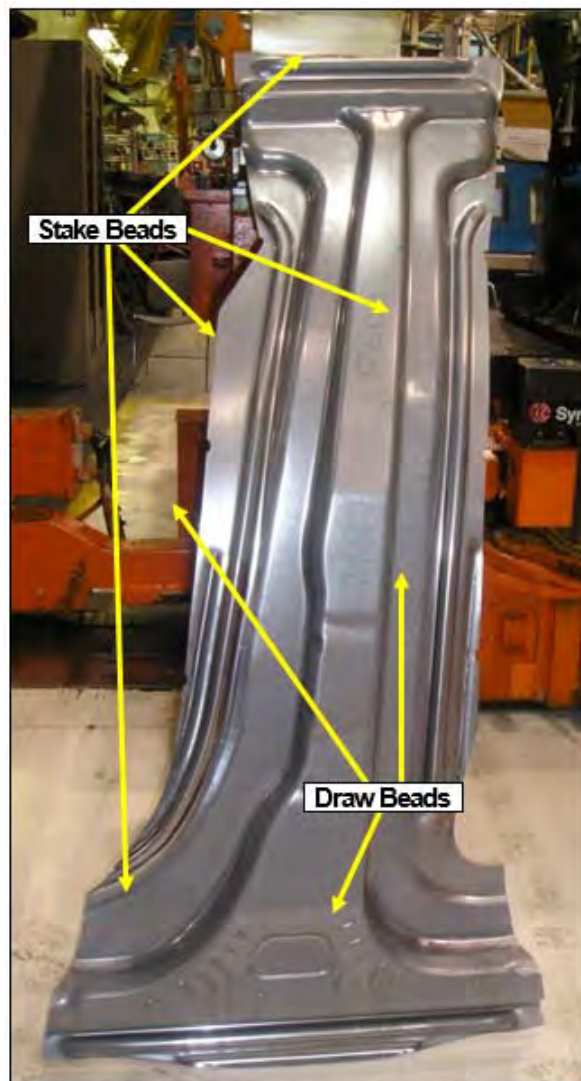


Figure 3.C-25: DP590 B-pillar with draw beads on the blankholder and stake beads on the punch.



Figure 3.C-26A: Stake beads machined into the punch of this DP780 die.

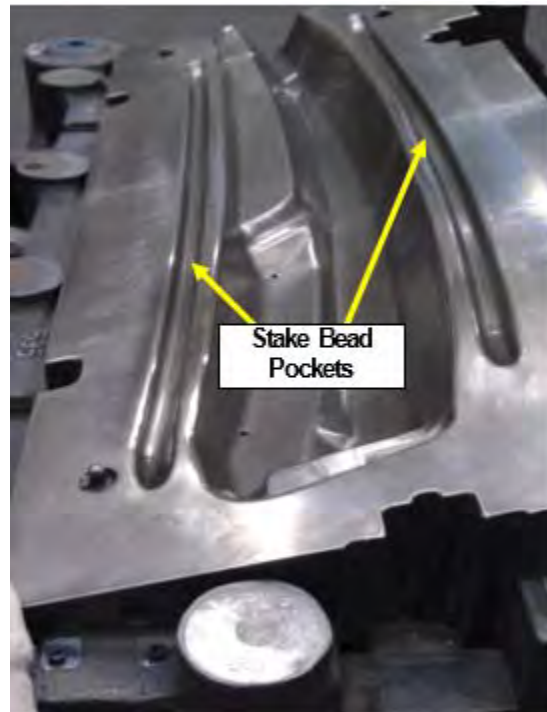


Figure 3.C-26B: Stake bead pockets machined into the upper draw die. Note that there are no draw beads on this blankholder.

The punch and upper binder in Figure 3.C-26A-B have no draw beads, and instead exhibit stake beads that engage very late in the press stroke. This solution is lower in cost but provides limited flexibility since the beads are machined into the die. In contrast, Figure 3.C-27 shows a die with removable stake bead inserts located on the punch – improved adjustability, but with added expense for machining the die and installing stake bead inserts.



Figure 3C-27: This die has adjustable stake beads, but they are located on the punch as inserts and do not retract during every press stroke. Note also that there are no draw beads on the blankholder.

An alternative approach to achieve the post forming 2% strain on the part involves an additional die or die station. The part is removed from the first die and inserted into a second die that locks the remaining flange. The part is then further deformed by 2%. This approach is expensive as an additional die is constructed for this operation, or if processed in a progressive die, an extra station needs to be added which increases the size and complexity of the progressive die.

These post-stretch forming operations normally require significantly higher forming forces and energy requirements to be effective for several reasons. The significantly higher work hardening rate of many AHSS grades means that once they have been pulled through a draw bead their yield strength has increased significantly. As stake beads are located inboard of draw beads, the stake bead must deform material with a much higher yield strength due to the work hardening created by the bending and straightening of the material while being pulled through the draw bead. As stake beads engage very late in the press stroke, their utilization has the same effective result as creating embossments. As discussed in Section 3.C.6.f. – Case Study for Press Energy, the last increment of punch travel required to finish embossing requires significantly higher energy for AHSS versus conventional mild or HSLA steel (see Figure 3.C-65 and 3.C-66). As the sidewalls have also been strengthened by work hardening during the forming process, inducing an additional 2% post forming strain into the part will also require higher forming forces and energy requirements. Even if the press is capable of generating the higher forces, caution must be taken not to neck down and tear the sheet metal bent over the punch radius.

A restrike operation may be required after trimming to ensure dimensional precision. The restrike die should sharpen the radius and provide sidewall stretch (post-stretch) of approximately 2%.

A case study on post-stretch was conducted on TRIP 450/800, DP 850/980, DP 450/750, DP 350/600, CM 490/590, and HSLA 350/450 steels using two specially designed dies^{L-1}. One die had conventional metal flowing from the flange without a bead. The second die had a recessed square stake bead in the flange that created a post-stretch near the end of the stroke. As expected, the side wall curl was very small with the post-stretch die (see Figures 3.C-28A-B). In addition, the material tensile strength did not have much effect on the amount of springback in the post-stretch die. This translates into a more robust process.

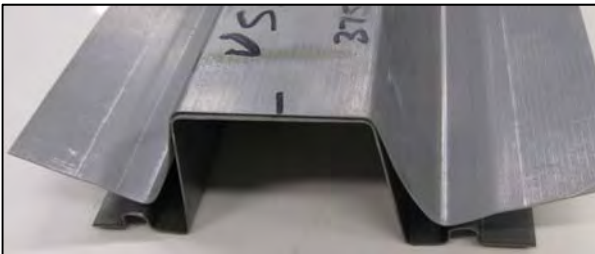


Figure 3.C-28A: Two DP 450/750 parts from the same coil formed in the same die, the only difference being that the bottom part had stake beads that engaged near the bottom of the press stroke to induce an additional 2% strain in the sidewall to control springback.



Figure 3.C-28B: Same two parts from a different angle.

OVER-FORMING: Many angular change problems occur when the tooling either is constructed to part print or has insufficient springback compensation. Over-forming or over-bending is required.

- Rotary bending tooling should be used where possible instead of flange wipe dies (see Figure 3.C-29). The bending angle can be easily adjusted to correct for changes in springback due to variations in steel properties, die set, lubrication, and other process parameters. In addition, the tensile loading generated by the wiping shoe is absent.

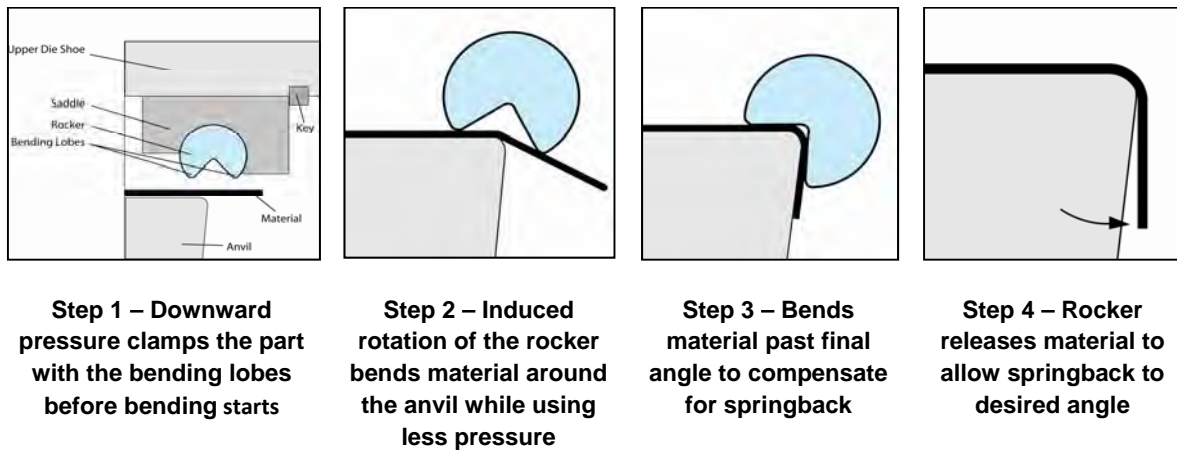


Figure 3.C-29: The above schematics show the four steps with a rotary bending tool.

- Multiple stage forming processes may be desirable or even required depending on the part shape. Utilize secondary operations to return a sprung shape back to part datum. Care must be taken though to ensure that any subsequent operation does not exceed the work hardening limit of the worked material. Use multi-stage computerized forming-process development to confirm strain and work hardening levels. Try to fold the sheet metal over a radius instead drawing or stretching.

- Cross section design for longitudinal rails, pillars, and cross members can enable greater springback compensation. The rear longitudinal rail cross section in sketch A of Figure 3.C-30 does not allow over-bend for springback compensation in the forming die. In addition, the forming will produce severe sidewall curl in AHSS channel-shaped cross sections. These quality issues can be minimized by designing a cross section that allows for over-bend during forming, as in sketch B. Sidewall curl is also diminished with the cross-sectional design. Typical wall opening angles should be 3-degrees for Mild steel, 6 degrees for DP 350/600 and 10 degrees for DP 850/1000 or TRIP 450/800. In addition, the cross section in sketch B will have the effect of reducing the impact shock load when the draw punch contacts the AHSS sheet. The vertical draw walls shown in sketch A require higher binder pressures and higher punch forces to maintain process control.

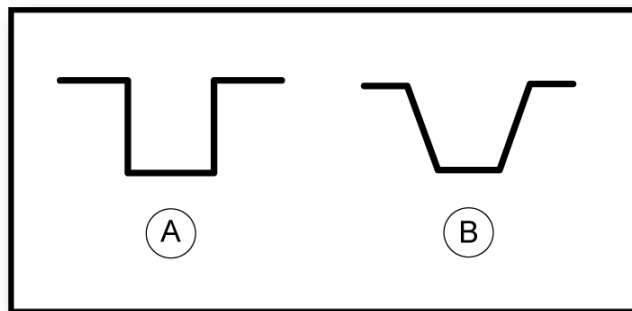


Figure 3.C-30: Changing rail cross section from A to B allows easier over-bending to reduce springback problems with AHSS.^{N-3}

- If over-bend must be incorporated for some parts to minimize angular change and rotary bending is not planned, use die radii less than the part radius and use back relief for the die/punch (Figure 3.C-31).
- If necessary, add one or two extra forming steps. For example, use pre-crown in the bottom of channel-type parts in the first step and flatten the crown in the second step to eliminate the springback at sidewall (Figure 3.C-32).

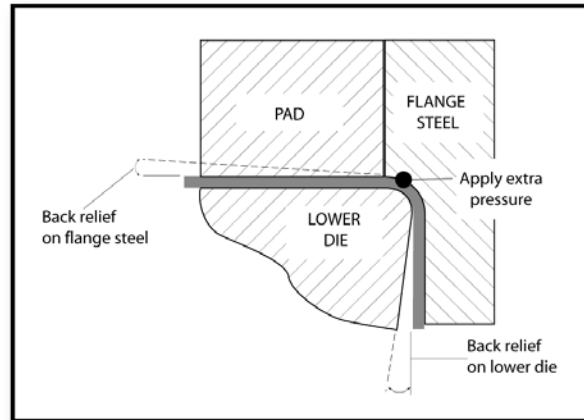


Figure 3.C-31: Over-bending is assisted when back relief is provided on the flange steel and lower die.^{A-2}

B. Reduce or Minimize the Elastic Stresses

The design of the process, and therefore the tooling design, can drastically affect the level of the elastic stresses in the part.

Forming the channel wall (Figure 3.C-33) shows four possible forming processes to create a hat-profile channel with different blankholder actions.

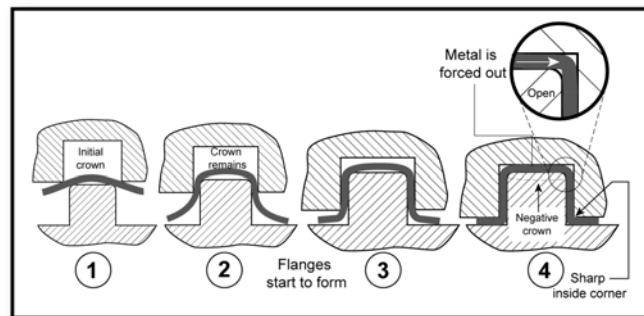


Figure 3.C-32: Schematic showing how bottom pre-crown can be flattened to correct for angular springback.^{A-3}

Descriptions of the four processes above:

- Draw is the conventional forming type with continuous blankholder force and all blank material undergoing maximum bending and unbending over the die radius. This forming mode creates maximum sidewall curl.
- Form-draw is a forming process in which the blank holder force is applied between the middle and last stage of forming. It is most effective to reduce the sidewall curl because bend-unbend deformation is minimized and during the last stage of forming a large tensile stress (post-stretch) can be created.
- Form process allows the flange to be formed in the last stage of forming and the material undergoes only a slight amount of bend-unbend deformation.
- Bend is a simple bending process to reduce the sidewall curl because the sidewall does not undergo one or more sequences of bend and unbend. However, an angular change must be expected.

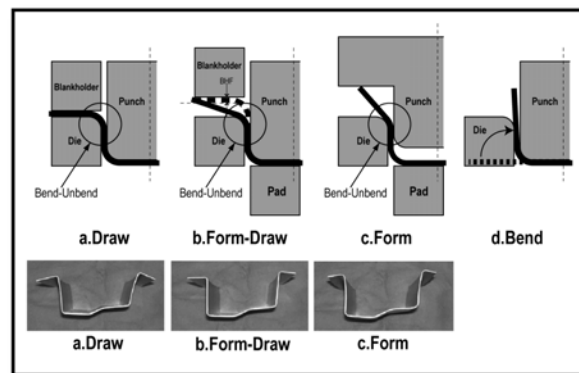


Figure 3.C-33: Four processes for generating a channel for bumper reinforcement create different levels of elastic stress and springback.^{K-5}

Guidelines for Draw and Stretch Form Dies

- Equalize depth of draw as much as possible.
- Binder pressure must be increased for AHSS. For example, DP 350/600 requires a tonnage factor 2.5 times greater than that required for mild steel of comparable thickness. Higher binder pressure will reduce panel springback.
- Maintain a 1.1t maximum metal clearance in the draw dies.
- Maintain die clearance as tight as allowed by formability and press capability to reduce unwanted bending and unbending (Figure 3.C-34).

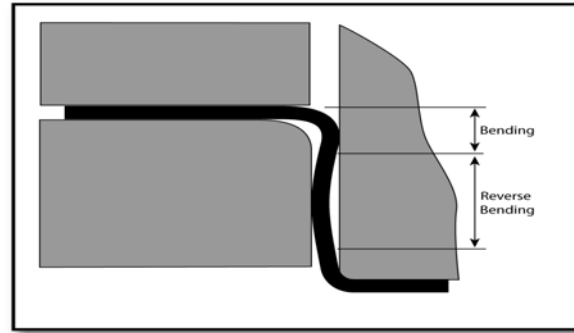


Figure 3.C-34: Reducing die clearance restricts additional bending and unbending as the sheet metal comes off the die radius to minimize angular change.^{Y-2}

Stretch-forming produces a stiffer panel with less springback than drawing. Potential depth of the panel is diminished for both processes as the strength of the material increases. Deeper AHSS stampings will require the draw process.

An extensive American Iron and Steel Institute study^{S-3} defined several tool parameters that reduced angular change (shown in Figure 3.C-35A) and side wall curl (see Figure 3.C-35B).

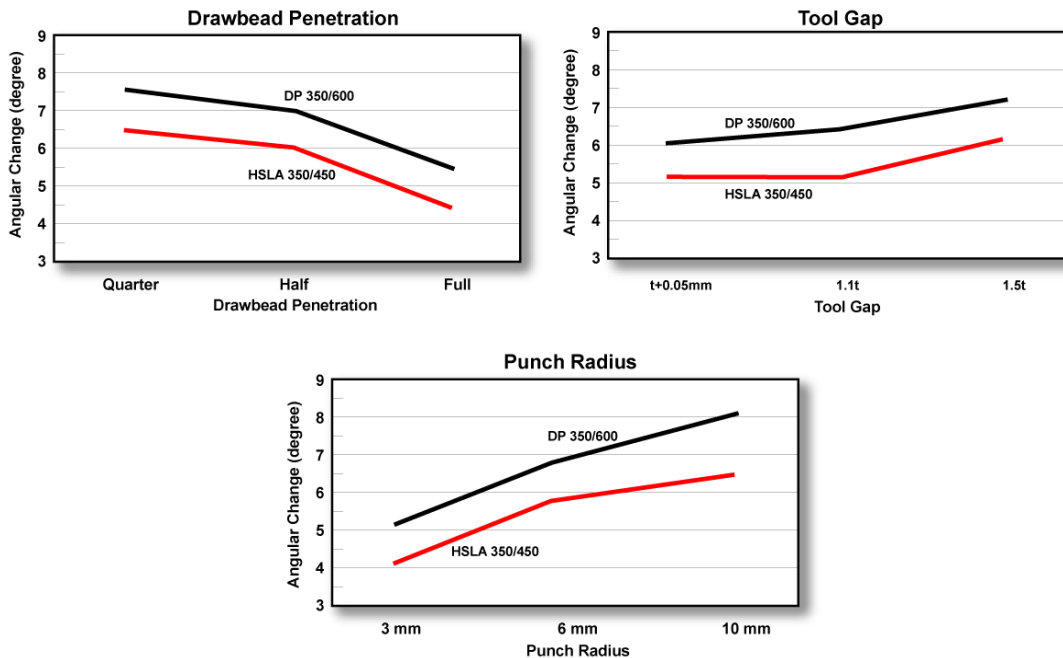


Figure 3.C-35A – The effect of tool parameters in angular change. The lower values are better.^{S-3}

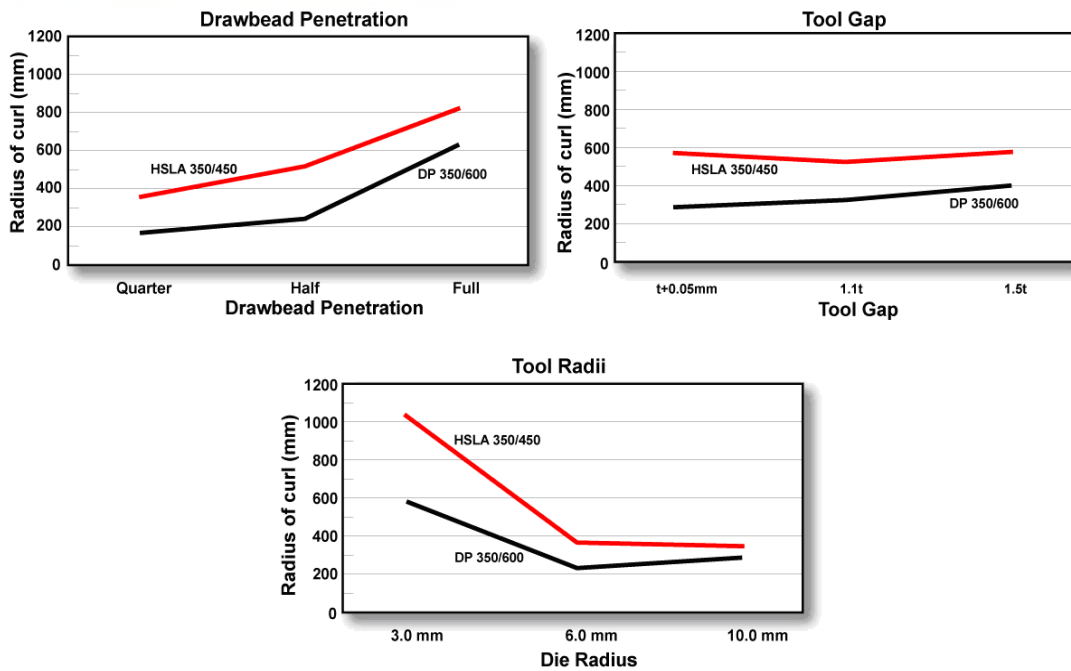


Figure 3.C-35B: The effect of tool parameters in sidwall curl. Higher values of radius of curl are better.^{S-3}

Guidelines for Form Die

- Set-up the die to allow for appropriate over-bend on sidewalls.
- Equalize the depth of forming as much as possible.
- Use a post-stretch for channel-shaped stampings. For less complex parts, one form die should be sufficient. For more geometrically complex parts, the first die will form the part with open sidewalls. The second die will finish the form in a restrike die with post-stretch of the sidewalls. Part geometry will determine the required forming process.
- Some complex parts will require a form die with upper and lower pressure pads. To avoid upstroke deformation of the part, a delayed return pressure system must be provided for the lower pad. When a forming die with upper pad is used, sidewall curl is more severe in the vertical flange than in the angular flange.
- Provide higher holding pressure. DP 350/600 requires a force double that needed for Mild steel.
- When using form dies, keep a die clearance at approximately 1.3t to minimize sidewall curl. Die clearance at 1t is not desirable since the sidewall curl reaches the maximum at this clearance.
- Do not leave open spaces in the die flange steels at the corners of the flanges. Fit the radius on both sides of metal at the flange break. Spank the flange radius at the bottom of the press stroke.
- Bottom the pad and all forming steels at the bottom of the press stroke.

- Design the punch radius as sharp as formability and product/style allow, while considering the limitations for AHSS. Figure 3.C-36 illustrates how the springback angle is reduced with smaller bend ratios, and is acceptable with conventional steel. The biggest concern with sharp radii on AHSS, however, is the local formability failure mode called shear fracture. Inside product feature radii should be a minimum of 3T for any AHSS at 590 or above. Die radii at draw beads, punch openings, etc., where the material is pulled under tension over a radius should be at least 5T for any AHSS over 590 and radius to thickness ratios may be even greater as strength levels continue to increase, roll forming excluded. To avoid problems due to specifying the wrong AHSS grade for the wrong application, bend test and HET data should be used in conjunction with close communication with the steel supplier when selecting the proper die radius for the intended AHSS material. In addition, sharp radii contribute to excessive thinning at the tangent to the radius when global formability failures are of concern.

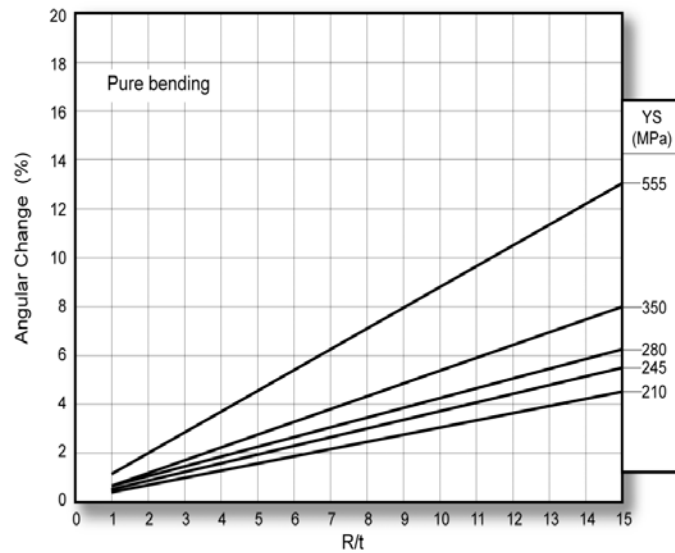


Figure 3.C-36: Angular changes are increased by YS and bend radius to sheet thickness ratio.^{S-2}

- To avoid problems due to specifying the wrong AHSS grade for the wrong application, bend test and HET data should be used in conjunction with close communication with the steel supplier when selecting the proper die radius for the intended AHSS material. In addition, sharp radii contribute to excessive thinning at the tangent to the radius when global formability failures are of concern.
- Curved parts with unequal length sidewalls in the fore-aft direction will develop torsional twist after forming. The shorter length wall can be under tension from residual forming stresses. Torsional twist is more pronounced with the higher strength steels. Conventional guidelines for normal steels can also be applied to AHSS to avoid asymmetry that accentuates the possibility for part twist. However, the greater springback exhibited by AHSS means extra caution should be taken to ensure symmetry is maintained as much as possible.
- Inner and outer motor-compartment rails also require an optimized cross-sectional design for AHSS applications. Sketch A in Figure 3.C-37 shows a typical rectangular box section through the inner and outer rails. This design will cause many problems for production due to sidewall curl and angular change. The hexagonal section in sketch B will reduce sidewall curl and twist problems, while permitting over-bend for springback compensation in the stamping dies.
- Springback computer simulations should be used whenever possible to predict the trend of springback and to test the effectiveness of solutions.

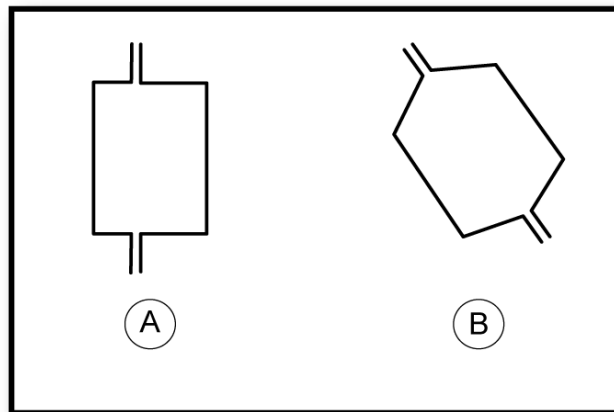


Figure 3.C-37: Changing rail cross section from A to B reduces springback problems with AHSS.^{N-3}

- Design the part and tool in such a way that springback is desensitized to variations in material, gauge, tools and forming processes (a robust system and process) and that the effects of springback are minimized rather than attempt to compensate for it.

C. Lock in the Elastic Stresses

- Where part design allows, mechanical stiffeners can be inserted to prevent the release of the elastic stresses and reduce various forms of springback. However, all elastic stresses not released remain in the part as residual or trapped stresses. Subsequent forming, trimming, punching, heating, or other processes may unbalance the residual stress and change the part shape. Twist also can be relieved by adding strategically placed vertical beads, darts, or other geometric stiffeners in the shorter length wall to equalize the length of line. Examples of various methods utilized to lock in elastic stresses to control springback can be seen in Figures 3.C-38 thru 3.C-42.

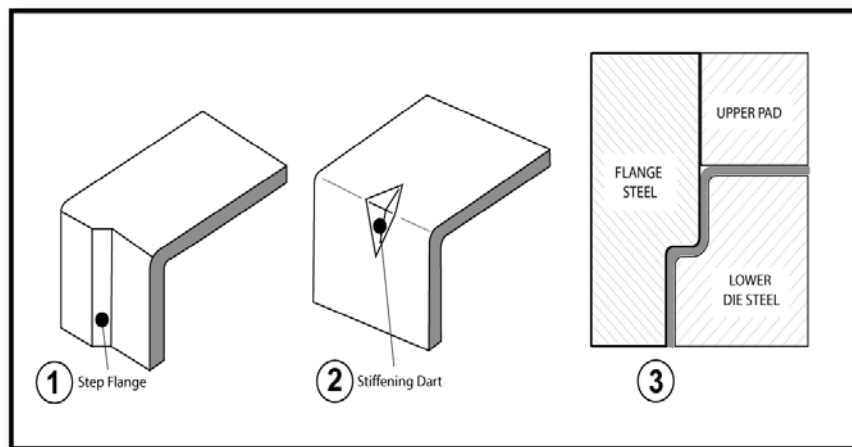


Figure 3.C-38: Mechanical stiffeners can be used to lock in the elastic stresses and the part shape.^{A-2}

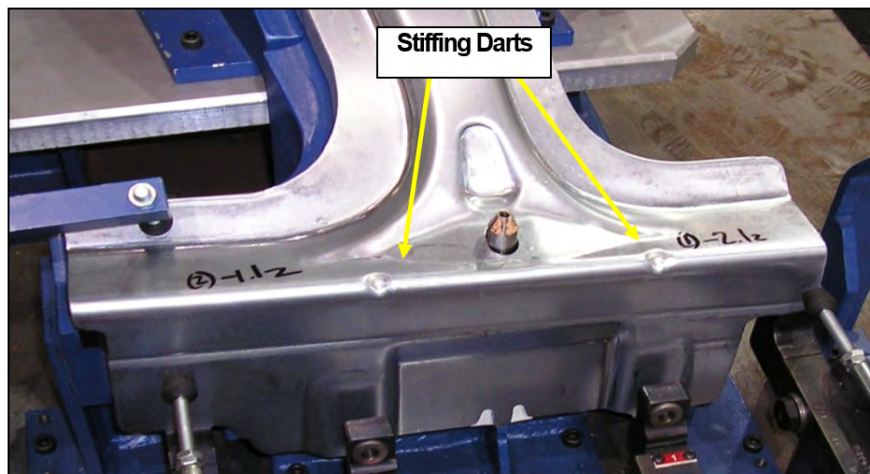


Figure 3.C-39: B-pillar where stiffening darts were added to help control springback.^{M-5}

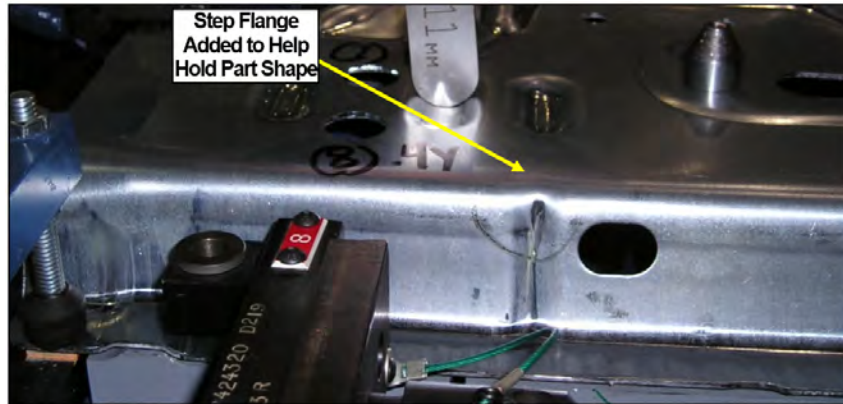


Figure 3.C-40: Step flange added to lock in elastic stresses on a draw wall. Figure 3-139A – The effect of tool parameters in angular change. The lower values are better.^{M-5}

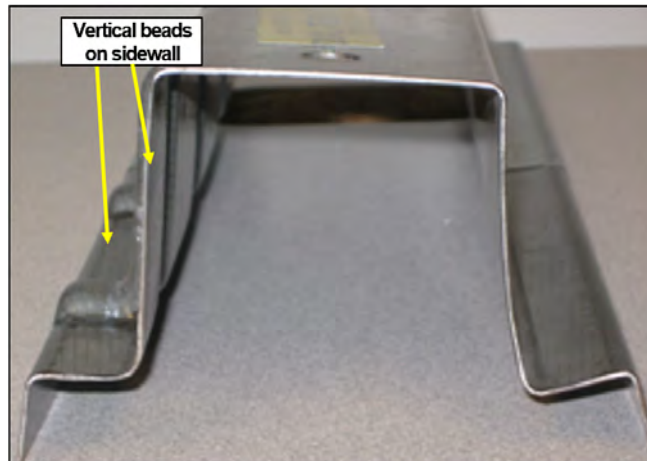


Figure 3.C-41: Hat section with vertical beads on one sidewall and a flat sidewall on the other side of the part. Springback/sidewall curl is noticeably less pronounced on the side with the vertical beads.^{M-7}



Figure 3.C-42: DP600 front rail upper reinforcements with vertical beads designed into the part geometry to help control springback.

3.C.3.e Key Points

- Angular change and sidewall curl escalate with increasing as-formed yield strength and decrease with increasing material thickness.
- For equal yield strengths, DP steels exhibit more angular change and sidewall curl than conventional HSLA steels. The springback behaviours of TRIP steels are between DP and HSLA steels.
- The sidewall curl appears to be more sensitive to the material and set-up in a channel draw test.
- The angular change decreased with smaller tooling radii and tool gap, but sidewall curl showed mixed results for smaller tooling radii and tool gap. Both angular change and sidewall curl were reduced with a larger drawbead restraining force but shear fracture becomes a concern when increasing restraining force and decreasing radii at the same time.
- Numerous process modifications are available to remove (or at least minimize and stabilize) the different modes of springback found in channels and similar configurations.

3.C.4. Blanking, Shearing, and Trim Operations

3.C.4.a. General Comments

AHSS exhibit high work hardening rates, resulting in improved forming capabilities compared to conventional HSLA. However, the same high work hardening creates higher strength and hardness in sheared or punched edges. In addition, laser cutting samples will also lead to highly localized strength and hardness increases in the cut edge. In general, AHSS can be more sensitive to edge condition because of this higher strength. Therefore, it is important to obtain a good quality edge during the cutting operation. With a good edge, both sheared and laser cut processes can be used to provide adequate formability.

To avoid unexpected problems during a program launch, production intent tooling should be used as early in the development as possible. For example, switching to a sheared edge from a laser-cut edge may lead to problems if the lower ductility, usually associated with a sheared edge, is not accounted for during development.

3.C.4.b. Trim Blade Design & Blanking Clearances

Cut, sheared, punched or trimmed sheet metal edges have reduced stretchability. All these processes generate a zone of high work hardening and a reduced n-value. This work hardened zone can extend one-half metal thickness from the cut edge. Therefore, the allowable edge stretchability is less than that predicted by the various forming limit curves. The DP and TRIP steels have islands of martensite located throughout the ferritic microstructure, including the shear zones. These hard particles act as crack initiators and further reduce the allowable edge stretch. These problems are minimized by using laser, EDM or water jet cutting devices that minimize the work hardening and loss of n-value.

Steel company research centers are conducting studies to improve the cutting process by modifying the cutting tool. One program^{S-9} evaluated the design of the punch. Instead of the traditional flat bottom punch, a bevelled design was used. Their conclusion stated the optimized bevel angle was between 3 and 6 degrees, the shear direction was parallel the rolling direction of the coil and a bevel clearance of 17% was used. The maximum shearing force was significantly reduced and the hole expansion ratio increased by 60% when compared to conventional flat punching process. These problems are increasing as the AHSS grades continue to become stronger.

Multiple studies have examined the trimmed edge quality based on various cutting conditions. These conditions included different clearances, shear angles, and rake angles on mechanical shearing operations as well as clearances on slitting operations. Laser cut, water jet cut and milled edges were also examined. A typical mechanically sheared steel edge has 4 main zones – rollover, burnish, fracture and burr (see Figure 3.C-43). Laser cutting, water jet cutting, EDM and milling are a different story as cold working is not the issue with these processes.

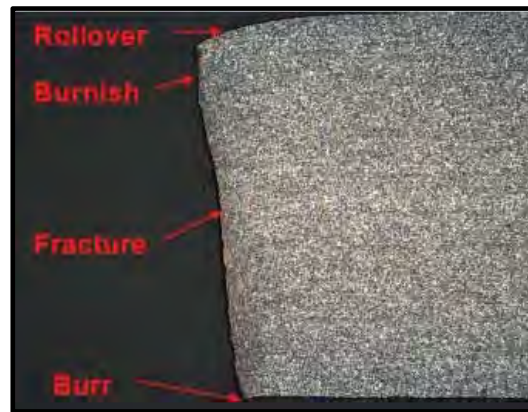


Figure 3.C-43: Cross section of a punched hole of DP780 showing the 4 main zones of a typical sheared edge.^{M-5}

Conventional mild and HSLA steels have historically used burr height as the main measure of edge quality. The typical practice: maintain burr height below 10% of metal thickness and slightly larger for thicker steel. This is because as burr height exceeds 10%, the trim steels need to be sharpened or

replaced, or clearances need to be changed. Greater burr height is associated with additional cold working and creates stress risers that can lead to edge splitting. These splits, however, are global formability related failures where the steel thins significantly at and around the split, independent of the local formability edge fractures associated with AHSS. Figure 3.C-44 shows a conventional BH210 steel grade liftgate with an excessive burr in the blank that led to global formability edge splitting in the draw die.



Figure 3.C-44: Excessive burr on blank (top) and a global formability split on the formed liftgate (bottom) due to excessive work hardening. Dull trim steels were the cause of this condition. ^{M-8}

Due to their progressively higher yield and tensile strengths, AHSS grades experience less rollover and smaller burrs (to be discussed in Section 3.C.2.c – Tool Wear, Clearances and Burr Height). They tend to fracture with very little rollover or burr. As such, detailed examination of the actual edge condition under various cutting conditions becomes more significant with AHSS as opposed to measuring burr height alone to determine edge quality. Multiple studies have been conducted to microscopically examine the actual sheared edges under various trimming conditions. Additionally, microstructural analysis and microhardness testing has been conducted to examine the work hardening effect after being cold worked. It was found that the ideal condition to combat local formability edge fractures for AHSS was to have a clearly defined burnish zone with a uniform transition to the fracture zone.

The fracture zone should also be smooth with no voids, secondary shear or edge damage (see Figure 3.C-45 for photos of an optimal edge condition). If clearances are too small, secondary shear can occur and the potential for voids due to the multiphase microstructure increases (see Figure 3.C-46 for edge with secondary shear due to small trim steel clearance).

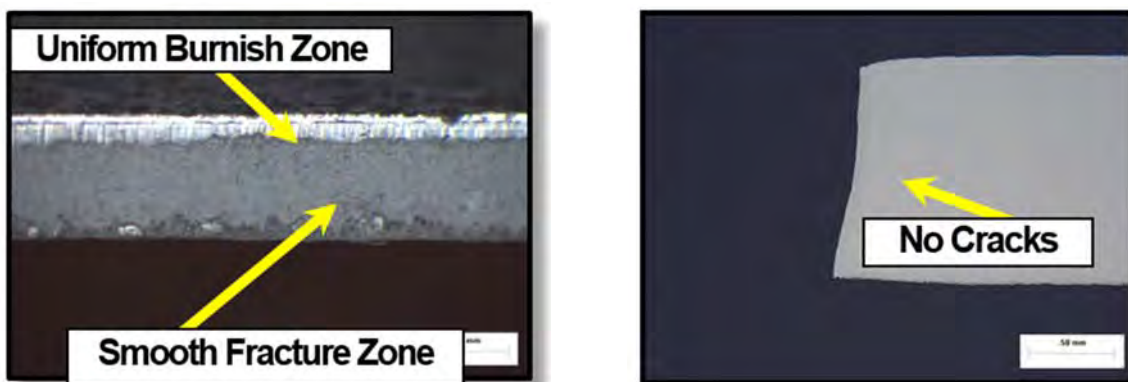


Figure 3.C-45: Ideal sheared edge with a distinct burnish zone and a smooth fracture zone (left) and a cross section of the same edge (right).

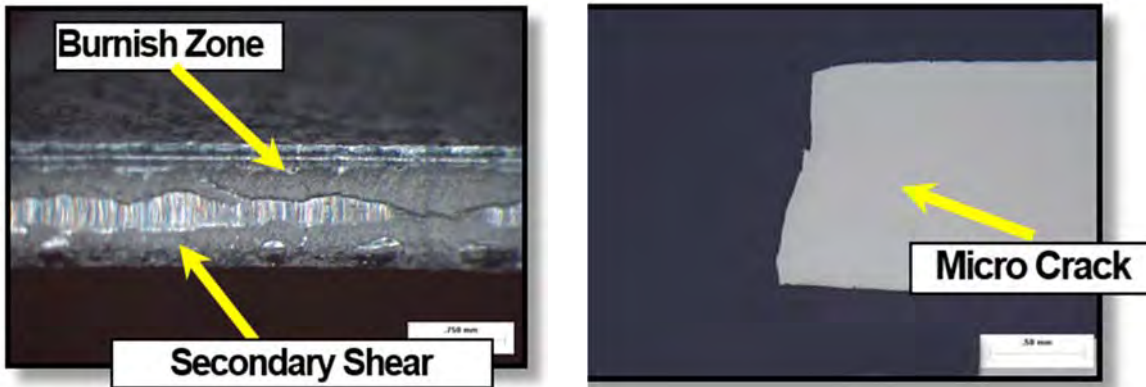


Figure 3.C-46: Sheared edge with the trim steel clearance too small (left) and a cross section of the same edge (right) showing a micro crack on the edge. This edge has what is called secondary shear due to the tight clearance and increases the odds that edge fracture will occur.

Clearances that are too large create additional problems that include excessive burrs and voids. A non-uniform transition from the burnish zone to the fracture zone is also undesirable. These non-ideal conditions create propagation sites for edge fractures. HET results and 2D tension test results show a strong correlation between edge condition, HER and percent elongation results. Microstructural analysis of blanked edges, trimmed edges and slit edges should be conducted on a routine basis to assess the edge condition, particularly after die sharpening, tooling modifications, die repair and set-up.

There are multiple causes for a poor sheared edge condition. They include, but are not limited to, the die clearance being too large or too small, a cutting angle that is too small, worn, chipped, or damaged tooling, improperly ground or sharpened tooling, improper die material, improperly heat treated die material, improper (or no) coating on the tooling, misaligned die sections, worn wear plates and out of level presses or slitting equipment. The higher loads required to shear AHSS with increasingly higher tensile strength also creates additional deflection of dies and processing equipment. Clearances measured under a static condition may change once the die, press or slitting equipment is put under load due to this deflection. As a large percentage of presses, levellers, straighteners, blankers and slitting equipment were designed years ago, the significantly higher loads required to process today's AHSS may exceed equipment beyond their design limits, dramatically altering their performance.

Figure 3.C-47 shows an edge fracture on a DP980 rocker panel. This panel experienced edge fractures during production, occurring in embossments along the edge of the part, with no evidence of necking at the fracture site. This is a classic local formability failure, reinforcing the need to closely inspect the conditions at the fracture zone of AHSS to determine whether the root failure is global or local formability. Process and die solutions are quite different based on the mode of failure.

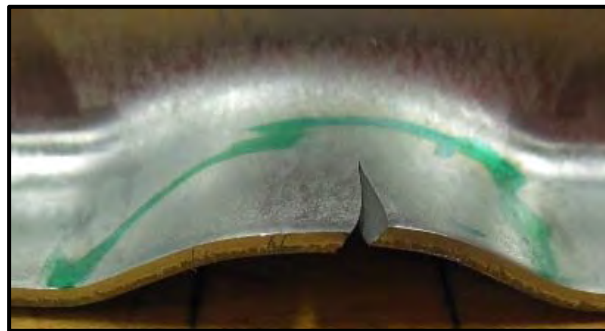


Figure 3.C-47: Classic local formability relates edge fracture on an embossment on a DP980 part..^{M-7}

This part was a typical rocker panel – a long rectangular hat section. The master coil was slit into several narrower coils (mults) before being shipped to the stamper and only a few coils experienced edge fractures, but all along the slit edge. Understanding that edge condition is critical with respect to multiphase AHSS, the edge condition of the “good” mults and the “bad” mults were examined under magnification. Figure 3.C-48 shows a photo of the slit edge on a lift of blanks that ran with no edge fractures. As can be seen, the edge condition has a uniform burnish zone with a uniform transition to the smooth fracture zone. Figure 3.C-49, however, shows a photo of the slit edge of a lift of blanks from the same coil that experienced 100% edge fracture at the embossments. This edge exhibits secondary shear as well as a thick burnish zone with a non-uniform transition from the burnish zone to the fracture zone.

A key learning is that maintenance of key process variables (such as clearance, tool condition) is critical to achieving long-term edge stretchability.



Figure 3.C-48: Slit edges on a lift of blanks that successfully produced DP980 rocker panels. Note the uniform transition from the burnish zone to the fracture zone with a smooth fracture zone as well. ^{M-7}

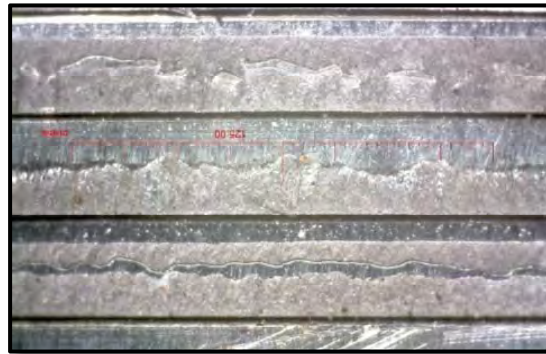


Figure 3.C-49: Slit edges on a lift of blanks from the same master coil that experienced edge fractures on all embossments on the edge of the part. Note the obvious secondary shear as well as the thicker, non-uniform transition from the burnish to the fracture zone. ^{M-7}

3.C.5. Computerized Die Tryout (Virtual Forming)

3.C.5.a. Short Explanation of Process

Using software to evaluate sheet metal formability has been in industrial use (as opposed to university and research environments) for more than a decade. The current sheet metal forming programs are part of a major transition to virtual manufacturing that includes analysis of welding, casting solidification, moulding of sheet/fibre compounds, automation, and other manufacturing processes.

Computer simulation of sheet metal forming is identified more correctly as computerized forming-process development or even computerized die tryout. The more highly developed software programs closely duplicate the forming of sheet metal stampings as they would be done physically in the press shop.

For conventional steels, these programs have proven to be very accurate in blank movement, strains, thinning, forming severity, wrinkles, and buckles. Prediction of springback generally provides qualitatively helpful results. However, the magnitude of the springback probably will lack some accuracy and will depend highly on the specific stamping, the input information, and user experience.

Traditionally the software uses the simple power law of work hardening that treats the n-value as a constant. For use with AHSS, the codes should treat the n-value as a function of strain. Most commercial software now can process the true stress-true strain curve for the steel being evaluated without the need for a constitutive equation. However, this capability is not present in some proprietary industrial and university software, and caution must be taken before using it to analyze AHSS stampings.

3.C.5.b. Advantages for AHSS Forming

Computerized forming-process development is ideally suited to the needs of current and potential users of AHSS. A full range of analysis capabilities is available to evaluate AHSS as a new stamping analysis or to compare AHSS stampings to conventional Mild steel stampings. These programs allow rapid what-if scenarios to explore different grades of AHSS, alternative processing, or even design optimization.

The potential involvement of software-based AHSS process development is shown in Figure 3.C-50. At the beginning of the styling to production cycle, the key question is whether the stamping can even be made. With only the 3D-CAD file of the final part and material properties, the One-Step or Inverse codes can rapidly ascertain strain along section lines, thinning, forming severity, trim line-to-blank, hot spots, blank contour, and other key information.

During selection of process and die design parameters, the software will evaluate how each new input not only affects the outputs listed in the previous paragraph, but also will show wrinkles and generate a press-loading curve. The most useful output of the analysis is observing (similar to a video) the blank being deformed

into the final part through a transparent die. Each frame of the video is equivalent to an incremental hit or breakdown stamping. Problem areas or defects in the final increment of forming can be traced

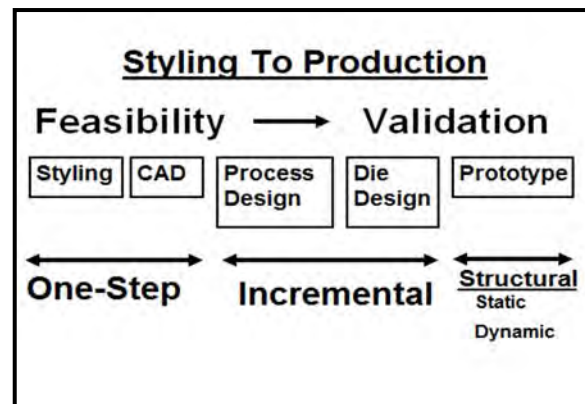


Figure 3.C-50: Schematic showing utilization of computerized forming-process development to assist in forming stampings from AHSS.

backwards through the forming stages to the initiation of the problem. The most comprehensive software allows analysis of multi-stage forming, such as progressive dies, transfer presses, or tandem presses. The effects of trimming and other offal removal on the springback of the part are documented.

Since many applications of AHSS involve load bearing or crash analyses, computerized forming-process development has special utilization in structural analysis. Previously the part and assembly designs were analysed for static and dynamic capabilities using CAD stampings with initial sheet thickness and as-received yield strength. Often the tests results from real parts did not agree with the early analyses because real parts were not analysed. Now virtual parts are generated with point-to-point sheet thickness and strength levels nearly identical to those that will be tested when the physical tooling is constructed. Deficiencies of the virtual parts can be identified and corrected by tool, process, or even part design before tool construction has even begun.

Many of these virtual forming codes are designed to evaluate the properties of AHSS. The actual **true** stress-strain curve must be entered into the simulation instead of a constitutive equation with a single n -value. Closer interaction with the steel supplier is required to obtain the exact properties of the type and grade to be supplied. The exact properties of TRIP steel can be difficult to determine as they change with strain path, temperature, amount of deformation, and other factors during forming. Although these virtual forming tools are good at predicting global formability related failures, they presently struggle to accurately predict local formability related failures such as edge and shear fracture. A major advantage of virtual forming tools is the ability to conduct Design of Experiments (DOE). In the physical press shop DOE's are very difficult to run on actual tooling. They require an excessive amount of time, are limited to very few variables, need to grind and weld tooling, and require different grades on metal to study effect of variable changes. In the virtual press shop all the variables can be changed with a stroke of the keyboard – none of the restrictions apply. Some codes use Monte Carlo variations. In one case study, the variations showed 85% of the time parts to print would be made. However, certain combinations of variables would cause 15% failures over the span of the run.

The main advantage of virtual forming codes is the opportunity to design and do die tryout on the computer before the first hard die is cut. Waiting to test out the viability of the part design, process, and die design until all the hard dies have been machined and inserted into the press has a major disadvantage. All the mating parts (usually from other suppliers) probably have already been made and approved. If your part does not work and requires major redesign, all the mating parts may already have blocked all your options. Running all the parts in the virtual world at the same time and comparing compatibility is a big step forward for the press shops and the final assembly station. The virtual press shop is even more important for AHSS because their higher strengths reduce the size of the formability window.

The codes generally can generate qualitative corrections for springback but not exact quantitative answers. The prime reason for this restriction is the lack of accurate data values to input into the computer. A prime example is a coefficient of friction. Depending on surface topography, localized tool pressure, amount of deformation, heat, and many other factors affecting the steel's status, the coefficient of friction not only varies from point to point on the stamping but changes during the forming process. A single coefficient of friction does not accurately describe its contribution to the springback process.

Actual case studies of automotive stampings can be found in the Auto/Steel Partnership Case Studies, which include virtual forming analysis as part of their stamping analyses, modifications, and Lessons Learned.

3.C.5.c. Key Points

- The virtual press shop allows one to create the stamping and die design without machining the first piece of die.
- A virtual tryout can detail areas of severe forming, buckles, excessive blank movement, and other undesirable deformation.
- Virtual forming codes cannot accurately predict local formability failures such as edge and shear fracture.
- Alternative “What-if” scenarios can be quickly explored with quick clicks on the keyboard – not hours of grinding and welding on a physical hard die.
- Mentally determining the outcome of the interaction of 30 or more inputs to the forming system is impossible. Understanding steels such as DP and TRIP that change properties when deformed under different forming conditions is even worse. The virtual forming codes are able to process this data to show how the final product will react.
- Observing the stamping being formed in a transparent die is a valuable troubleshooting tool provided by virtual forming.
- The virtual forming codes do not accurately predict springback or the success of springback correction procedure because of the lack of accurate data everywhere in the stamping during the entire forming operation. However, users report reduction in recuts of the die from 12 or more to 3 or 4 based on information from the code.
- Design of Experiments (DOE) studies are very limited in the physical press shop because of the large number input changes required by the process. Virtual forming makes the changes and computations at computer speed.

3.C.6. Press Requirements

3.C.6.a. Servo Presses^{A-10}

AHSS products have significantly different forming characteristics and these challenge conventional mechanical and hydraulic press forming. Some forming characteristics associated with AHSS products that differ from their conventional draw-quality, low-carbon steel counterparts include:

- Lower formability/ductility
- Variations in through-coil properties
- Difficulty in local formability fracture predictions (conventional mild, IF, BH and HSLA fracture mechanics do not apply well with AHSS).
- Higher forming loads
- High contact pressures cause higher temperatures at die-steel interface, requiring high performance lubricants and tool steel inserts with advanced coatings
- Increased springback

These challenges lead to issues with the precision of part formation and stamping line productivity. The stamping industry is developing more advanced die designs as well as advanced manufacturing techniques to help reduce fractures and scrap associated with AHSS stamped from traditional presses. A servo driven press is a significant option that has promising results when forming AHSS and correcting the above issues.

Characteristics of Servo Presses

A servo press is a press machine that uses a servomotor as the drive source. The advantage of the servomotor is that it can control both the position and speed of the output shaft compared a constant cycle speed. In conventional mechanical presses, the press cycles at constant speed and press loads develop slowly, building power to their maximum force at bottom dead center (180-degree crank), and then they reverse direction. In comparison, the servo press uses software to control press speed and position, which is much more flexible.

Servo presses have a closed-loop feedback system to more accurately control cycle rate and loads, hence delivering a key advantage, which is the application of very high forming loads early in the stamping stroke. New forming techniques have been developed utilizing these features, and automakers are finding that with the use of the servo press, more complex part geometries can be achieved while maintaining dimensional precision.

Servo presses have only been around for about 10 to 15 years, and so are considered “new technology” for the automotive industry. Recent growth in the use of servo presses in the automotive manufacturing industry parallels the increased use of AHSS in the structure of new automobiles.

There are multiple variations of the servo press, such as mechanical servo press where the power of the motor is delivered by a rotating mechanism such as a crank, or by a direct drive mechanism as with a ball screw. There also is a hydraulic servo press where the power of the motor is delivered by way of hydraulic pressure. The high-powered servo motor allows for direct driving of the mechanical press without using a flywheel and clutch. The fundamental driving mechanisms remain the same as

conventional presses. A cut-away of a servo press is shown below in Figure 3.C-51 to give a better understanding on the servo mechanism.

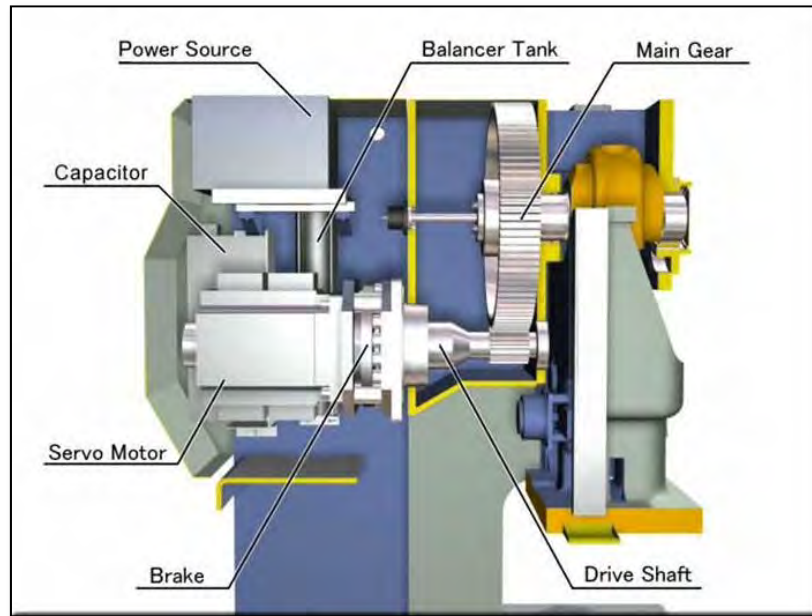


Figure 3.C-51: The Servo Press Cut-away ^{A-9}

Types of Servo Presses

1) Servo motor and ball screw driven press: These servo presses employ ball screws to reduce the friction on the screws. Unlike traditional screw presses, this press does not require a clutch/flywheel and the slide velocity can be altered throughout forming. A notable feature of the ball screw type servo press is that the maximum force and slide speed are available at any slide position. This can be applied to almost all the forming methods. This capability proves to be very useful for forming with a long working stroke such as an extrusion, and for forming that requires a high-speed motion at the end of the formation.

The torque capacity of the servo motor, the load carrying capacity of the ball screw, and the reduction of the belt drive limit the maximum load. One solution to increase the power of the ball screw driven servo press is to increase the number of motors and driving axles (spindles). The only problem with this solution is the cost increases tremendously. Figure 3.C-52 shows a mechanism of hybrid servo press.

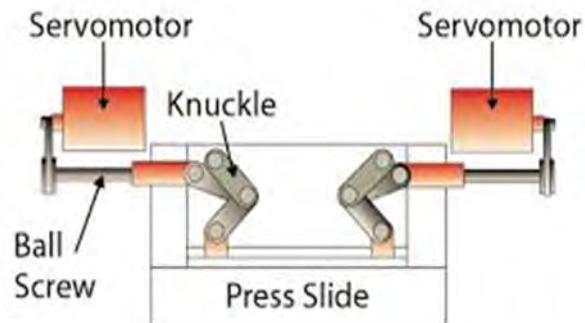


Figure 3.C-52: Operating mechanism of a hybrid servo press ^{M-5}

2) Servomotor driven crank press: This press provides a lower-cost alternative compared to ball screw style servo presses. Crank presses have a high torque servomotor directly attached to the press drive shaft. A few press manufacturers developed c-Frame presses, which combine the servo driving

mechanism with the conventional press structure. These presses are visually similar to mechanical presses, but the servo motor replaces the flywheel, clutch, and main motor. When the main shaft rotates at a constant speed, the stroke-time curve mirrors that of a conventional mechanical press. To increase power (for higher forming loads), crank presses are coupled with two connecting rods.

3) Servomotor driven linkage press: Linkage mechanisms are often used for presses to reduce the slide velocity and increase the load capacity of a given motor torque near the bottom dead center. Servomotor driven linkage presses prove to be advantageous in increasing the approaching and returning speeds by slowing down the slide speed in the working region within the stroke. They also have the advantage of maintaining high load capabilities through a considerably long working stroke.

4) Hybrid servo press: The knuckle joint and the linkage mechanisms are used to increase the press power with the crank shaft mechanism, and they can be combined with the ball screw mechanisms for servo presses.

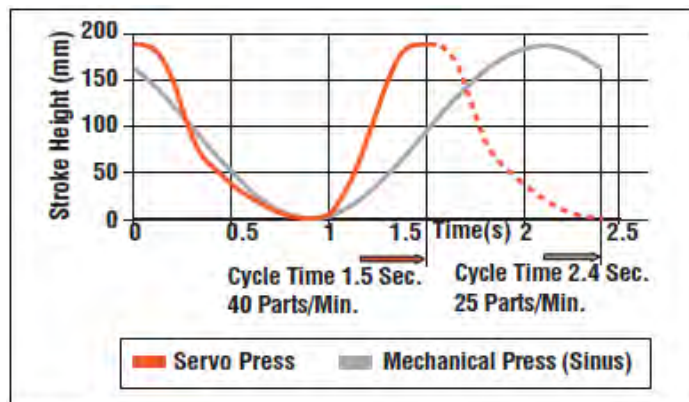
5) Servomotor driven hydraulic press: These hydraulic presses have been developed because the high-power servomotors achieve higher slide speed compared with the conventional servo press with flow control valves.

Advantages of Servo Presses

Servo press technology has many advantages compared to mechanical presses when working with AHSS materials. Press manufacturers and users claim advantages in stroke, speed, energy usage, quality, tool life and uptime; these of course are dependent upon part shape and forming complexity.

1) Adjustable Stroke: The servo press has an adjustable stroke; the slide motion can be programmed to exert the required press load for deep draw stampings and then switch to different program routines to allow for shallow part stampings, or even blanking. This makes the servo press very versatile.

2) Speed: Compared to a standard mechanical press, servo presses manufacturers claim up to 37% increased cycle rates, which translates into better stamping plant productivity. Figure 3.C-53 shows cycle rates for comparable stroke heights for both a servo press and a traditional mechanical press.



**Figure 3.C-53: Cycle Rates for Servo
and Mechanical Presses ^{M-5}**

3) Energy Savings: The servo press has no continuously driven flywheel, cutting the costs of energy consumption. This is especially true in large capacity presses. The installed motor power is greater than that of a mechanical press whose capacity is comparable. However, throughout the stamping operation, the servo-driven motor is used only while the press is moving since the servo press has no continuously driven flywheel. Also contributing to nominal energy savings is the dynamic braking operation of the servo driven motor. Through this operation, the braking energy is transferred back into the power system. It is also possible to install an external energy storage feature to make up for energy peaks while reducing the nominal power drawn from the local power supply system (in cases where it is economically justified).

Figure 3.C-54 shows a comparison between a servo press and a traditional mechanical press with respect to energy use and storage. In a servo press, energy from deceleration of the slide is stored in an external device and tapped when the press motion requires more than 235 HP for each motor. The stored energy (maximum of 470 HP) is thus used during peak power requirements, enabling the facility power load to remain nearly constant, around 70 HP.

4) Quality: Better forming stability translates into fewer part rejections.

5) Longer tool life: Decreasing the tool impact speed while reducing the cycle time at the same time reduces impact loading, thus maximizing tool life. Lubrication effectiveness has been observed, and using pulsating or oscillating slide motion can extend the working limit.

6) Uptime: Synchronized clutching and extended brake life allow for less frequent maintenance and better equipment uptime.

Slide Motion

Another key attribute (and advantage) of the servo press is the free motion of the slide. The slide of a servo press is capable of the following motions:

1) Reverse motion of the slide: The slide moves downward at a pre-set speed, and alternatively rises in the middle. After rising a bit, the slide then moves downward again, and the system repeats this motion. When the slide motion changes from downward to upward, the forming forces become negligible and the elastic deformation of dies and machine recover. This has the potential to mitigate “springback” that is associated with the forming of higher strength materials in traditional mechanical presses. By holding pressure at the bottom of the stroke, releasing the pressure and then reapplying it, multiple stamping hits can be made in just one cycle, setting the form of the product and eliminating the need for secondary operations.

2) Variable speed slide & acceleration/deceleration: The speed of the slide movement can be modified throughout the stroke. The touch speed of upper and lower dies can be decreased to avoid the impact, and after forming, the upward slide movement can change quickly. The slide speed in the forming stage can be accelerated, decelerated, or held constant as necessary. Through the use of these slide movements, the frictional characteristics between dies and blank sheet materials are expected to change, but these behaviors are not clear and are under further investigation.

3) Stationary function of the slide: The slide motion can be programmed to stop at bottom dead center. Leveraging this feature, coining pressure can be applied to the blank sheet steel at the bottom dead center to ensure shape and dimensional accuracy of the product formed.

4) Die cushion: Servo presses incorporate variable die cushion by numerical control. A pressure sensor within the servo die cushion (similar to that of a hydraulic cushion often used in mechanical presses) controls the position of the die cushion. This allows for the optimization of metal flow in the

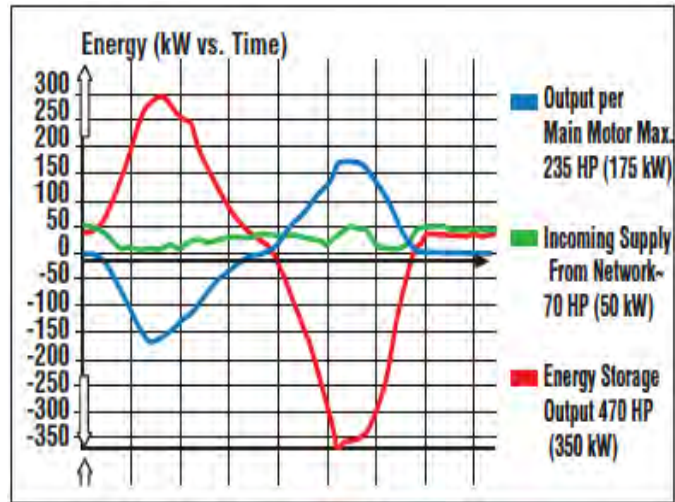


Figure 3.C-54: Energy vs. Displacement for Servo Press M-5

flange between the die and the blank holder. Additionally, servo-driven die cushions can also be used to regenerate energy when the cushion is pushed downward by the upper die and slide.

Figure 3.C-55 shows the difference between the motions of mechanical presses versus servo driven presses. Here the flexibility of controlling the slide motion is noted. The slide motion of the servo press can be programmed for: more parts per minute, decreased drawing speed to reduce quality errors, and dwelling or re-striking at bottom dead center to reduce springback.

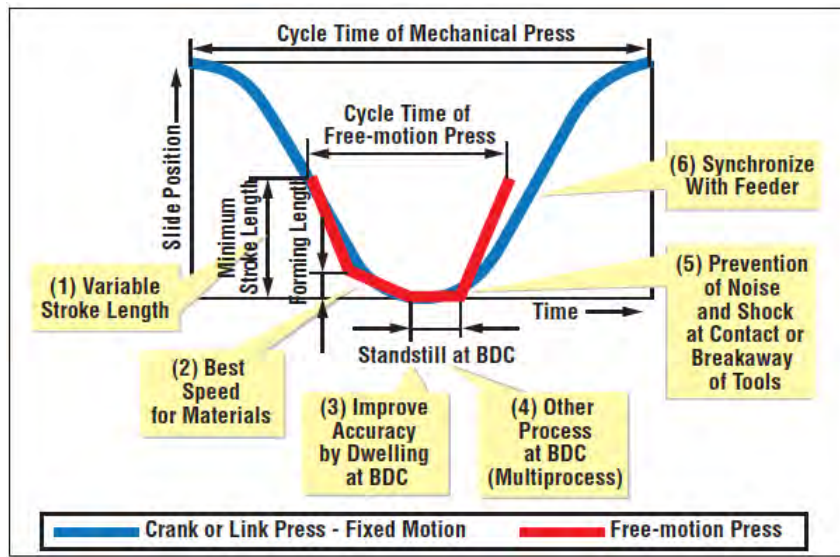


Figure 3.C-55: Comparison of Press Signatures ^{M-3}

In summary, the servo press has demonstrated advantages for the forming of complex geometries with AHSS products. Additionally, they show the potential for many business advantages, including more efficient energy utilization and enhanced productivity. Research studies are continuing to be conducted to explore the full potential of servo presses, providing robust applications with AHSS.

3.C.6.b. Force versus Energy

Both mechanical and hydraulic presses require three different capacities or ratings – maximum force, energy, and power. The most common press concern when forming higher strength steels is whether the press is designed to withstand the maximum force required to form the stamping. Therefore, press capacity (for example, 1000 kN) is a suitable number for the mechanical characteristics of a stamping press. Capacity, or tonnage rating, indicates the maximum force that the press can apply. However, the amount of force available depends on whether the press is hydraulic or mechanically driven. Hydraulic presses can exert maximum force during the entire stroke as their tonnage is generated via hydraulic fluid, pumps and cylinders. Mechanical presses exert their maximum force at a specific displacement usually measured at ½” above bottom dead center (BDC). At increased distances above bottom dead center, the press capacity is reduced due to the continued loss of mechanical advantage.

Figure 3.C-56 shows a typical press-force curve for a 600-ton mechanical press. As can be seen, when the press is approximately 3" off BDC the maximum tonnage rating is only 250 tons, not 600 tons. Air cushions and nitrogen cylinders are common on single action mechanical presses to give them a double action; the initial tonnage spikes up while the press is still several inches off BDC upon initial contact with the blankholder, and setting of the draw beads. This increases the chances of the mechanical press being damaged. Figure 3.C-57 shows the potential negative consequences when a mechanical press exceeds the rated capacity early in the press stroke.

Energy consumption inherent in sheet metal forming processes is related to the true stress-true strain curve and it depends on the yield strength and the work hardening behaviour characterized by the n-value. The energy required for plastically deforming a material (force times distance) corresponds to the area under the true stress-true strain curve. Figure 3.C-58 shows the true stress-strain curves for two materials with equal yield strength - HSLA 350/450 and DP 350/600. Many other true stress-true strain curves can be found in Figures 3.B-1 through 3.B-7.

The higher work hardening of the DP grade requires higher press loads when compared to the HSLA at the same sheet thickness. However, the use of AHSS is normally coupled with a reduced thickness for the stamping and the required press load would be decreased or compensated. The higher n-values also tend to flatten strain gradients and further reduce the peak strains. The required power is a function of applied forces, the displacement of the moving parts, and the speed. The energy rating of a press is also a function of applied press load and the distance through which the load is applied. For example, pushing 200 tons through 3" of deep drawing requires 600 in.-tons of energy. Changing the part to AHSS could require 500 tons of force working through the same 3" distance expending 1500 in.-tons of energy. Each stroke of the press will expend a given amount of energy, all of which needs to be replaced.

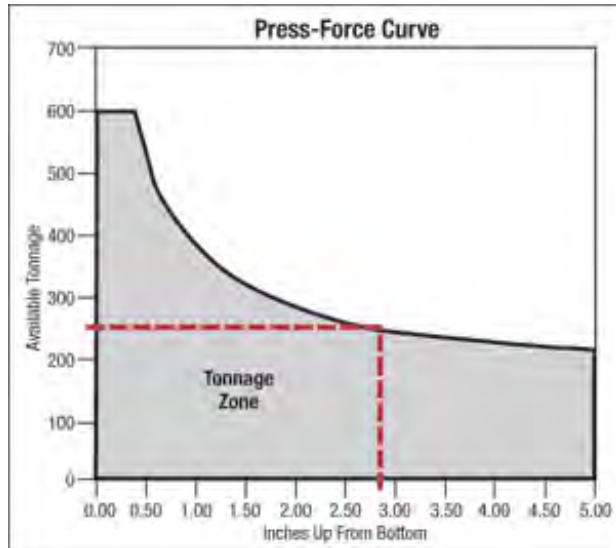


Figure 3.C-56: Schematic showing the maximum rated tonnage capacity of a 600 ton mechanical press based on the position of the slide compared to bottom dead center reference. ^{M-5}



Figure 3.C-57: Broken connecting rod on a mechanical press. ^{M-5}

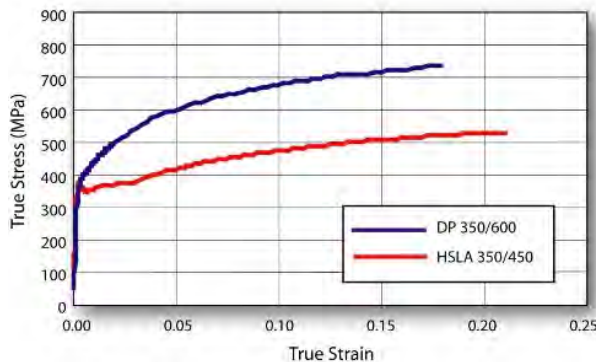


Figure 3.C-58: True stress-strain curves for two materials with equal yield strength. ^{T-3}

The size of the main motor, mass and rotation speed of the flywheel become critical. The main motor, along with its electrical connections, is the only source of energy for the press and it must have sufficient power to supply the demands of the stamping operation. As the flywheel is an energy storage device, it must be able to store and deliver the required energy when needed. The stored energy varies by the square of the speed; thus, a large amount of energy can be stored in the flywheel when the press is running at full speed. If using AHSS requires press speeds to slow down due to heat generation and formability concerns, insufficient energy requirements could lead to the press stalling. Figure 3.C-59 shows a press-energy curve for a 600-ton mechanical press. The graph illustrates how the available energy of the press diminishes to 25% of rated capacity when its speed is reduced from 24 strokes/min to 12 strokes/min.

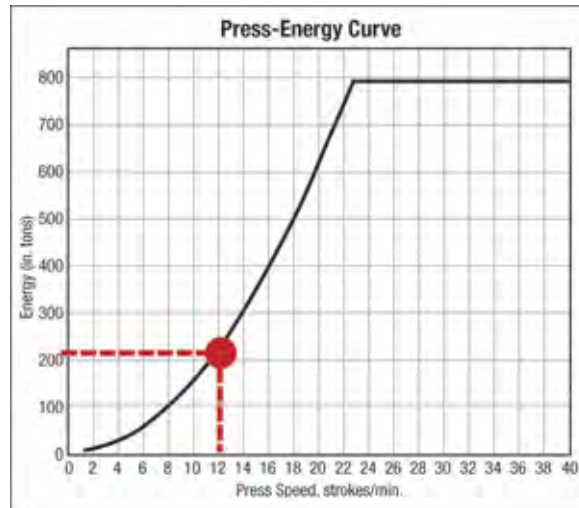


Figure 3.C-59: A press-energy curve for a 600 ton mechanical press.

Predicting the press forces needed initially to form a part is known from a basic understanding of sheet metal forming. Different methods can be chosen to calculate drawing force, ram force, slide force, or blankholder force. The press load signature is an output from most computerized forming-process development programs, as well as special press load monitors.

Example: Press Force Comparisons

The computerized forming process-development output (Figure 3.C-60) shows the press forces involved for drawing and embossing Mild steel approximately 1.5 mm thick, conventional HSLA, and DP 350/600. It clearly shows that the forces required are dominated by the embossing phase rather than by the drawing phase.

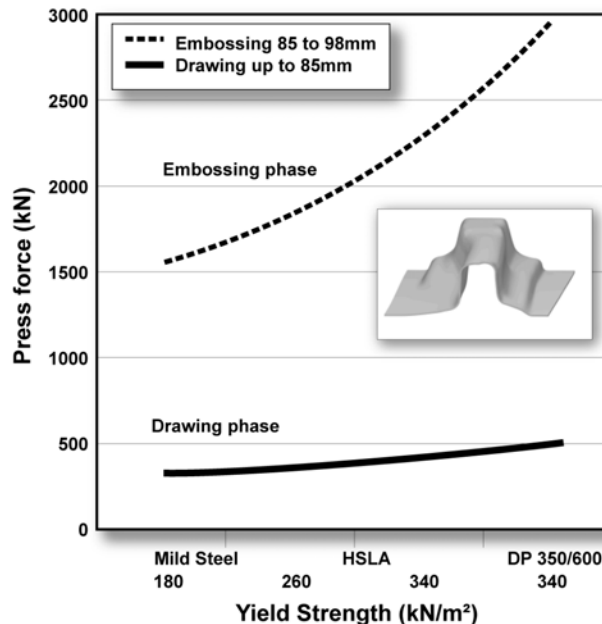


Figure 3.C-60: Data demonstrates that embossing dominates the required press force rather than the drawing force.^{H-3}

Sometimes the die closing force is an issue because of the variety of draw-bead geometries that demand different closing conditions around the periphery of the stamping.

Example: Press Energy Comparisons

A similar analysis (Figure 3.C-61) shows the press energy required to draw and emboss the same steels shown in Figure 3.C-60. The energy required is also dominated by the embossing phase rather than by the drawing phase, although the punch travel for embossing is only a fraction of the drawing depth.

3.C.6.c. Prediction of Press Forces Using Simulative Tests

Relative press forces from Marciniak stretching tests showed AHSS grades require higher punch forces in stretch forming operations (Figure 3.C-62). However, applying the stretch forming mode for CP grades is not common due to the lower stretchability of CP grades.

3.C.6.d. Extrapolation from Existing Production Data

Relationships between thickness and UTS can be used as a quick extrapolation calculation of press loads for simple geometries. Figure 3.C-63 shows the measured press loads for the production of a cross member with a simple hat-profile made of HSLA 350/450 and DP 300/500 steels of the same thickness.

Using the following equation, the press load F2 for DP 300/500 was estimated from the known press load F1 from HSLA 350/450, shown in Table 3.C-2.^{T-3}

F2 is proportional to (F1) x (t₂/t₁) x (R_{m2}/R_{m1})

Where:

- F1 Old Measured Drawing Force
- F2 New Estimated Drawing Force
- t₁ Old Material Thickness
- t₂ New Material Thickness
- R_{m1} Old Tensile Strength
- R_{m2} New Tensile Strength

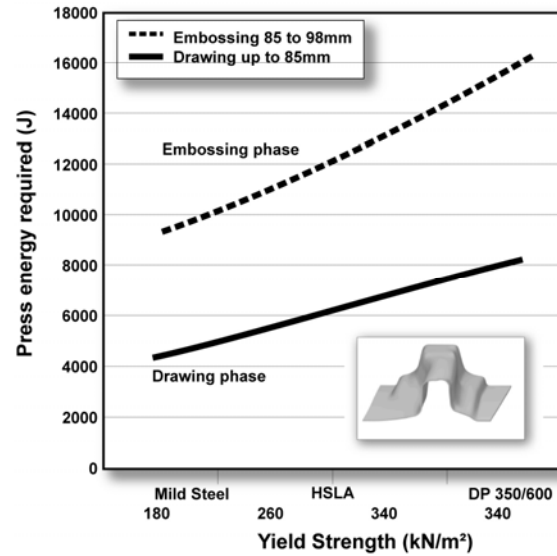


Figure 3.C-61: Data showing the energy required to emboss a component is greater than for the drawing component.^{H-3}

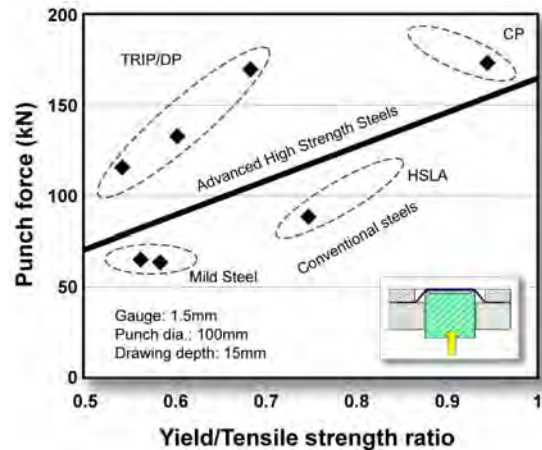


Figure 3.C-62: Punch forces from Marciniak cup-stretch forming tests for AHSS and conventional steel types.^{H-3}

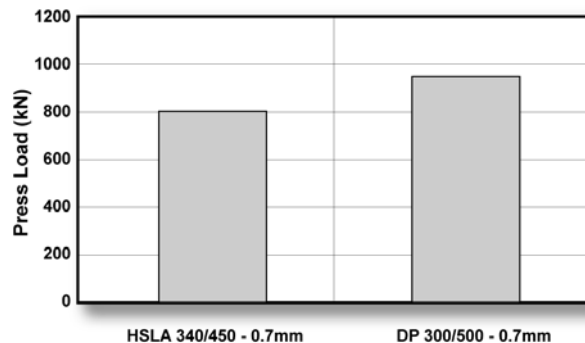


Figure 3.C-63: Measured press load for a Hat-Profile Cross Member.^{T-3}

**Table 3.C-2: Press load F2 estimated for DP 300/500 from the known press load F1
from HSLA 350/450**

Steel Type 33B	Thickness (mm) t	Measured Drawing Force [kN] F	UTS (approx.) (MPa) R _m	Estimated Drawing Force [kN]
1 = HSLA	0.7	F1 = 791	433	
2 = DP	0.7	934	522	F2 = 953

The data above compares the measured drawing force and the estimated drawing force for the DP 300/500 using the formula. A good correlation between measured and predicted drawing force was obtained. Although it is possible to estimate the drawing force using this extrapolation technique, the accuracy is rather limited and often overstates the load. Therefore, the calculation should be viewed as an upper boundary.

3.C.6.e. Computerized Forming-Process Development

Rules of thumb are useful to estimate press loads. A better evaluation of press loads, such as draw force, embossment force, and blank holding force, can be obtained from computerized tools. Many of the programs enable the user to specify all of the system inputs. This is especially important when forming AHSS because the high rate of work hardening has a major effect on the press loads. In addition, instead of using a simple restraining force on blank movement, analyses of the physical draw beads must be calculated.

Another important input to any calculation is the assumption that the tools are rigid during forming, when the tools deform elastically in operation. This discrepancy leads to a significant increase in the determined press loads, especially when the punch is at home position. Hence, for a given part, the draw depth used for the determination of the calculated press load is an important parameter. For example, if the nominal draw depth is applied, press loads may be overestimated. The deflection (sometimes called breathing) of the dies is accentuated by the higher work hardening of the AHSS.

Similarly, the structure, platens, bolsters, and other components of the press are assumed to be completely rigid. This is not true and causes variation in press loads, especially when physical tooling is moved from one press to another.

If no proven procedure for computerized prediction is available, validation of the empirical calculations is recommended. Practical pressing tests should be used to determine the optimum parameter settings for the simulation. Under special situations, such as restrike operation, it is possible that computerized analyses may not give a good estimation of the press loads. In these cases, computerized tools can suggest forming trends for a given part and assist in developing a more favourable forming-process design.

Most structural components include design features to improve local stiffness. Features requiring embossing processes are mostly formed near the end of the ram cycle. Predicting forces needed for such a process is usually based on press shop experiences applicable to conventional steel grades. To generate comparable numbers for AHSS grades, computerized forming process-development is recommended.

3.C.6.f. Case Study for Press Energy

The following study is a computerized analysis of the energy required to form a cross member with a hat-profile and a bottom embossment at the end of the stroke (Figure 3.C-64). Increasing energy is needed to continue punch travel. The complete required energy curves are shown in Figure 3.C-65 for Mild, HSLA 250/350, and DP 350/600 steels. The three dots indicate the start of the embossment formation at a punch movement of 85 mm.

The last increment of punch travel to 98 mm requires significantly higher energy, as shown in Figure 3.C-66. Throughout the punch travel however, the two higher strength steels appear to maintain a constant proportional increase over the Mild steel.

3.C.6.g. Setting Draw Beads

A considerable force is required from a nitrogen-die cushion in a single-acting press to set draw beads in AHSS before drawing begins. The nitrogen-die cushion may be inadequate for optimum pressure and process control. In some cases, binder separation may occur because of insufficient cushion tonnage, resulting in a loss of control for the stamping process and excessive wrinkling of the part or addendum.

The high impact load on the cushion may occur several inches up from the bottom of the press stroke. Since the impact point in the stroke is both a higher velocity point and a de-rated press tonnage, mechanical presses are very susceptible to damage due to these shock loads. Additional flywheel energy is dissipated by the high shock loads well above bottom dead center of the stroke.

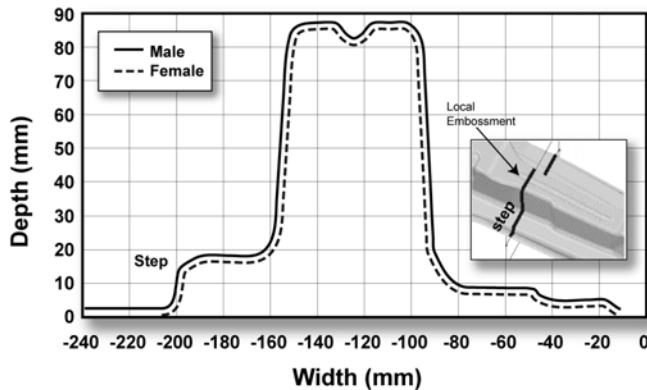


Figure 3.C-64: Cross section of a component having a longitudinal embossment to improve stiffness locally.^{H-3}

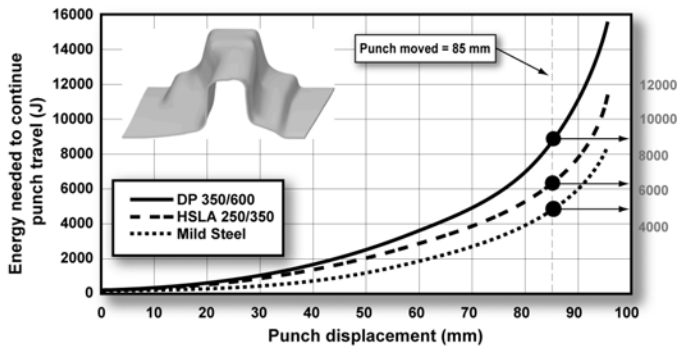


Figure 3.C-65: Computerized analysis showing the increase in energy needed to form the component with different steel grades. Forming the embossment begins at 85 mm of punch travel.^{H-3}

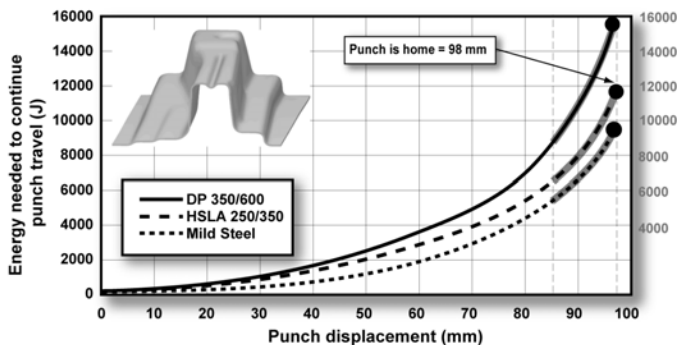


Figure 3.C-66: A further increase in energy is required to finish embossing.^{H-3}

Staggering the heights of the nitrogen cylinders so they do not all engage at the same time is one way to reduce the shock load (see Figure 3.C-67).



Figure 3.C-67: Staggered nitrogen cylinders designed to reduce the initial shock load when setting draw beads by engaging at different depths in the press stroke. ^{M-5}

A double-action press will set the draw beads when the outer slide approaches bottom dead center where the full tonnage rating is available and where the slide velocity is substantially lower. This minimizes any shock loads on die and press with resultant load spikes less likely to exceed the rated press capacity.

3.C.6.h. Key Points

- **Press loads are increased for AHSS steels primarily because of their increased work hardening and increased strength levels.**
- **More important than press force is the press energy required to continue production. The required energy can be visualized as area under the true stress–true strain curves.**
- **High forming loads and energy requirements in a typical hat-profile cross member with a strengthening bead in the channel base are due to the final embossing segment of the punch stroke compared to the pure drawing segment.**
- **DP 350/600 requires about twice the energy to form hat-profile cross member than the same cross member formed from Mild steel.**
- **While several punch force approximation techniques can be used for AHSS, the recommended procedure is computerized forming-process development.**

3.C.7. Straightening and Precision Levelling AHSS

The first operation when unwinding a coil is straightening to ensure flatness before further processing. There are two main types of equipment used to create a flat coil – a straightener and a precision leveller. In some respects, these two types of equipment are similar, but a precision leveller has additional capabilities.

Straighteners - All coils must be wound under tension to avoid “soft” or collapsed coils. As a result, tension and compression stresses are induced into the strip during the coiling process, and these can contribute to blank or part distortion in subsequent processes. Straighteners are designed to eliminate these stresses and create flat material; the objective is to relieve the residual stresses in the outer 20% of the strip. Straightening of coils is accomplished by bending the strip around a set of rolls to alternately stretch and compress the upper and lower surfaces of the steel to erase coil set or crossbow. Critical parameters include roll diameter, roll spacing, backup rolls, roll material type, gear design, backup rolls, overall system rigidity, and power requirements.

The higher the material's yield strength, the more force is required to relieve those residual stresses. Thus, equipment capability needs to be considered when processing AHSS products. Figure 3.C-68 shows a schematic of a straightener working the outer 20% of the steel strip.

Figure 3.C-69 depicts coil set and crossbow conditions.

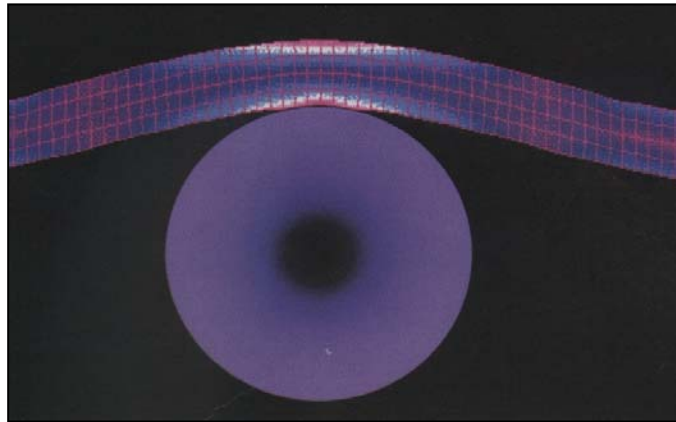
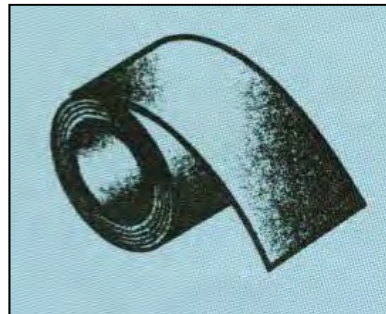
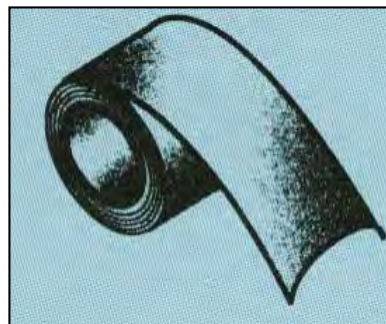


Figure 3.C-68: Schematic of a straightener roll working the outer 20% of the steel strip. ^{M-5}



Coil Set



Crossbow

Figure 3.C-69: Schematic of a coil with a coil set and crossbow conditions, that can be removed with a straightener. ^{M-5}

When utilizing a straightener, the two critical steel variables are the yield strength and the thickness. Straighteners have a series of rolls that progressively flex the strip to remove the residual stresses. These rolls have an entry and exit gap that need to be adjusted when thickness and yield strengths vary. Figure 3.C-70 shows a schematic of a typical set of straightener rolls required to obtain a flat strip. These gaps should be adjusted based on the yield strength and thickness of the material. Many equipment manufacturers have generated tables to guide the operator as to the best settings for various yield strength-thickness combinations.^{M-5}

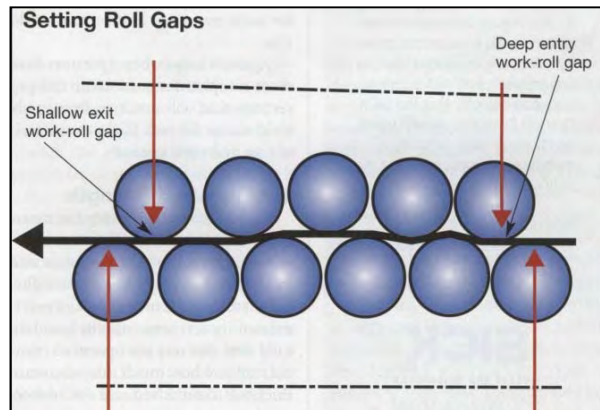


Figure 3C-70: Schematic of a set of straightener rolls indicating the 2 main adjustments – entry and exit gaps. ^{M-5}

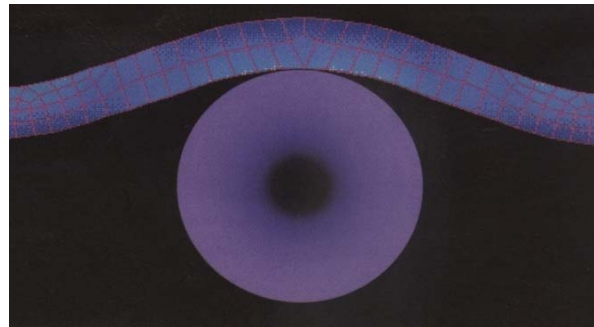


Figure 3.C-71: Schematic of a precision leveller roll working the outer 50% portion of a steel strip. ^{M-5}

Precision Levellers – Although precision levellers can perform all the functions of a straightener, they have additional capabilities. They can remove coil set and crossbow conditions and are capable of correcting other shape issues in coils that can create manufacturing problems in subsequent operations, for example, edge waves and center buckles.

Edge waves and distortion requires exceeding the yield strength of the steel strip at levels of 50% or more of the cross section of the strip and may increase the potential for work hardening the steel strip, negatively affecting formability. Figure 3.C-71 shows a schematic of a precision levelling roll working 50% of the cross section of the steel strip. This process can take out edge waves and center buckles if properly adjusted.

Design and Processing Implications

The progressively higher yield strengths for AHSS are challenging the capabilities of straighteners and precision levellers that were not designed for flattening these high strength materials. Equipment manufacturers have been studying and developing solutions to address this issue. There are a series of components related to the design of straighteners and precision levellers that need to be considered:

Roll Diameter – Straightener rolls for AHSS generally may need to be smaller in diameter than those used for mild steel, providing a smaller radius around which to bend the material. This is because AHSS must be bent more severely to exceed its higher yield strength.

Roll Spacing – Work roll center-spacing may need to be closer for AHSS than for comparable mild steels. Closer spacing means that more force is required to back-bend the material, requiring greater power for processing.

Roll Support – Larger journal diameters with larger radii and bearing capacity may be needed to withstand the greater forces and higher power required to straighten AHSS.

Roll Material – Higher strength materials and special heat treatment may need to be employed to insure rolls can withstand greater stresses for longer periods without experiencing fatigue failure.

Roll Depth Penetration – The upper rolls have to have enough travel to be able to penetrate the lower fixed rolls sufficiently in order to yield AHSS. This penetration may need to be as much as 50 to 60 percent greater than for mild steels.

Gear Sizes – Wider gear faces may be required as well as stronger outboard support of journals and idler shafts to produce higher gear power ratings required for flattening AHSS.

Gear Positioning – Closer roll center spacing requires higher power transmission and results in a smaller gear-pitch ratio, which reduces gear power ratings.

Gear Materials – Gears that drive the rolls should be produced from heat treated high strength materials to produce smooth running, chatter free roll drive for long life under high loads.

Given the greater force requirements for straightening AHSS, work roll deflection becomes a concern. Excessive work roll deflection results in undesirable side effects such as edge waves, increased journal stresses and premature gear failure. Backup rollers prevent excessive work roll deflection. Increased frame rigidity is also vital to ensuring the effectiveness of the backup rolls to prevent work roll deflection when processing AHSS. Equipment manufacturers have also developed design solutions that address processing of AHSS. As an example, several manufacturers have designed equipment with removable cartridges. These cartridges have different roll diameters, roll spacing, etc., and can be rolled in and out when switching from AHSS to conventional steels. This also allows for off-line roll cleaning and maintenance.

3.D. Die Surface Treatments and Lubrication

3.D.1. Die Surface Treatments

3.D.1.a. Surface Hardening vs. Surface Coating

Good tooling materials and high-performance die surface treatments are necessary to maximize tool life. Substrate hardening and/or surface coatings can be applied to manage wear, but with AHSS, the combination of these processes is desirable. A substrate treatment changes the physical structure of the base metal of the die. These “harden” the substrate to a certain depth, and normally require a re-treatment after a measured amount of production (number of hits) due to die wear. Examples include ion-nitriding, flame hardening, induction hardening, and furnace hardening. A surface coating adds a layer of material to the surface, in what is described as a non-metallurgical bond. Examples of surface coatings include chrome plating, physical vapor deposition and chemical vapor deposition.

Figure 3.D-1 shows the effect on surface hardness for more traditional surface treatments, including nitriding and chrome plating. ^{N-6} These have distinct advantages over non-treated dies, however they may still be ineffective against the heavy shear forces encountered when forming AHSS products.

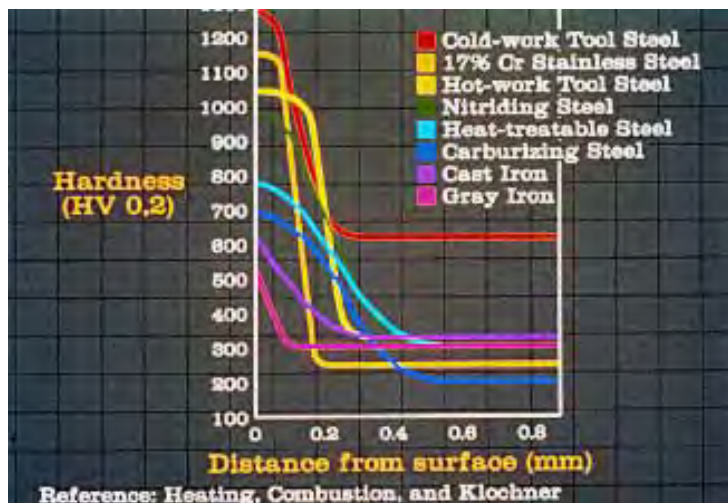


Figure 3.D-1: Punch hardness and surface depth for various surface treatments. ^{N-6}

Coatings are used to reduce friction between the blank sheet metal and the surface of the die and thus lower the shear forces that lead to unwanted wear on the die. They are applied on the tool substrate via micron-level thickness. The various coating processes are applied at various temperatures, ranging from ambient to very high temperatures.

Surface coatings are recommended for DP 350/600 and higher grades. When coatings are used, it is important that the substrate has sufficient hardness/strength to avoid plastic deformation of the tool surface - even locally. Therefore, a separate surface hardening, such as nitriding, can be used before the coating is applied. Before coating, it is important to use the tool as a pre-production tool to allow the tool to set, and to provide time for tool to adjust. Surface roughness must be as low as possible before coating. R_a values below $0.2 \mu\text{m}$ are recommended.

Physical vapor deposition (PVD) describes a variety of vacuum deposition methods that can be used to produce extremely thin films of a hard compound onto the die surface (See Figure 3.D-2). PVD uses a physical process, such as heating or sputtering, to produce a vapor of material, which is then

deposited on the object that requires the coating. Common industrial coatings applied by PVD are: titanium nitride (TiN), chromium nitride (CrN), and titanium aluminum nitride (TiAlN). The PVD process is conducted at relatively low temperature, which minimizes the risk of measurable die component shape variation (distortion) or surface oxidation. Deposition usually occurs between 210° C and 400° C.

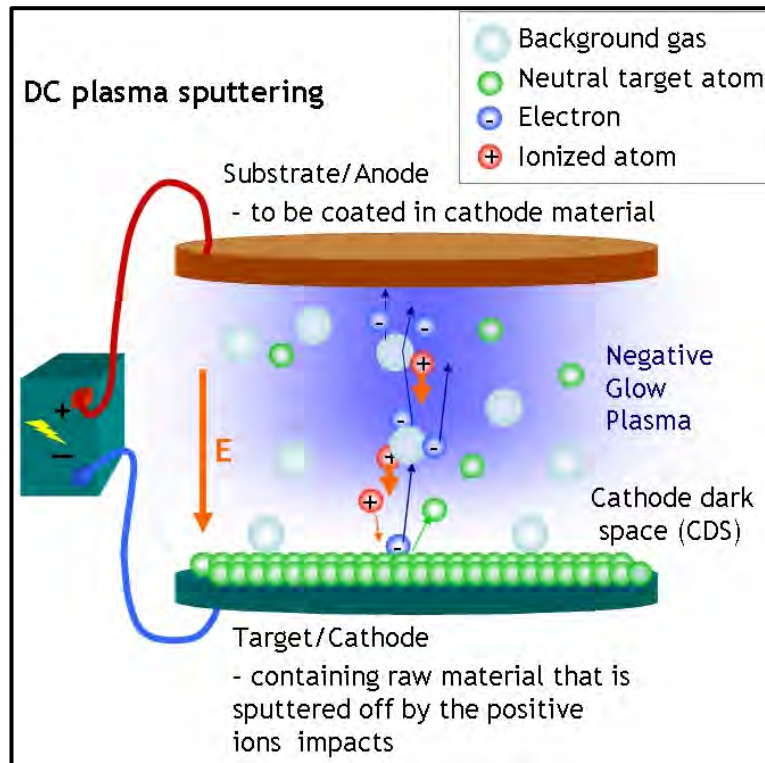


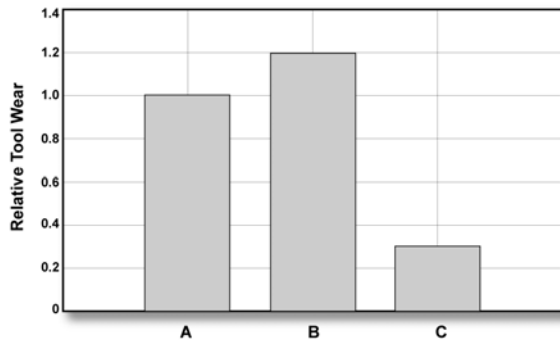
Figure 3.D-2: The Physical Vapor Deposition (PVD) process. ^{W-12}

Chemical Vapor Deposition (CVD) is an atmosphere controlled process conducted at elevated temperatures (~1050° C) in a CVD reactor. During this process, thin-film coatings are formed as the result of reactions between various gaseous phases and the heated surface of substrates within the CVD reactor. As different gases are transported through the reactor, distinct coating layers are formed on the tooling substrate, and the results look extremely promising.

For example, a new Chemical Vapor Deposition (CVD) coating was developed to reduce abrasive wear during stamping of AHSS materials. This coating contains certain combinations of individual coating layers of titanium carbide (TiC), titanium carbonitride (TiCN), and titanium nitride (TiN). Multilayer structures such as this CVD coating are found to work much better than traditional coatings and thus help to maximize the longevity of the tool and die materials. CVD costs double that of an alternative coating, Physical Vapor Deposition (PVD), because the high temperature processing of CVD includes pre- and post-treatments, but in certain applications, the improvement in die life justifies the cost.

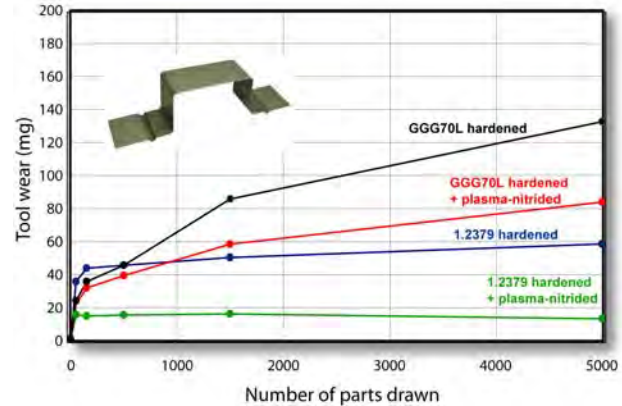
Figure 3.D-3 shows the relative tool wear when punching Mild steel with conventional tool steel (A) and punching of DP 350/600 with an uncoated (B) and coated (C) PM tool steel.

Research on different surface treatments for a hat-profile drawing with draw beads showed a similar effect of coated surfaces on a cast iron die and a tool steel die (Figure 3.D-4).



- A = Mild steel formed with 1.2363 tool steel dies (X100CrMoV5/1; US A2; Japan SKD 12)
- B = DP 350/600 steel formed with 1.3344 tool steel dies (carbon 1.20%, vanadium 3%)
- C = DP 350/600 steel formed with 1.3344 tool steel dies + hard surface CVD

Figure 3.D-3: Tool wear results for different tool steels and surface treatments using Mild steel with A2 dies (A) for a reference of 1^{H-2} Tests B and C show tool wear for DP 350/600 formed in uncoated (B) and coated (C) PM dies.



- GGG70L = Spheroid graphite bearing cast iron, flame hardened
- 1.2379 = Tool steel (X155CrMo12/1; US D2; Japan SKD 11)

Figure 3.D-4: Surface treatment effects on tool wear, DP steel EG, 1mm.^{T-3}

3.D.2. Lubricant Overview

Lubrication is an important input to almost every sheet metal forming operation. The lubricants have the following interactions with the forming process:

1. Control metal flow from the binder.
2. Redistribute strains over the punch.
3. Maximize/minimize the growth of strain gradients (deformation localization).
4. Reduce surface damage from die wear (galling and scoring).
5. Remove heat from the deformation zone.
6. Change the influence of surface coatings.

All these effects become more important as the strength of the sheet metal increases. Therefore, special attention to lubrication is required when considering AHSS.

3.D.2.a. AHSS Energy, Heat and Lubrication

Higher strength steels (both conventional and AHSS) have less capacity for stretch (less work hardening or n-value than Mild steels) over the punch or pullover plug to generate the required length of line. As the steel strength increases, more metal must flow from the binder into the die to compensate for the loss of length of line for a required stamping depth. Tensile stresses are applied to the metal under the binder in the radial direction (perpendicular to the die radius) to pull the metal towards the die radius. Compressive stresses can form in the circumferential direction (parallel to the die radius) as the

blank reduces its circumferential length. While this compression usually happens in box corners, it also can happen in sidewall features that shorten the length of line while moving into the stamping. Metal flowing uncontrolled into a sidewall also can generate compressive circumferential stresses. These compressive stresses tend to buckle the binder metal rather than uniformly increase the local thickness. This buckling is following the law of least energy-forming mode in sheet metal forming. Less energy is required to form a local hinge (a buckle) using only few elements of the sheet metal compared to uniformly in-plane compressing the metal to generate an increase in thickness for a large number of elements.

Weight reduction programs use higher strength steels to reduce the sheet metal thickness. The thinner sheet metal is more prone to buckling than thicker steels. Therefore, part designs utilizing AHSS with thinner sheets can require significantly higher blankholder forces to flatten buckles that form. Since restraining force is a function of the coefficient of friction (C.O.F.) times the blankholder force, the restraining force increases and metal flow decreases. We learned in the press section that deforming Advanced High-Strength Steels requires more energy (see Figure 3.C-58). This combination results in higher contact pressure between the metal and the die, and higher interface temperatures. Counter measures include an improvement in lubrication with a lower coefficient of friction, and the ability to maintain viscosity at elevated temperatures; other process changes may be required to calm the pressures and temperature effects.

Higher forming energy causes both the part and the die to increase in temperature. For example, a study by Irmco¹⁻⁵ measured the temperatures on stampings produced from 350 MPa and 560 MPa steels, with a production rate of 13 strokes per minute. Table 3.D-1 clearly shows that increasing strength levels result in higher part temperatures.

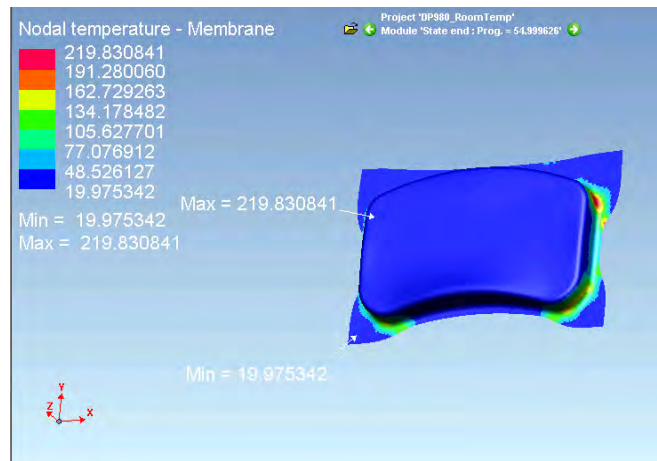
Table 3.D-1: Stamping Temperatures for High Strength Steels

Steel Strength	Press Rate	Temperature
HSLA 350	13 spm	100 ° C
HSLA 560	13 spm	138 ° C

The die temperatures are also significantly higher, and most conventional water-based or oil-based lubricants suffer viscosity reduction, with a corresponding increase in the coefficient of friction.

Ohio State University⁰⁻¹ has performed many lubricant studies with AHSS steels; Figure 3.D-1 shows the temperature profile on a DP900 stamping.

The highest temperatures are found on the die opening radius, and exceed 200°C, reinforcing that part and die temperatures increase with increasing material strength. Without high-temperature additives, the lubricant effectiveness deteriorates and galling results, followed by scoring of the sheet metal and dies. All these events increase blankholder restraining force and defeat the goal of more metal flowing into the die. As production speed increases (the number of parts per minute), the amount of heat generated increases, with a corresponding increase in sheet metal and die temperature.



**Figure 3.D-3: Temperature distribution
for DP 900 Steel.**

One key to solving the heat problem when forming higher strength steels is application of a better lubricant. The chemistries of these better lubricants are less prone to viscosity changes and lubricant breakdown. Water-based lubricants disperse more heat than oil-based lubricants. Some parts may require tunnels drilled inside the tooling for circulating cooling liquids. These tunnels target hot spots (thermal gradients) that tend to localize deformation leading to failures.

3.D.2.b. New Lubricants for AHSS Stampings

Special emphasis by some lubricant companies to provide a stable, low C.O.F. lubricant is the dry (barrier) lubricant. These lubricants (mainly polymer based) separate the sheet metal from the die. The dry lube C.O.F. for the same sheet metal and die combination can be 0.03 compared to a good wet lubricant C.O.F. of 0.12 to 0.15. That means doubling the blankholder force to maintain very flat binders for joining purposes will still reduce the binder restraining force by one-half or more. That reduction in binder restraining force now allows much more metal flow into the die, resulting in a reduction in the amount of punch stretching required to form the part. Ultimately, forming strains may be lowered from the FLC red failure zone to well into the green safe zone. Fuchs Lubricants^{F-4} provides the guidelines in Table 3.D-2 for lubricant selection for AHSS, as shown in the below table.

Table 3.D-2: Lubricant Selection Guide for AHSS

Neat Oils	<ul style="list-style-type: none"> • Most severe forming conditions evolve to using Neat oils because of their overall performance, characterized by good heat retention and film strength • They are difficult to remove, and can cause issues in post processing • Utilized for poor condition dies, heavy gauge materials, or with high strength steels characterized by poor elongations. Recommended for AHSS > 980 MPa.
Water-based Synthetics	<ul style="list-style-type: none"> • For use where heat reduction is primary concern • Use on HSLA and AHSS < 980 MPa • Very thin viscosity and poor film strength requires frequent reapplication (high volume sprays and flooding).
Soluble Oils	<ul style="list-style-type: none"> • Characterized by heat-resistant viscosity and substantial film strength. • Significant extreme pressure additives • Easy to clean, excellent for post-processing

They report that additives to Extreme Polymer (EP) lubricants creates a protective barrier or film between the sheet metal and die. At elevated temperatures, the EP breaks down and deposits a metallic salt layer, which acts as a further temperature insulator (analogous to a surface coating on the die) and allows continued functionality of the lubricant. The complete separation of sheet metal and die by the barrier lubricant also means isolation of any differences in coating characteristics. Finally, a known and constant C.O.F. over the entire stamping greatly improves the accuracy of Computer Forming-Process Development (computerized die tryout).

Fuchs^{F-4} has developed the list of lubricants and applications in Table 3.D-3 as another guide for users of AHSS:

Table 3.D-3: Lubricants and Typical Automotive Applications^{F-4}

Tuf Draw 2806 M100	Structural, passenger cradle component parts
Eco Draw HVRG8	Seat components and rails
Eco Draw BG9	DP 980 applications
Montgomery DB 4265 C	Primarily used with HSLA – BIW parts
Eco Draw HVE1	HSLA components such as engine cradles
Renoform OL 8190	Most severe forming applications

3.D.2.c. Key Points

- Lubrication helps control metal flow from the binder towards the die radius and into the part. Because many high strength parts have less stretch over the punch, different lubricant characteristics must enable additional metal flow in the binder.
- Increased metal strength and reduced sheet thickness for weight reduction require greater press energy and hold down forces. The increased energy to form many AHSS causes both part and die to increase in temperature. Increased temperature usually causes reduced lubricant viscosity and even lubricant breakdown resulting in galling and scoring.
- Maintaining metal flow in the binder requires a robust lubricant with a lower coefficient of friction, and resistance to temperature degradation.
- The dry barrier lubricants have several characteristics capable of reducing forming problems when making parts with AHSS. EP lubricants are another group of temperature resistant products.

3.E. Other Steel Processing Technologies

From the steel portfolio, a primary formed blank or tube is produced, and this can be from any of the following:

- Conventional single steel grade and thickness sheet
- Tailor (laser) welded blank
- Laser welded tube, both constant and variable thickness
- Laser welded coils
- Tailor rolled coils
- Laser blanked coils
- High-frequency induction welded tubes
- Variable walled tubes

From the primary formed blank or tube, a number of manufacturing processes are then utilized to produce the final part. They include:

- Cold forming processes, such as conventional stamping and roll forming
- Hot stamping, both direct and in-direct

These were described in Section 3.B. – Sheet Forming.

Section 3.C. captures steel processing technologies for flat blanks and metal tubes, and also provides an overview of the Hydroforming process.

3.E.1. Laser (Tailor) Welded Blanks

A laser welded blank is two or more sheets of steel seam-welded together into a single blank which is then stamped into a part. Laser welded blank technology allows for the placement of various steel grades and thicknesses within a specific part, placing steel's attributes where they are most needed for part function, and removing weight that does not contribute to part performance. For example, Figure 3.E-1 shows a laser welded body side aperture (outer) with multiple grades and thicknesses. This technology allows for a reduction in panel thickness in non-critical areas, thus contributing to an overall mass reduction of the part.

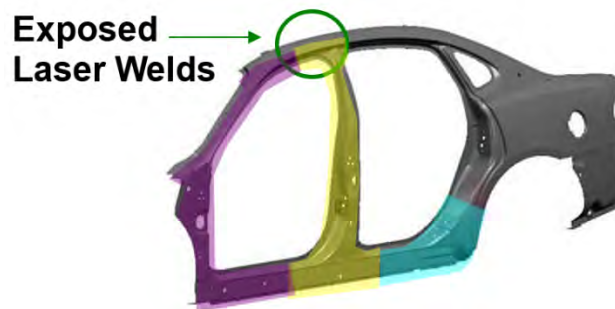


Figure 3.E-1: Future body-side outer with exposed laser welds and multi-piece construction.^{A-17}

There are several advantages to a laser welded blank, compared with conventional blanks made from a single grade and part thickness. They include:

- Superior vehicle strength and rigidity
 - Consolidation of parts, where one blank can replace a number of different parts
 - Lower vehicle and part weight
 - Reduced steel usage
 - Improved safety
 - Elimination of reinforcement parts
 - Elimination of assembly processes
 - Reduction in capital spending for stamping and spot-welding equipment
 - Reduced inventory costs
-
- Improved dimensional integrity (fit and finish)
 - Achievement of high performance objectives with lower total costs
 - Reduction in Noise, Vibration, and Harshness (NVH)
 - Elevated customer-perceived quality

3.E.2. Laser Welded Coil

Laser welded coil is a process (Figure 3.E-2) of producing a continuous coil of steel from individual, separate coils of varying thickness and grades. The basic process takes separate coils, prepares their edges for contiguous joining, and laser welds these together into one master coil. The new strip is then readied for other blanking, or to be used as a continuous feed into a transfer press line.

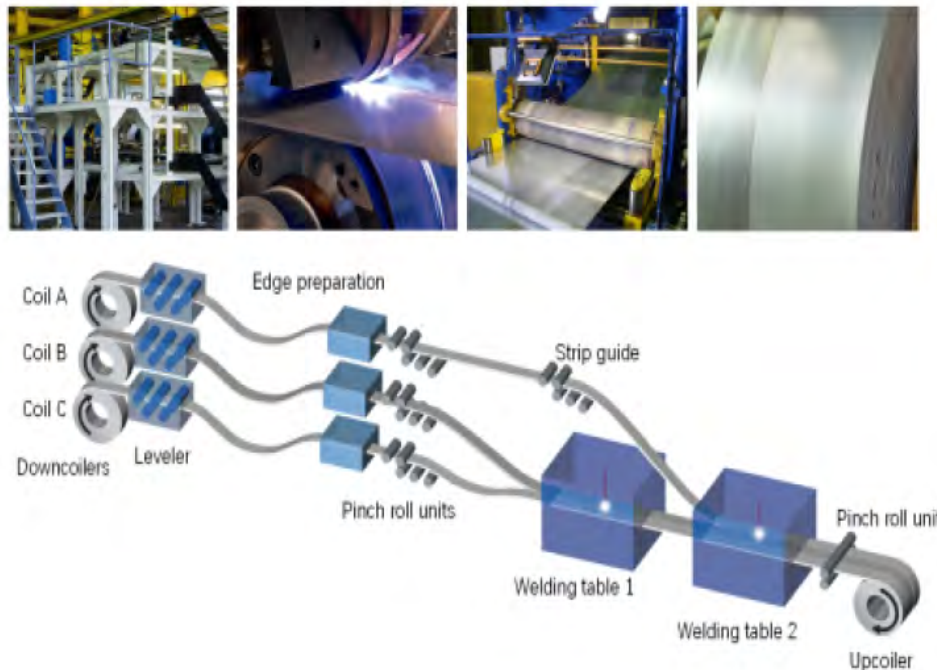


Figure 3.E-2: Laser welded coil process. ^{A-17}

Potential use of a laser welded coil in an automotive application, using a pro-die-stamping process, includes the following:

1. Roof frames
2. Roof bows
3. Side members
4. Reinforcements
5. Seat cross members
6. Exhaust systems

3.E.3. Tailor Rolled Coil

This is a manufacturing process of flexible cold strip rolling by varying the gap between two rolls, allowing for different strip thicknesses in the direction of rolling. Figure 3.E-3 illustrates the manufacturing principles. The accurate measuring and controlling technology guarantees the strip thickness tolerances.

A tailor rolled coil can be either used for blanking operations (for stamping or tubular blanks), or can be directly fed into a roll-forming line.

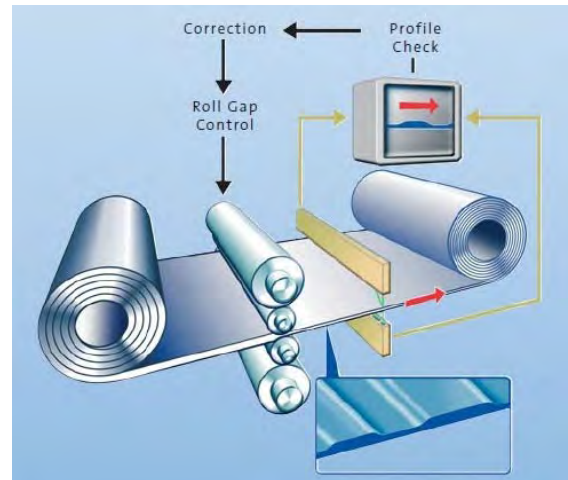


Figure 3.E-3: The principle of producing a Tailor Rolled Coil. ^{M-7}

3.E.4. Laser Blanking

As discussed in Section 3.B.3.b – Edge Stretching Limits, a comparison of various mechanical sheared edges with water jet, laser cut and milled edges showed that laser cut edges had percent elongations that approached that of the ideal milled edge. As a response to increasing AHSS volumes and strength levels, multiple companies have developed laser blanking lines, where a coil is blanked via a laser or series of lasers to produce blanks. These new lines are capable of cutting blanks on a high-volume basis.

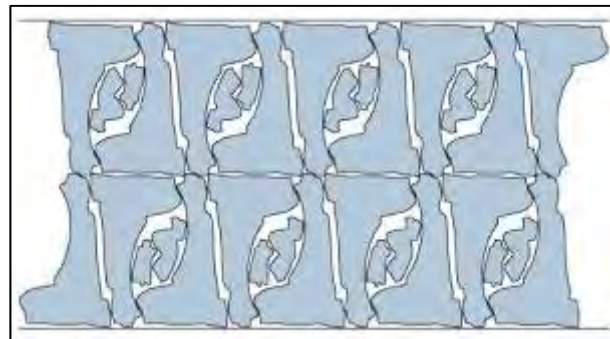


Figure 3.E-4: Schematic of 3 different blanks to be laser blanked from the same coil to minimize engineered scrap. Not only is engineered scrap minimized, but the superior edge condition significantly reduces the potential for edge fracture. ^{M-7}

There are several advantages to this approach when processing AHSS. Improved edge condition to combat edge fracture is a significant one. Additional savings can be achieved through the elimination of expensive blank die construction and tooling maintenance costs (no blank die is needed and no expensive tool steels are required – AHSS usually requires more durable and more expensive tool steels). Less floor space is needed because there are no blank dies to store. There is also the opportunity to optimize material utilization through either blank nesting optimization or blanking two or more different blanks out of the same steel strip. Figure 3.E-4 shows an example of optimized laser blank nesting of three different blanks from the same coil. Fast production changes can be made to

increase uptime as there are no blank dies to remove and replace. Blank contours can easily be modified after production launch as well. As many AHSS grades are rolling direction sensitive with respect to edge and shear fracture, alternative nesting can potentially optimize the blank orientation to minimize these types of local formability failures.

The decision for laser blanking should be made during development, in order maximize overall process efficiency and avoid building a blank die or other nonessential tooling Figure 3.E-5 shows a typical laser blanking line specifically designed to process AHSS.



Figure 3.E-5: Laser blanking line specifically designed to process AHSS. As described in Section 3.C.7. – Straightening and Precision Leveling AHSS, there is even a cartridge designed straightener (far left) specifically designed to insure blanks are flat after processing.

3.E.5. Traditional Tube Forming

3.E.5.a High Frequency Welded Tubes

Welded tubes are commonly produced from flat sheet material by continuous roll forming and a high frequency welding process. These types of tubes are widely used for automotive applications, such as seat structures, cross members, side impact beams, bumpers, engine subframes, trailing arms, and twist beams. Currently AHSS tubes up to grade DP 700/1000 are in commercial use in automotive applications.

Tube manufacturing involves a sequence of processing steps (for example roll forming, welding, calibration, shaping) that influence the mechanical properties of the tube. During the tube manufacture process, both the YS and the UTS are increased while the total elongation is decreased. Subsequently, when manufacturing parts and components, the tubes are then formed by operations such as flaring, flattening, expansion, reduction, die forming, bending and hydroforming. The actual properties of the tube dictate the degree of success to which these techniques can be utilized.

Published data on technical characteristics of tubes made of AHSS are limited. For example, the ULSAB-AVC programme^{W-8} deals only with those tubes and dimensions applied for the actual body structure (Table 3.E-1).

Table 3.E-1: Examples of properties of as-shipped straight tubes for ULSAB-AVC project.^{W-8}

Steel Grade	Min. YS (MPa)	Min. UTS (MPa)	Typical Total EL (%) [*]
MS 950/1200	1150	1200	5-7
DP 500/800	600	800	16-22
DP 280/600	450	600	27-30

The earlier ULSAC study^{W-9} resulted in design and manufacturing of demonstration hardware, which included AHSS tubes made of DP 500/800 material (Figure 3.E-6). The ULSAC Engineering Report provides the actual technical characteristics of those two tube dimensions used in the study: 55x30x1.5mm and \varnothing 34x1.0mm.



Figure 3.E-6: ULSAC study door (left) and DP500/800 lower (center) and outer belt reinforcement tubes (right)

The work hardening, which takes place during the tube manufacturing process, increases the YS and makes the welded AHSS tubes appropriate as a structural material. Mechanical properties of welded AHSS tubes (Figure 3.E-7) show welded AHSS tubes provide excellent engineering properties.

Compared to HSLA steel tubes, the AHSS tubes offer an improved combination of strength, formability, and good weldability. AHSS tubes are suitable for structures and offer competitive advantage through high-energy absorption, high strength, low weight, and cost efficient manufacturing.

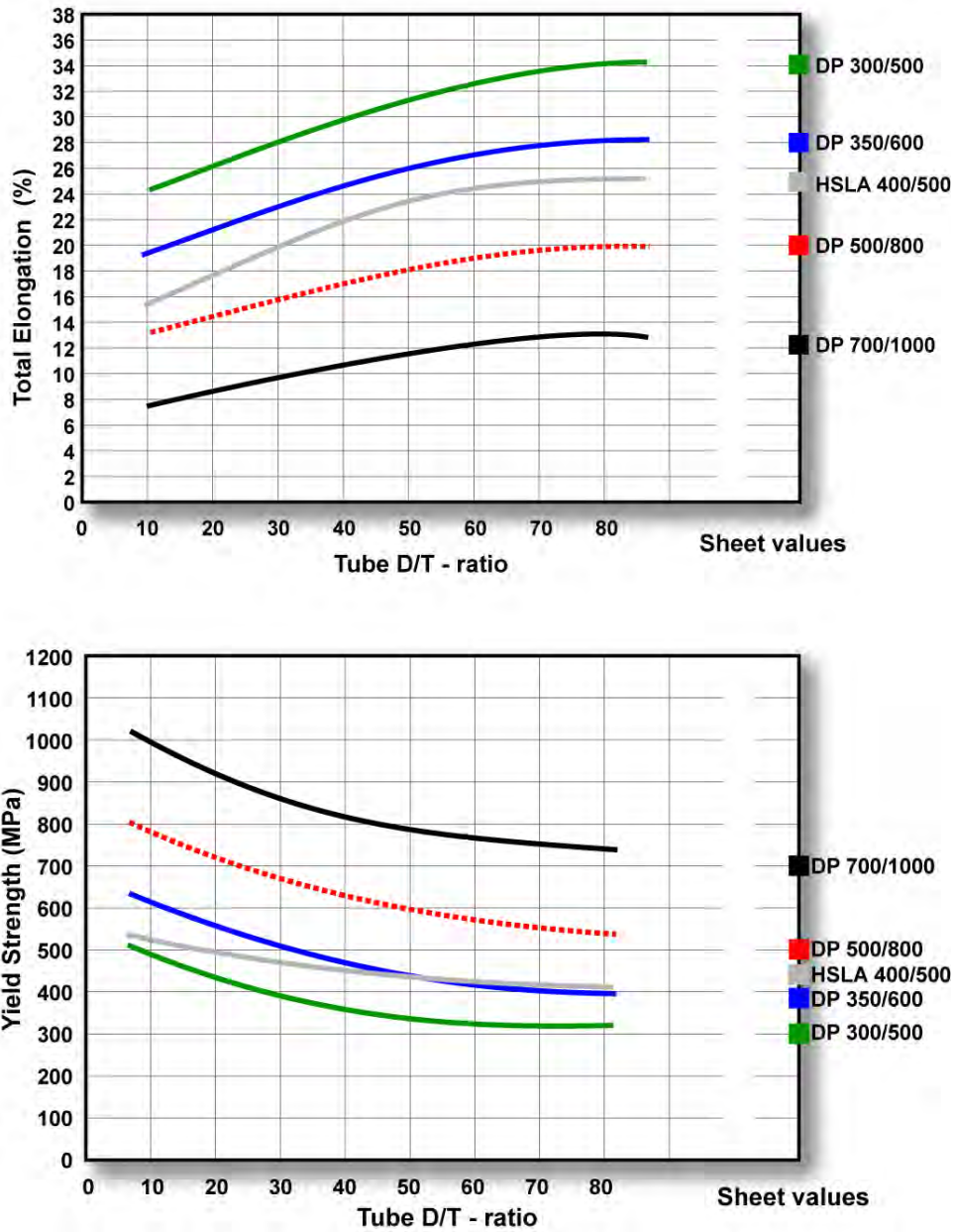


Figure 3.E-7: Anticipated Total Elongation and Yield Strength of AHSS tubes.^{R-1}

The degree of work hardening, and consequently the formability of the tube, depends both on the steel grade and the tube diameter/thickness ratio (D/T) as shown in Figure 3.E-8. Depending on the degree of work hardening, the formability of tubular materials is reduced compared to the as-produced sheet material.

Bending AHSS tubes follows the same laws that apply to ordinary steel tubes. One method to evaluate the formability of a tube is the minimum bend radius, which utilizes the total elongation (A_5) defined with proportional test specimen by tensile test for the actual steel grade and tube diameter.

The minimum Centerline Radius (CLR) is defined as:

$$CLR = 50 \times \frac{D}{A_5}$$

Computerized forming-process development utilizes the actual true stress-true strain curve, which is measured for the actual steel grade and tube diameter. Figure 3.D-3 contains examples of true stress-true strain curves for AHSS tubes.

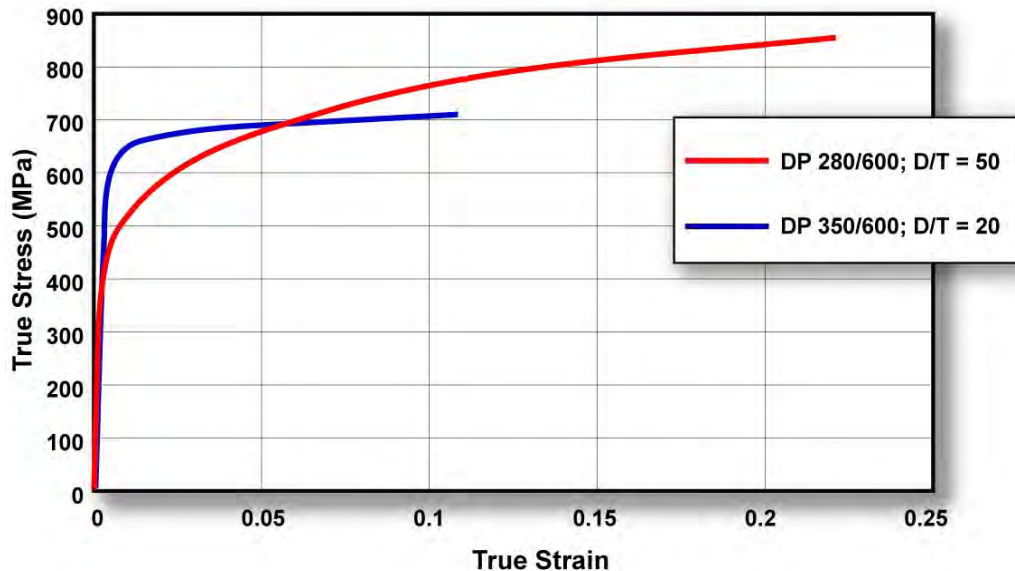


Figure 3.E-8: Examples of true stress-true strain curves for AHSS tubes.^{R-1}

However, it is important to note that the bending behaviour of tube depends on both the tubular material and the bending technique. The weld seam is also an area of non-uniformity in the tubular cross section. Thus, the weld seam influences the forming behaviour of welded tubes. The first recommended procedure is to locate the weld area in a neutral position during the bending operation.

The characteristics of the weld depend on the actual steel sheet parameters (that is chemistry, microstructure, strength) and the set-up of the tube manufacturing process. Figures 3.E-9 and 3.E-10 provide examples of the forming of AHSS tubes.



Figure 3.E-9: Hydroformed Engine Cradle made from welded DP 280/600 tube with YS \approx 540 N/mm²; TS \approx 710 N/mm²; Total Elongation \approx 34%. Draw bending, Centerline Bending Radius = 1.6 x D, Bending Angle > 90 Degrees.^{R-1}



Figure 3.E-10: Bending test of welded DP 350/600 tube with YS \approx 610 N/mm²; TS \approx 680 N/mm²; Total Elongation \approx 27%. Booster bending, Centerline Bending Radius = 1.5 x D, Bending Angle = 45 Degrees.^{R-1}

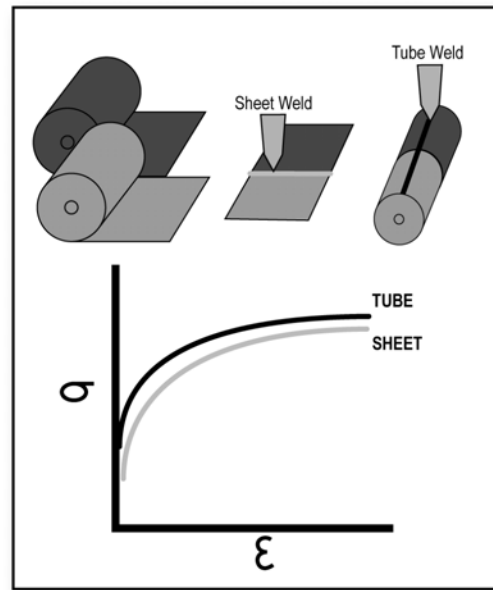
3.E.5.b. Laser Welded Tailored Tubes

Tube products for chassis applications produced by conventional HF weld process (as previously described) receive their properties during traditional tube making processes (such as roll-forming and widely used HF-welding).

For body structures, thin-wall tube sections are recommended as a replacement for spot-welded box-shape components. To meet further demands for even thinner gauges (with different metal inner and outer surface coatings in all AHSS grades that are more sensitive to work hardening) an alternative manufacturing process is required to maintain the sheet metal properties in the as-rolled sheet conditions.

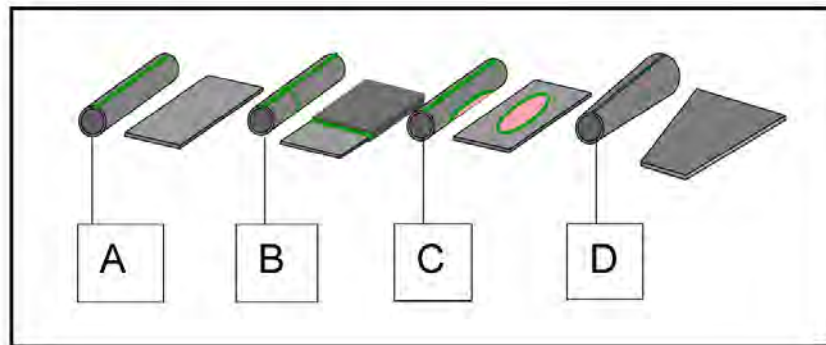
Laser welding, used extensively for tailored welded blanks, creates a very narrow weld seam. Sheet metals with dissimilar thickness and/or strengths are successfully used to achieve required weight savings by eliminating additional reinforcement parts. Further weld improvements have been made during the steadily increasing series-production of laser welded blanks.

Part consolidation utilizing hydroforming is one strategy to simultaneously save both cost and weight. With hydroforming technology, the next step in tubular components is to bring the sheet metal into a shape closer to the design of the final component without losing tailored blank features (Figure 3.E-11).



Figures 3.E-11: Mechanical properties of tailored tubes are close to the original metal properties in the sheet condition.^{G-1}

The tailored tube production process allows the designer to create complex variations in shape, thickness, strength, and coating. (Figure 3.E-12). The shape complexity, however, is limited by the steel grades and mechanical properties available.



Figures 3.E-12: Laser welded, tailored tube examples and required pre-blank shapes.^{F-1}
A) 1-piece cylindrical tube - B) 2-piece tailored tube - C) Patchwork tube - D) 1-piece conical tube

Conical tailored tubes, designed for front rail applications, with optimized lightweight and crash management are one opportunity to cope with auto body-frame architecture issues. In frontal crash and side impacts the load paths have a key importance on the body design as they have a major bearing on the configuration of the structural members and joints. Figure 3.E-13 is an example of a front-rail hydroformed prototype. The conical tailored tubes for this purpose take advantage of the high work hardening potential of TRIP steel.



Figure 3.E-13: Front-rail prototype based on a conical tube having 40 mm end to end difference in diameter.^{F-2}

3.E.5.c. Variable (Multiple) Walled Tubes

Variable, or Multiple Walled Tubes (MWT), is a proprietary process where tubes are fabricated with varied wall thicknesses along the length, to satisfy specific functional requirements that vary with length. The MWT process produces the varied tube thicknesses, in discrete steps, in a single formed tube. The wall thickness can vary on either the inside or outside of the tube. Figure 3.E-14 shows an example tube profile.

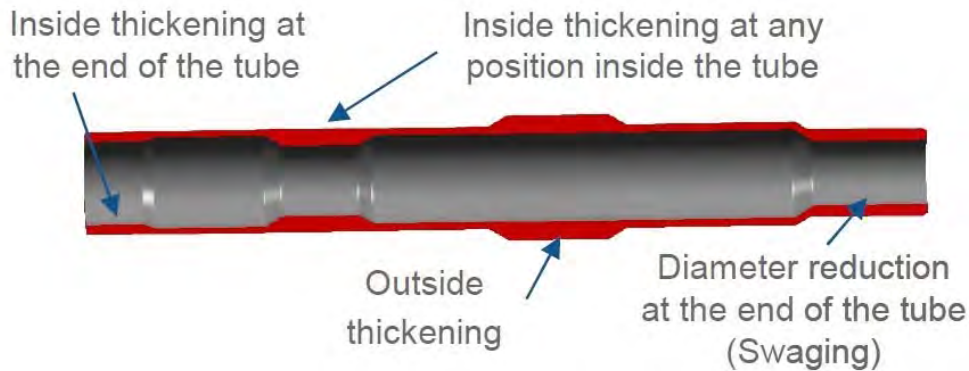


Figure 3.E-14: Multiple walled tube showing varying wall thickness

However, other approaches to a MWT that have been applied to production vehicles are, laser welding of a tailor welded blank, (also known as a tailor laser welded tube) and a tailor rolled blank laser welded into a tube with the laser welded tube process.

3.E.5.d. Key Points

- Due to the cold working generated during tube forming, the formability of the tube is reduced compared to the as-received sheet.
- The work hardening during tube forming increases the YS and TS, thereby allowing the tube to be a structural member.
- Laser welded tubes create a very narrow weld seam.
- The weld seam should be located at the neutral axis of the tube, whenever possible during the bending operation.

3.E.6. Hydroforming Tubes

3.E.6.a. Pre-Form Bending

As discussed in the previous section, AHSS will initially work harden (increase strength) during the initial tube making process and then continue to work harden more with each forming step in the hydroforming process. For example, tube manufacturing involves a sequence of processing steps - roll forming, welding, calibration, shaping. During the tube manufacturing process, both the YS and the UTS increase while the total elongation and residual stretchability decrease. The same is true during the pre-form bending of the tube. In the area of the tube where the pre-form bending stresses are concentrated, the YS and the UTS will increase in the deformation zone while the total elongation and stretchability decrease locally. When considering production of a hydroformed part, both product and tool designs must account for these increased strengths and reduced formability parameters.

Careful consideration is required to avoid exceeding the available total elongation for bending limits or forming limits - especially for stretchability formations in the finished part that are located in the area of a pre-form bend. Refer to Figure 3.E-7 for anticipated elongation values for several illustrative high strength steels formed into tubes of various D/T ratios.

The deformation available for the pre-form bend process and the subsequent hydroforming process will depend on the material selected, tube D/T ratio, tube manufacturing process, centreline radius of the pre-form bend, and the included angle of the bend. Referring to Figure 3.E-7 of the previous section, tubes of higher strength AHSS will have limited elongation available. Therefore, analysis of part designs is required to avoid exceeding the various forming limits imposed by the chosen material.

Automotive roof rail sections have incorporated hydroformed parts for several years. The ULSAB-AVC^{W-8} also used this type of construction. More recent vehicles have used much higher strength AHSS to improve roof strength (Figure 3.E-15).

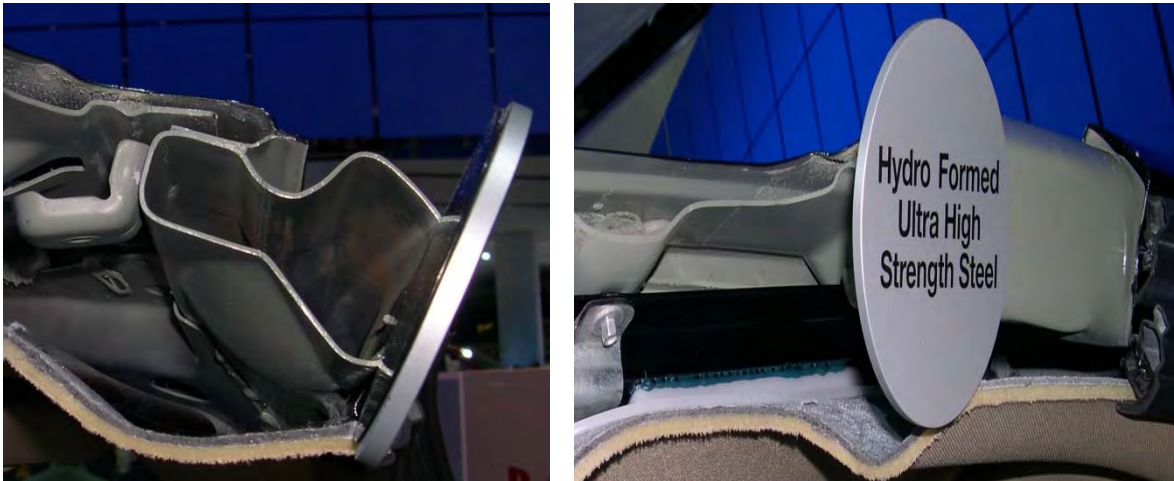


Figure 3.E-15: North American 2008 truck roof rail using AHSS hydroformed section.^{P-1}

3.E.6.b. Forming

The hydroforming process for tubes usually involves expanding the tube diameter from 3% to 30% depending on the design, materials selected and pressures available for forming. Tube production commonly utilizes one of three basic methods of hydroforming tubes. The first two are low-pressure and high-pressure processes. The low-pressure begins with a tube whose circumference is slightly less than the final circumference of the finished geometry. After placing the tube in an open die, the tube is pressurized. As the die closes, the circumference of the tube changes shape to conform to the closing die. The pressure is sufficient to prevent the tube from buckling during the shape change. The key is very little increase in the circumference to allow high strength and reduced formability metals to achieve tighter radii without failure. This low-pressure process is suitable for tubes made from AHSS.

The second process is high-pressure tube hydroforming. Here the tube is placed in the die and the die is closed. Pressurizing the tube now causes the metal to stretch as the circumference increases to conform to the inner circumference of the die – often with tight radii in corners and product features. Higher strength steels may be unable to expand sufficiently to fill the die geometry or create small radii without failure. Furthermore, high pressure could be necessary to obtain the correct geometry with minimum springback or fewer wrinkles compared to low pressure hydroforming.

A third process reduces the severity of circumferential expansion by “end feeding.” Special end pistons push additional material into the die cavity from the tube end to provide more material for higher expansion of the tube circumference. This method of tube circumference expansion involves bi-directional strain. The end feeding is beneficial for hydroforming tubes from AHSS.

Hydroforming AHSS tubes require highly developed forming limit charts that utilize tube D/T, degree of pre-form bend, and final geometrical shape. Currently, these data are limited for AHSS beyond DP steels with a tensile strength greater than 600 MPa. The availability of forming limit charts will improve as new applications develop rapidly. To assist with very early process and die design, computerized forming-process development is an excellent tool for examining the validity of applying different AHSS to potential part designs.

Figures 3.E-16 and 3.E-17 illustrate two hydroformed production parts.



Figure 3.E-16: This duplicate of Figure 3-167 shows the two potential problem areas (circled) for a hydroformed Engine Cradle made from welded DP 280/600 tube .^{R-1}

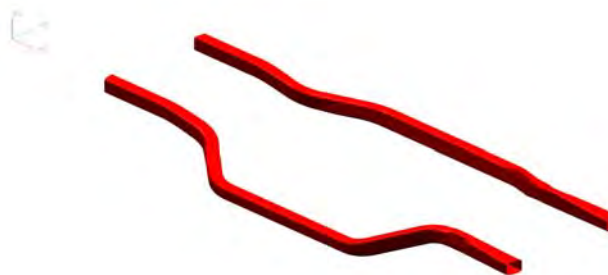


Figure 3.E-17: Opel Speedster, Pontiac Solstice and Saturn Sky main body side rail: Tube DIA 132 mm, Gauge 1.8 mm, D/T = 73, Finished length 4070mm, DP 350/600.^{A-7}

3.E.6.c. Post Forming Trimming

For trimming and piercing, the same general cautions utilized for stamped AHSS parts apply to hydroformed AHSS parts. Since AHSS have higher tensile strength than conventional high-strength steels, engineering the trim tools to withstand higher loads is a requirement. Proper support for the trim stock during the trim operation also is very important to minimize edge cracking. Laser trimming, which is common for hydroformed parts, is still an excellent choice. However, evaluating the hardening effects of the laser beam on the trimmed edge is required.

3.E.6.d. Design Considerations

Today, hydroformed parts are widely used for automotive applications, such as seat structures, cross members, side impact beams, bumpers, engine subframes, trailing arms, roof rails and twist beams. Currently, AHSS tubes up to grade DP 700/1000 are in commercial use in automotive applications. In general, the same design guidelines that support hydroforming of conventional steels apply to AHSS. However, additional attention to the available elongation for forming and to part function is required as part design and manufacturing processes are developed.

3.E.6.e. Key Points

- **Tube hydroforming is a current production process for making numerous structural parts.**
- **Those AHSS tubes with higher yield and tensile strengths but lower total elongations and stretchability limits will limit some hydroformed tube designs.**
- **The total summation of forming deformation is required from all stages of product development, which includes creating the initial tube, pre-bending, hydraulic circumferential expansion, and forming of local features.**
- **AHSS tube trimming and piercing have similar cautions as AHSS stamped part trimming and piercing.**

3.F. Process Maintenance and Quality Control

AHSS applications are growing, where the high strength body components help meet crash requirements, and thinner sections achieve weight reduction for improved fuel economy and lower overall emissions. Both higher strength and thickness reduction contribute to lower overall formability, higher forces, greater temperatures and accelerated die wear, and each of these outcomes reduce the size of the manufacturing window. To manage all of these challenges, the pressroom must implement advanced process control measures in order to minimize normal process variation, as the process is now less tolerant of this variation. The same holds true for die and recipe maintenance.

Understanding this reality, it's important to make process decisions that enhance the forming window – this includes better die materials, surface treatments, surface coatings and data-based lubricant specification. Cross-functional communication is required to create awareness among employees in the level of process discipline critical to success. Controlling the inputs of the stamping process

become vital to achieving predictable outputs, therefore process recipes should be defined and fixed across all shifts. This is the spirit behind process control, which defines the relationship between key inputs and outputs of the stamping process; Figure 3.F-1 shows critical stamping inputs, such as the steel, lubricant, press and die conditions. All of these contribute to final part outputs, and thus need to be well-documented, maintained and understood for process reliability and repeatability.

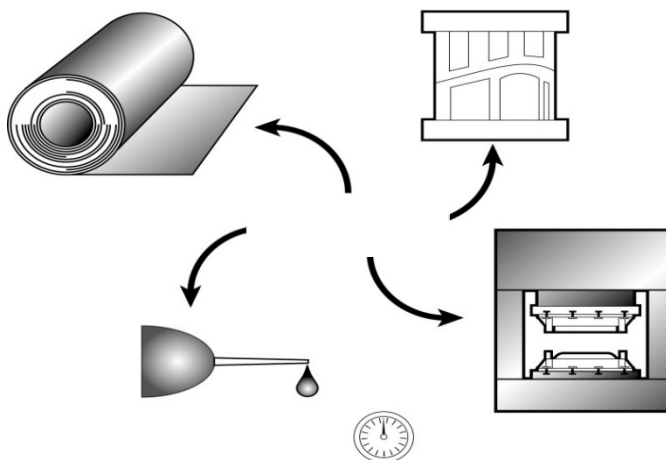


Figure 3.F-1: Stamping pressroom critical inputs including the steel, lubricant, press and die.

3.F.1 Reference Panels

Reference Panels are ideal for AHSS processes, and effectively establish process control of the forming operation.

A reference panel is a draw shell that documents input settings and process outputs (forming strains, draw-in lines, trim scrap) at the time the panel was formed. It thus serves as a useful reference for each die-set, to compare to the current operational panel and process, ensuring that all inputs are stable. Visual changes in panel appearance or measured changes in strains or draw-in lines allow rapid detection of input variation, and process adjustments to be incorporated prior to incurring unacceptable panels (scoring, distortion, buckles or splits).

The use of reference panels should be part of a Formability System, characterized by systematic panel reviews, recipe confirmations, and die improvement / die maintenance planning. As an example, production realities are such that reference panels won't be used if they are not stored in a protective rack, near the floor (so access is easy). Figure 3.F-2 shows an example reference panel rack system in a North American stamping plant.



Figure 3.F-2: Door Outer Reference Panel and Storage Rack

All affected employees need to be trained on the importance of this tool, so panels are preserved and not discarded during housekeeping events. And a disciplined panel review process aligns production and trade personnel to ensure that the reference panels are used during each part run.

Draw-in or thickness templates allow for formability measures on panels in very precise and consistent locations. Measuring these outputs on a regular basis (every part run) enables a determination of process stability and trends, which becomes important towards scheduling PM. Examples of draw-in templates are shown below in Figure 3.F-3.



Figure 3.F-3: Draw-in template for draw panel; cutout allows for accurate, repeatable measurement.

Because AHSS products are susceptible to edge shearing from trim and pierce operations, these operations require advanced tooling and more frequent PM intervals. All die maintenance will be critical, requiring more frequent polishing, insert replacement (or reconditioning), surface treatment assessments to plan repair or reapplication, etc. Finally, tool and die personnel should attempt to define the size of the forming window with split-buckle analysis, varying shut height while maintaining all other variables constant to determine when unacceptable buckles or necking initiate. This information is then used to develop input (recipe) settings that achieve production stability and robustness.

3.F.2. Key Points

- **Process control and die maintenance become more critical with AHSS products, because the manufacturing window is significantly smaller compared to conventional steels.**
- **Reference panels are great tools that allow the detection of process drift and variation, but their use must be systematized and operating practices to adopt their use need to be integrated on the pressroom floor.**
- **More frequent die PM intervals should be anticipated with AHSS. This includes the trim and flanging operations, also susceptible to more rapid deterioration due to the high forces involved with cutting and moving these very high strength steels.**

3.G. In-Service Requirements

The microstructure of DP and TRIP steels increase the sheet metal forming capability, but also improve energy absorption in both a crash environment.

3.G.1. Crash Management

DP and TRIP steels with ferrite as a major phase show higher energy absorbing property than conventional high-strength steels, particularly after pre-deformation and paint baking treatments. Two key features contribute to this high energy-absorbing property: high work hardening rate and large bake hardening (BH) effect.

The relatively high work-hardening rate, exhibited by DP and TRIP steels, leads to a higher ultimate tensile strength than that exhibited by conventional HSS of similar yield strength. This provides for a larger area under the true stress-strain curve, and results in greater energy absorption when deformed in a crash event to the same degree as conventional steels. The high work hardening rate also causes DP and TRIP steels to work harden during forming processes to higher in-panel strength than similar YS HSS, further increasing the area under the stress-strain curve and crash energy absorption. Finally, the high work-hardening rate better distributes strain during crash deformation, providing for more stable, predictable axial crush that is crucial for maximizing energy absorption during a front or rear crash event.

The relatively large BH effect also increases the energy absorption of DP and TRIP steels by further increasing the area under the stress-strain curve. The BH effect adds to the work hardening imparted by the forming operation. Conventional HSS do not exhibit a strong BH effect and therefore do not benefit from this strengthening mechanism.

Figure 3.G-1 illustrates the difference in energy absorption between DP and TRIP steels as a function of their static (traditional tensile test speed) yield strength.

Figure 3.G-2 shows calculated absorbed energy plotted against total elongation for a square tube component. The absorbed energy remains constant for the DP and TRIP steels but the increase in total elongation allows for formation into complex shapes. For a given crash-critical component, the higher elongations of DP and TRIP steels do not generally increase energy absorption compared to conventional HSS if all materials under consideration have sufficient

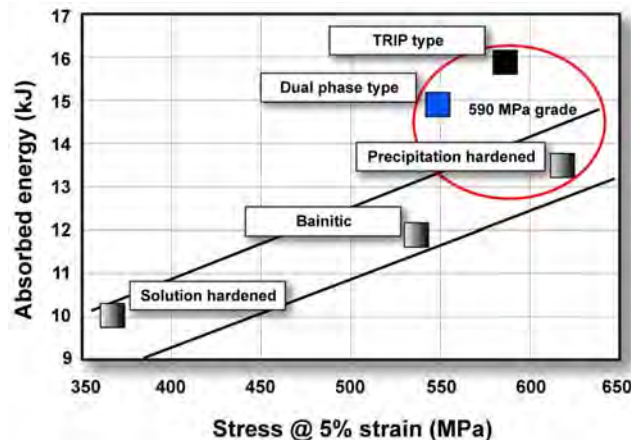


Figure 3.G-1: Absorbed energy for square tube as function of static yield strength.^{T-2}

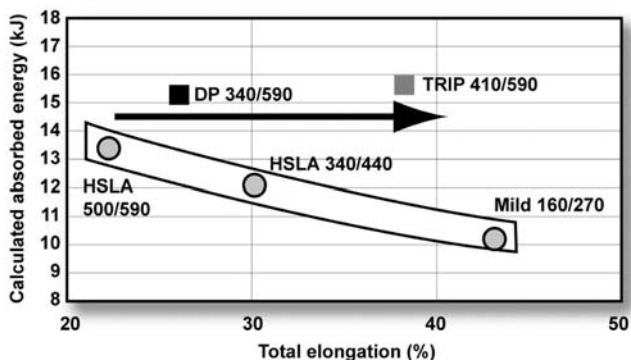


Figure 3.G-2: Calculated absorbed energy for a square tube as a function of total elongation.^{T-2}

elongation to accommodate the required crash deformation. In some applications, the DP and TRIP grades could increase energy absorption over that of a conventional HSS if the conventional steel does not have sufficient ductility to accommodate the required crash deformation and splits rather than fully completing the crush event. In the latter case, substituting DP or TRIP steel, with sufficient ductility to withstand full crash deformation, will improve energy absorption by restoring stable crush and permitting more material to absorb crash energy.

High Strain Rate Property Test Methods for Steel and Competing Materials

During recent years the global steel industry collaboratively prepared recommended practices to be incorporated into International Standards Organization (ISO) standards for high strain rate test methods.^{Y-3} The need for such test methods was based on the following points:

- Strain rate effect is an important issue for crash worthiness
- Steel has favorable strain rate effect properties whereas aluminum does not
- Common test methods around the world prior to this effort were not well established

3.G.2. Fatigue

The fatigue strength of DP steels is higher than that of precipitation-hardened steels or fully bainitic steels of similar yield strength for many metallurgical reasons. For example, the dispersed fine martensite particles retard the propagation of fatigue cracks. For TRIP steels, the transformation of retained austenite can relax the stress field and introduce a compressive stress that can also improve fatigue strength. Figures 3.G-3 and 3.G-4 illustrate the improvements in fatigue capability.

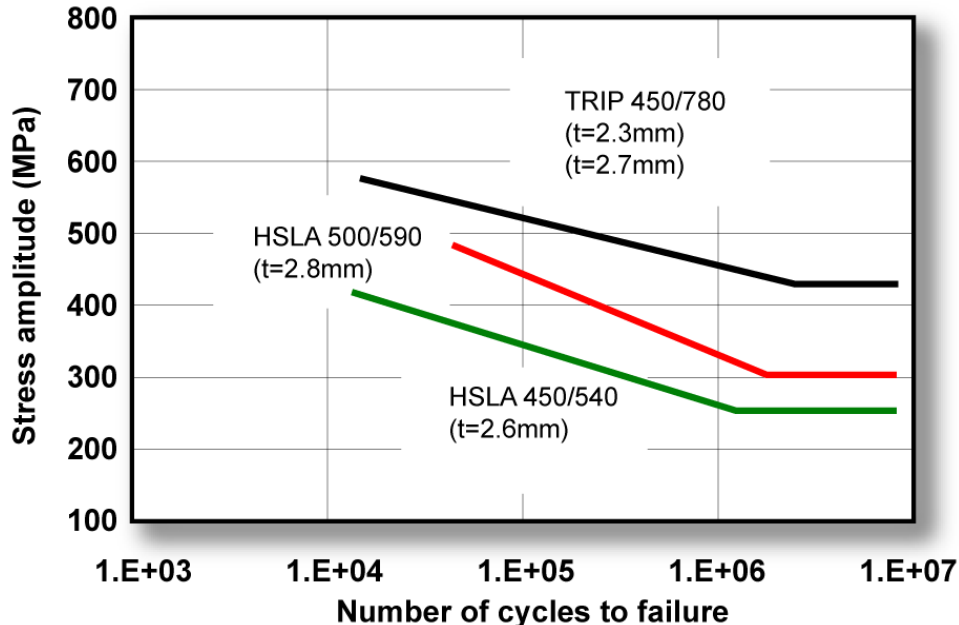


Figure 3.G-3: Fatigue characteristics of TRIP 450/780 steel compared to conventional steels.^{T-1}

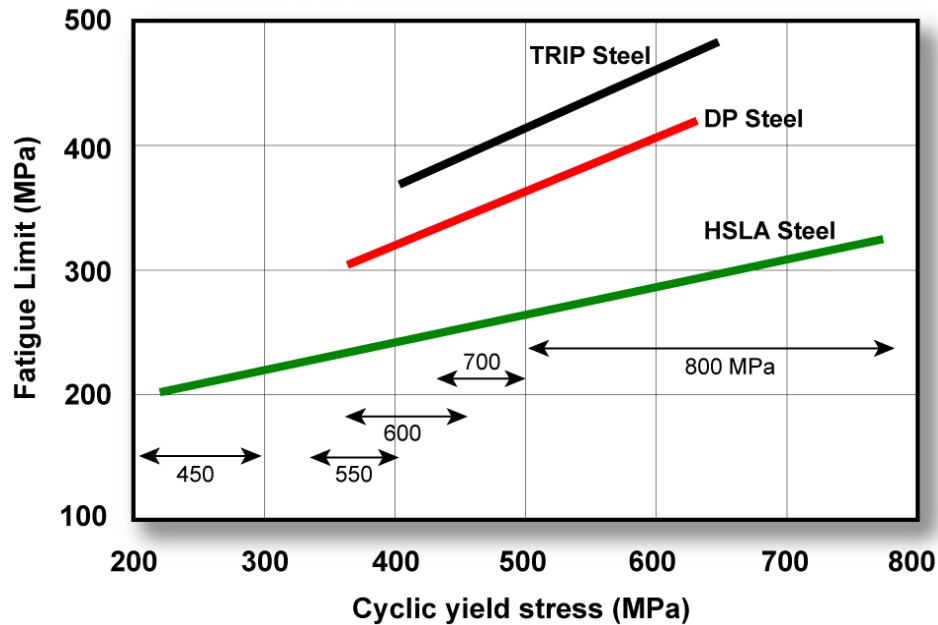


Figure 3.G-4: Fatigue limit for AHSS compared to conventional steels.^{T-2}

3.G.3. Key Points

- DP and TRIP steels have increased energy absorption in a crash event compared to conventional HSS because of their high tensile strength, high work hardening rate, and large BH effect.
- The greater ductility of DP and TRIP steels permit use of higher strength, greater energy absorbing capacity material in a complex geometry that could not be formed from conventional HSS.
- DP and TRIP steels have better fatigue capabilities compared to conventional HSS of similar yield strength.

SECTION 4 – JOINING

4.A. Introduction

The unique physical characteristics of Advanced High Strength Steels (AHSS) present some challenges to welding and bonding processes. AHSS differ from mild steels by chemical composition and microstructure, and it's important to note that their microstructures will change from welding operations. For example, intensive localized heat associated with some welding processes causes a significant change in the local microstructure, and hence affect properties. Due to fast Cooling Rates (CR) typical in welding, it is normal to see martensite and/or bainite microstructures in the weld metal and in the Heat-Affected Zone (HAZ).

When joining AHSS, production process control is important for successful assembly. Manufacturers with highly developed joining control methodology will experience no major change in their operations. Others may require additional checks and maintenance. In certain instances, modifications to equipment or processing methodologies may be required for successful joining of AHSS.

The coating methods for AHSS are similar to those for mild steels. Welding of either AHSS or mild steels with coatings will generate fumes. The amount and nature of fumes will depend on the coating thickness, coating composition, joining method, and fillers used to join these materials. The fumes may contain some pollutants. The chemical composition of fumes and the relevant exhaust equipment must meet appropriate regulatory standards. Thicker coatings and higher heat inputs cause more fumes. Additional exhaust systems should be installed. While welding AHSS (with or without metallic or organic coatings and oiled or not oiled) gases and weld fumes are created similar to mild steels. The allowed fumes or gases must comply with respective national rules and regulations.

4.B. Joining Processes

Considering recent developments of hybrid approaches to welding, there are now over 100 types of welding processes available for the manufacturer or fabricator to choose from. The reason that there are so many processes is that each process has its list of advantages and disadvantages that make it more or less appropriate for a given application. Arc welding processes offer advantages such as portability and low cost, but are relatively slow and use a considerable amount of heating to produce the weld. High energy density processes such as laser welding generally produce low heat inputs and fast welding speeds, but the equipment is very expensive and joint fit-up needs to be ideal. Solid-state welding processes avoid many of the weld discontinuities produced by those requiring melting (fusion), but they may be expensive and often are restricted to limited joint designs. Resistance welding processes are typically very fast and require no additional filler materials, but are often limited to thin sheet applications or very high-production applications such as in the automotive industry.

Most welding processes produce a weld (metallic bond) using some combination of heat, time, and/or pressure. Those that rely on extreme heat at the source such as arc and high energy density processes generally need no pressure and relatively small-to-medium amounts of time. The following section introduces joining processes that are applicable to AHSS automotive applications, while describing unique process attributes.

4.C. Resistance Welding Processes

4.C.1. Fundamentals and Principles of Resistance Welding

Resistance welding processes represent a family of industrial welding processes that produce the heat required for welding through what is known as joule ($J = I Rt$) heating. Much in the way a piece of wire will heat up when current is passed through it, a resistance weld is based on the heating that occurs due to the resistance of current passing through the parts being welded. Since steel is not a very good conductor of electricity, it is easily heated by the flow of current and is an ideal metal for resistance welding processes. There are many resistance welding processes, but the most common is Resistance Spot Welding (RSW) (Figure 4.C-1). All resistance welding processes use three primary process variables – current, time, and pressure (or force). The automotive industry makes extensive use of resistance welding, but it is also used in a variety of other industry sectors including aerospace, medical, light manufacturing, tubing, appliances, and electrical.

The RSW process is often used as a model to explain the fundamental concepts behind most resistance welding processes. Figure 4.C-2 shows a standard RSW arrangement in which two copper electrodes apply force and pass current through the sheets being welded. If the sheets are steel, the resistance to the flow of current of the sheets will be much higher than the copper electrodes, so the steel will get hot while the electrodes remain relatively cool. But another important characteristic exists that is critical to most resistance welding processes – the contact resistance between the parts (or sheets) being welded. As indicated on the figure, the highest resistance to the flow of current is where the sheets meet ("Resistance" 4). This fact allows a weld nugget to begin forming and grow exactly where it is needed – between the sheets.

The figure depicts the flow of current from one electrode to the other as an electrical circuit that contains seven "resistors". Resistors 1 and 7 represent the bulk resistance of the copper electrodes, Resistors 2 and 6 represent the contact resistance between the electrodes and the sheets, Resistors 3 and 5 represent the bulk resistance of the sheets, and Resistor 4, as mentioned, represents the contact resistance between the sheets. Another fact that works strongly in the favor of resistance welding of steel is that as the steel is heated, its resistivity relative to copper increases even more. So, the initial contact resistance effectively heats the surrounding area which is in turn heated more rapidly because its resistance is higher since it is hotter. As a result, heating and weld nugget formation can occur quite rapidly. A typical weld time for RSW of steel is approximately 1/5 of a second. The current required in resistance welding is much higher than arc welding, and it is in the range of 8-15 kA.



Figure 4.C-1: RSW.

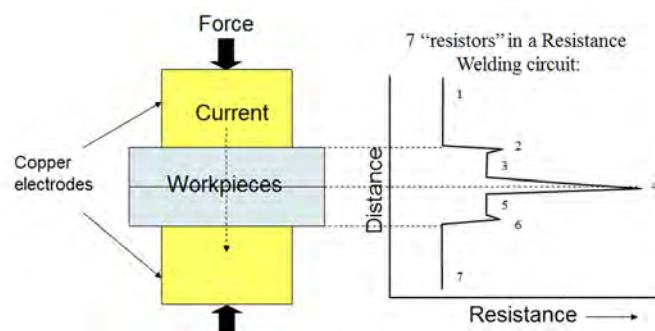


Figure 4.C-2: Resistances associated with steel resistance spot welds.

In addition to RSW, three other common resistance welding processes are Resistance Seam (RSEW), Projection (RPW), and Flash Welding (RFW) (Figure 4.C-3). The RSEW process uses two rolling electrodes to produce a continuous-welded seam between two sheets. It is often the process of choice for welding leak tight seams needed for automotive fuel tanks. RPW relies on geometrical features machined or formed on the part known as projections to create the required weld current density. RFW is very different from the other processes in that it relies on a rapid succession of high-current-density short current pulses which create what is known as flashing. During flashing, molten metal is violently expelled as the parts are moved together. The flashing action heats the surrounding material which allows a weld to be created when the parts are later brought together with significant pressure. Other important resistance welding processes which are not shown include High-Frequency Resistance Welding (HFRW) (used for producing the seams in welded pipe), and Resistance Upset Welding (RUW).

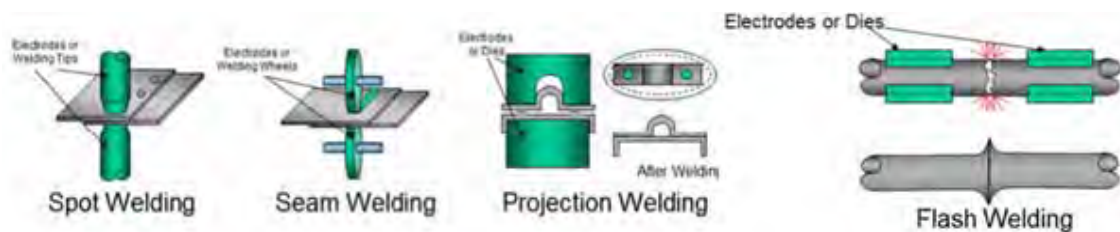


Figure 4.C-3: Common resistance welding processes.

Most welding processes produce welds that provide strong visible evidence of weld quality, so visual examination is often an important approach to verifying the quality of the weld. However, with most resistance welding processes visible examination is not possible due to the "blind" weld location between the sheets or parts being welded. As a result, maintaining weld quality with processes such as RSW is highly dependent on what is known as a lobe curve (Figure 4.C-4), which is basically a process window for RSW. The lobe curve represents ranges of weld current and time that will produce a spot weld nugget size that has acceptable mechanical properties for the intended application. So, weld quality monitoring with resistance welding processes relies highly on the ability to monitor parameters such as current and time. During production, if a weld is made with parameters that fall outside of the lobe curve, the weld is considered unacceptable. Ultrasonic testing is also often used in the automotive industry for Nondestructive Testing (NDT) of the blind location of RSW.

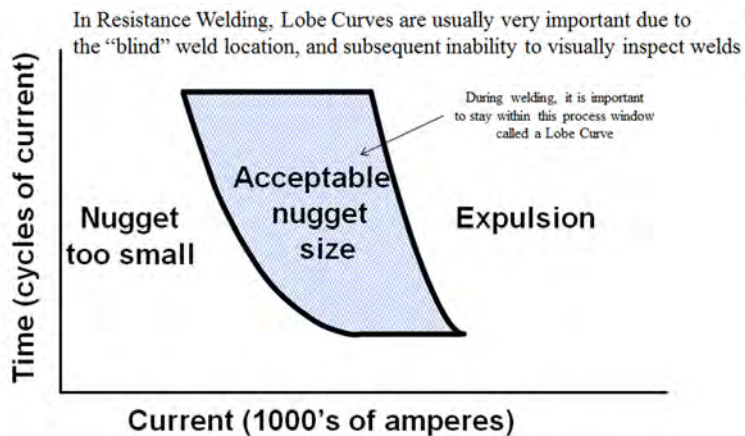


Figure 4.C-4: Resistance welding lobe curve.

Electrode geometry is a very important consideration with RSW. Figure 4.C-5 shows three common shapes, but there are many more options available including unique custom designs for specific applications. The basic electrode geometry is usually selected to improve the electrical-thermal-mechanical performance of an electrode. This is generally a geometry in which the cross-sectional area increases rapidly with distance from the workpiece, thereby providing a good heat

sink. The choice of shape may also include considerations such as accessibility to the part and how much surface marking of the part is acceptable. The diameter of the electrode contact area is also a consideration. Too small an area will produce undersized welds with insufficient strength, while too large an area will lead to unstable and inconsistent weld growth characteristics.



Figure 4.C-5: Typical RSW electrode geometries (left), example geometries used by automotive manufacturers (right).

Electrodes must be able to conduct current to the part, mechanically constrain the part, and conduct heat from the part. They must be able to sustain high loads at elevated temperatures, while maintaining adequate thermal and electrical conductivity. The choice of electrode alloy for a given application is often dictated by the need to minimize electrode wear. When electrodes wear, they typically begin to "mushroom", or grow larger in diameter. Electrode wear is accelerated when there is an alloying reaction between the electrode and the part, a common problem when welding Aluminum (Al) and coated steels. As the electrode diameter increases, the current density decreases, resulting in a decrease in the size of the weld. Since the strength of a spot-welded joint is directly related to the size of the weld nugget, electrode wear can be a big problem.

A range of Copper (Cu)-based or refractory-based electrode materials are used depending on the application. The Resistance Welding Manufacturers Association (RWMA) sorts electrode materials into three groups: A, B, and C. Group A contains the most common Cu-based alloys (see Table 4.C-1), Group B contains refractory metals and refractory metal composites, and Group C contains specialty materials such as dispersion-strengthened copper. Within the groups, they are further categorized by a class number. The general rule of thumb is as the class number goes up, the electrode strength goes up but the electrical conductivity goes down. When electrical conductivity goes down, the electrode heats more easily, resulting in premature electrode wear. The choice of electrode material involves many factors, but generally higher strength electrodes will be selected when higher strength materials are being welded. It is also important that the electrical and thermal conductivities of the electrode are much higher than those of the material being welded.

Table 4.C-1: Minimum mechanical and physical properties of Cu-based alloys for RWMA electrodes.^{A-18}

Group A ^a Copper Base Alloys		Hardness Rockwell			Conductivity %IACS ^b			Yield Strength ^c , ksi (5% Ext. Under Load)			Ultimate Tensile Strength, ksi			Elongation % in 2-in. or 4-in. Diameters		
Size Range		Class			Class			Class			Class			Class		
in.	mm	1	2	3	1	2	3	1	2	3	1	2	3	1	2	3
Diameter – Round Rod Stock (Cold Worked)																
Up to 1	Up to 25	65 HRB	75 HRB	90 HRB	80%	75%	45%	45	55	90	60	65	95	13%	13%	9%
Over 1 to 2	Over 25 to 51	60 HRB	70 HRB	90 HRB	80%	75%	45%	45	55	90	55	59	92	14%	13%	9%
Over 2 to 3	Over 51 to 76	55 HRB	65 HRB	90 HRB	80%	75%	45%	45	55	90	50	55	88	15%	13%	9%
Thickness – Square, Rectangular, and Hexagonal Bar Stock (Cold Worked)																
Up to 1	Up to 25	55 HRB	70 HRB	90 HRB	80%	75%	45%	45	45	90	60	65	95	13%	13%	9%
Over 1	Over 25	50 HRB	65 HRB	90 HRB	80%	75%	45%	45	40	90	50	55	90	14%	13%	9%
Thickness - Forgings																
Up to 1	Up to 25	55 HRB	65 HRB	90 HRB ^d	80%	75%	45%	45	45	50	60	55	94	12%	13%	9%
Over 1 to 2	Over 25 to 51	50 HRB	65 HRB	90 HRB ^d	80%	75%	45%	45	45	50	50	55	90	13%	13%	9%
Over 2	Over 51	50 HRB	65 HRB	90 HRB ^d	80%	75%	45%	45	40	50	50	55	88	13%	13%	9%
Castings																
All	All	NA	55 HRB	90 HRB	NA	70%	45%	NA	20	45	NA	45	75	NA	12%	5%

a All materials are In fully heat-treated condition unless otherwise specified. Round rod up to 1 in (25 mm) diameter is fully heat-treated and cold worked.

b International Annealed Copper Standard (IACS). Conductivity= $\frac{1}{0.0058 \text{ (Resistivity)}}$ where: Conductivity is expressed in %IACS and resistivity is in the units $\mu\Omega \text{ cm}$.

c Yield strength (YS) listed is typical – actual can be higher or lower.

d Hot worked and heat treated – but not cold worked.

The two most commonly used electrodes are the Class 1 and 2 electrodes of Group A. Class 1 electrodes [99% copper, 1% cadmium; 60 ksi UTS (forged); conductivity 92% International Annealed Copper Standard (IACS)] offer the highest electrical and thermal conductivity, and are typically used for spot welding Al alloys, magnesium alloys, brass, and bronze. Class 2 [99.2% copper, 0.8% chromium; 62 ksi UTS (forged), 82% IACS] electrodes are general-purpose electrodes for production spot and seam welding of most materials. IACS refers to a copper standard to which the electrodes are compared. Pure Cu has an IACS number of 100%.^{A-11, P-6, O-1}

In summary, most resistance welding processes offer the following advantages and limitations:

- Advantages:
 - Can weld most metals, but works best with steel
 - Extremely fast welding speeds are possible (a typical spot weld is produced in 1/5 of a second)
 - Very good for automation and production because of the “self-clamping” aspect of the electrodes
 - No filler materials required
 - RSW and RSEW are ideal for welding of thin sheets
- Limitations:
 - Equipment is much more expensive than arc welding equipment
 - Welds cannot be visually inspected (except for RFW and RUW welds)
 - The requirement for extremely high currents creates high power line demands
 - Equipment is not portable
 - Mechanical properties such as tensile and fatigue of welds made from processes

- Electrode wear
- such as spot welding can be poor due to the sharp geometrical features at the edge of the weld

4.C.2. RSW Procedures

In general, if any type of AHSS [Dual-Phase (DP), Transformation-Induced Plasticity (TRIP), Complex Phase (CP), Ferritic Bainitic (FB), or Martensitic (MS)] is used for the first time, the user should take the welding schedules applied to mild steel and then:

- Increase the electrode force by 20% or more depending on YS.
- Increase weld time as appropriate.

If these changes are insufficient, try these additional changes:

- A multi-pulse welding schedule (several pulses or post heating).
- Larger tip diameter and/or change the type of electrode.
- Increase the minimum weld size.

When resistance welded, AHSS require less current than conventional mild steel or HSLA because AHSS have higher electrical resistivity. Therefore, current levels for AHSS are not increased and may even need to be reduced depending on material chemical composition. However, most AHSS grades may require higher electrode forces for equivalent thickness of mild steels because electrode force depends on material strength. If thick mild steel or HSLA steel (of the same thickness) is replaced by an equivalent thickness of AHSS, the same forces may be required during assembly welding.

AHSS often have tighter weld windows (welding parameters that give acceptable welds) when compared to mild steels, as shown in the Figure 4.C-6.

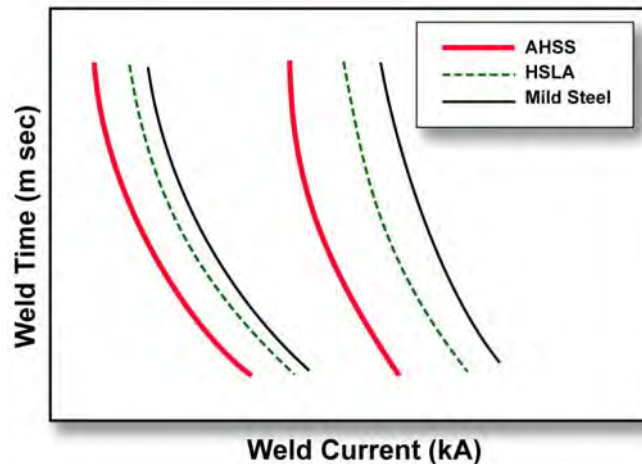


Figure 4.C-6: Schematic weld lobes for AHSS, HSLA, and mild steel with a shift to lower currents with increased strength.

The current range (kA) for AHSS of 600-1400MPa during RSW is shown in Figures 4.C-7 and 4.C-8. The process window for RSW of AHSS is influenced by the electrode force and welding time used in a major way. The current range increases by an average of 500 A for every additional 500 N of electrode force (Figure 4.C-7). The current range also increases by an average of 250 A for each additional 40 ms of welding time (Figure 4.C-8). Extra amounts of electrode force and welding time lead to increased current range, allowing for a wider process window.

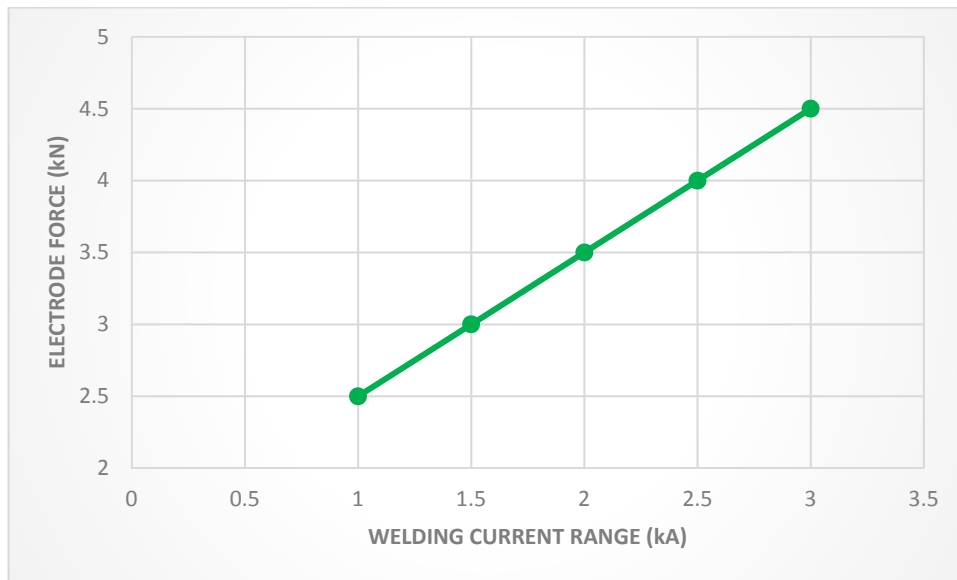


Figure 4.C-7: RSW with AHSS, current range for varying electrode force (Cap Type B 16/6, 6-mm tip diameter, single pulse, 340-ms weld time, 250-ms hold time, plug failures.). [19]

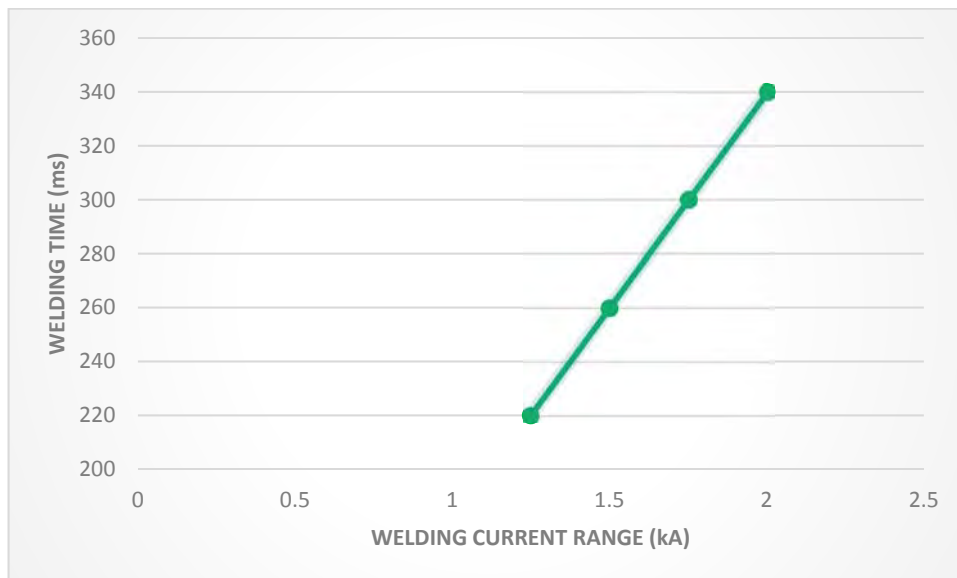


Figure 4.C-8: RSW with AHSS, current range for varying weld time (Cap Type B 16/6, 6-mm tip diameter, single pulse, 3.5-kN electrode force, 250-ms hold time, plug failures.).⁰⁻¹

A more extensive weld study^{T-5} of three DP HDGA (45/45 g/m²) coated steels showed similar welding behavior for all three steels. The 1.6-mm-thick steels were DP 340/590, DP 420/780, and DP 550/980. To characterize the welding behavior of the steels, useful current ranges and static weld tensile tests were performed. The useful current range is the difference between the welding current required to produce a minimum button size (I_{min}) and the current that causes expulsion of weld metal (I_{max}). In this study, the $4\sqrt{t}$ as the minimum button diameter was used, where “t” is the nominal sheet thickness. This is generally used in the automotive and steel industries. The weld current range was 2.2 kA for the DP 340/590 and DP 420/780 and 2.5 kA for the DP 550/980 steel (Figure 4.C-9). These current ranges are sufficiently wide to weld successfully the DP steels. The study also found no weld imperfections, which means these three DP steels are weldable with simple, easy to use welding parameters.

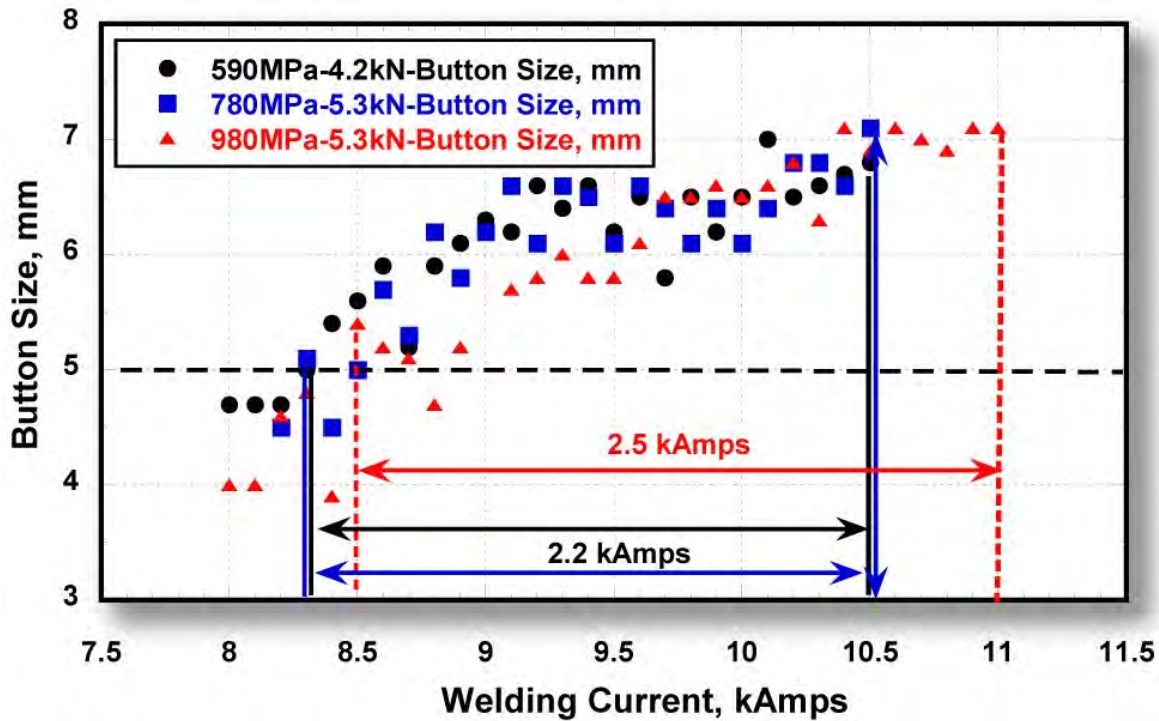


Figure 4.C-9: Welding current ranges for 1.6-mm HDGA DP steels with minimum tensile strengths of 590, 780, and 980 MPa.^{T-5}

Average reported weld hardness was 380 HV for the DP 340/590 and 415 HV for the other two. Again, all three DP steels had similar weld hardness distributions. The study also concluded that weld fracture mode alone is not a good indicator of weld integrity and performance. The load to fracture should be considered more important in judging weld integrity.

A second study^{T-6} compared two 1.6-mm-thick HDGA (45/45 g/m²) steels: DP 420/700 and TRIP 420/700. The weld current range for 18 cycles weld time was similar: 1.4 kA for the DP 420/700 and 1.5 kA for the TRIP 420/700. The average weld hardness was 400 HV for both steels. The study concluded that acceptable welds with no imperfections can be produced in both steel grades. Both steel grades are readily weldable with easily adoptable welding parameters. Weld tensile strength differences between the two steels were small and not considered statistically significant.

Weld schedules (Figure 4.C-10) with pulsed current profiles for AHSS can have weld-current ranges similar to mild steel. Even though there is no increased tendency for weld expulsion with AHSS, avoiding weld expulsion is highly desirable with AHSS. Loss of nugget material can affect weld-nugget size and strength.

Spot Welding of Galvanized TRIP 400/700 parameters settings, schematic

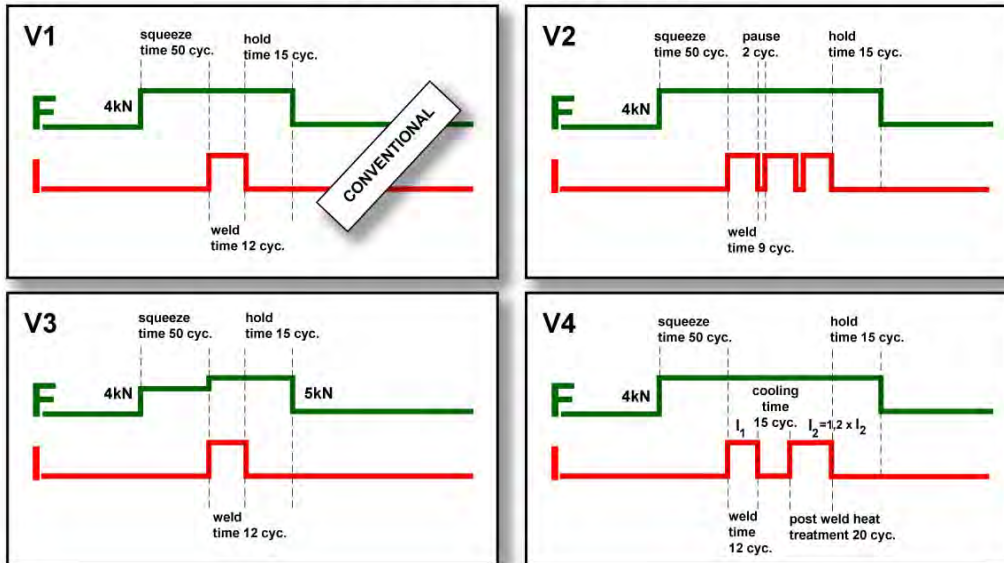


Figure 4.C-10: Schematics of optimized weld schedules for AHSS.^{B-1}

Post annealing (tempering pulse weld schedule) of TRIP steel may alter weld fracture mode and weld current range (Figure 4.C-11). However, since studies have shown that the occurrence of partial or IF fractures does not necessarily indicate poor weld quality, the use of pulsed current is not required to improve weld quality. Further, the effect of current pulsing on tensile and fatigue properties, as well as the electrode tip life, is not known. Therefore, users should perform their own evaluations regarding the suitability of such modified parameters.

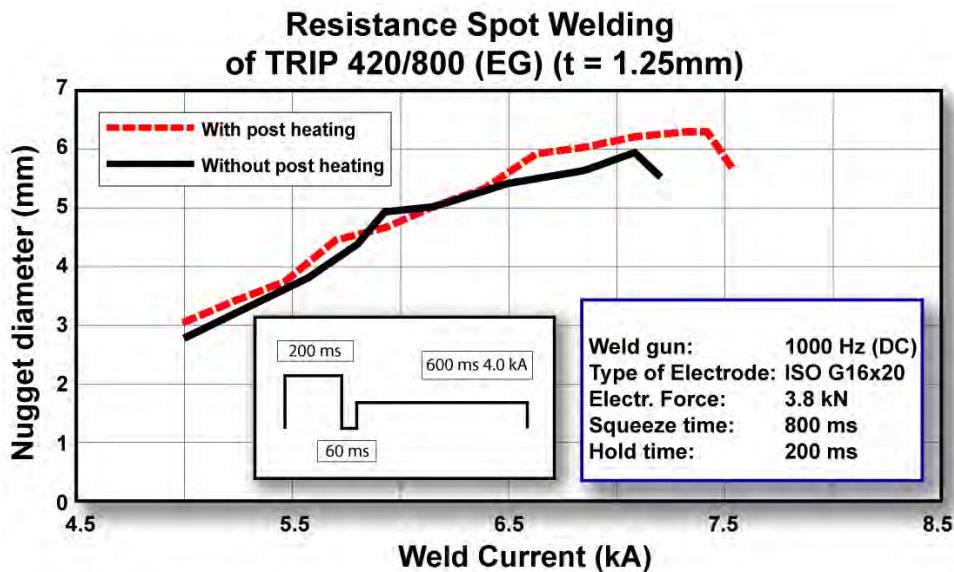


Figure 4.C-11: Post annealing may enlarge weld current range.^{B-1}

Additional work using Quench and Partition (Q&P) 980 showed less current required than conventional steels because it has higher electrical resistivity. Due to ultra-high base material (BM) strength, it needs higher electrode force than conventional steels which have equivalent thickness. The weld lobe of 1.6-mm Q&P 980 is shown in Figure 4.C-12 with the pulsed weld time and force of 5.8 kN. The yellow zone of this figure shows the fracture mode of full button (FBF) when peel tested. Some pictures of these weld spots' fracture mode are captured in Figure 4.C-13, for diameters of 6.0 to 7.7 mm.

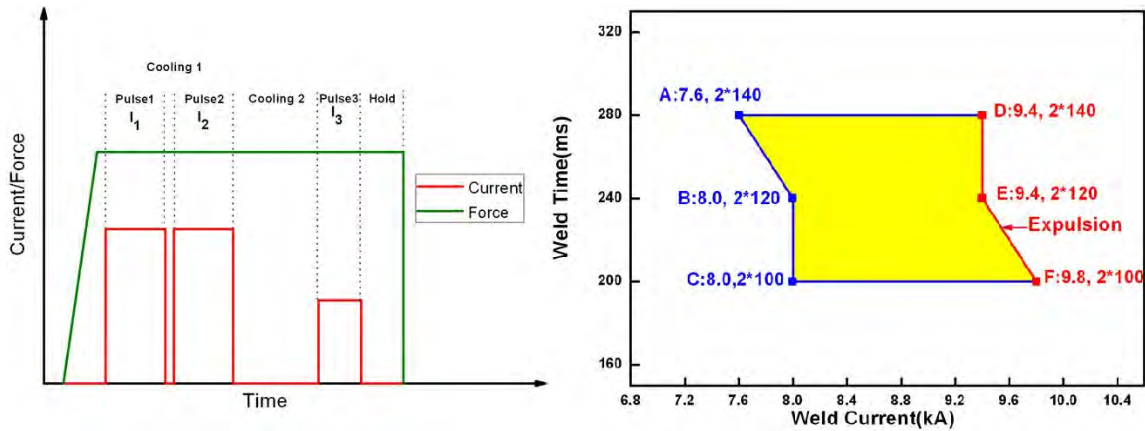


Figure 4.C-12: Pulsed current profile and weld lobe of 1.6-mm Q&P 980. ^{B-4}



Figure 4.C-13: Fracture mode of weld spots in yellow zone. ^{B-4}

Hardness measurements and cross sections through the spot weld different zones can be identified as depicted in Figure 4.C-14. In a first step, the spot-welded joint can be subdivided into

three zones: weld, HAZ, and BM. The weld is covered by the HAZ, where the melting temperature is not reached but high enough to change the microstructure. This region is dominated by inhomogeneous properties due to the different temperature and cooling gradients. Considering the hardness measurements of AHSS 3 sample, even a softening in the HAZ compared to the BM can be observed. Finally, the HAZ is surrounded by the BM, which does not show any local changes within the structure. These modifications of microstructure in the HAZ and weld are essential for the load-bearing capacity because the strength and ductility are drastically changed in comparison to the BM. Normally a high hardness is related to high strength and less ductility.

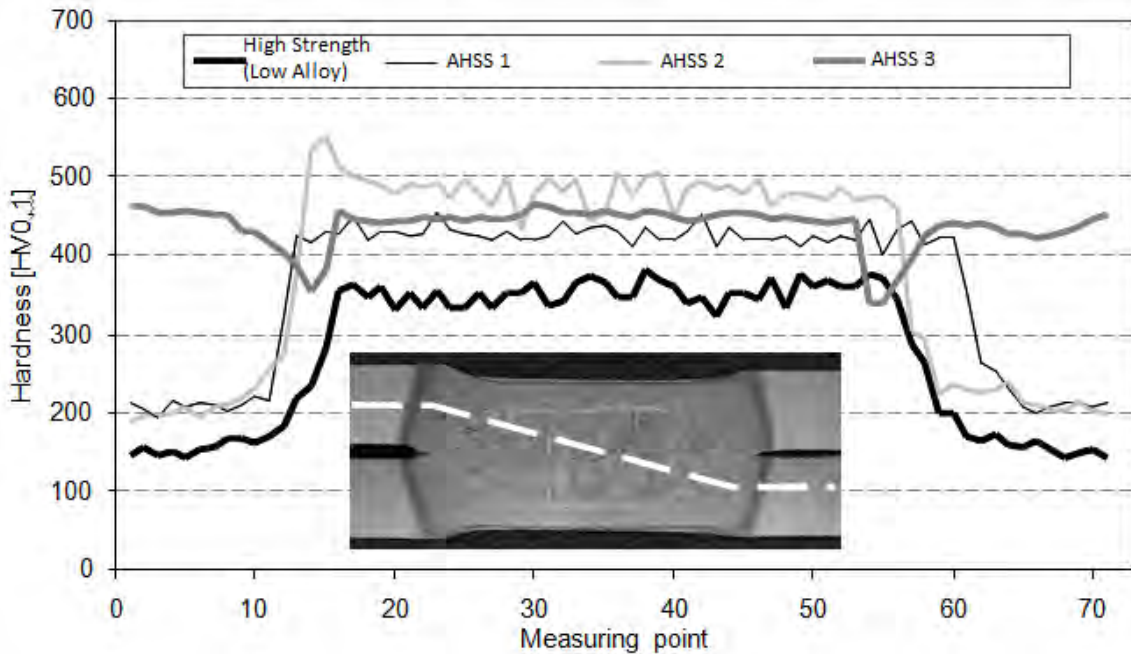


Figure 4.C-14: Hardness distribution through spot welds of various strength steels.^{P-7}

Weld spot micrograph and microhardness of 1.6-mm Q&P 980 is shown in Figure 4.C-15, in which no weld defects, such as cracks, shrinkage void, pore, no fusion, deep indentation, etc. were found. Hardness testing is typically performed as shown in Figure 4.C-16 (diagonal traverse across the weld from BM of top coupon to BM of bottom coupon) using a suitable instrument for micro-indentation hardness testing (Vickers or Knoop).

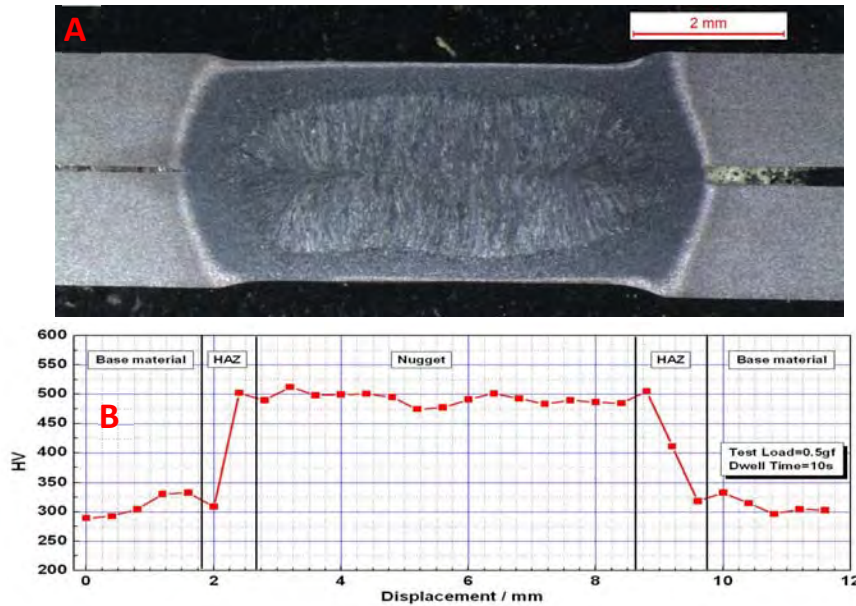


Figure 4.C-15: Weld spot micrograph and microhardness of 1.6-mm DP 980. ^{B-4}

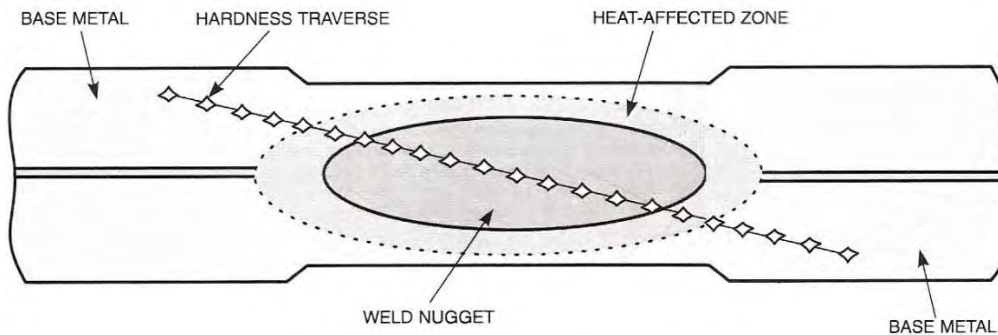
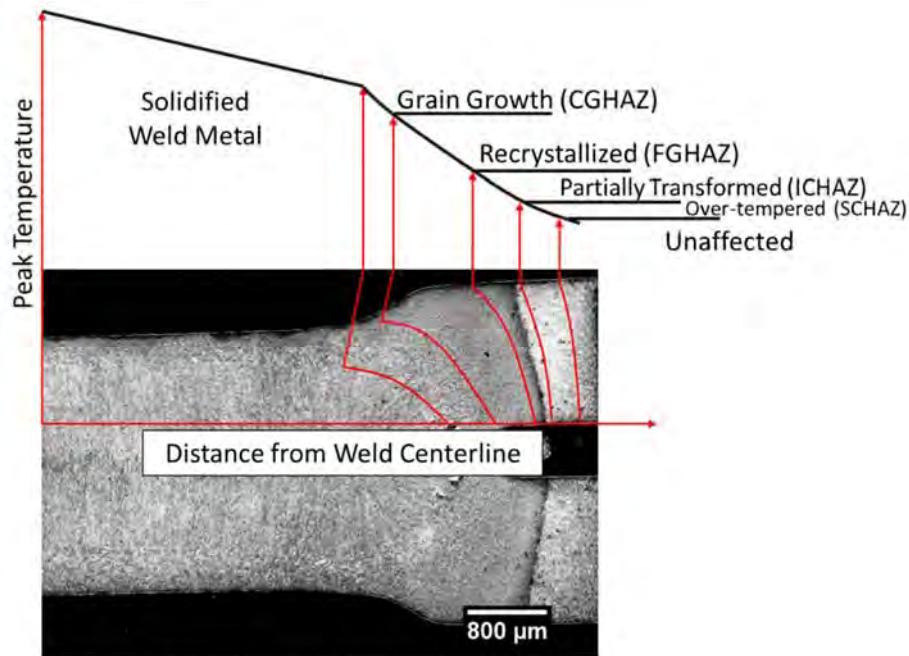


Figure 4.C-16: Typical cross-sectioned weld and hardness traverse. ^{A-13}

The different hardness values seen in a typical cross-sectioned weld depict different microstructural regions^{P-8}. Figure 4.C-17 shows the temperature distribution of a typical 2T weldment of hot stamped boron steel. At the solidified weld nugget, we see the highest temperatures and steadily decrease toward the unaffected base metal. The weld metal, coarse grain heat affected zone, fine grain heat affected zone, and unaffected base metal are made up of martensitic microstructure. The base metal has this microstructure due to the heat treatment (hot stamping) process. The weld metal, coarse grain heat affected zone, and fine grain heat affected zone are exposed to austenitizing temperature upon welding, and are cooled rapidly reforming the martensite microstructure. The subcritical heat affected zone has a unique microstructure of over-tempered martensite. In this region, the peak temperature re below the Ac1, causing the base metal martensitic microstructure to decompose into ferrite and cementite. Micrographs of the different weld regions can be seen in Figure 4.C-18.



Adapted from Easterling, *Introduction to the Physical Metallurgy of Welding*, 1992.

Figure 4.C-17: Temperature distribution of a typical 2T RSW of hot stamped boron steel.^{P-8}

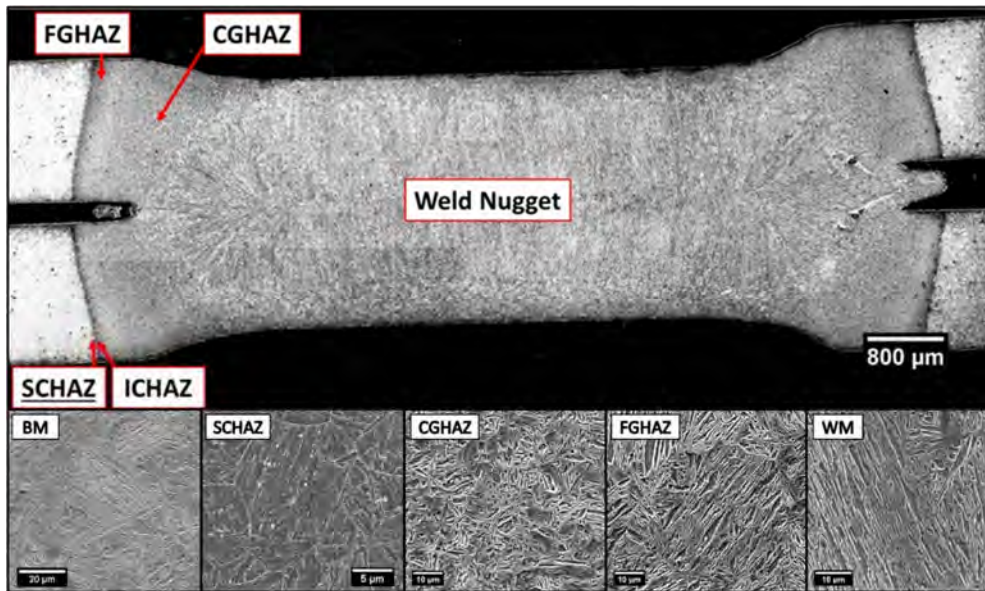


Figure 4.C-18: Different microstructures seen throughout the HAZ of a 2T hot stamped boron steel joint.^{P-8}

In summary, Tables 4.C-2 and 4.C-3 provide the AWS C1.1 Spot Welding Parameter Guidelines. These general guidelines can be used to approximate which parameters can be used to begin the RSW process of a specific part thickness. From the recommended parameters, changes can be made on a specific stack-up to ensure an acceptable strength and nugget size for a particular application. Additional, more complicated RSW parameter guidelines using a pulsation welding schedule with AC 60 Hz for welding AHSS is included in Table 4.C-4.

Table 4.C-2: Spot welding parameters for low-carbon steel 350-700 MPa (AHSS).^{A-14}

Spot-Welding Parameters for Bare, Galvanneal, and Galvanized Low-Carbon Steel 350-700 MPa (50-108 ksi) Ultimate Tensile											
Metal(e) Thickness [mm (in.)]	Electrode(f)		Net Electrode Force [kN (lb)]	Coated Weld(h) Time (cycles)	Bare Weld(h) Time (cycles)	Coated Weld Current (Approx) (A)	Bare Weld Current (Approx) (A)	Minimum Contact Overlap [mm (in.)]	Minimum Weld Spacing [mm (in.)]	Nugget Diameters(i)	
	Face Diameter [mm (in.)]	Shape(g)								Minimum Satisfactory [mm (in.)]	Setup [mm (in.)]
0.51 (0.020)	4.76 (0.187)	a,b,e	2.00 (500)	10	7	8,500	6,500	11.2 (0.44)	9.5 (0.37)	3.0 (0.12)	4.6 (0.18)
0.64 (0.025)	4.76 (0.187)	a,b,e	2.22 (600)	11	8	9,500	7,500	11.9 (0.47)	15.9 (0.63)	3.3 (0.13)	4.6 (0.18)
0.76 (0.030)	6.35 (0.250)	a,b,e	2.42 (650)	12	9	10,500	8,500	11.9 (0.47)	15.9 (0.63)	3.6 (0.14)	5.1 (0.20)
0.89 (0.035)	6.35 (0.250)	a,b,e,f	2.89 (700)	13	9	11,500	9,500	13.5 (0.53)	19.0 (0.75)	4.1 (0.16)	6.4 (0.25)
1.02 (0.040)	6.35 (0.250)	a,b,e,f	3.11 (800)	13	10	12,500	10,500	13.5 (0.53)	19.0 (0.75)	4.3 (0.17)	6.4 (0.25)
1.14 (0.045)	6.35 (0.250)	a,b,e,f	3.34 (900)	14	11	13,000	11,000	15.0 (0.59)	20.3 (0.94)	4.8 (0.19)	6.4 (0.25)
1.27 (0.050)	7.94 (0.313)	a,b,e,f	3.56 (1000)	16	12	13,500	11,500	15.0 (0.59)	20.3 (0.94)	5.1 (0.20)	7.9 (0.31)
1.40 (0.055)	7.94 (0.313)	a,b,e,f	4.56 (1100)	17	13	14,000	12,000	16.0 (0.63)	27.0 (1.06)	5.3 (0.21)	7.9 (0.31)
1.52 (0.060)	7.94 (0.313)	a,b,e,f	5.16 (1200)	18	14	15,000	13,000	16.0 (0.63)	27.0 (1.06)	5.6 (0.22)	7.9 (0.31)
1.78 (0.070)	7.94 (0.313)	a,b,e,f	5.60 (1400)	22	16	16,000	14,000	16.8 (0.66)	30.0 (1.18)	6.1 (0.24)	7.9 (0.31)
2.03 (0.080)	7.94 (0.313)	a,b,e,f	6.23 (1600)	25	18	17,000	15,000	18.3 (0.72)	34.9 (1.37)	6.6 (0.26)	7.9 (0.31)
2.29 (0.090)	9.52 (0.375)	a,b,e,f	7.72 (2100)	31	20	18,000	15,000	19.8 (0.78)	39.7 (1.56)	6.9 (0.27)	9.5 (0.37)
2.67 (0.105)	9.52 (0.375)	a,b,e,f	8.01 (2250)	35	23	19,500	16,500	21.3 (0.84)	42.7 (1.68)	7.1 (0.28)	9.5 (0.37)
3.05 (0.120)	9.52 (0.375)	a,b,e,f	9.34 (2100)	42	26	21,000	18,000	22.4 (0.88)	46.0 (1.81)	7.6 (0.30)	9.5 (0.37)

- (a) Use of coated parameters recommended with the presence of a coating at any faying surface.
- (b) These recommendations are based on available weld schedules representing recommendations from resistance welding equipment suppliers and users.
- (c) For intermediate thicknesses parameters may be interpolated.
- (d) Minimum weld button shear strength determined as follows:
 - $ST = (-6.36E-7 \times S^2 + 6.58E-4 \times S + 1.674) \times S \times 4 t^{1.5} / 1000$
 - ST = Shear Tension Strength (kN)
 - S = BM Tensile Strength (MPa)
 - t = Material Thickness (mm)
- (e) Metal thicknesses represent the actual thickness of the sheets being welded. In the case of welding two sheets of different thicknesses, use the welding parameters for the thinner sheet.
- (f) Welding parameters are applicable when using electrode materials included in RWMA Classes 1, 2, and 20.
- (g) Electrode shapes listed include: A-pointed, B-domed, E-truncated, F-radiused. Figure 2 shows these shapes.
 - The use of Type-B geometry may require a reduction in current and may result in excessive indentation unless face is dressed to specified diameter.
 - The use of Type F geometry may require an increase in current.
- (h) Welding parameters are based on single-phase AC 60 Hz equipment.
- (i) Nugget diameters are listed as:
 - Minimum diameter that is recommended to be considered a satisfactory weld.
 - Initial aim setup nugget diameter that is recommended in setting up a weld station to produce nuggets that consistently surpass the satisfactory weld nugget diameter for a given number of production welds.

Table 4.C-3: Spot welding parameters for low-carbon steel >700 MPa (AHSS).^{A-14}

Spot-Welding Parameters for Bare, Galvanneal, and Galvanized Low-Carbon Steel >700-MPa (102-ksi) Ultimate Tensile											
Metal(e) Thickness [mm (in.)]	Electrode(f)		Net Electrode Force [kN (lb)]	Coated Weld(h) Time (cycles)	Bare Weld(h) Time (cycles)	Coated Weld Current (Approx) (A)	Bare Weld Current (Approx) (A)	Minimum Contact Overlap [mm (in.)]	Minimum Weld Spacing [mm (in.)]	Nugget	
	Face Diameter [mm (in.)]	Shape (g)								Minimu m Satisfact ory [mm (in.)]	Setup [mm (in.)]
0.51 (0.020)	4.76 (0.187)	a,b,e	2.00 (500)	12	8	7,500	5,500	11.2 (0.44)	9.5 (0.37)	3.0 (0.12)	4.6 (0.18)
0.64 (0.025)	4.76 (0.187)	a,b,e	2.22 (600)	13	10	8,500	6,500	11.9 (0.47)	15.9 (0.63)	3.3 (0.13)	4.6 (0.18)
0.76 (0.030)	6.35 (0.250)	a,b,e	2.42 (650)	14	11	9,500	7,500	11.9 (0.47)	15.9 (0.63)	3.6 (0.14)	5.1 (0.20)
0.89 (0.035)	6.35 (0.250)	a,b,e,f	2.89 (700)	15	11	10,500	8,500	13.5 (0.53)	19.0 (0.75)	4.1 (0.16)	6.4 (0.25)
1.02 (0.040)	6.35 (0.250)	a,b,e,f	3.11 (800)	16	12	11,500	8,500	13.5 (0.53)	19.0 (0.75)	4.3 (0.17)	6.4 (0.25)
1.14 (0.045)	6.35 (0.250)	a,b,e,f	3.34 (900)	17	13	12,000	10,000	15.0 (0.59)	20.3 (0.94)	4.8 (0.19)	6.4 (0.25)
1.27 (0.050)	7.94 (0.313)	a,b,e,f	3.56 (1000)	19	14	12,500	10,500	15.0 (0.59)	20.3 (0.94)	5.1 (0.20)	7.9 (0.31)
1.40 (0.055)	7.94 (0.313)	a,b,e,f	4.56 (1100)	20	16	13,000	11,000	16.0 (0.63)	27.0 (1.06)	5.3 (0.21)	7.9 (0.31)
1.52 (0.060)	7.94 (0.313)	a,b,e,f	5.16 (1200)	22	17	14,000	12,000	16.0 (0.63)	27.0 (1.06)	5.6 (0.22)	7.9 (0.31)
1.78 (0.070)	7.94 (0.313)	a,b,e,f	5.60 (1400)	26	19	15,000	13,000	16.8 (0.66)	30.0 (1.18)	6.1 (0.24)	7.9 (0.31)
2.03 (0.080)	7.94 (0.313)	a,b,e,f	6.23 (1600)	30	21	16,000	14,000	18.3 (0.72)	34.9 (1.37)	6.6 (0.26)	7.9 (0.31)
2.29 (0.090)	9.52 (0.375)	a,b,e,f	7.72 (2100)	37	24	17,000	14,000	19.8 (0.78)	39.7 (1.56)	6.9 (0.27)	9.5 (0.37)
2.67 (0.105)	9.52 (0.375)	a,b,e,f	8.01 (2250)	42	28	18,500	15,500	21.3 (0.84)	42.7 (1.68)	7.1 (0.28)	9.5 (0.37)
3.05 (0.120)	9.52 (0.375)	a,b,e,f	9.34 [2400]	50	31	20,000	17,000	22.4 (0.88)	46.0 (1.81)	7.6 (0.30)	9.5 (0.37)

- (a) Use of coated parameters recommended with the presence of a coating at any faying surface.
- (b) These recommendations are based on available weld schedules representing recommendations from resistance welding equipment suppliers and users.
- (c) For intermediate thicknesses parameters may be interpolated.
- (d) Minimum weld button shear strength determined as follows:
 - $ST = (-6.36E-7 \times S^2 + 6.58E-4 \times S + 1.674) \times S \times 4 t^{1.5} / 1000$
 - ST = Shear Tension Strength (kN)
 - S = BM Tensile Strength (MPa)
 - t = Material Thickness (mm)
- (e) Metal thicknesses represent the actual thickness of the sheets being welded. In the case of welding two sheets of different thicknesses, use the welding parameters for the thinner sheet.
- (f) Welding parameters are applicable when using electrode materials included in RWMA Classes 1, 2, and 20.
- (g) Electrode shapes listed include: A-pointed, B-domed, E-truncated, F-radiused. Figure 2 shows these shapes.
 - The use of Type-B geometry may require a reduction in current and may result in excessive indentation unless face is dressed to specified diameter.
 - The use of Type F geometry may require an increase in current.
- (h) Welding parameters are based on single-phase AC 60 Hz equipment.
- (i) Nugget diameters are listed as:
 - Minimum diameter that is recommended to be considered a satisfactory weld.
 - Initial aim setup nugget diameter that is recommended in setting up a weld station to produce nuggets that consistently surpass the satisfactory weld nugget diameter for a given number of production welds.

**Table 4.C-4: AHSS bare-to-bare, bare-to-galvanized,
Galvanized-to-galvanized RSW parameters for pulsating AC 60 Hz.**

Thickness (mm)	Weld Force (kN)	Approx. Weld Current (kA)	Number of Pulses	Pulse Time (cycles)	Cool Time (cycles)
AHSS Bare to Bare FSC - AC 60-Hz Welder Controls					
0.6-1.0	2.6	8	1	9	0
1.0-1.6	3.6	9	1	11	0
1.6-2.3	4	10.5	2	7	1
2.3-2.6	5	11.5	3	8	2
AHSS Bare to Galvanized FSC - AC 60-Hz Welder Controls					
0.6-1.0	2.6	9	1	10	0
1.0-1.3	3.6	9.5	1	12	0
1.3-2.4	4	10.5	3	7	1
2.4-2.6	4	11.5	4	7	2
AHSS Galvanized to Galvanized FSC - AC 60-Hz Welder Controls					
0.6-1.0	2.3	10	1	14	0
1.0-1.3	2.6	10.5	1	16	0
1.3-2.0	3.6	11.5	3	8	2
2.0-2.6	4	12.5	4	7	2

4.C.3. Heat Balance - Material Balance - Thickness Balance

As discussed earlier, the heat input in RSW is defined as:

$$\text{Heat Input} = I^2Rt$$

where:

- I Welding current
- R IF and bulk resistance between two sheets
- t Welding time

The heat input must be changed depending on the gauge and grade of the steel. Compared to low strength steel at a particular gauge, the AHSS at the same gauge will need less current. Similarly, the thin gauge material needs less current than thick gauge. Controlling the heat input according to the gauge and grade is called heat balance in RSW.

For constant thickness, Table 4.C-5 shows steel classification based on strength level. With increasing group numbers, higher electrode force, longer weld time, and lower current are required for satisfactory RSW. Material combinations with one group difference can be welded with little or no changes in weld parameters. Difference of two or three groups may require special considerations in terms of electrode cap size, force, or type of power source.

Table 4.C-5 - Steel classification for RSW purposes. ^{A-11}

Group	Minimum Tensile Strength (MPa)	Typical Products
1	<350	Mild 140 YS/270 TS BH 180 YS/300 TS BH 210 YS/320 TS BH 240 YS/340 TS
2	350-500	BH 260 YS/370 TS HSLA 280 YS/350 TS HSLA 350 YS/450 TS DP 300 YS/50 0TS
3	>500-800	DP 350 YS/600 TS TRIP 350 YS/600 TS DP 500 YS/800 TS TRIP 500 YS/800 TS CP 700 YS/800 TS
4	>800	DP 700 YS/1000 TS MS 950 YS/1200 TS MS 1150 YS/1400 TS MS 1250 YS/1520 TS HF 950 YS/1300 TS

For a particular steel grade, changes in thickness may require adoption of special schedules to control heat balance. When material type and gage are varied together, specific weld schedules may need to be developed. Due to the higher resistivity of AHSS, the nugget growth occurs preferentially in AHSS. Electrode life on the AHSS-side may be reduced due to higher temperature on this side. In general, electrode life when welding AHSS may be similar to mild steel because of lower operating current requirement due to higher bulk resistivity in AHSS. This increase in electrode life may be offset in production due to poor part fit up created by higher AHSS springback. Frequent tip dressing will maintain the electrode tip shape and help achieve consistently acceptable quality welds.

4.C.4. Welding Current Mode

AHSS can be welded with power sources operated with either AC or DC types (Figure 4.C-18). Middle-Frequency Direct-Current (MFDC) has an advantage over conventional AC due to both unidirectional and continuous current. These characteristics assist in controlling and directing the heat generation at the interface. Current mode has no significant difference in weld quality. It should be noted that both AC and DC can easily produce acceptable welds where thickness ratios are less than 2:1. However, some advantage may be gained using DC where thickness ratios are over 2:1, but welding practices must be developed to optimize the advantages. It also has been observed that nugget sizes are statistically somewhat larger when using DC welding with the same secondary weld parameters than with AC. Some studies have shown that welding with MFDC provides improvements in heat balance and weld process robustness when there is a thickness differential in AHSS (as shown in Figure 4.C-19). DC power sources have been reported to provide better power factors and lower power consumption than AC power sources. Specifically, it has been reported that AC requires about 10% higher energy than DC to make the same size weld.^{L-7}

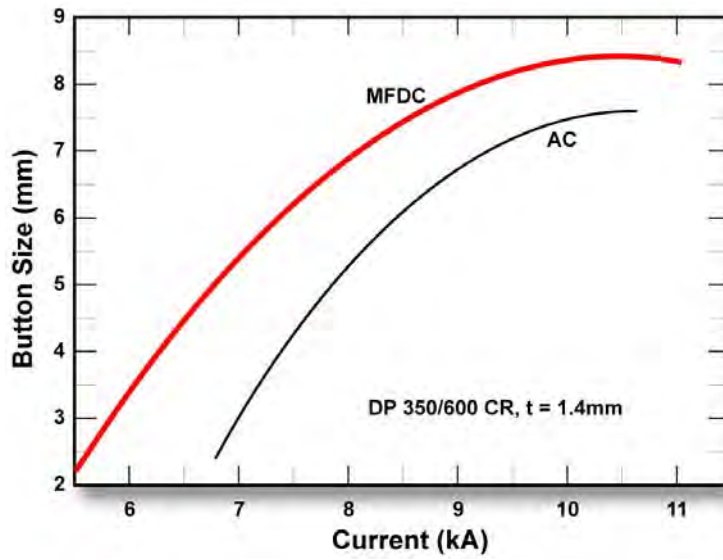
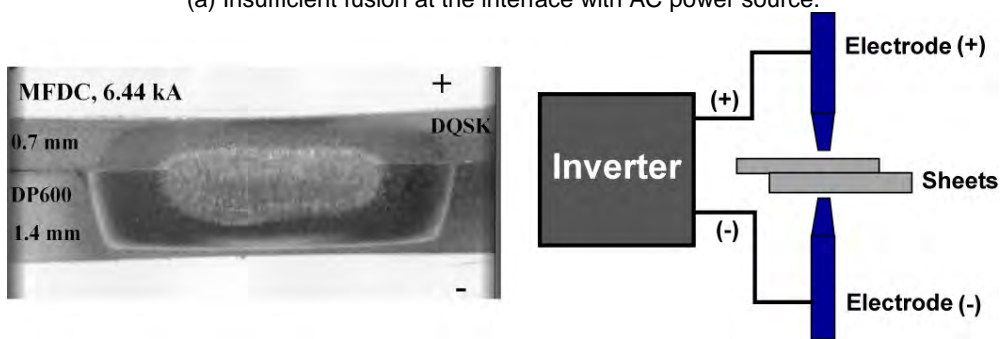


Figure 4.C-18: Range for 1.4-mm DP 350/600 CR steel at different current modes with a single pulse.^{L-2}



(a) Insufficient fusion at the interface with AC power source.



(b) Button size of 3.5 mm with DC power source

Figure 4.C-19: Effect of current mode on dissimilar-thickness stack-up^{L-2}

Consult safety requirements for your area when considering MFDC welding for manual weld gun applications. The primary feed to the transformers contains frequencies and voltages higher than for AC welding.

4.C.5. Electrode Geometry

Although there are differences in weld process depending on weld tip material and shape (truncated cone and dome shape), AHSS can be welded with all weld tip shapes and materials. Dome-shaped electrodes ensure buttons even at lower currents due to higher current densities at the center of the dome shape (Figure 4.C-20). The curve of dome-shaped electrodes will help to decrease the effect of electrode misalignment. However, dome electrodes might have less electrode life on coated steels without frequent tip dressing. Due to round edges, the dome electrode will have fewer tendencies to have surface cracks when compared to truncated electrode.

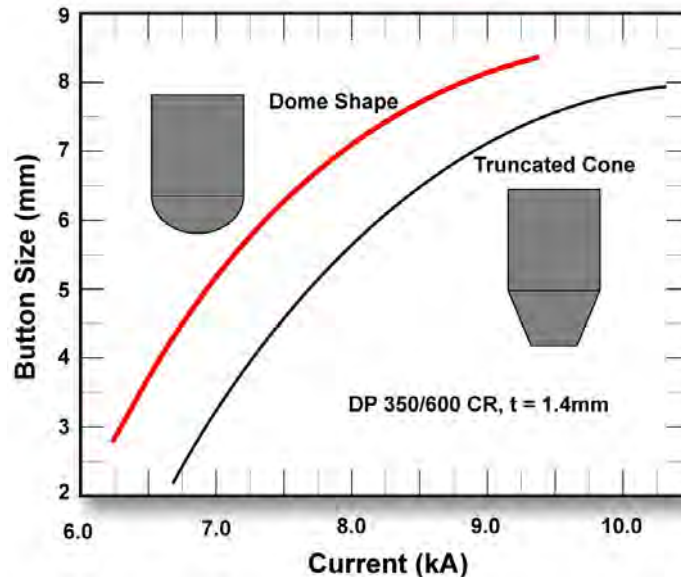


Figure 4.C-20: Effect of electrode geometry on current range using AC power mode and single pulse.^{L-2}

4.C.6. Part Fit-Up

Resistance welding depends on the interfacial resistance between two sheets. Good and consistent fit-up of parts is important to all resistance welding. Part fit-up is even more critical to the welding of AHSS due to increased YS and greater springback. In case of poor or inconsistent part fit-up, large truncated cone electrodes are recommended for both AHSS and conventional steels. The larger cap size will have large current range, which might compensate for the poor part fit-up. Also, progressive electrode force and upslope can be used to solve poor part fit-up.

4.C.7. Coating Effects

One of the methods by which the coatings are applied to the steel sheet surface is through a process called Hot Dipped Galvanizing (HDG). In this process, continuous coils of steel sheet are pulled at a controlled speed through a bath containing molten Zinc (Zn) at ~ 460° C. The Zn reacts with the steel and forms a bond. The excess liquid metal sticking on the sheet surface as it exits the bath is wiped off using a gas wiping process to achieve a controlled coating weight or thickness per unit area.

As mentioned earlier, AHSS are commercially available with HDGA or HDGI coatings. The term “galvanize” comes from the galvanic protection that Zn provides to steel substrate when exposed to a corroding medium. A Galvannealed (GA) coating (HDGA) is obtained by additional heating of the Zn-

coated steel at 450-590°C (840-1100°F) immediately after the steel exits the molten Zn bath. This additional heating allows iron (Fe) from the substrate to diffuse into the coating. Due to the diffusion of Fe and alloying with Zn, the final coating contains about 90% Zn and 10% Fe. Due to the alloying of Zn in the coating with diffused Fe, there is no free Zn present in the GA coating.

A study^{T-7} was undertaken to examine whether differences exist in the RSW behavior of DP 420/800 with a HDGA coating compared to a HDGI coating. The RSW evaluations consisted of determining the welding current ranges for the steels with HDGA and HDGI coatings. Shear and cross-tension tests also were performed on spot welds made on steels with both HDGA and HDGI coatings. Weld cross sections from both types of coatings were examined for weld quality. Weld micro hardness profiles provided hardness variations across the welds. Cross sections of HDGA and HDGI coatings, as well as the electrode tips after welding, were examined using a Scanning Electron Microscope (SEM). Composition profiles across the coating depths were analyzed using a glow-discharge optical emission spectrometer to understand the role of coating in RSW. Contact resistance was measured to examine its contribution to the current required for welding. The results indicated that DP 420/800 showed similar overall welding behavior with HDGA and HDGI coatings. One difference noted between the two coatings was that HDGA required lower welding current to form the minimum nugget size. This may not be an advantage in the industry given the current practice of frequent electrode tip dressing. Welding current range for HDGA was wider than for HDGI. However, the welding current range of 1.6 kA obtained for HDGI coated steel compared to 2.2 kA obtained for the HDGA coated steel is considered sufficiently wide for automotive applications and should not be an issue for consideration of its use (Figure 4.C-21).

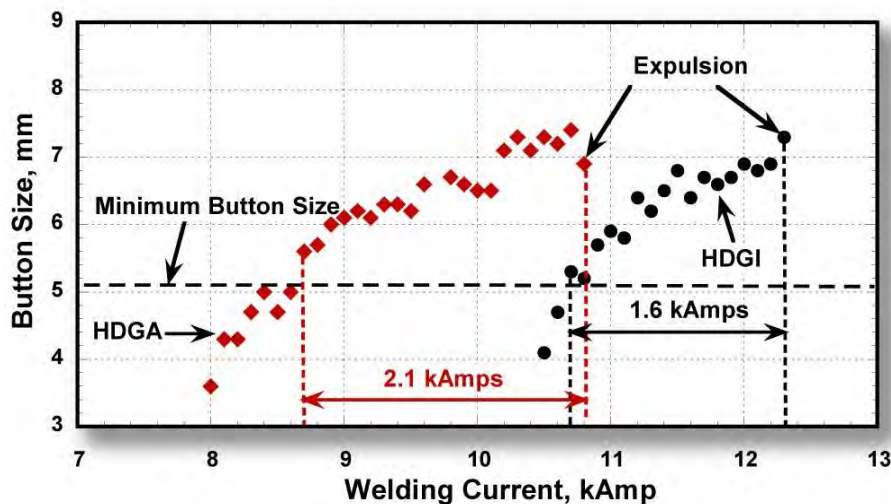


Figure 4.C-21: Welding current ranges for 1.6-mm DP 420/800 with HDGA and HDGI coatings.^{T-7}

As was mentioned briefly in Section 4.D.1, electrode wear is a larger issue when welding coated steels. In high-volume automotive production of Zn-coated steels, the rate of electrode wear tends to accelerate compared to the rate when welding uncoated steels. The accelerated electrode wear with coated steel is attributable to two mechanisms. The first mechanism is increasing in the electrode contact area (sometimes referred to as mushrooming effect) that results in decreased current density and smaller weld size. The second mechanism is electrode face erosion/pitting due to chemical interaction of the Zn coating with the Cu alloy electrode, forming various brass layers. These layers tend to break down and extrude out to the edges of the electrode (Figure 4.C-22). To overcome this electrode wear issue, the automotive industry is using automated electrode dressing tools and/or weld schedule adjustments via the weld controller. Typical adjustments include increase in welding current and/or increase in electrode force, while producing more welds. Research and development work has been conducted to investigate alternative electrode material and geometries for improving electrode life.

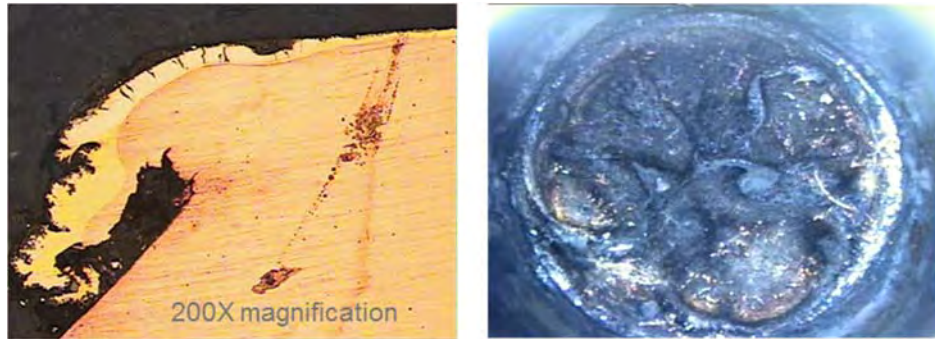


Figure 4.C-22: Erosion/pitting and extrusion of brass layers on worn RSW electrode.^{U-2}

The resistance weldability of coated steels can also cause problems. In many applications, more intricate welding schedules are used to ensure welds meet the size and strength requirements. Studies have been conducted to determine the nugget growth and formation mechanisms to properly select parameters for each pulse of a three-pulse welding schedule^{J-2} (Figure 4.C-23). The first pulse, high current and short weld time, is used to mitigate the effects of the coating on welding and develop contact area at the sheet-to-sheet interface. The second pulse, low current long weld time, is used to grow the weld nugget and minimize internal defects. The third pulse, medium current and long weld time, is used to grow the weldability current range and maximize the nugget diameter.

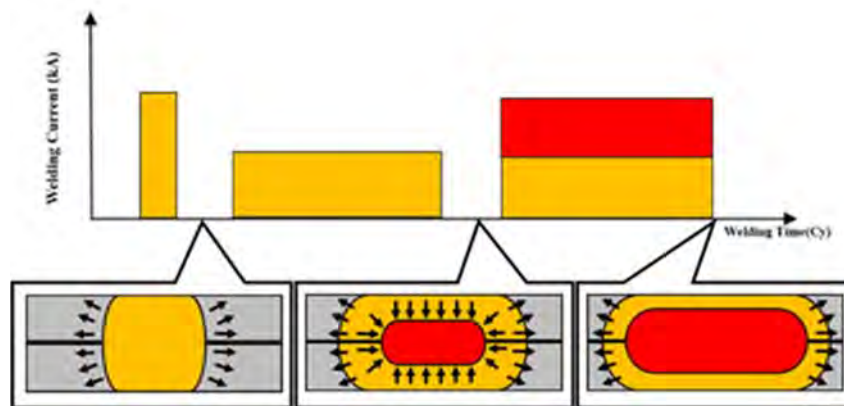


Figure 4.C-23: Weld growth mechanism of optimized three-pulse welding condition.^{J-2}

4.C.8. Judging Weldability Using Carbon Equivalence (CE)

Existing Carbon Equivalent (CE) formulas for RSW of steels do not adequately predict weld performance in AHSS. Weld quality depends on variables such as thickness, strength, loading mode, and weld size. New formulae are proposed by various entities. Because there is no universally accepted formula, use of any one CE equation is not possible and users should develop their own CE equations based on their experience.

4.C.9. Process Simulation

The advantages of numerical simulations for resistance welding are obvious for saving time and reducing costs in product developments and process optimizations. Today's modeling techniques can predict temperature, microstructure, stress, and hardness distribution in the weld and HAZ after welding. Commercial modeling software is available which takes into account material type, various current modes, machine characteristics, electrode geometry, etc. An example of process simulation

results for spot welding of 0.8-mm DC 06 low-carbon steel to 1.2-mm DP 600 steel is shown in Figure 4.C-24. Obviously, this technique can apply to dissimilar thicknesses, material types, and geometries. Application of adhesives is also being used with these simulations.

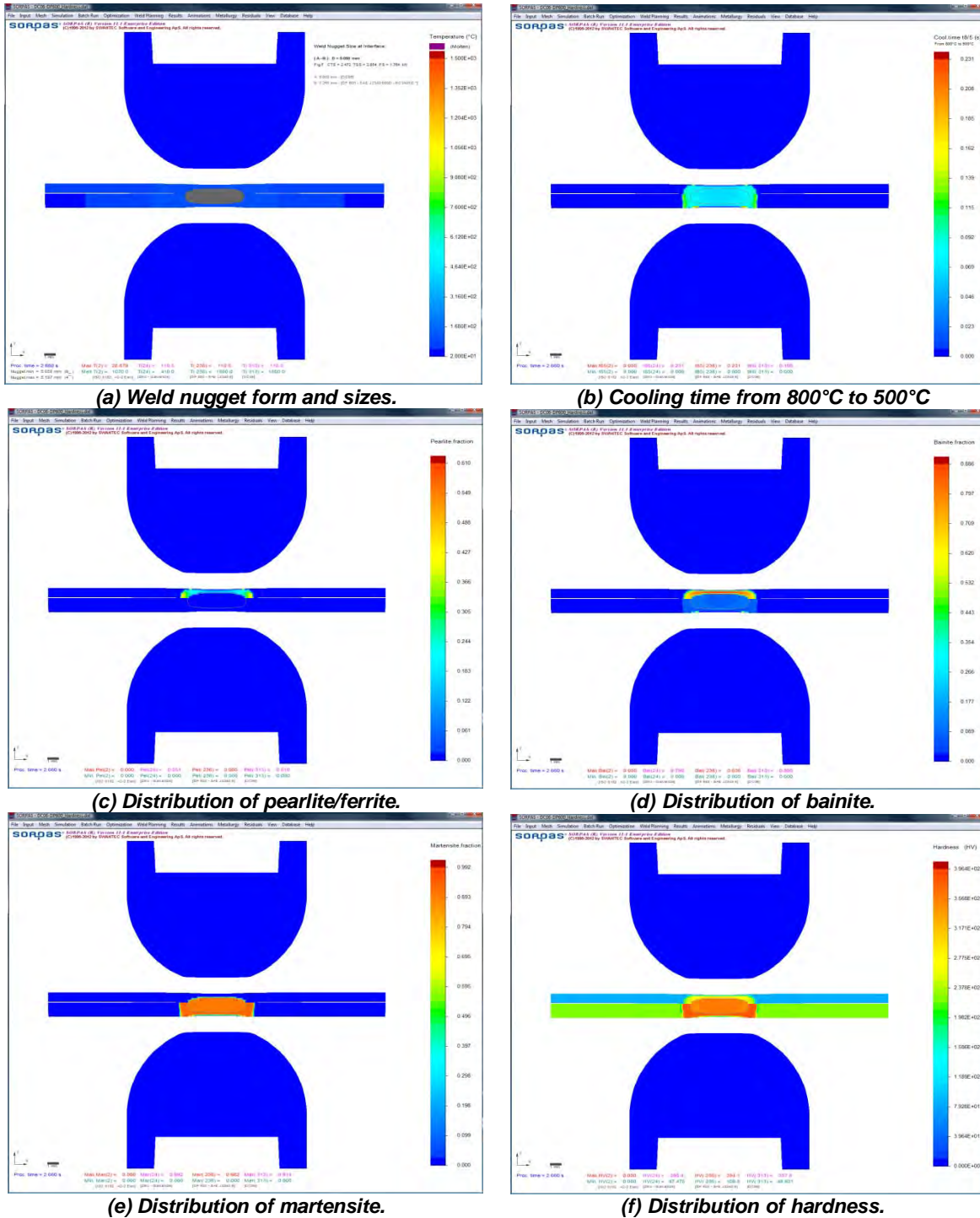


Figure 4.C-24: Simulation results with microstructures and hardness distribution for spot welding of 0.8-mm DC06 low-carbon steel to 1.2-mm DP 600 steel.^{Z-1}

4.D. Resistance Spot Welding Joint Test Performance

Acceptable weld integrity criteria vary greatly among manufacturers and world regions. Each AHSS user needs to establish their own weld acceptance criteria and the characteristics of AHSS resistance spot welds. AHSS spot weld strength is higher than that of the mild steel for a given button size (Figure 4.C-24). It is important to note that partial buttons (plugs) or IF fractures (IF not defined?) do not necessarily characterize a failed spot weld in AHSS. IF fractures may be typical of smaller weld sizes in Mild steel or in all weld sizes in AHSS. Reference is made to the new Specification AWS/ANSI D8.1 Weld Quality Acceptance for additional details (Figures 4.D-1 through 4.D-4).

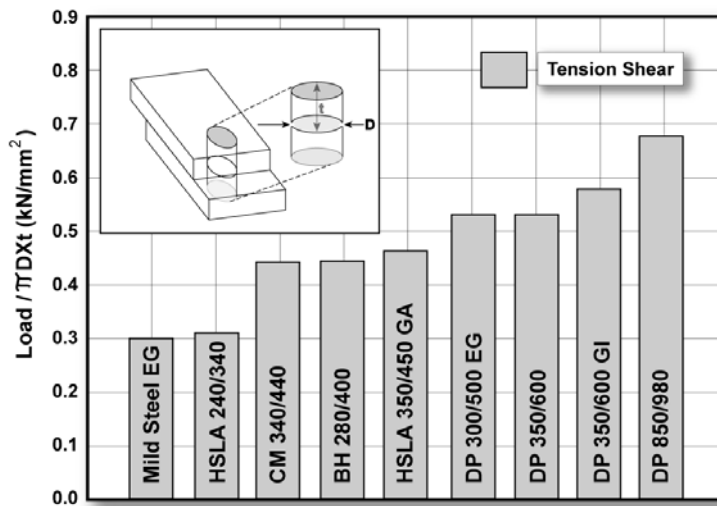


Figure 4.D-1: Load-bearing capacity of spot welds on various cold-rolled steels^{L-2} (Steel type, grade, and any coatings are indicated on the bars.)

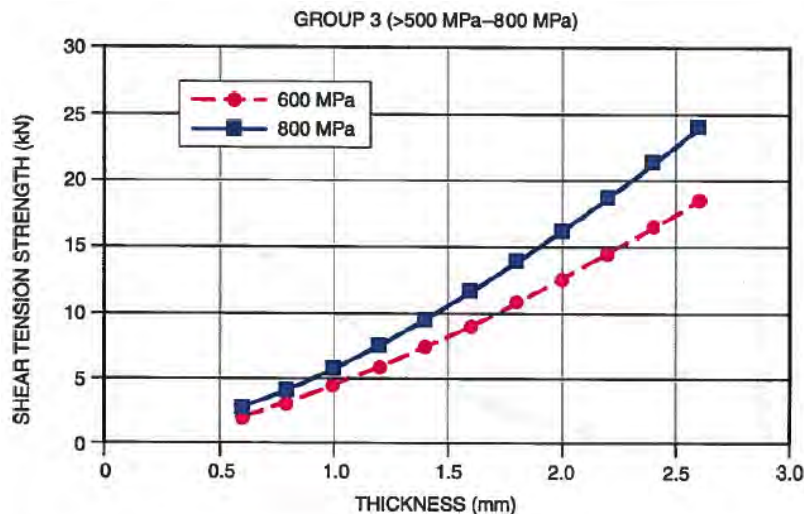


Figure 4.D-2: Representative minimum shear tension strength values for Group 3 steels. ^{A-13}

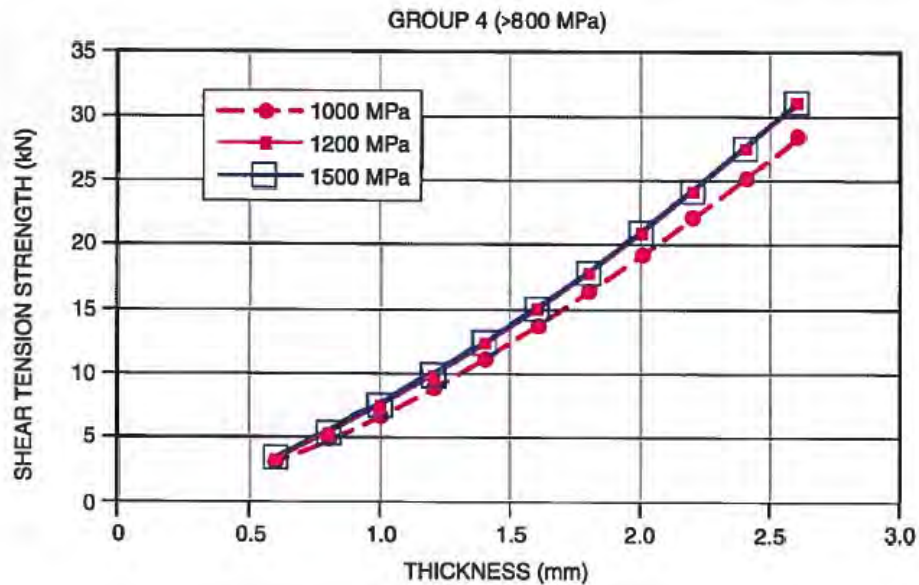


Figure 4.D-3: Representative minimum shear tension strength values for Group 4 steels. ^{A-13}

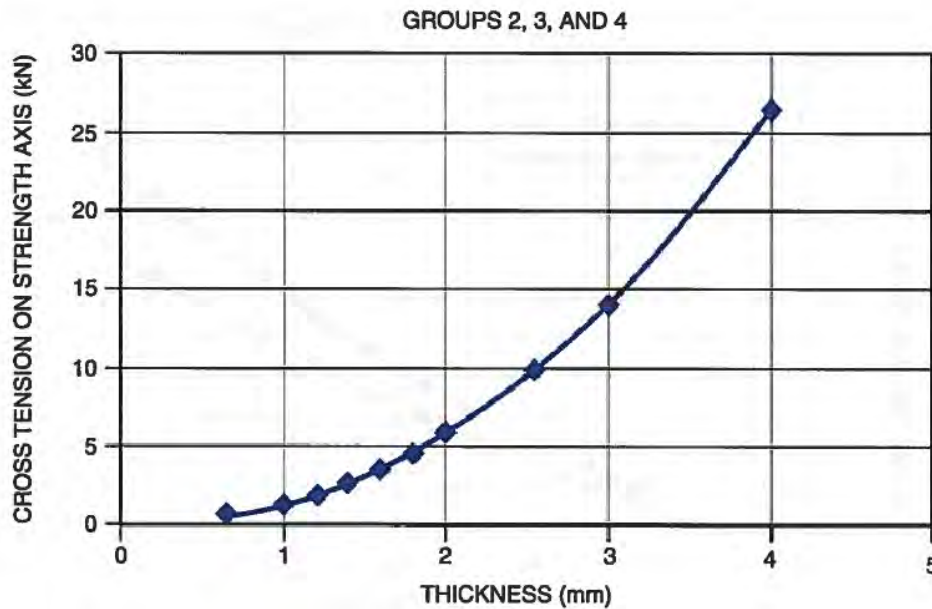


Figure 4.D-4: Minimum Cross-Tension Strength (CTS) values for Group 2, 3, and 4 steels. ^{A-13}

4.D.1. Destructive and In-Process Weld Testing

Peel and chisel testing of resistance spot welds in AHSS may produce fracture through the weld during destructive or teardown testing. This type of fracture becomes more common with increasing sheet thickness and BM strength. Weld metal fracture may accompany significant distortion of the metal immediately adjacent to the weld during testing. Such distortion is shown in Figures 4.D-5 and 4.D-6. Under these conditions weld metal fracture may not accurately predict serviceability of the joint. Weld performance of AHSS depends on microstructure, loading mode, loading rate, and degree of

constraint on the weld.

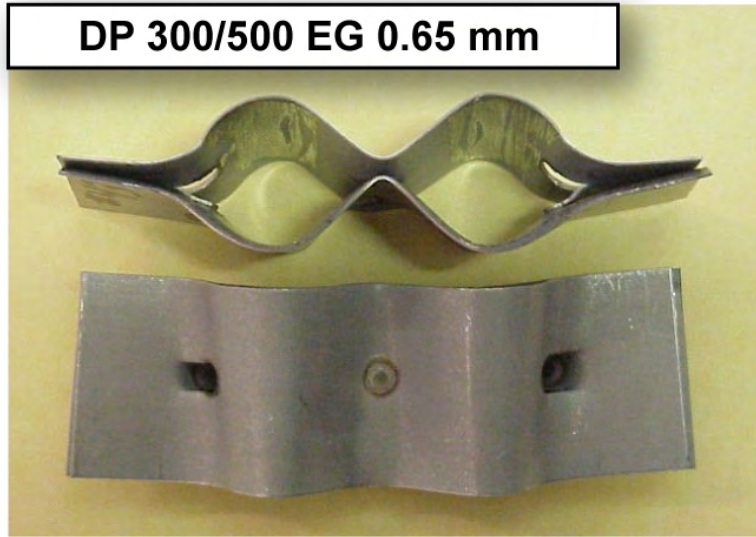


Figure 4.D-5: Example of laboratory dynamic destructive chisel testing of DP 300/500 EG 0.65-mm samples.^{M-1}

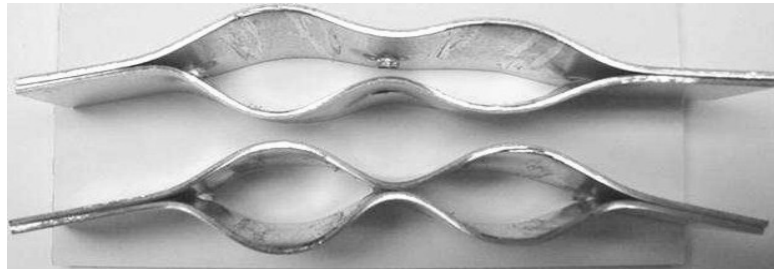


Figure 4.D-6 - Example of laboratory dynamic destructive chisel testing of DP 350/600 GI 1.4-mm samples.^{M-1}

Additionally, because of inherent stiffness of AHSS sheets, “nondestructive” chisel testing (Figure 4.D-6) on AHSS spot-welded panels will deform the panel permanently and may promote weld metal fracture. Therefore, this type of in-process weld check method is not recommended for AHSS with thicknesses greater than 1.0 mm. Alternative test methods should be explored for use in field-testing of spot welds in AHSS.



Figure 4.D-6: Semi-destructive chisel testing in 0.8-mm DP 300/500 EG.^{M-1}

Ultrasonic nondestructive spot weld testing has gained acceptance with some manufacturers. It still needs further development before it can replace destructive weld testing completely. Some on-line real-time systems to monitor the resistance welding are currently available and are being used in some weld shops.

4.D.2. Shear-Tension Strength of Welds and Fracture Modes

The AHSS weld tensile strength is proportional to material tensile properties and is higher than mild steel spot weld strength (Figure 4.D-7).

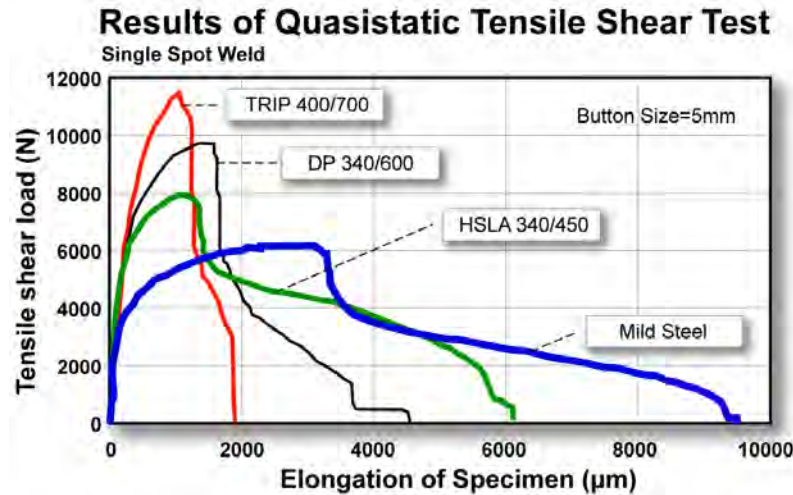
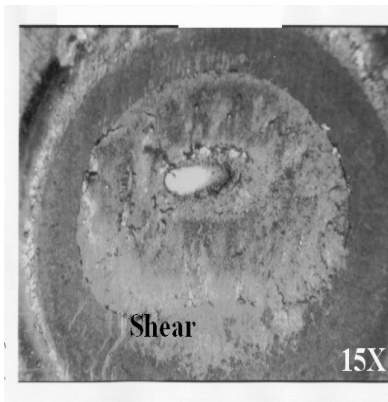


Figure 4.D-7: Tensile shear strength of single spot welds.^{L-4}

While testing thick AHSS spot welds (from small button size to expulsion button) the fracture mode during shear-tension testing may change from IF to button pull out or plug (as shown in Figure 4.D-6). Despite IF fractures [Figure 4.D-8 (a)], welds in AHSS may show high load-bearing capacity. In thin-gage steels, the fracture is often in a button or plug (Figure 4.D-9).



(a) IF fracture (low currents)



(b) Fracture by button pull out (high currents)

Figure 4.D-8: Fracture modes in thick (1.87-mm) DP 700/980 CR during tension-shear testing.

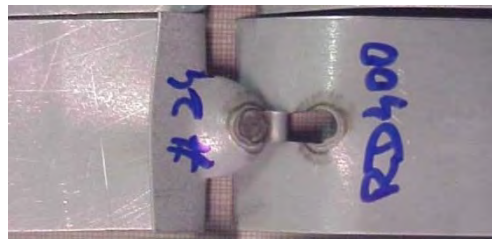


Figure 4.D-9: Fracture modes in thin (0.65-mm) DP 300/500 EG during tension-shear testing.^{L-2}

In a recently published study^{L-6}, Finite-Element Modeling (FEM) and fracture mechanics calculations can be used to predict the RSW fracture mode and loads in shear-tension tests of AHSS. The results were compared to those obtained for an IF steel. The results of the work confirmed the existence of a competition between two different types of fracture modes, namely FBF pull-out and interfacial (IF) fracture. The force required to cause a complete weld button pull-out type fracture was found to be proportional to the tensile strength and to the thickness of the BM as well as the diameter of the weld. The force to cause an IF weld fracture was related to the fracture toughness of the weld, sheet thickness, and weld diameter. For High-Strength Steels (HSS), it was determined that there is a critical sheet thickness above which the expected fracture mode could transition from pull-out to IF fracture. In this analysis, it was shown that, as the strength of the steel increases, the fracture toughness of the weld required to avoid IF fracture must also increase. Therefore, despite higher load-carrying capacity due to their high hardness, the welds in HSS may be prone to IF fractures. *Tensile testing showed that the load-carrying capacity of the samples that failed viral FI fracture was found to be more than 90% of the load associated with a FBF pull-out. This indicates that the load-bearing capacity of the welds is not affected by the fracture mode.* Therefore, the mode of fracture should not be the only criteria used to judge the quality of spot welds. The load-bearing capacity of the weld should be the primary focus in the evaluation of the shear-tension test results in AHSS.

Presently, some steel sheets have tensile strengths of 1,500 MPa or more. Such steels are subjected primarily to hot-press forming. The strengths of spot-welded joints are illustrated in Figure 4.D-10. The tensile shear strength of welded joints tends to increase with increasing steel sheet strength. Conversely, the Cross-Tension Strength (CTS) of welded joints tends to decline when the steel sheet strength is 780 MPa or more. This is thought to occur for the following reason. With increasing steel sheet strength, the stress concentration at the nugget edge increases, and nugget ductility and toughness decrease. When the amount of any added element [such as Carbon (C)] is increased in order to secure the desired steel sheet strength, the hardness of the weld metal (nugget) obtained increases; this, in turn, causes the nugget toughness to decrease. Nugget toughness also decreases when the contents of embrittling elements (P and S) are increased. The following equation of equivalent carbon content has been proposed to express the effects of these elements has been known.

$$C_{eq} (spot) = C + \frac{Si}{30} + \frac{Mn}{20} + 2P + 4S \leq 0.24 (\%) \quad (1)$$

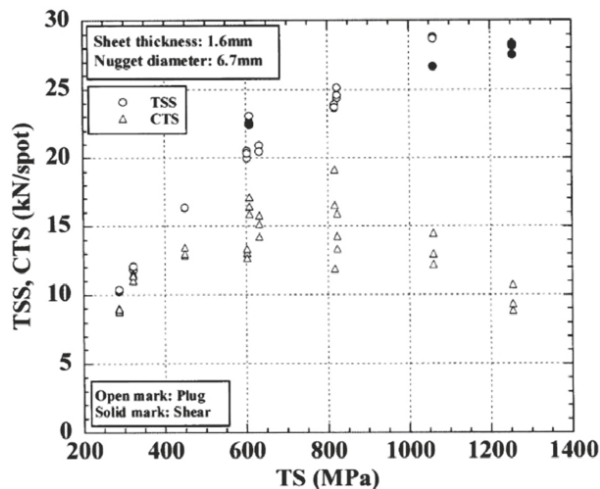


Figure 4.D-10: Effect of tensile strength of steel sheet on TSS and CTS of spot-welded joints.

It is believed that C, Silicon (Si), and Manganese (Mn) contribute to the increase in nugget hardness and Phosphorus (P) and Sulfur (S) contribute to the increase in segregation, thereby causing a decline in nugget toughness. The threshold value on the right-hand side represents the strength of a welded joint and the soundness of the fracture mode in a cross-tension test. When the C_{eq} (spot) is within the range indicated by the above equation, fracture always occur outside the nugget (plug fracture) and CTS is high. However, attempts have been made to enhance CTS by controlling the composition of steel sheet appropriately. It was reported that even when the steel sheet strength is maintained constant, the strength of the weld increases as C content decreases and the Si content increases. This is thought to occur for the following reason. With the increase in C content, the hardness of the weld increases and the sensitivity of the fracture to the stress concentration at the nugget end increases, thereby causing CTS to decline. By contrast, as the content of Si – a hardenability element – is increased, the region that is quench-hardened by Si widens, that is, the change in hardness in the region from the nugget to the BM becomes milder, thereby improving CTS.

According to a well-known material mechanics model, it is expected that the CTS of the spot-welded joints will improve with the increase in steel sheet strength. However, this contradicts the observed phenomenon. Therefore, a cross-tension test was considered based on fracture mechanics and attempted to clarify the dominant factors of CTS.

Understanding the fracture of spot-welded joints in the cross-tension test as a problem of crack propagation from around the nugget, the problem was studied using an elastic-plastic fracture mechanics model in order to obtain a general understanding of fracture, from the ductile fracture to the brittle fracture. According to elastic-plastic fracture mechanics, it is assumed that the crack starts to propagate when the crack propagation driving force (J) around the nugget under a tensile load reaches the fracture toughness (J_C) of the nugget edge. Therefore, it was attempted to derive the value of J and measure the value of J_C of the edge during the cross-tension test.

Figure 4.D-11 shows the distribution of maximum principal stress at the nugget edge under a load of 4 kN. The broken line in the figure indicates the fusion line. It is clear that the virtual crack in the edge opened during the deformation. The decline in potential energy that was caused by the opening was divided by the crack area to obtain the value of J . Figure 4.D-12 shows the dependence of the J -value on nugget diameter under a load of 5 kN, obtained for each of the two types of cracks. It is clear that, in either cracking direction, the J -value under the same load decreases with the increase in nugget diameter. According to the analysis result obtained for a nugget diameter of $3\sqrt{t}$, the J -value when the crack was allowed to propagate in the IF direction was slightly larger than that when the crack was allowed to propagate in the sheet thickness direction. However, for larger nugget diameters (4 and $5\sqrt{t}$), the J -value when the crack was allowed to propagate in the sheet thickness direction became larger than that when the crack was allowed to propagate in the IF direction.

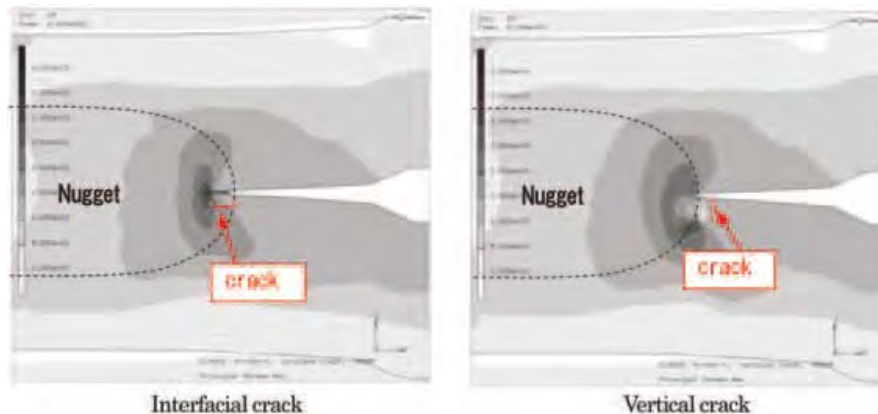


Figure 4.D-11: Deformed state and distribution of maximum principal stress at edge of nugget under the load of 4 kN.^{N-5}

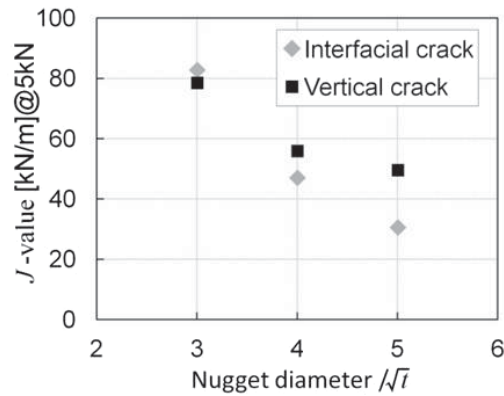


Figure 4.D-12: Dependence of J-value on nugget diameter under the load of 5 kN.^{N-5}

In Figure 4.D-13, the fractured 0.30% C specimen revealed a grain boundary fracture at the edge and a cleavage fracture surface inside the nugget.

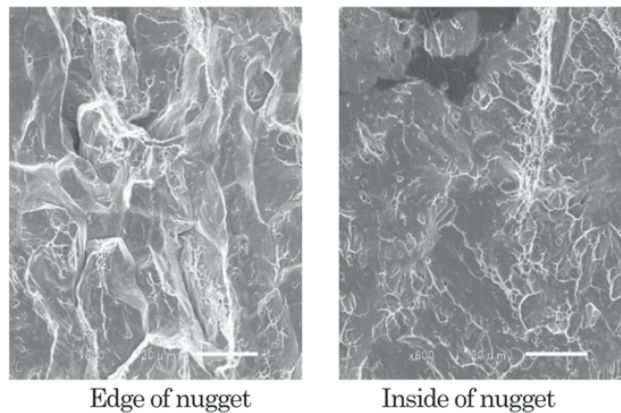


Figure 4.D-13: SEM images of fracture surface of miniature CT specimens after testing (0.30 mass % C).^{N-5}

The CTS of welded joints was 2.4 kN for the 0.30% C steel sheet and 6.6 kN for the 0.13% C steel sheet, the ratio between them being 0.38. According to the fracture toughness test results, the fracture stress ratio [J_C (0.30% C)/ J_C (0.13% C)]; the square root of J is proportional to stress) is 0.35. Thus, the above ratio was close to the test result. The 0.30% C joint subjected to the cross-tension test revealed a grain boundary fracture at the edge and a cleavage fracture surface inside the nugget.

4.D.3. Fracture Mode

Several automotive and national specifications are using the criterion of fracture modes as an indication of weld quality in production when using AHSS. During peel and chisel testing, results vary from FBF appearance to a complete interface fracture. An example of the various fracture modes experience by the automotive industry is shown in Figure 4.D-14.

Peel and Chisel Criteria - Failure Modes



Figure 4.D-14: Peel and chisel test fracture modes in automotive industry.

There is an approximate relationship between hardness and fracture mode in resistance spot-welded joints. It is found that peel-type loading of resistance spot-welded joints (e.g., coach peel, cross-tension tensile, and chisel testing) begins to produce partial plug and IF fractures at hardness levels exceeding 450 Hardness Value (HV). The relationship between post-weld hardness and fracture mode in peel-type loading is illustrated in Figure 4.D-15. It can be seen that there are no set levels of hardness, where one type of fracture mode changes to another type of fracture mode. Instead, there is much overlap between the hardness levels, where specific fracture mode types occur. This indicates that post-weld hardness is not the only factor determining fracture mode.

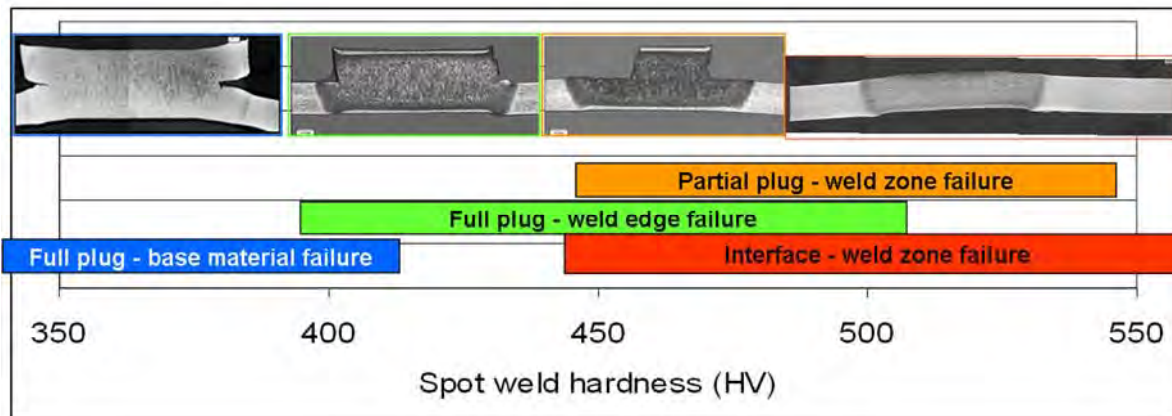


Figure 4.D-15: Schematic relationship between RSW hardness and failure mode in peel-type loading.

There are various approaches to predict the fracture of spot welded joints by detailed numerical simulations. However, there are many issues such as the adequate recording of different fracture modes or a numerical methodology for dissimilar welds, which mostly appear in automotive structures. Therefore, a new simulation approach has been developed managing to close the existing gap. This method is based on different damage criteria for each spot weld zone (BM, HAZ, and weld) in order to capture all relevant fracture modes. The model parameters are identified via an inverse method on the basis of simple standardized test (tensile shear tests and peel test), which makes the application efficient. All relevant fracture modes (IF fracture and plug fracture) can be detected. A precise prediction of spot welds behavior for similar and dissimilar joints were demonstrated. The results show that the material parameters determined for one sheet thickness are transferable to investigations with differing sheet thicknesses. Consequently, the experimental effort to characterize substitute spot weld models for full car crash simulations can be reduced.

The determination of the specific model parameters for a similar weld combination of DP automotive application steel with a low yield stress and large ultimate strength was presented (thickness of 1.5 mm, ferrite matrix with areas of martensite). A characterization of the plastic flow behavior for each zone is required. For the BM a tensile test provides the flow curve in the region of uniform elongation. In order to capture the plastic flow behavior of the transformed zones in a physical manner, the BM curve is scaled by the averaged hardness change in the HAZ and the weld. To determine the Gurson model parameters for the HAZ, a static peel test is done. This loading results in a high stress concentration in the vicinity of the notch which leads to fracture initiation and evolution in the HAZ. The numerical damage parameters for the HAZ are fitted according to the experiment (Figure 4.D-16).

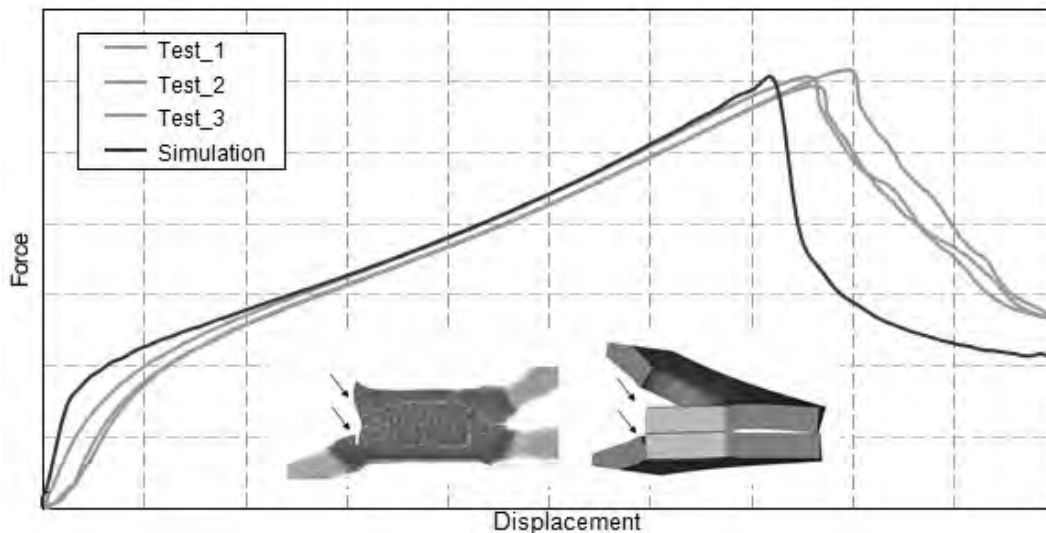


Figure 4.D-16: Parameter fitting for HAZ via peel test for DP steels.^{P-7}

4.D.4. Fatigue Strength of Spot Welds

In a comparative study^{L-6} of the spot weld fatigue strength of various steels grades, some of which included grades such as 1.33-mm Fully Stabilized (FS) 300/420 (HDGA), 1.35-mm DP 340/600 (HDGA), 1.24-mm TRIP 340/600 (HDGA), and 1.41-mm TRIP 340/600 (HDGA), it was concluded that BM microstructure/properties have relatively little influence on spot weld fatigue behavior (Figure 4.D-17). However, DP 340/600 and TRIP 340/600 steels have slightly better spot weld fatigue performance than conventional low-strength Aluminum-Killed Drawing Quality (AKDQ) steels. Further, it was found that the fatigue strength of spot welds is mainly controlled by design

factors such as sheet thickness and weld diameter. Therefore, if down-gauging with HSS is considered, design changes should be considered necessary to maintain durability of spot-welded assemblies.

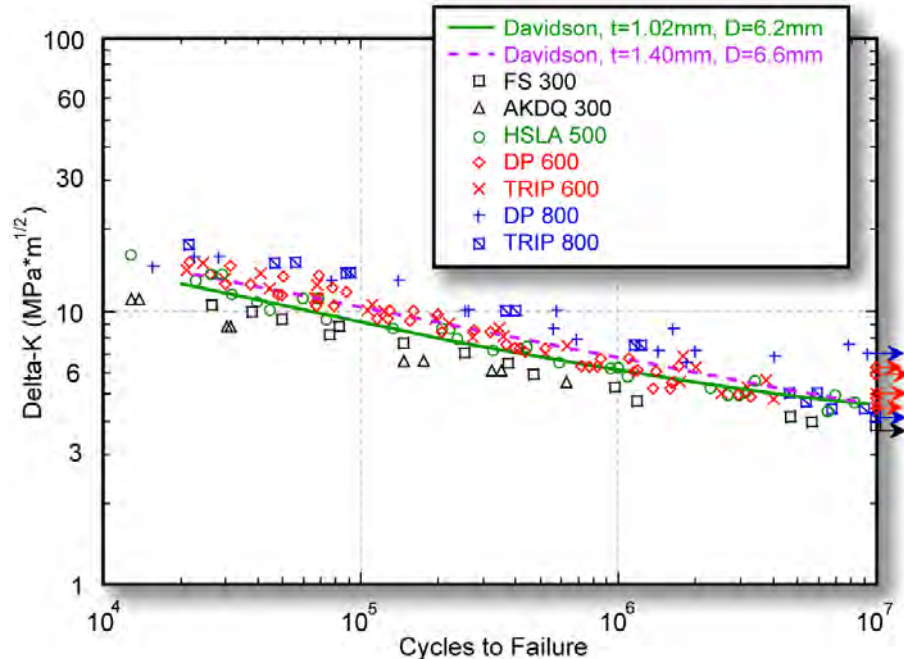


Figure 4.D-17: Tensile-shear spot weld fatigue endurance curves for various HSS
(The data are normalized to account for differences in sheet thickness and weld size. Davidson's data in the plot refer to historical data.^{L-6}).

Similar to mild steel, an increase in the number of welds in AHSS will increase the component fatigue strength (Figure 4.D-18). Multiple welds on AHSS will increase the fatigue strength more than mild steel.

Influence of Number of Welds on the Fatigue Behaviour of Resistance Spot Welded Specimens

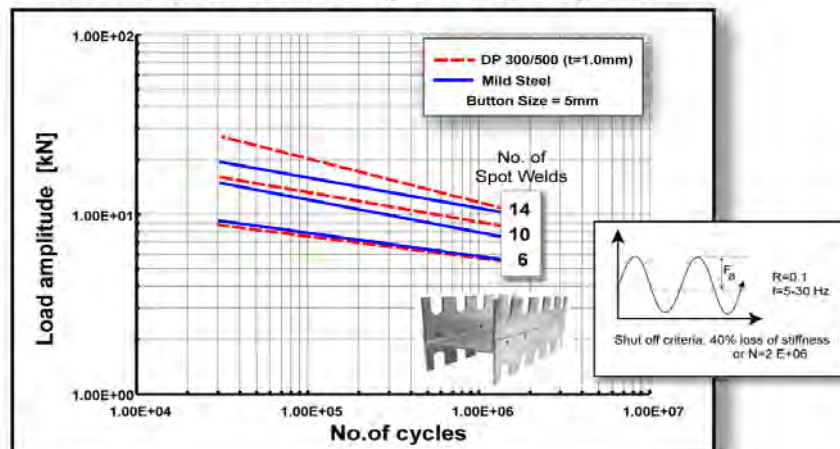


Figure 4.D-18: Effect of increase in number of welds in mild steel and DP steel components.^{S-4}

Figure 4.D-19 is a representative best-fit curve based on numerous data points obtained from mild steel, DP steels with tensile strengths ranging from 500 to 980 MPa, and MS steel with a tensile strength of 1400 MPa. The curve indicates that the fatigue strength of single spot welds does not depend on the BM strength.

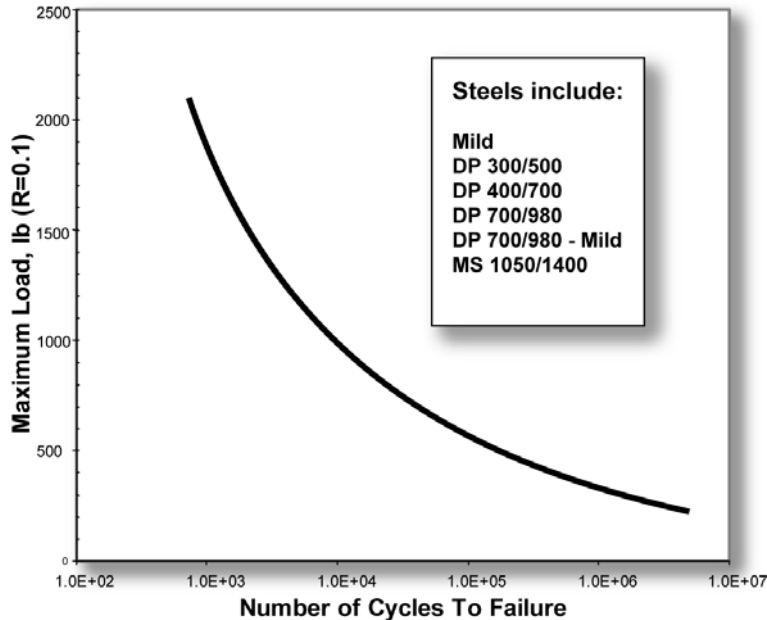


Figure 4.D-19: A best-fit curve through many data points for MS, DP steels, and MS steel (Fatigue strength of single spot welds does not depend on BM strength.^{L-2})

4.D.5. Improvement in CTS by Post-Heat Conduction

As described, the joint strength in the peeling direction begins to decrease when the BM strength exceeds 780 MPa. They found that the CTS of HSS joints could be improved by using appropriate conditions for post-heat conduction. Unlike the conventional tempering process in which the weld is tempered after a sufficient cooling time (i.e., after completion of martensite transformation of the weld), the post-heat conduction process incorporates a short cooling time; hence, it will not cause significant decline in productivity. The post-heat conduction process is described in detail below.

Figure 4.D-20 illustrates the effect of cooling time on CTS. It is clear that CTS reaches a peak for a cooling time of 6 cycles and improves when the post-heat conduction time is increased, even when the cooling time is increased to 35 cycles. With the aim of investigating why CTS improved, as described above, the conditions of solidification segregation were analyzed, for example, Mn, Si, and P. An example of P segregation is shown in Figure 4.D-21. When post-heat conduction was not performed at all or was performed using the conditions under which CTS did not improve [as shown in Figure 4.D-21(b)], the segregation of P in the same part decreased markedly. One reason for this is thought to be as follows. The element that was solidification-segregated during regular conduction was diffused during the post-heat conduction. As described in the preceding section, it is believed that the toughness of the nugget edge increased, thereby helping to enhance CTS.

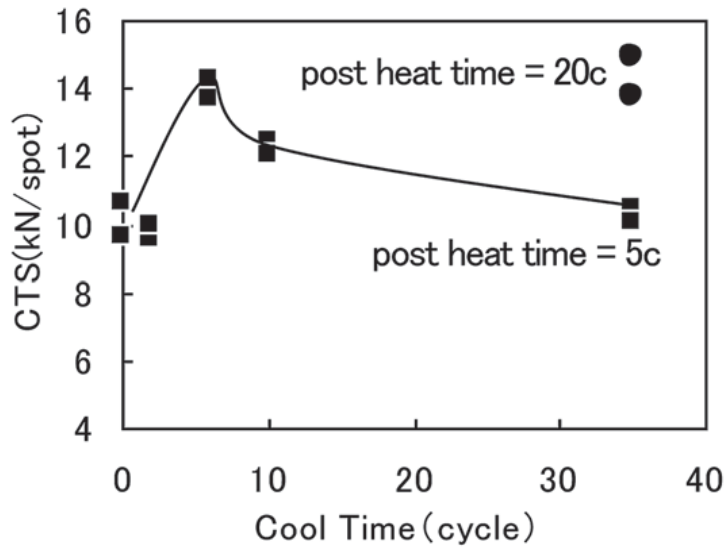


Figure 4.D-20: Effect of cool time on CTS (HS, 2-0-mm sheet thickness, $5\sqrt{t}$ nugget diameter).^{N-5}

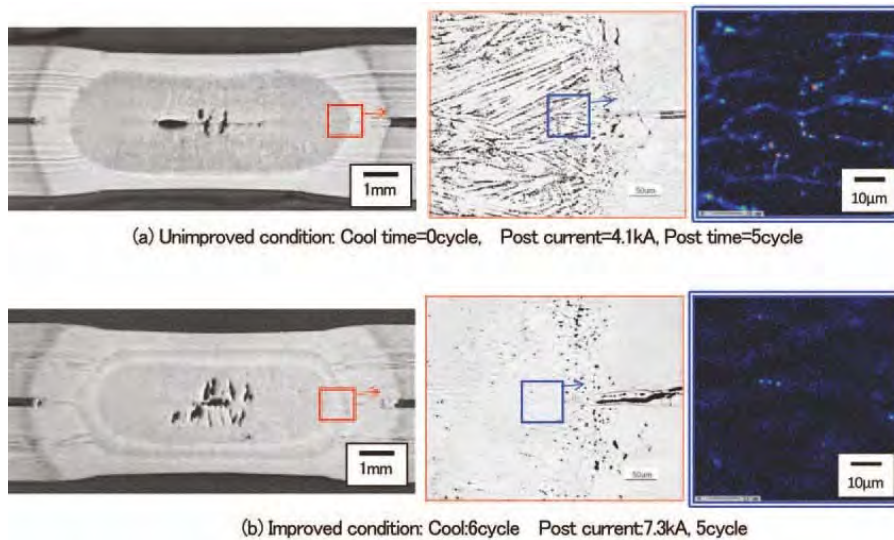


Figure 4.D-21: Effect of post-heat conditions on microstructure and solidification segregation at edge of nugget.^{N-5}

The effect of post-heat conduction in easing such solidification segregation is supported by other researchers. It should be noted that the hardness of the nugget interior remains the same, regardless of whether the post-heat conduction is implemented. Therefore, the above improvement in CTS cannot be attributed to the effect of tempering. Conversely, the application of post-heat conduction increased the degree and width of softening of the HAZ. From the standpoint of fracture mechanics, the degree of influence of the widening of soft HAZ on the improvement in CTS was estimated to be about 4%. Therefore, the improvement in CTS by post-heat conduction can be attributed mainly to the enhancement of fracture toughness by the easing of solidification segregation.

Figure 4.D-22 shows comparison of CTS between with and without pulse pattern at the nugget diameter. The strength became higher when welded with pulse pattern, especially when the pulse current was between 8 and 9 kA. These results suggest that the pulsation pattern achieved adequate reduction in solidification segregation and soften the HAZ.

4.D.6. Embrittlement Phenomenon

It has been a long-standing challenge to extend the usage of the very high-strength steels in hydrogen-rich environments, given that these steels are prone to Hydrogen Cracking, due to their increased mechanical strength. Hydrogen embrittlement (HE) is known to be a premature fracture caused by a small amount of hydrogen atoms concentrated at highly stressed regions inside susceptible high tensile strength materials. (See examples in Figure 4.D-23.)

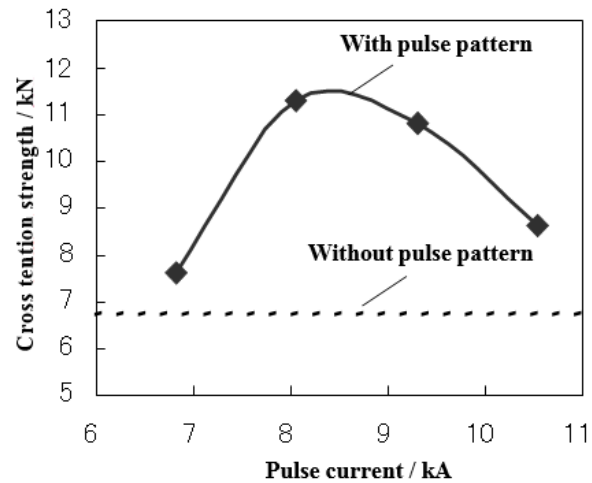


Figure 4.D-22: Comparison of CTS between with and without pulse pattern.^{J-1}

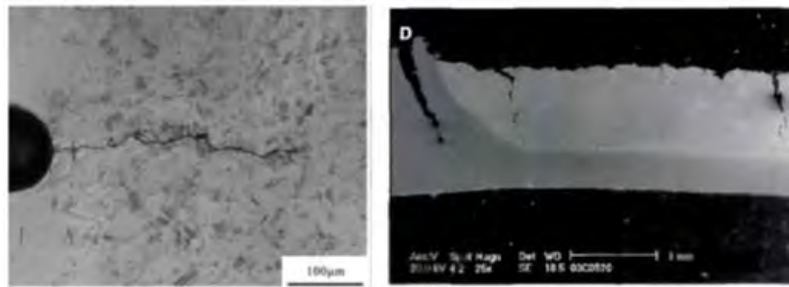


Figure 4.D-23: Examples of hydrogen embrittlement (HE) failure in RSW.

The factors controlling the occurrence of HE, susceptible microstructure, stress, and the presence of hydrogen, are well known and have been sufficiently quantified to develop procedures that minimize its occurrence mostly in arc welding thicker gage steels. When advanced high strength steel (AHSS) with tensile strength over 980 MPa are applied in automotive applications, there is a small risk that hydrogen embrittlement fracture (sometime called delayed fracture) may occur after welding, while a vehicle is in use. Although there have been no reports that automotive parts made of AHSS have fractured due to hydrogen embrittlement, a risk assessment of delayed fracture for AHSS is considered necessary to ensure the safety of the automotive body and encourage wider use of UHSS sheets.

Another common embrittlement phenomenon involves the zinc coating discussed previously. Resistance spot welding is dependent on the interfacial contact resistance between the electrodes and the material. During welding, a metal with a lower melting point, such as zinc can penetrate in a liquid state into the grain boundaries of the material. By the end of the welding process, liquid metal embrittlement (LME) can become a problem due to the ductility of the grain boundary being reduced by the impeding tensile stress. (Example can be seen in Figure 4.D-24.) Also, brittle intermetallic compounds, such as Cu_5Zn_8 , are created by the reaction with the Cu electrode and the material at the high temperature, which promotes LME or surface cracking.

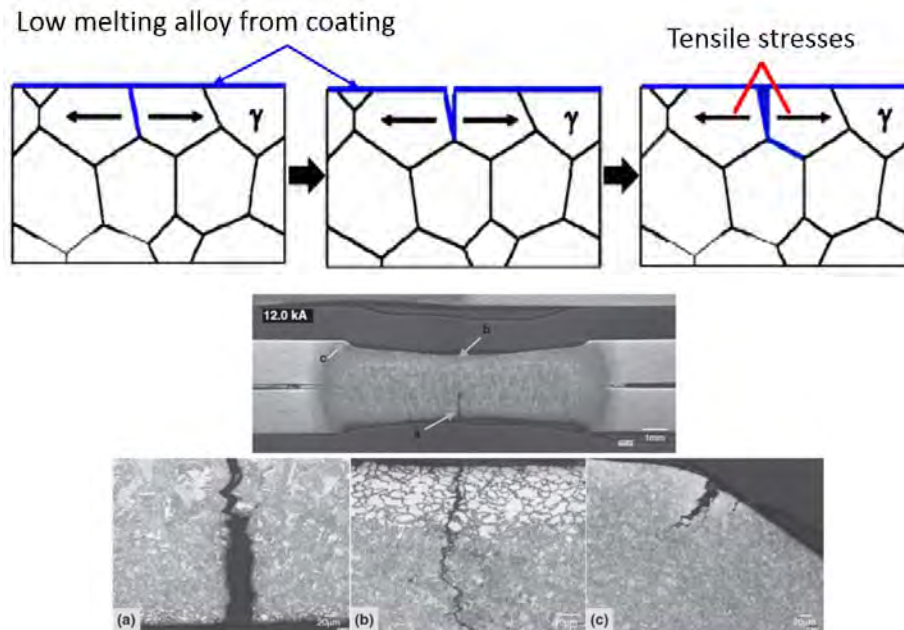


Figure 4.D-24: Description of (top image) and actual example (bottom) of the LME phenomenon in zinc coated AHSS.

There are many research papers investigating and analyzing Liquid Metal Embrittlement in mild steel and AHSS. LME is not unique to automotive AHSS steels or RSW, but is discovered in other ferrous materials, heat treatment and other welding processes. In spot welding AHSS, the complex microstructure and the greater spring back behavior of AHSS eventually lead to weld discontinuities such as LME.

In summary, LME cracking may occur when a combination of tensile stress, liquid metal and susceptible microstructure exist. Studies are being performed to evaluate whether LME is mitigated by today's automotive RSW processes, where the volume of welds significantly exceeds engineering requirements, or whether the occurrence of LME actually affects in-use properties at all.

4.E. Spot Welding of Three Steel Sheets with Large Thickness Ratios

Car parts such as side panels are fabricated by spot welding three steel sheets together. When the outer steel sheet is a thin sheet of mild steel and the reinforcement steel sheets are thick sheets of HSS (that is, when there is a large thickness ratio between the sheets), it is often difficult to spot weld such sheets together. The term “thickness ratio” as used herein refers to the total thickness of the three steel sheets divided by the thickness of the thinnest steel sheet. Nuggets obtained by spot welding of three steel sheets are illustrated in Figure 4.E-1 (a). In the spot welding of three steel sheets with a large thickness ratio, it is difficult to form a nugget at the interface between thin and thick steel sheets, as shown in Figure 4.E-1 (b). The reason for this is that in spot welding, because of heat removal by the water-cooled electrode, the fusion progresses from the thickness center of the three steel sheets toward the outside, except for the heat generated by contact resistance at the steel sheet surfaces in the early stages of welding time. In addition, in view of the dimensional accuracies of actual members, it is necessary to set appropriate welding conditions when there is a gap between steel sheets. In practice, the proper welding current range is as shown in Figure 4.E-2. However, the welding current range is often narrower in one-step spot welding.

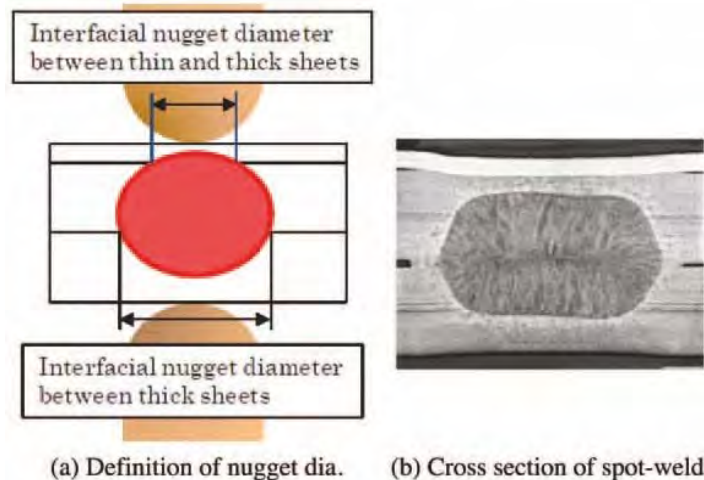


Figure 4.E-1: Three sheets spot welded.^{N-5}

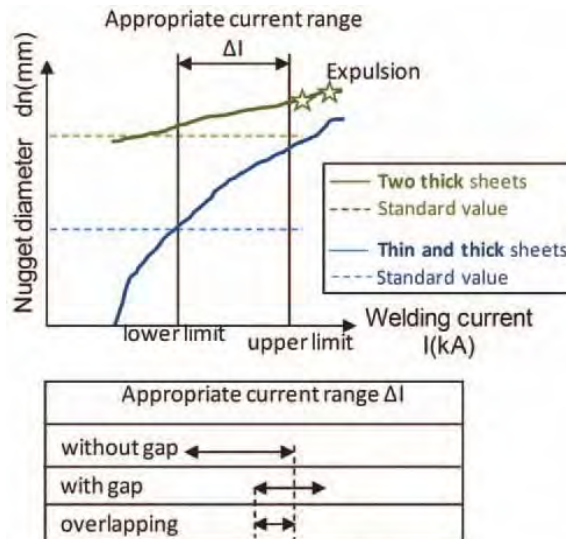


Figure 4.E-2: Weldability lobe of three sheets spot welded.

As a means of solving the above problem when there is no gap between the steel sheets, a method has been proposed in which the diameter of the electrode tip at the thin-sheet side is reduced and the welding force and current are varied during the welding time. In addition, a two-step pulsating current welding method (Figure 4.E-3) has been proposed in which neither the electrode diameter nor the welding force are changed. This method is described briefly below. Initially, during the first welding step, a relatively large welding current is passed to generate heat by using the contact resistance at the interface between the thin and thick steel sheets and that between the thick steel sheets. This method does not positively use the contact resistance that is effective when the electrode force is low. Since the method can be applied even under a high electrode force, it is particularly effective when there is a gap between the steel sheets to be welded together.

An experiment was conducted by using the above technology. The materials used were a 0.6-mm-thick sheet of mild steel and two 1.6-mm-thick sheets of HSS (980 MPa class). Spacers 1.4-mm thick were inserted at intervals of 40 mm between the thin and thick steel sheets and between the thick steel sheets. A servomotor-driven, single-phase AC welder was used for the test. The electrode used was a Cr-Cu dome radius type with a 40-mm tip upper radius and 6-mm tip lower diameter. The welding force was 3.43 kN. To evaluate the diameter of fusion at the interface between the thin and thick sheets, which determines the proper current range, a chisel test was conducted at the interface and evaluated the plug diameter.

The test results are illustrated in Figure 4.E-4. The horizontal axis represents the first step welding current for one-step welding (welding time $t_1 = 18$ cycles) and the second-step welding current for two-step welding (first welding time $t_1 = 18$ cycles, second welding time $t_2 = 8$ cycles) or pulsation welding [$t_1 = 18$ cycles, $t_2 = (5\text{-cycle heat}/2\text{-cycle cool}) \times 5$]. For one- or two-step welding, the welding current range was less than 1 kA. Conversely, with pulsation, it was possible to secure a proper welding range of 3 kA or more (about 1.8 kA when there was no gap between the steel sheets).

In addition to the two-step pulsating current welding method (Figure 4.E-4), preheating the sheets at 20-25% of the normal current before beginning the impulses can be effective when joining three layers of extremely different thicknesses. Figure 4.E-5 shows a weld cross section using preheating prior to three impulses.

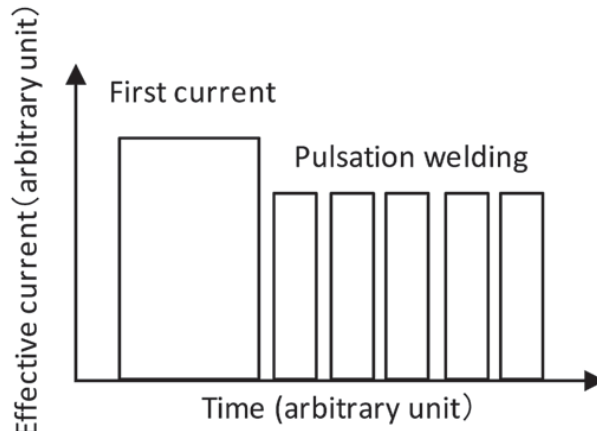


Figure 4.E-3: Image of welding current pattern.

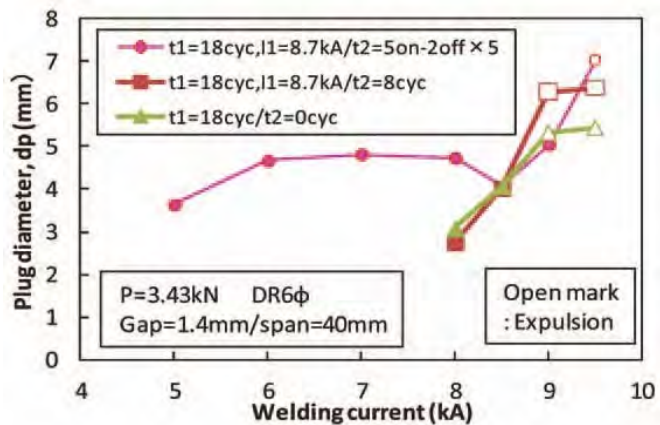


Figure 4.E-4: Current ranges for different welding current patterns.

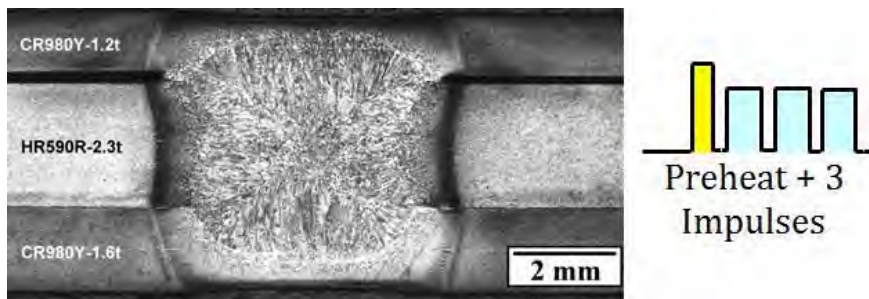


Figure 4.E-5: Cross section of three sheet spot weld including preheating prior to pulsations.^{C-6}

Another solution to RSW three sheets is when the Fusion Zone (FZ) formation process is controlled by setting the welding current and welding force during welding in multiple steps; this is referred to as Intelligent Spot Welding. (ISW). Using this approach, nugget formation between a thin sheet and thick sheet becomes possible when reduced welding force is applied. In Step 1 of the welding process, a FZ is reliably formed between the thin sheet and thick sheet by applying conditions of low welding force, short welding time, and high current. In the subsequent Step 2, a FZ is formed between the two thick sheets by apply high welding force and a long welding time. The results are shown in Figure 4.E-6, in which welding is performed with the edge of three steel sheets positioned directly under the electrodes, and the behavior of FZ formation at the edge of the sheets was observed with a high-speed video camera. Condition (a) is welding under a constant welding force and condition (b) is ISW. In condition (a), a nugget was formed between the two thick sheets, but the nugget failed to grow to the thin sheet-thick sheet joint, and the two sheets were not welded. However, condition (b) shows that nuggets have formed between both the thin and thick sheet and between the two thick sheets. The optimal welding current range for Step 2 can be determined from nugget formation between the two thick sheets, resulting in a wide available current range equal to or greater than that in joint welding of two thick sheets.

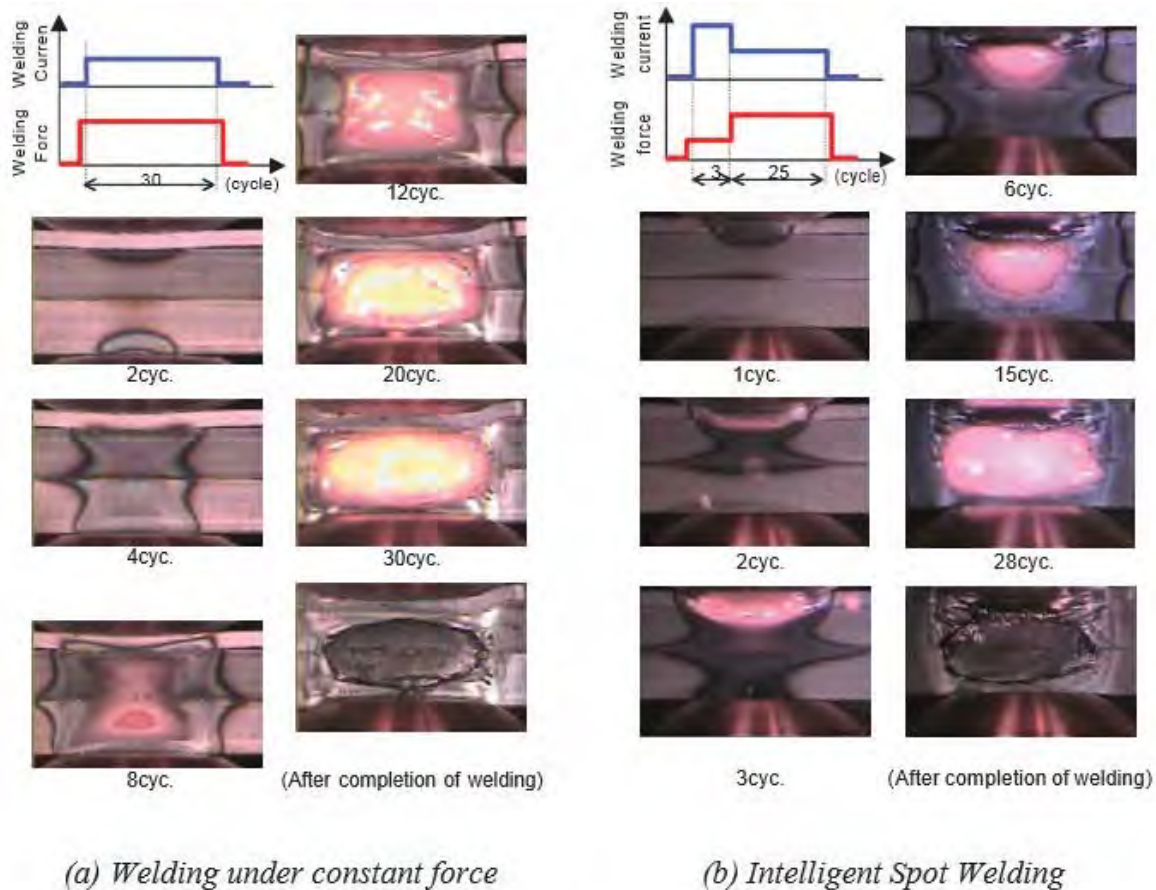


Figure 4.E-6: Results of observation of FZ formation phenomenon in RSW of three-sheet joint by high-speed video camera.^{J-1}

4.F. Application of Spot Welding to Hollow Members

In spot welding of car bodies, the so-called direct spot welding (in which the welding current is passed while two or more steel sheets are pressed against each other) by the welding electrodes is used most commonly. However, for those parts with closed cross sections, it may become necessary to drill a working hole through which the electrodes for direct spot welding of the steel sheets can be passed. In this case, the decline in rigidity of the drilled part being compensated for by using a thicker steel sheet or providing a reinforcing member will inevitably increase the weight of the car body. Therefore, attempts were made to reduce the steel sheet thickness (weight) and secure the required stiffness simultaneously without drilling any hole in the steel sheets. Indirect spot welding was used, in which the steel sheets are pressed and welded by a couple of electrodes from one side at the same time. Because the steel sheets are pressed by electrodes from one side, the weld sinks and the area of contact between the steel sheets increases (the current density decreases) if an excessive force is applied, making it difficult to perform fusion welding. Conversely, if an excessively large current is applied, the local current density between the electrodes increases because of a shunt current, causing a crack or explosion.

Studies were made for various welding conditions for the combination of a hollow member with a 1.6-mm wall thickness and a sheet-formed member with a 0.7-mm thickness. By using an electrode with a specially designed tip and a DC power supply in combination, indirect spot welding could be performed of the above members without requiring any special pattern of conduction or pressing, even in the presence of a gap between the members or the presence of shunts (existing welding points). An example of the cross section of an indirect spot weld is illustrated in Figure 4.F-1, which clearly indicates that a sufficiently large nugget was formed.

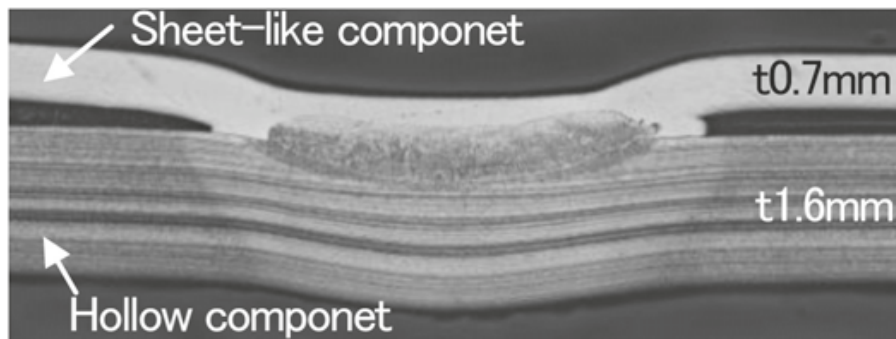


Figure 4.F-1: Cross section of indirect spot weld for hollow and sheet-like components.

For the indirect RSW with single-side access of the welding electrode, the variable controls of electrode force and current during welding were developed to promote the weld nugget formation. Experiments as well as numerical simulations were conducted to study the welding phenomena and optimize the welding process. It was verified that the nugget was stably formed with the developed process even when shunting was large. Figure 4.F-2 describes the effect of variable current and force on the promotion of weld nugget formation.

At the first stage with low welding current and high electrode force, the electric conduction with sufficient load at weld preheats the sheet, which promotes contacting area between the electrode and upper sheet and thus inhibits the expulsion from the surface. Meanwhile, contacting area between upper and lower sheets is also promoted forming the stable conduction path. Subsequently, at the second stage with high welding current and low electrode force, the nugget formation is effectively promoted with a heated region concentrated at the center in weld, avoiding the further penetration of welding electrode into the upper sheet and thus maintaining the current density.

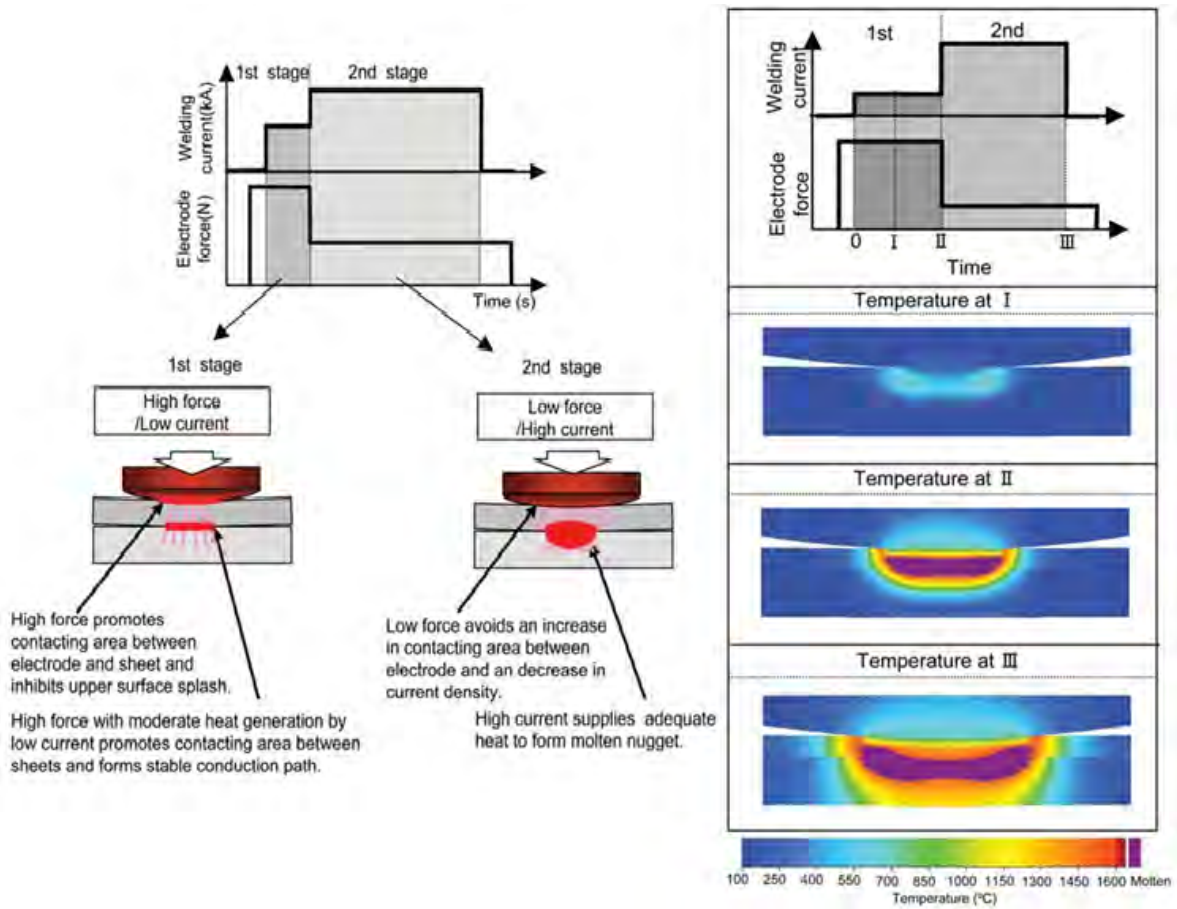


Figure 4.F-2: Concept of nugget formation process of variable current and force control for single-sided RSW.^{J-1}

4.G. Arc Welding Processes

4.G.1. Fundamentals and Principles of Arc Welding

This section serves as an introduction to all the arc welding processes. The common features and important concepts and terminology of this family of processes are reviewed, with more process-specific details provided in the sections covering the specific processes.

Arc welding refers to a family of processes that rely on the extreme heat of an electric arc to produce a weld. They may or may not rely on additional filler metal to create the weld. Although generally considered “low-tech”, arc welding continues to be very popular primarily due to its low equipment cost and high flexibility. Some of the key discoveries that led to modern arc welding include the discovery of the electric arc in the 1820s (Davies), the first welding patent using a carbon electrode in 1886, and the first covered electrode in 1900 (Kjellberg).

The most common arc welding processes today are illustrated in Figure 4.G-1. The abbreviations refer to American Welding Society (AWS)^{A-11} terminology as follows:

- EGW – ElectroGas Welding
- FCAW – Flux-Cored Arc Welding
- GMAW – Gas Metal Arc Welding
- GTAW – Gas Tungsten Arc Welding
- PAW – Plasma Arc Welding
- SAW – Submerged Arc Welding
- SMAW – Shielded Metal Arc Welding
- SW – Arc Stud Welding

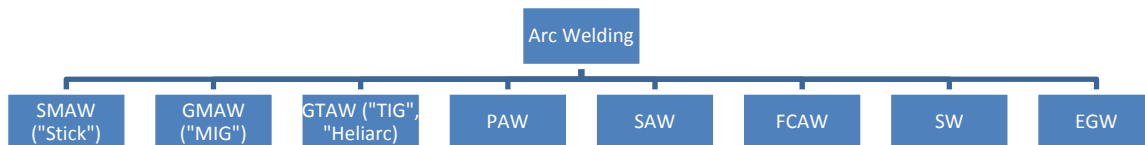


Figure 4.G-1: Common arc welding processes.

Whereas the welding engineer should always use proper AWS terminology during formal communications, in reality, the use of slang terminology for SMAW, GMAW, and GTAW processes is very common. Thus, where appropriate the “slang” terminology is included in italics.

With all arc welding processes, the initiation of an arc basically completes (or closes) an electrical circuit consisting of the ground and work cables, the welding torch, the workpiece or parts to be welded, and the secondary of the welding power supply. Voltages provided by the power supply are commonly either 60 or 80 V. Such voltages are high enough to establish and maintain an arc, but low enough to minimize the risk of electric shock. Once the arc is struck, actual arc voltages commonly range between 10 and 35 V. Direct Current (DC) is most common, but Alternating Current (AC) is sometimes used. Pulsed DC is becoming a common feature in modern welding power supplies. The electrical polarity used during arc welding is very important, but it has different effects with different processes. The effect of polarity on heat input is especially important with GTAW and GMAW, but the effects are opposite. With GTAW, direct-current electrode negative (DCEN) produces the greatest amount of heat into the part and is the most common polarity. However, with GMAW, direct-

current electrode positive (DCEP) produces the greatest amount of heat into the part and is used almost exclusively with this process (Figure 4.G-2).

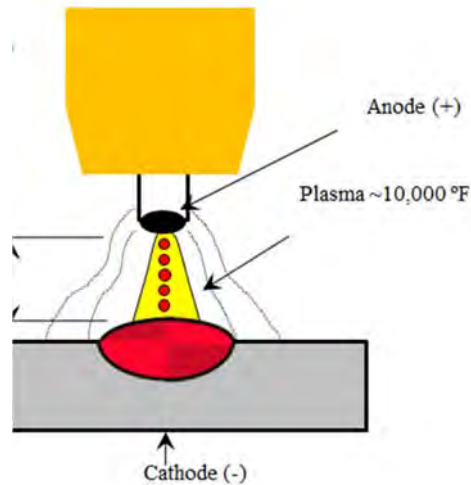


Figure 4.G-2: DCEP – common with GMAW.

The heat input during arc welding is primarily a function of weld travel speed and current, based on the following equation:

$$Net\ Energy\ Input = Arc\ Efficiency\ Factor \times \left[\frac{(Voltage \times Current)}{Speed} \right] \quad (2)$$

Although voltage appears to play a prominent role in the heat input equation, it is a parameter that is chosen primarily to create the most stable arc, not to affect heat input.

AWS filler metal classifications vary somewhat depending on the process. A common example is the classification system for SMAW electrodes, “EXXX” where “E” stands for electrode, the two digits following the E give the minimum deposited weld metal tensile strength in kips per square inch (ksi) (there will be a third digit if the strength is 100 ksi or higher), the third “X” provides information on what welding positions that electrode can be used for, and the final “X” provides information about the coating type. The electrode and filler metal classification schemes will be covered in more detail in the subsequent chapters covering each of the arc welding processes.

4.G.1.a. Shielding

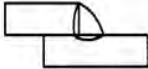
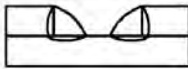
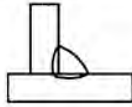
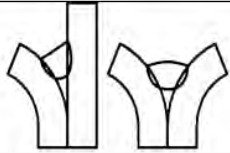
When metals are heated to high temperatures approaching or exceeding their melting point, diffusion rates are accelerated and the metals become very susceptible to contamination from the atmosphere. Elements that can be most damaging are oxygen, nitrogen, and hydrogen, and contamination from these elements can result in the formation of embrittling phases (such as oxides and nitrides), and porosity. To avoid this contamination, the metal must be shielded as it solidifies and begins to cool. The arc welding processes all rely on either a gas or a flux, or a combination of both for shielding. The way these processes are shielded is their main distinguishing feature from one another.

Processes such as GMAW, GTAW, and PAW rely solely on gas shielding. Shielding gasses protect by purging the susceptible metal from atmospheric gasses. The GMAW process commonly uses argon (Ar), carbon dioxide (CO₂), or blends of Ar and CO₂. CO₂ gas produces more spatter and a rougher weld appearance. It can produce fast welding speeds, is readily available, and is cheap.

Additions of CO₂ or small amounts of O₂ to Ar can improve puddle flow. The choice of shielding gas for GMAW plays a major role in the type of molten metal transfer mode from the electrode to the weld puddle.

4.G.1.b. Weld Joints and Weld Types for Arc Welding

The selection of a proper weld joint and weld type is a very important aspect of arc welding. The joint refers to how the workpiece or parts that are being welded are arranged relative to each other, and weld type refers to how the weld is formed in the joint. Specifically in arc welding, there are numerous joint types, but only two weld types, a fillet and a groove weld. A fillet weld offers the advantage of requiring no special joint preparation because the geometry of the joint provides the appropriate features to place the weld. Groove welds facilitate the creation of full-penetration welds which are often required in critical applications. The choice of weld and joint type is often dictated by the design of the component being welded, but will play a major role in the properties of that joint. The thickness of the parts being welded, as well as the material and type of welding process being used may also affect the choice of weld or joint type. Some very common arc welding joints and weld types are shown in Figure 4.G-3. Basic welding positions are shown in Figure 4.G-4. It is recommended that all welding joints be positioned for welding in either the flat or horizontal position whenever possible. The horizontal or vertical plane of the flat and horizontal joint may vary up to a maximum of 10 degrees.

Joint Type	Weld Type	Combination of Weld and Joint Type
Lap	Fillet	
Lap	Single/Double-Sided Slot Weld	
T-Joint	Fillet Weld	
Corner/Butt	Flare Bevel/Flare V-Groove Weld	

**Figure 4.G-3: Typical arc welding joint and weld types for automotive sheet steel applications
Need to add BUTT weld to table.**

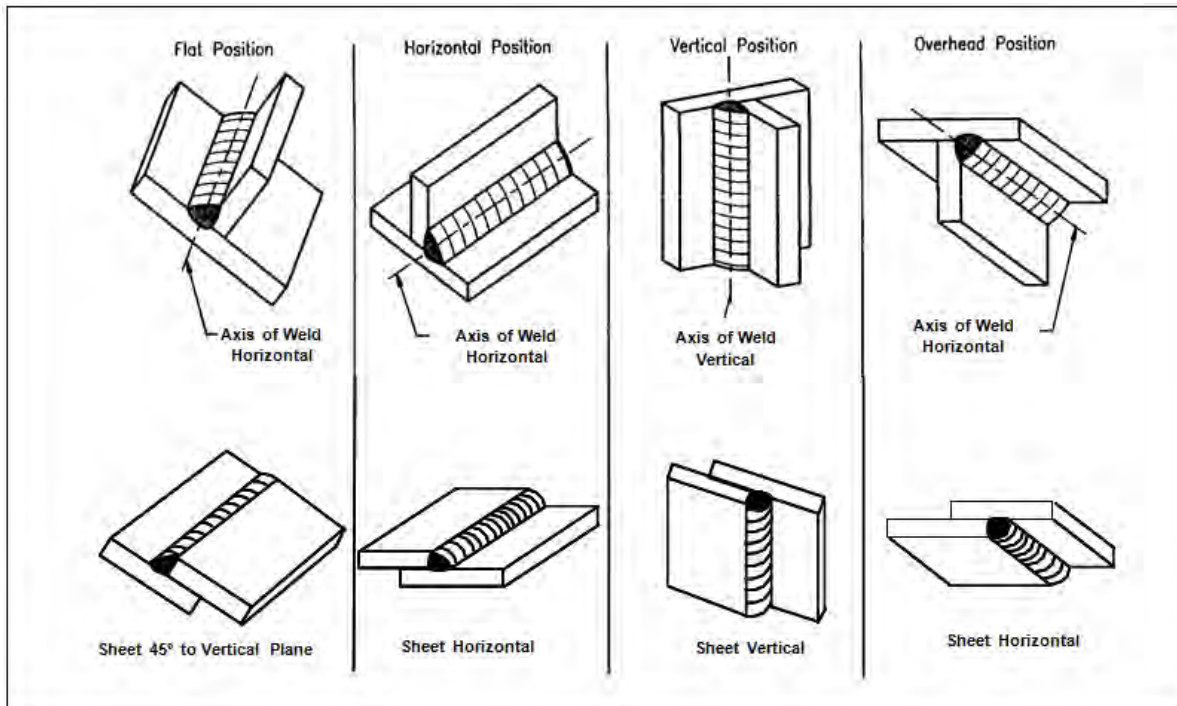


Figure 4.G-4: Basic arc welding positions.

4.G.1.c. Electrode Feed Rate

When using the semiautomatic arc welding processes such as GMAW electrode feed rate (or wire feed speed) determines both deposition rate and current. Higher feed rates increase weld metal deposition, and increase current since melting rates at the end of the wire must increase as the wire feed speed increases. As a result, with the semiautomatic processes, current is typically adjusted by changing the wire feed speed since the two are relatively proportional. Typical wire feed speeds are between 100 and 500 inches per minute (ipm).

4.G.1.d. Welding Travel Speed

Travel speed refers to how fast the welding arc is moving relative to the workpiece. The heat input equation clearly shows that travel speed, like current, plays a direct role in the amount of heat into the part. Faster speeds produce less heat into the part and reduced weld metal deposit. The choice of travel speed is typically driven by productivity, with the obvious desire to usually weld as fast as possible. Travel speed is independent of current and voltage, and may be controlled by the welder or mechanized. Typical travel speeds range between 5 and 100 ipm.

4.G.1.e. Arc Welding Safety

There are many hazards associated with arc welding that are not only important concerns for the welder, but for personnel working around any arc welding operations. This section will provide a very brief overview of the most common hazards of which the welding personnel should be aware. It is strongly recommended regarding safety in arc welding and other welding and associated processes to refer to the American National Standards Institute (ANSI) Document Z49.1, "Safety in Welding, Cutting, and Allied Processes" (Figure 4.G-5).

Ultraviolet radiation from the arc can damage the eyes and burn the skin in the same way skin is burned from the sun. This requires the use of proper shielding for the eyes and protective clothing to cover any exposed skin. Personnel working near arc welders should be careful not to glance at an open arc without proper shielding. Sparks and spatter during welding mandate the need for proper eye protection for anyone near the welding operation. Additional protective helmets are needed for the welder. Although the low voltages used in arc welding are relatively safe, proper electrical safety must be exercised at all times, including grounding of parts and equipment and avoiding damp conditions.

Welding fumes can be hazardous to the welder when inhaled over long periods of times so proper ventilation is paramount. Shielding gases can produce suffocation in enclosed spaces, such as when welding in tanks. Ar is heavier than air, and in the absence of proper ventilation, will displace oxygen when it fills a room. Helium is lighter than air producing a similar risk for overhead welding. Compressed shielding gas bottles can explode when mishandled or abused, or an arc strike can weaken the bottle, leading to an explosion. Hot metal is always a hazard with fusion welding processes like arc welding. When working around a welding operation, one should always assume that any piece of metal is hot. Welding arcs and associated hot metal spatter are ready sources for ignition of flammable materials in the vicinity of welding. Many fires have been started by careless welders who are not aware of any combustible material.^{A-11, P-6}

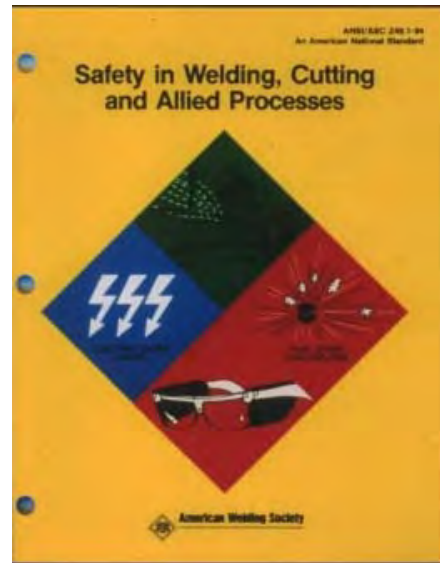


Figure 4.G-5: ANSI Document Z49.1 covers safety of welding and allied processes.

4.G.2. Arc Welding Procedures

Conventional arc welding (for example GMAW, TIG, and plasma) can be used for AHSS in a similar way to mild steels. The same shielding gases can be used for both AHSS and mild steels. For automotive applications, a design gap tolerance (G) of $0-0.5$ mm is allowed for all weld joints, as illustrated in Figure 4.G-6. An edge trim tolerance (E_t) of ± 0.5 mm is required where the edge is part of the weld joint, as shown in Figure 4.G-7. The variation in edge location causes variation in alignment of the electrode wire with the weld joint, as shown in Figure 4-60. Misalignment of the electrode may cause poor weld shape, improper fusion and burn-through. To control this variable, the trim tolerance at the weld joint must be held to ± 0.5 mm and the electrode must maintain a root joint alignment tolerance of ± 0.5 mm.

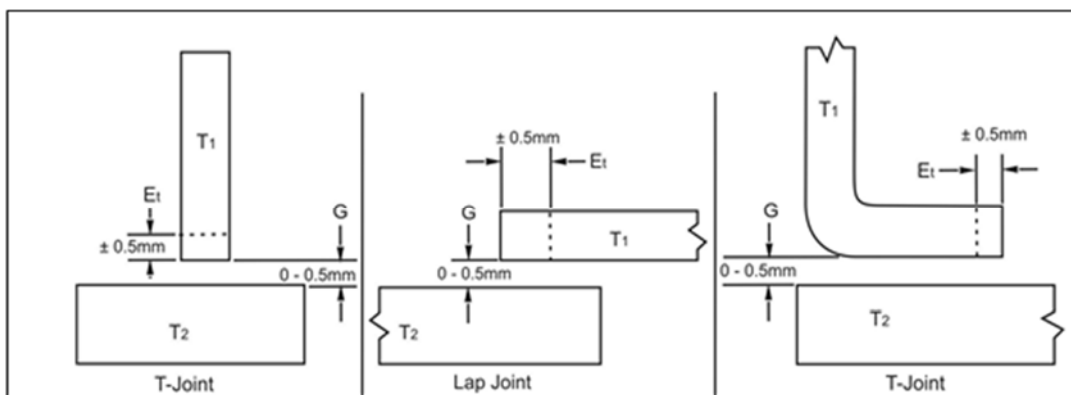


Figure 4.G-6: Joint design tolerance.^{A-12}

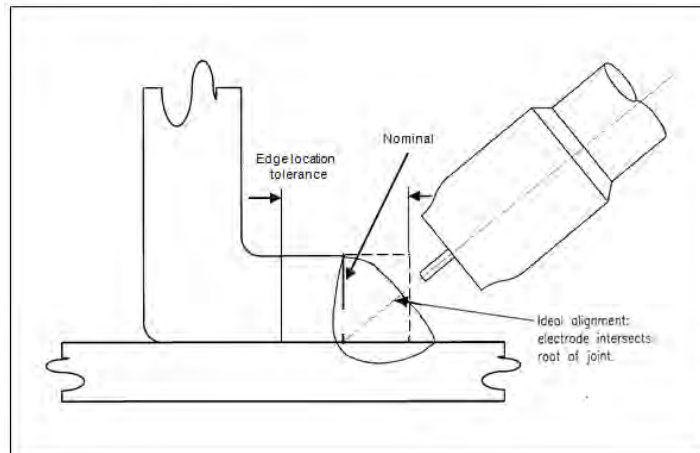


Figure 4.G-7: Edge location tolerance for fillet weld in a lap joint.^{A-12}

A tolerance stack-up review must be performed on all GMAW joints. The worst-case maximum designed gap including tolerance stack-up shall not exceed what is listed in Figure 4.G-8. It is preferable to target the smallest possible gap (the thickness of the thinnest sheet or 1.5 mm, whichever is smaller).

High-stress areas defined by CAE analysis and/or functional testing should be reviewed for weld optimization. Figure 4.G-9 illustrates techniques used to reduce the fillet weld stress concentration and to improve weld performance. These techniques include placing the weld start/stop away from corners and other high-stress areas, avoiding abrupt weld line direction changes when possible, etc.

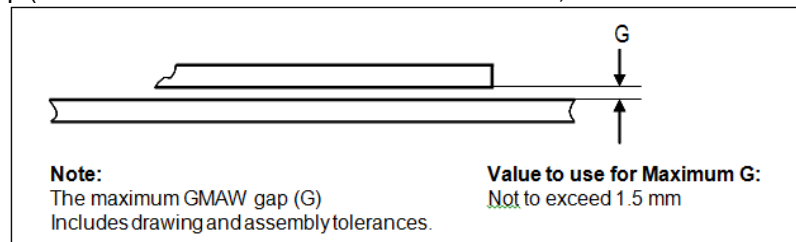


Figure 4.G-8: Maximum GMAW welding gap.^{A-12}

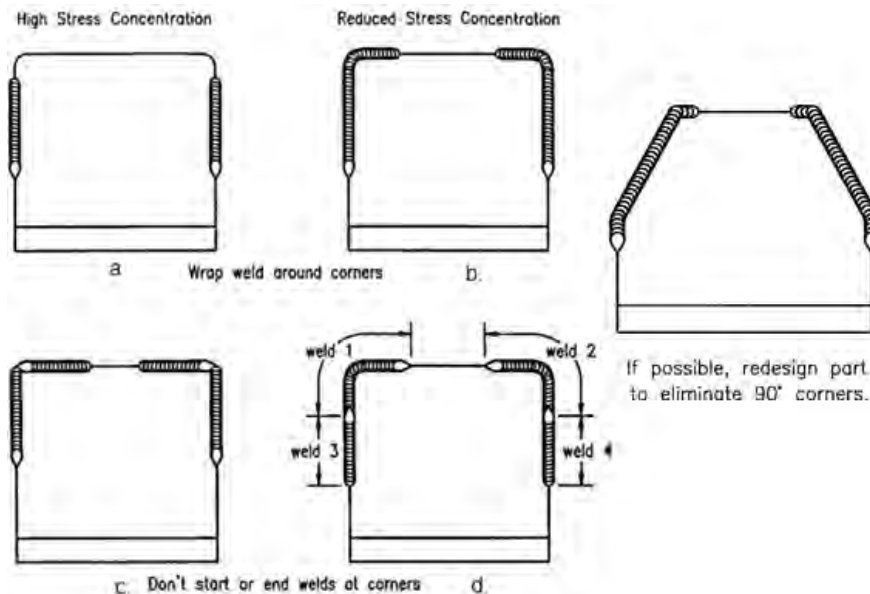


Figure 4.G-9: Reducing weld stress concentrations.^{A-12}

Intermittent welds that are properly sequenced can help keep joints closed by reducing the heat input which reduces distortion.

Meanwhile, intermittent welds also introduce weld starts and weld stops, both of which are stress risers. Similar to continuous welds, weld start/stops of intermittent welds should be placed away from high stress areas. Intermittent welds are specified by the center-to-center distance (i.e., pitch) and weld length, as shown in Figure 4.G-10.

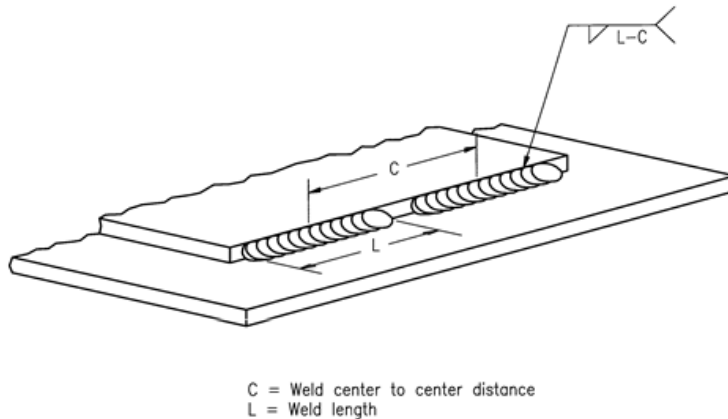


Figure 4.G-10: Intermittent fillet weld spacing.^{A-12}

Despite the increased alloying content used for AHSS, there are no increased welding imperfections compared with mild steel arc welds. Changing from mild steel to AHSS may also result in a change of arc blow. The strength of the welds for AHSS increases with increasing base metal strength and sometimes with decreasing heat input. Depending on the chemical composition of AHSS [for example, mild Steels and DP steels with high martensite content and strength levels more than 800 MPa], the strength of the weld joint may be reduced in comparison to the base metal strength due to small soft zones in HAZ (Figure 4.G-11). For CP and TRIP grades, no soft zones occur in HAZ due to the higher alloying content for these steels in comparison to DP and mild steels.

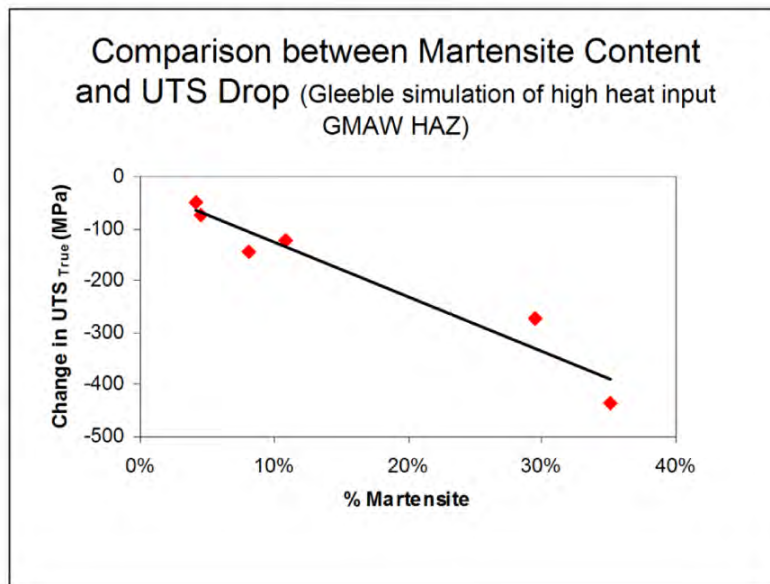


Figure 4.G-11: Relationship between martensite content and reduction in true ultimate tensile strength (UTS) (Data obtained by thermomechanical simulation of high heat input GMAW HAZ.^{D-1}).

Higher strength filler wires are recommended for welding of AHSS grades with strength levels higher than 800 MPa (Figure 4.G-12 for single-sided welded lap joint and Figure 4.G-13 for butt joints). It should be noted that higher strength fillers are more expensive and, more importantly, less tolerant to the presence of any weld imperfections. When welding AHSS to lower strength or mild steel, it

is recommended that filler wire with 70 ksi (482 MPa) strength be used. Single-sided welded lap joints are normally used in the automotive industry. Due to the unsymmetrical loading and the extra bending moment associated with this type of joint, the strength of this lap joint is lower than that of the butt joint.

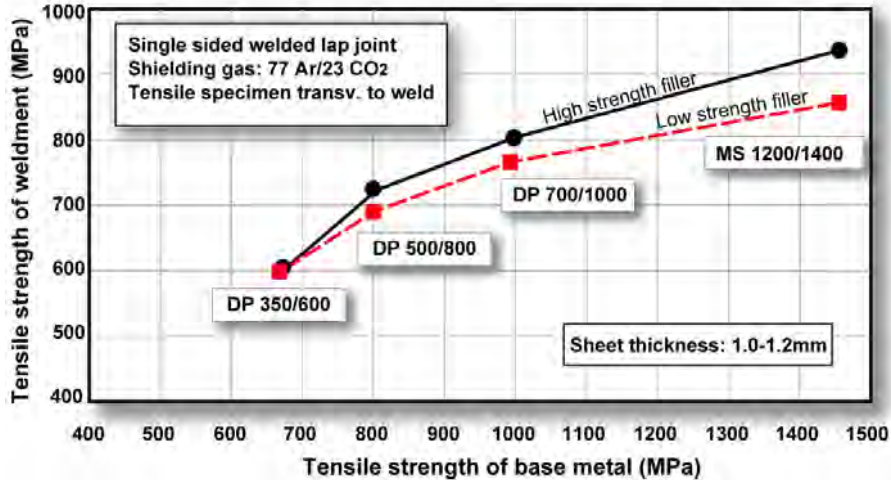


Figure 4.G-12: Influence of filler metal strength in arc welding of DP and mild steels. (Tensile strength is 560 MPa for low strength and 890 MPa for high-strength fillers. Fracture position in HAZ for all cases except DP 700/1000 and MS 1200/1400 combination with low-strength filler where fracture occurred in weld metal. Tensile strength equals peak load divided by cross-sectional area of sample.^{C-3})

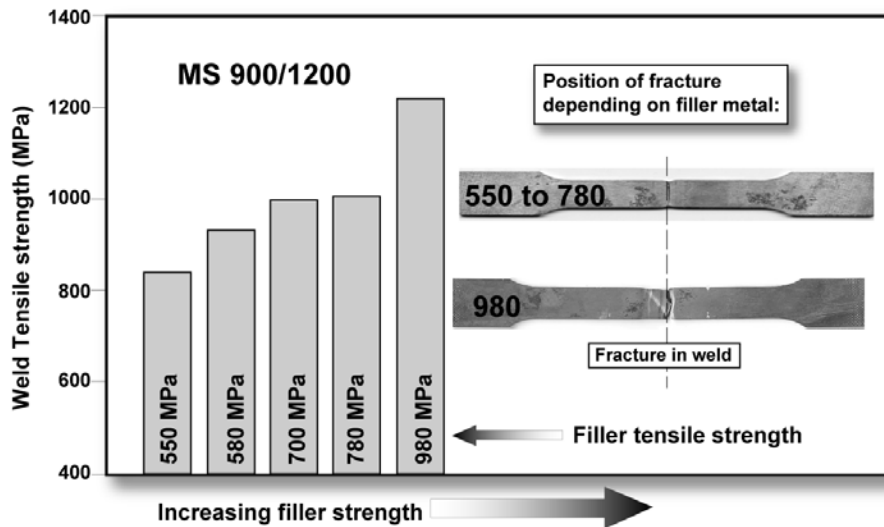


Figure 4.G-13: Influence of filler metal strength in GMAW (butt) welding on weld strength for MS steel. (Filler metal tensile strength range is 510-950 MPa.^{B-1})

Arc welds are normally used in local areas of vehicles where the loads are high. As required with all GMAW of any grade of steel, care should be taken to control heat input and the resulting weld metallurgy. The length of the GMA welds is often quite short. The reduction in strength for some of the AHSS GMA welds, in comparison to BM, can be compensated by increasing the length of the weld.

By adjusting the number and length (that is the total joined area) of welds, the fatigue strength of the joint can be improved. The fatigue strength of an arc-welded joint, in general, tends to be better than that of a spot-welded joint (Figure 4.G-14).

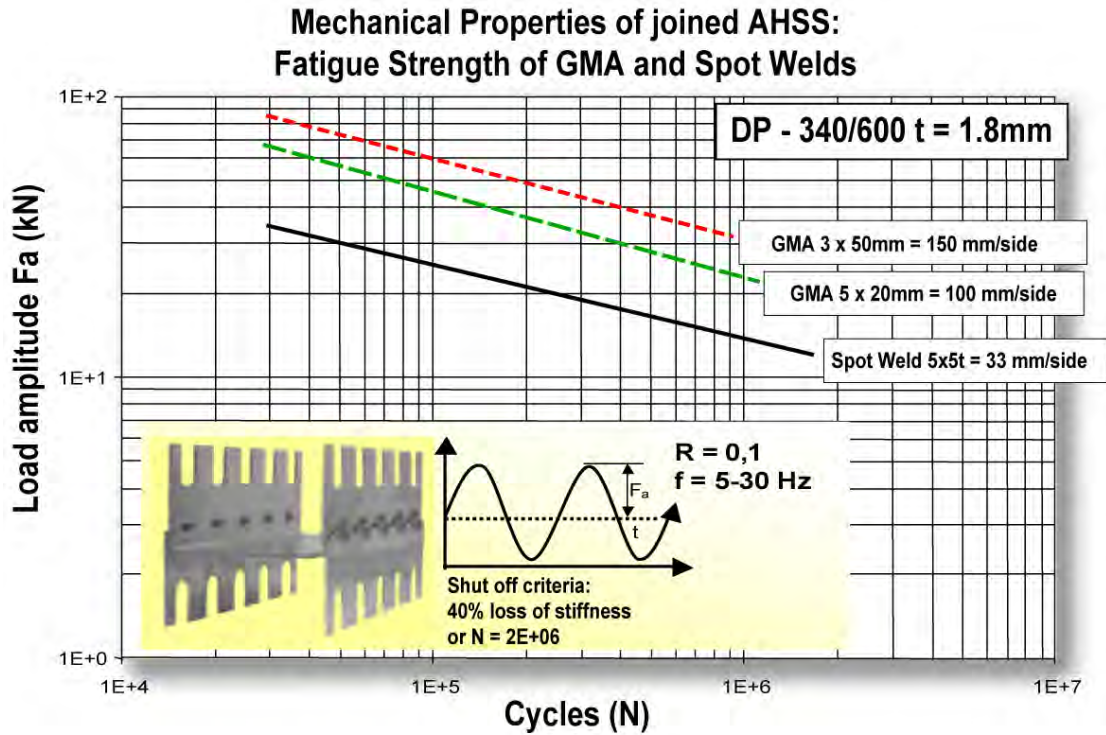


Figure 4.G-14: Fatigue strength of GMA-welded DP 340/600 compared to spot welding.^{L-2}

4.H Gas Metal Arc Welding (GMAW)

GMAW (Figure 4.H-1), commonly referred to by its slang name “MIG” (metal inert gas welding) uses a continuously fed bare wire electrode through a nozzle that delivers a proper flow of shielding gas to protect the molten and hot metal as it cools. Because the wire is fed automatically by a wire feed system, GMAW is one of the arc welding processes considered to be semiautomatic. The wire feeder pushes the electrode through the welding torch where it makes electrical contact with the contact tube, which delivers the electrical power from the power supply and through the cable to the electrode. The process requires much less welding skill than SMAW or GTAW, and produces higher deposition rates.

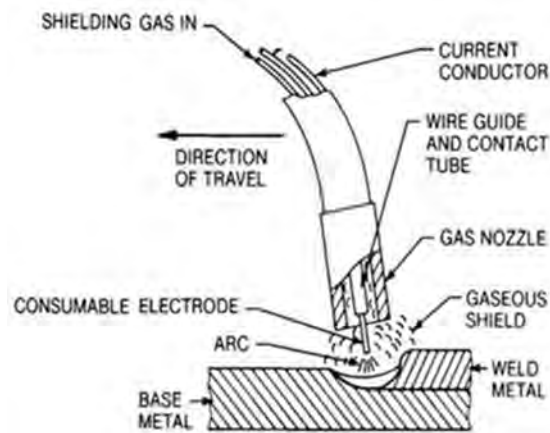


Figure 4.H-1: GMAW

The basic equipment components are the welding gun and cable assembly, electrode feed unit, power supply, and source of shielding gas. This set up includes a water cooling system for the welding gun which is typically necessary when welding with high duty cycles and high current.

GMAW became commercially available in the late 1940s offering a significant improvement in deposition rates and making welding more efficient. Deposition rates are much higher than for SMAW and GTAW, and the process is readily adaptable to robotic applications. Because of the fast welding speeds and ability to adapt to automation, it is widely used by automotive and heavy equipment manufacturers, as well as a wide variety of construction and structural welding, pipe and pressure vessel welding, and cladding applications. It is extremely flexible and can be used to weld virtually all metals. Relative to SMAW, GMAW equipment is a bit more expensive due to the additional wire feed mechanism, more complex torch, and the need for shielding gas, but overall it is still relatively inexpensive.

GMAW is “self-regulating”, which refers to the ability of the machine to maintain a constant arc length at all times. This is usually achieved using a constant-voltage power supply, although some modern machines are now capable of achieving self-regulation in other ways. This self-regulation feature results in a process that is ideal for mechanized and robotic applications.

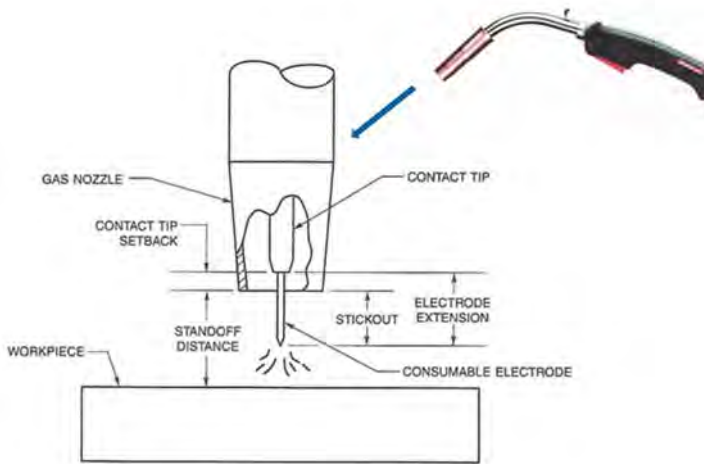
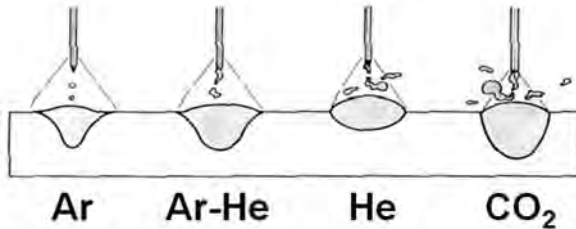


Figure 4-69: Common GMAW terminology



**Figure 4.H-2: Effect of shielding gas on weld profile
Convey addition of O₂ and CO₂ to indicated gases**

result in excessive spatter build-up on the nozzle and contact tip. Various gases are being used for shielding the in GMAW process. The most common ones include argon (Ar), helium (He), and carbon dioxide (CO₂) and combinations of these. Figure 4.H-2 illustrates the effect of the shielding gas on the weld profile.

AWS A5.18 is the carbon steel filler metal specification for SMAW, and includes both filler metal for both GMAW and GTAW. A typical electrode is shown on Figure 4.H-3. The “E” refers to electrode and the “R” refers to rod which means the filler metal can be used either as a GMAW electrode which carries the current, or as a separate filler metal in the form of a rod that could be used for the GTAW process. The “S” distinguishes this filler metal as solid (vs. the “T” designation which refers to a tubular GCW electrode or “C” for composite electrode), the number, letter, or number/letter combination which follows the S refers to a variety of information about the filler metal such as composition, recommended shielding gas, and/or polarity.

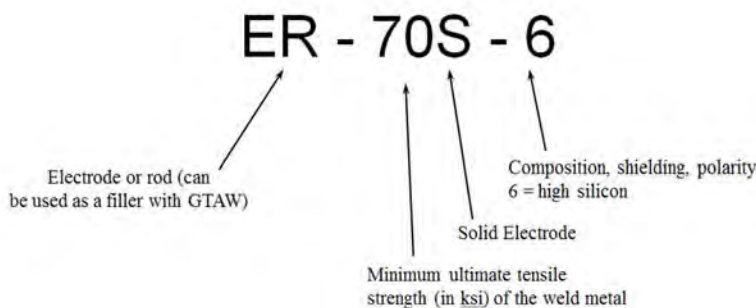


Figure 4.H-3: Typical AWS A5.18 electrode.

Figure 4.H-2 provides important GMAW terminology. Of particular importance is electrode extension. As shown, electrode extension refers to the length of filler wire between the arc and the end of the contact tip. The reason for the importance of electrode extension is that the longer the electrode extension, the greater the amount of resistive (known as I²R) heating that will occur in the wire. Resistive heating occurs because the steel wire is not a good conductor of electricity. This effect can become significant at high currents and/or long extensions, and can result in more of the energy from the power supply being consumed in the heating and melting of the wire, and less in generating arc heating. As a result, significant resistive heating can result in a wider weld profile with less penetration or depth of fusion. The stand-off distance is also an important consideration. Distances that are excessive will adversely affect the ability of the shielding gas to protect the weld. Distances that are too close may

In summary, the GMAW process offers the following advantages and limitations:

- Advantages:
 - Higher deposition rates than SMAW and GTAW
 - Better production efficiency vs. SMAW and GTAW since the electrode or filler wire does need to be continuously replaced
 - Since no flux is used there is minimal post-weld cleaning required and no possibility for a slag inclusion
 - Requires less welder skill than manual processes
 - Easily automated
 - Can weld most commercial alloys
 - Deep penetration with spray transfer mode
 - Depending on the metal transfer mode, all position welding is possible

- Limitations:
 - Equipment is more expensive and less portable than SMAW equipment
 - Torch is heavy and bulky so joint access might be a problem
 - Various metal transfer modes add complexity and limitations
 - Susceptible to drafty conditions

4.H.1. GMAW Procedures

Despite the increase alloying content used for Q&P 980, there is no increased welding defect type or rate compared with mild steel GMAW welds. Figure 4.H-4 is the microhardness profile of 1.6-mm Q&P 980's GMAW weld joint. Both welded seam and HAZ are all less than 500 HV, and there is no obvious softened zone in HAZ.^{B-4}

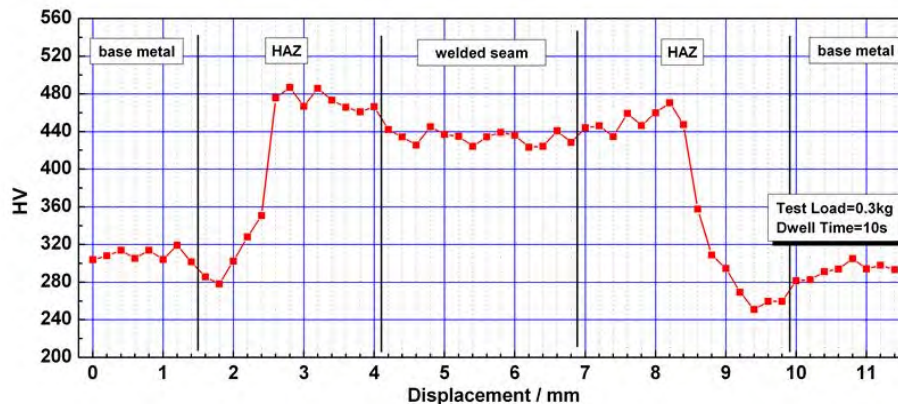


Figure 4.H-4: Microhardness profile of 1.6-mm DP 980's GMAW weld joint.^{B-4}

GMAW was used on three steels studied under a range of conditions. The left represents the FZ location and the middle is the HAZ. The figures show various degrees of HAZ hardening and softening depending on material grade and other conditions. The highest hardness occurs in the near HAZ, while the softest point is in the far HAZ. DP 980 shows the greatest degree of HAZ hardening and softening. The nominally high CR condition is a combination of low heat input and heat sink. The plots show that CR tends to have the largest effect on the DP steels, with the TRIP steel being somewhat less affected. Pre-strain has the largest effect on the TRIP BM, increasing the BM hardness by about 25%. The hardness of the softest location of the TRIP 780 HAZ is also increased by pre-strain, although degree of softening (about 20%) is not significantly changed. Pre-straining

increased the DP 780 BM hardness by only about 10%. Pre-straining did not affect the peak HAZ hardness for either material. Post-baking did not appear to have a significant influence on the HAZ hardness profiles of the DP 780 material or the TRIP 780 material, regardless of pre-strain condition (Figures 4.H-5 through 4.H-7).

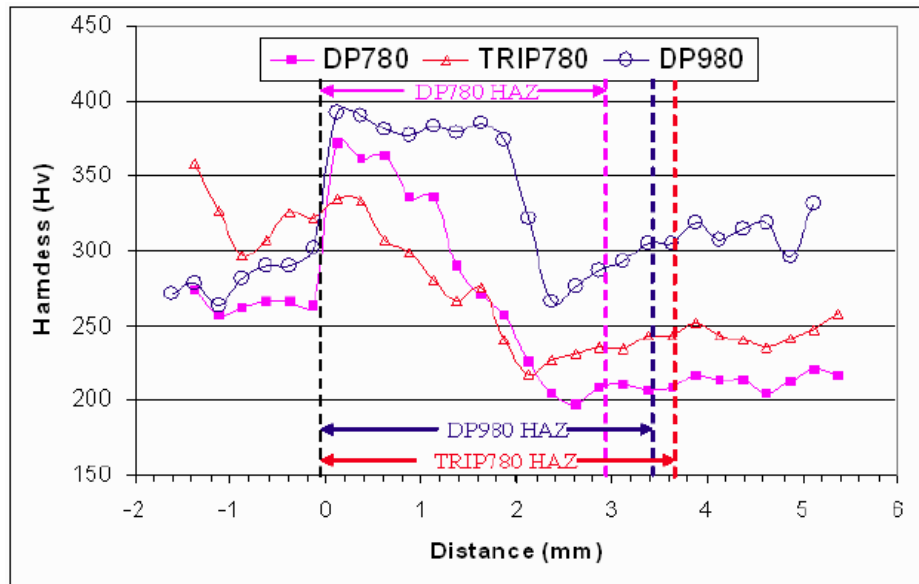


Figure 4.H-5: Hardness profiles of DP 780, TRIP 780, and DP 980 lap welds produced with the nominally high CR, no pre-strain or post-baking.^{P-7}

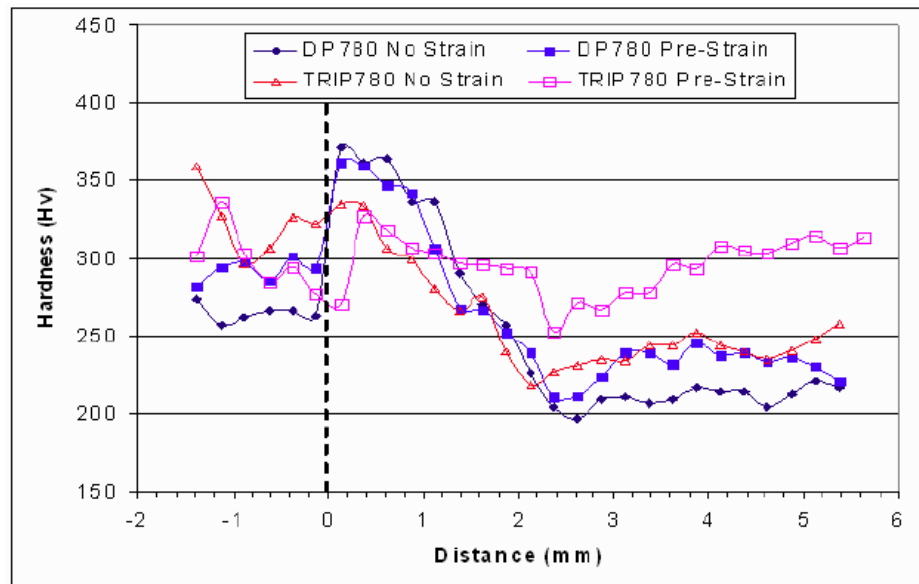


Figure 4.H-6: Hardness profiles of DP 780 and TRIP 780 welds produced both with and without pre-strain for the high CR condition.^{E-1}

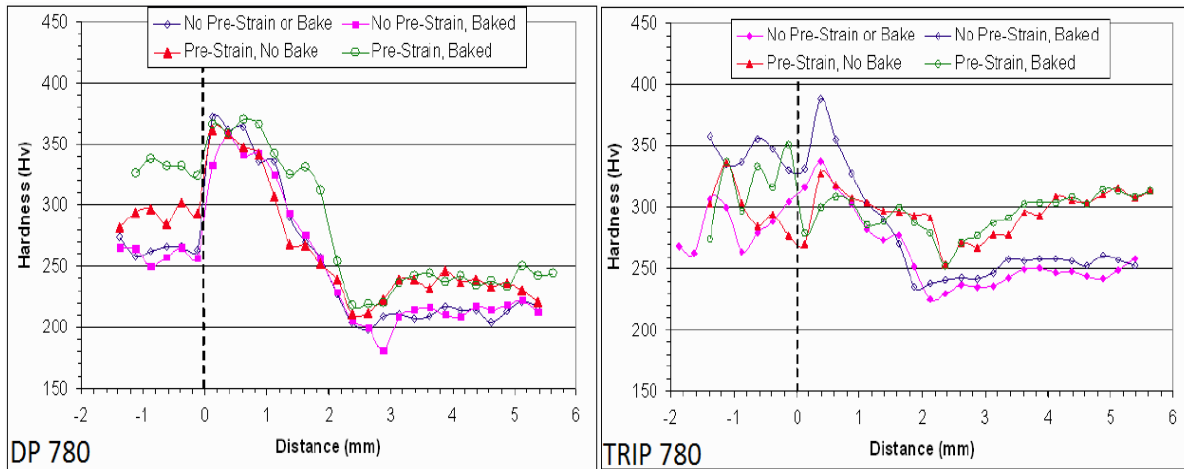


Figure 4.H-7: Hardness profiles of DP 780 and TRIP 780 welds produced both with and without post-baking for both pre-strained sheet and not pre-strained sheet for the nominally high CR condition.^{E-1}

TRIP 780 lap joint static tensile results for different filler metal and CR conditions are shown in Figure 4-76. The results are expressed in terms of joint efficiency and the strain at peak load. The data indicates joint efficiencies ranged from about 50% to about 98%. Strains at peak load ranged from less than 3% to nearly 8%. Fracture occurred either in the far HAZ or at the weld fusion boundary. Filler metal strength had no discernable effect on the tensile properties. Figure 4.H-8 shows static tensile test results of the TRIP 780 butt joints. All the welds failed in the softened region of the far HAZ with joint efficiencies in excess of 89%. On average, welds made using higher CR experienced higher strains during loading than those made using lower CR. As was the case with the lap welds, filler metal strength did not appear to influence the static tensile properties. The abbreviations of high and low “CR” indicate high and low CR used for each weld.

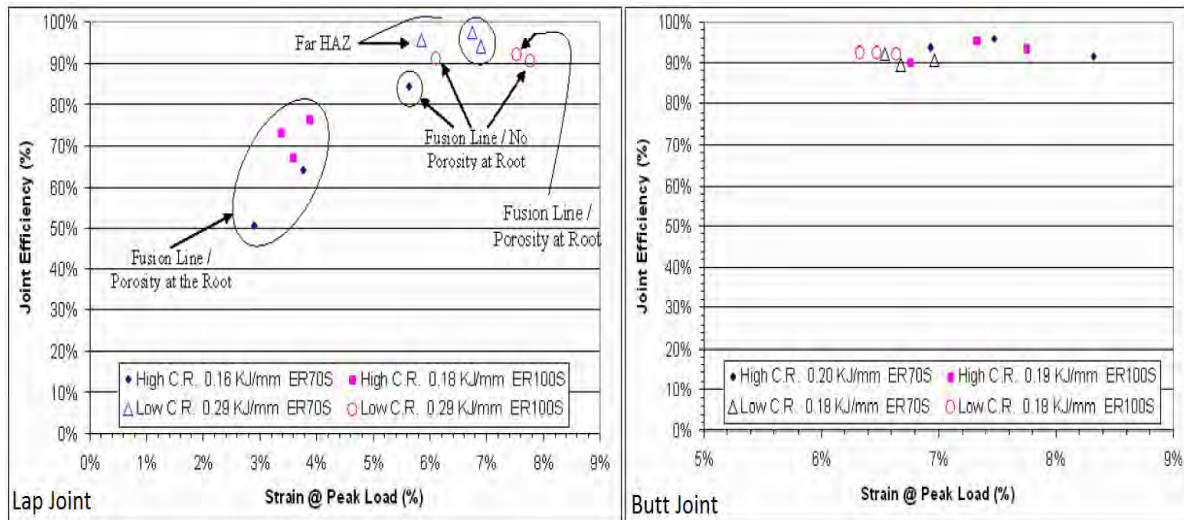


Figure 4.H-8: Static tensile test results of TRIP 780 lap and butt joints.^{E-1}

The static tensile test results of the DP 780 butt welds are shown in Figure 4.H-9. All welds failed in the softened region of the far HAZ. As shown, the high CR welds had joint efficiencies in excess of 90%. The high CR welds also appear to have slightly greater strains at peak load.

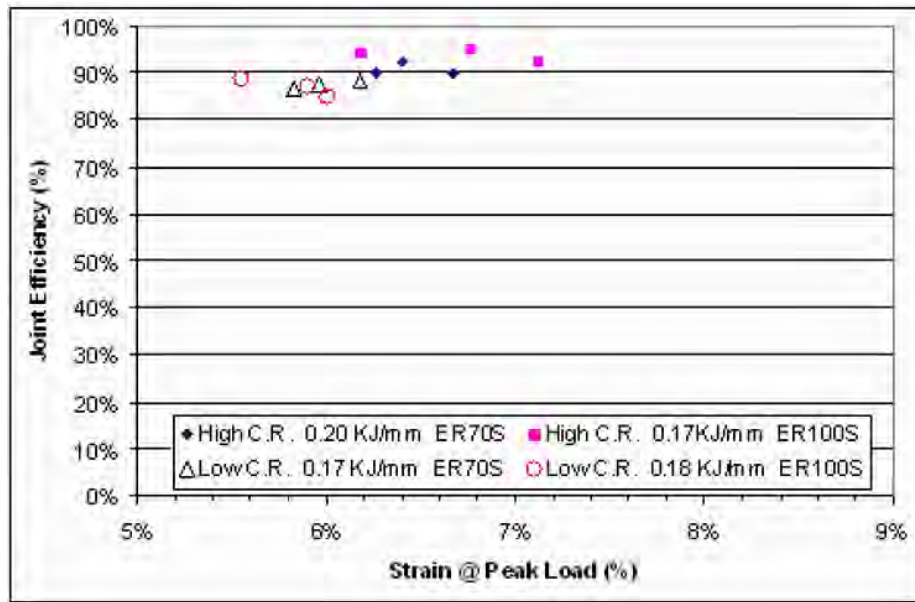


Figure 4.H-9: Static tensile test results of DP 780 butt joints.^{E-1}

Figure 4.H-10 (left) shows the TRIP 780 lap joint dynamic tensile results for different filler metal and CR conditions. UTS ranged from 372 to 867 MPa (54 to 126 ksi) and strain at peak load ranged from less than 1% to over 5%. The high CR lap joints had lower strengths and strains at peak load. These welds failed along the fusion line presumably due to porosity present at the root. All the low CR lap welds produced with the ER70S-6 wire failed in far HAZ of the bottom sheet. Of the low CR lap joints produced with the ER100S-G wire, two dynamic tensile specimens failed in the softened region of the far HAZ, and one failed along the fusion line of the top sheet without the presence of porosity at the weld root. Analysis of Figure 4.H-10 (left) indicates that filler metal strength did not have a distinguishable effect on the dynamic tensile test results. Figure 4.H-10 (right) shows the dynamic tensile test results of the TRIP 780 butt joints. All failed in the softened region of the far HAZ. The UTS of the butt joints ranged from 840 to 896 MPa (122 to 130 ksi), and strain at peak load was generally between 3 and 4%. The figure indicates that neither filler metal strength nor CR condition had a distinguishable effect on the dynamic tensile test results of the butt joints.

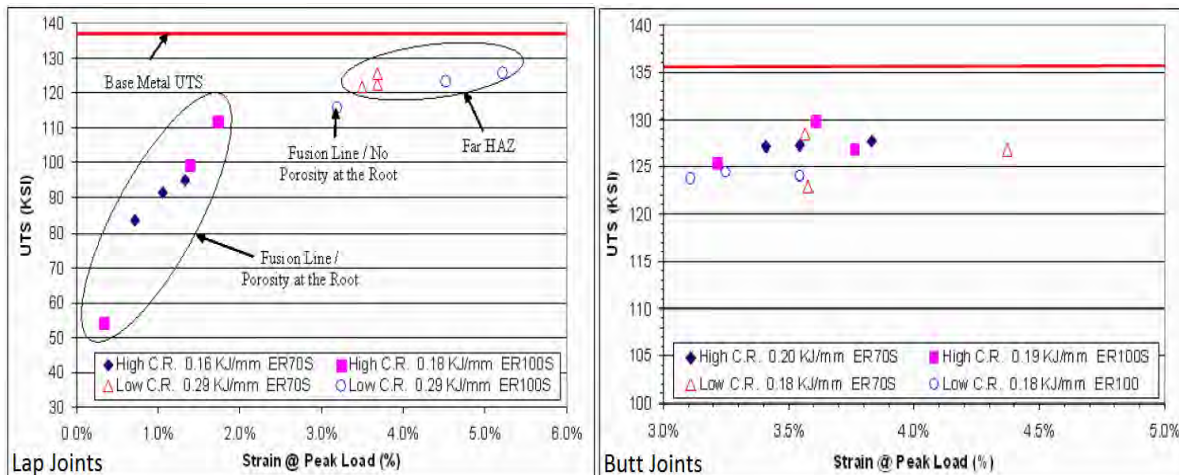


Figure 4.H-10: Dynamic tensile test results of TRIP 780 lap joints and butt joints.^{E-1}

The dynamic tensile test results of the DP 780 butt joints are shown in Figure 4.H-11. All failed in the softened region of the far HAZ. UTS ranged from 841 to 910 MPa (122 to 132 ksi), and strain at peak load ranged from 2.25% to less than 4.0%. It should be noted that similar UTS were obtained for the DP 780 and TRIP 780 butt joints. On average, TRIP 780 butt joints had slightly higher strain at peak load. Neither filler metal strength nor CR condition appears to have a distinguishable effect on the dynamic tensile properties.

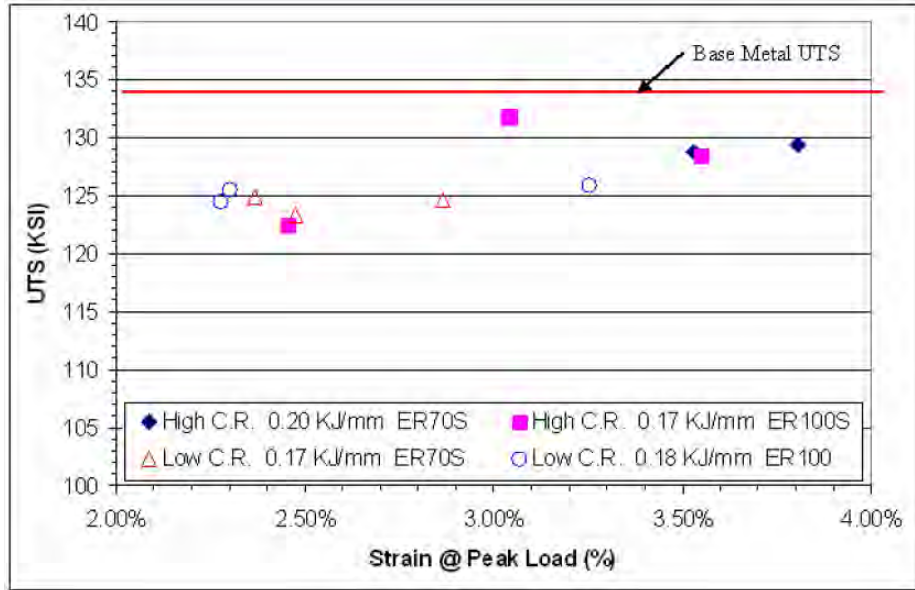


Figure 4.H-11: Dynamic tensile test results of DP 780 butt joints.^{E-1}

4.1. Arc Stud Welding

Arc stud welding is an arc welding process designed to quickly and efficiently attach a stud to a plate. The welded stud typically acts as a threaded attachment site or an anchor. The process uses a constant-current power supply, and a gun (Figure 4.1-1) that positions the stud as it is being welded. A ceramic ferrule protects the weld area from the atmosphere and helps shape the weld.

The weld sequence is shown in Figure 4.1-2. When the operator pulls the trigger, the stud first touches the part (A) and then is drawn away (B) while the voltage is applied initiating an arc. The heat of the arc melts the end of the stud as well as the BM below the stud. Steel studs typically use a small ball of Al placed at the end of the stud that melts and vaporizes in arc. The vaporized Al acts as a deoxidizer to protect the molten metal. The stud is then immediately plunged into the BM (C) which creates the weld while it expels contaminants and oxidized material through the ferrule holes, and squeezes out molten metal into the ferrule cavity. The entire weld sequence typically lasts less than a second. The final step involves removing the ferrule by breaking it with a hammer to reveal the weld (D). The process requires no special operator skill.

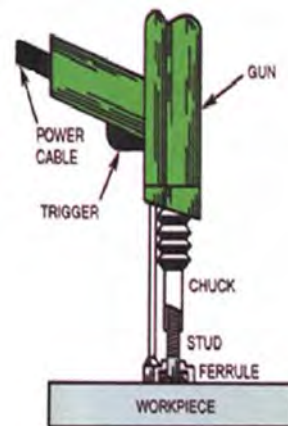


Figure 4.1-1: Arc stud welding gun in position to weld.

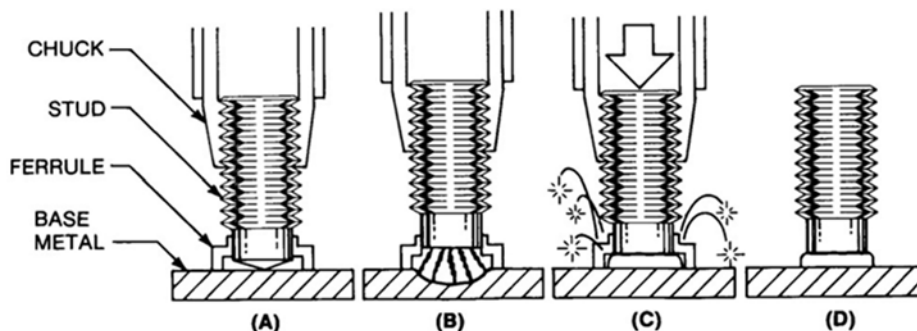


Figure 4.1-2: arc stud welding steps.

Arc stud welding is used in a wide variety of applications and industry sectors, including automotive manufacturing, shipbuilding, and bridge and building construction. Figure 4.1-3 shows the wide variety of studs possible. It is expected that welding studs on AHSS are typically free of any specific material issues.

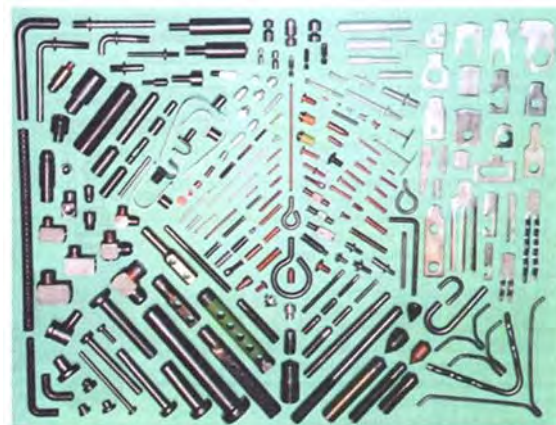


Figure 4.1-3: A wide variety of studs is available.

4.1.1 Gas Arc Stud Welding

Gas arc stud welding (Figure 4.1-4) is an excellent process, but its application must be a good match. The key advantage of gas arc stud welding is that no ferrule is used. Many customers are tempted by this because of the lower initial cost and the lower cost of cleanup. However, because the flash is uncontrolled, the molten metal may spread over a wider area creating an issue for mating parts.

Gas arc stud welding is often used with robotics. Because of the extra material handling requirement of the ferrule, gas arc stud welding is often chosen. The precise nature of robotic systems work well with the gas arc option.¹⁻⁴

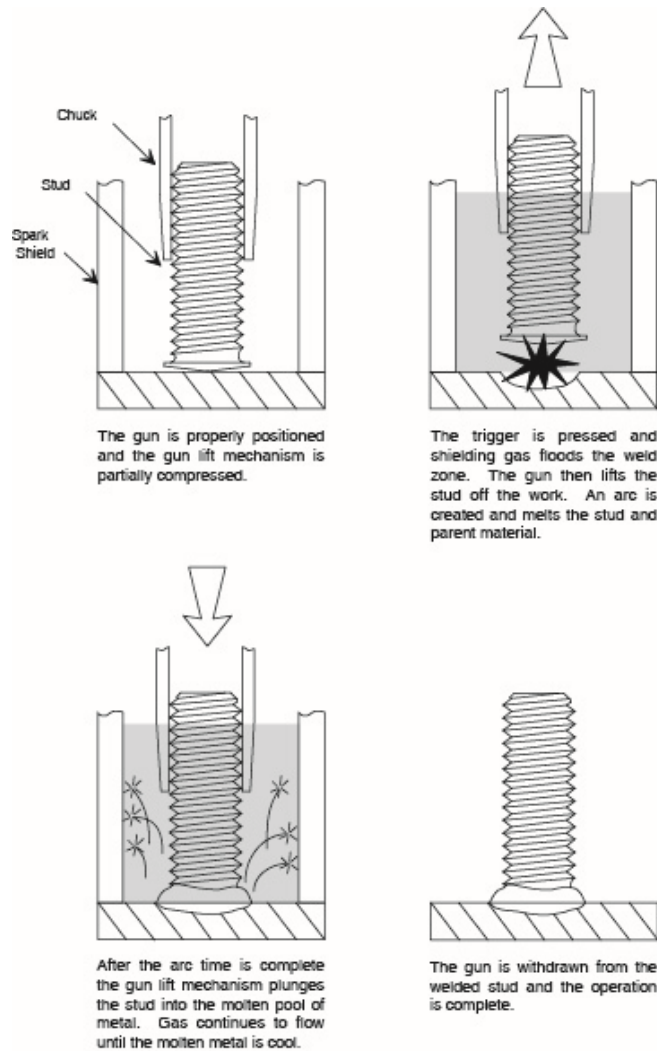


Figure 4.1-4: Gas arc stud welding process.¹⁻⁴

4.J. High Energy Density Welding Processes (Laser Welding)

4.J.1 Fundamentals and Principles of High Energy Density Welding Processes

High energy density welding processes are those that focus the energy needed for welding to an extremely small size area. This allows for very low overall heat input to the workpiece, which results in minimal BM degradation, residual stress, and distortion. Welding speeds can be very fast. The two main processes known for extreme energy densities are laser (Figure 4.J-1) and Electron Beam Welding (EBW).

As shown in Figure 4.J-2, energy densities of focused laser and electron beams can approach and exceed 10^4 kW/cm². These energy densities are achieved through a combination of high power and beams that are focused to an extremely small diameter. Diameters as small as a human hair (0.05 mm) are possible. PAW offers greater energy density than conventional arc welding processes, and is sometimes referred to as the “poor man’s laser”.

High energy density processes produce weld profiles of high depth-to-width ratio, as compared to other welding processes (Figure 4.J-3). As a result, much greater thicknesses can be welded in a single pass, especially with EBW. The figure also illustrates the fact that high energy density processes can produce a weld with minimal heating to the surrounding area as compared to the other processes. However, the high depth-to-width ratio weld profile is much less forgiving to imperfect joint fit-up than the profile produced by arc welding processes.

Laser and EBW processes are used in a wide variety of industry sectors. Very high weld speeds are possible and the welds are usually aesthetically pleasing. Laser welding is very adaptable to high-speed production so it is common in the automotive sector. The ability to precisely locate welds on smaller sensitive components with minimal heat input makes laser welding very attractive to the medical products industry.



Figure 4.J-1: Laser welding.

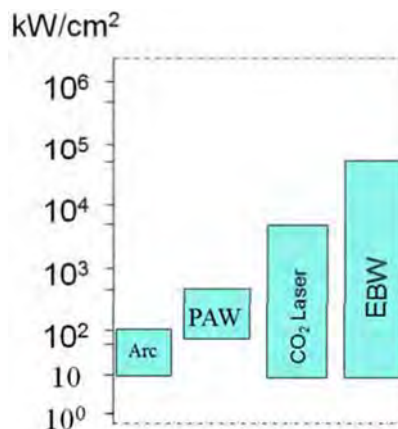


Figure 4.J-2: Power densities of various welding processes.

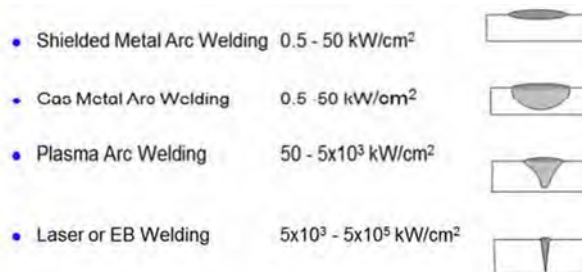


Figure 4.J-3: Comparison of typical weld profiles.

When welding with high energy density processes, the laser or EB is focused along the joint line of the workpieces to be welded. The extreme power density of the beam not only melts the material, but causes evaporation. As the metal atoms evaporate, forces in the opposite direction create a significant localized vapor pressure. This pressure creates a hole, known as a keyhole, by depressing the free surface of the melted metal. The weld solidifies behind the keyhole as it progresses along the joint (Figure 4.J-4). This method of welding known as keyhole welding is the most common approach to laser and EB, and produces the characteristic welds of high depth-to-width ratio. There are some cases where the keyhole mode is not used. This mode is known as conductive mode welding. Conductive mode welds have a weld profile closer to that of an arc weld.^{A-11, P-6}

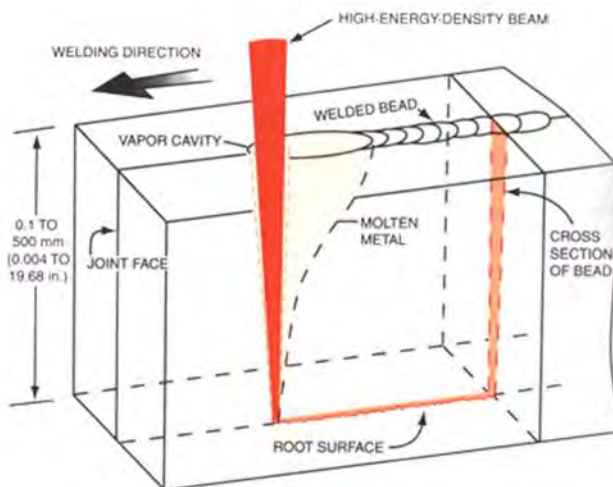


Figure 4.J-4: Keyhole mode welding.

4.J.2 Laser Beam Welding

The word “laser” is an acronym for “light amplification by stimulated emission of radiation.” Lasers produce a special form of light (electromagnetic energy) consisting of photons that are all of a single coherent wavelength. Light of this form can be focused to extremely small diameters allowing for the creation of the high-energy densities used for welding. The laser beam itself is not useful for welding until it is focused by a focusing lens.

Lasers vary in the quality of the beam produced. A high-quality beam will diffract less when focused, providing for the creation of a smaller spot size. Reflective lenses are important to lasers as well since they are used in the optical cavity where the beam is generated, as well in the beam delivery systems for some lasers. For these reasons, optics play a major role in laser beam welding.

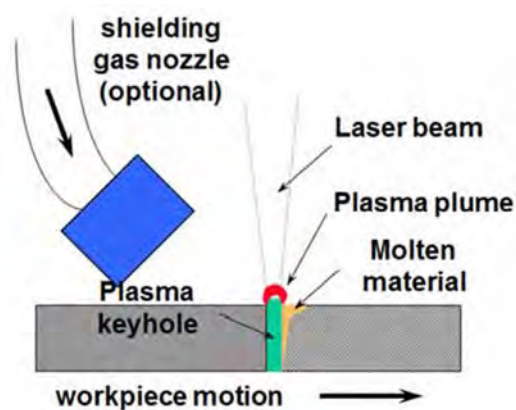


Figure 4.J-5: Laser beam welding.

Laser beam welding (Figure 4.J-5) does not require additional filler metal and shielding gas is optional. When the beam hits the workpiece, it melts and vaporizes metal atoms, some of which are ionized by the intense beam. This creates what is known as a plume (or plasma) over the weld area that can sometimes interfere with the beam. In these cases, shielding gas may be used to deflect the plume.

The choice of laser type depends on cost, the type and thickness of material to be welded and the required speed and penetration. Lasers are distinguished by the medium used to generate the laser beam, and the wavelength of laser light produced. Although there are many types of lasers, the

common lasers for welding include the Nd:YAG, fiber, disk solid-state lasers, and the gas-based CO₂ laser. The lasing medium in solid-state lasers are crystals (Nd:YAG and disk lasers) or fibers (fiber laser) that have material added (doped) that will “lase” when exposed to a source of energy, whereas the lasing medium in the CO₂ laser is a gas blend consisting of CO₂, He, and N₂ gas. In all cases, “lasing” occurs when the atoms/molecules of the medium are excited to a higher energy state through the introduction of additional energy (known as pumping). When this occurs, photons are emitted, which, in turn, excite other atoms/molecules. This results in a cascade of photons that travel in coherent waves of a single wavelength, the two properties that laser light is known for.

CO₂ lasers produce wavelengths of 10.6 μm, while the wavelength of the solid-state lasers is 1.06 μm. CO₂ lasers are generally less expensive, but the longer wavelength of light does not allow its beam to be delivered through fiber optic cables which reduces its versatility. Its light is also more reflective, which limits its use with highly reflective metals such as Al. The solid-state lasers are generally more compact and require less maintenance than the CO₂ laser. They are more conducive to high-speed production since their beams can be delivered through long lengths of fiber optic cable which can then be attached to a robot. Some of the solid-state lasers such as the fiber laser produce beams of outstanding quality. However, the shorter wavelength of these lasers requires additional safety precautions regarding eye protection.

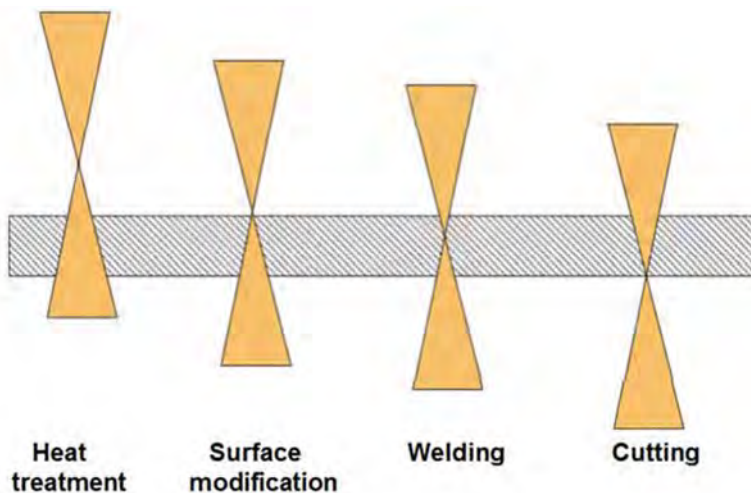


Figure 4.J-6: Focusing of the laser beam.

The choices of focus spot size, focus spot location in the joint, and focal length are all important considerations when laser beam welding. Usually, a small focus size is used for cutting and welding, while a larger focus is used for heat treatment or surface modification. As indicated in Figure 4.J-6, the location of the beam’s focal point can also be varied based on the application. When welding, it is common to locate the focal point somewhere near the center of the joint. But cutting applications benefit from placing the focal point at the bottom of the joint. Weld

spatter onto the focusing lens can sometimes be a problem, especially when there are contaminants on the surface of the parts being welded. Approaches to minimizing the spatter problem include choosing a long focal length lens which keeps the lens a safe distance from the weld area, or the use of an air “knife” to protect the lens. ^{A-11, P-6}

In summary, the advantages and limitations of laser beam welding are as follows:

- Advantages:
 - High energy density process allows for low overall heat input which produces minimal BM degradation, residual stress, and distortion
 - Fast welding speeds
 - No filler metal required
 - Relatively thick ($\frac{3}{4}$ in.) single-pass welds can be made
 - Concentrated heat source allows for the creation of extremely small weld sizes needed for small and intricate components
 - Easily automated, especially with lasers that are conducive to fiber optic delivery
 - Since there is no bulky torch as with most arc welding processes, laser beam welding is capable of welding joints with difficult accessibility

- Limitations:
 - Equipment is very expensive
 - Portability is usually low
 - Requires very tight joint fit-up and accurate positioning of the joint relative to the beam
 - Metals that are highly reflective such as Al are difficult to weld with some laser beam welding processes
 - High weld CR may create brittle microstructures when welding certain steels
 - Laser plume may be a problem
 - Energy efficiency of lasers is poor
 - Some lasers require special (and expensive) eye protection
 - Laser beam welding is complex and requires significant training and knowledge

4.J.3. Laser Welding Procedures

Common laser welding applications in the automotive industry include most of the part systems as shown in Figure 4.J-7.

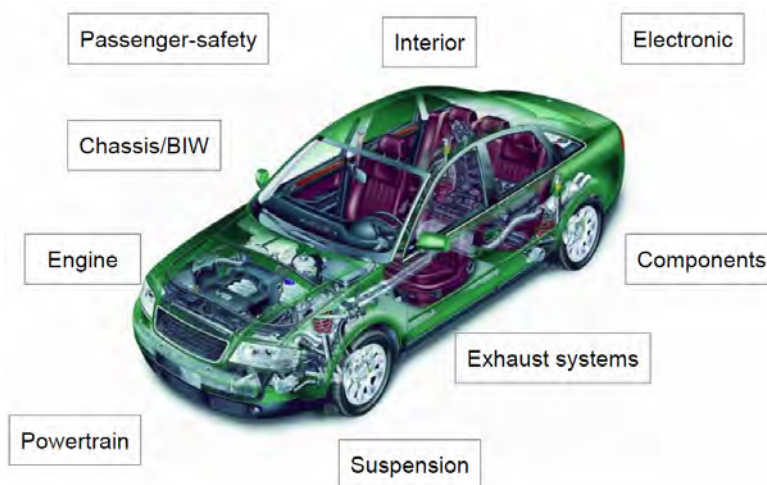


Figure 4.J-7: Common automotive applications using laser welding^{T-9}

4.J.3.a. Butt Welds and Tailor-Welded Products

AHSS grades can be laser butt-welded and are used in production of tailored products (tailor-welded blanks and tubes). The requirements for edge preparation of AHSS are similar to mild steels. In both cases, a good quality edge and a good fit-up are critical to achieve good-quality welds. The blanking of AHSS needs higher shear loads than mild steel sheets (see Section 3.B.7. – Blanking, Shearing and Trim Operations).

If a tailored product is intended for use in a forming operation, a general stretchability test such as the Erichsen (Olsen) cup test can be used for assessment of the formability of the laser weld. AHSS with tensile strengths up to 800 MPa show good Erichsen test values (Figure 4.J-8). The percent stretchability in the Erichsen test = 100 × the ratio of stretchability of weld to stretchability of BM.

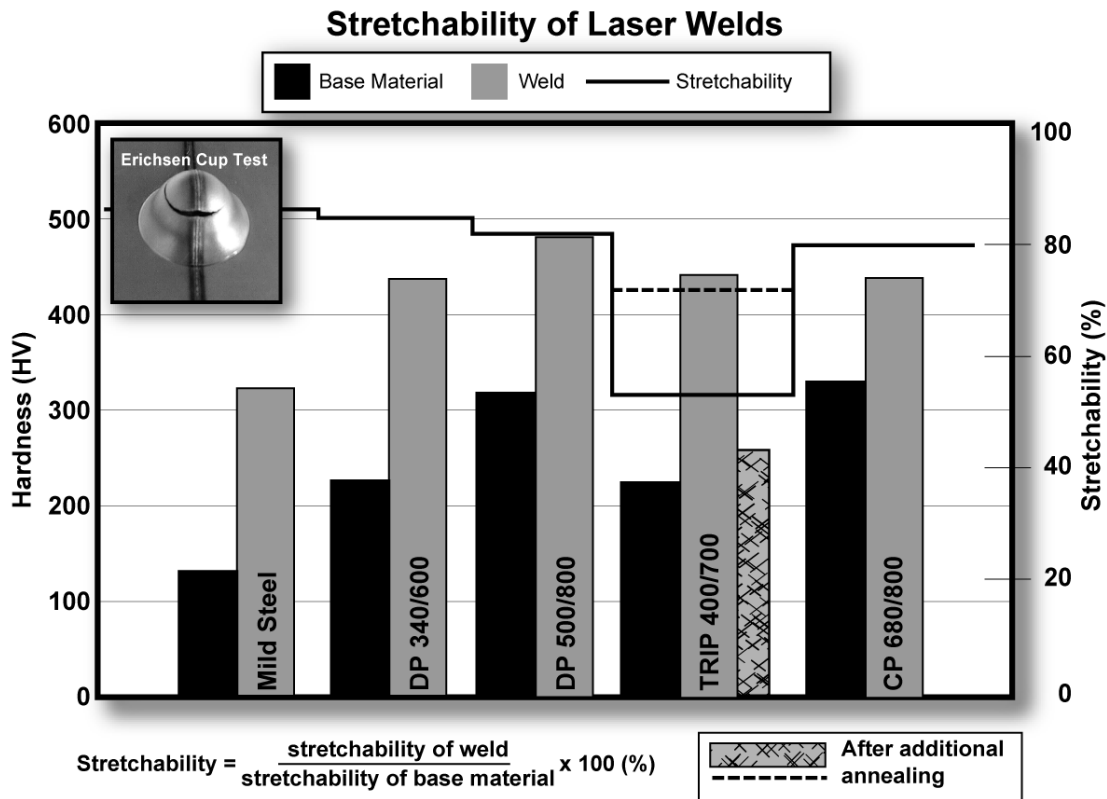


Figure 4.J-8: Hardness and stretchability of laser butt welds with two AHSS sheets of the same thickness (Erichsen test values describe the stretchability.^{B-1})

The hardness of the laser welds for AHSS is higher than for mild steels (Figure 4.J-9). However, good stretchability ratios in the Erichsen test can be achieved when the difference in hardness between weld metal and BM is only slightly higher for AHSS compared to mild steels. If the hardness of the weld is too high, a post-annealing treatment (using HF-equipment or a second laser scan) may be used to reduce the hardness and improve the stretchability of the weld.



Figure 4.J-9: Improved stretchability of AHSS laser welds with an induction heating post-Heat treatment (Testing performed with Erichsen cup test ^{T-3})

Laser butt-welded AHSS of very high strength (for example MS steels) have higher strength than GMAW welded joints. The reason is that the high CR in the laser welding process prompts the formation of hard martensite and the lower heat input reduces the soft zone of the HAZ.

Laser butt-welding is also used for welding tubes in roll-forming production lines as an alternative method for HF induction welding.

4.J.3.b. Assembly Laser Welding

Automotive applications use a variety of welding joint designs for laser welding in both lap joint and seam butt joint configurations as shown in Figure 4.J-10. Lap joints and seam butt joint configurations use different characteristics. Seam welds on butt joints need less power from the machine than lap joints due to the smaller weld fusion area, producing less distortion and a smaller HAZ. Butt joint configurations are more cost efficient. However, the fit up for seam welds can be more difficult to obtain than those of lap joints. Also, lap joints tend to provide a larger process window.

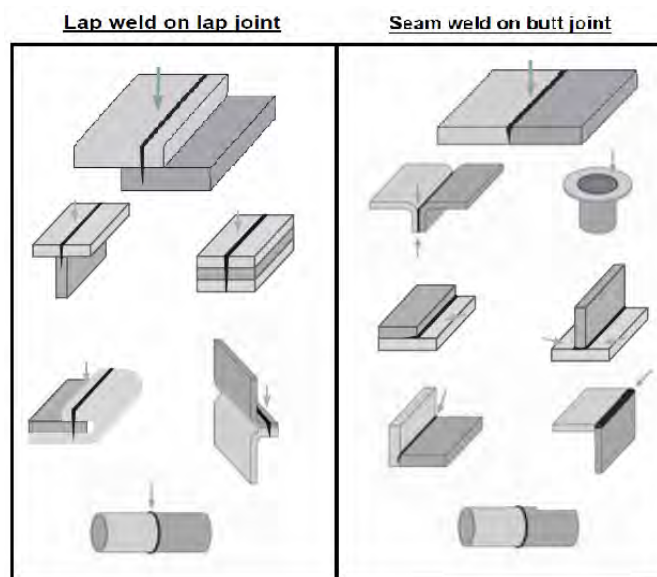


Figure 4.J-10: Common seam and joint types for laser welding of automotive applications^{T-9}

When seam welding butt joint configurations, a general guideline for fit-up requirements include a gap of 3-10% the thickness of the thinnest sheet being welding and an offset of 5-12% thickness of the thinnest sheet. A guideline for lap joints can require a gap of 5-10% the thickness of the top sheet being welded (Figure 4.J-11). These general guidelines are not absolute values due to the change of variables such as the focus spot size, the edge geometry for butt welds, strength requirements, etc.

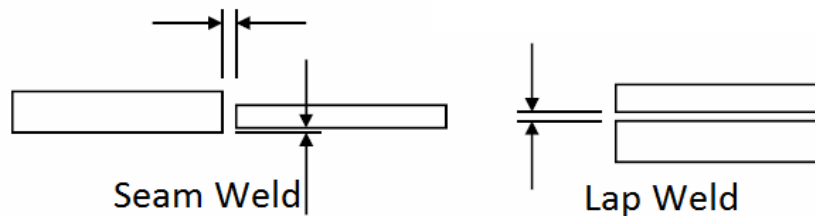


Figure 4.J-11: Fit-up requirements for butt joint and lap joint configurations in laser welding^{T-9}

Laser welding is often used for AHSS overlap joints. This type of weld is either a conventional weld with approximately 50% penetration in the bottom sheet or an edge weld. Welding is performed in the same way as for mild steels, but the clamping forces needed for a good joint fit-up are often higher with AHSS than for mild steels. To achieve good laser-welded overlap joints for Zn-coated AHSS, a small intermittent gap (0.1-0.2 mm) between the sheets is recommended, which is identical to Zn-coated mild steels. In this way, the Zn does not get trapped in the melt, avoiding pores and other imperfections. An excessive gap can create an undesirable underfill on the topside of the weld. Some solutions for lap joint laser welding Zn-coated material are shown in Figure 4.J-12.

Joining of Tubular Hydroformed Parts Laser welding of zinc-coated steels

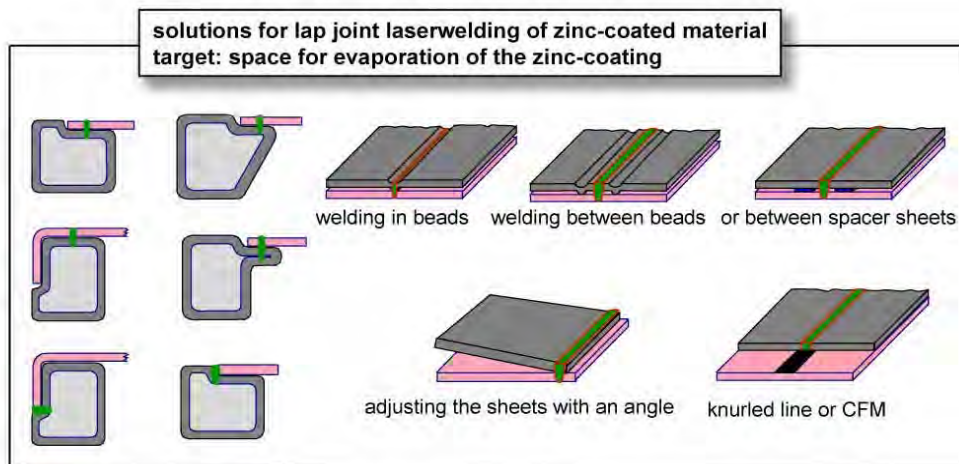


Figure 4.J-12: Laser welding of Zn-coated steels to tubular hydroformed parts^{L-3}

Recent studies^{L-5} have shown welding Zn-coated steels can be done without using a gap between the overlapped sheets. This is accomplished using dual laser beams. While the first beam is used to heat and evaporate the Zn coating, the second beam performs the welding. The dual laser beam configuration combines two laser-focusing heads using custom-designed fixtures.

4.J.3.c. Remote Laser Welding

Remote scanner welding is used for many automotive applications, including seating (recliners, frames, tracks, and panels), BIW (trunks, rear panels, doors /hang on parts, side walls, and pillars) and interior (IP beams, rear shelf/hat rack) (Figure 4.J-13). Compared to conventional laser welding, remote scanner welding has several advantages. Those include a reduced cycle time (via reduction of index time), programmable weld shapes (ability to customize weld shape to optimize component strength), large stand-off (longer protection glass life), and reduced number of clamping fixtures (via reduced number of stations). Remote laser welding, or "welding on the fly", combines a robot and scanner optics to position the focused laser beam on the workpiece on the fly. The robot arm guides the scanner optics along a smooth path about half a meter over the workpiece. Extremely nimble scanning mirrors direct the focal point in fractions of a second from weld seam to weld seam. A fiber-delivered, solid-state laser is the source of the joining power far away from the processing station. The scanning optic or Programmable Focusing Optic (PFO) at the end of the laser's fiber-optic cable is the central element for precise positioning of the laser's focus point on the component to be welded. Inside the PFO, two scanner mirrors direct the beam through a "flat field" optic, which focuses the beam onto a common focus plane no matter where it is in the work envelope of the PFO. The PFO is also equipped with a motorized lens that allows the focus plane to be moved up and down in the Z-axis. The repositioning of the focused laser beam from one end of the entire work envelope to the other takes about 30 ms.^{T-9}

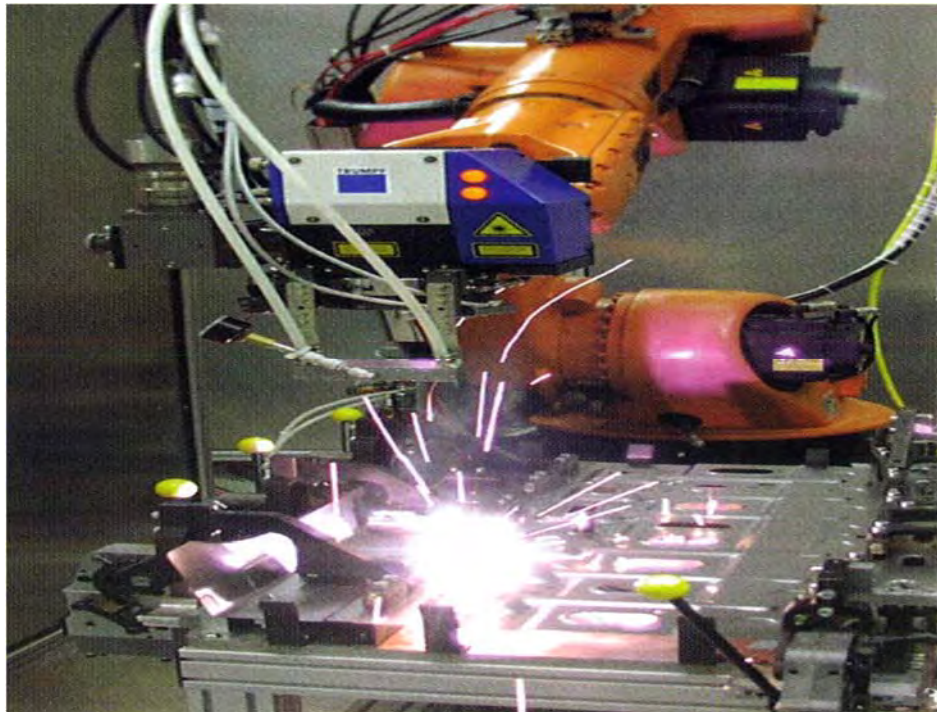


Figure 4.J-13: Remote laser welding of automotive applications^{T-9}

There are three basic preconditions for welding on the fly. First, a solid-state laser is needed as the beam source. Solid-state lasers enable delivery of the laser beam through a highly flexible fiber optic cable, which is required when joining components in 3D space with a multi-axis robot. Second, a laser with excellent beam quality and the appropriate power is required. Beam quality is the measure of focus-ability of a laser, and the long focal lengths required for remote welding necessitate superior beam quality (i.e., 4 to 8 mm-mrad) to achieve the appropriate focused spot size (i.e., about 0.6 mm) at the workpiece. For remote welding in automotive body production, typically about 4 to 6 kW of laser power is used. The third essential precondition is precise positioning of the weld seams, which requires axis synchronization between the robot and the scanner control. This allows the weld shape programmed in the scanner control for a specific shape weld to have proper shape with the robot moving

at various speeds over the part to be welded. Some control architectures use "time" synchronization. The problem here is that if the robot speed is changed for any reason, the weld shape will also change because the axes are not synchronized. ^{T-9}

4.J.3.d. Body-in-White (BIW) Joining

Laser-based solutions can offer a high- and cost-effective improvement potential for steel-based BIW joining. The laser joining design's stiffness increases in direct relation to the laser weld length. Also, at low process time, there is up to a +14% torsional stiffness increase without any additional joining technique, shown in Table 4.J-1.

Table 4.J-1: Stiffness performances comparison for several joining designs^{A-16}

Joining design	Average Torsional Stiffness (Nm/deg)	Scatter % (5 samples)	Baseline % average
Spot weld	805	4,5	REFERENCE
C-weld	869	5,1	+8%
Laser stitch	896	2,5	+11%
Continuous laser weld	921	2,3	+14%
Spot weld bonded joint	961	0,6	+19%
Adhesive bonding	964	2,4	+20%

Laser weld shape optimization can help to homogenize performances and increasing the laser weld shape factor leads to a signification reduction of IF fracture risk (Figure 4.J-14).

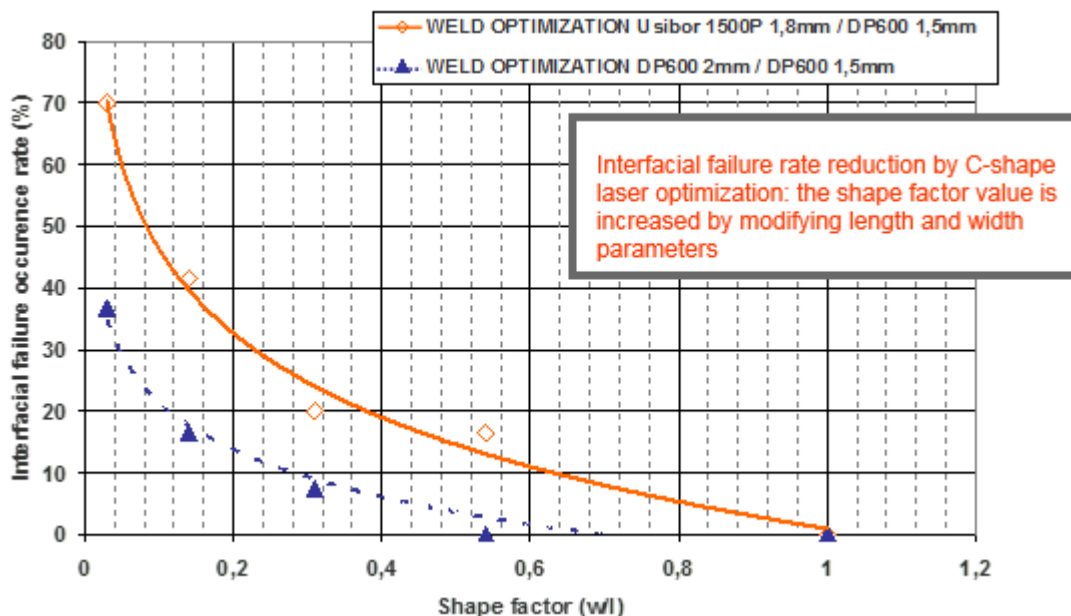


Figure 4.J-14: Impact of laser weld design optimization on fracture type^{A-16}

DP 800* has the advantage of weight reduction and equally good properties when laser welding as the

DP 800. The absolute strength of DP 800 is slightly higher, but the ductility for the DP 800¹ is greater, shown in Figure 4.J-15.

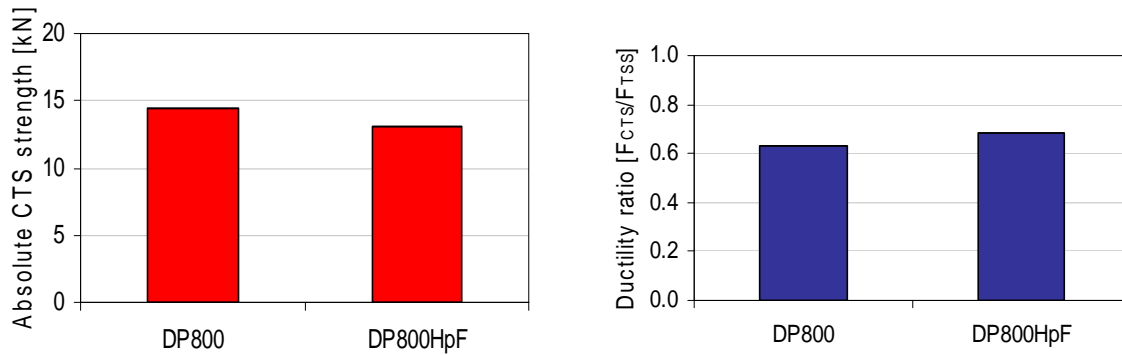


Figure 4.J-15: Absolute strength and ductility of DP 800 and DP 800.*^{T-10}

Figure 4.J-16 shows a cross-tension test in which both materials fail outside the weld zone, DP 800 failing entirely in the HAZ and DP 800* failing partly in the HAZ and partly in the BM.



Figure 4.J-16: Cross-tension testing of DP 800 and DP 800*^{T-10}

Figure 4.J-17 is the microhardness profile of 1.6-mm Q&P 980's laser weld joint. Microhardness of both welded seam and HAZ are all higher than BM, and there is no obvious softened zone in HAZ.

¹ DP 800 with additional retained austenite and associated bainite.

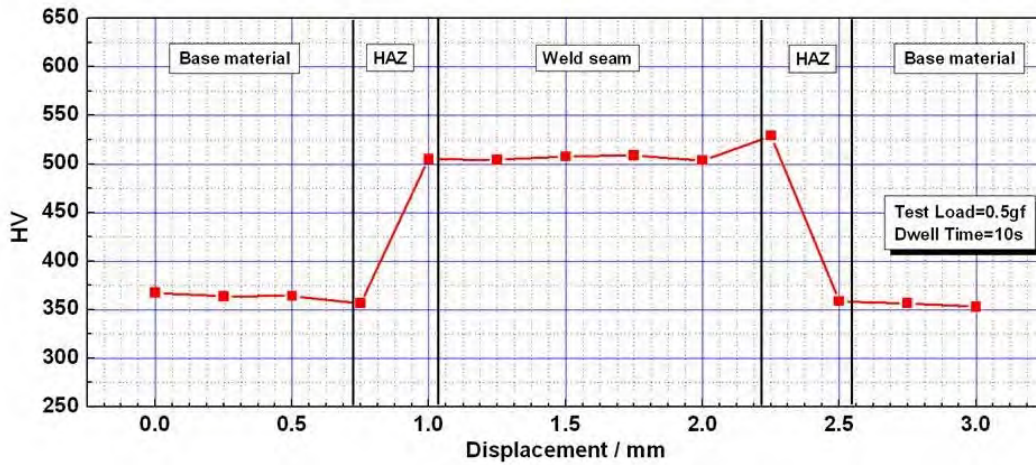


Figure 4.J-17: Microhardness profile of 1.6-mm Q&P 980's laser weld joint^{B-4}

Figure 4.J-18 is Erichsen test result for the BM and weld seam of 1.6-mm Q&P 980, showing good stretchability.

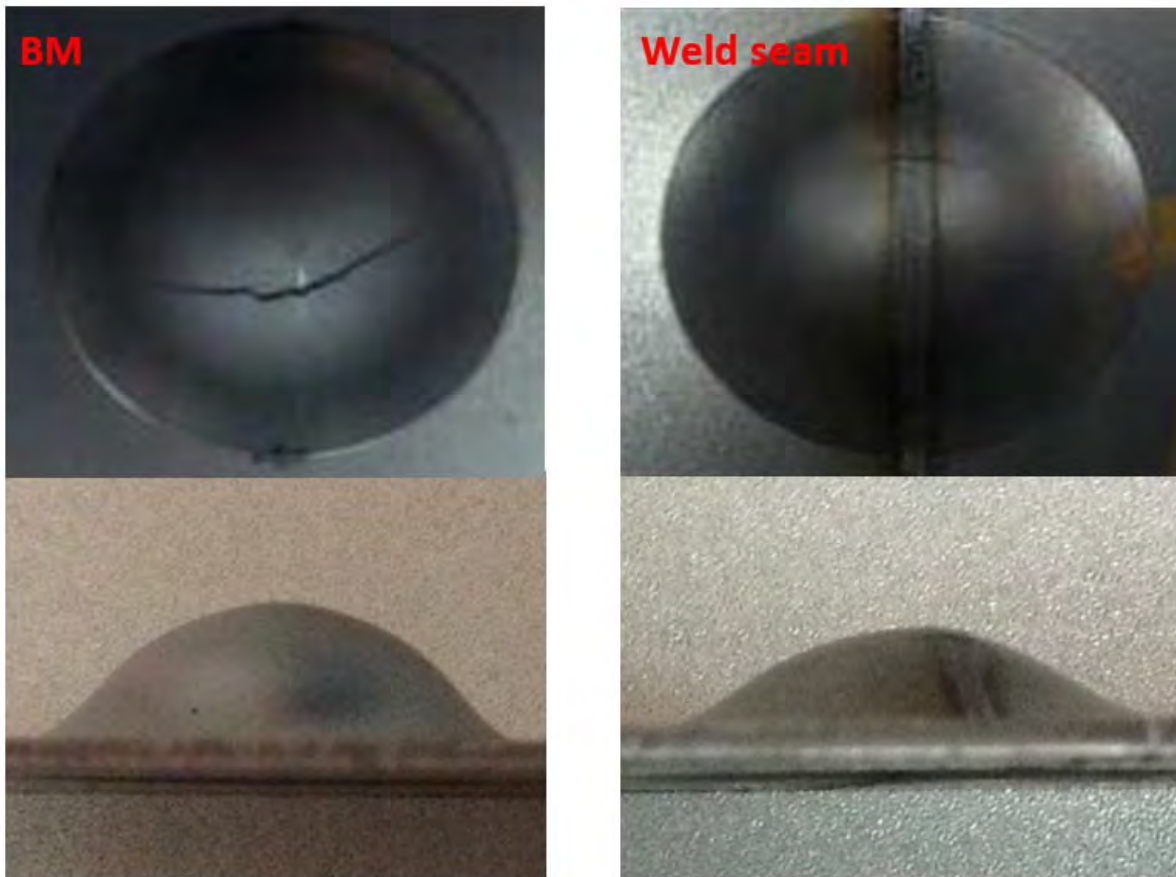


Figure 4.J-18: Erichsen test result of 1.6-mm Q&P 980, laser welded^{B-4}

4.K. Hybrid Welding Processes

4.K.1. Fundamentals and Principles of Hybrid Welding

Recent developments in welding include approaches that could be considered novel, as well hybrid, or those that combine more than one established process. A sampling of these unique approaches will be reviewed here. A hybrid process that is being extensively developed known as hybrid laser welding combines both the laser beam and GMAW processes (Figure 4.K-1). This approach uses a head that carries both the laser focusing optics and the GMAW gun. The laser beam creates a keyhole near the leading edge of the puddle. The motivation for this concept is that the best features of each process can be combined (Figure 4.K-2) to create an even better process for certain applications. Laser beam welding provides the capability for deep-penetrating single-pass welds at high speeds, but requires precise joint fit-up and doesn't produce weld reinforcement which can add strength to the joint. When combined with GMAW, these limitations are eliminated. The laser beam also helps stabilize the arc, which can be of particular benefit when welding Titanium (Ti).

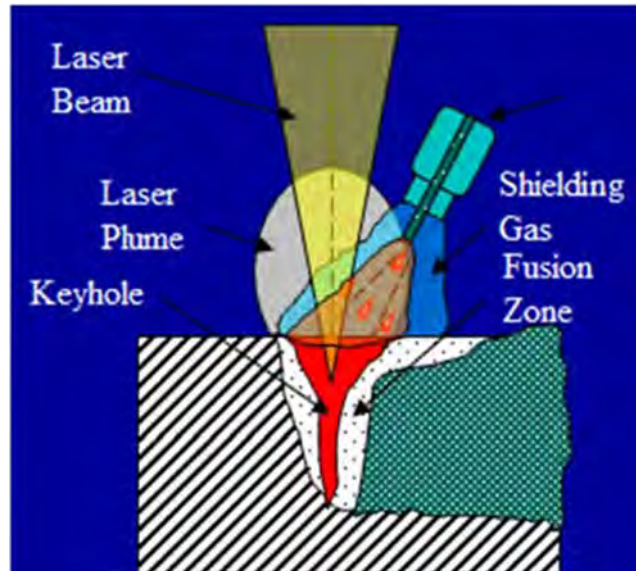


Figure 4.K-1: Hybrid laser welding.

PAW, GTAW and GMAW have also been combined into a hybrid process. The benefits are similar to the laser hybrid welding approach, but the equipment has the potential to be much less expensive. The combination of FSW with ultrasonic energy is being explored as an approach to creating friction stir welds with greatly reduced forces, and therefore, smaller machines. [1] [2]

4.K.2. Hybrid Welding Procedures

As with mild steels, AHSS-hybrid joints can be made by combining adhesive bonding with RSW, clinching, or self-piercing riveting. These hybrid joints result in higher strength values (static, fatigue, and crash) than the spot welding alone (Figure 4.K-3). If local deformation and buckling can be avoided during in-service applications of weld bonding/adhesive hybrid joining, the potential for component performance is enhanced.

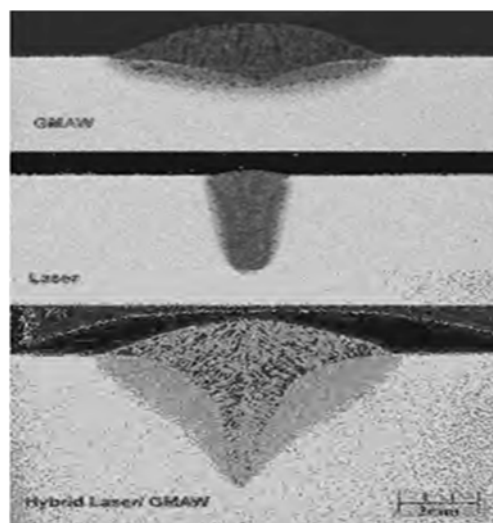


Figure 4.K-2: Hybrid laser welding combines the best features of laser beam and GMAW (top GMAW, middle LBW, bottom hybrid).

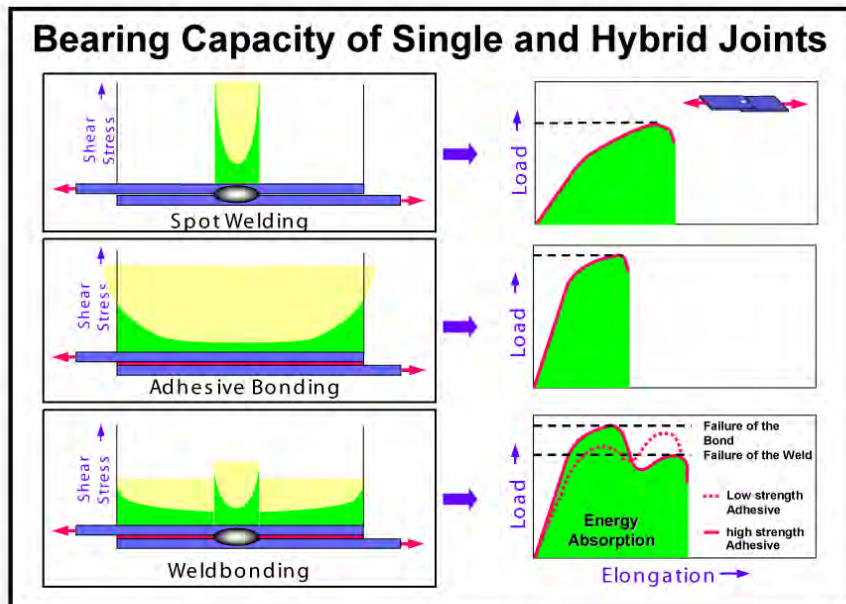


Figure 4.K-3: Comparison of bearing capacity for single and hybrid Joints^{B-3}

4.K.2.a. Hybrid Laser and MIG Welding

In hybrid welding process parameters such as stick out and torch angle are very important to decide overall joint performance. A model has been developed to predict the penetration and toe length under similar heat input conditions, shown in Figure 4.K-4. The gap, stickout and angle shows synergic agreement with penetration and toe length but the interactions among them can show disagreement.

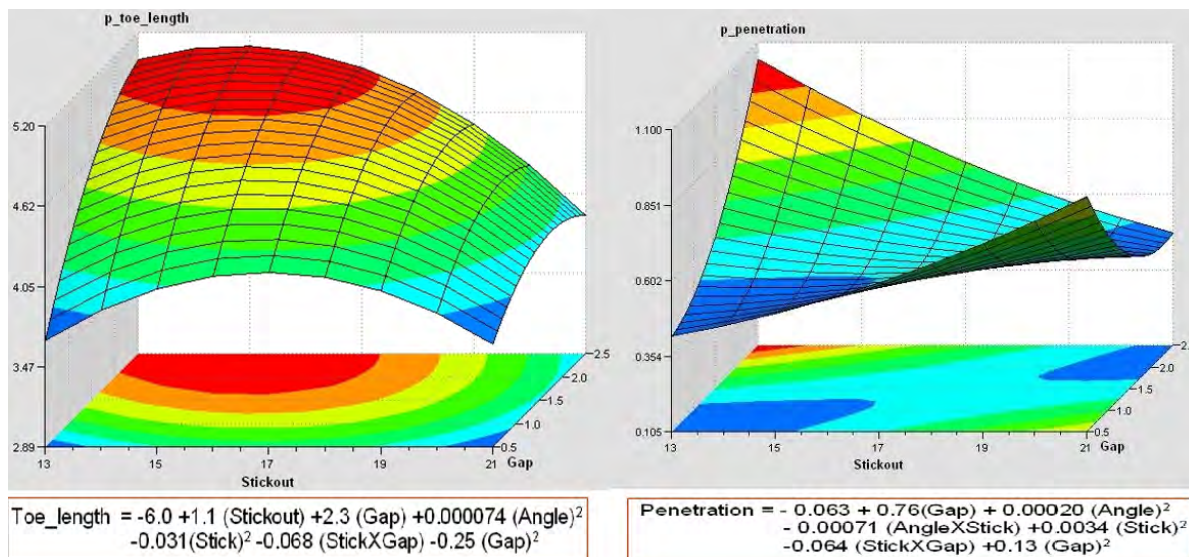


Figure 4.K-4: Effects of toe length and penetration^{T-10}

The weld joint strength increases with the increase in wire feed rate for a given laser power shown in Figure 4.K-5.

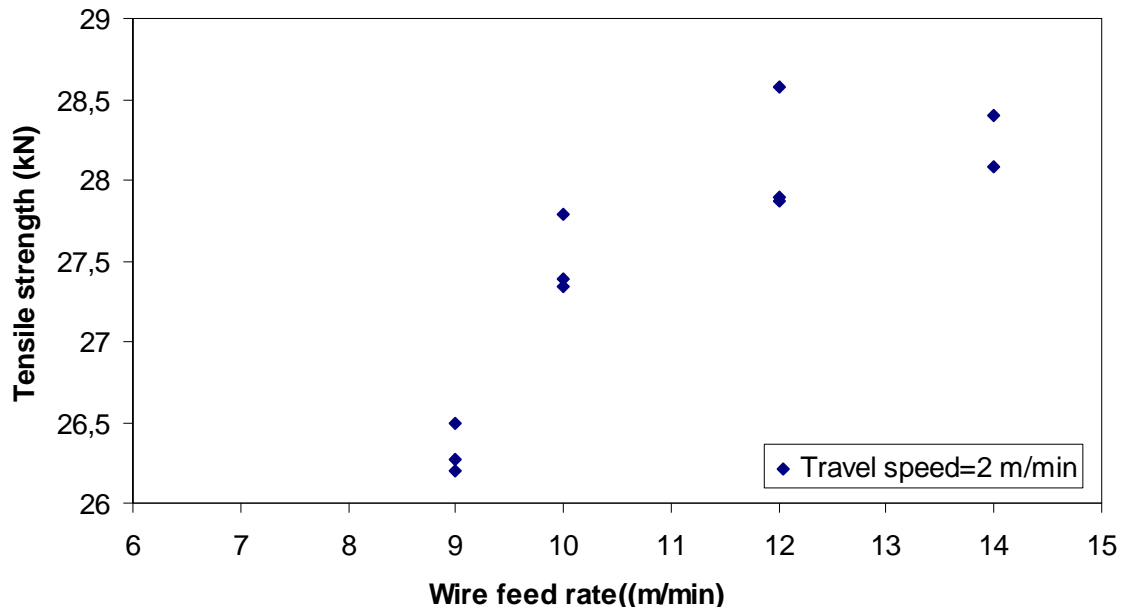


Figure 4.K-5: Wire feed rate versus tensile strength of hybrid laser and MIG welds ^{T-10}

4.K.2.b. Hybrid RSW and Adhesives

Many automotive joining BIW applications are using the combination of RSW together with adhesives to obtain superior joint performance. This combination is referred to as WB. Figure 4.K-6 shows a tensile shear test for resistance spot welds, adhesives, and weld bonds. There were trends of fracture strength increasing slightly with material strength with the spot welds. Also, the fracture strength was very high, increasing significantly with increasing material strength for adhesive bonds. The fracture strength was the highest for welded bonds and increased significantly with increasing material strength.

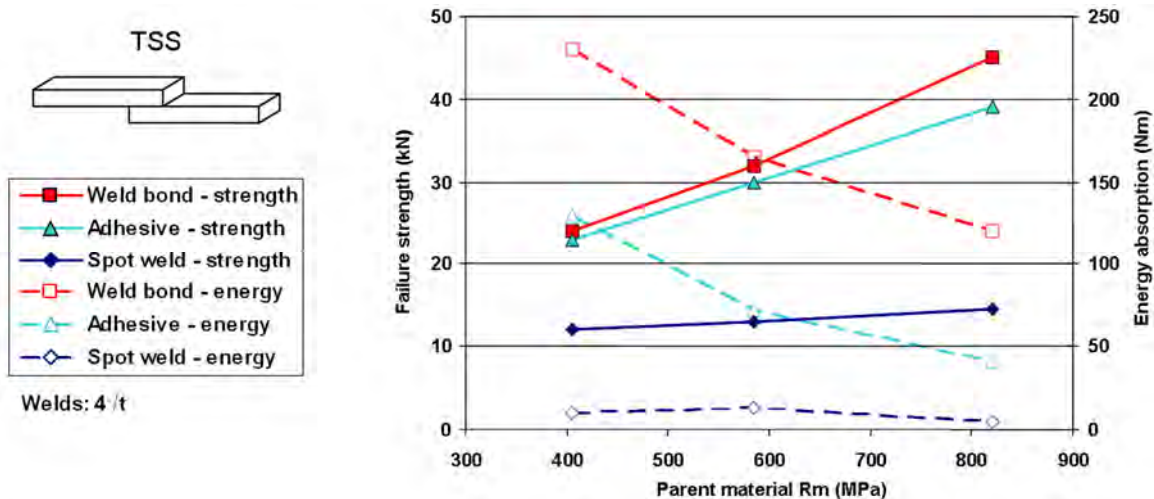


Figure 4.K-6: TSS failure strength and energy absorption for all joints and materials ^{T-10}

Figure 4.K-7 represents a peel test for the same samples. Trends observed were fracture strength increasing slightly with material strength, but is lower than the other joining methods for spot welds. Fracture strength for adhesive bonding is greater than Weld Bonding (WB) and spot welding. Energy absorption was not very sensitive to material strength. The bond using adhesive alone had poor failure strength as well as poor energy absorption.

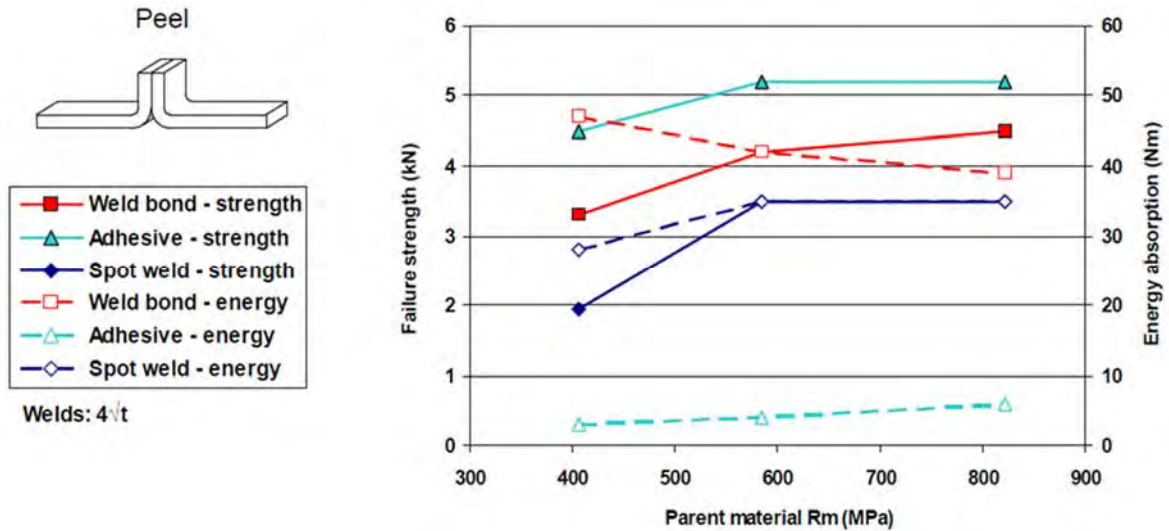


Figure 4.K-7: Peel strength data for all joint types T-10

Figure 4.K-8 shows cross tensile results for the three samples. Spot welds showed fracture strength reaching a maximum for DP 600. Adhesive fracture strength increased slightly with increasing material strength. The welded bond's fracture strength was greater than the other joint types and increased significantly with increasing material strength.

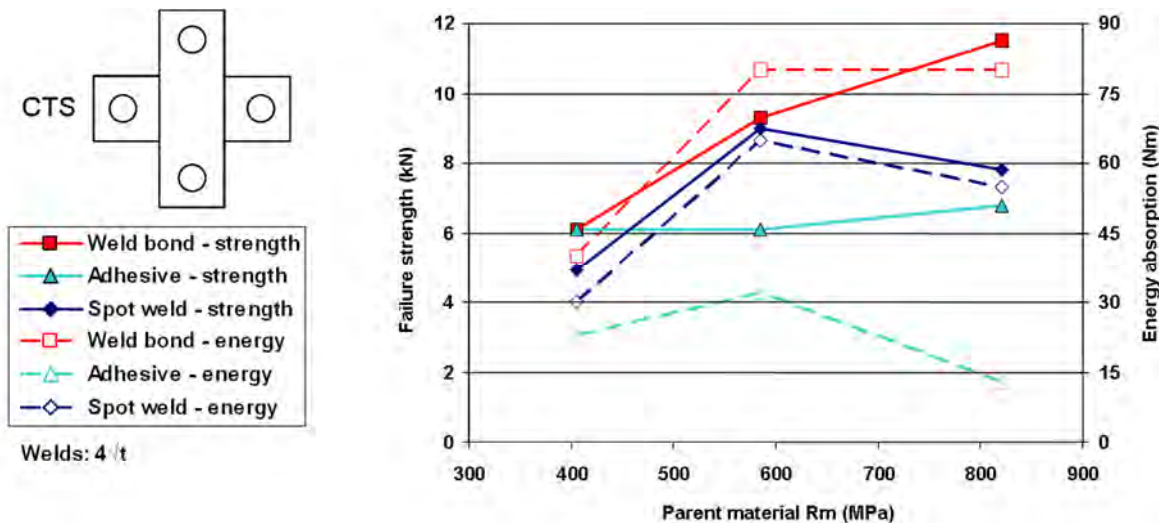


Figure 4.K-8: CTS fracture strength and energy absorption for all joints and materials T-10

Figure 4.K-9 shows the fatigue testing performed in tensile shear mode on DP 800 material (1.2-mm gage). Spot welds showed the lowest fatigue properties of the test samples. While the weld-bonded samples performed much better than conventional spot welds, they were still weaker than the adhesive joints. Adhesive had the best fatigue performance. The parent material properties had little

influence upon the fatigue properties of spot welds because the spot weld itself acts as a fatigue crack initiator.

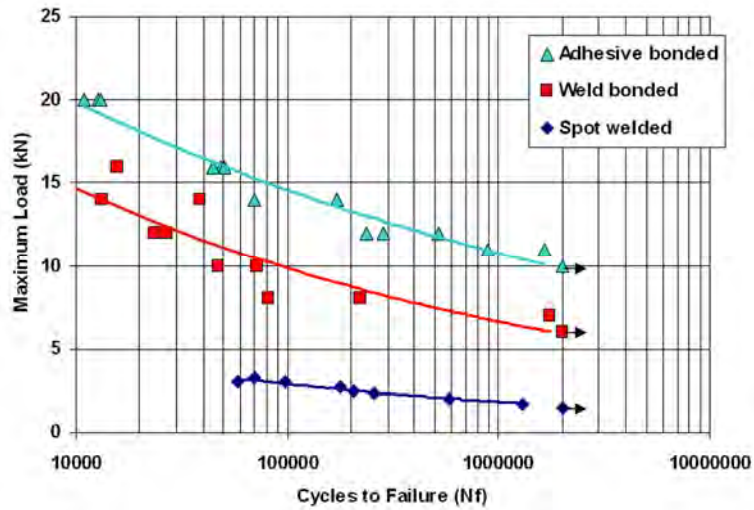
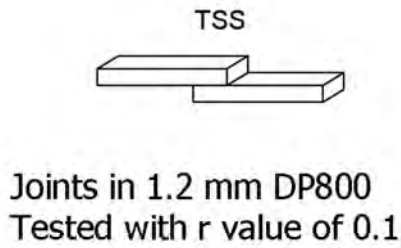


Figure 4.K-9: DP 800 fatigue results ^{T-10}

Hybrid Riveting Adhesive

Some BIW applications consider using self-piercing riveting combined with adhesive bonding in place of RSW with adhesive. Figure 4.K-10 is an example of tensile shear results for the various joint types. The self-piercing riveting with adhesive joints exhibited higher static strength than the other joint types.

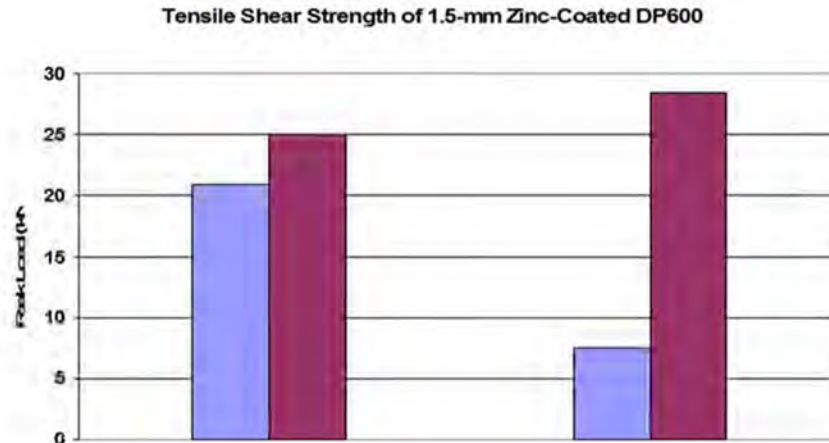


Figure 4.K-10: Tensile shear strength of 1.5-mm DP 600 RSW, weld-bonded, SPR, SPR with adhesive.

4.L. Solid-State Welding Processes

Solid-State welding refers to a family of processes that produce welds without the requirement for molten metal. Solid-state welding theory emphasizes that the driving force for two pieces of metal to spontaneously weld (or form a metallic bond) to each other exists if the barriers (oxides, contaminants, and surface roughness) to welding can be eliminated. All solid-state welding processes are based on this concept, and use some combination of heat, pressure, and time to overcome the barriers. Approaches include friction, diffusion, explosion, and ultrasonic welding.

Since there is no melting, there is no chance of forming defects such as porosity or slag inclusions which are only associated with fusion welding processes. Solid-state welding processes also require no filler materials, and in some cases, can be quite effective at welding dissimilar metals that cannot be welded with conventional processes due to metallurgical incompatibilities. The equipment is typically very expensive, and some processes involve significant preparation time of the parts to be welded. Most of these processes are limited to certain joint designs, and some of them are not conducive to a production environment. NDT processes do not always work well with solid-state welding processes because of the difficulties of distinguishing a true metallurgical bond with these techniques.

4.L.1. Friction Welding Processes

This family of processes relies on significant plastic deformation or forging action to overcome the barriers to solid-state welding. Frictional heating dominates at the beginning of the process, followed by the heating due to plastic deformation once the forging action begins. The friction welding processes which use rotation of one part against another are inertia and continuous (or direct)-drive friction welding. These are the most common of the friction welding processes and are ideal for round bars or tubes. In both inertia and Continuous-Drive (CD) friction welding, one part is rotated at high speeds relative to the other part (Figure 4.L-1). They are then brought together under force creating frictional heating which softens (reduces the YS) the material at and near the joint to facilitate the forging action, which, in turn, produces further heating. Following a sufficient amount of time to properly heat the parts, a high upset force is applied which squeeze the softened hot metal out into the “flash”. Any contaminants are squeezed out as well as the weld is formed. The flash is usually removed immediately after welding while it is still hot.^{A-11, P-6}

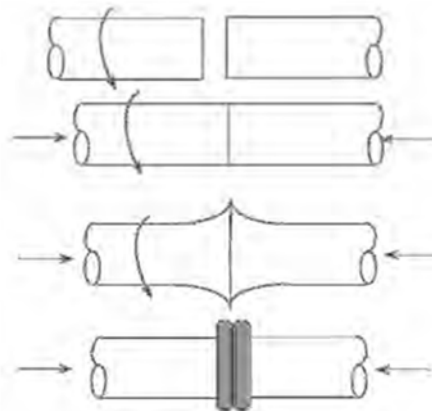


Figure 4.L-1: Basic steps of both inertia and CD friction welding.

4.L.1.a. Friction Stir Welding (FSW)

FSW is a revolutionary new friction welding process that was developed in the early 1990s by the British Welding Institute (TWI). Whereas processes such as inertia and CD friction welding are primarily limited to round parts, FSW (Figure 4.L-2) produces solid-state friction welds using conventional joint design such as butt joints. FSW relies on the frictional heat created when a special non-consumable pin tool is rotated along the joint against the top of the two pieces being welded. As the process begins, frictional heating softens (or plasticizes) metal at the joint, facilitating a stirring action of plasticized metal. Further heating that is generated by the plastic deformation becomes the main source of heating as the weld progresses.

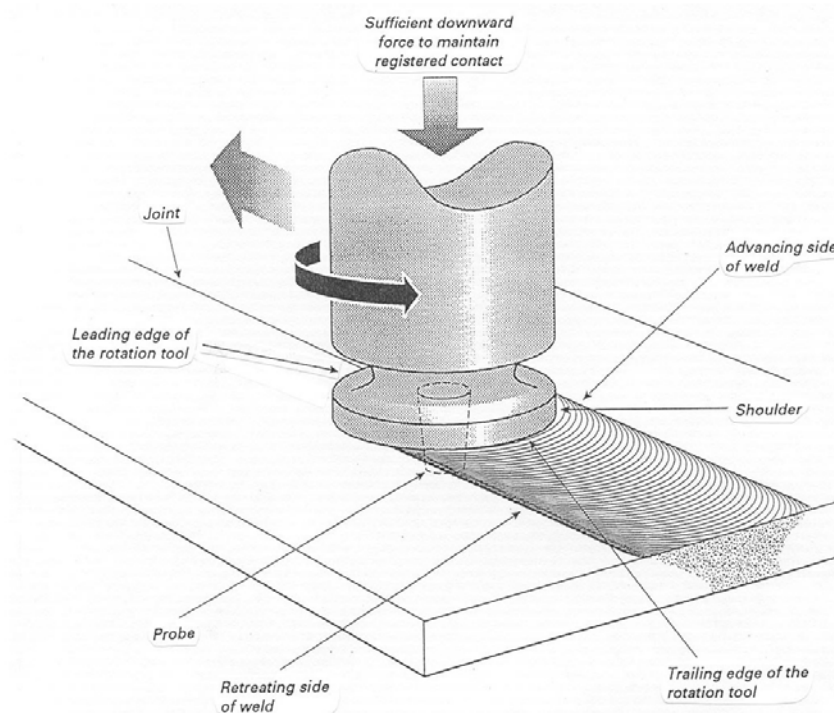


Figure 4.L-2: FSW.

The pin tool for FSW consists of a shoulder and pin. The shoulder rests on the surface of the plates and provides most of the frictional heating. The pin partially penetrates the joint of the plates being welded. Within the stir zone itself, the plasticized hot metal flows around the pin and coalesces to form a weld. The primary purpose of the pin is to control the stirring action. A wide variety of pin tool designs and materials have been studied, including the use of Tungsten (W)-based materials, threaded pins, and cupped shoulders. As indicated on Figure 4.L-3, a slight push angle (<5 degrees) relative to the travel direction is typically used. Weld travel speeds are much slower than typical arc welding speeds. The process has limited industrial applications since it is still under development, especially in tool development. ^{A-11, P-6}



Figure 4.L-3: FSW typically uses a slight push angle.

The FSW of hard metals (steel, Ti, Ni) has been made possible due to advancements in both tool design and tool materials. Tool material choices for AHSS applications include ceramic-based Polycrystalline Cubic Boron Nitride (PCBN) and refractory based Tungsten-Rhenium alloy (W-Re). PCBN is chosen because it is extremely wear resistant and has good thermal management. W-based material is chosen because it is very tough at room and welding temperatures and it is capable of being used for thick sections of steels.

Mechanical properties for FSW of AHSS cross-weld tensile specimens showed fully consolidated weld joints without discontinuities, but showed a drop-in weld ductility of about 10%, as seen in Figure 4.L-4.

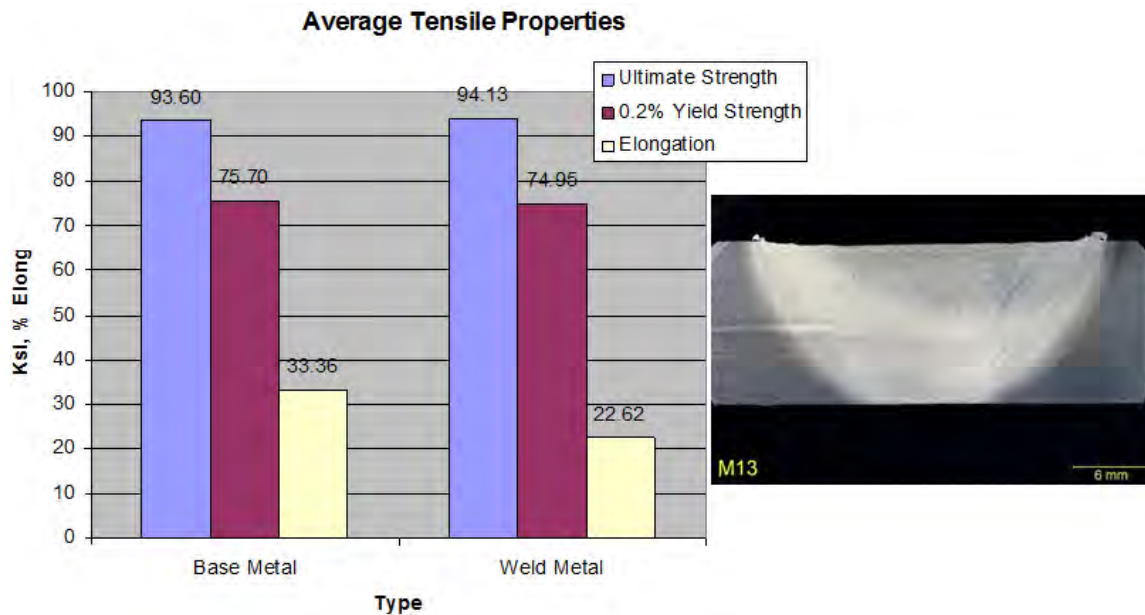


Figure 4.L-4: Mechanical properties of FSW for HSS.

A variation of the FSW process is friction stir spot welding. This process was specifically developed for some automotive applications, including joining of AAl), Al-to-steel, and AHSS. The process steps are similar to FSW without the linear movement, thus creating a “spot”-type joint (Figure 4.L-5).⁰⁻¹

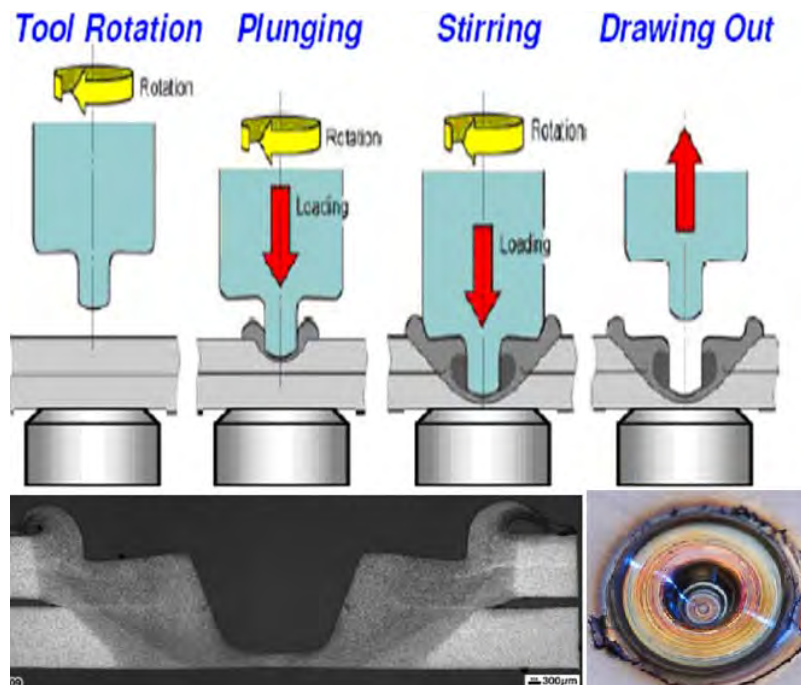


Figure 4.L-5: Process steps for friction stir spot welding (top) with the resultant weld profile (bottom).⁰⁻²

In summary, the advantages and limitations of friction welding processes are listed below.

- Advantages:
 - No melting means no chance for solidification-related defects
 - Filler materials are not needed
 - Very few process variables result in a very repeatable process
 - In the case of CD friction welding, can be deployed in a production environment
 - Fine grain structure of friction welds typically exhibits excellent mechanical properties relative to the BM, especially when welding Al
 - No special joint preparation or welding skill required

- Limitations:
 - Equipment is very expensive
 - Limited joint designs, and in the case of CD and inertia welding, parts must be symmetric
 - FSW is very slow, and not conducive to high-speed production

4.L.2. HF Welding

4.L.2.a Fundamentals and Principles of HF Welding

HF welding processes rely on the properties of HF electricity and thermal conduction, which determine the distribution of heat in the workpieces. HF contact welding and high-frequency induction welding are used to weld products made from coil, flat, or tubular stock with a constant joint symmetry throughout the length of the weld. Figure 4.L-6 illustrates basic joint designs used in HF welding. Figures 4.L-6 (A) and (B) are butt seam welds; Figure 4.L-6 (C) is a mash seam weld produced with a mandrel, or backside/inside bar. Figure 4.L-6 (D) is a butt joint design in strip metal; and Figure 4.L-6 (E) shows a T-joint. Figures 4.L-6 (F) and (G) are examples of helical pipe and spiral-fin tube joint designs. Figure 4.L-6 (J) illustrates a butt joint in pipe, showing the placement of the coil. Figure 4.L-6 (K) shows a butt joint in bar stock.

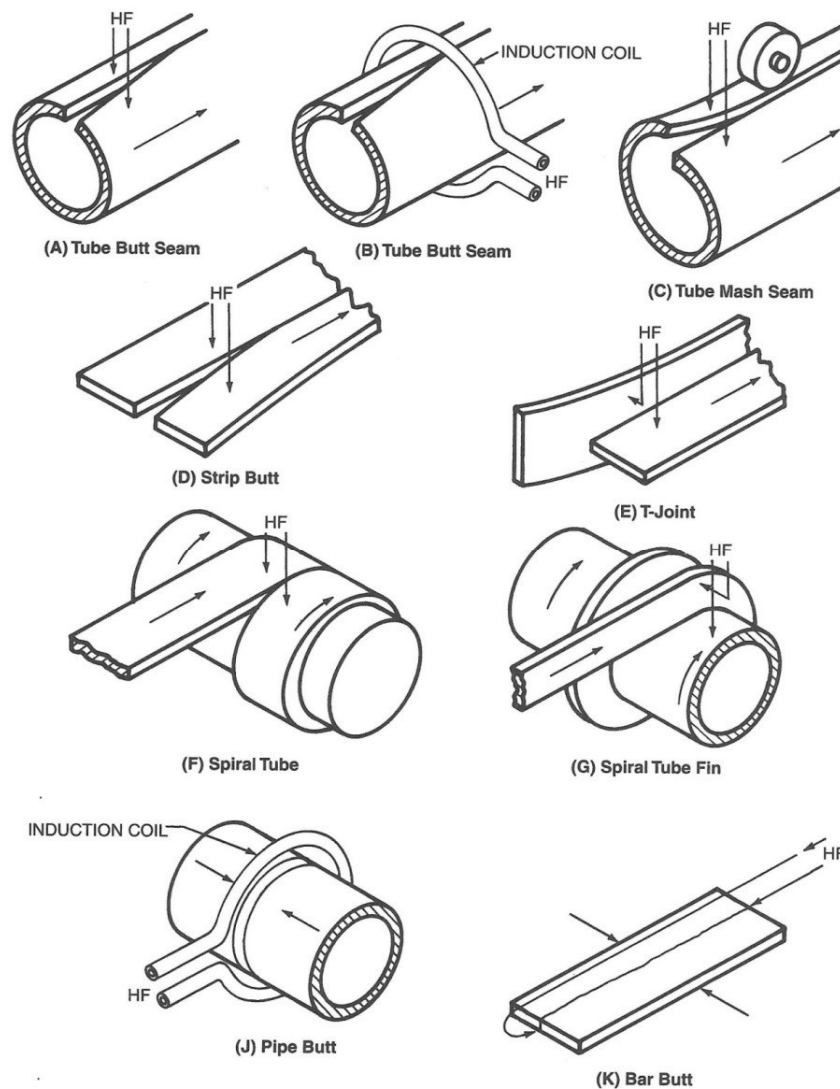


Figure 4.L-6: Basic joint designs for HF welds in pipe, tube, sheet, and bar stock.

HF current in metal conductors tends to flow at the surface of the metal at a relatively shallow depth, which becomes shallower as the electrical frequency of the power source is increased. This commonly is called the *skin effect*. The depth of electrical current penetration into the surface of the conductor also is a function of electrical resistivity, and magnetic permeability, the values of which depend on temperature. Thus, the depth of penetration also is a function of the temperature of the material. In most metals, the electrical resistivity increases with temperature; as the temperature of the weld area increases, so does the depth of penetration. For example, the resistivity of low-carbon steel increases by a factor of five between room temperature to welding temperature. Metals that are magnetic at room temperature lose the magnetic properties above the Curie temperature. When this happens, the depth of penetration increases drastically in the portion of metal that is above the Curie temperature while remaining much shallower in the metal that is below the Curie temperature. When these effects are combined in steel heated at a frequency of 400 kHz, the depth of current penetration is 0.05 mm (0.002 in.) at room temperature, while it is 0.8 mm (0.03 in.) at 800°C (1470°F). The depth of current penetration for several metals as a function of frequency is shown in Figure 4.L-7.

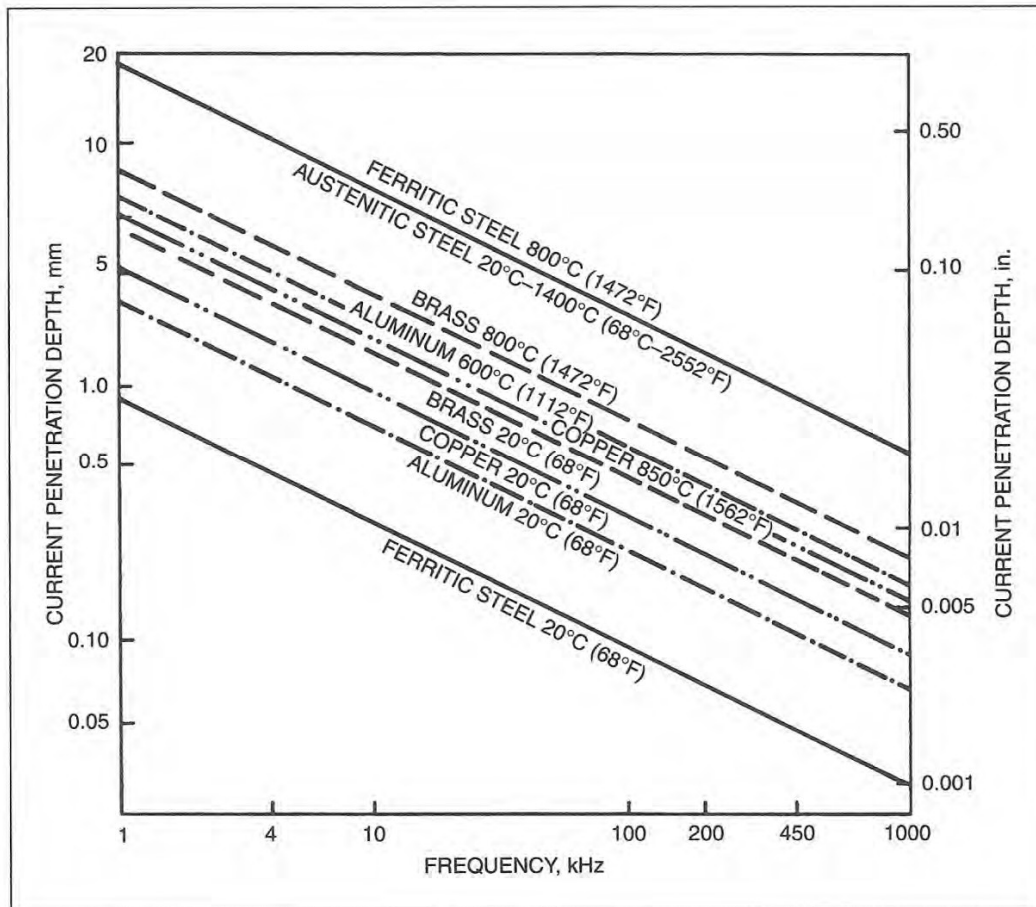


Figure 4.L-7: Effect of frequency on depth of penetration into various metals at selected temperatures.

The second important physical effect governing the HF welding process is thermal conduction of the heat generated by the electric currents in the workpiece. Control of the thermal conduction and of the penetration depth provides control of the depth of heating in the metal. Because thermal conduction is a time-dependent process, the depth to which the heat will conduct depends on the welding speed and the length of the electrical current path in the workpiece. If the current path is shortened or the welding speed is increased, the heat generated by the electric current in the workpiece will be more concentrated and intense. However, if the current path is lengthened or the welding speed is reduced, the heat generated by the electric current will be dispersed and less intense. The effect of thermal conduction is especially important when welding metals with high thermal conductivity, such as Cu or Al. It is not possible to weld these materials if the current path is too long or the welding speed is too slow. Changing the electrical frequency of the HF current can compensate for changes in welding speed or the length of the weld path, and the choice of frequency, welding speed, and path length can adapt the shape of the HAZ to optimize the properties of the weld metal for a particular application^{A-11, A-15}

4.L.2.b. Advantages/Disadvantages of HF Welding

A wide range of commonly used metals can be welded, including low-carbon and alloy steels, ferritic and austenitic stainless steels, and many Al, Cu, Ti, and Ni alloys.

Because the concentrated HF current heats only a small volume of metal at the weld interface, the process can produce welds at very high welding speeds and with high energy efficiency. HFRW can be

accomplished with a much lower current and less power than is required for low-frequency or direct-current resistance welding. Welds are produced with a very narrow and controllable HAZ and with no superfluous cast structures. This often eliminates the need for Post-Weld Heat Treatment (PWHT).

Oxidation and discoloration of the metal and distortion of the workpiece are minimal. Discoloration may be further reduced by the choice of welding frequency. Maximum speeds normally are limited by mechanical considerations of material handling, forming and cutting. Minimum speeds are limited by material properties, excessive thermal conduction such that the heat dissipates from the weld area before bringing it to sufficient temperature, and weld quality requirements. The high process speed may also become a disadvantage if process settings are incorrect, as scrap can be generated at very high rates.

Considering the high processing speeds, with the high equipment cost required for HF welding, it is important to understand the amount of product needs for economic justification.

The fit-up of the surfaces to be joined and the way they are brought together are important if high-quality welds are to be produced. However, HF welding is far more tolerant in this regard than some other processes.

Flux is almost never used, but can be introduced into the weld area in an inert gas stream. Inert gas shielding of the weld area generally is needed only for joining highly reactive metals such as Ti or for certain grades of stainless steel.^{A-11, A-15}

4.L.2.c. Induction Seam Welding of Pipe and Tubing

The welding of continuous-seam pipe and tubing is the predominant application of HF induction welding. The pipe or tube is formed from metal strip in a continuous-roll forming mill and enters the welding area with the edges to be welded slightly separated. In the weld area, the open edges of the pipe or tube are brought together by a set of forge pressure rolls in a vee shape until the edges touch at the apex of the vee, where the weld is formed. The weld point occurs at the center of the mill forge rolls, which apply the pressure necessary to achieve a forged weld.

An induction coil, typically made of Cu tubing or Cu sheet with attached water-cooling tubes, encircles the tube (the workpiece) at a distance equal to one to two tube diameters ahead of the weld point. This distance, measured from the weld point to the edge of the nearest induction coil, is called the *vee length*. The induction coil induces a circumferential current in the tube strip that closes by traveling down the edge of the vee through the weld point and back to the portion of the tube under the induction coil. This is illustrated in Figure 4.L-8.

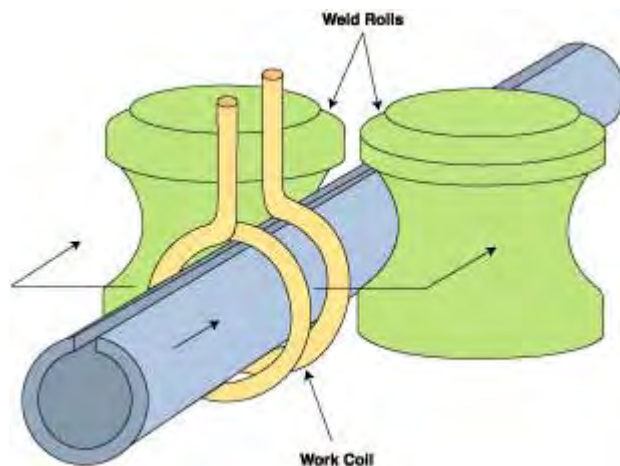


Figure 4.L-8: HF induction seam welding of a tube.

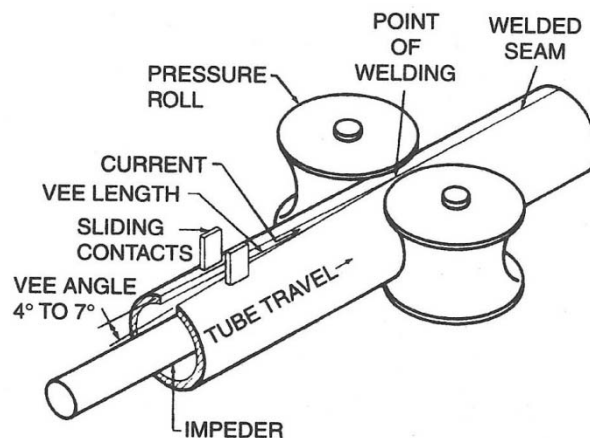
The HF current flows along the edge of the weld vee due to the proximity effect (see Fundamentals), and the edges are resistance-heated to a shallow depth due to the skin effect.

The geometry of the weld vee is such that its length usually is between one and one half to two tube diameters long. The included angle of the vee generally is between 3 and 7 degrees. If this angle is too small, arcing between the edges may occur, and it will be difficult to maintain the weld point at a fixed location. If the vee angle is too wide, the proximity effect will be weakened causing dispersed heating of the vee edges, and the edges may tend to buckle. The best vee angle depends on the characteristics of the tooling design and the metal to be welded. Variations in vee length and vee angle will cause variations in weld quality.

The welding speed and power source level are adjusted so that the two edges are at the welding or forge temperature when they reach the weld point. The forge rolls press the hot edges together, applying an upset force to complete the weld. Hot metal containing impurities from the faying surfaces of the joint is squeezed out of the weld in both directions, inside and outside the tube. The upset metal normally is trimmed off flush with the BM on the outside of the tube, and sometimes is trimmed from the inside, depending on the application for the tube being produced.^{A-11, A-15}

4.L.2.d. Contact Seam Welding of Pipe and Tubing

The HF contact welding process provides another means of welding continuous seams in pipe and tubing. The process essentially is the same as that described above for induction welding and is illustrated in Figure 4.L-9. The major difference is that sliding contacts are placed on the tube adjacent to the unwelded edges at the vee length. With the contact process, the vee length generally is shorter than that used with the induction process. This is because the contact tips normally can be placed within the confines of the forge rolls where the induction coil must be placed sufficiently behind the forge rolls, so that the forge rolls are not inductively heated by the magnetic field of the induction coil. Because of the shorter vee lengths achievable with the contact process, an impeder often is not necessary, particularly for large-diameter tubes where the impedance of the current path inside the tube has significant inductive reactance.



Note: Vee length extends from point of welding to sliding contacts.

Figure 4.L-9: Joining a tube seam with HFRW using sliding contacts.

An impeder, which is made from a magnetic material such as ferrite, generally is required to be placed inside the tube. The impeder is positioned so that it extends about 1.5 to 3 mm (1/16 to 1/8 in.) beyond the apex of the vee and the equivalent of one to two workpiece diameters upstream of the induction coil. The purpose of the impeder is to increase the inductive reactance of the current path around the inside wall of the workpiece. This reduces the current that would otherwise flow around the inside of the tube and cause an unacceptable loss of efficiency. The impeder also decreases the magnetic path length between the induction coil and the tube, further improving the efficiency of power transfer to the weld point. The impeder must be cooled to prevent its temperature from rising above its Curie temperature, where it becomes nonmagnetic. For ferrite, the Curie temperature typically is between 170 and 340°C (340 and 650°F).^{A-11, A-15}

4.L.3. HF Induction Welding Procedures

As discussed earlier, HFIW is the main welding technology for manufacturing cold-formed welded steel tubes. Welded tubes are normally made from flat sheet material by continuous roll forming and the HFIW process. The tubes are widely used for automotive applications, including seat structures, cross members, side-impact structures, bumpers, subframes, trailing arms, and twist beams. A welded tube can be viewed as a sheet of steel having the shape of a closed cross section.

Two features distinguish the welded tube from the original sheet material:

1. The work hardening which takes place during the tube-forming process.
2. The properties and metallurgy of the weld seam differ from those of the BM in the tubular cross section.

Good weldability is one precondition for successful HF welding. Most DP steels are applicable as feed material for manufacturing of AHSS tubes by continuous roll forming and the HFIW process. The quality and the characteristics of the weld depend on the actual steel sheet characteristics (such as chemistry, microstructure, and strength) and the set-up of the tube manufacturing process. Table 4.L-1 provides some characteristics of the HF welds in tubes made of DP 280/600 steel.

For DP 280/600 the hardness of the weld area exceeds the hardness of the BM (Figure 4.L-10). There is a limited or no soft zone in the transition from HAZ to BM. The nonexistent soft zone yields a HF weld that is stronger than the BM (Table 4.L-1). This is an essential feature in forming applications where the tube walls and weld seam are subject to transverse elongation, such as in radial expansion and in hydroforming.

Table 4.L-1: Transverse tensile test data for HFIW DP 280/600 tube.^{R-1}

Sample	YS MPa	TS MPa	Tot. EL % (in 50 mm)	Tot. EL % (in 80 mm)	Uniform EL %
Tube Transversal 1	447	697	33.3	23.6	16.1
Tube Transversal 2	446	683	34.7	24.7	16.9
Weld Transversal 1*	473	695	29.9	18.2	13.2
Weld Transversal 2*	476	687	30.4	16.9	12.9

Note: The fracture takes place outside the weld and HAZ.

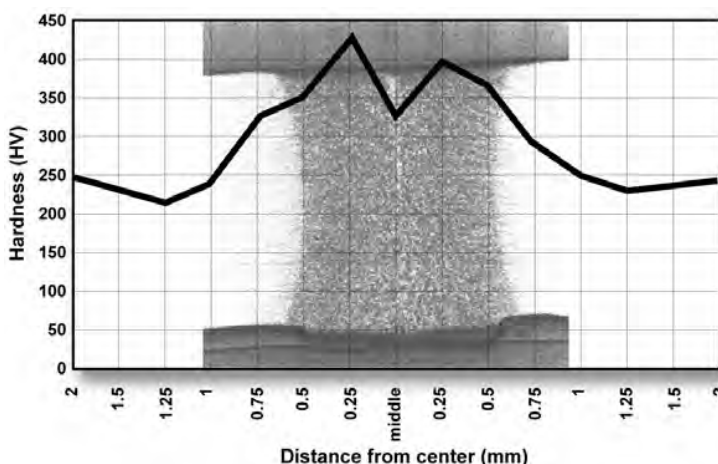


Figure 4.L-10: Weld hardness of a HF weld in a DP 280/600 tube.^{R-1}

Figures 4.L-11 and 4.L-12 contain additional examples of the hardness distribution across HF welds in different materials compared to mild steel.

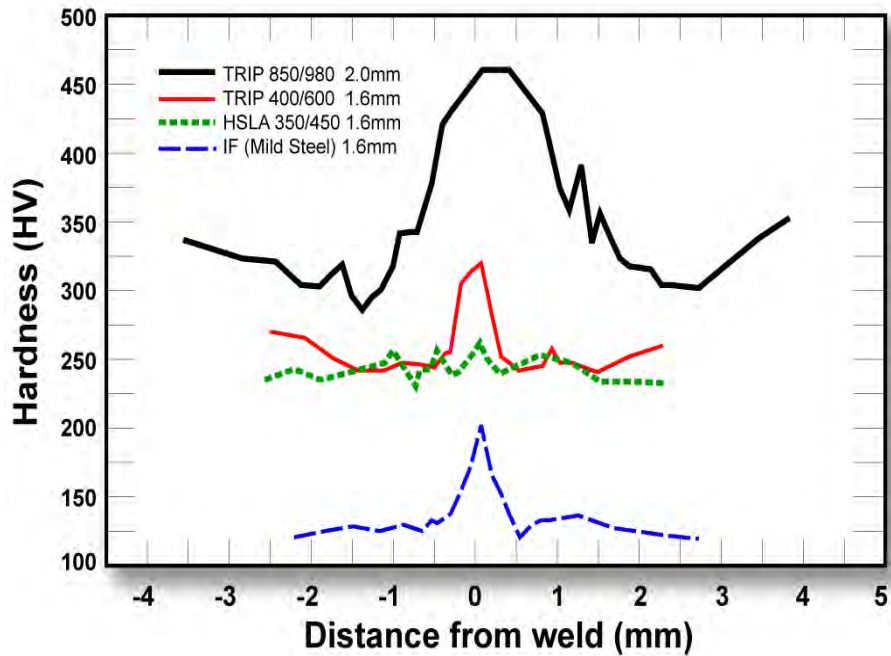


Figure 4.L-11: Hardness variation across induction welds for various types of steel.^{M-1}

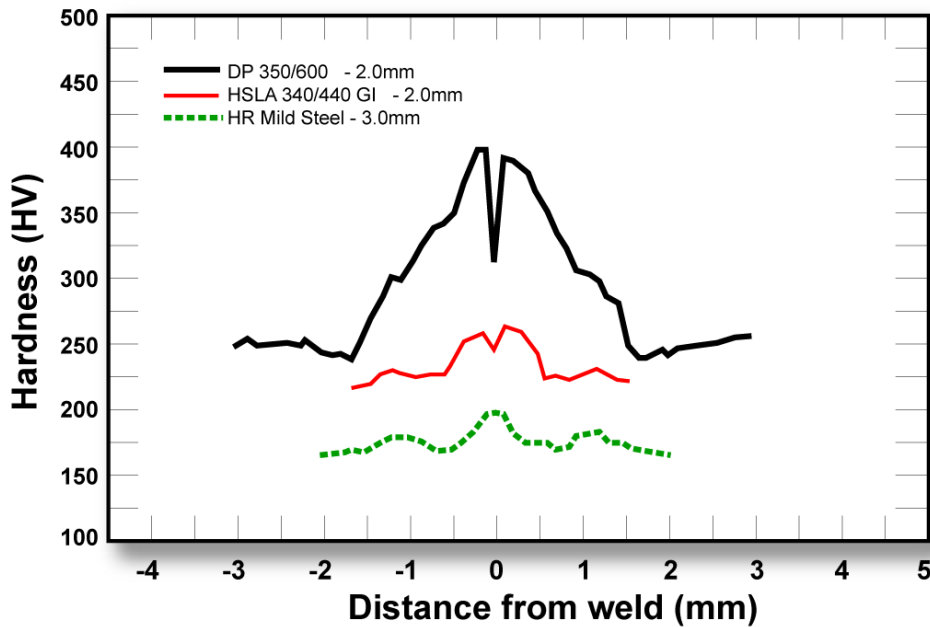


Figure 4.L-12: Hardness variation across induction welds of DP 350/600 to mild steel.^{D-1}

4.L.4. Safe Practices

The health and safety of the welding operators, maintenance personnel, and other persons in the welding operations must be considered when establishing operating practices. The design, construction, installation, operation, and maintenance of the equipment, controls, power sources, and tooling should conform to the requirements of the United States Department of Labor in *Occupational Safety and Health Standards for General Industry*, (29) CFR Part 1910, Subpart Q.1.

The HF power source must also conform to the requirements of the Federal Communication Commission (FCC) as stated in Title 47, Part 15 concerning the radio frequency emissions from industrial, scientific and medical sources. Responsibility for complying with FCC standards is undertaken by the power source manufacturer and does not pose a problem for the end user of the equipment, if the power source is installed following the manufacturer's recommendations. Information manuals provided by the manufacturers of equipment must be consulted, and recommendations for safe practices must be strictly followed. State, local, and company safety regulations also must be followed. The American Welding Society (AWS) document *Safety in Welding, Cutting, and Allied Processes*, ANSI Z49.1: 2005 covers safe practices specifically for the welding industry.

Voltages produced by HF power sources with solid-state inverter power sources (as high as 3,000 V) and voltages produced vacuum-tube oscillators (as high as 30,000 V) can be lethal. Proper care and precautions must be taken to prevent injury while working on HF generators and related control systems.

Modern power sources are equipped with safety interlocks on access doors and automatic safety grounding devices that prevent operation of the equipment when access doors are open. The equipment should never be operated with panels or high-voltage covers removed or with interlocks and grounding devices bypassed.

HF currents are more difficult to ground than low-frequency currents, and ground lines should be as short as possible to minimize inductive reactance. All leads between the power source and the contacts or induction coil should be totally enclosed in an insulated or grounded structure and constructed in a way that minimizes Electromagnetic Interference (EMI). Also, care should be taken to prevent the HF magnetic field around the coil and leads from induction heating of the adjacent metal mill components.

The weld area should be protected so that operating personnel cannot come in contact with any exposed contacts or induction coils while these devices are energized. Injuries to personnel from direct contact with HF voltages, especially at the upper range of welding frequencies, may produce severe local tissue damage.

4.M. Magnetic Pulse Welding (MPW)

MPW is a solid-state process that uses electromagnetic pressure to accelerate one workpiece to produce an impact against another workpiece. The metallic bond created by this process is similar to the bond created by explosion welding. MPW, also known as electromagnetic pulse or magnetic impact welding, is highly regarded for the capability of joining dissimilar materials.

4.M.1. Physics of the Process

Electromagnetic metal processing was developed in the late 1800s, and in succeeding years most applications for this technology were in metal forming. It was not recognized as a viable welding process, but a substantial renewal of interest has occurred recently in the further development of this technology for welding.

Fundamentally, both metal forming and welding use the same underlying physics. The process is driven by the primary circuit. A significant amount of energy, usually between 5 and 200 kJ, (1,124- and 44,962-lb force) is stored in capacitors charged to a high voltage that may range between 3,000 and 30,000 V. The capacitors are then discharged through low-inductance and highly conductive bus bars into a coil, or actuator. The resulting current takes the form of a damped sine wave, characterized as a ringing inductance-resistance-capacitance (LRC) circuit. Peak currents during this process range between tens of thousands and millions of Amperes (A), with pulse widths on the order of tens of microseconds. This creates an extremely intense transient magnetic field in the vicinity of the coil. The magnetic field induces eddy currents in any conductive materials nearby, in the opposite direction to the primary current. The opposing fields in the coil and workpiece result in a high repulsion force. This force drives the flyer, or driver, workpiece (the workpiece closest to the driving coil) at high velocity toward the target, the stationary workpiece, resulting in a high impact between the two metals.

The impact pressure drives away the surface contaminants and provides for the intimate contact of clean surfaces across the weld interface. Metallic bonding results from this contact. A schematic of the process is shown in Figure 4.M-1.

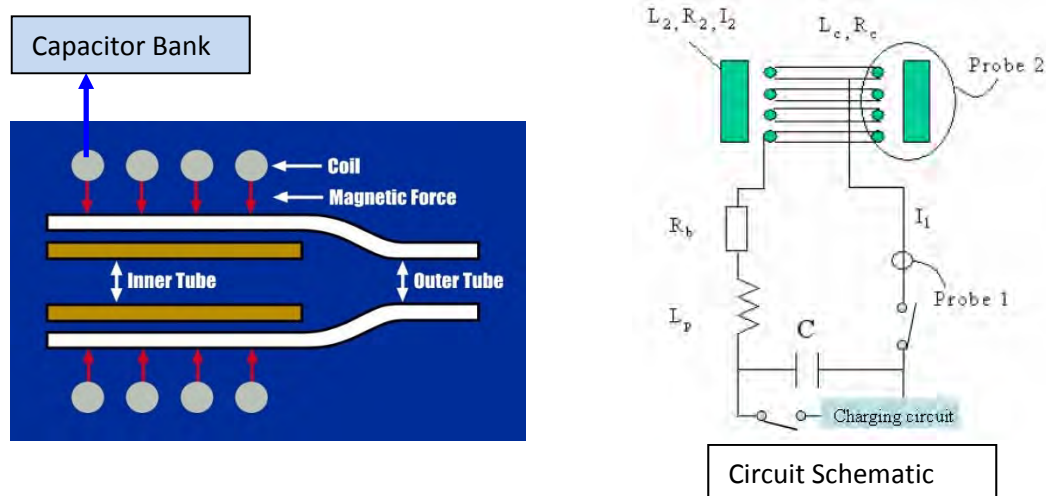


Figure 4.M-1: Basic diagram of the MPW process.

The following three elements are fundamental to achieving good magnetic pulse-welded joints:

1. Correct welding machine parameters.
2. Consideration of metal or material properties.
3. Relative positioning of the flyer and the target workpieces.

Welding machine parameters determine the frequency and magnitude of the current waveform. High frequencies typically are favored for MPW. If the frequency is too low, the buildup of eddy currents in the flier workpiece will not be sufficient to achieve the velocities necessary for impact joining. The frequency is directly related to the electrical characteristics (LRC) of the circuit, including the capacitors and coil. Low system capacitances and inductances favor HF characteristics.

The properties of the workpiece metal, particularly of the flier, also contribute to determining the weldability of a given metal. Properties to be considered include electrical conductivity and strength. Metals with high electrical conductivity and low strength are most easily welded with the magnetic pulse process. Higher electrical conductivity facilitates greater induced currents in the flier workpiece, with correspondingly greater magnetic pressures. Lower YS facilitate displacements of the flier at lower magnetic pressures, and are easier to accelerate to the required speed for welding. Carbon steel also can be welded when adjustments are made to the system power and frequency. Metals with relatively low electrical conductivity, such as austenitic stainless steels, are almost impossible to directly weld with the magnetic pulse process. They are readily welded, however, with the use of a driver plate. The driver plate is essentially a band of conductive material (typically Cu) wrapped around the low-conductivity flier. During welding, the driver reacts with the coil, pushing the actual flier to the necessary velocities for metallic bonding.^{A-11}

4.M.2. Power Source

The essential component of a MPW system is a capacitor bank. The energy stored in the system can be determined from the size (capacitance) of the bank and the charge voltage using the following equation:

$$E = \frac{CV^2}{2} \quad (3)$$

where:

- E = Energy
- C = Capacitance
- V = Voltage

The energy is provided to the capacitors by a dedicated charging system. The capacity of the charging system largely controls the time required to charge the bank between subsequent welds. The charging circuit generally is actively cooled, allowing repeated use during production applications.

As previously mentioned, energy is transferred from the capacitors to the coil with an assembly of bus bars. Two considerations are key in the design of the bus bar assembly: it must have low inductance (in general, the majority of the system inductance should be at the coil), and low resistance contacts. When in use, the capacitors are charged relatively slowly to a predefined voltage. Once this voltage is reached, a fast-action switch is used to allow current flow to the coil. Switching typically is done using solid-state Silicon-Controlled Rectifiers (SCRs).^{A-11}

4.M.3. Tubular Structures

MPW has great potential for joining tubular structures for automotive and aerospace applications and for fluid-carrying tubes. Examples of MPW tubular applications are shown in Figure 4.M-2. The process has several advantages that can significantly reduce manufacturing costs, summarized as follows:

1. HS joints can be produced that are stronger than the BM.
2. Leak-tight welds can be made.
3. High welding speeds, in the millisecond range make the process readily adapted to automation.
4. Dissimilar metals and difficult-to-weld materials, such as 303 stainless steel, can be joined.
5. Cold processing enables immediate handling.
6. Welds are made with no HAZ and minimum distortion.
7. Post-cleaning operations and PWHTs are unnecessary.
8. The process is cost efficient because no filler metals or shielding gases are needed, and environmental costs are reduced.

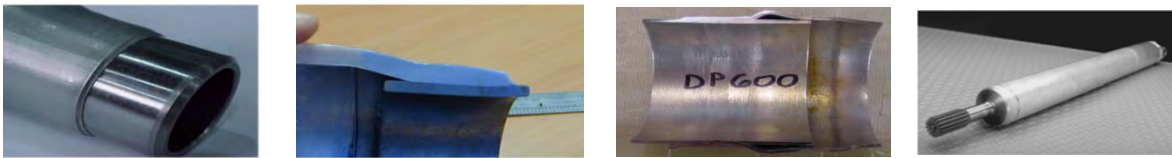


Figure 4.M-2: Examples of MPW tubular applications.

4.M.4. Applications

MPW has been successfully applied to various similar and dissimilar metal combinations. Materials with high conductivity, such as Al and Cu, are the easiest to weld with the magnetic pulse process. Al has been successfully welded to steel and stainless steel. Cu has been successfully welded to steel and stainless steel.

MPW has been used to join fuel pipes, fuel filters, exhaust system components, power cables, and for the construction of automotive body parts. The development of new applications of the MPW process continues, with the goal of advancing these applications to mass production. The process is achieving increased recognition for applications across the industrial spectrum.^{A-11}

4.M.5. Safe Practices

The potential hazards of MPW include mechanical and electrical risks, noise, flash, and fumes.

4.M.5.a. Mechanical

The welding machine should be equipped with appropriate safety devices to prevent injury to the operator's hands or other parts of the body. Initiating devices, such as push buttons or foot switches, should be arranged and guarded to prevent inadvertent actuation.

Machine guards, fixtures, and operating controls must prevent the operator from coming in contact with the coil and workpiece, and must block or deflect the weld jet associated with the process.

4.M.5.b. Electrical

All doors and access panels on machines and controls must be kept locked or interlocked to prevent access by unauthorized personnel. The interlocks should interrupt the power and discharge all the capacitors through a suitable resistive load when the panel door is open.

4.M.5.c. Personal Protection

Appropriate guards should be in place to isolate the operator from the process. Operating personnel should wear ear protection when the welding operations produce high noise levels.

Additional information on safe practices for welding is provided in the latest edition of ANSI *Safety in Welding, Cutting, and Allied Processes*, Z49.1 published by AWS. This document is available online at www.aws.org.

4.N. Brazing and Soldering

4.N.1. Fundamentals and Principles of Brazing and Soldering

Brazing and soldering are joining processes that use a filler metal that melts at temperatures below the melting temperature of the BM being joined. Because the processes do not depend on BM melting, they are not considered welding processes. Per AWS, the process is considered brazing when the filler metal melts above 450°C, and soldering when the filler metal melting temperatures are below 450°C.

Brazing and soldering both depend highly on the ability of the molten filler metal to wet and flow through the joint through capillary action. Capillary action refers to a force of attraction that can occur between a liquid and a solid. A classic approach to verifying capillary action is to dip a small-diameter tube into a liquid and observe the extent to which the liquid rises up the tube (Figure 4.N-1). If there is good capillary action, the liquid will rise quite high into the tube, seemingly defying gravity. This same concept applies to joint gaps during brazing and soldering. If good capillary action is not achieved, the joint may not be completely filled. Many factors affect capillary action, including the joint gap distance, uniformity of temperature throughout the joint, viscosity of the molten braze filler metal, cleanliness of the braze surface (affects wetting), and gravity.

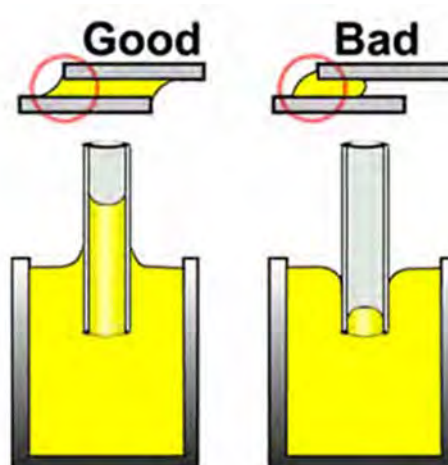


Figure 4.N-1: Approach to verifying capillary action.

One big advantage of processes that do not require BM melting is that both metals and non-metals (ceramics and composites) can be joined. Brazing is also used to join metals to non-metals. There are numerous brazing and soldering filler metals compositions available, as well as various forms including pastes and inserts. Fluxes are often used to help the capillary action through cleaning, deoxidizing, and affecting the surface tension between the liquid braze material and the material being brazed. Since joint strength is directly related to the area of the joint, the processes are most conducive to overlapping joints which allow for the creation of large joint areas. The gap used during brazing is a critical aspect to the process – gaps too large or too small will cause problems. There is a wide variety of equipment and approaches including furnaces, dip tanks (baths), induction coils, and torches. The GMAW process is also used for brazing mainly in the automotive industry, also known as MIG brazing. Laser brazing is being used in some decorative applications. The applications for brazing and soldering are diverse, and are frequently the processes of choice when welding is not a viable option.^{A-11, P-6}

In summary, the advantages and limitations of brazing and soldering are as follows:

- Advantages:
 - Ability to join non-metals and metals-to-non-metals
 - Minimal BM degradation and distortion
 - Can be relatively economical when conducted in “batch” operations

- Limitations:
 - Processes are often slow and labor intensive
 - Joint strength depends on size of joint area so joint designs are limited
 - Significant joint preparation usually required
 - Equipment can be expensive
 - BM erosion can be a problem with some brazing operations
 - Joints typically exhibit poor ductility
 - Service temperature will be limited, especially with joints that are soldered

4.N.2. Brazing Procedures

There are several brazing processes being applied in automotive manufacturing, mostly in BIW applications. These includes GMA brazing, plasma brazing and laser brazing. Designers need to consider the strength of the brazing filler material as it is usually lower in strength than the steel structure it is applied to. These various brazing processes can be used to eliminate molding, sealers, and adhesives in automotive show surfaces as their final joint appearance may be appealing. An example of this application for the General Motors (GM) Cadillac roof to body side is shown in Figure 4.N-2. Typical joint designs used for these processes include fillet and flare V-bevel groove (Figure 4.N-3). These processes can be easily automated for high-volume manufacturing.^{O-1}

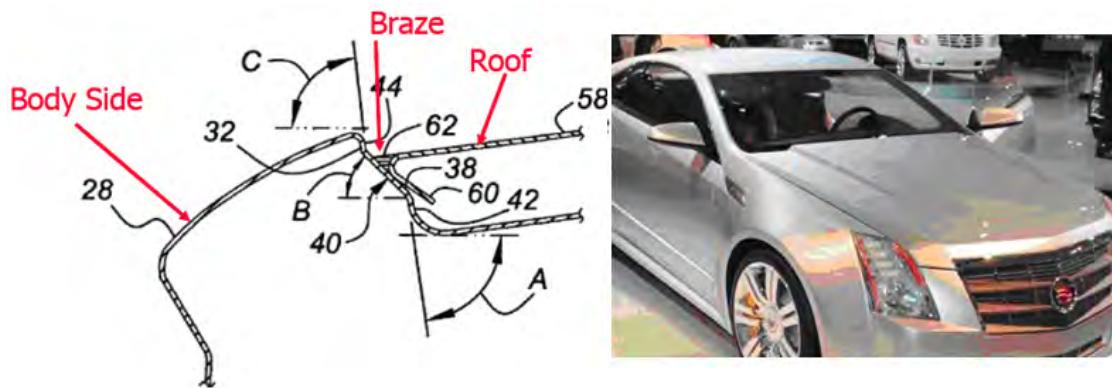


Figure 4.N-2: Laser brazing application for roof to body side in GM Cadillac.^{G-6}

Brazing can be used to join Zn-coated AHSS. Today there are many commercial grades of arc braze materials that can be used for AHSS without any additional corrosion issues. The most common braze material is SG-CuSi₃ (Table 4.N-1) mainly due to the wide melting range, which reduces the risk for imperfections during the brazing. To increase joint strength, braze materials with a higher amount of alloying elements are available at higher costs.

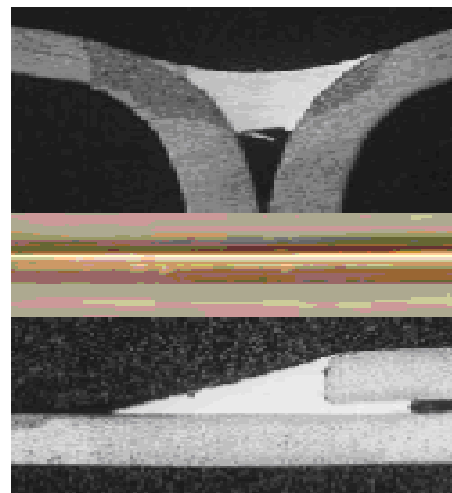


Figure 4.N-3: Fillet and flare V-bevel groove joint designs for laser brazing applications.

Table 4.N-1: Properties for the braze material SG-CuSi₃ used in brazing.^{T-3}

Braze Material	YS (MPa)	Tensile Strength (MPa)	Elongation (%)	Melting Range (°C)
SG-CuSi ₃	250	350	40	965-1035

Results from tensile-shear testing and peel testing of the braze material SG-CuSi₃ (Figure 4.N-4) show that the brazed joint strength for SG-CuSi₃ is somewhat lower than the BM, except for DP 340/600 in tensile peel condition.

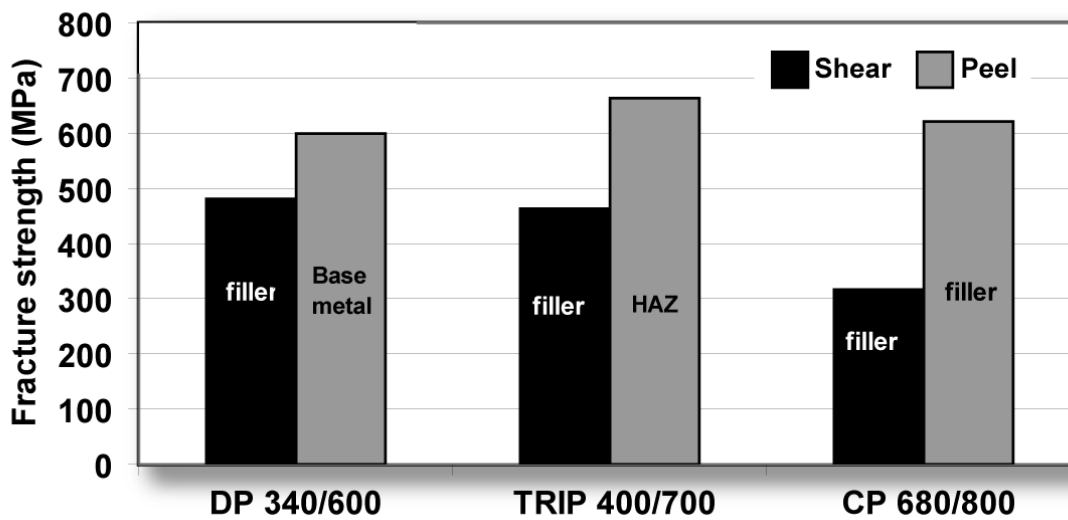


Figure 4.N-4: Tensile-shear (fillet weld on lap joint) and tensile peel tests (flange weld) for the braze material SG-CuSi₃ of DP 340/600 (1.0 mm), TRIP 400/700 (1.0 mm), and CP 680/800 (1.5 mm) (shielding gas: Ar.^{T-3}).

4.O. Adhesive Bonding

4.O.1. Fundamentals and Principles of Adhesive Bonding

Adhesive bonding is a joining process for metals and non-metals that uses an adhesive or glue, typically in the form of a liquid or a paste. It offers the major advantage of being able to join a wide array of materials, but is limited by joint strength and applicable service conditions. Many of the fundamentals are similar to brazing and soldering, in particular the need for wetting and capillary action, and overlapping joint designs that rely on joint area for strength. Adhesives are categorized as thermosetting or thermoplastic. Thermosetting adhesives require a chemical reaction to cure and cannot be remelted once cured. They are the most common adhesives for structural applications. Thermoplastic adhesives soften when heated and harden when cooled, a process that can be continually repeated. They are generally not used for structural applications because of their poor mechanical properties (in particular, creep) and decomposition that can occur at relatively low temperatures.

Surface preparation is usually a very important and time-consuming step prior to applying the adhesive, and typically includes cleaning and deoxidizing procedures. Further steps may be taken such as the application of a coating. Adhesives may be applied a variety of ways, including caulking and spray guns, dipping, rollers, and brushes. Curing may be accelerated by heating or some other energy source. In addition to joining, adhesives may be used for many other reasons including sealing, electrical insulation, and sound suppression. Some of the larger users of adhesive bonding include the automotive, appliance, and electrical/electronics industry sectors.

4.O.2. Adhesive Bonding Procedures

The bond strength of an adhesive is constant, and in design applications, is proportional to the area covered by the adhesive. The adhesive joint strength will be unchanged and analysis of the joint should be comprehensive. In general, the use of AHSS with high-strength structural adhesives will result in higher bond strength than for mild steel if the same sheet thickness is applied (Figure 4.O-1). Reduction of sheet thickness will decrease the strength because more peel load will occur. The true mechanical load in the component part must be considered. If higher joint strengths are needed, the overlapped area may be enlarged. Adhesives with even higher strength are under development.

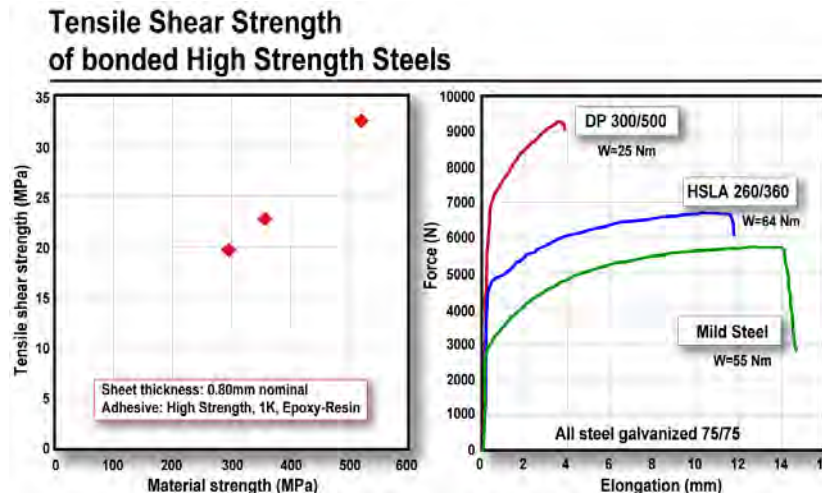


Figure 4.O-1: Effect of material strength on bond strength (W is the integral of the force/elongation curve.^{B-2}).

Joining of AHSS with adhesive bonding is a good method to improve stiffness and fatigue strength in comparison to other joining methods (spot welding, mechanical joining, arc welding, and laser welding). Due to the larger bonding area with adhesive bonding, the local stresses can be reduced and therefore the fatigue strength is increased. These improvements in stiffness and fatigue strength are important factors to consider at the design stage, especially in those cases when AHSS is used to decrease the weight of a component.

4.P. Mechanical Joining

Examples of mechanical joining in automotive manufacturing are clinching and self-piercing riveting. The process steps and typical equipment for both processes are shown in Figure 4.P-1. A simple round punch presses the materials to be joined into the die cavity. As the force continues to increase, the punch side material is forced to spread outward within the die side material.

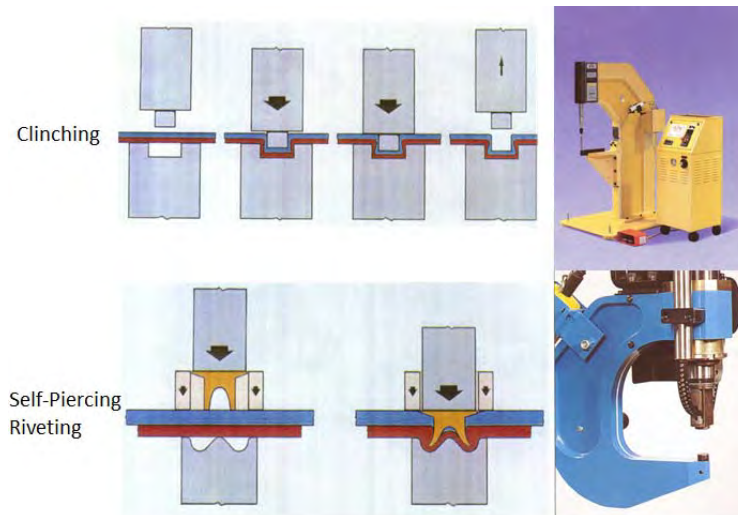


Figure 4.P-1: Process steps and equipment for mechanical joining in automotive industries.

This creates an aesthetically round button, which joins cleanly without any burrs or sharp edges that can corrode. Even with galvanized or aluminized sheet metals, the anti-corrosive properties remain intact as the protective layer flows with the material. Table 4.P-1 shows characteristics of different mechanical joining methods.

Table 4.P-1: Characteristics of mechanical joining systems.^{T-12}

Factor	Clinching	Self-Piercing Rivet	Spot Welding
Base material suitability	Most materials with reasonable ductility; harder materials use semi-piercing tooling	Most materials with reasonable ductility	Most sheet steels; Aluminium alloys more difficult
Metals coatings, e.g., zinc	Can be joined	Can be joined	More difficult for thick coatings and if passivated
Organic coatings/lubricants	Thick coatings can affect joint properties	Thick coatings can affect joint properties	Only thin, weldable coatings possible
Dissimilar metals	Possible	Possible	Metallurgical compatibility necessary; Al to steel not possible
Joint shear strength	Medium	High	High
Joint peel strength	Low	Medium	Medium
Fatigue Performance	Medium	High	Low
Cosmetic appearance	Hole one side, button on the other	Flush one side, button normally on the other	Slight indent both sides; Coatings damaged
Corrosion issues	Low susceptibility	Low susceptibility but special coatings required on steel rivets	Low susceptibility but some damage to protective coatings
Basic equipment cost	Low to medium	Medium to high	Medium to high
Consumables	None	Rivets	Electrodes
Cost per joint	Low	High	Medium
Workplace environment	Good	Good	Possible weld splash and fume

In a recent study conducted to assess the feasibility of clinch joining advanced HSS^{T-8}, it was concluded that 780-MPa DP and TRIP steels can be joined to themselves and to low-carbon steel (see Figure 4.P-2). However, 980 DP steel showed tears when placed on the die side (Figure 4.P-3). These cracks were found at the ferrite- martensite boundaries (Figure 4.P-4). However, these tears did not appear to affect the joint strength. More work is needed to improve the local formability of 980 MPa tensile strength DP steel for successful clinch joining.

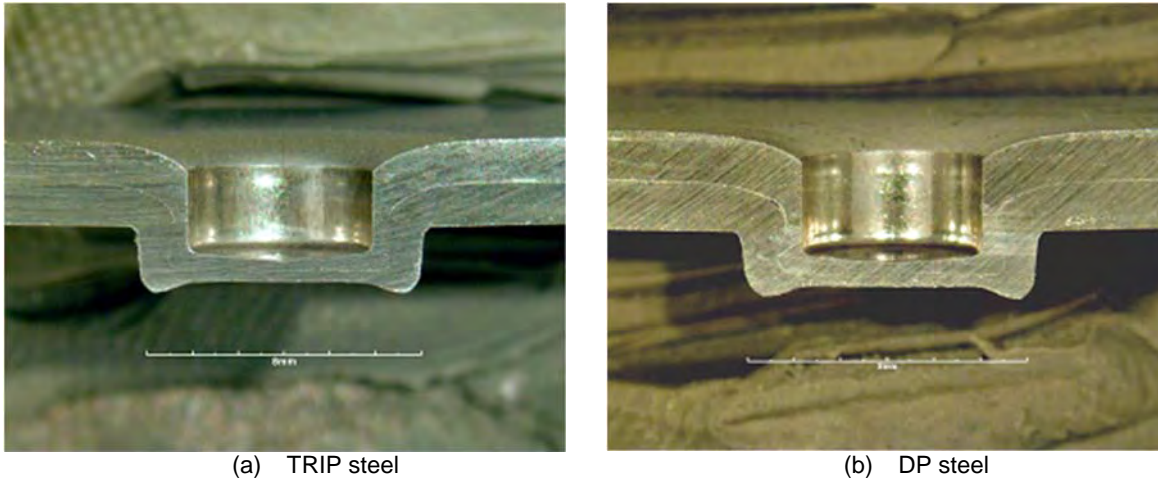


Figure 4.P-2: Cross sections of successful clinch joints in 780-MPa tensile.

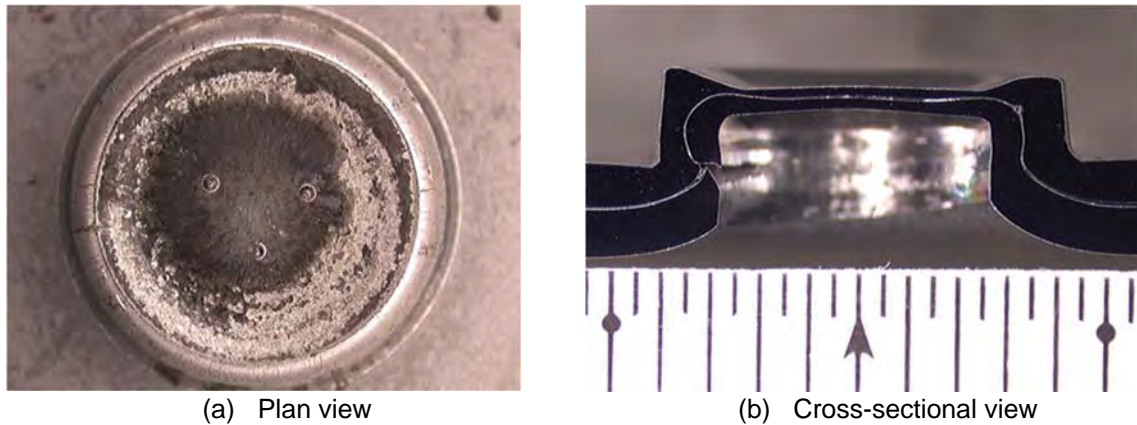


Figure 4.P-3: Clinch joint from 980-MPa tensile strength DP steel showing tears on the die side.

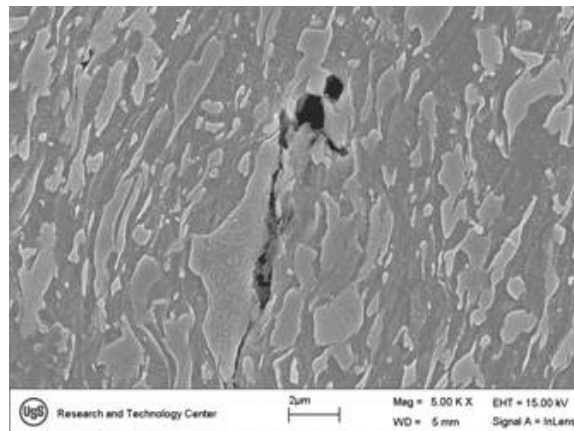


Figure 4.P-4: SEM views of tears found in 980-MPa tensile strength DP steel clinch joints.

Circular clinching without cutting and self-piercing riveting (existing half-hollow-rivets) are not recommended for materials with less than 40% hole expansion ratio (λ) as shown in Figure 4.P-5. Clinching with partial cutting may be applied instead.

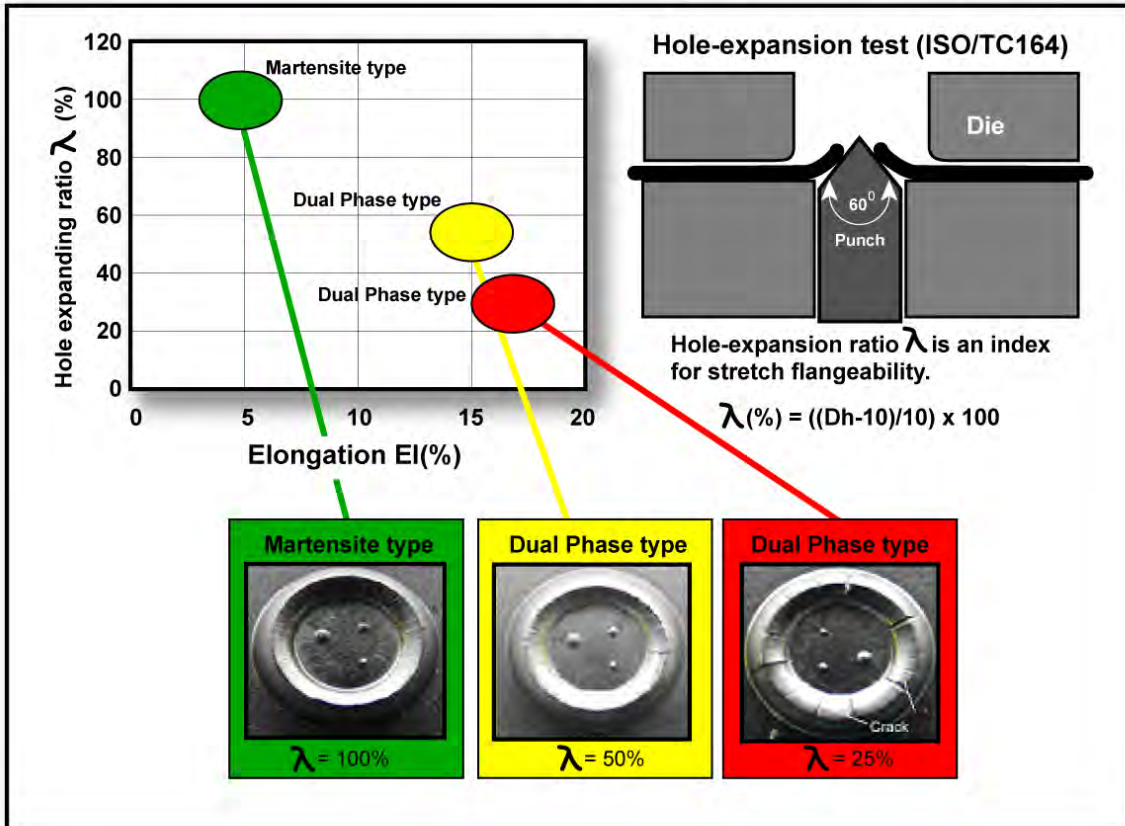


Figure 4.P-5: Balance between elongation and stretch flangeability of 980-MPa tensile-strength class AHSS and surface appearance of mechanical joint at the back side.^{N-1}

Warm clinching and riveting are under investigation for material with less than 12T total elongation. As with any steel, equipment size and clinch/pierce force are proportional to the material strength and tool life is inversely proportional to material strength.

The strength of self-piercing riveted AHSS is higher than for mild steels. Figure 4.P-6 shows an example of a self-piercing rivet joining two sheets of 1.5-mm-thick DP 300/500. AHSS with tensile strengths greater than 900 MPa cannot be self-piercing riveted by conventional methods today.

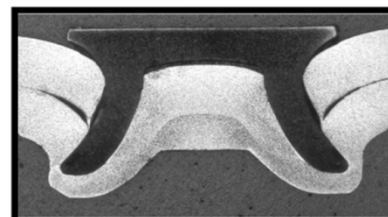


Figure 4.P-6: Example of DP 300/500 with a self-piercing rivet.^{G-2}

Self-piercing rivet joints are typically similar or slightly weaker in strength when compared to spot welds. It is largely dependent on the punch-die size, design, and rivet size. However, self-piercing rivets usually perform better in fatigue loading compared to spot welds because there is no notch effect such as what exists in spot-welded joints [Figure 4.P-7 (left)]. Although clinch joining is being used in several automotive applications, their performance is lower as shown in Figure 4.P-7 (right). Thus, they are not recommended for critical joints in automotive manufacturing.

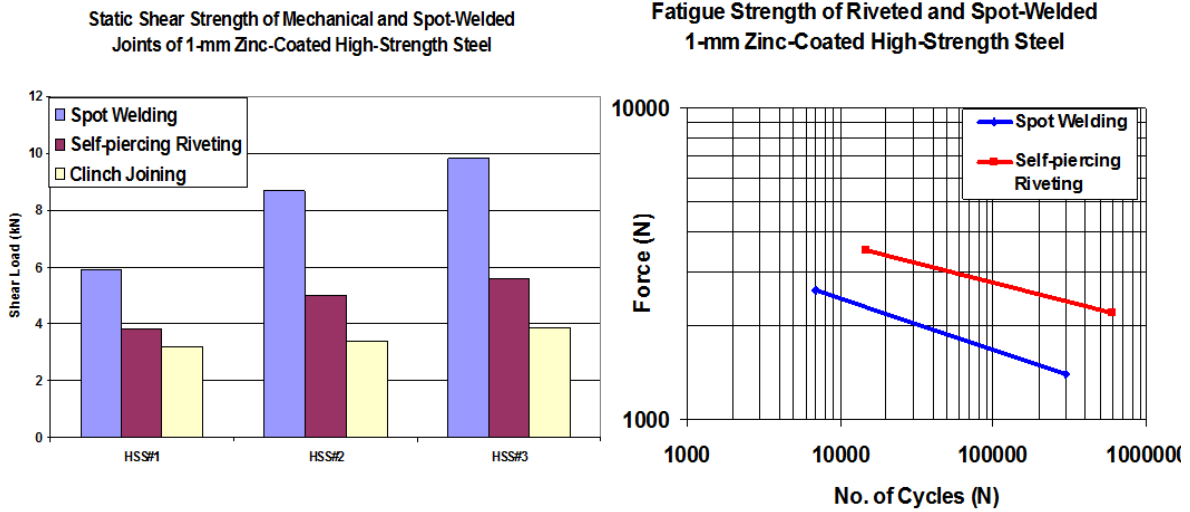


Figure 4.P-7: Strength performance for various mechanical joining methods

Self-piercing rivets can also be combined with adhesives to result in increased initial stiffness, YS, failure loads and fatigue strength when compared to spot welds using adhesives (Figure 4.P-8).

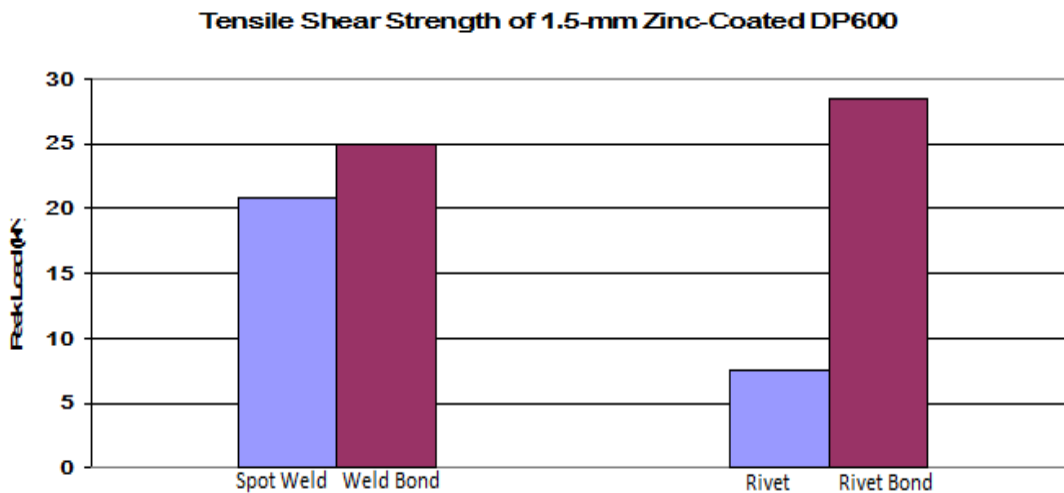


Figure 4.P-8: Tensile shear strength of SPR with adhesives and RSW with adhesives.

4.Q. Material Issues for Field Weld Repair and Replacement

The American Iron and Steel Institute (AISI), in cooperation with North American Original Equipment Manufacturers (OEMs), has undertaken studies to understand the influences of “in field” repair practices on some AHSS.^{A-5} Studies have been completed for DP, MS, and TRIP steels. In particular, the effects of GMAW and a practice called “flame straightening” were examined.

Test results indicate that GMA welding is acceptable as a repair method for AHSS - including DP, MS, and TRIP. Mechanical properties were within the expected range for each material in close proximity to the repair weld and, therefore, were considered acceptable.

Flame straightening consists of heating a portion of the body or frame structure that has been deformed in a collision to 650°C (dull cherry red) for 90 s and then pulling the deformed portion of the structure to its original position. This heating cycle then could be applied twice. Test results indicated that “flame straightening” should NOT be used to repair AHSS such as DP, MS, and TRIP. The heating cycle was found to cause degradation of the mechanical properties of as-formed (work-hardened) body parts.

Therefore, repair of AHSS parts using GMAW in the field may be acceptable. In any event, the OEM's specific recommendations for the material and vehicle should be followed.

4.R. Joint Performance In-Use

In static or in dynamic conditions, the spot weld strength of UHSS may be considered as a limiting factor. The stress concentration at the localized spot weld (Figure 4.R-1) may induce fracture of the joint, directly impacting the behavior of the module. Figure 4.R-1 shows a simulation of the predicted Von Mises stress distribution in a cross-tension test sample that was subjected to a load of 450 N. Figure 4.R-2 includes the dynamic cross-tension test results for 1.2 mm DP 780 and DP 980 steels. For this example, FBF pull-out fractures occurred at all weld sizes in both the grades. Figure 4.R-3 is a photograph of a lightweight front end crash-tested vehicle. A side view of the passenger side of the vehicle is shown in the left photograph. A close up of the area outlined in the left photo shows typical buckling of panels in between spot welds (shown by arrows).

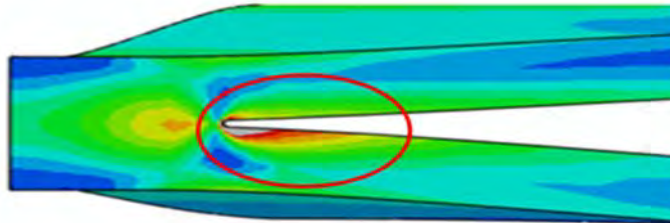


Figure 4.R-1: Example of model-predicted von Mises stress distribution in a cross-tension test sample subjected to a 450 N load.^{U-3}

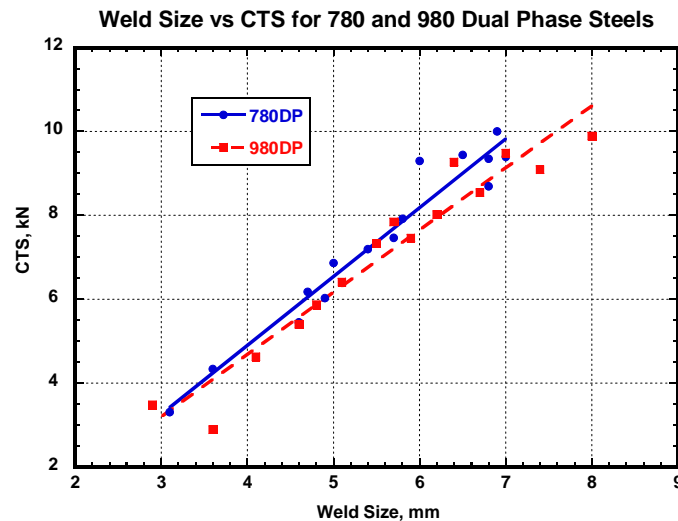


Figure 4.R-2: Cross-tension test results for 1.2-mm DP 780 and DP 980 steels.^{U-3}

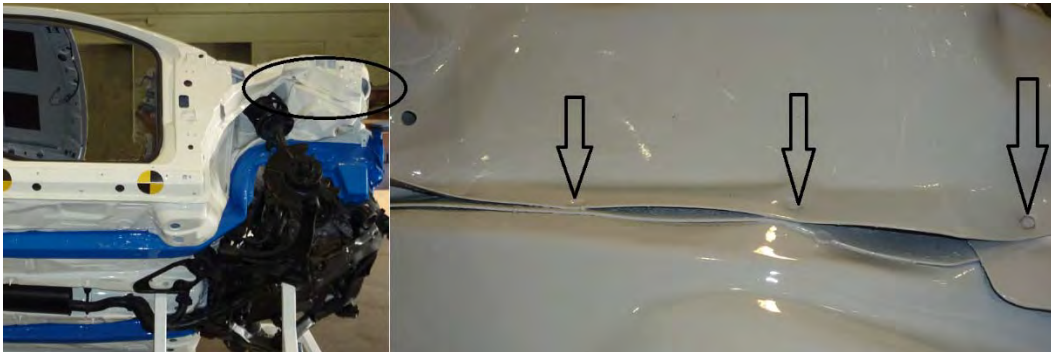


Figure 4.R-3: Photograph of a lightweight front-end crash-tested vehicle.^{U-3}

A solution to improve the spot weld strength is to add a HS adhesive to the weld. Figure 4.R-4 illustrates the strength improvement obtained in static conditions when crash adhesive (Betamate 1496 from Dow Automotive) is added. The trials are performed with 45-mm-wide and 16-mm adhesive bead samples.

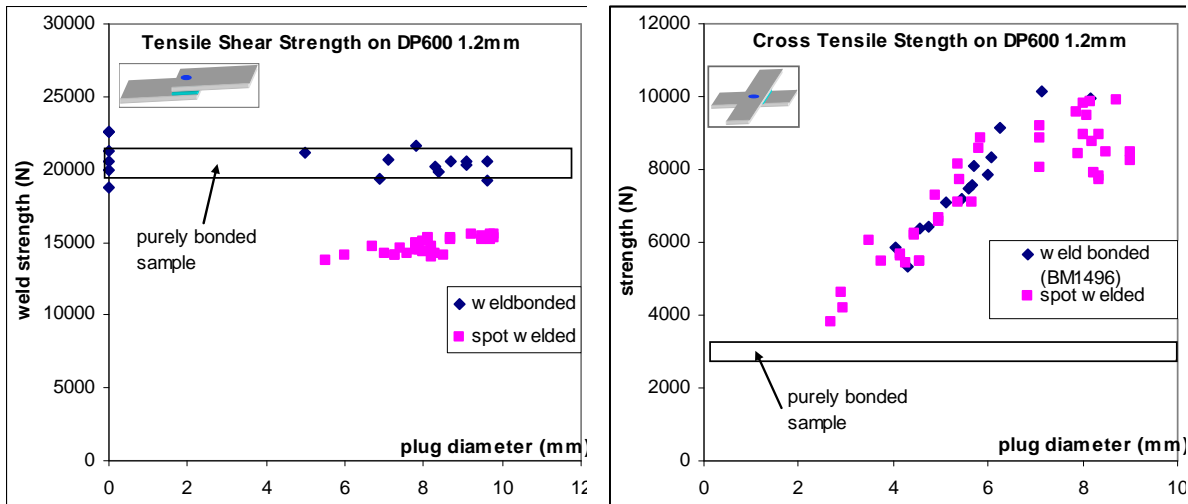


Figure 4.R-4: TSS and CTS on DP 600. A-16

Another approach to improve the strength of welds is done by using laser welding instead of spot welding. The technologies based on remote welding optics have been introduced and a high productivity can be obtained. The effective welding time is maximized and a wide variety of weld geometries becomes feasible. Compared to spot welding, the main advantage of laser welding, regarding mechanical properties of the joint, is the possibility to adjust the weld dimension to the requirement. One may assume that, in tensile shear conditions, the weld strength depends linearly of the weld length (Figure 4.R-5).

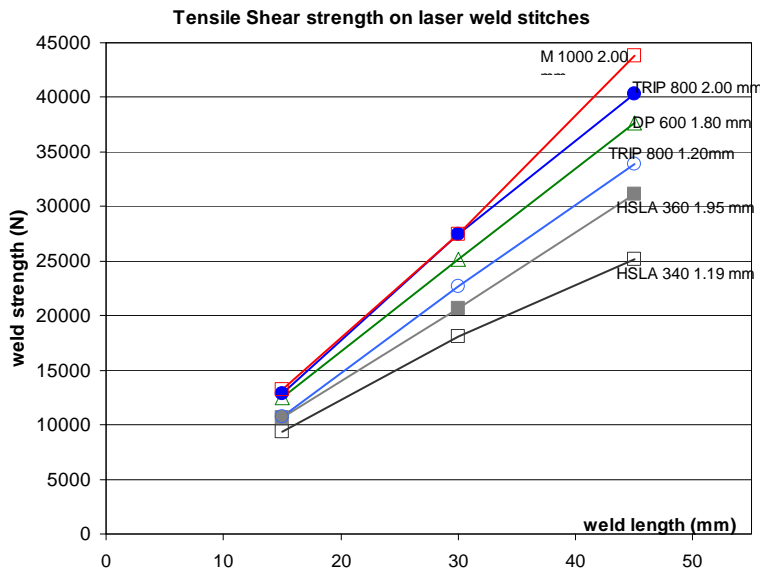


Figure 4.R-5: Tensile-shear strength on laser weld stitches of different length. A-16

Comparing spot weld strength with laser weld strength cannot be restricted to the basic tensile shear test. Tests were performed to evaluate the weld strength in both quasi-static and dynamic conditions under different solicitations, on various UHSS combinations. The trials were performed on a high-speed testing machine, at 5 mm/min for the quasi-static tests and 0.5 m/s for the dynamic tests (pure shear, pure tear or mixed solicitation) (Figure 4.R-6). The strength at failure and the energy absorbed during the trial have been measured. It should be noticed that the energy absorbed depends also on the deformation of the sample. However, as all the trials were made according to the same sample geometry, the comparison of the results is relevant. Laser stitches were done with a 27-mm length. C- and S-shape welds were performed with the same overall weld length. This leads to various apparent length and width of the welds. A shape factor, expressed as the ratio width/length of the weld, can be defined according to Table 4.R-1.

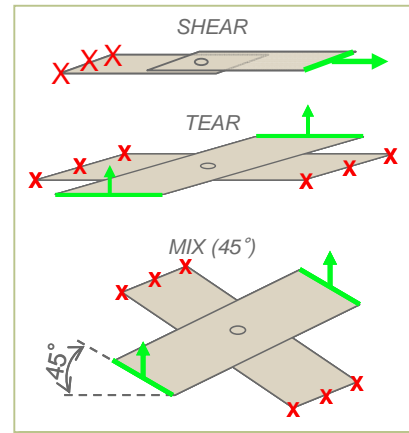



Figure 4.R-6: Sample geometry for quasi-static and dynamic tests. ^{A-16}

Table 4.R-1: Shape factor definition. ^{A-16}

	Length of Fused Zone (mm)	Shape Length l (mm)	Shape Width W (mm)	Shape Factor = w/l
Linear stitch	27	27	1	0.04
C-shape	27	16	5	0.31
S-shape	27	14.7	5	0.34

The weld strength at failure can be easily described with an elliptical representation, with major axes representing pure shear and normal solicitation (Figure 4.R.7). For a reference spot weld corresponding to the upper limit of the weldability range, globally similar weld properties can be obtained with 27-mm laser welds. The spot weld equivalent length of 25-30 mm has been confirmed on other test cases on UHSS in the 1.5- to 2-mm range thickness. It has also been noticed that the spot weld equivalent length is shorter on thin mild steel (approximately 15-20 mm). This must be considered in case of shifting from spot to laser welding on a given structure. There is no major strain rate influence on the weld strength; the same order of magnitude is obtained in quasi-static and dynamic conditions.

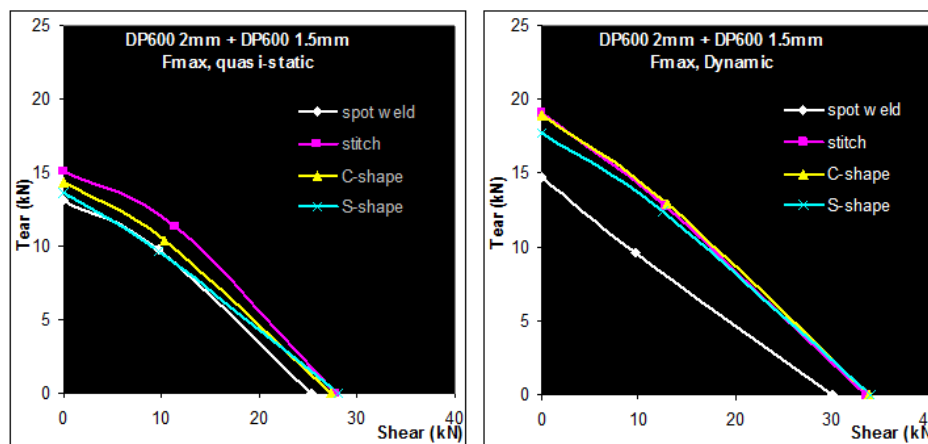


Figure 4.R-7: Quasi-static and dynamic strength of welds, DP 600 2 mm+1.5 mm. ^{A-16}

The results in terms of energy absorbed by the sample are seen in Figure 4.R-8. In tearing conditions, both the strength at fracture and energy are lower for the spot weld than for the various laser welding procedures. In shear conditions, the strength at fracture is equivalent for all the welding processes. However, the energy absorption is more favorable to spot welds. This is due to the different fracture modes of the welds. IF fracture is observed on the laser welds under shearing solicitation (Figure 4.R-9). Even if the strength at failure is as high as for the spot welds, this brutal failure mode leads to lower total energy absorption.

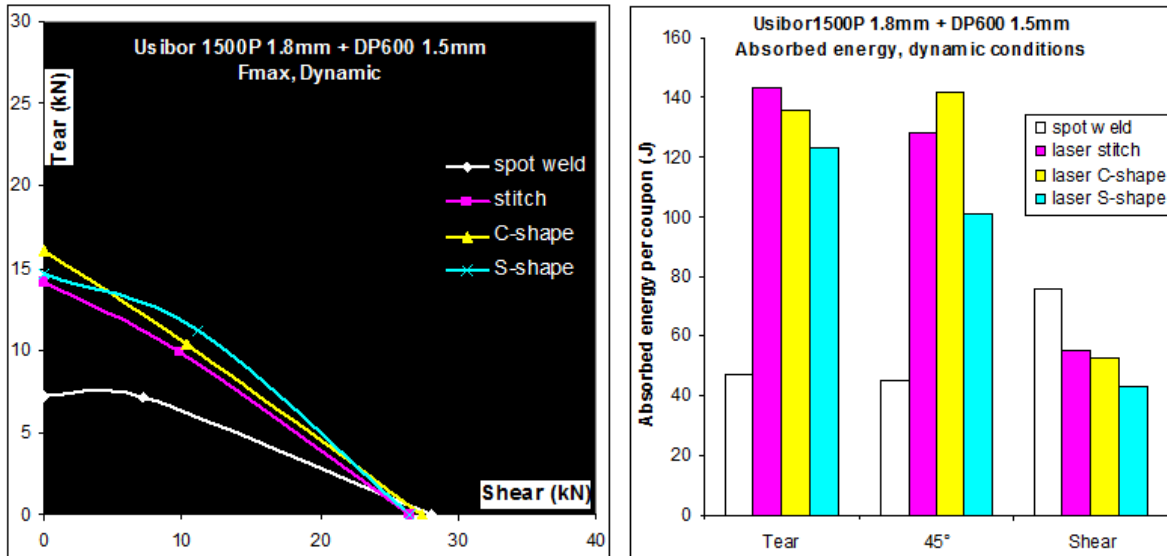


Figure 4.R-8: Strength at fracture and energy absorption of Usibor1500P 1.8-mm + DP 600 1.5-mm samples for various welding conditions. ^{A-16}



Figure 4.R-9: IF fracture mode (left), "plug-out" fracture mode (right). ^{A-16}

Figure 4.R-10 represents the energy absorbed by omega-shaped structures and the corresponding number of welds that fail during the frontal crash test (here on TRIP 800 grade). It appears clearly that laser stitches have the highest rate of fracture during the crash test (33%). In standard spot welding, some weld fractures also occur. It is known that UHSS are more prone to partial IF fracture on coupons, and some welds fail as well during the crash test. By using either Weld-Bonding or adapted laser welding shape, there is no more weld fractures during the test, even if the parts are severely crashed and deformed. As a consequence, higher energy absorption is also observed.

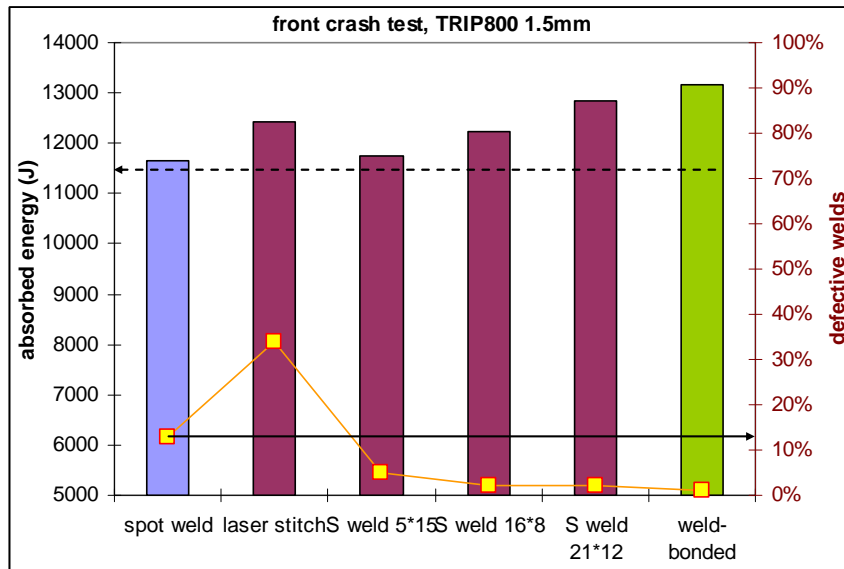


Figure 4.R-10: Welding process and weld shape influence on the energy absorption and weld integrity on frontal crash tests. ^{A-16}

Regarding stiffness, up to 20% improvement can be obtained. The best results are obtained with continuous joints, and particularly using adhesives. Adhesive bonding and weld-bonding lead to the same results of the stiffness improvement only being due to the adhesive, not to the additional welds.

Figure 4.R-11 shows the evolution of the torsional stiffness with the joining process.

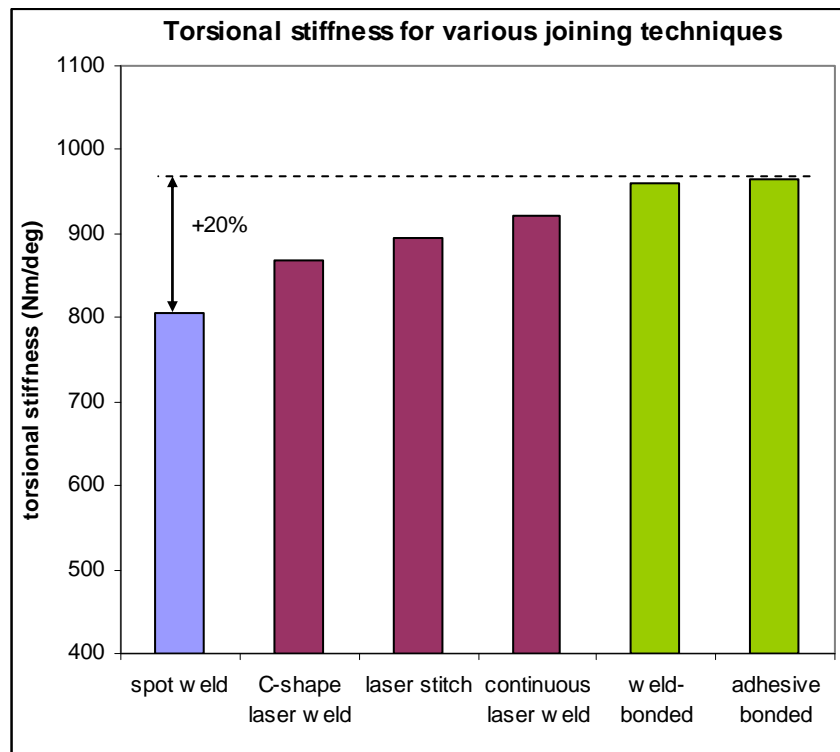


Figure 4.R-11: Evolution of the torsional stiffness with the joining process. ^{A-16}

Optimized laser joining design leads to same performances as a weld bonded sample regarding fracture modes seen in Figure 4.R-12.

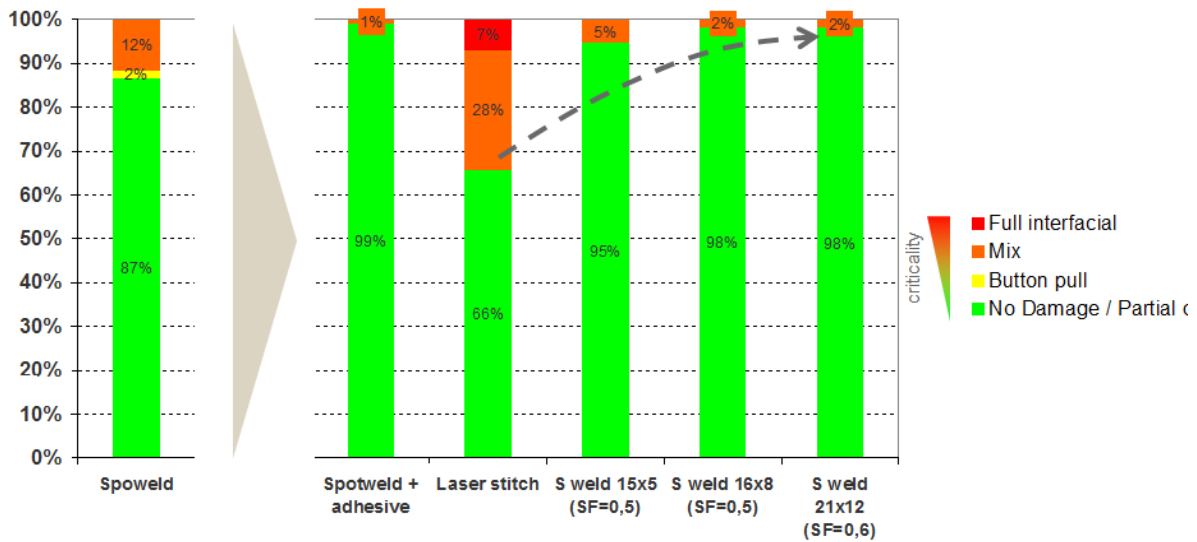


Figure 4.R-12: Validation test case 1.2-mmTRIP 800/1.2-mm hat-shaped TRIP 800.

Top-hat crash boxes were tested across a range of AHSS materials including DP 1000. The spot weld's energy absorbed increased linearly with increasing material strength. The adhesives were not suitable for crash applications as the adhesive peels open along the entire length of the joint. The welded bond samples perform much better than conventional spot welds. Across the entire range of materials there was a 20-30% increase in mean force when WB was used. The implications of such a large increase in crash performance are very significant. The results show that when a 600 MPa steel is weld bonded it can achieve the same crash performance as a 1000 MPa steel in spot-welded condition. It is also possible that some down gauging of materials could be achieved, but as the strength of the crash structure is highly dependent upon sheet thickness only small gage reductions would be possible.

Figure 4.R-13 shows the crash results for spot-welded and weld-bonded AHSS.

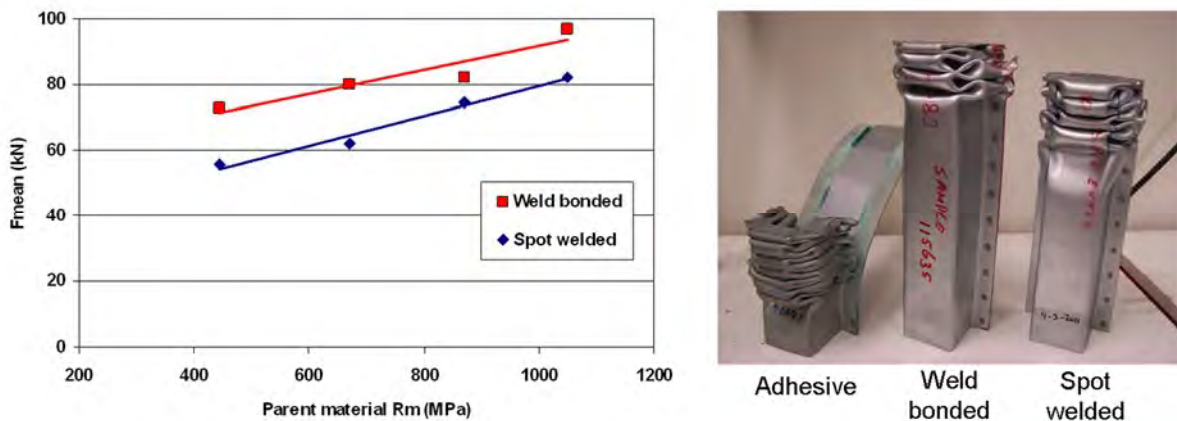


Figure 4.R-13: Crash results for spot-welded and weld-bonded AHSS.

4.S. Joint Performance Comparisons

There are numerous welding processes available for the welding of AHSS in automotive applications. Each of these processes has advantages and disadvantages that make them more or less applicable for particular applications. These qualities include joint efficiency, joint fit-up and design, joint strength, and stiffness, fracture mode, and cost effectiveness (equipment cost, production rates, etc.). The following data can allow for comparisons to be made for automotive application welding and joining processes, as well as possible repair substitutions.

Many tests were performed using lap and coach joints, reduced specimen overlap distance, and adjusted weld sizes to more closely represent typical joints consistent with automotive industry acceptance criteria. The tests were aimed at providing a baseline reference for a wide variety of welding and joining processes and material combinations. In general, there was no correlation between joint efficiency, normalized energy, and normalized stiffness. Joint efficiency was calculated by dividing the peak load of the joint by the peak load of the parent metal. Some processes, joint configurations and material combinations have high joint efficiency and energy, while others result in high joint efficiency but low energy. Few processes showed high values for all metrics across all materials and joint configurations (Figure 4.S-1). It was observed that peak loads tended to increase, on average, as material strength increased for lap joints (Figure 4.S-2). However, joint efficiency generally decreased as material strength increased. Therefore, joint strength did not increase in proportion to parent material strength increase for most of the processes and materials studied. Coach joints generally showed lower joint efficiency and stiffness than lap joints (Figure 4.S-3). Process and material combinations should be selected based on the required performance, joint design, and cost.^{A-12}

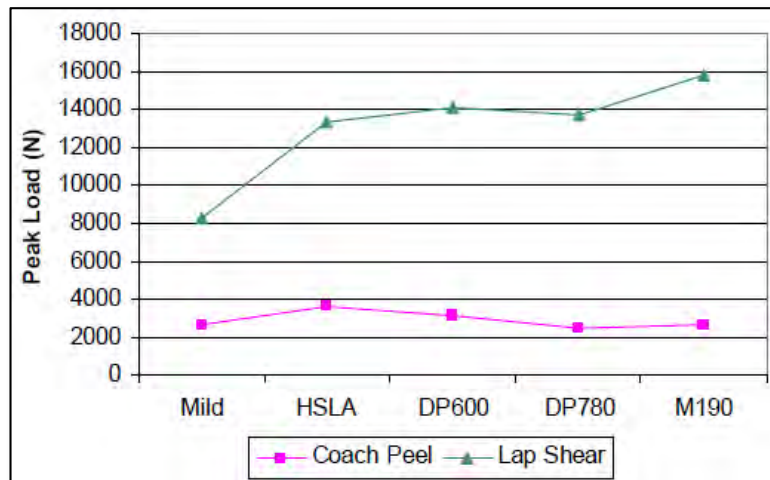


Figure 4.S-1: Average peak loads (all processes combined).^{A-12}

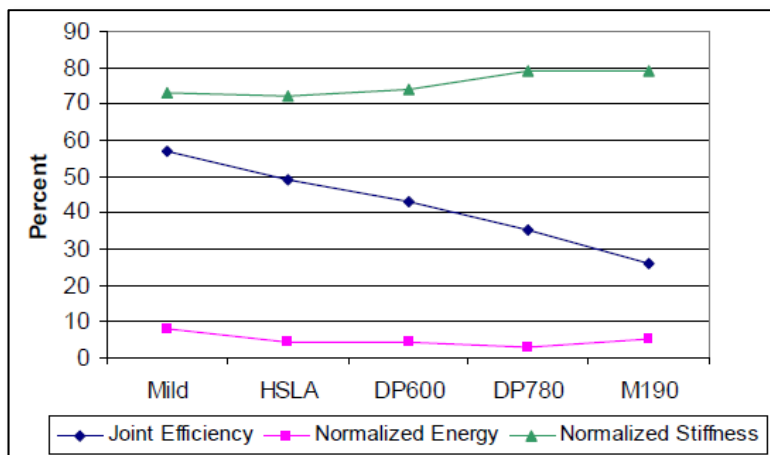


Figure 4.S-2: Lap shear average joint efficiency, normalized energy and stiffness (all processes combined).^{A-12}

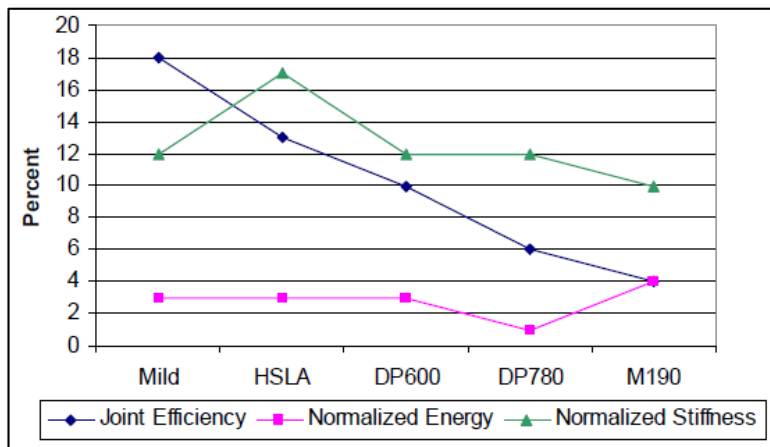


Figure 4.S-3: Coach peel average joint efficiency, normalized energy and stiffness (all processes combined).^{A-12}

4.S.1. All Processes General Comparison

Numerous tests were performed using the most popular automotive joining processes including RSW, GMAW/brazing, laser welding/brazing, mechanical fasteners, and adhesive bonding. Joint efficiency and normalized energy of all the processes were compared for HSLA steels, DP 600 samples, DP 780 samples, and M190 samples. Joint efficiency was calculated as the peak load of the joint divided by the peak load of the parent metal. Energy was calculated as the area under the load/displacement curve up to peak load.

The materials used consisted of 1.2-mm EG HSLA, 1.2-mm galvanized DP 600, 1.0-mm GA DP 780, and 1.0-mm EG M190. The testing configuration matrix (Table 4.S-1) lists the materials and process combinations studied. The tolerance of weld lengths is $\pm 10\%$. Lap-shear joints were centered in the overlap for all processes except lap fillet welds and brazes. Coach-peel joints were centered in the overlap for all processes (Figure 4.S-4).^{A-12}

Table 4.S-1: Lap-shear (left) and coach-peel (right) test configuration matrix ^{A-12}

	1.2 mm GI Mild	1.2 mm EG HSLA	1.2 mm GI DP600	1.0 mm GA DP780	1.0 mm EG M190		1.2 mm GI Mild	1.2 mm EG HSLA	1.20 mm GI DP600	1.0 mm GA DP780	1.0 mm EG M190
Parent Metal	2	2	2	2	2		0	0	0	0	0
Resistance Spot Weld (AWS D8.1M)	5	5	5	5	5		5	5	5	5	5
A/SP RSW Starting Schedule (AC)	5	5	5	5	5		5	5	5	5	5
A/SP RSW Starting Schedule (DC)	5	5	5	5	5		5	5	5	5	5
* Laser (15mm lap)	5	5	5	5	5		5	5	5	5	5
* Laser (20mm lap)	5	5	5	5	5		5	5	5	5	5
* Laser (25mm lap)	5	5	5	5	5		5	5	5	5	5
* Laser (15mm lap fillet)	5	5	5	5	5		5	5	5	5	5
* Laser (20mm lap fillet)	5	5	5	5	5		5	5	5	5	5
* Laser (25mm lap fillet)	5	5	5	5	5		5	5	5	5	5
* Laser (staple geometry)	5	5	5	5	5		5	5	5	5	5
* Laser Mig (15mm lap fillet)	5	5	5	5	5		5	5	5	5	5
* Laser Mig (20mm lap fillet)	5	5	5	5	5		5	5	5	5	5
* Laser Mig (25mm lap fillet)	5	5	5	5	5		5	5	5	5	5
* Laser Braze (15mm lap fillet)	5	5	5	5	5		5	5	5	5	5
* Laser Braze (20mm lap fillet)	5	5	5	5	5		5	5	5	5	5
* Laser Braze (25mm lap fillet)	5	5	5	5	5		5	5	5	5	5
* GMAW (AWS D8.8M - 15mm fillet)	5	5	5	5	5		5	5	5	5	5
* GMAW (AWS D8.8M - 20mm fillet)	5	5	5	5	5		5	5	5	5	5
* GMAW (AWS D8.8M - 25mm fillet)	5	5	5	5	5		5	5	5	5	5
* Manual GMAW (AWS D8.8M - 15mm fillet)	5	5	5	5	5		5	5	5	5	5
* Manual GMAW (AWS D8.8M - 20mm fillet)	5	5	5	5	5		5	5	5	5	5
* Manual GMAW (AWS D8.8M - 25mm fillet)	5	5	5	5	5		5	5	5	5	5
* Arc Braze (15mm lap fillet)	5	5	5	5	5		5	5	5	5	5
* Arc Braze (20mm lap fillet)	5	5	5	5	5		5	5	5	5	5
* Arc Braze (25mm lap fillet)	5	5	5	5	5		5	5	5	5	5
* Plasma Braze (15mm lap fillet)	5	5	5	5	5		5	5	5	5	5
* Plasma Braze (20mm lap fillet)	5	5	5	5	5		5	5	5	5	5
* Plasma Braze (25mm lap fillet)	5	5	5	5	5		5	5	5	5	5
* GMAW - Plug Weld (10mm hole)	5	5	5	5	5		5	5	5	5	5
* Arc Braze - Plug Joint (10mm hole)	5	5	5	5	5		5	5	5	5	0
* GMAW - Arc Spot	5	5	5	5	5		5	5	5	5	0
Hemlok Rivet	5	5	5	5	5		5	5	5	5	5
Self Pierce Rivet	5	5	5	5	0		5	5	5	5	0
Fracture Toughened Adhesive A	5	5	5	5	5		5	5	5	5	5
Fracture Toughened Adhesive B	5	5	5	5	5		5	5	5	5	5
Fracture Toughened Adhesive C	5	5	5	5	5		5	5	5	5	5
RSW/Adhesive A	5	5	5	5	5		5	5	5	5	5
RSW/Adhesive B	5	5	5	5	5		5	5	5	5	5
RSW/Adhesive C	5	5	5	5	5		5	5	5	5	5
SPR/Adhesive A	5	5	5	5	0		5	5	5	5	0
SPR/Adhesive B	5	5	5	5	0		5	5	5	5	0
SPR/Adhesive C	5	5	5	5	0		5	5	5	5	0

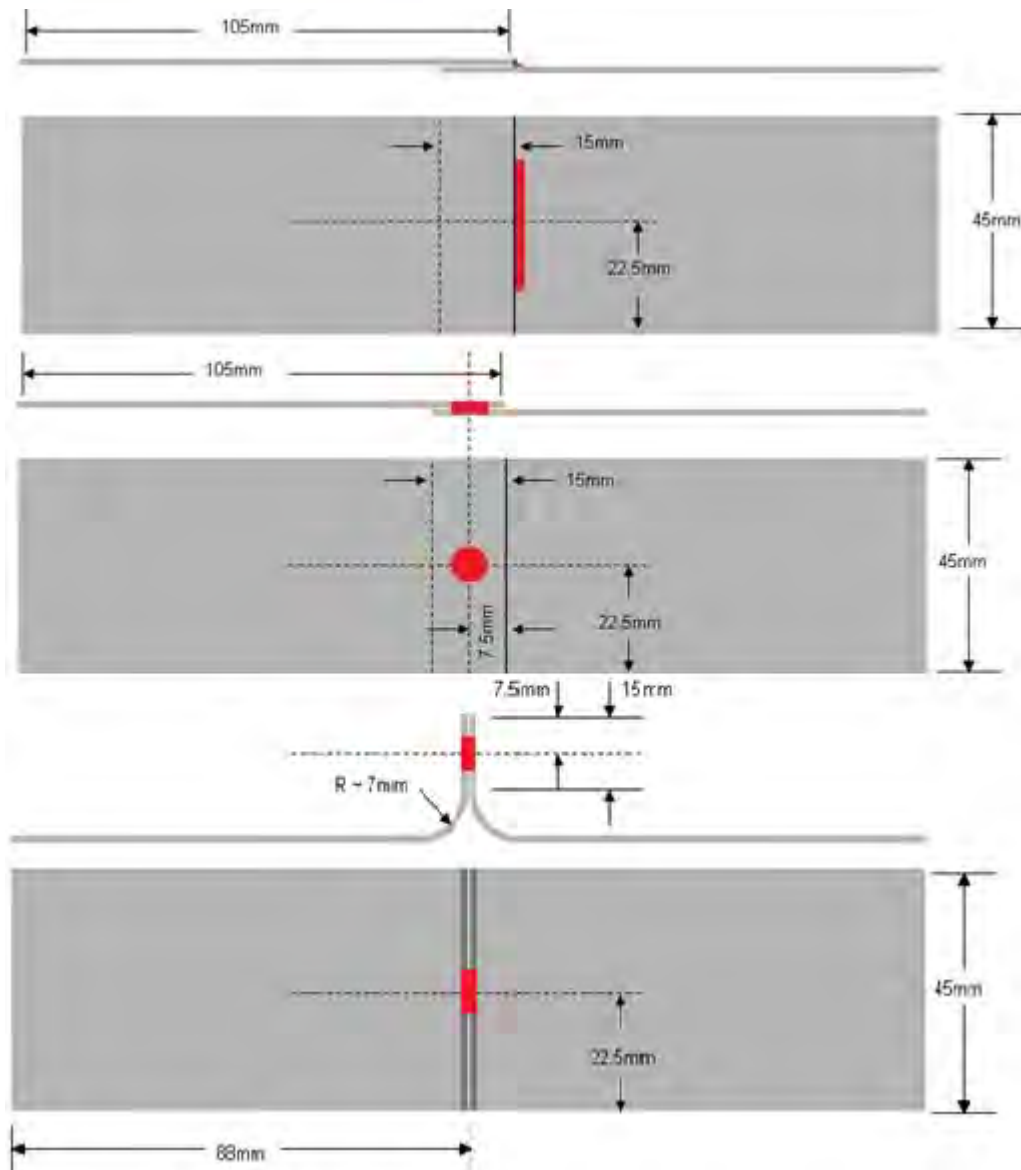


Figure 4.S-4: Lap-shear and coach-peel set-up.^{A-12}

DP 600 samples, DP 780 samples, and M190 samples. Joint efficiency was calculated as the peak load of the joint divided by the peak load of the parent metal. Energy was calculated as the area under the load/displacement curve up to peak load.

Self-piercing riveting with adhesive gave the greatest overall joint efficiency for the HSLA lap shear tests, while laser obtained the largest normalized energy (Figure 4.S-5).

Self-penetrating riveting with adhesive gave the greatest overall values for both joint efficiency and normalized energy for lap shear testing of DP 600 samples (Figure 4.S-6). However, coach peel testing of DP 600 obtained the best results with laser welding (Figure 4.S-7).



Figure 4.S-6: Joint efficiency and normalized energy of DP 600 lap shear for all processes.^{A-12}

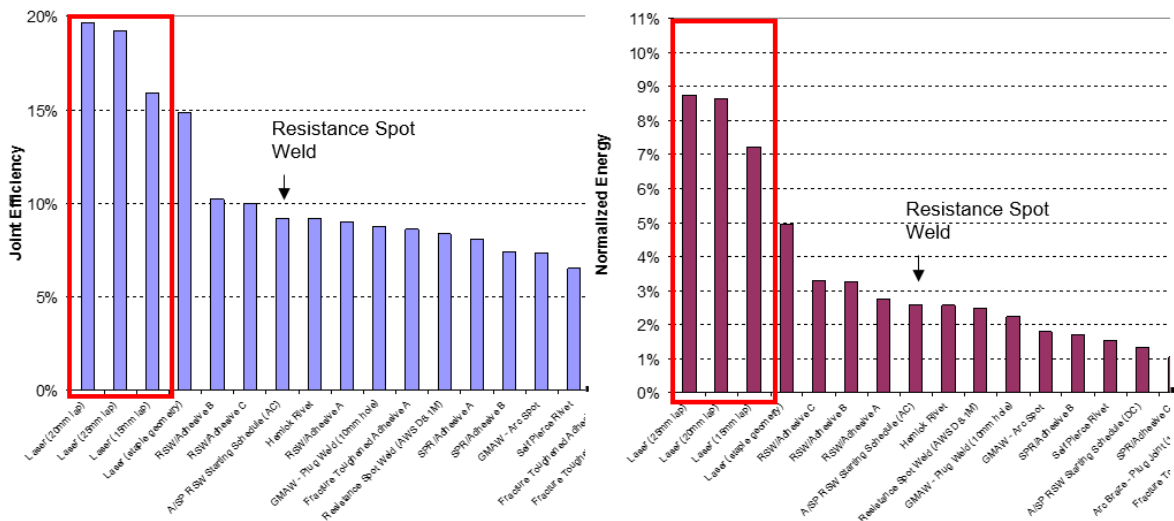


Figure 4.S-7: Joint efficiency and normalized energy of DP 600 coach peel for all processes.^{A-12}

For the DP 780 lap-shear test, the best results out of all the tested processes were from laser/MIG welding, leading in both joint efficiency and normalized energy (Figure 4.S-8). Full laser welding produced the best results for coach-peel tests of the DP 780 samples (Figure 4.S-9).

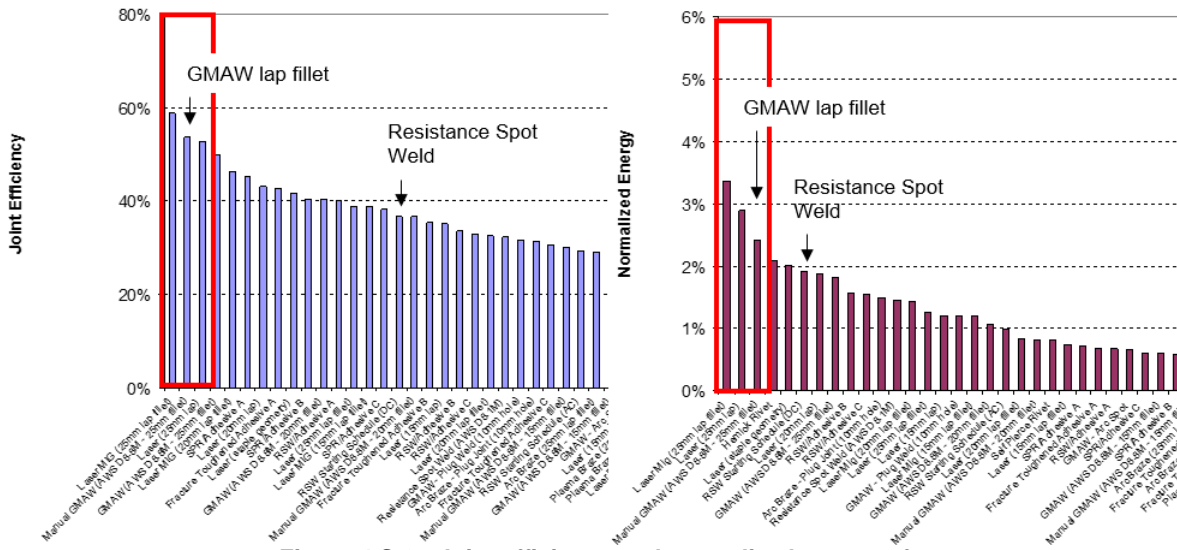


Figure 4.S-8: Joint efficiency and normalized energy of DP 780 lap shear for all processes.^{A-12}

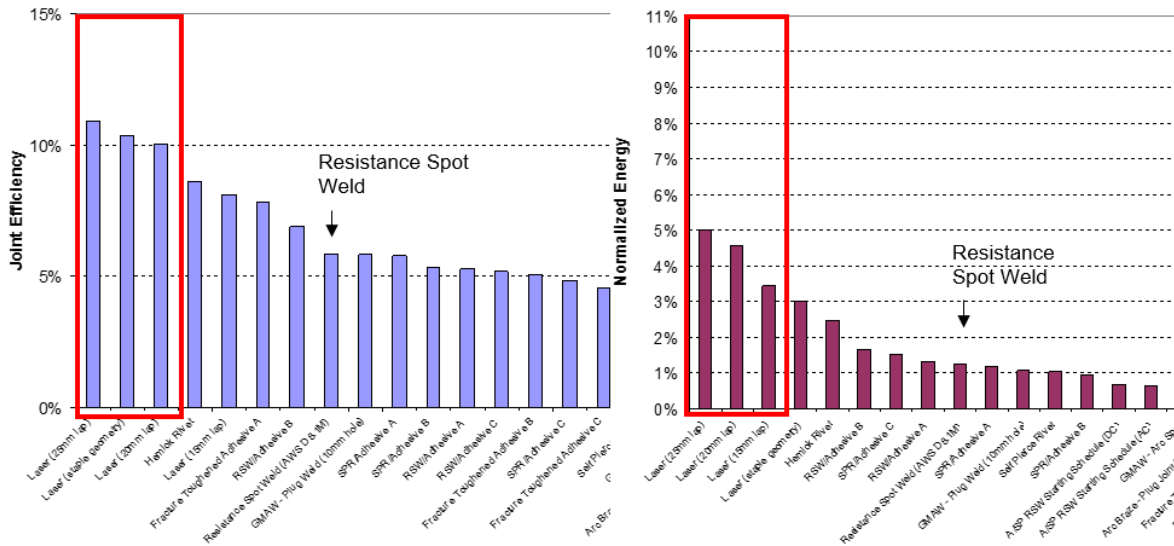


Figure 4.S-9: Joint efficiency and normalized energy of DP 780 coach peel for all processes.^{A-12}

The M190 lap-shear samples had the best joint efficiency using RSW with adhesive, but full laser welding gave better normalized energy (Figure 4.S-10). The coach peel tests also had the best normalized energy with full laser welding. The best joint efficiency of the coach peel tests was produced from laser welding with staples (Figure 4.S-11).

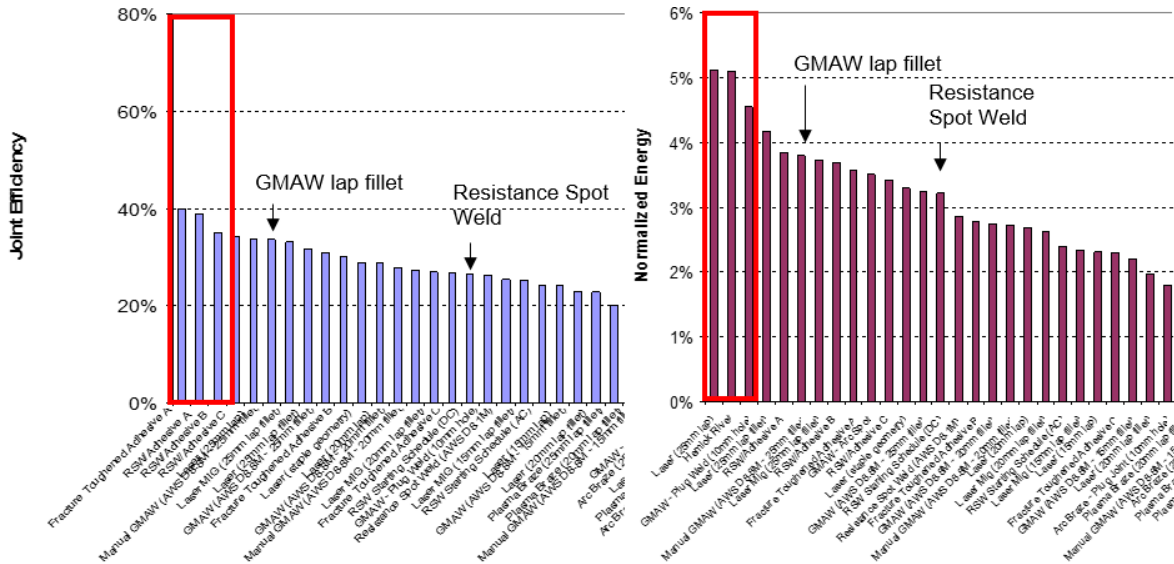


Figure 4.S-10: Joint efficiency and normalized energy of M190 lap shear for all processes.^{A-12}

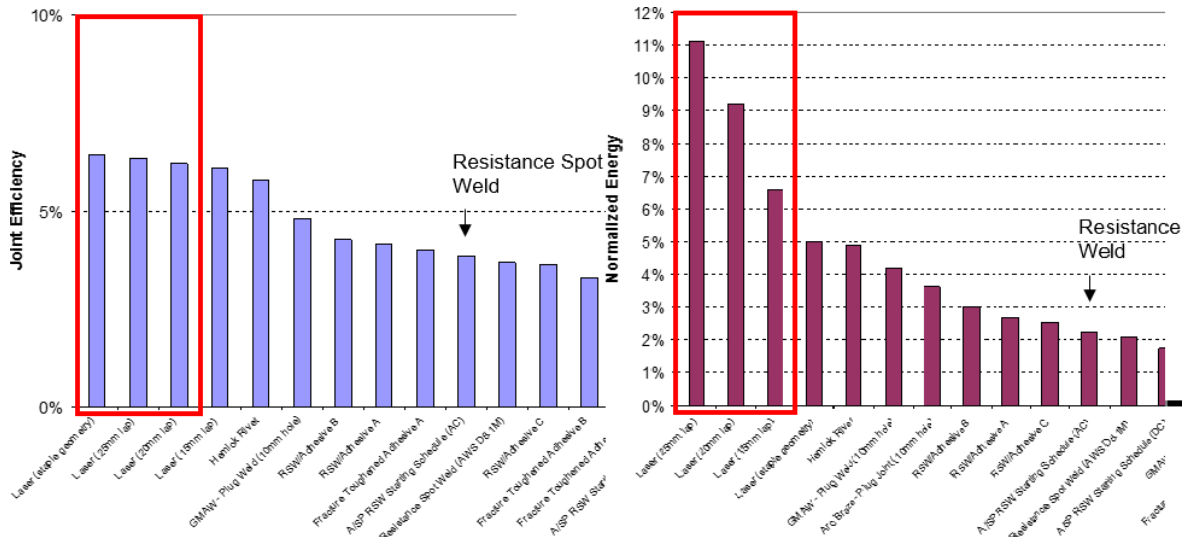


Figure 4.S-11: Joint efficiency and normalized energy of M190 coach peel for all processes.^{A-12}

4.S.2. Spot Welding Compared to Spot/Laser Welding Mixture

4.S.2.a. Cost Effectiveness

When automotive manufacturers are weighing the advantages and disadvantages of RSW to those of a spot/laser welding mixture process, cost effectiveness is a major concern. Spot/laser mixture welding has 38% lower operation cost compared to full spot welding because the laser installation performs more welds than a spot welding robot. Also, there are fewer robots to maintain and less consumables. The global cost is similar, but the spot/laser solution is about 4% less expensive overall. Figure 4.S-12 shows a cost comparison of spot welding and spot/laser welding.

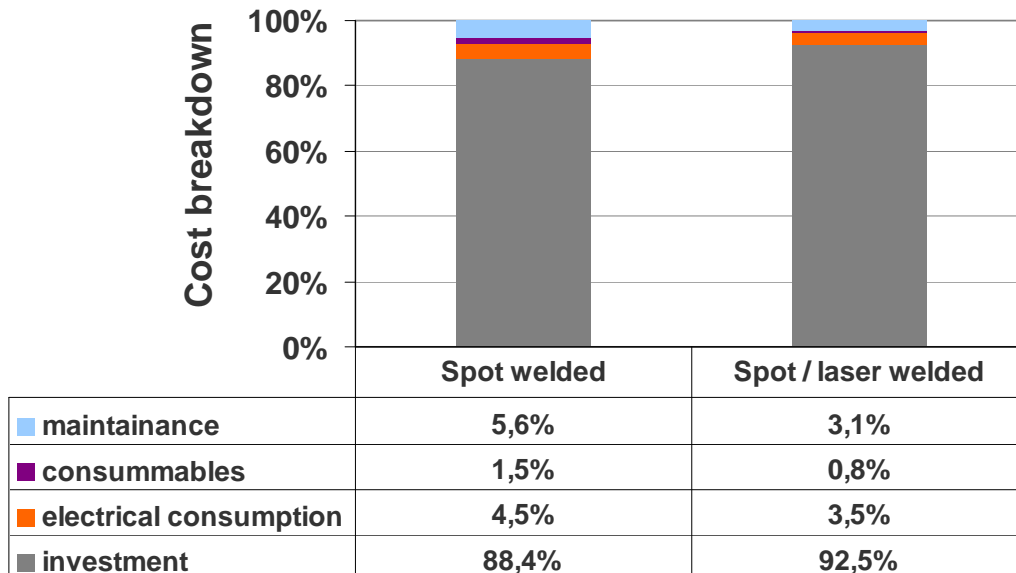


Figure 4.S-12: Cost comparison of spot welding and spot/laser welding.^{A-16}

4.S.3. GMAW Compared to Laser Welding

When comparing the advantages and disadvantages of GMAW to those of laser welding in automotive applications, joint efficiency is a key subject. Numerous welds were made using both processes on 15- and 25-mm-thick pieces of materials varying in strength. All results showed that laser welding continuously had greater joint efficiency than GMAW (Figure 4.S-13).

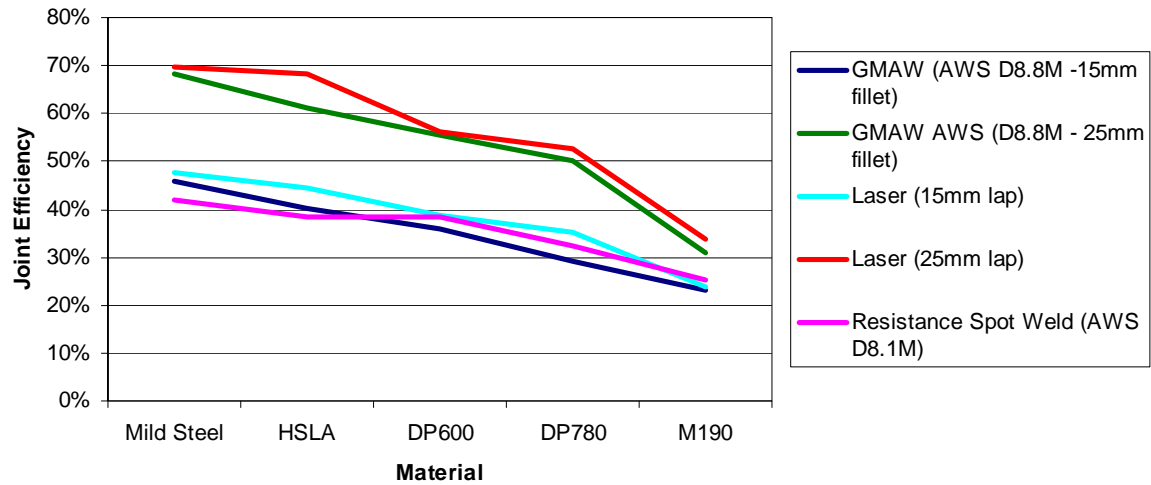


Figure 4.S-13: Joint efficiency of GMAW and laser welding for various steel strengths.

SECTION 5 – GLOSSARY

WorldAutoSteel acknowledges contributions from the AHSS Applications Guidelines Group of the Auto Steel Partnership (A/SP) in the development of this glossary.

A

AHSS (Advanced High-Strength Steel): A series of high-strength steels containing microstructural phases other than ferrite and pearlite. These other phases include martensite, bainite, retained austenite, and/or austenite in quantities sufficient to produce unique mechanical properties. Most AHSS have a multi-phase microstructure.

AKDQ (Aluminium-Killed Draw-Quality steel): A highly formable grade of mild steel that is usually aluminum deoxidized and commonly used around the world for a large number of sheet metal stampings. See Mild Steel.

Alloy: A material composed of two or more chemical elements of which at least one is an elemental metal. The resultant material combines the physical attributes of the ingredient elements.

Angular change: Springback resulting from a change in sheet metal curvature at the punch radius. The springback angle describes the resulting change in flange position.

Anisotropy: Variations in one or more physical or mechanical properties with direction.

Normal anisotropy – A condition where a property in the sheet thickness direction differs in magnitude from the same property in the plane of the sheet. The common measurement is r_m or the mean r -value of plastic strain ratios taken at 0°, 45°, 90°, and 135° to the coil rolling direction.

Planar anisotropy – A condition where a property varies with direction in the plane of the sheet. The planar variation in plastic strain ratio (Δr) indicates the tendency of the sheet metal to ear during deep drawing.

Plastic strain ratio – A measure of plastic anisotropy (r) defined by the ratio of the true width strain to the true thickness strain in a tensile test.

Austenite: A face-centered cubic crystalline phase, also known as gamma (γ). At room temperature, it is a feebly magnetic homogenous phase consisting of a solid solution of no more than 2% carbon and significant amounts of manganese and/or nickel. It has an inherently high n -value and high elongation, therefore providing improved formability over other crystalline structures of comparable strength. It is the primary phase of steel at elevated temperatures after solidification prior to cooling, but is not present in conventional steels at room temperature. With proper alloying, high temperature austenite can be rapidly quenched to produce martensite.

Retained austenite - Austenite present in the microstructure at room temperature resulting from proper chemistry and heat-treating. With sufficient subsequent cold work, this retained austenite can transform into martensite.

B

Bainite: A mixture of α -iron and very fine carbides that has a needle-like structure and is produced by transformation of austenite. Replacing the ferrite with bainite helps strengthen the steel.

Bake hardening index: The change in yield strength created in a tensile test sample given a 2% stretch and then followed by a typical automotive paint bake cycle.

BH (Bake Hardening steel): A low carbon, cold formable sheet steel that achieves an increase in strength after forming due to a combination of straining and age hardening. Increasing the temperature accelerates the aging-hardening process.

Batch (box) annealed steel: A large stationary mass of cold worked steel coils heated and slowly cooled within the surrounding furnace to return the steel microstructure to a more formable condition and desired size of undeformed grains.

Binder: The upper and lower holding surfaces that control sheet metal flow into the draw die cavity and prevent wrinkling. Often, the terms blankholder, binder ring or holddown are used.

Blank: A pre-cut sheet metal shape ready for a stamping press operation.

Developed blank - A flat sheet steel blank with a profile that produces a finished part with a minimum of trimming operations. Blank cutting dies produce this type of blank for form dies.

Rough blank - A flat sheet steel blank with a rectangular, trapezoidal, or chevron periphery. Shear lines or cutoff dies produce these blanks for draw die or stretch-form die applications.

Blankholder: The part of the draw die's binder that has pressure adjustment. Other names are binder or holddown.

Programmable blankholder - A blankholder actuated by a press or die cushion programmed to vary the pressure profile during the draw die process. AHSS stampings can often benefit from a variable cushion pressure profile during the press stroke.

Buckling: A bulge, bend, kink or other wavy condition of the workpiece caused by compressive stresses.

Burr: The rough, sharp protrusion above the surface of a stamped, pierced, or slit edge of metal which is exacerbated by worn trim steels or improper die or knife clearance. Although unavoidable in metal cutting except with fine blanking, it should be minimized due to problems it causes with edge stretching & forming, handling, and contact issues.

C

Carbide (Iron Carbide): A hard iron-carbon phase (Fe_3C) that is formed during solidification (primary carbides) or during cooling (cementite).

Carbon Equivalent: The amount of carbon, manganese, chromium, molybdenum, nitrogen and other elements that have the same effect on a steel's weldability as a steel containing carbon without these elements using various carbon equivalent prediction formulas.

CM (Carbon Manganese steel): High-strength steels with strength increased primarily by solid solution strengthening.

Clearance: 1. The space, per side, between the punch and die. Also called breakage on trim and/or pierce dies. 2. The space between any two details to avoid interference.

Clinching: Mechanical joining operation where the punch forces two sheets of metal to spread outward in the die and interlock.

Coining: A closed die squeezing operation in which all surfaces of the sheet metal are confined or restrained, resulting in a well defined imprint of the die on the workpiece. Also called bearing or hard marks.

CP (Complex Phase steel): Steel with a very fine microstructure of ferrite and higher volume fractions of hard phases and further strengthened by fine precipitates.

Computerized forming simulation: More accurately titled as computerized forming-process development, computerized die tryout, or virtual sheet metal forming. Forming the virtual stamping in the computer provides validation of product, process, and die design information before beginning construction of hard tooling. Applications include determination whether the initial product design can be formed, evaluation of various product and process design options, and acquisition of additional production requirements, such as maximum required press load and blank size/shape.

Continuous annealed steel: Steel that is unwrapped as it is pulled through a long continuous furnace and then through a cooling or quench region to recrystallize the microstructure and obtain the desired physical properties. The alternative annealing method is batch annealing. Also can be used for transformation strengthening (martensite formation).

Cup drawing: A press forming operation in which a sheet metal blank (usually circular) forms a cup shaped part (often cylindrical).

Curl (sidewall): Springback resulting from metal bending and unbending over a radius and/or drawbead. Curl is characterized by an average radius of curvature.

D

Die clearance: The gap or distance between the die surfaces as the press is in operation.

Double action press: A press with inner and outer slides to activate draw dies. Usually, the outer slide drives the blankholder and the inner slide drives the punch.

Draw bead: A small ridge of metal on the blankholder to restrain the flow of sheet steel into the die cavity.

Active draw bead - Draw beads that are separate from the binder. They are usually below the surface of the binder at the beginning of the press stroke and are mechanically lifted near the bottom of the press stroke to increase restraint of the sheet metal flow off the binder.

Square lock bead - A small, square-shaped ridge of metal on the blankholder to prevent metal flow off the binder in stretch-form dies.

Draw development: The process of developing a die-setup for the stamping (including the flange trim angles, addendum sheet metal, and binder surfaces) to design a draw die and subsequent trim die operation.

Draw die: A die in which sheet metal circumferentially compresses (minor axis) on the binder and radially elongates (major axis) when pulled off the binder and into the die cavity by the punch. Most automotive body draw die stampings will have circumferential compression located primarily in the corners of the stamping. Draw stampings for parts such as cups and cans will have circumferential compression around the entire punch line. Automotive body panel draw die processes normally require a rough blank, draw beads on the binder, and subsequent trim

die operations to remove the binder offal. The term is also used colloquially to identify the first die in a multiple stage forming process used to produce a stamped part.

Cushion draw die - A draw operation performed in a single-action press with blankholder force supplied by an air, nitrogen, or hydraulic pressure cushion.

Double action draw die - A draw die actuated by a double action press that has separate slides to drive the die punch and blankholder.

DQSK (Draw-Quality Special-Killed steel): A highly formable grade of mild steel that is usually aluminum deoxidized. Also called Aluminium-Killed Draw-Quality (AKDQ) steel. See Mild Steel.

DP (Dual Phase steel): Steel consisting of a ferrite matrix containing a hard second phase, usually islands of martensite.

Ductility: The property of a material that permits it to sustain permanent deformation in tension without rupture.

E

Elastic deformation: Deformation that will return to its original shape and dimensions upon removal of the load or stress.

Elastic limit: The maximum stress to which a material may be subjected and yet return to its original shape and dimensions upon removal of the stress.

Elastic recovery: The reaction of sheet metal to the release of elastic and residual stresses. The reaction increases as the strength of the steel increases.

Elongation: The amount of permanent plastic deformation in a tensile test or any segment of a sheet metal stamping.

Local elongation: The percent of permanent stretch deformation in a localized area over a very short gauge length. It is highly affected by the material microstructure. Local elongation is commonly measured by a conical hole expansion test and expressed as a percentage increase (λ) in hole diameter.

Total elongation - A measure of ductility obtained from a tensile test. Values are the final gage length minus original gage length divided by the original gage length and then changed to percent. Different regions of the world use different gauge lengths and specimen widths.

Uniform elongation - A measure of ductility obtained from a tensile test. Values are the gage length at maximum load (UTS) minus original gage length divided by the original gage length and then changed to percent.

Embossing: Forming or displacing a section of metal without metal flow from surrounding sheet metal.

Engineering strain: The percent unit elongation obtained by the change in length divided by the original length.

Engineering stress: The unit force obtained when dividing the applied load by the original cross-sectional area.

Erichsen test: A spherical punch test that deforms a piece of sheet metal, restrained except at the centre, until fracture occurs. The height of the cup at fracture is a measure of ductility. This test is similar to the Olsen test.

F

Ferrite (α): A body-centered cubic crystalline phase of steel. It is the microstructure of pure iron, and can have this lattice structure with up to .022%% carbon in solid solution.

FB (Ferritic-Bainitic steel): Steel with a microstructure containing ferrite and bainite. The bainite provides strength and replaces the islands of martensite in DP and TRIP steels to provide improved edge stretchability.

Filler metal: Metal added during arc welding that is available in the form of rods, spooled wire, or consumable inserts.

Formability: The ability of a material to stretch or draw without fracture.

Forming: Changing the shape of a metal piece which does not intentionally reduce the metal thickness and which produces a useful shape.

Form die: A die process capable of producing part surface contours as well as peripheral flanges. Usually, a developed blank is used which reduces or eliminates the need for subsequent trim die operations.

Draw-action form die - A form die in which an external pressure pad (similar to a binder) controls compression and buckles on flanges during the deformation process. This type of die normally utilizes a developed blank, which eliminates the need for a following trim die operation. Draw beads are not used.

Open-end form die - A die process similar to a draw die, but with little or no compression of the sheet metal due to the absence of closed corners at the ends of the stamping. A rough blank is used and a subsequent trim die operation is necessary, similar to that required for the draw die process. Draw beads often are used. Rails and channel shaped parts frequently are stamped this way.

Post-stretch form die - A form die with the sheet metal stamping locked out and stretched over the post or punch shortly before the press reaches bottom dead centre. This post-stretch reduces residual stresses that cause springback and other distortions in HSS stampings.

Stretch-form die - A die similar to a draw die with the sheet metal restrained by lock beads on the binder surface. A rough blank is used. The sheet undergoes biaxial stretch to form the part. Subsequent trim die operations are required to remove the lock beads.

FLC (Forming Limit Curve): An empirical curve showing the different combinations of biaxial strain levels beyond which failure (local necking) may occur in sheet metal forming. The strains are given in terms of major and minor strains measured from ellipses previously imprinted as circles on the undeformed sheet metal.

FRW (Friction Welding): Welding process that uses frictional heating between the parts to be welded.

FSW (Friction Stir Welding): Welding process that uses a rotating tool to generate frictional heating to mostly produce linear welds.

FSSW (Friction Stir Spot Welding): A variation of FSW to produce spot welds.

G

GMAW (Gas Metal Arc Welding): An arc welding process that uses a continuously fed consumable electrode and a shielding gas. Common GMAW processes are MIG (metal inert gas) welding and MAG (metal active gas) welding.

GTAW (Gas Tungsten Arc Welding): An arc welding process that uses tungsten electrode; sometimes referred to as TIG welding.

H

HAZ (Heat Affected Zone): The zone adjacent to the weld fusion zone where heat generated by the welding process changes base metal properties and grain size.

Heat balance: The phenomenon in resistance spot welding of balancing the heat input during the weld based on the gauge and grade of steel.

HF Welding (High Frequency Welding) or HFRW (High Frequency Resistance Welding): A resistance welding process uses high frequency current to generate continuous seam welds in tube and pipe mills.

HHE (High Hole Expansion steel): A specific customer application requirement to improve local elongation for hole expansion and stretch flanging operations. A variety of special steel types may meet these specific specifications.

HSLA (High-Strength, Low-Alloy steel): Steels that generally contain microalloying elements such as titanium, vanadium, or niobium to increase strength by grain size control, precipitation hardening, and solid solution hardening.

HSS (High-Strength steel): Any steel product with initial yield strength greater than 210 MPa or a tensile strength greater than 270 MPa.

HET (Hole expansion test): A formability test in which a tapered (usually conical) punch is forced through a punched or drilled and reamed hole forcing the metal in the periphery of the hole to expand in a stretching mode until fracture occurs.

HF (Hot-Formed steel): A quenchant steel that is heated to transform the microstructure to austenite and then immediately hot-formed and in-die quenched. Final microstructure is martensite. HF steel provides a combination of good formability, high tensile strength, and no springback issues. Most common HF steels are boron based.

Hybrid joining: Combining adhesive bonding with resistance spot welding, clinching or self-piercing rivets to increase joint strength.

I

IF (Interstitial-Free steel): Steel produced with very low amounts of interstitial elements (primarily carbon and nitrogen) with small amounts of titanium or niobium added to tie up the remaining interstitial atoms. Without free interstitial elements, these steels are very ductile and soft, will not age or bake harden, and will not form strain (Lüder's) lines during forming due to the absence of YPE (yield point elongation).

Impact Line (Marks): The line or marks on the part that is caused by impact of the flanging steel or draw ring. Its size can be controlled by the size of the radius on the flange steel or draw ring. Also called draw line.

IS (Isotropic steel): A ferritic type of microstructure modified so the Δr value is approximately zero to minimize any earing tendencies.

K

K-value: Determined from the plot of log true stress versus log true strain, K is the value of true stress at a true strain of 1.0. The K-value is an important term in the power law equation $\sigma = KE^n$.

ksi: An English unit of measure for thousands of pounds per square inch. One ksi = 6.895 MPa. MPa and ksi are units of measure for stress in materials and pressure in fluids.

L

LBW (Laser Beam Welding): a welding technique used to join multiple pieces of metal through the use of a laser. The beam provides a concentrated heat source, allowing for narrow, deep welds and high welding rates. The process is frequently used in high volume applications, such as in the automotive industry.

Locking Bead: A bead or projection designed to prevent metal flow in a forming operation (usually found in stretch-form dies).

Low Spot: A local inboard condition on a panel that results in a shallow area adjacent to strained metal. Undesirable on outer skin panels.

Limiting Draw Ratio (LDR): An expression of drawability given by the highest drawing ratio (blank diameter divided by punch diameter) without cup failure. The Swift cup test often is the required series of tests utilized to measure the LDR.

M

Major strain: Largest positive strain at a given point in the sheet surface measured from a circle grid. The major strain is the longest axis of the ellipse. The press shop term often is major stretch.

MS (Martensitic steel): A body-centered tetragonal crystalline phase of steel. It is the primary strengthening phase in Dual Phase steels and Martensitic steels are 100% martensite. It is a hard phase that can form during the quenching of steels with sufficient carbon equivalents. Martensite can also be formed by the work hardening of austenite.

MPa (Mega Pascal): A metric measure of stress in materials and pressure in fluids. One MPa = 0.145 ksi.

MAG (Metal Active Gas): See Gas Metal Arc Welding (GMAW).

Metal gainer: A preformed area of the stamping that temporarily stores surplus material which is subsequently used to feed metal into an area that normally would be highly stretched and torn. Alternatively, the term is used to describe a post-forming operation where surplus material is permanently stored in stamped shapes to prevent buckles.

MIG (Metal Inert Gas): - See Gas Metal Arc Welding (GMAW).

Microstructure: The contrast observed under a microscope when a flat ground surface is highly polished, and then thermally or chemically etched. The contrast results from the presence of grain boundaries and different phases, all of which respond differently to the etchant. A photomicrograph is a picture of the resulting microstructure.

MFDC (Mid-Frequency Direct Current): MFDC has the advantage of both unidirectional and continuous current.

Mild steel: Low strength steels with essentially a ferritic microstructure and some strengthening techniques. Drawing Quality (DQ) and Aluminium-Killed Draw-Quality (AKDQ) steels are examples and often serve as a reference base because of their widespread application and production volume. Other specifications use Drawing Steel (DS), Forming Steel (FS), and similar terms.

Minor strain: The least strain at a given point in the sheet surface and always perpendicular to the major strain. In a circle grid, the minor strain is the shortest axis of the ellipse. The press shop term often is minor stretch.

MP (Multi-phase steel): See AHSS (Advanced High Strength Steels).

MPW (Magnetic Pulse Welding): A welding process that uses high electromagnetic force to generate impact type weld.

Multiple stage forming: Forming a stamping in more than one die or one operation. Secondary forming stages can be redraw, ironing, restrike, flanging, trimming, hole expansion, and many other operations.

N

n-value: The work hardening exponent derived from the relationship between true stress and true strain. The n-value is a measure of stretchability. See work hardening exponent.

Instantaneous n-value - The n-value at any specific value of strain. For some AHSS and other steels, the n-value changes with strain. For these steels, a plot of log true stress versus log true strain allows measurement of the slope of the curve at each point of strain. These slope measurements provide the n-value as a function of strain.

Terminal n-value - The n-value at the end of uniform elongation, which is a parameter influencing the height of the forming limit curve. In the absence of an instantaneous n-value curve, the n-value between 10% elongation and ultimate tensile strength (maximum load) from a tensile test can be used as a good estimate of terminal n-value.

Necking: A highly localized reduction in one or more dimensions in a tensile test or stamping.

Diffuse necking - A localized width neck occurring in tensile test specimens that creates the maximum load identified as the ultimate tensile strength (UTS).

Local necking - A through-thickness neck that defines the forming limit curve and termination of useful forming in the remainder of the stamping. No deformation takes place along the neck. Further deformation within the local neck leads to rapid ductile fracture.

O

Overbend: Increasing the angle of bend beyond the part requirement in a forming process to compensate for springback.

Over/Undercrown: A type of springback affecting the longitudinal camber of stampings such as rails and beams.

P

Pearlite: A lamellar mixture or combination of ferrite and carbide.

Plastic deformation: The permanent deformation of a material caused by straining (stretch, draw, bend, coin, etc.) past its elastic limit.

Post-annealing: An annealing cycle given to a stamping or portion of the stamping to recrystallize the microstructure and improve the properties for additional forming operations or in-service requirements.

PFHT (Post-Formed Heat-Treatable steel): Heating and quenching formed stampings off-line in fixtures to obtain higher strengths. A broad category of steels having various chemistries is applicable for this process.

Post-stretch: A stretch process added near the end of the forming stroke to reduce sidewall curl and/or angular change resulting from the stamping process. Active lock beads, lock steps, or other blank locking methods prevent metal flow from the binder to generate a minimum of 2% additional sidewall stretch at the end of the press stroke.

Preformed Part: A partially formed part which will be subjected to one or more subsequent operations. Usually done after a blank die and prior to going into a draw die.

Press: A machine having a stationary bed or anvil and a slide (ram or hammer) which has a controlled reciprocating motion toward and away from the bed surface and at right angle to it. The slide is guided in the frame of the machine to give a definite path of motion.

Press Slide: The main reciprocating member of a press, guided in the press frame, to which the punch or upper die is fastened. Sometimes called the ram, press ram, slide, plunger, or platen.

Process capability: The variation of key dimensions of parts produced from a die process compared to the part tolerances.

Process variation: Two components make up process variation. One is the variation caused by differences in run-to-run press and die setups. The second is the part-to-part variation within the same run caused by process variables such as lubrication, cushion pressures, die temperatures, non-uniform material, etc.

Punch: The male member of a complete die. Punches are divided into three categories: 1. Cutting punches - effect cutting of the stock material, also called perforator and pierce punch. 2. Non-cutting - the act to form deform the stock material. 3. Hybrid punches - both cutting and non-cutting functions are combined in the same punch.

Punchline: The line between the draw die binder and the draw die punch in the plan view of the die drawing.

Q

Quasi-static: Traditionally the strain rate during a tensile test, which is very slow compared to deformation rates during sheet metal forming or a crash event.

R

Recoil: The distortion of a part along the flange line where the part lifts off the die steel. This is caused by insufficient pad pressure or by a pad that gives insufficient part coverage.

Redrawing: Second and following drawing operations in which the part is deepened and reduced in cross-sectional dimensions.

Residual stresses: Elastic stresses that remain in the stamping upon removal of the forming load, due to non-uniform deformation or temperature gradients from rapid cooling or welding. Residual stresses are trapped stresses because the final geometry of the stamping does not allow complete release of all elastic stresses. **Restrike die:** A secondary forming operation designed to improve part dimensional control by sharpening radii, correcting springback, or incorporation of other process features.

RSW (Resistance Spot Welding): Spot welding is a process in which contacting metal surfaces are joined by the heat obtained from resistance to electric current. Work-pieces are held together under pressure exerted by electrodes. Typically the sheets are in the 0.5 to 3 mm thickness range.

R-Value: see Anisotropy.

r_m -

Δr -

S

Scoring: A build-up of metal from a sheet metal part on the surface of a steel. Also can be worn grooves in the surface of a steel.

Servo Press: A servo press is a press machine that uses a servomotor as the drive source; the advantage of the servomotor is that it can measure both the position and speed of the output shaft, and vary these vs. having a constant cycle speed. In conventional mechanical presses, the press cycles at constant speed and press loads develop slowly, building power to their maximum force at bottom dead center (180 degree crank), and then they reverse direction. In comparison, the servo press uses software to control press speed and power, thus is much more flexible.

Sheared edge stretchability: Reduced residual stretchability of as-sheared edges due to the high concentration of cold work, work hardening, crack initiators, and pre-cracking at the sheared interface.

Shrink flanging: A bending operation in which a narrow strip at the edge of a sheet is bent down (or up) along a curved line that creates shrinking (compression) along the length of the flange.

Sidewall curl: Springback resulting from metal moving over a radius or through draw beads. Curl is characterized by an average radius of curvature.

Simulative formability tests: These tests provide very specific formability information that is significantly dependent on deformation mode, tooling geometry, lubrication conditions, and material behaviour. Examples include hemispherical dome tests, cup tests, flanging tests, and other focused areas of formability.

Single action press: A press with a single slide to activate the die.

Skid Lines: Lines seen on the finished part when the stock slips on a draw punch. This is caused by the die not being timed correctly or when the forming of a shape is at such an off angle.

SMAW (Shielded Metal Arc Welding): An arc welding process that uses coated electrodes, sometimes referred to as Stick Welding.

Solid-State Welding: Welding processes that generate a weld with no evidence of melting in the weld interface.

Spalling: The breaking off of flake - like metal particles from a metal surface.

Springback: The extent to which metal in the stamping deviates from the designed or intended shape after undergoing a forming operation. Also the angular amount a metal returns toward its former position after being bent a specified amount.

Spring-back Allowance: The allowance designed into a die for bending metal a greater amount than specified for the finished piece, to compensate for spring-back.

Strain gradient: A change in strain along a line in a stamping. Some changes can be very severe and highly localized and will have an accompanying increase in thickness strain.

Strain Hardening: The increase in strength of a metal caused by plastic deformation at temperatures which are lower than the recrystallization temperature. **Strain rate:** The amount of strain per unit of time. Used in this document to define deformation rate in tensile tests, forming operations, and crash events.

Stress Cracking: The fracturing of parts which have retained residual stresses from cold forming, heat treating, or rapid cooling.

SF (Stretch Flangeable steel): A specific customer application requirement to improve local elongation for hole expansion and stretch flanging operations. A variety of special steel types may meet these specific specifications.

Stretch flanging: A bending operation in which a narrow strip at the edge of a sheet is bent down (or up) along a curved line that creates stretching (tension) along the length of the flange.

Stress Relief (Relieving): A heat treating process which is used to reduce residual stresses in steel that have resulted from welding, carburizing or nitriding.

T

Tempering pulse: A post-weld heat treatment or post-annealing to improve the weld fracture mode and the weld current range.

TS (Tensile Strength): Also called the ultimate tensile strength (UTS). In a tensile test, the tensile strength is the maximum load divided by the original cross-sectional area.

TRIP (Transformation-Induced Plasticity steel): A steel with a microstructure of retained austenite embedded in a primary matrix of ferrite. In addition, hard phases of martensite and bainite are present in varying amounts. The retained austenite progressively transforms to martensite with increasing strain.

True strain: The unit elongation given by the change in length divided by the instantaneous gage length.

True stress: The unit force obtained from the applied load divided by the instantaneous cross-sectional area.

TWIP (Twinning-Induced Plasticity steel): A high manganese steel that is austenitic at all temperatures – especially room temperature. The twinning mode of deformation creates a very high n-value, a tensile strength in excess of 900 MPa, and a total elongation in excess of 40%.

Twist: Twist in a channel defined as two cross-sections rotating differently along their axis.

U

UTS (Ultimate Tensile Strength): See Tensile Strength.

UFG (Ultra fine grain steel): Hot-rolled, higher strength steel designed to avoid low values of blanked edge stretchability by replacing islands of martensite with an ultra-fine grain size. An array of very fine particles can provide additional strength without reduction of edge stretchability.

ULSAB-AVC (UltraLight Steel Auto Body – Advanced Vehicle Concepts): Information is available at www.worldautosteel.org.

ULSAC (UltraLight Steel Auto Closures): Information is available at www.worldautosteel.org.

W

Work hardening exponent: The exponent in the relationship $\sigma = K\epsilon^n$ where σ is the true stress, K is a constant, and ϵ is the true strain. See n-value.

Wrinkling: A wavy condition on metal parts due to buckling under compressive stresses.

Y

YS (Yield Strength): The stress at which steel exhibits a specified deviation (usually 0.2% offset) from the proportionality of stress to strain and signals the onset of plastic deformation.

SECTION 6 – REFERENCES

A

- A-1.** Body Systems Analysis Team, “Automotive Sheet Steel Stamping Process Variation,” Auto/Steel Partnership (Summer 1999) www.a-sp.org.
- A-2.** High Strength Steel (HSS) Stamping Design Manual, Auto/Steel Partnership (2000).
- A-3.** High Strength Steel (HSS) Stamping Design Manual, Auto/Steel Partnership (1997).
- A-4.** Courtesy of M. Munier, Arcelor.
- A-5.** American Iron and Steel Institute, “Advanced High-Strength Steel Reparability Studies: Phase I Final Report and Phase II Final Report,” www.autosteel.org.
- A-6.** Auto/Steel Partnership, “Advanced High Strength Steel Guidelines,” www.a-sp.org (November 1, 2007).
- A-7.** American Iron and Steel Institute, Great Designs in Steel, Seminar Presentation.
- A-8.** ULSAB-AVC Consortium. (2001, Jan). *ULSAB-AVC (Advanced Vehicle Concepts) Overview Report*. Retrieved from <http://www.autosteel.org/Programs/ULSAB-AVC.aspx>.
- A-9.** Courtesy of AIDA America.
- A-10.** Dr. T. Altan, Professor at Ohio State University.
- A-11.** AWS, “Welding Handbook – Welding Processes, Part 2,” American Welding Society (2007).
- A-12.** Courtesy of Auto/Steel Partnership and AET Integration.
- A-13.** AWS D8.1, “Specification for Automotive Weld Quality – Resistance Spot Welding of Steels,” American Welding Society (2013).
- A-14.** AWS C1.1, “Recommended Practices for Resistance Welding,” American Welding Society (2012).
- A-15.** ASM International, “Welding, Brazing and Soldering,” The Materials Information Society (2008).
- A-16.** Courtesy of ArcelorMittal.
- A-17.** Auto\Steel Partnership Advanced High-Strength Steel Applications Design and Stamping Process Guidelines – Section 2 – Lessons learned from Advanced High Strength Steel Case Studies (2010)
- A-18.** AWS – AWS D8.6:2005, Table 2, Page 4.
- A-19.** L. W. Austin and J. L. Lindsay, “Continuous Steel Strip Electroplating,” slide course, American Electroplaters and Surface Finishers Society, 1989
- A-20.** Courtesy of Auto/Steel Partnership

B

B-1. H. Beenken, "Joining of AHSS versus Mild Steel," Processing State-of-the-Art Multi-phase Steel; European Automotive Supplier Conference, Berlin (September 23, 2004).

B-2. H. Beenken et al, "Verarbeitung Oberflächenveredelter Stahlfeinbleche mit Verschiedenen Füge-techniken," Große Schweißtechnische Tagung 2000, Nürnberg, (September 27, 2000). DVS-Berichte Bd. 209, Schweißen und Schneiden (2000).

B-3. H. Beenken, "Hochfeste Stahlwerkstoffe und ihre Weiterverarbeitung im Rohbau," Füge-technologien im Automobilleichtbau, AUTOMOBIL Produktion, Stuttgart, (March 20, 2002).

B-4. Courtesy of Baosteel and Posco Steel.

C

C-1. B. Carlsson et al, "Formability of High Strength Dual Phase Steels," Paper F2004F454, SSAB Tunnpålar AB, Borlänge, Sweden (2004).

C-2. B. Carlsson, "Choice of Tool Materials for Punching and Forming of Extra- and Ultra High Strength Steel Sheet," 3rd International Conference and Exhibition on Design and Production of Dies and Molds and 7th International Symposium on Advances in Abrasive Technology, Bursa, Turkey (June 17-19, 2004).

C-3. V. Cuddy et al, "Manufacturing Guidelines When Using Ultra High Strength Steels in Automotive Applications," EU Report (ECSC) R585 (January 2004).

C-4. D. Corjette et al, "Ultra High Strength FeMn TWIP Steels for Automotive Safety Parts," SAE Paper 2005-01-1327 (2005).

C-5. Corus Automotive. (2009, Dec) *Pocket book of steel: Your reference guide to steel in the automotive industry*. Retrieved from http://www.tatasteela.com/file_source/StaticFiles/Microsites/Automotive/Publications/Book%20of%20steel/Book%20of%20Steel%203rd%20Ed_lowres.pdf.

C-6. Courtesy of China Steel.

D

D-1. Courtesy of A. Lee, Dofasco Inc.

D-2. Abraham, A. Ducker Worldwide. (2011, May). [Future Growth of AHSS](#) [PowerPoint presentation at Great Designs in Steel Seminar - 2011].

E

E-1. Edison Welding Institute and the Ohio State University, "Effect of Material and GMAW Process Conditions on AHSS Welds," Sheet Metal Welding Conference XII.

F

F-1. T. Flehmig et al, "A New Method of Manufacturing Hollow Sections for Hydroformed Body Components," International Body Engineering Conference, Detroit, USA (2000).

F-2. T. Flehmig et al, "Thin Walled Steel Tube Pre-bending for Hydroformed Component – Bending Boundaries and Presentation of a New Mandrel Design," SAE Paper 2001-01-0642, Detroit, USA (2001).

F-3. Courtesy of FCA North America LLC.

F-4. Courtesy of Fuchs Lubricants.

G

G-1. J. Gerlach et al, "Material Aspects of Tube-hydroforming," SAE Paper 1999-01-3204, Detroit, USA (1999).

G-2. S. Göklü, "Innovative Fügetechnologien beim Einsatz Neuartiger Stahlwerkstoffe für den Schienenfahrzeugbau," Fügen und Konstruieren im Schienenfahrzeugbau, SLV Halle, (May 21, 1997).

G-3. S. Göklü et al, "The Influence of Corrosion on the Fatigue Strength of Joined Components from Coated Steel Plate," *Materials and Corrosion* 50, p.1 (1999).

G-4. Geyer, R. (2008, Sept 15). "Parametric Assessment of Climate Change Impacts of Automotive Material Substitution." *Environmental Science & Technology*, 42 (18), 6973-6979.

G-5. Green Car Congress (September 5, 2012). MQB-based 7th Generation VW Golf up to 100 kg Lighter and 23% More Fuel Efficient Than Predecessor.

G-6. Courtesy of General Motors Corporation.

H

H-1. R. Hilsen et al, "Stamping Potential of Hot-Rolled, Columbium-Bearing High-Strength Steels," *Proceedings of Microalloying 75* (1977).

H-2. B. Högman et al, "Blanking in Docol Ultra High Strength Steels," *Verschleißschutztechnik*, Schopfheim, Germany (2004) and G. Hartmann "Blanking and Shearing of AHS Steels – Quality Aspects of Sheared Edges and Prediction of Cutting Forces," ACI Conference; Processing State-of-the Art Multiphase Steels, Berlin, Germany (2004).

H-3. G. Hartmann, "Das Spektrum Moderner Stahlfeinbleche-Festigkeiten und Auswirkungen auf die Umformung" *Verschleißschutztechnik*, Schopfheim, Germany (2004).

H-4. Published 03/28/2017 Copyright © 2017 SAE International doi:10.4271/2017-01-0306 saeeng.saejournals.org Hance, B., "Practical Application of the Hole Expansion Test," *SAE Int. J. Engines* 10(2):2017, doi:10.4271/2017-01-0306

I

- I-1.** R. Mohan Iyengar et al, "Implications of Hot-Stamped Boron Steel Components in Automotive Structures," SAE Paper 2008-01-0857 (2008).
- I-2.** Global Comparison of Passenger Car and Light Commercial Vehicle Fuel Economy/GHG Emissions Standards; February 2014 Update, International Council for Clean Transportation (ICCT). www.theicct.org
- I-3.** Insurance Institute for Highway Safety. <http://www.iihs.org/> [Web resources].
- I-4.** Image Industries. <http://www.imageindustries.com/welding-processes/gas-arc-welding-process/> [Web Resources].
- I-5.** Courtesy of Irmco (Jeff Jeffery).

J

- J-1.** Courtesy of JFE Steel Corporation
- J-2.** C. Ji, M. Kimchi, Y. Kim and Y. Park, "The application of pulsed current in resistance spot welding of zn-coated hot-stamped boron steels," in *Advances in Resistance Welding*, Miami, FL, 2016.

K

- K-1.** A. Konieczny, "Advanced High Strength Steels – Formability," 2003 Great Designs in Steel, American Iron and Steel Institute (February 19, 2003), www.autosteel.org.
- K-2.** S. Keeler, "Increased Use of Higher Strength Steels," PMA Metalforming magazine (July 2002).
- K-3.** A. Konieczny, "On the Formability of Automotive TRIP Steels", SAE Technical Paper No. 2003-01-0521 (2003).
- K-4.** T. Katayama et al, "Effects of Material Properties on Shape-Fixability and Shape Control Techniques in Hat-shaped Forming," Proceedings of the 22nd IDDRG Congress, p.97 (2002).
- K-5.** Y. Kuriyama, "The Latest Trends in Both Development of High Tensile Strength Steels and Press Forming Technologies for Automotive Parts," NMS (Nishiyama Memorial Seminar), ISIJ, 175/176, p.1 (2001).
- K-6.** A. Konieczny and T. Henderson, "On Formability Limitations in Stamping Involving Sheared Edge Stretching," SAE Paper 2007-01-0340 (2007).
- K-7.** M. Kupper, K. Eckhardt, GM Opel, from proceedings of the 2014 Aachen Body Engineering Days.
- K-8.** Courtesy of Kia Motors.

L

- L-1.** S-D. Liu, "ASP HSS Load Beam Springback Measurement Data Analysis," Generalety Project Report #001023 (May 27, 2004).
- L-2.** S. Lalam, B. Yan, "Weldability of AHSS," Society of Automotive Engineers, International Congress, Detroit (2004).
- L-3.** R. Laurenz, "Bauteilangepasste Fügetechnologien," Fügetechnologien im Automobilbau, Ulm (February 11, 2004).
- L-4.** R. Laurenz, "Spot Weldability of Advanced High Strength Steels (AHSS)," Conference on Advanced Joining, IUC, Olofstrøm (February 2, 2004).
- L-5.** F. Lu and M. Forrester, Proceedings of the 23rd International Congress on Applications of Lasers and Electro Optics (2002).
- L-6.** T. M. Link, "Tensile Shear Spot Weld Fatigue of Advanced High Strength Steels," Paper presented at the 45th MWSP Conference, Page 345, Vol. XLI (2003).
- L-7.** W. Li and E. Feng, "Energy Consumption in AC and MFDC Resistance Spot Welding" paper presented at the XI Sheet Metal Welding Conference, American Welding Society, Detroit Chapter (May 11-14, 2004).

M

- M-1.** Courtesy of S. Lalam, Mittal Steel.
- M-2.** M. Merklein and J. Lechler, "Determination of Material and Process Characteristics for Hot Stamping Processes of Quenchable Ultra High Strength Steels with Respect to a FE-based Process Design." SAE Paper 2008-01-0853 (2008).
- M-3.** K. Miyoshi, "Current Trends in Free Motion Presses," Nagoya, Japan.
- M-4.** M. McCosby, "Hot Dipped Coating Technology – Galvannealing and GA Products" (2006) – U. S. Steel Research and Technology Center.
- M-5.** Courtesy of P. Mooney archives
- M-6.** H. Mohrbacher, "Advanced metallurgical concepts for DP steels with improved formability and damage resistance" – NiobelCon bvba
- M-7.** P. Mooney, "Design and Application Related Considerations for AHSS" – 3S – Superior Stamping Solutions, LLC training seminar
- M-8.** P. Mooney, "Stamping Technology Seminar" – 3S – Superior Stamping Solutions, LLC training seminar

N

- N-1.** Courtesy of K. Yamazaki, Nippon Steel Corporation.
- N-2.** M. F. Shi, Internal National Steel Corporation report.
- N-3.** J. Noel, HSS Stamping Task Force, Auto/Steel Partnership.
- N-4.** National Highway Traffic Safety Administration.
<http://www.nhtsa.gov/Laws+&+Regulations/Vehicles?rulePage=0> [Web resources].
- N-5.** Courtesy of Nippon Steel
- N-6.** Courtesy of the National Plasma Nitriding Center.

O

- O-1.** Courtesy of the Ohio State University
- O-2.** Courtesy of Oak Ridge National Laboratory and Ford Motor Company

P

- P-1.** C. Potter, American Iron and Steel Institute, Southfield, MI
- P-2.** Courtesy of Posco, South Korea
- P-3.** P.E. International, GaBi Professional Database 2013 - Aluminium ingot mix IAI (2010),
<http://gabi-documentation-2013.gabi-software.com/xml-data/processes/eee56f32-df9d-47ac-ad4d-4e733eb18921.xml>
- P-4.** Patterson, J., Alexander, M., Gurr, A. (2011, May 20). "Preparing for a Low Carbon Vehicle Society"; Report Number RD/11.124801.4, Low Carbon Vehicle Partnership Study.
- P-5.** Parsons, W. (May, 2012). "Body Structure Light Weighting at Cadillac", *Great Designs in Steel* conference presentation
- P-6.** D. Phillips, Manuscript "Welding Engineering: An Introduction," Wiley (to be published 2014)
- P-7.** D. Pieronek (Forschungsgesellschaft Krafftahwesen), A. Marx (Dortmunder OberflächenCentrum) and R. Röttger (ThyssenKrupp), "Numerical Failure Prediction of Resistance Spot Welded Steel Joints," NAFEMS Seminar (2010).
- P-8.** Andrea Peer, Ying Lu, Tim Abke, Menachem Kimchi, and Wei Zhang "Deformation Behaviors of Subcritical Heat-affected Zone of Ultra-high Strength Steel Resistance Spot Welds." in 9th International Seminar & Conference on Advances in Resistance Spot Welding. Miami, (3 2016). Paper No. 12.
- P-9:** The Phoenix Group (2016), "The Science of Sheet Metal Formability".

R

R-1. Courtesy of P. Ritakallio, Rautaruukki Oyj.

R-2. D. J. Radakovic and M. Tumuluru, "Predicting Resistance Spot Weld Fatigue Failure Modes in Shear Tension Tests of Advanced High Strength Automotive Steels," *Welding Journal*, Vol. 87 (April 2008).

S

S-1. M. Shi et al, "Formability Performance Comparison between Dual Phase and HSLA Steels," *Proceedings of 43rd Mechanical Working and Steel Processing*, Iron & Steel Society, 39, p.165 (2001).

S-2. M. Shi, "Springback and Springback Variation Design Guidelines and Literature Review," National Steel Corporation Internal Report (1994).

S-3. S. Sadagopan and D. Urban, "Formability Characterization of a New Generation of High Strength Steels," American Iron and Steel Institute (March 2003).

S-4. Singh et al, "Selecting the Optimum Joining Technology," p.323 and "Increasing the Relevance of Fatigue Test Results," *MP Materialprüfung*, 45, 7-8, p.330 (2003).

S-5. Courtesy of D. Eriksson, SSAB Tunnpåt AB.

S-6. Steel Market Development Institute Automotive Market Program. www.autosteel.org. [Web resources].

S-7. Shaw, J. R. and Zuidema, B. K. (2001). "New High Strength Steels Help Automakers Reach Future Goals for Safety, Affordability, Fuel Efficiency and Environmental Responsibility" *SAE Paper* 2001-01-3041.

S-8. Tom Stoughton, General Motors Research, GDIS 2013 and other papers.

S-9. Hua-Chu Shih, Constantin Chirac, and Ming Shi, "The Effects of AHSS Shear Edge Conditions on Edge Fracture," *Proceedings of the 2010 International Conference on Manufacturing Science and Engineering*, MSEC2010-34062

S-10. M. Shih, "Laser Cutting to Improve AHSS Edge Stretchability," *SAE Paper* 2014-01-0994

S-11. M. Shih, M. Shi, D. Zeng, C. Xia, Development of Shear Fracture Criterion for Dual Phase Steel Stamping – 2009 SAE International 2009-01-1172

S-12. M. Shih, M. Shi, C. Xia, D. Zeng, "Experimental Study on Shear Fracture of Advanced High Strength Steels Part II" – 2009 International Conference on Manufacturing Science and Engineering

S-13. M. Shih, "Die Wear and Galling in Stamping DP 980 Steels" – Great Designs in Steel 2015

T

- T-1.** M. Takahashi et al, "High Strength Hot-Rolled Steel Sheets for Automobiles," Nippon Steel Technical Report No. 88 (July 2003).
- T-2.** M. Takahashi, "Development of High Strength Steels for Automobiles," Nippon Steel Technical Report No. 88 (July 2003).
- T-3.** Courtesy of ThyssenKrupp Stahl.
- T-4.** Courtesy of TOX PRESSOTECHNIK GmbH & Co. KG, Weingarten.
- T-5.** M. Tumuluru, "Resistance Spot Welding of Coated High-Strength Dual-Phase Steels," Welding Journal (August 2006).
- T-6.** M. Tumuluru, "A Comparative Examination of the Resistance Spot Welding Behavior of Two Advanced High Strength Steels," SAE Paper 2006-01-1214 (2006).
- T-7.** M. Tumuluru, "The Effect of Coatings on the Resistance Spot Welding Behavior of 780 MPa Dual Phase Steel", Welding Journal, Vol. 86 (June 2007).
- T-8.** M. Tumuluru and S. Gnade, "Clinch Joining of Advanced High Strength Steels," Paper presented at the MS&T Conference, Detroit, MI (September 2007).
- T-9.** Courtesy of TRUMPF
- T-10.** Courtesy of TATA Steel
- T-11.** Courtesy of ThyssenKrupp Steel Europe
- T-12.** Courtesy of The Welding Institute, United Kingdom, <http://www.twi-global.com/technical-knowledge/faqs/process-faqs/faq-how-do-clinching-and-self-piercing-riveting-compare-with-spot-welding-for-sheet-materials/> [Website Reference]

U

- U-1.** M. Ueda and K. Ueno, "A Study of Springback in the Stretch Bending of Channels," Journal of Mechanical Working Technology, 5, p.163 (1981).
- U-2.** Courtesy of United States Council for Automotive Research LLC
- U-3.** Courtesy of US Steel Corporation (M. Tumuluru and D. J. Radakovic)

V

- V-1.** Courtesy of C. Walch, voestalpine Stahl GmbH.
- V-2.** Courtesy of M. Peruzzi, voestalpine Stahl GmbH.

W

- W-1.** International Iron and Steel Institute, UltraLight Steel Auto Body - Advanced Vehicle Concepts (ULSAB–AVC) Overview Report (2002), www.worldautosteel.org.
- W-2.** www.worldautosteel.org.
- W-3.** J. Wu et al, “A Failure Criterion for Stretch Bendability of Advanced High Strength Steels,” SAE Paper 2006-01-0349 (2006).
- W-4.** M. Walp et al, “Shear Fracture in Advanced High Strength Steels,” SAE Paper 2006-01-1433 (2006).
- W-5.** WorldAutoSteel. <http://www.worldautosteel.org/> [Web resources].
- W-6.** WorldAutoSteel. (April 16, 2013) *Steel Eliminates Weight Gap With Aluminium For Car Bodies*. Retrieved from [www.worldsteel.org/2013 press releases](http://www.worldsteel.org/2013_press_releases).
- W-7.** WorldAutoSteel. (2011) *FutureSteelVehicle – Final engineering report*. Retrieved from <http://www.autosteel.org/Programs/Future%20Steel%20Vehicle.aspx>.
- W-8.** WorldAutoSteel (2002) ULSAB-AVC (Advanced Vehicle Concepts) Engineering Report. Retrieved from <http://www.worldautosteel.org/projects/ulsab-avc-2/>.
- W-9.** WorldAutoSteel. (2001) ULSAC Engineering Report. Retrieved from <http://www.worldautosteel.org/projects/ulsac-2/ulsac/>.
- W-10.** G. Walters, Hot Dipped Coating Technology – Coating Bath Hardware (2006) – U. S. Steel Research and Technology
- W-11.** Photo courtesy of Worthington Specialty Processing.
- W-12.** Photo courtesy of WikiBooks, https://en.wikibooks.org/wiki/Microtechnology/Additive_Processes [Web resources]

Y

- Y-1.** B. Yan, “High Strain Rate Behavior of Advanced High-Strength Steels for Automotive Applications,” 2003 Great Designs in Steel, American Iron and Steel Institute (February 19, 2003), www.autosteel.org.
- Y-2.** K. Yoshida, “Handbook of Ease or Difficulty in Press Forming,” Translated by J. Bukacek and edited by S-D Liu (1987).
- Y-3.** B. Yan (Mittal Steel, USA), Y. Kuriyama and A. Uenishi (Nippon Steel Corporation), D. Cornette (Arcelor), M. Borsutzki (ThyssenKrupp Stahl), C. Wong, SAE Paper 2006-01-0120 - *Recommended Practice for Dynamic Testing for Sheet Steels - Development and Round Robin Tests*

Z

- Z-1.** W. Zhang (SWANTEC Software and Engineering ApS), A. Chergue (ThyssenKrupp Steel Europe) and C Valentin Nielsen (Technical University of Denmark), “Process Simulation of Resistance Weld Bonding and Automotive Light-weight Materials,” 7th International Seminar on Advances in Resistance Welding (2012).